TECHNICAL UNIVERSITY IN ZVOLEN

Faculty of Wood Sciences and Technology
Department of Fire Protection
Department of Chemistry and Chemical Technologies
and
Faculty of Ecology and Environmental Sciences
Department of Environmental Engineering

Book of Proceedings

International Scientific Conference

Earth in a trap? 2018

Analytical Methods in Fire and Environmental Sciences

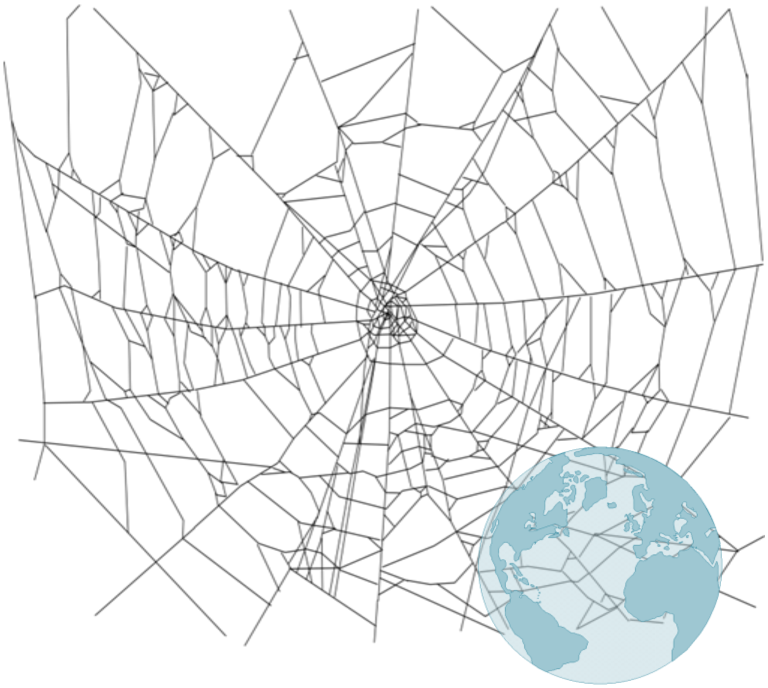

23rd – 25th May, 2018
Salamandra Hotel
Horný Hodrušský tajch, Hodruša-Hámre
Slovak Republic

Book of Proceedings

International Scientific Conference

Earth in a trap? 2018: Analytical Methods in Fire and Environmental Sciences

23rd – 25th May, 2018

ISBN 978-80-228-3062-1

Editors: Tatiana Bubeníková, Veronika Veľková

Technical editors: Rastislav Veľas, Martin Bednár

Published by Technical University in Zvolen, Slovak Republic, 2018

INTERNATIONAL SCIENTIFIC COMMITTEE

prof. Magdaléna BÁLINTOVÁ, Ph.D.
Technical University of Košice, Slovak Republic

prof. Adriana EŠTOKOVÁ, Ph.D.
Technical University of Košice, Slovak Republic

pplk. Štefan GALLA, Ph.D.
Fire and Rescue Service, Slovak Republic

prof. František KAČÍK, Ph.D.
Technical University in Zvolen, Slovak Republic

prof. Danica KAČÍKOVÁ, Ph.D.
Technical University in Zvolen, Slovak Republic

assoc. prof. Andrea MAJLINGOVÁ, Ph.D.
Technical University in Zvolen, Slovak Republic

assoc. prof. Linda MAKOVICKÁ-OSVALDOVÁ, Ph.D.
University of Žilina, Slovak Republic

assoc. prof. Jozef MARTINKA, Ph.D.
Slovak University of Technology in Bratislava, Slovak Republic

prof. Ph.D. Verica MILANKO
Visoka tehnička škola strukovnih studija, Serbia

assoc. prof. Andrei NIKULIN
Saint Petersburg Mining University, Russia

plk. Zděnek RÁŽ
Technical Institute of Fire Protection in Prague, Czech Republic

Dr. habil. Tamas RÉTFALVI
University of Sopron, Hungary

prof. Dagmar SAMEŠOVÁ, Ph.D.
Technical University in Zvolen, Slovak Republic

prof. Ph.D. Branko SAVIC
Visoka tehnička škola strukovnih studija, Serbia

prof. Maroš SOLDÁN, Ph.D.
Slovak University of Technology in Bratislava, Slovak Republic

prof. Quiang XU
Nanjing University of Science and Technology, China

EDITOR`S FOREWORD

The conference “Earth in Trap?” began writing its history in 2006 with the main theme “Analysis of components of environment“. The aim of the conference was to create a forum for the exchange of knowledge and discussion of experts in the field of environment contamination solution. The event found a positive response in the scientific community, both in research and practice. Each year of the conference brought presentations of quality scientific work, stimulated discussion, opened new possibilities for problem solving, new contacts were established and cooperation started on projects.

The year 2016 opened new era of the conference direction. Applications of analytical methods in environmental engineering expanded also to fire engineering. Quality analysis is a basic element of identifying and defining the problem and the basis of its solution. Protection of the environment, fire protection of persons and property, fire and accident investigation, testing of new materials whose dynamic development and use extends to all spheres of human life are areas where the need for quality analytical methods is becoming more and more striking.

The aim of the conference is to provide a space for scientific and professional community to present new knowledge and discussion on the use of modern analytical methods in fire and environmental sciences, to point out to problems in developing new methods, innovation of classical methods to satisfy the needs of science and practice. The organizational committee is glade that the contact of scientific approach with the praxis has become a tradition of the conference.

The Book of Proceedings consists of scientific papers of authors from five countries, represents the latest state of the knowledge at the area of applications of analytical methods in fire and environmental engineering.

Organizational committee

WE ARE GRATEFUL FOR THE SUPPORT:

AMEDIS

HERMES
LabSystems

®
O.K. SERVIS
BioPro
s.r.o.
www.biopro.cz

Earth in a Trap? 2018
Analytical Methods in Fire and Environmental Science

Content

Earth in a Trap? 2018
Analytical Methods in Fire and Environmental Science

Earth in a Trap? 2018
Analytical Methods in Fire and Environmental Science

Earth in a Trap? 2018
Analytical Methods in Fire and Environmental Science

The influence of modification of spruce wooden sawdust on heavy metal absorption

Magdalena Balintova[a][*] – Stefan Demcak[a]

[a]Technical University of Kosice, Faculty of Civil Engineering, Institute of Environmental Engineering, Vysokoskolska 4, 042 00 Kosice, Slovakia

---

Abstract

The contamination of wastewater by heavy metal is a world-wide environmental problem. For this purposes low-cost adsorbents obtained from plant wastes or semi-products of various industries as a replacement of costly conventional methods as precipitation, ion exchange, and adsorption are also applied. The removal of heavy metals by adsorption onto low-cost waste materials has recently become the subject of considerable interest. Natural materials that are available in large quantities, or certain waste products from industrial or agricultural operations, can be used as inexpensive adsorbents.

The aim of this article is a study of absorption properties of natural and modified spruce wooden sawdust. Modification of spruce sawdust was carried out by sodium hydroxide and potassium hydroxide. The efficiency of heavy metals removal was tested on the model solutions with concentration of 10 $mg.L^{-1}$ cooper, zinc, and iron, respectively. Changes of the functional groups of sorbents was analysed by infrared spectrometry. Absorption properties of spruce wood sawdust and their two modifications were studied by colorimetric method. Changes of pH values in solutions after the absorption experiments were determined too.

Keywords: Biosorption; alkaline treatment; heavy metals removal

---

[*] Corresponding author. Tel.: +421-55-602-4274; fax: +421-55-602-4274; e-mail: magdalena.balintova@tuke.sk.

1. Introduction

The discharge of various kinds of pollutants, including heavy metals into the environment is still large problem and in some areas of the world it has even increasing character. The pollution of rivers and water reservoirs due to the disposal of heavy metals has been an increasing worldwide concern for the last few decades [1]. Heavy metals are one of the most dangerous environmental pollution. They are a menace for both the people and the whole ecosystem due to their toxicity and mutagenic, immunogenic, carcinogenic, teratogenic action [2]. Metals are accumulated very easily in living organisms that is why their harmful effect may appear even at very low concentrations [3, 4]. Most commonly used treatment processes heavy metals removal are chemical precipitation, membrane filtration, ion-exchange, adsorption, absorption, and precipitation with adsorption/ absorption [5].

The cost effective alternative technologies are important for removal of metals from contaminated waste water. Natural materials that are available in large quantities or have origin from waste products at industrial or agricultural operations may have potential as an inexpensive sorbents [6, 7]. Due to their low costs, these sorbents can be used without expensive regeneration in comparison to the industrial sorbents. Cost is an important parameter for comparing the sorption materials, but cost information is seldom reported, and the price of individual sorbents varies depending on the level of processing and local availability [8]. In general, a sorption can be assumed as a low-cost technology if it requires minimal processing, sorbent is abundant in nature, or is a by-product or waste material from another industry. Improving of sorption capacity may compensate the cost of additional processing. Sorbents are insoluble materials or mixtures of materials used to clean liquids through the mechanism of absorption, or adsorption, or both. Although they may be used as the sole clean-up method in small contamination, sorbents are most commonly used to remove final traces [4, 9].The use of low-cost adsorbents like wood sawdust has been investigated as a replacement of current costly methods [10]. Sawdust is mainly waste by-product of the timber industry that is either used as cooking fuel or a packing material; however, it can be used as a low-cost adsorbent of heavy metals, principally due to its lignocelluloses composition. Natural materials or waste products from certain industries with a high capacity for heavy metals can be obtained, employed, and disposed of with little cost [8, 11, 12].

The paper deals with a study of natural and modified spruce wooden sawdust absorption properties for removal of copper, zinc and iron ions from model solutions. The spruce wooden sawdust was modified by 1 M sodium hydroxide and potassium hydroxide, respectively and they were used for comparison of absorption properties with untreated wooden sawdust. The IR spectra of natural and modified spruce sawdust were studied for characterization of present functional groups, which can be responsible for metal binding and for study of the intensity changes of the selected functional groups of alkali modified sawdust.

2. Material and methods

The wooden sawdust of spruce was dried and sieved, and the fraction with particle size max. 2.0 mm was used for adsorption experiments and modification by hydroxides. Modification of spruce sawdust was carried out by 1M solutions of NaOH and KOH, where 200 mL of the appropriate hydroxide was mixed with 20 g of spruce sawdust for 24 h. After 1 day the modified sawdust were filtered, washed by deionised water and dried.

1 g of each dry adsorbent was mixed with 100 mL of each model solutions containing 10 mg.L^{-1} copper, zinc, and iron cations, respectively. The model solutions were prepared by dissolution of their sulphate salts in deionised water. Batch adsorption experiments were carried out on static conditions with interaction time 24 h. After absorption, sawdust mixtures were filtrated.

Concentrations of appropriate ions were determined by colorimetric method by Colorimeter DR 890. The pH values of solutions were also measured by pH meter inoLab pH 730. The IR spectra of dried spruce sawdust were studied for characterization of present functional groups, which can be responsible for metal binding by Bruker Alpha Platinum-ATR spectrometer (Bruker Optics, Ettingen, Germany). Also the efficiency of ion removal was calculated using the following equation:

$$\eta = ((c_0 - c_e)/c_0) \cdot 100\%, \qquad (1)$$

where η is efficiency of ion removal (%), c_0 is the initial concentration of appropriate ions (mg.L^{-1}) and c_e is equilibrium concentration of ions (mg.L^{-1}).

3. Results and discussions

3.1. Infrared spectra of wooden sawdust

Metal adsorption capacity of wooden sawdust could be influenced by various factors but is closely linked to the surface structures of –COH, –COOH, –NH, –NH_2, and –NH_3 functional groups which are present in organic materials [11]. Functional groups in spruce wood sawdust were determined using FTIR spectroscopy. The IR spectra of natural and alkali modified wooden sawdust are shown in Fig. 1. According to literature [13] we can suppose that the structure of wooden sawdust is mainly formed by cellulose, hemicellulose, and lignin. The FTIR spectrum of natural and modified sawdust showed several major intense bands that can be divided to 2 significant areas around wavenumbers 3,600–2,800 cm^{-1}; and 1,750–800 cm^{-1}.

The strong broad –OH stretching (3,650–3,000 cm^{-1}) and C–H stretching of methyl and methylene groups (3,000–2,800 cm^{-1}) are present in Fig. 1. The ending of strong boarded peak centred at wavenumber around 3,337 cm^{-1} could be also attributed to amine (–NH) functional groups. For the presence of hemicelluloses is the typical stretching band around at 1,736 cm^{-1} caused by presence of C=O from the acetyl groups [14]. Infrared spectra of lignin in wooden sorbent materials revealed characteristic bands at 1,503 and 1,454 cm^{-1} (correspond to aromatic skeletal vibrations of lignin) and at 1,320 cm^{-1} (syringyl and guaiacyl condensed lignin). The wavenumbers at 1422, 1367, 1315, 1153, 1024 and 894 cm^{-1} appertain to cellulose that occurs in two forms in crystalline (at 1315 cm^{-1}) and in amorphous (at 894 cm^{-1}) [15]. Functional groups of aromatics, carboxylic acids and alkyl halides were described at wavenumber 829 cm^{-1} [14].

The influence of the treatment have occurred intensification of strong broad –OH stretching at wavenumber centred at 3,337 cm^{-1} and creating of wide peak –OH deformation functional group at wavenumber 3,337 cm^{-1}. The potassium hydroxides considerably increase of hydroxyl functional groups intensity of spruce wood sawdust. The differences were also observed at wavenumbers of 3,000–2,800 cm^{-1} where the asymmetric C–H stretch were rearranged to symmetric, resulting in alignment of the triple peak at the wavenumber 2,883 cm^{-1}.

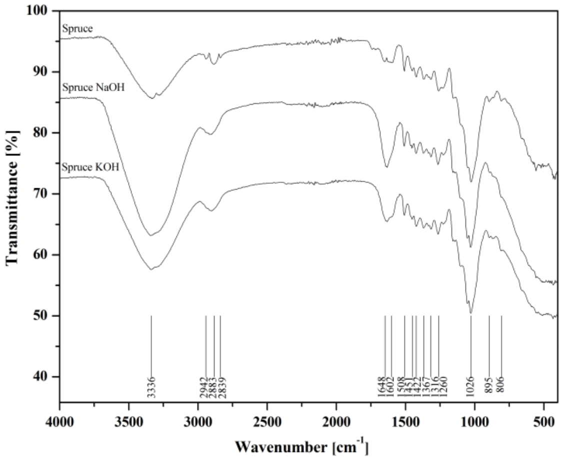

Fig. 1. Infrared spectra of natural and modified spruce wooden sawdust.

3.2. Adsorption experiments

Results of absorption experiments for solutions with concentrations of 10 mg.L^{-1} cations are shown in Table 1. Authors [16] investigated of metals removal by various sawdust adsorptions as appear to be a promising adsorbent for metals removal from wastewater with potentially more economical than current removal processes. Spruce wooden sawdust used for absorption were capable to removal the ions. The natural non-modified spruce exhibits suitable effect on absorption of copper, zinc and iron ions from solution with efficiencies about 80 %. The influence of alkali modification enhanced the absorption efficiency of copper and zinc ions from model solution. As it shown from FTIR spectra, the sodium hydroxide considerably increased of hydroxyl functional groups intensity that it resulting to increasing of absorption properties of spruce wooden sawdust to efficiency about 88 % for copper and zinc ions. In case of iron removal, the influence of hydroxides caused significant decreasing of efficiency to values under 0.5 %. It was caused by forming of organic-metallic dyes solved in solution without possibility of sorption. Changes of pH values in solutions were observed after sorption too. The alkaline modification had the effect to significant increase to pH values in all causes.

Table 1

Results of sorption experiments with spruce wooden sawdust (initial concentration of heavy metal ions in solutions c_0= 10 mg.L^{-1})

Sorbent	Cu^{2+} Initial pH= 5.8			Zn^{2+} Initial pH= 5.4			Fe^{2+} Initial pH= 5.4				
	c_e [mg.L^{-1}]	η [%]	pH	c_e [mg.L^{-1}]	η [%]	pH	Fe^{2+} c_e [mg.L^{-1}]	Fe^{3+} c_e [mg.L^{-1}]	Fe_{total} c_e [mg.L^{-1}]	Fe_{total} η [%]	pH
Spruce	1.90	81.0	4.9	3.00	70.0	5.3	3	-	3	70.0	5
Spruce_NaOH	1.27	87.3	7.7	1.20	88.0	7.9	0.3	9.7	10	<0.5	7.5
Spruce_KOH	2.78	72.2	7.8	2.59	74.1	8.3	0.2	9.8	10	<0.5	7.6

4. Conclusions

Presented study showed that modification of spruce wood sawdust by hydroxides increase absorption capacity for copper and zinc ions. The using of alkali spruce wooden sawdust modification for iron ions removal from solution is not suitable due to forming of organic-metallic dyes. This pollution has a negative influence on water treatment. Modified spruce wooden sawdust increases the pH values in solution. It was caused by releasing of the bonded hydroxides from the modified sawdust.

The infrared spectrometry showed changes of functional groups due to an alkaline modification of spruce wooden sawdust. The potassium hydroxides considerably increase of hydroxyl functional groups intensity of spruce wood sawdust. The differences were also observed at the wavenumbers about 2, 883 cm^{-1}, where the asymmetric C-H stretch in natural spruce wooden sawdust was rearranged to symmetric C-H stretch.

Acknowledgments

This work has been supported by the Slovak Grant Agency for Science (Grant No. 1/0563/15).

References

[1] H. Aydın, Y. Bulut, Ç. Yerlikaya, Journal of Environmental Management 87 (2008) 37.

[2] H. Hybská, D. Samešová, Ecotoxicology, Technical University in Zvolen, Zvolen, (2015).

[3] W.W. Ngah, M.A.K.M. Hanafiah, Bioresource technology 99 (2008) 3935.

[4] M. Ahmaruzzaman, Advances in Colloid and Interface Science 166 (2011) 36.

[5] M. Arora, B. Kiran, S. Rani, A. Rani, B. Kaur, N. Mittal, Food Chemistry 111(2008) 811.

[6] A. Shukla, Y.H. Zhang, P. Dubey, J.L. Margrave, S.S. Shukla, Journal of Hazardous Materials 95 (2002) 137.

[7] D. Samešová, H. Hybská, A. Ďuricová, 15th International multidisciplinary scientific geoconference SGEM: Ecology and environmental protection, (2015) 275.

[8] S.E. Bailey, T.J. Olin, R.M. Bricka, D.D.A. Adrian, Water research, 33 (1999) 2469.
[9] F. Fu, Q. Wang, Journal of environmental management 92(2011) 407.
[10] S. Ricordel, S. Taha, I. Cisse, G. Dorange, Separation and purification Technology 24 (2001) 389.
[11] G. Crini, Bioresource technology 97 (2006) 1061.
[12] K.S. Low, C.K. Lee, S.C. Liew, Process Biochemistry 36 (2000) 59.
[13] L. Kidalova, N. Stevulova, E. Terpakova, Pollack Periodica 10 (2015) 123.
[14] P. Zhang, S.J. Dong, H.H. Ma, B.X. Zhang, Y.F. Wang, X.M. Hu, Industrial Crops and Products 76(2015) 688.
[15] M.S. Rahman, M.A.Sc. Thesis, Dalhousie University, Canada, 2007.
[16] Y. Bulut, Z. Tez, Journal of Environmental Sciences 19 (2008) 160.

Changes of expanded polystyrenes macromolecular characteristics at thermal degradation

Martin Bednár[a*] – Tatiana Bubeníková[a] – Danica Kačíková[a] – František Kačík[a,b]

[a]*Faculty of Wood Sciences and Technology, Technical University in Zvolen, T. G. Masaryka 24, 960 53 Zvolen, Slovakia*

[b]*Faculty of Forestry and Wood Sciences, Czech University of Life Sciences in Prague, Kamýcká 1176, Praha 6 - Suchdol, 16521 Czech Republic*

Abstract

The study of expanded polystyrenes degradation is important because of their possible deterioration at higher temperatures. The influence of thermal loading in the temperature range from 140 °C to 200 °C on the expanded polystyrenes EPS 100F and EPS-Grey Wall (EPS GW) molecular weight changes was investigated. Size exclusion chromatography (SEC) with two PLgel MIXED B columns and tetrahydrofuran as a mobile phase were used for determination of molecular weights, degree of polymerisation (DP), polydispersity index (PDI) and molecular weight distribution (MWD). The degree of polymerisation (DP) decreases at the temperature above 140 °C in EPS 100F, polystyrene EPS GW has relatively good stability up to temperature of 180 °C, then its DP value rapidly drops. At 200 °C, molecular weight dropped by 90% for EPS 100F, and by 73% for EPS GW, respectively. At lower temperatures the polystyrene depolymerisation is slow and chain-end reaction prevails, at higher temperatures (140 °C for EPS 100F, and 180 °C for EPS GW, respectively) the drop of molecular weight is rapid and random cleavage of bonds is dominant.

Keywords: SEC; polystyrene; thermal degradation; degree of polymerisation; polydispersity index; molecular weight distribution

---

[*] Corresponding author. Tel.: +421 944 431 803; e-mail: bednar.mtn@gmail.com.

1. Introduction

Polystyrene is in several countries most produced material. The improvement of thermal stability and flammability performance of widely used thermoplastics is a major concern both industries and in an academic world. Consequently, modification of polystyrene, being one of the most commercialized thermoplastic, by addition of flame retardants is crucial [1, 2].

Brominated flame retardants being compatible and having small influence on mechanical properties have been used in polymer industry widely to reduce fire damage and harm. The most common brominated flame retardants are polybrominated biphenyls, polybrominated diphenyl oxides/ethers, tetrabromobisphenol-A and polybrominated epoxy resins. However, evolution of toxic brominated compounds during recycling, incineration, or in fires of such materials, provoked strong limitations in their use [3].

The nanoparticles can be used as flame retardant additives or fillers for polystyrenes and the addition of small percentage of nanoparticles with conventional flame retardants seemed to improve the flame-retardant performance. Addition of nanoparticles not only affects flame characteristics but also thermal behavior [2].

Expanded polystyrene is wide used material well-known from many of application from packaging of goods by household application to construction. Expanded polystyrenes are used as thermal insulation of buildings around the world. There are many of application in construction, one of the well-known is ETICS. One of the mostly used type of polystyrenes used in Slovakia for ETICS was EPS 100F it is white table of expanded polystyrene, on the other hand today there is modified polystyrene EPS Grey Wall (EPS GW) which is modified by graphite nanoparticles. EPS GW is a high quality expanded polystyrene of grey colour. The graphite particles integrated within the insulation reflects radiant heat and significantly improves insulation capability of EPS GW than traditional white EPS of the same thickness. Uhl and Wilkie [4] observed by thermogravimetry that modification of polystyrene by graphite nanoparticles has large impact to its thermal stability.

Macromolecular characteristics of polymers (e.g. polydispersity index (PDI), molecular weight distribution (MWD) and degree of polymerisation (DP)) have important influence on their mechanical and chemical properties. The aim of this work was therefore to investigate changes of macromolecular characteristics at thermal degradation of expanded polystyrenes.

2. Experimental

A 50 mm EPS 100F and EPS Grey Wall (EPS GW) polystyrenes from Isover (Saint-Gobain Construction Products) in self-extinguishing rendering with a polymer-based retarder, designated especially for outside systems of thermal insulation (ETICS) with enhanced insulating capability, were tested. Thermal loading of 0.1 g polystyrene samples was performed in 20-mL headspace vials in the temperature range from 140 °C to 200 °C and compared with the sample treated at the temperature of 20 °C using an Agilent Headspace Autosampler 7697A. Molecular weights (MW), polydispersity index (PDI = M_w/M_n) and molecular weight distribution (MWD) of polystyrene samples were analysed by size exclusion chromatography (SEC) using Agilent 1200 series equipment with two PLgel 10 µm MIXED B, 300 × 7.5 mm columns preceded PLgel 10µm Guard column 50 × 7.5 mm (Agilent), mobile phase tetrahydrofuran (flow rate 1 mL min^{-1}), temperature 35 °C, diode array detector. System was calibrated with polystyrene standards with molecular weights from 500 to 1,110,000 g mol^{-1} [5]. Measurements were performed on four replicates.

3. Results and discussion

Reduction in the polystyrene molecular weight has been observed by several authors, whereas the changes depended on its initial molecular weight and thermal exposure (temperature, time). However, thermal degradation of polystyrene is a complex process. According to Kruse et al. [6] polystyrene undergoes to numerous reactions, including bond fission, chain-end β-scission, midchain β-scission, 1,5-hydrogen transfer, 1,3-hydrogen transfer, radical addition, radical recombination, etc. As a result, the molecular weight decreases, and low-molecular compounds are formed. The formation of hazardous substances at the thermal loading of indoor polystyrene boards (e.g. styrene, α-methylstyrene, toluene, xylenes, ethylbenzene) was observed [7]. At higher temperatures, polystyrene degradation is initially rapid as a result of random cleavage of bonds, slowing down as it progresses, with the monomers cleaving off of the ends of the chain predominating [8-11]. From our results (Tab. 1, 2, Fig. 1, 2) is evident that degree of polymerisation (DP) of EPS 100F polystyrene decreases rapidly linear in the whole temperature region over the temperature of 140 °C, on the other hand DP of EPS GW show only little linear decrease up to the temperature of 180 °C, following with rapidly drop of its value. Molecular weights of the original (untreated) samples were about 190,000 g mol^{-1}, which is consistent with data published for EPS 100F polystyrene, in the range of 150,000 to 300,000 g mol^{-1} [11]. At 200 °C, this weight dropped to about 18,500 g mol^{-1}, i.e. it changed by 90% for EPS 100F, and to about 50,800 g mol^{-1}, i.e. it changed by 73% for EPS GW, respectively (Tab. 1, 2). At lower temperatures is polystyrene depolymerisation slow and chain-end reaction prevails, at higher temperatures (140 °C for EPS 100F, and 180 °C for EPS GW, respectively) the drop of molecular weight is rapid and random cleavage of bonds is dominant. The constancy of the ratio of the average degree of polymerization (DP_z/DP_w) is an indication of the homogeneity of the depolymerisation [12, 13]. In our case, the ratio remains fairly constant in whole temperature range for both polystyrenes, which indicates that no different reaction type, e.g. crosslinking, occurs. This idea is supported by constant values of polydispersity index (PDI) in both samples.

Table 1

Changes of molecular weights (MW) (M_n number-average MW; M_w weight-average MW; M_z z-average MW), M_{z+1} z+1-average MW), polydispersity index (PDI), and degree of polymerization (DP) in EPS 100F polystyrene

T (°C)	**M_n (g mol^{-1})**	**M_w (g mol^{-1})**	**M_z (g mol^{-1})**	**M_{z+1} (g mol^{-1})**	**PDI**	**DP**
20	77,283	190,234	371,634	585,829	2.46	1,829
	(2,076)	(1,087)	(251)	(3,678)	(0.05)	(10)
140	61,422	155,733	302,536	478,324	2.55	1,497
	(7,672)	(4,871)	(3,263)	(6,255)	(0.24)	(47)
160	36,705	86,377	156,860	242,601	2.35	830
	(101)	(943)	(4,997)	(16,628)	(0.02)	(9)
180	17,319	44,257	86,270	138,853	2.56	426
	(13)	(247)	(739)	(2,470)	(0.01)	(2)
200	6,931	18,563	38,173	60,828	2.68	178
	(389)	(309)	(240)	(236)	(0.11)	(3)

Note: Data in brackets represent standard deviation.

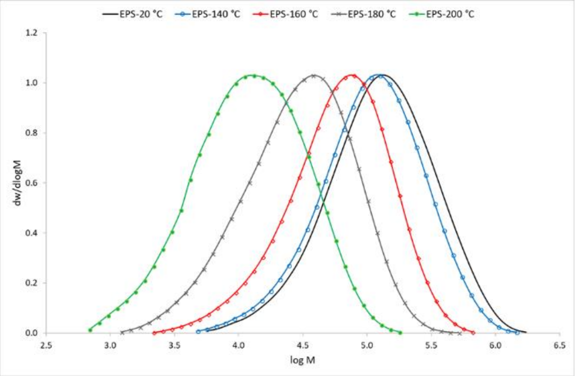

Fig. 1.
Molecular weight distribution (MWD) of EPS 100F polystyrene at different temperature of thermal treatment

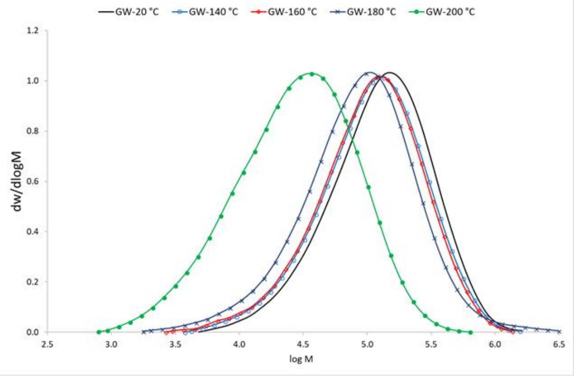

Fig. 2.
Molecular weight distribution (MWD) of EPS GW polystyrene at different temperature of thermal treatment

Table 2

Changes of molecular weights (MW) (M_n number-average MW; M_w weight-average MW; M_z z-average MW), M_{z+1} z+1-average MW), polydispersity index (PDI), and degree of polymerization (DP) in EPS GW polystyrene

T (°C)	**M_n (g mol^{-1})**	**M_w (g mol^{-1})**	**M_z (g mol^{-1})**	**M_{z+1} (g mol^{-1})**	**PDI**	**DP**
20	83,098 (2,556)	191,171 (1,538)	342,095 (6,245)	521,441 (19,764)	2.30 (0.06)	1,838 (15)
140	73,565 (672)	172,522 (725)	319,248 (4,514)	498,749 (14,196)	2.35 (0.03)	1,659 (7)
160	68,761 (2,092)	165,284 (1,207)	306,973 (4,764)	482,219 (16,516)	2.4 (0.06)	1,589 (12)
180	54,350 (1,263)	147,460 (1,358)	388,297 (13,569)	968,968 (20,268)	2.6 (0.26)	1,418 (13)
200	17,389 (879)	50,821 (1,098)	107,691 (2,769)	179,674 (10,264)	2.93 (0.09)	489 (11)

Conclusions

The influence of thermal loading in the temperature range from 140 °C to 200 °C on the expanded polystyrenes EPS 100 F and EPS GW molecular weight changes was investigated. The degree of polymerisation (DP) decreases linearly at the temperature above 140 °C in EPS 100F, polystyrene EPS-GW has relatively good stability up to temperature of 180 °C, then his DP value rapidly drops. At 200 °C, molecular weight dropped by 90% for EPS 100F, and by 73% for EPS GW, respectively. At lower temperatures is polystyrene depolymerisation slow and chain-end reaction prevails, at higher temperatures (140 °C for EPS 100F, and 180 °C for EPS GW, respectively, the drop of molecular weight is rapid and random cleavage of bonds is dominant. Polymer molecular weight determination will play an important role in the development of new polymer materials, ongoing processing / production over the polymer's lifecycle and its performance in the finished product, thus information obtained in this work may be useful for further utilization of thermally degraded polystyrenes.

Acknowledgments

This work was supported by the Slovak Scientific Grant Agency VEGA under contracts No. 1/0493/18 (50%) and No. 1/0806/2017 (50%).

References

[1] N. Pajaro, K. Caballer, J. Olivero-Verbel, Ambiente e Agua. 4 (2014) 610.
[2] H. Kaya, C. Kayna, J. Hacaloglu, J. Anal. Appl. Pyrol. 120 (2016) 194.
[3] H. Kaya, J. Hacaloglu, J. Anal. Appl. Pyrol. 105 (2014) 301.
[4] F. M. Uhl, C. A. Wilkie, Polym. Degrad. Stabil. 76 (2002), 111.
[5] F. Kacik, S. Podzimek, K. Vizarova, D. Kacikova, I. Cabalova, Cellulose. 23 (2016) 357.
[6] T. M. Kruse, O. S. Woo, H.-W. Wong, S. S. Khan, L. J. Broadbelt, Macromolecules. 35 (2002) 7830.
[7] Veľková, V., Kamenská, V., Bubeníková, T., Kačíková, D. Fire Protection, Safety and Security 2017, International Scientific Conference on Fire Protection, Safety and Security, Zvolen, Slovakia, May 03-05 (2017) 248.
[8] T. M. Kruse, H.-W. Wong, L. J. Broadbelt, Ind. Eng. Chem. Res. 42 (2003) 2722.
[9] C. L. Beyler, M. M. Hirschler, In: SFPE handbook of fire protection engineering. Vol. 2. Section 1, Chapter 7 (2002) 111-131. National Fire Protection Association.
[10] O. S. Woo, L. J. Broadbelt. Catal. Today. 40 (1998) 121.
[11] F. Sonnenberg, Annual Meeting of the American Foundry Society (AFS), 107th Casting Congress, Milwaukee, US, Apr 26-29, 2003; 113 (2003) 1213.
[12] X. Zou, N. Gurnagul, T. Uesaka, J. Bouchard, Polym. Degrad. Stabil. 43 (1994) 393.
[13] F. Kačík, D. Kačíková, M. Jablonský, S. Katuščák, Polym. Degrad. Stabil. 94 (2009) 1509.

Examination of Fuels of Selected Cellulose Materials on the Basis of Determination the Flash Point Ignition Temperature and Self-ignition Temperature

Iveta Coneva[a*]

[a]*Department of Fire Engineering, Faculty of Security Engineering, University of Žilina, Str. 1. mája 32, 026 01 Žilina, Slovak Republic*

Abstract

Fire protection issues as part of public protection is justified in preventing and minimizing the likelihood of fires and their consequences, and even in different categories of buildings sucha s.: industrial, manufacturing and technological buildings, warehouses and others. In the technologies of production and processing of cellulosic materials, eg: paper - namely tissue paper from basic raw materials, associated with treatment and disposal of unwanted printing dyes belongs, to the most risky in terms of fire. During bleaching process contact of flammable input raw materials (e.g. waste paper, cellulose) with strong oxidizing agent – hydrogen peroxide takes place. Hydrogen peroxide itself is not flammable but significantly supports burning process and thus increases fire danger in pulping operation at pulp cellulose preparing and in technological process of production tissue paper products: hygienic toilet paper, hygienic napkins and handkerchiefs. Used bleaching agent, hydrogen peroxide, is possible to substitute by other more suitable and more fire safety substance in practice. This substance is an enzyme that causes more effective enzymatic bleaching of waste paper input raw material. The goal of experimental investigation was verification and comparison of effect of bleaching agents (hydrogen peroxide and enzyme) on cellulose material inflammability. Subjects of tests werw input raw material samples – waste paper, wood pulp and intermediary product – tissue paper. Namely, following fire technical parameters: flash ignition temperature and self-ignition temperature of selected cellulose materials were determined and compared by method in STN ISO 871:1999 Plastics. Determination of ignition temperature using a hot-air furnace. Theoretical and practical investigations based on experiments concerning combustion of cellulose materials bring new knowledge.

Key words: burning of cellulose materials; waste paper; tissue paper; flash ignition temperature; self-ignition temperature

---

[*] Corresponding author. Tel.:+421 41 513 6755; Mobil:+421905636015; e-mail:iveta.coneva@fbi.uniza.sk.

1. Introduction

Protection of the population is a complex of preparation and in emergencies and crisis situations practically implemented measures. The measures are in line with current legislation and ensure utmost protection of health, life and animal population, material and cultural values as well as the environment, taking into account the economic capacity of the state. Public protection measures are carried out individual components Integrated Rescue System, especially Fire and Rescue SR. Fire in the different buildings and their subsequent localization and disposal are also part of the complex issue of public protection. Current legislation in force stipulates that fire safety topic solved almost in each building structure because it is necessary to secure not only sufficient level of fire safety but also protection of health and lives of people [1], [2]. Structural fire safety depends on many factors:e.g. on amount and type of flammable products, materials and substances placed in those.

In building structures and in technologies, too, flammable cellulose materials are present frequently [3-25], (for example wood, wood pulp, cellulose, paper, waste paper, tissue paper, etc.) Presence of cellulose materials as well as products significantly influences burning process thus i tis important to know their fire technical parameters [3-25], for example the flash ignition temperature and self-ignition temperature [9], [10], [12]. Values of the flash ignition temperature and self-ignition temperature are determined by the standardized method STN ISO 871:1999 Plastics: Determination of ignition temperature using a hot-air furnace [9], [10], [12]. Measured results can serve for comparison and assessment of fire origin possibility in technology of tissue products [3-25] production focused on a bleaching process by two different methods- the peroxide one and the enzymatic one. Effect of used bleaching agents (hydrogen peroxide and enzyme) on inflammability of completed tissue products [3-25] will be evaluated: that finally affects solving of fire protection topic in various building structures, namely in technological process of tissue product production [9], [10], [12].

2. Inflammability in a hot-air furnace

Fire technical characteristics - flash ignition temperature and self-ignition temperature of selected cellulose materials are to be determined and compared by method of STN ISO 871:1999 Plastics: Determination of ignition temperature using a hot-air furnace. This standard STN ISO 871 refers to the laboratory method of determination of ignition temperature using a hot-air furnace [3], [4], [9], [10], [12], [26-32]. This method is not used for description or evaluation of fire hazard nor fire risk of materials, products or equipment under specific fire conditions. Results of this test can be used as elements of fire hazard estimation when all factorsb relating to fire hazard estimation in any specific case are taken into account. Tests carried out under this method conditions have relevant significance at comparison of relative flammability characteristics of different materials. Obtained results represent the lowest temperature of ambient atmosphere when inflammability of material occurs under test conditions. Measured values allow arranging materials according to their susceptibility for inflammability under common use conditions. Determination of inflammability in a hot-air furnace is a suitable test also for polymeric materials on cellulose base [3], [4], [9], [10], [12], [26-32].

Flash ignition temperature (FIT) is the lowest temperature at which, under specified test conditions, sufficient flammable gases are emitted to ignite momentarily on application of a pilot flame [9],[10],[12],[14].

Spontaneous-ignition temperature (SIT) is the lowest temperature at which, under specified test conditions, ignition is obtained by heating in the absence of any additional ignition source [9],[10],[12],[14].

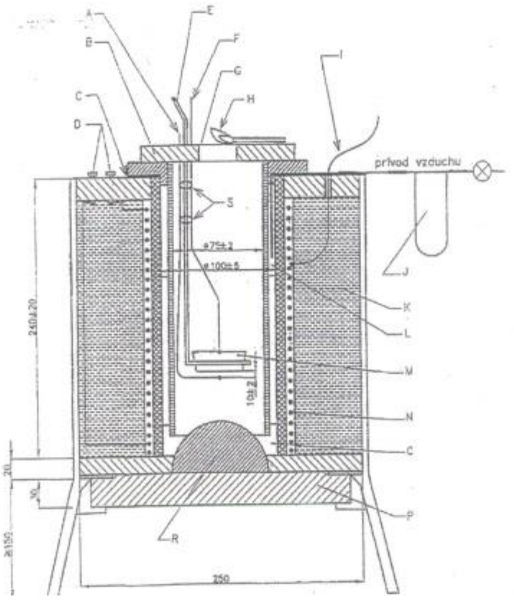

Fig. 1. Cross-section of the hot-air furnace [9]

A – thermocouple TC_2, B – fire-resistant disc cover,
C – sealing ring, D – terminals of heating spiral,
E – support rod, F – thermocouple TC_1, G – opening (diameter 25 mm), H – pilot flame,
I – thermocouple TC_3,
J – air-flow meter, K – mineral fibre wool,
L – air-flow tangential to cylinder, M – specimen pan, N – 50-turns of No 16 Nichrome wire in heat resistant tunnel, O – three distant blocks to spice inner tube location and support it,
P – thermal insulation, R – inspection plug, S – metal fastening clamps

2.1. Principle of the test, testing apparatus and specimens

A specimen of the material (Table 1) is heated in the hot-air furnace within a heating chamber using various temperatures. Flash ignition temperature is determined by is determined with a small pilot flame directed at the opening in the top of the furnace to ignite evolved gases. The spontaneous-ignition temperature is determined in the same manner as the flash-ignition temperature, but without the pilot flame [9],[10],[12],[26-32].The hot-air furnace and its cross-section is in Figure 1as a part of testing apparatus intended for determination of inflammability according to the STN ISO [9],[12]. The goal of investigation is verification and comparison of bleaching agents (hydrogen peroxide and enzyme) effect on inflammability of cellulose materials. Subjects of test are specimens of input raw materials – waste paper, and intermediary product – tissue paper [12],[33],[34] detailed referred to in the Table 1.

2.2. Preparation of tested specimens

Prior to the test, Specimens A, B, C, D, E were adjusted in roll forms with the mass (3,0 ± 0,2) g and tied by a wire and conditioned at the temperature (23 ± 2) oC and the relative humidity (50 ± 5) % for 40 hours in accordance with ISO 291 [12],[34].

Table 1

Essential data on cellulose materiál specimens [12],[33],[34]

Specimen identification	Essential data	Note (represented by)
A - input raw material	Mixture of waste paper; group quality C[a] – input raw material; better quality types	white newspaper; journals and newspaper with minimum text, pieces of paper sheets and cut white colourstripes printed by minimum text
B - input raw material	Mixture of waste paper; group quality B[a] – input raw material; middle quality types	journals and newspapers, pieces of paper sheets and cut white up to yellow colour stripes printed by text
C - intermediary product from 100 % wood pulp	Tissue paper –intermediary product made from 100 % wood pulp	non-bleached tissue paper suitable for production of final hygienic tissue products
D - intermediary product from waste paper bleached by enzyme	Tissue paper –intermediary product made from mixtures of waste paper (C[a] 30 % + 70 %B[a]) by enzymatic bleaching	tissue paper made from mixtures of waste paper bleached with enzyme and suitable for production of final hygienic tissue products
E - intermediary product from waste paper bleached by peroxide	Tissue paper –intermediary product made from mixtures of waste paper(C[a] 30 % + 70 %B[a]) by peroxide bleaching	tissue paper made from mixtures of waste paper bleached with peroxide and suitable for production of final hygienic tissue products

[a] Note:

Waste paper according to the standard STN EN 643 is divided into four main groups in which more subgroups are defined; the A group: types of lower quality; the B group: types of middle quality; the C group: higher quality types; and the D group: types containing sulphates [12],[33], [34].

B[a] – mixture of waste paper from the B group: middle quality types, actually it was represented by old newspapers [12],[33],[34].

C[a]- mixture of waste paper from the C group: middle quality types, actually it was represented by a mixture of printing scraps with bright multi-coloured colours [12],[33],[34].

3. Evaluation of experimental results and discussion

Measured values of the flash ignition temperature and spontaneous ignition temperature of cellulose material specimens are referred to in the table 2 and shown in graphic from in the Figure 2 [12], [34].

Table 2

Measured values of the flash ignition temperature and spontaneous ignition temperature of cellulose material specimens [12],[34]

Specimen - material	**Essential data**	**Flash ignition temperature [ºC]**	**Spontaneous ignition temperature [ºC]**
A - input raw material	Mixture of waste paper; group quality C^a – input raw material; better quality types	310	430
B - input raw material	Mixture of waste paper; group quality B^a – input raw material; middle quality types	320	410
C-intermediary product from 100 % wood pulp	Tissue paper – intermediary product made from 100 % wood pulp	270	420
D-intermediary product from waste paper bleached by enzyme	Tissue paper – intermediary product made from mixtures of waste paper (C^a 30 % + 70 % B^a) by enzymatic bleaching	310	410
E-intermediary product from wast paper bleached by peroxide	Tissue paper – intermediary product made from mixtures of waste paper (C^a 30 % + 70 % B^a) by peroxide bleaching	260	410

3.1 Discussion on experimental results – flash ignition temperature

Measured values of the flash ignition temperature (referred to in the Table 2 and the Figure 2),result in following: the highest flash ignition temperature value has the specimen B – 320 ºC (mixture of waste paper; group quality B) and the lowest one has the specimen E – 260 ºC (tissue paper made by peroxide bleaching). The specimen A – 310 ºC (mixture of waste paper; group quality C) reaches value comparable with the specimen B. Results of measured values of specimens B, A, D, and C, actually B – 320 ºC; A - 310 ºC; D - 310 ºC (tissue paper made by enzymatic bleaching); and C - 270 ºC (tissue paper made without bleaching) are higher than the value of the specimen E - 260 ºC. The flash ignition temperatures of the waste paper raw material – specimens B - 320 ºC and A - 310 ºC reached higher values probably due to presence of printing colouring. The specimen D - 310 ºC (tissue paper made by enzymatic bleaching) reaches also high value of the flash ignition temperature when compared with specimen C - 270 ºC (tissue paper made without bleaching) and specimen E – 260 ºC (tissue paper made by peroxide bleaching. The difference between the flash ignition temperature of the specimens D vs. E is 50 ºC that is not negligible [12],[34]. Probably more intensive bleaching processes at peroxide bleaching case may cause lower flash ignition temperature values for the specimen E; this means increasing of relative flammability of the Specimen E comparing with the specimen D that was bleached by enzyme. Based on measured values, it can be supposed that enzymatic bleaching of waste paper compared with the peroxide one, decreases flammability hazard of tissue paper, material intended for further processing and probably will decrease also flammability of final tissue products. It can be also stated that bleaching methods affect change of flash ignition temperature values as well as significantly change of relative flammability of all cellulose material specimens if naked heat source (flame) is used as an initiation source [3], [4], [12], [26-34].

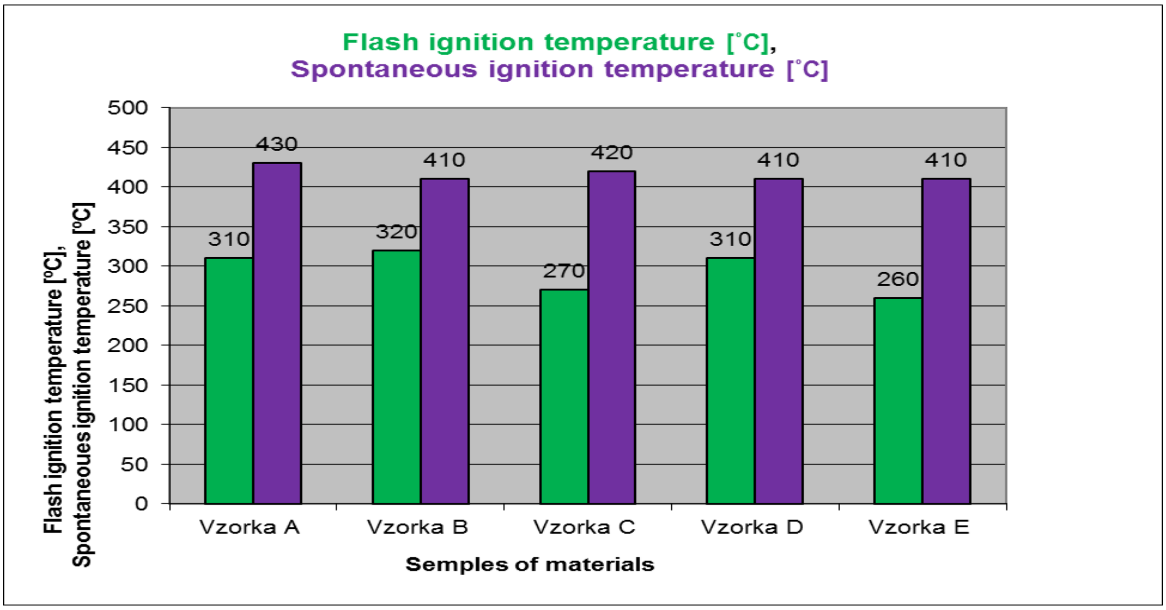

Fig. 2. Chart of measured values of the flash ignition temperature and spontaneous ignition temperature of cellulose material specimens [12], [34]

3.2. Discussion on experimental results – spontaneous ignition temperature

Measured values of the spontaneous ignition temperature (referred to in the Table 2 and the Figure 2), result in following: the highest spontaneous ignition temperature value has the specimen A – 430 °C (mixture of waste paper; group quality C); followed by the specimen C – 420 °C (tissue paper made without bleaching) and the lowest value of the spontaneous ignition temperature reached specimens B, D, and E; specimen B – 410 °C (mixture of waste paper; group quality B); specimen D – 410 °C (tissue paper made by enzymatic bleaching); and specimen E – 410 °C (tissue paper made by peroxide bleaching). Measured spontaneous ignition temperature values of the input raw material – waste paper are higher in the specimen A – 430 °C than this in the specimen B – 410 °C; the specimen A contains more printing colourings than the specimen B that probably leads to increasing of the spontaneous ignition temperature value. This means that the specimen A will ignite at higher temperature of the ambient air flowing around than the specimen B. Tissue paper – intermediary material being further processed in final hygienic products reached the highest spontaneous ignition temperature value for the specimen C – 420 °C followed by identical values of specimens D and E – 410 °C [12],[34]. Based on resulting values of the specimens D and E, it can be supposed that bleaching processes do not significantly influence the change of the spontaneous ignition temperature when compared with resulting values of the specimens A, B, and C. Values of samples D and E are only slightly lower (by 10 °C up to 20 °C) when compared with the specimens A, B, and C. It can be supposed that applying bleaching methods (specimens D and E) only slightly decreases the spontaneous ignition temperature and thus slightly increases relative flammability when compared with the specimen C represented by tissue paper without any bleaching. Overall, it can be quoted that bleaching methods have not significant effect on change of spontaneous ignition temperature values or on significant change of relative flammability of all cellulose material specimens if radiant heat source is used as an initiation source [3], [4], [12], [26-34].

3.3. Discussion on experimental results

Comparison of determined parameter values: the flash ignition temperature and the spontaneous ignition temperature of cellulose material specimens are referred to in the Table 2 and the Figure 2. The flash ignition temperature values of cellulose materials are within the range from 260 °C up to 320 °C; these flash ignition temperature values of particular specimens A, B, C, D, and E are referred to in the Table 2 and the Figure 2 – the graph. Determined values of the spontaneous ignition temperature of cellulose material specimens are within the range from 410 °C up to 430 °C; these values of particular specimens A, B, C, D, and E are referred to in the Table 2 and the Figure 2 – the graph. Measured values of the spontaneous ignition temperature of cellulose material specimens A, B, C, D, and E are by 110 °C up to 150 °C higher than values of the flash ignition temperature of identical specimens [12],[34].

Lower values of the flash ignition temperature can be explained by naked direct ignition source (propane flame) having higher initiation energy than indirect ignition source – hot air flow (radiant heat) used for determination of the spontaneous ignition temperature. Flash ignition, flame burning and following extinction of the same cellulosic material occur first, at lower temperatures than the spontaneous ignition and continuous flame burning [12],[26-34].

4. Conclusions

Determined values of the fire technical characteristics: the flash ignition temperature and the spontaneous ignition temperature were measured according to the standard STN ISO 871[9], [12]. Based on determined results (Tables 1 and 2 and Figure 2), it can be stated that input raw material specimens - waste paper A and B, namely specimen A – waste paper of quality group C and specimen B – waste paper of quality group B, reached the highest values of monitored fire technical characteristics: the flash ignition temperature and the spontaneous ignition temperature. It can be assumed that presence of dyers, fillers, gluing agents and other additives decreases relative flammability of waste paper. Based on comparison of determined values of the fire technical characteristics of the specimens D and E (Table 2 and Figure 2), the specimen D – tissue paper made by enzymatic bleaching; and the specimen E - tissue paper made by peroxide bleaching, it can be stated that tissue paper made from waste paper by enzymatic bleaching is less flammable than that made by peroxide bleaching. At the same time, it can be assumed that also final tissue hygiene products made by enzymatic bleaching are less flammable than tissue products made by peroxide bleaching [12].

Applying of enzymatic bleaching method (enzyme) during pulping when compared with peroxide bleaching method (hydrogen peroxide) decreases flammability of tissue paper and final tissue products that consequently affects decreasing of fire origin danger in the technological process of tissue product production. Measured results will contribute in practice to solving topic concerning decreasing of fire origin danger in paper-processing industry, namely at production of tissue paper and tissue hygienic products – toilet paper, hygienic handkerchiefs, napkins and dish-cloths. By suitable technology arrangement and treatment of selected characteristics of cellulose materials, fire danger relating to their technology processing and storage as well as flammability of final tissue products can be reduced.

Investigation of fire technical characteristics of treated products based on polymeric cellulose materials can contribute to increasing of fire safety in various building structures, especially in technological processes of production and storage [3], [4], [12], [26-36].Study of properties, especially fire-technical characteristics of different substances and materials that are found in industry, it is possible to prevent fires that are common undesirable incidents [3], [4], [12], [26-36]. Adverse crises situations are part of the solution to a complex issue of the protection of the population and critical infrastructure protection [35],[36].

References

[1] Balog, K., 1989: Požiarne nebezpečenstvo plastov používaných v stavebníctve. In:Horľavosť materiálov a nebezpečné pôsobenie splodín horenia. Bratislava: MV a ŽP SR a SŠP 1989, s.12

[2] Poledňák, P., 2000: The Protection of Dikes in Crises Situations. In: 11 th InternationalScientific and Technological Military Engineering Conference on Engineering and Management in Crises Situations. Military University of Technology, Warsawa 2000

[3] Můllerová, J., Orinčák , M., Coneva, I., 2016: Detoxification of ContaminatedEnvironment by Physico-Chemical Methods. In: SGEM 2016: Ecology, Economics, Education and Legislation: 16th International Multidisciplinary Scientific GeoConference SGEM 2016: www.sgem.org.SGEM2016 Conference Proceedings: 28 June – 6 July, 2016, Albena, Bulgaria. Book 5,Volume I. – Sofia: STEF92 Technology, 2016 – ISBN: 978-619-7105-65—0, ISSN:1314-2704. -[8] s., 239-246 pp, DOI:10.5593/SGEM2016/B51/S20.032

[4] Můllerová, J., Coneva, I., 2016: Thermal degradation of polymeric material based oncellulose by differential scanning calorimetry (DSC). In: SGEM 2016: Ecology, Economics, Education and Legislation: 16th International Multidisciplinary Scientific GeoConference SGEM 2016: www.sgem.org.SGEM2016 Conference Proceedings: 28 June – 6 July, 2016, Albena, Bulgaria. Book 5 Volume I., 765-770 pp – Sofia: STEF92 ECOLOGY AND ENVIRONMENTAL PROTECTION, 2016 – ISBN: 978-619-7105-65-0. -[6] s., ISSN 1314-2704, DOI: 10.5593/SGEM2016/B51/S20.102

[5] Blažej, A., Krkoška, P., 1989: Technológia výroby papiera. In. ALFA Bratislava.Bratislava 1989, ISBN 80-05-00119-3

[6] Hnětkovský, V. a kol.,1983:Papírenská příručka. In. STNL Praha. Praha 1983

[7] Bučko, J.,1997: Chemické spracúvanie dreva. Zvolen. TU Zvolen, 1997 ISBN 80- 228-0663-3

[8] Coneva, I., Lusková, M., 2006: Nebezpečenstvo použitia peroxidu vodíka vo výrobnomprocese. In:Ochrana pred požiarmi a záchranné služby, [elektronický zdroj] 2. vedecko-odborná konferencia s medzinárodnou účastku. Žilina 2006. KPI FŠI ŽU Žilina. s.25 - 33, ISBN 80-8070-539-9

[9] STN ISO 871 : 1999. Plasty. Stanovenie zápalnosti v teplovzdušnej peci. 1999

[10] Littomerický,V.: Prehľad skúšok horľavosti vykonaných na PTEÚ MV SR v Bratislave

[11] Coneva, I., Čahojová, Ľ., 2004: Vyhodnotenie štatistických údajov o papierenskom priemysle. In: Fórum mladých odborníkov protipožiarnej ochrany [elektronický zdroj], 5. medzinárodný odborný seminár. Zvolen, 2004. Zborník referátov, Zvolen: Technická univerzita, 2004,ISBN80-228-1354-0

[12] Coneva, I., 2008: Nebezpečenstvá vzniku požiaru pri výrobe produktov na báze celulózy [dizertačná práca: elektronický zdroj - CD] / Iveta Coneva; školiteľ Kateřina Orlíková.- VŠB – TU Ostrava, ČR, Fakulta bezpečnostního inženýrství,Katedra požární ochrany; študijný odbor: Požární ochrana a bezpečnost průmyslu, doktorský študijný program: Požární ochrana a bezpečnost, Ostrava: 2008, - 158 s. + Autoref. 34 s.

[13] Filipi, B., 2003: Náuka o materiály. 1. vyd. Ostrava : Edice SPBI Spektrum, 2003. 18-19 s. ISBN 80-86034-11-6

[14] STN EN ISO 13 943: 2000. Požiarna bezpečnosť. Slovník, apríl 2000

[15] Balog, K., Kvarčák, M., 1999: Dynamika požáru. 1. vyd. Ostrava : Edice SPBI Spektrum, sv. 22,1999. ISBN 80-86111 44-X

[16] Orlíková, K., Štroch, P., 1999: Chémie procesu horení. 1. vyd. Ostrava : Edice SPBI Spektrum,1999. ISBN 80-611139-3

[17] Bártlová, I., 2000: Nebezpeční látky I. 1. vyd. Ostrava : Edice SPBI Spektrum, sv. 24, 2000, 151 s., ISBN 80-8611160-1

[18] Osvald, A., 1996: Hodnotenie požiarnej bezpečnosti materiálov a výrobkov z dreva.Zvolen: TU DF,1996, 103 s. ISBN 80-28-0595-5

[19] Balog, K., 1999: Samovznietenie. 1. vyd. Ostrava : Edice SPBI Spektrum, 1999. ISBN 80-86111-45-8

[20] Steinleitner, M.D. A kol., 1990: Požárne a bezpečnostne technické charakteristické hodnoty nebezpečných látek.Zväz PO ČSSR, Praha, 1990

[21] Coneva, I., 2006: Skladovanie základnej vstupnej suroviny – zberového papiera vo výrobnej prevádzke.In. Crisis management, roč. 5, č.1, ŽU Žilina FŠI, 2006. 17-20 s. ISSN 1336-0019

[22] Kačíková, D., Netopilová, M., Osvald, A., 2006: Drevo a jeho termická degradácia. In. SPBI Ostrava. Ostrava 2006, ISBN 80 86634-78-7

[23] Fengel, D., Wegener, G., Wood, P., 1984: Chemistry, Ultrastructure, Reactions. Berlin, New York: Walter de Gruyter,1984. p.613

[24] Funaoka, M., Kako, T., Abe, I., 1991: Condensation of lignin dutiny heating of wood. In: Wood Science and Technology 24, 1991. p. 277-288

[25] Rowell, R.M., Dusoty, A.R., Degroot, F.W., Shafizadef,F., 1984 :Bonding fire retardants to wood: Part I. Thermal behavior of chemical bonding agents. In: Wood and Fiber Science, 16 (2),1984, p. 214-223

[26] Zachar, M., Majlingová, A., Martinka, J., Xu, Qiang, Balog, K., Dibdiaková, J., Poledňák, P., RYBAKOWSKI, M., 2014: Impact of oak wood ageing on the heat release rate and the yield of carbon monoxide during fire. European journal of environmental and safety sciences: scientific journal of the European Science and Research Institute and the Association

of Fire Engineering. 2014. zv. Vol. 2, č. issue 1, s. 1--4. ISSN 1339-472X

[27] Balog, K., Tureková, I., 2000: Sledovanie vplyvu retardačních úprav na tepelnú degradáciu celulózy. In. CO-MAT-TECH 2000, 8. medzinárodná vedecká konferencia, Trnava 2000, KEBI MTF TU Trnava, s. 299-304, ISBN 80-227-2117-4

[28] Orémusová, E., 2007: Hodnotenie teploty vzplanutia vybraných druhov PUR pien. Krízový manažment X/2007. Žilina :FŠI, Žilinská univerzita v Žiline 2007. s. 90-93. ISSN 1336-0019

[29] Orémusová, E., 2008: Teplota vznietenia poťahových textílií na báze bavlny a vlny. In. Ochrana pred požiarmi a záchranné služby. 3. vedecko-odborná konferencia s medzinárodnou účasťou. Žilina: Katedra požiarneho inžinierstva FŠI ŽU v Žiline 2008, s. 136-140, ISBN 978-80-8070-856-6

[30] Marková, I., 2003: Hodnotenie horľavosti látok uplatňujúcich sa v izolačnej alebo tvarovej vrstve čaluneného výrobku. Čalúnnické dni 2004. Tu vo zvolene, s. 16-20. IBN 80-288-1316-8

[31] Tureková, I., 2003: Valuation of combustibility od selected polymers. In CO-MAT-TECH 2003. Bratislava: STU, 2003: ISBN 80-227-1949-8

[32] Tureková, I., Balog, K., Michalíková, A., 2002: Vplyv kyseliny trihydrogénboritej na horenie tepelne namáhanej celulózy. In: CO-MAT-TECH 2002, MtF STU Trnava. 2002. str. 390 – 394

[33] STN EN 643: 1999. Zberový papier.1999

[34] Coneva, I.: Vzorka a materiály z výrobnej firmy tissue výrobkov

[35] Dvořák, Z., Boc, K., Vidríková, D., 2014: Informačný portál ochrany kritickej infraštruktúry v Slovenskej republike In: Civilná ochrana : revue pre civilnú ochranu obyvateľstva. – ISSN 1335-4094. - Roč. 15, č. 4 (2014), s. 54-56.

[36] Šimák, L., 2013: Základná terminológia na úseku prevencie závažných priemyselných havárií. Vedecký redaktor: Miloslav Seidl. In: Prevencia závažných priemyselných havárií : (vedecká monografia). - Žilina: Žilinská univerzita, 2013. - ISBN 978-80-554-0786-9. - S. 9-28.

Earth in a Trap? 2018
Analytical Methods in Fire and Environmental Science

Influence of the temperature on the load-bearing capacity of timber connections with steel fasteners

Tomasz Domański[a*] – Kamil Kmiecik[a]

[a]*Cracow University of Technology, The Faculty of Engineering, ul. Warszawska 24, Cracow 31-155, Poland*

Abstract

This paper presents a summary of results from numerical studies on the fire behavior of timber connections with steel members. The finite element software ANSYS was used to make a three-dimensional thermal model of the connections. Then the FE model was used to analyze the heat flow within the connections under standard ISO-fire exposure. To estimate the load-bearing capacity of the connections exposed to the standard fire, the failure modes from the literature were used. The calculations take into account the reduction of the cross-section caused by charring and the reduction of steel strength at elevated temperatures.

Keywords: fire safety; timber joints; thermal anaysis; steel plates; fastener

---

[*] Corresponding author, e-mail: doman@pk.edu.pl.

1. Introduction

Timber is a building material often used in constructions. The increasing use of wood in structures has been recently noticeable. There are many advantages of using this material, such as good environmental influence, aesthetic values, high energy efficiency and quick erection time. One of the most important issues concerning the design of timber structures is the fire safety requirement. The fire resistance of timber constructions can be determined using standard fire test, such as ISO 834 [1], it is calculated by methods included in EN 1995-1-2 [2].

Timber connections are usually the weakest parts in any timber structure, especially in fire conditions. Heat is conducted deep into the wood cross section from outside surfaces and primarily by the metal elements. It causes faster charring of timber elements. The fire resistance of timber connections depends on the charring of the wood and on the reduction of strength of the steel fasteners. The analysis of the fire performance of timber connections is complex because there are many parameters, such as geometry of the connection, different fastener arrangements and variability of the properties of wood and steel at elevated temperatures.

Wood is a combustible material. When timber is subjected to high temperature, it undergoes physical, chemical and structural changes. At first, timber heats up and the moisture will begin to evaporate. When wood is exposed to high temperature, the pyrolysis takes place when the temperature of wood is around 300 °C. These phenomena cause loss in mass and they decrease the mechanical and strength properties. The char layer is not able to carry any loads. In the reduced section, the stress increases. At the same time, the inner part of the cross section heats up, which causes the decrease of material properties. EN 1995-1-2 [2] assumes a reduction in the cross section by the charring while the charring rate is constant. Therefore the remaining cross section which is still load bearing can be defined.

Currently, prediction the structural behavior of wood in fire conditions is gaining importance due to the development of multi-storey timber structures [3]. Therefore, the numerical simulations using the finite element method are effective tools to examine the performance of timber structures exposed to fire. The main issues in simulations of timber connections under fire are modelling of the pyrolysis and the influence of steel elements on the temperature distribution. This paper focuses on wood-steel-wood connections. In this type of joints, a steel plate is slotted in the timber members and the connection is held together with steel bolts and dowels. The ANSYS [4] program was used to carry out the thermal simulations. The connections were exposed to the ISO fire.

2. Heat transfer and thermal properties

In modeling the wood-steel-wood connections in fire, three types of heat transfer processes should be considered as:

- Heat conduction in the element
- Heat exchange between steel and wood members
- Convective and radiative heat transfer from fire to element boundary.

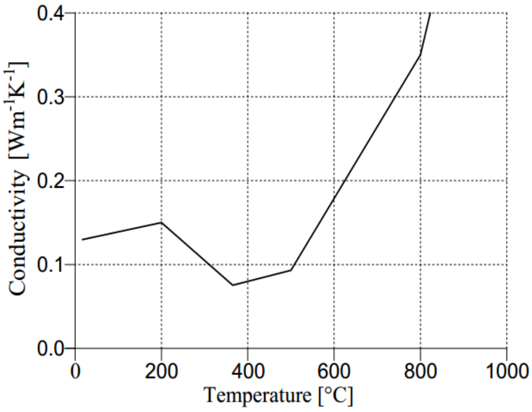

Fig. 1. Temperature-thermal conductivity relationship for wood and the char layer, based on EN-1995-1-2 [2]

The transient heat conduction within the connection members was modeled using three-dimensional linear interpolation heat transfer element. The governing partial differential equation should be defined as follows:

$$\frac{\partial}{\partial x}\left(\lambda_x \frac{\partial T}{\partial x}\right)+\frac{\partial}{\partial y}\left(\lambda_y \frac{\partial T}{\partial y}\right)+\frac{\partial}{\partial z}\left(\lambda_z \frac{\partial T}{\partial z}\right)+\dot{Q}=\rho c\frac{\partial T}{\partial t}$$

where T(K) is temperature, $\lambda_{x,y,z}$ (W/mK) are thermal conductivities in x, y, z directions, $\dot{Q}$ (W/m^3) is internally generated heat, ρ (kg/m^3) is density, c (J/kgK) is specific heat, and t (s) is time.

Thermal actions are given by the heat flux to the surface of the member. In fire conditions, the net heat flux should consist of heat transfer by radiation and convection. The equation is given by:

$$q'' = h_c(T_f - T_s) + \Phi\varepsilon_{eff}\sigma(T_f^4 - T_s^4)$$

where h_c (W/m^{2}K) is the convection coefficient, Φ is the configuration factor, σ is the Stefan-Boltzmann constant, ε_{eff} is the effective emissivity, T_s (K) is the surface of the member temperature and T_f (K) is the fire temperature. The convection coefficient h_c for the standard fire is 25 W/m^{2}K [5]. In the standard fire test, the configuration factor Φ can be taken as 1.0. The efficient emissivity ε_{eff} should be defined as:

$$\varepsilon_{eff} = \frac{\varepsilon_f \varepsilon_s}{\varepsilon_f + \varepsilon_s - \varepsilon_f \varepsilon_s}$$

where ε_f is emissivity of the furnace, ε_s is the surface emissivity.

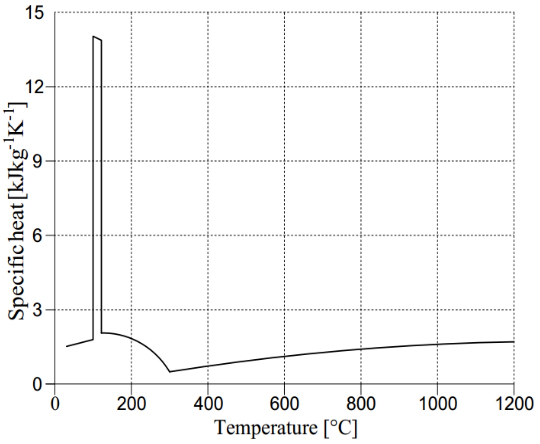

Fig. 2. Temperature-specific heat relationship for wood and the charcoal, based on EN 1995-1-2 [2]

For the standard ISO 834 fire curve, the fire temperature T_f (°C) at time is given by [6]:

$$T_f = 20 + 345 \times \log_{10}(8t+1)$$

Furthermore, the heat transfer between members in FE model should be defined with proper contact properties. Gaps between steel elements and wood members are assumed to be sufficiently narrow. Heat transfer between members is restricted to be radiation and conduction through air:

$$q''_G = k_{air}\frac{\Delta T}{L} + 4\sigma\bar{T}^3\Delta T \Big/ \left(\frac{1}{\varepsilon_H}+\frac{1}{\varepsilon_C}-1\right)$$

where $\Delta T = T_H - T_C$, k_{air} is the thermal conductivity of air, L is the thickness of air layer, ε_C is the cold interface emissivity and ε_H is the hot interface emissivity. The thermal conductivity of air is given as [9]:

$$k_{air} = 0.024 + 7.05\times10^{-5}T_{air} - 1.59\times10^{-8}T_{air}^2$$

where T_{air} is the air temperature (°C).

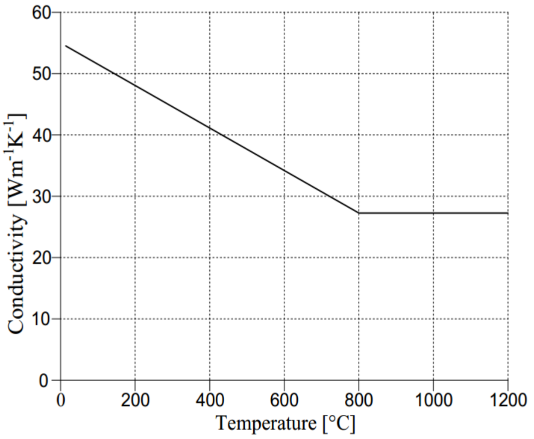

Fig. 3. Thermal conductivity of carbon steel as a function of the temperature, based on EN 1993-1-2 [7]

2.1. Thermal properties of wood

The thermal properties of wood are varied considerably with temperature. Figures 1 and 2 show the thermal conductivity and specific heat versus temperature. The thermal conductivity values of the char layer increase at temperatures exceeding 500°C.

This is due to the effect of cracks and shrinkage of the char layer. The large spike at 100°C represents the heat required to evaporate the moisture in wood. Moisture evaporates at about 100°C and wood turns to char over 300°C. The density is not constant at elevated temperature. It drops to about 90% when the temperature reaches 100°C and to about 20% when the wood turns to char when the temperatures exceeds 300°C.

2.2. Thermal properties of steel

Thermal properties of steel at elevated temperature are well researched. The thermal conductivity of steel according to temperature is shown in Figure 3. The specific heat of steel according to temperature is shown in Figure 4. The peak value of specific heat at about 735°C results from a metallurgical change. The density of steel is remaining essentially constant with temperature.

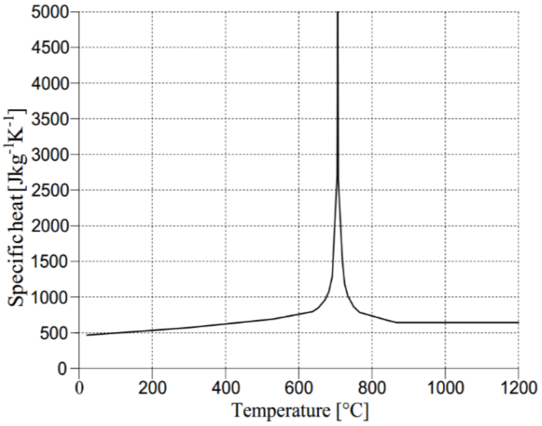

Fig. 4. Specific heat of carbon steel as a function of the temperature, based on EN 1993-1-2 [7]

3. Thermal analysis

3.1. Finite Element Model validation

Before using the model to conduct heat transfer simulations, the wood material and thermal properties at high temperatures implemented in the Finite Element software should be validated. The evaluation was conducted using the FE program ANSYS Workbench. The fire tests of König [8] were used to validate used software. König's tests were performed on four unprotected timber specimens. Wood members had a moisture content of 12% and the timber density was about 425 kg/m^3. König performed fire tests under ISO 834 fire and temperatures were measured in a depth of 6, 18, 30 and 42 mm from the exposed surface.

Figure 5 shows a comparison of the results obtained from modeling with the results of the fire tests of König. Modelling results are in good agreement with König's fire tests.

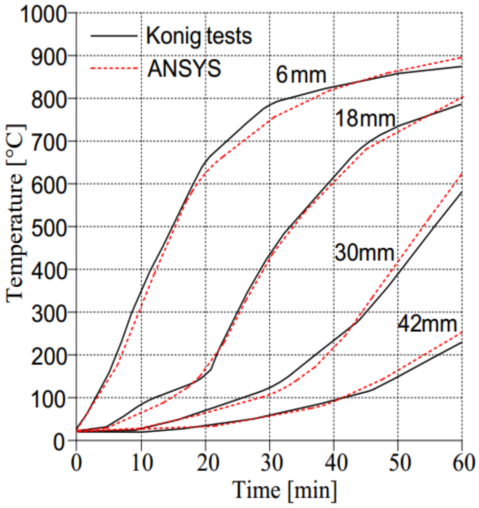

Fig. 5. Temperature as a function of time at different timber depths under ISO-fire

3.2. Numerical study on heat transfer

The subject of the research are the wood-steel-wood timber connections. The geometry of the modeled connections is shown in Figure 6. The joints are made of wood C20 class and steel fasteners M10 cl.4.6. The elements have the following dimensions of the cross-section: 300 x 300 mm (a) 150 x 150 mm (b).

The main objective of modelling the connections using FE method was to determine the influence of steel elements on the temperature distribution in wood-steel-wood timber joints [9,10]. The ISO 834 fire was applied on four sides of the specimens.

The temperature distribution of the timber member with steel elements is shown in Figure 9. Due to the high thermal conductivity of steel, the heat flux through the steel elements leads to higher temperatures of the wood interior. It causes a quick reduction of the net section.

4. Mechanical analysis

4.1. Design methods according to Eurocode 5

EN 1995-1-2 [1] provides only some issues of connection design due to fire conditions in timber constructions. Design rules apply to laterally loaded connections with various types of fasteners (bolts, nails, dowels, etc.) exposed to the ISO standard fire [6]. According to Eurocode 5, the maximum fire resistance time which can be determined is 60 minutes. EN 1995-1-2 [1] proposes two methods for calculating the resistance of timber joints exposed to fire:

- Application of simplified rules
- Reduced load method.

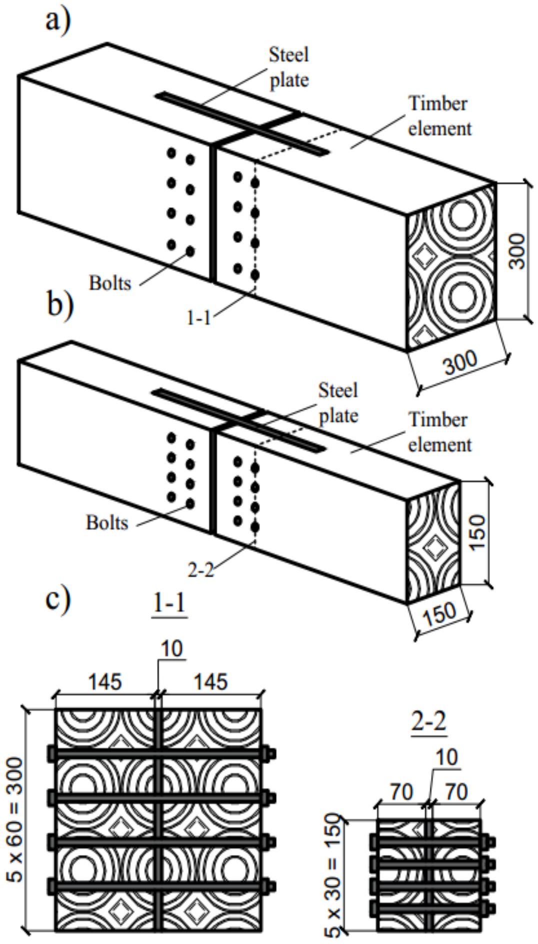

Fig. 6. Geometry of the modelled connections:
a) connection 1, b) connection 2, c) cross-sections 1-1 and 2-2

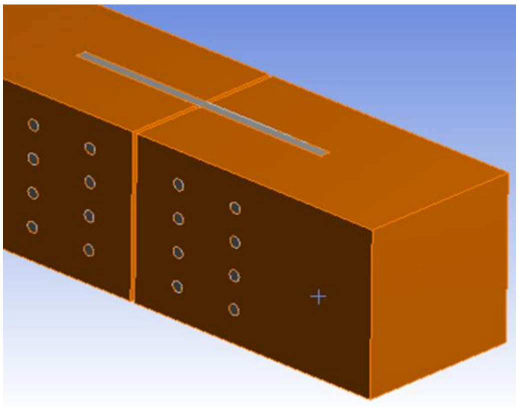

Fig. 7. Finite element heat transfer models of the connections

According to the first approach, fire resistance of unprotected joints with dowels is assumed to be 20 min. For connections with other connector types the fire resistance is considered to be 15 min. Fire resistance periods, greater than those above, but not exceeding 30 minutes, can be achieved by increasing the edge distance, as well as the thickness and width of the side members.

The reduced load method assumes, that the load bearing capacity of the joint exposed to fire is achieved by reducing the room temperature capacity via a conversion factor η. The conversion factor includes the design fire resistance of the unprotected connection and a parameter k, which depends on the joint type.

Fig. 8. An example of a similar connection

Specifications for calculations the resistance of connections with axially loaded screws under elevated temperatures are also presented. The above take into consideration the configuration of the connection, the edge distance and the embedment depth of the screws.

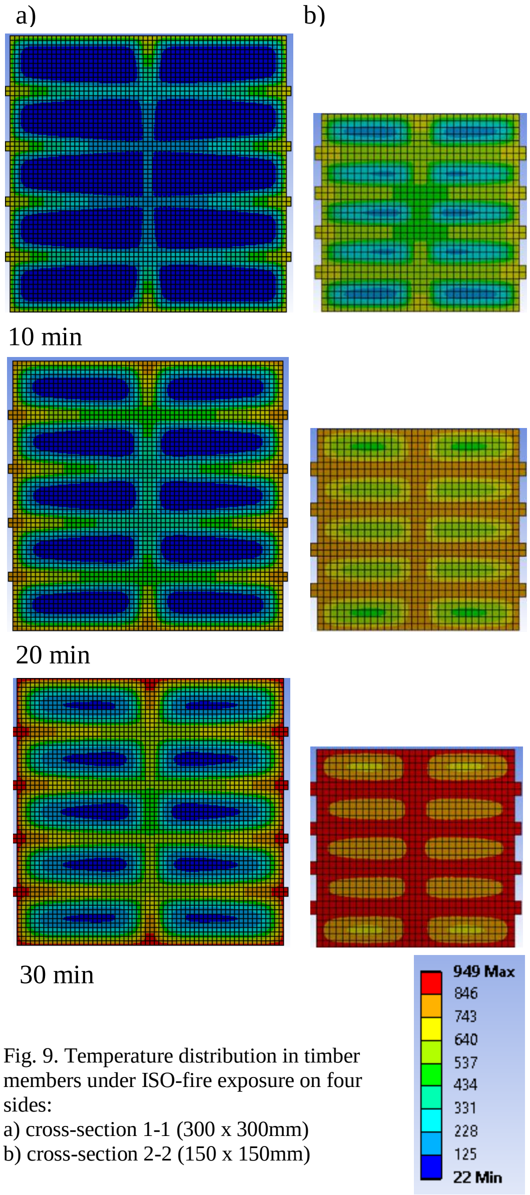

Fig. 9. Temperature distribution in timber members under ISO-fire exposure on four sides:
a) cross-section 1-1 (300 x 300mm)
b) cross-section 2-2 (150 x 150mm)

4.2. Failure modes

Wood-steel-wood connections loaded in tension can fail in different modes. The failure modes depends on connection types, geometry and the number, diameter and configuration of fasteners. Possible failure modes can be described as follows:

- Bearing failure
- Net tension failure
- Splitting of wood
- Shear-out failure
- Group shear-out failure

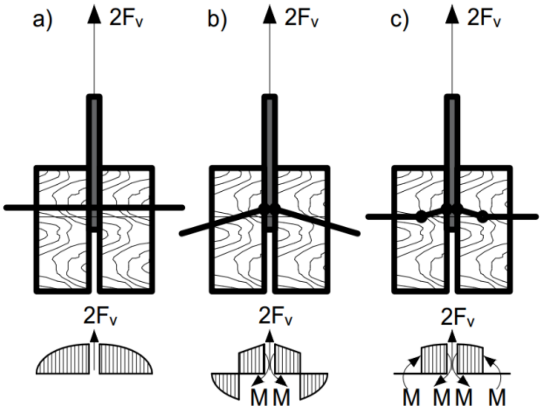

Fig. 10. Failure models of WSW connections in fire:
a) Mode I b) Mode 2, c) Mode III

The first failure mode takes place due to wood embedment failure in the contact area, with steel yield of fasteners. Other failure modes are brittle [11]. Possible bearing failure modes for wood-steel-wood timber connections is shown in Figure 10. In many cases failure is a combination of different modes.

In fire tests for WSW connections, first two failure modes were observed as main failure modes: elongation of fastener holes due to wood crushing and deformation of fasteners [12,13]. This is due to the charring of wood members and the rapid temperature increasing in steel elements. The third failure mode is of the least importance in this analysis, because this destruction can occur when the timber side elements are very thick.

EN 1995-1-1 [14] gives simplified formulas:

$$F_{v,Rk,I} = f_{h,1,k} t_1 d$$

$$F_{v,Rk,II} = f_{h,1,k} t_1 d \left[\sqrt{2 + \frac{4M_{y,Rk}}{f_{h,1,k} d t_1^2}} - 1 \right] + \frac{F_{ax,Rk}}{4}$$

$$F_{v,Rk,III} = 2{,}3\sqrt{M_{y,Rk} f_{h,1,k} d} + \frac{F_{ax,Rk}}{4}$$

$$F_{v,Rk} = \min(F_{v,Rk,I}, F_{v,Rk,II}, F_{v,Rk,III})$$

Table 1

Load-bearing capacity per shear plane per fastener in fire conditions

Duration of fire [min]	**Load-carrying capacity per fastener for the failure model [kN]**						**$F_{V,Rk}$ [kN]**	
	Mode I		Mode II		Mode III			
	a	b	a	b	a	b	a	b
0	81,5	39,3	34,5	17,8	15,1	15,1	15,1	15,1
5	70,2	28,1	29,9	13,5	14,3	14,3	14,3	13,5
10	59,1	16,9	25,3	9,8	13,8	13,8	13,8	9,8
15	47,8	4,2	20,9	4,5	12,9	12,9	12,9	4,5
20	36,5	0	16,3	0	11,7	11,7	11,7	0
25	25,3	0	11,9	0	10,3	10,3	10,3	0
30	14,1	0	8,4	0	8,6	8,6	8,4	0

Where $F_{v,Rk,i}$ is the load-bearing capacity per shear plane per fastener for i failure mode (kN), $f_{h,1,k}$ is the embedment strength in timber member (MPa), t_1 is the smaller of the thickness of the timber side member (mm), d is the fastener diameter (mm), $M_{y,Rk}$ is the fastener yield moment (kNm), and $F_{ax,Rk}$ is the withdrawal capacity of the fastener (kN).

4.3. Load-bearing capacity of the connections in fire conditions

The wood-steel-wood connections have to meet the design rules and requirements of Eurocode 5. The main functions used in strength equations are the diameter, the yield strength and the embedment strength of the fasteners. During fire exposure, the timber section is reduced. Also steel fasteners reduce strength. The steel yield strength at elevated temperatures is adopted from EN 1993-1-2 [2].

Table 1 contains load-bearing capacity per shear plane per fastener for the failure models at time intervals of 5 min in the ISO fire exposure. As expected, the first two are the main failure modes for estimating the load-bearing capacity of the connection in fire conditions.

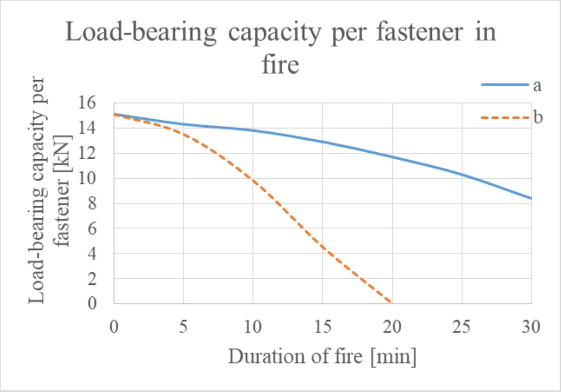

Fig. 11. Load-bearing capacity per fastener in fire conditions

5. Conclusions

In this paper, a thermal analysis of the timber connections with steel elements were carried to determine the influence of steel members on the temperature distribution in timber cross-section under fire exposure. The FE model can provide good predictions of the temperatures within timber connections with steel elements.

The dimensions of the wood side members have a significant influence on the load-bearing capacity of timber connections with steel members in fire conditions.

References

[1] ISO834 Fire resistance tests-elements of building construction, Part 1: general requirements, International Organization for Standardization, Switzerland, 1999.

[2] EN 1995 1-2 Eurocode 5: Design of timber structures, Part 1-2: structural fire design, CEN, Brussels, Belgium, 2004.

[3] D. Barber, Determination of fire resistance ratings for glulam connectors within US high rise timber buildings, Fire Safety Journal, 91 (2017) 579-585.

[4] ANSYS® Academic Research Mechanical, Release 19.0

[5] EN 1991 1-2 Eurocode 1: actions on structures, Part 1-2: General actions – actions on structures exposed to fire, CEN, Brussels, Belgium, 2003.

[6] P. Racher, K. Laplanche, D. Dhima, A. Bouchair, Thermo-mechanical analysis of the fire performance of dowelled timber connection, Engineering Structures, 32 (2010) 1148-1157.

[7] EN 1993-1-2 Eurocode 3: Design of steel structures, Part 1-2: General rules - Structural fire design, CEN, Brussels, Belgium, 2005.

[8] J. Konig, L.Wallei, One-dimensional charring of timber exposed to standard and parametric fires in initially unprotected and post-protection fire situations. Rapport I 9908029, Swedish Institute for Wood Technology Research, Stockholm, Sweden, 1999.

[9] M. Audebert, D. Dhima, M. Taazount, A. Bouchair, Numerical investigations on the thermo-mechanical behavior of steel-to-timber joints exposed to fire, Engineering Structures, 33 (2011) 3257-3268.

[10] V.D. Thi, M. Khelifa, M. Oudjene, M. El Ganaoui, Y. Rogaume, Finite element analysis of heat transfer through timber elements exposed to fire, Engineering Structures, 143 (2017) 11-21.

[11] L. Peng, J. Mehaffey, M. Mohammad, Predicting the fire resistance of wood-steel-wood timber connections, Fire Technology, 47 (2009) 1101-1119.

[12] C. Maraveas, K. Miamis, E. Matthaiou, Performance of timber connections exposed to fire, Fire Technology, 51 (2013) 1401-1432.

[13] P. Moss, A. Buchanan, M. Fragiacomo, C. Austruy, Experimental testing and analytical prediction of the behavior of timber bolted connections subjected to fire, Fire Technology, 46 (2010) 129-148.

[14] EN 1995 1-1 Eurocode 5: Design of timber structures, Part 1-1: General rules and rules for buildings, CEN, Brussels, Belgium, 2004.

The impact of the exterior wall surface finish on the separation distance

Katarína Dúbravská[a] – Jaroslava Štefková[b]

[a] *Department of fire protection, Technical University in Zvolen, T. G. Masaryka 24, Zvolen, Slovakia*

[b] *Institute of foreign languages, Technical University in Zvolen, T. G. Masaryka 24, Zvolen, Slovakia*

Abstract

Surface finish of the outer side of an external wall is not considered at its classification as a construction member, however itis considered at demining clearances. It is considered when separation distances are determined. It is also taken into account when the size of the partially fire open exterior wall area is determined in case if there is more than 100 MJ heat released from 1 m^2. The paper discusses the impact of the surface finish of an external wall on the final separation distance. The comparison of five alternatives was evaluated – mineral wool insulating system, 120 mm polystyrene insulation system, 200 mm polystyrene insulation system, exterior siding - wooden and stone veneer placed on a part of the exterior wall. The procedure of determination of separation distances is described in STN 920 0201-4. The standard states that separation distance from the fire compartment is determined on the base of a length and height of the exterior wall due to the fire compartment, the type of construction member, the ratio of the fire open exterior walls and fire risk.

I tis clear that the lowest values of separation distance were achieved by the alternatives whose surface finish was formed from non-combustible materials (insulation system with mineral wool, exterior cladding from artificial stone). In case of the alternatives where polystyrene was used, the separation distances vary. This insulation material suggest that beside the kind of material used for surface finish, it is necessary to look at its thickness, density, calorific value and heat release per unit area (HRRPUA).

Keywords: surface finish; separation distance; heat release per unit area; partial fire open exterior area

---

1. Introduction

While dealing with the fire safety of a structure, the fire spreadbetween individual compartments inside the building is considered, but not meeting the separation distances can also lead towards the spread of fire to neighbouring structures.

By Mózer [5], from the viewpoint of separation distances there are two ways how the fire is spread – radiation heat thorough fire open exterior walls or by falling embers from the burning construction. The vital condition to eliminate the fire spread from the burning building is stating separation distances [4]. The Regulation of the Ministry of the Interior No. 94/2004 defines separation distance as a perpendicular distance between the surfaces of the fire open exterior wall or between the surface of the comparison plane of fire open exterior walls, a fire compartment, or open technology area or open storage to a fire risk area.

The separation distances are stated by the STN 92 0201-4 [15] norm. The procedure refers specifically to:

- a fire compartment
- a fire compartment made by a residential unit in a residential building,
- a fire compartment in a residential unit in a accommodation building,
- open storage,
- open technological facilities.

The values of the separation distance for a fire compartment are determined on the basis of [5]:

- the size of fire open areas in the fire compartment,
- spatial density of the thermal flow from the fire compartment (depending on the fire risk),
- dimensions of the bordering constructions of the fire compartment,
- the type of construction assembly (increasing the value of the fire risk depending on the type of construction assembly),
- probability of the fire spread by the firebrands from the burning constructions.

By Kucbel [3], the fire open area is the part of an external wall or a roof shield, which does not limit (or limits only partially) the heat spread and does not restrain the fire spread away the structure or a fire compartment.

STN 920201-4 [15] states that the fire open areas can be completely or partially fire open areas or fire open areas of the roof shield. Completely fire open areas include areas of openings impossible to close or openings which do not meet required criteria.

If the construction does not meet the requirements of the fire resistance which are imposed on it, this construction is also considered completely fire open area.

Partially fire open wall area is according to STN 920201-4 [15] the area which includes:

a) external wall or its part or a roof shield which meets the criteria of partially fire open area according to STN 73 0855 [12];
b) external wall or its part which meets the fire requirements but its outer side has flammable surface and it is able to release bigger amount of heat than 100 MJm^{-2} from 1 m^2;
c) an opening closed by a construction which meets criteria of the partially fire open area according to STN 73 0855 [12].

This paper focuses on the requirement of the caser b) in the above-mentioned definition for partially fire open area. In practice, it means that the area of the external wall where the insulation system with combustible insulation materials or where there is a combustible exterior siding are applied are calculated in into the partially fire open wall area.

By Osvald a Falchbart [8], the application of the combustible material on the facade means the fire spreads faster in vertical as well in horizontal direction.

2. Methodology

2.1. Methodology of calculation

The procedure of stating the separation distances is described in STN 920201-4 [15] and in other related literature. The procedure to determine separation distances was summarised by Kucbel [3] into the following points:

- the total area S_p of the external wall or roof shield with length l and height h_u is determined,

- the area of fire open areas S_{po} is determined,
- the ratio of the fire open areas to the area of external wall in percent according to the equation:

$$p_o = \frac{S_{po}}{S_p} . 100 \ (\%)$$

where S_{po} is the fire open area (m^2);

S_p the area of the external wall (m^2) which includes the fire open areas.

In Table 3 in STN 920201-4 [15] the separation distance is determined depending on height h_u, length l, ratio p_o, and calculated fire risk p_v, or equivalent time of the fire duration.

If there are completely fire open exterior wall areas S_{po1}, partially fire open areas S_{po2}, and fire open areas in roof shield, the total fire open area S_{po} is determined from the ratio of the heat flow density of individual areas according to the equation [15]:

$$S_{po} = S_{po1} + S_{po2}.k_{10} + S_{po3}.k_{11}$$

where S_{po}size of fire open areas (m^2);
S_{po1} completely fire open area (m^2);
S_{po2} partially fire open area (m^2);
S_{po3} fire open area of the roof shield (m^2);
k_{10} coefficient of partially fire open areas;
k_{11} coefficient of fire open areas of roof.

Fire open areas are defined according to the heat spread limiting as follows [5]:

- completely fire open area is considered that part of the external wall which does not meet the requirements of fire resistance according the class of fire safety of the fire compartment which it confines. At the same time, it also includes all the openings which are impossible to enclose against fire (windows, doors, others).

Partially fire open area S_{po2} is considered:

- the area of the external wall or closure if they meet the requirements of partially open as in
- the area of the external wall whose outer side has surface finish from the materials which are able to ignite and release more than 100 MJ of heat from 1 m^2 .

The spatial amount of released heat from the combustible materials in the outer surface is calculated by this equation [15]:

$$Q = \sum_{i}^{j} M_i . H_i$$

where Q amount of heat (MJ.m^{-2});
M_i spatial weight of the combustible material placed on the outer surface of the external wall (kg.m^{-2});
H_i calorific value of the i-thcombustible material on the outer surface of the external wall.

Kupilík [4] mentions the possibility of fire spread the cause of which is falling of firebrands of burning building constructions made of construction member D3. In this case:

- the separation distance is determined based on the previous equation,
- the value of 0.36-muiltiple of the height, which is identical with the height of the fall of a firebrand of the burning building.

The final separation distance is then considered the higher one.

2.2. Description of the individual alternatives

The basis of the alternatives is created by the structure with the identical layout and construction arrangement which is made of construction members of D1 kind and is included in the non-combustible construction assembly. By STN 92 0201-2 [14], the surface finish is not considered at classification of the construction member. The difference of individual alternatives is particularly in the surface finish treatment of the external wall (see alternative description).

In the facility there is the shop with textiles, adjacent storage room, office, hallway, kitchen and toilets. The due fire compartment is imposed by calculated fire risk 110 kg.m^{-2}.

The description of the external construction from which the separation distance is calculated follows:

- wall length 18 m, wall height 3.2 m,
- plastic windows 1.5x1.5 m,
- plastic doors 1.5x2.31 m,
- exterior trimsaround the openings 350 mm wide.

The description of the alternatives of surface finish is following:

- Alternative 1 –the thermal insulation of mineral wool is applied against the complete area of the external wall (Fig.1).
- Alternative 2 –the contact insulation system with polystyrene is appliedagainst the complete surface of the exterior wall,

the polystyrene thickness is 200 mm Fig.1).

- Alternative 3 –the contact insulation system with polystyrene is appliedagainst the complete surface of the external wall, the polystyrene thickness is 200 mm (Fig.1).
- Alternative 4 – windows and doors are framedwith32 mm thick wooden trim (Fig.2).
- Alternative 5 – windows and doors are framed with the 25 mm thick stone veneertrim Fig.2).

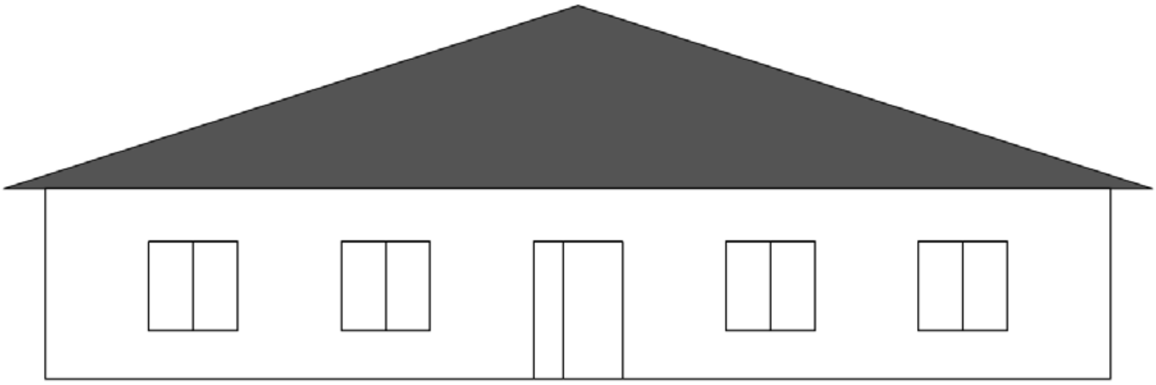

Fig. 1 External wall with the surface finish against the entire wall

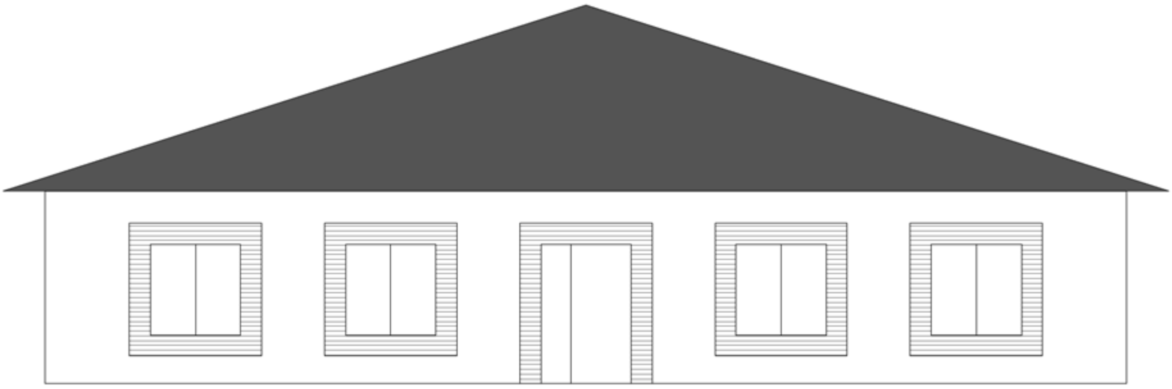

Fig. 2 External wall with the surface finish placed only against a part of it

As Rumiantcev et al. [10] states the insulation systems and decorative materials applied on the outer side of the external walls have various functional and constructional solutions and may well demonstrate their properties also from the fire safety viewpoint.

Thermal insulation, decorative and exterior materials are briefly described in Table 1.

Table 1

Properties of insulating and decorative materials [5], [12], [16]

Material	Thickness (m)	Density (kg.m^{-3})	Calorific value	Reaction to fire classification
Expanded polystyrene	120	20	40	E
Expanded polystyrene	200	20	40	E
Mineral insulation	140	35	-	A1
Wood siding	32	470	17	D
Stone veneer siding	25	-	-	A1

Table 2

Spatial amount of released heat [5], [12], [16]

Surface finish	Thickness of surface finish (mm)	Density	Calorific value	Spatial weight of the combustible material (kg.m^{-2})	Spatial amount of released heat (MJ.m^{-2})
Mineral insulation	140	-	-	-	-
Polystyrene	120	20	40	2.40	96.00
Polystyrene	200	20	40	4.00	160.00
Wood siding	32	470	17	15.04	255.68
Stone veneer siding	25	-	-	-	-

3. Results and discussion

Completely fire open areaS_{po1} which is made up by the area of openings – windows and doors, is all alternatives the same. It regards the same design solution of the structure.

The differences in individual alternatives are caused namely by the figure of partially fire open area S_{po2}. It refers to coefficient which respects also surface finish of the external wall. As it is mentioned above, surface finish is taken into account and calculated in if it is possible to ignite and release more than 100 MJ of heat from 1m^2 according to STN 920201-4[15]. The data on the released heat from the combustible material placed on the outer surface are summarised in the Table 2.

Spatial amount of released heat depends on the calorific heat of the combustible material and the thickness of the surface finish. The influence of the thickness the spatial weight M_i and the spatial amount of released heat Q is given in the Table 2.

Polystyrene with the thickness of 120 mm has M_i = 2,4 kg.m^{-2} and Q = 96 MJ.m^{-2}. Polystyrene with the thickness of 200 mm has M_i = 4,00.m^{-2} and Q = 160 MJ.m^{-2}.

If there is the insulation system with mineral wool applied on the external wall, fire open areas are created only by the area of openings (completely fire open area). The insulation material is of A1 class of the reaction to fire, i.e. does not contribute to fire development.

The main parameter of the insulation system with polystyrene is the thickness of the insulation material. In Table 3, there are given data about the size of fire open areas. It is not found as partially open area for the polystyrene of 120 mm thickness, density of 20kg.m^{-3} and the calorific value of 40 MJ.kg^{-1}. The reason for this judgement is that this surface finish does not release more than 100 MJ.m^{-2}. The spatial amount of released heat for this finish is 96 MJ.m^{-2}.

The surface finish of 200 mm thick polystyrene of 20 kg.m^{-3} density and calorific value 40 MJ.kg^{-1} is found as partially fire open area as it releases 160 MJ.m^{-2}.

The size of the fire open area is 28.26 m^2 for the Alternative 3. The total sum of fire open areas created by adding completely fire open areas and partially fire open areas multiplied by the coefficient k_{10} accounting for 0.35.

When using polystyrene of the thickness below 120 mm, the separation distance is 3.5 m. When using polystyrene of the thickness below 200 mm, the separation distance is 3.5 m. As it has been mentioned, the thickness of the material causes the difference. By Mózer [5], the boundary thickness for the polystyrene is 125 mm with 20 kg.m^{-3} density and calorific value 40 MJ.kg^{-1}.If the thickness of the material exceeds the 125 mm then the surface finish is taken into the calculations of the partially fire open area.

According to Pastor et al. [9], ETICS (contact insulation system with polystyrene) is purposefully designed to improve the properties of constructions from the point of thermal insulation. However, at the same they mention that most of the materials used is combustible and can considerably contribute to the fire development and surface spread of fire. In case of the ETICS use, i tis necessary to apply fire barriers. Sternová et al.[11] remark that fire barriers shall be of 200 mm height, from at leastA2 class of reaction to fire for insulation materials, in contact system of insulation in at least A2-s1,d0. Zhou at al. [18] investigated how horizontal fire barrier influences further spread of fire across the surface of the exterior wall.

Pastor et al. [9] investigated performance of insulation materials under fire loading. The tested materials were mineral wool and polystyrene. As they state the mineral wool insulation kept its properties under fire loading test, the temperature.

Table 3

Separatione distance

Surface finish	Area of external wall S_p	Size of the fire open areas S_{po}	Completely fire open areas S_{po1}	Partially fire open area S_{po2}	Ratio of fire open areas	Separation distance
Mineral insulation	57.60	11.50	11.50	0.00	19.97	3.50
Polystyrene 120 mm	57.60	11.50	11.50	0.00	19.97	3.50
Polystyrene 200 mm	57.60	27.66	11.50	46.10	47.98	9.80
Wood siding	57.60	15.96	11.50	12.75	27.71	7.20
Stone veneer siding	57.60	11.50	11.50	0.00	19.97	3.50

The outcomes for the ETICS did not get such favourable values [9].

A special chapter describes exterior and decorative siding. These can be place against whole wall or only its part. Also in this case, it is the material which matters, its density, thickness, calorific value. For alternatives 4 and 5, the exterior siding is applied only against a part of the wall – 350 mm along the opening (Fig.2). When wood is applied, the material mostly refers to spruce wood. Some authors (Čabalová et al. [1],Oremusová and Čepec [6], Osvald et al.[7], Kačíková et al. [2]) investigated the wood behaviour under thermal loading or under fire loading. The particular material releases 255.68 MJ.m^{-2} of heat. Fire open areas are created by the completely fire open areas and partially open areas, which only includes the area of decorative wood siding.

In case of mineral wool surface finish and stone veneer siding, the amount of released heat is not considered because itis assumed that that materials from A1class of the reaction to fire it does not contribute to fire. The fire open areas are created by completely fire open areas. The separation distance is 3.5 m.

In all cases, a significant factor influencing the separation distance is presented by type of facility which is present in the fire compartment (for a non-manufacturing facility there is calculated a fire risk).

4. Conclusions

Surface finish. regardless to the thickness. is not considered in classification of the construction member. The combustibility of the surface finish material its flammability and calorific value is therefore considered in stating the separation distances. Their task is to stake the fire hazardous space. Conformation to separation distances shall prevent spread of fire between the structure and surrounding objects.

Determining the separation distances, the type of facility (fire risk) is taken into account, the length and width of external wall of the due fire compartment and the ratio of fire open areas. I tis the last parameter which considers the surface finish of the external wall, in the item of partially fire open area.

The paper dealt with the influences of the type of insulating system and exterior siding on separation distances. Apparently, the best results were achieved by mineral insulation among the insulation systems and stone veneer side from siding materials. Itis caused by the class of reaction to fire of these materials, additionally, they will not ignite. ;From the point of view of separation distances, the same results were achieved by polystyrene 120 mm thick. It is questionable if the insulation material will meet the requirements from the thermal insulation point of view. The highest values of separation distances were achieved for the polystyrene of 200 mm thickness. The value of the spatial amount of heat was lower than for the wood siding, but contrary to the wood siding, this material was applied against the whole wall.

Considering the choice of insulation material, mineral wool presents a better option. It is non-combustible material. Considering polystyrene, it is necessary to look at its thickness. When applying contact insulation system with polystyrene there must be also applied fire barriers which are required for A2 class of reaction to fire. In these circumstances there must be placed the stripe made of mineral insulation. Choosing decorative and exterior siding it is necessary to focus the attention on material composition. Wood siding had the highest value of spatial amount of released heat. When applying such siding we should minimize the area of external wall where it is applied.

Acknowledgments

This work was supported by the Cultural and Educational Grant Agenca of the Ministry of Education, Science, Research and sport of the Slovak Republic on the basis of the project no KEGA 009TUZV-4/2017.

References

[1] Čabalová, F. Kačík, D. Kačíková, M. Oravec, Acta Facultatis Xylologiae Zvolen 55(2) (2013) 59.
[2] D. Kačíková, F. Kačík, P. Hrnčiarik, Delta 5(10) (2011) 16.
[3] J. Kucbel, Fire safety of buildings, vol.1, STU , Bratislava, 2003.
[4] V. Kupilík, Building structures from a fire aspect, vol. 1, Grada Publishing, Praha, 2006
[5] V. Mózer, Bases of fire safety of buildings, vol. 1, EDIS, Žilina, 2015
[6] M. Oremusová, R. Čepec, Delta 6(12) (2012) 8.
[7] Osvald, Wood Research 62(4) (2017) 565.
[8] Osvald, J. Flachbart, Crisis Management 2 (2017) 55.
[9] E. Pastor et al., International Conference on Applications of Structural fire Engineering Location, Conf.., Dubrovnik, 15-16 Oct., 2015; Applications of Structural Fire Engineering-Series (2017)
[10] Rumiantcev, A. Zhukov, D Zelenshikov, A. Chkunin, K. Ivanov, Y. Sazonova, 5th International Scientific Conference on Integration, Patnership and Innovation in Construction Science and Education, Moscow, 16-17 Oct., 2016; MATEc Web of Conferences 86 (2016)
[11] Z. Sternová, P. Hlavenka, Principles of designing the ETICS for fire protection in the renovation of buildings, vol. 2, Jaga Group, Bratislava, 2015
[12] STN 73 0824 Fire protection of buildings. Heating value of flammable substances (1992)
[13] STN 73 0855 Fire resistance test of external walls (1980)
[14] STN 92 0201-2 Structural fire protection. Common regulations. Part 2: Building constructions (2017)
[15] STN 920201-4 Structural fire protection. Common regulations, Part 4: Separation distance (2000)
[16] STN EN 13501-1 +A1/Z1 Fire classification of construction products and building elements. Part 1: Classification using data from reaction to fire tests(2017)
[17] The Regulation of the Ministry of the Interior No. 94/2004 of the Slovak Republic laying down the technical requirements for fire safety in the construction and use of buildings, as amended

[18] L. Zhou, A. Chen, X. Liu, F. Zhang, Springer Science+Business Media 52 (2016) 649.

Earth in a Trap? 2018
Analytical Methods in Fire and Environmental Science

Investigation of zones of fatigue falure of screws

K. Epifantsev[a]* - T. Mishura[a]

[a]*St. Petersburg State University Aerospace Instrumentation 190000, St. Petersburg, Russia. Bolshaya Morskaya Street 67*

Abstract

In recycling technology screw - the main working element for processing waste machines - extruders. From the quality of its production depends the productivity of the shop and the integrity of the machine body. When refining a multicomponent raw material, which is Refuse Derived Fuel - this is the general name for alternative fuels obtained from recycling. As raw material, almost any organic material is used: cellulose, rubber, plastic, leather, its substitutes. The study used an example based on work with RDF-raw materials of the Janino Refuse Processing Plant. Leningrad region. It is when working with such highly abrasive waste that it becomes necessary to increase the service life of screw augmentedly by using new processing technologies, since metal components and hard-to-break silicates can occur in the composition of this raw material.
It research very important, because the priority project of the Russian Government, will be implemented from 2017 to 2025 with the key aim of reducing the environmental footprint from municipal solid waste disposal and mitigating environmental risks of an accumulated environmental damage [4]. The priority project involves the construction of five environment-friendly facilities for the thermal processing of municipal solid waste (waste incineration plants), four of them to be built in the Moscow Region and one facility to be built in the Republic of Tatarstan.
An alternative to waste incineration is municipal waste recycling by moulding in extrusion machines to make pellets to be further used in the fuel or construction industries. The profitability of a waste recycling facility is dependent on a sound choice of extrusion equipment with the best value for money [5].

Keywords: fatigue failure; screw; refuse processing; deflected mode; mode of deformation

---

* Corresponding author. Tel.: +7-963-373-7759; e-mail: epifancew@gmail.com.

1. Introduction

The development of non-destructive testing in Saint-Petersburg State University of aerospace instrumentation (SUAI) is reflected in the appearance of new terms that are used in practice, scientific papers and technical descriptions. Non-destructive control increasingly contacts with adjacent areas involved in assessing the actual technical condition of the facilities, determining the possibility of their further operation and the terms of safe operation (resource problem). In this paper, the methods of nondestructive testing of industrial objects, as well as various types of this method, such as magnetic, electric, which are used to create new laboratory work in the educational process. In In this paper, a finite element method was used to study the auger in the program Cosmos Works[10].

2. Materials and study methods

When modeling extruders for waste processing, much attention is paid to designing and testing the work of the auger, the main working member involved in grinding, heating and preparing for molding a plastic mass. the mass through the matrix (Fig. 1).

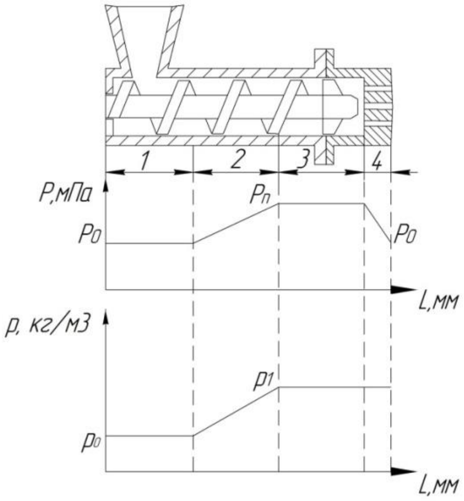

Fig. 1 – Graph of functioning of pressure in extruder screw

The auger compresses the mass to the accumulation point m. Pp, after which, it becomes possible to create the pressure p1 necessary to pass Only when there is a balance on both sides of the extruder, the mass can come out of the die dies. However, if the extruder is conventionally divided into 4 work areas, at the moment of increasing pressure P, MPa and the maximum loading of the screw p kg / m3, a maximum pressure area is created (in Figure 1 zone "2"), which is capable of deforming the auger.

In an auger machine, an increase in mass consumption requires an increase in the speed of the screw, and a corresponding increase in the loading of the screw by the material. At the same time, the pressure (Fig. 1) rises to Pn, because the increased feed rates lead on the same matrix to increased friction in the die dies, which adversely affects also the maximum abrasive area for screw turns. With the auger manufacturing technology - welding the turns to the shaft by welding in CO_2, cracks and loosening of the screw turns (Fig. 2).

Fig. 2 – Screw defects - tears

Naturally during the operation for forming RDF raw materials, it was assumed that the following load acts on the extruder screw: the torque on the coupling shaft produced by the engine is 5000 N.

The temperature of the raw material heating inside the extruder reaches 500 C°. It is necessary to determine the zones with the greatest accumulation of load, displacement, deformation (Fig. 3). Thus, creating the parameters that are as close as possible to the real operating conditions, it is possible to detect the most loaded zones of the structure during the research and thus to improve the screw design in the stage of design and selection of materials.

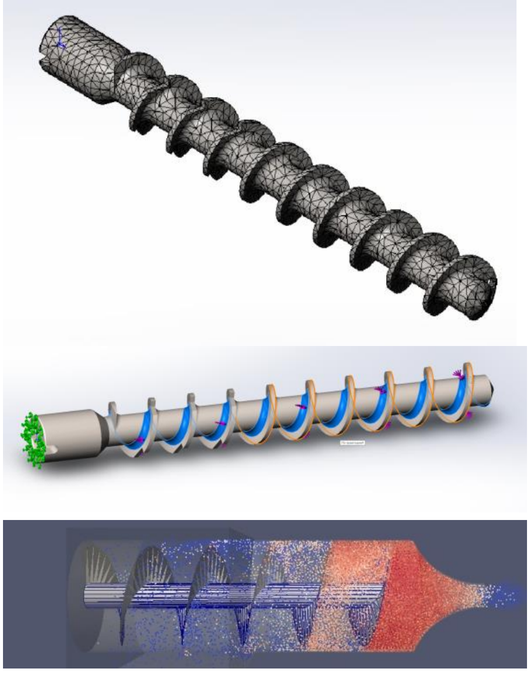

Fig. 3 – Screwing the auger into a grid using the finite element method, indicating the strength of the action on the screw.

3. Results and Discussions

The process of molding the biomass is accompanied by a sufficiently high pressure, which is necessary for the destruction of the residual fibers and the compaction of the processed batch. Along with the negative effect of pressure on the turns of the auger, with an unbalanced, unbalanced shape of the screw, the energy spent on molding.

The Solid works software allows to simulate methods for diagnostics on the basis of application of virtual measuring instruments with minimal systematic error. This creates ideal conditions for the creation of new technologies in the field of innovation and the development of tools for express diagnostics of most technological processes.

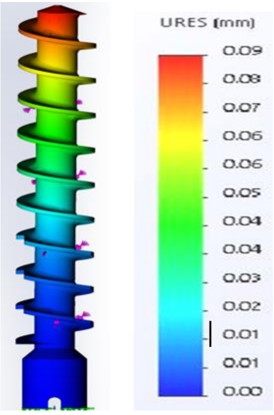	Testing and check screw for tensile metall
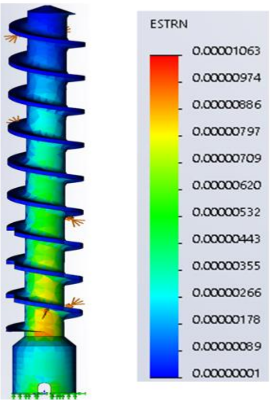	Testing and check screw for deformation metall
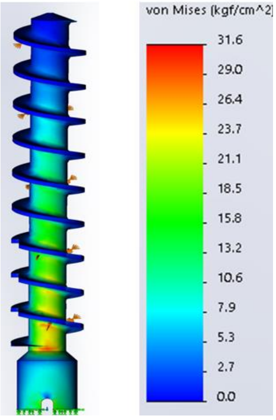	Testing and check screw for stress of metall

Fig. 4 – Results of testing screw.

Summary

In Fig 5 -6 will be see results of experiment.

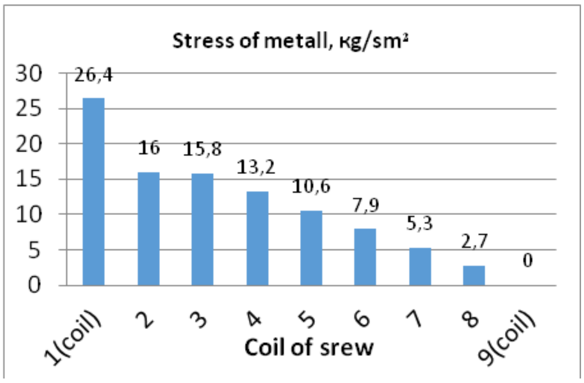

Fig 5 – Results of stress

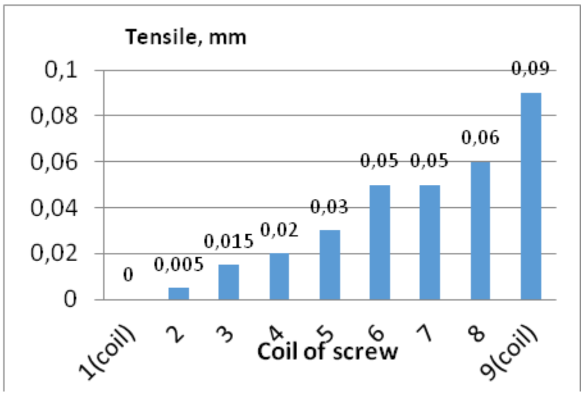

Fig 6 – Results of tensile

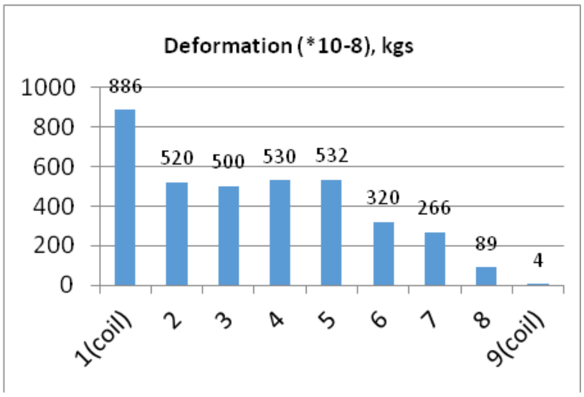

Fig 7 – Results of Deformation screw

Thus the software allowed to identify the most dangerous areas in the zone of bright red colors, which can become a zone of fatigue destruction of the screw and bring to the blocking of the machine. In addition, these parts are subject to the most wear and the process of highly abrasive action, which will cause a decrease in pressure inside the machine body, and thus deterioration in the quality of the molded pellets.

The stress and strain are inversely proportional to the displacement, which proves the maximum coefficient of pressure on the screws in this region. Therefore, the 7th and 8th turns must be welded together with the additional reinforcement rib in order to compensate the stresses

Acknowledgments

The results of this work were marked on the The grant for young scientists (Government of St. Petersburg, 2017), Scholarship of the President SP-2381.2018.1

References

[1] Qingqing, H. Recent trends in rock dust modifications for improved dispersion and coal dust explosion mitigation // R. Honaker / Journal of Loss Prevention in the Process Industries, Volume 41, 2016, Pages 121–128.

[2] Qingqing, H. Optimized reagent dosage effect on rock dust to enhance rock dust dispersion and explosion mitigation in underground coal mines // R. Honaker / Powder Technology, Volume 301, 2016, Pages 1193–1200.

[3] Title 30 – Mineral Resources. Vol. 1, parts 1–199. Washington: U.S. Government Printing Office, 2009. 767 p.

[4] Title 30 – Mineral Resources. Vol. 2, parts 600-699. Washington: U.S. Government Printing Office, 2009. 750 p.

[5] Title 30 – Mineral Resources. Vol. 3, parts 700 to end. Washington: U.S. Government Printing Office, 2009. 750 p.

[6] Order No. 440 dated 19 November 2013 on Approval of the Coal Mine Safety Rules Federal Industrial Safety Rules and Regulations / Federal Service for Ecological, Technological, and Nuclear Supervision [electronic resource], accessed at: http://docs.cntd.ru/document/499060050 (accessed on 18 February 2017).

[7] Lindenau, N. I., Origin, Prevention, and Suppression of Spontaneous Fires in Coal Mines // Maevskaya V. M., Krylov V. F., M.: Nedra, 1977. 387 p.

[8] Yinlin, J. A comparative study of dust control practices in Chinese and Australian longwall coal mines // Ting R., Peter W., Zhijun W., Zhaoyang M., Zhimin W. / International Journal of Mining Science and Technology, Volume 26, Issue 2, 2016, Pp. 199–208.

[9] Lebecki, K. Gas in mines. Katowice: The Main Institution Gornictwa, 2004. 399 p.

[10] European Standard EN 13205. Workplace Environment: Assessment of the Productivity of Air-Borne Particle Concentration Meters. German version.

[11] European Standard EN 481: 1991. Determination of Conventions on a Fraction Part for Suspended Solids Measurement in the Workplace. German version.

[12] International Standard ISO 7708: 1995. Air Quality. Determination of Fractions by Particle Size for Hygiene-Related Fractions.

Thermal analysis as a useful analytical tool in environmental and civil engineering

Adriana Estokova[a]*

[a] *Technical University of Kosice, Faculty of Civil Engineering, Institute of Environmental Engineeering, Department of Material Engineering, Vysokoskolska 4, 042 00 Kosice, Slovakia*

Abstract

Thermal analysis is a set of methods that are used for various purposes in a whole range of areas. Recently, its importance and practical application also increase in environmental engineering. This contribution aims to highlight the use of these techniques for research purposes on selected issues in the field of environmental science. The paper presents an application of thermal analysis to study the durability of concrete in aggressive environments, to examine hemp fibers prior to their application to light composites, or to analyze the resistance of polystyrene boards to thermal stress. The results confirm that thermal analysis could be also used in non-traditional areas of research.

Keywords: concrete*;* DSC; TGA; DTA; building materials; durability

---

---

[*] Corresponding author. Tel.: +421-55-602-4265; e-mail: adriana.estokova@tuke.sk.

1. Introduction

Thermal analysis includes a variety of physico-chemical techniques to analyze a wide range of materials including metals, polymers, food, cosmetics, organic and inorganic substances, biological molecules and biopolymers, soil and geological samples. The analyzed material is subjected to a selected temperature mode (heating, cooling or constant temperature or a combination thereof) and corresponding material properties such as temperature, weight, dimensions and others are monitored. The heat load of the can be dynamic (heating or cooling) or static (at a constant temperature depending on time).

For the study of solid materials, the most commonly the dynamic methods are used where the sample is heated or cooled at a constant temperature rate according to a preset program. The test specimens are exposed to a predetermined temperature program in a special crucibles under the specified atmospheric conditions (air, inert atmosphere) while graphically recording the temperature or time changes of the monitored parameter. These dependencies, which are characteristic of the behavior of each material, can be used to analyze

- Structural changes (glass transition temperature, melting / crystallization, evaporation, sublimation, solid phase transition)
- Mechanical properties (elastic behavior, damping)
- Thermal properties (expansion / shrinkage, specific heat capacity, melting / crystallization temperature, coefficient of expansion)
- Chemical reactions (decomposition and temperature stability in various gaseous environments, chemical reactions in solutions or gas phase, gas reaction, dehydration) [1].

Currently there are a number of thermal analysis methods, among the most used are thermogravimetric analysis (TGA), differential thermal analysis (DTA) and differential scanning calorimetry (DSC). The simplest method of thermal analysis is thermogravimetric analysis. In this method, a small amount of sample (milligrams to grams) is subjected to heating, and a change in weight is monitored on a precision balance. Thus, TGA can be used to evaluate the thermal or thermal-oxidative stability of a material. In a desired temperature range, if a sample is thermally stable, there will be no observed mass change. By analyzing the degradation steps of the material it is possible to evaluate its composition, moisture content, organic and inorganic matter content [2].

Differential thermal analysis (DTA) combines the ease of measurement of heating or cooling curves with the quantitative features of calorimetry. The principle of DTA is the observation of temperature effects (exothermic or endothermic) in the sample, which are associated with its physical or chemical changes in continuous linear heating or cooling [3]. The sample under test is heated together with the temperature-inert standard. Most of this is made of alumina or other substances or compounds (e.g., potassium nitrite, potassium chromate, carbon barium, quartz and others). Temperature is measured continuously as for heating or cooling curve determinations, and the differential temperature measurement permits the calculation of the heat flow difference between reference and sample, which are kept in almost identical environments.

Differential scanning calorimetry (DSC) is one of the most widely used thermal analysis methods with both solid and liquid samples being tested in a very wide temperature range. It measures endothermic (heat flow to the sample) and exothermic (heat flow from the sample) transitions as a function of temperature. Transitions are characterized by glass transition, melting, crystallization, kinetics, onset of oxidation, and thermal capacity [4]. The DSC method measures the differences between the amount of heat supplied and the reference materials and sample during the predefined temperature program. As reference, an inert material (i.e., a material in which no phase changes are made in the selected temperature mode), typically an empty crucible, is used.

Simultaneous measurement of multiple properties during one experiment are also often performed.

Simultaneous thermal analysis (STA) is abbreviated for the methods e.g. TG/DTA, TG/DSC etc.

Application of thermal analysis methods has been reported in field of environmental engineering over the years rarely [5-8]. Nowadays, the thermal analysis technics are successfully used for a wide range of research in environmental engineering such as sludge characterization within the waste water management [9,10], sediment investigation regarding its environmental safety [11,12], soil quality examining [13,14] or environmental properties of materials and technologies [15,16].

The paper aims to report the other applications of the thermal analysis in environmental and civil engineering. The special attention was paid to investigation of the cement composites and their durability, hemp fibres and their applications into the concretes as well as fire resistibility of polymer materials in constructions.

2. Material and Methods

2.1. Thermal analysis

To investigate the thermal stability and thermal behavior of various samples, STA 449 Jupiter F3 thermal analyzer (Netzsch, Germany) was used. Temperature interval ranged from 25 to 1000 °C, various heating rates from 2.5 to 40 K/min were applied (polystyrene), however, most of measurements have been performed at the heating rate of 10 K/min (concretes, hemp fibres). The measurements proceeded under both nitrogen and natural atmosphere using simultaneous thermal analysis in DSC/TG mode. The Al_2O_3 crucibles represented the reference inert material. The mass of the samples analyzed varied in dependence on the material properties from 7 to 40 mg.

2.2. Materials

Concrete composites of various compositions, with various waste materials and supplementary cementitious materials have been investigated using thermal analysis. The incorporation of waste into concrete allows saving the raw materials and natural sources together with reducing the landfilled waste amounts.

Hemp fibers original and chemically treated have been analyzed prior their applications to the concretes and built-in composites as well.

Expanded polystyrene (EPS) insulation boards have been analyzed in terms of their thermal resistance and stability.

3. Results

3.1. Concrete durability study

Thermal analysis was used to study potential differences in thermal behavior of the concrete sample before and after a corrosion experiment while the sample was exposed to sulfuric acid of (pH = 3). The record of the first derivative of the TG/TGA curves - differential thermogravimetry (DTG) curves of the concrete composite with silica fume addition under nitrogen atmosphere are presented in Fig. 1. The DTG curve (Fig.1) consists of three peaks where mass loss was recorded: 100˚C - 150˚C: release of crystallized water and water dehydration from the pores (C-S-H, etringit); 450 ° C - 550 ° C: dehydroxylation of calcium hydroxide and degradation of C-S-H gels, 700°C-850°C: decarbonation of $CaCO_3$. The DTG curve shows the decomposition of concrete sample with silica fume after sulfate exposure at a lower temperature

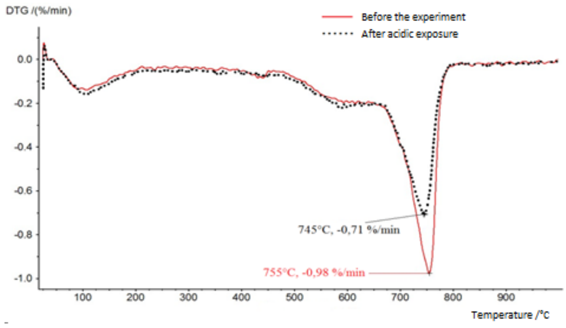

Fig. 1. DTG curves of concrete composite with silica fume before and after the acidic exposure.

(745 °C), compared to the sample before the corrosion test (755 ° C). In this respect, the sample after acidic corrosion was found to decompose earlier.

This finding was clearly confirmed also by DSC curves as it is seen in Fig. 2.

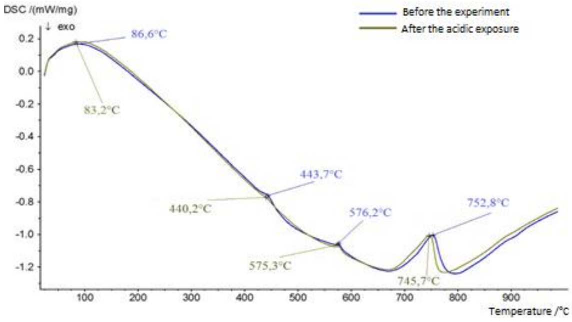

Fig. 2. DSC curves of concrete composite with silica fume before and after the acidic exposure.

From the DSC curves, it is clear that the major decomposition peaks in sample after acidic corrosion are shifted to lower temperatures compared to the sample before the experiment. This fact indicates a lower thermal stability of the sample after acidic exposure.

3.2. Thermal behaviour of hemp fibres

Another environmental approach is developing the light composites based on natural plant materials such as hemp. The study of thermal stability of hemp hurds was very important due to its subsequent incorporation into composite materials and use of the products thus prepared for various construction purposes. Fig. 3 shows details of DSC curves of hemp hurds in the most important temperature range of 250–500 °C.

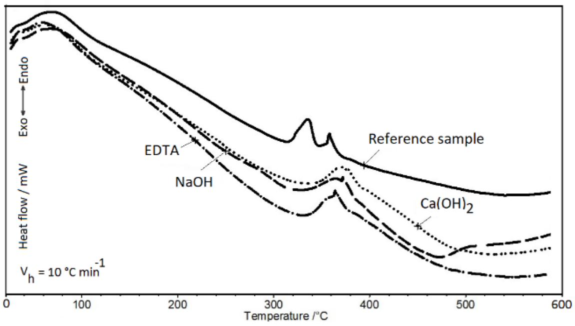

Fig. 3. DSC curves of referential and chemically treated hemp hurds [17].

As seen from the DSC results, curves for modified fibres have a different course in depending on the used agents (NaOH – Sodium hydroxide, EDTA - Ethylenediaminetetraacetic acid, $Ca(OH)_2$ – Calcium hydroxide) compared to the referential sample. In case of all treated samples, the onset of temperature degradation of the components of hemp hurds was observed at higher temperatures in comparison to the reference sample without any modification [17].

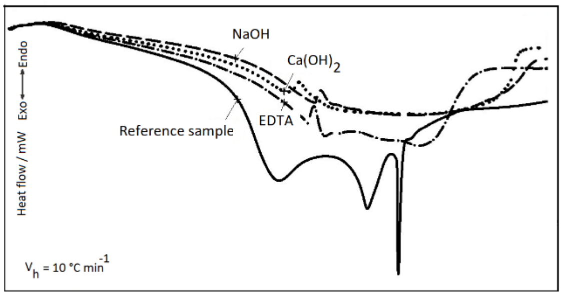

Fig. 4. DSC curves of referential and chemically treated hemp hurds [18].

The thermal analysis performed under air atmosphere provided different DSC curves of the same hemp fibres, original and chemically modified, as seen in Fig.4. In addition to the decomposition peaks, the oxidation processes occurred. Thermal stability and behavior of the hemp fibres was very useful when considering the resistivity of the hemp composites against a fire.

3.3. Polystyrene decomposition

Decomposition of the polymer materials is of importance due to both stability and safety reasons. Polymers, when decomposed, could release dangerous pollutants to the air and thus negatively affect human health. Thermal analysis is definitely very important tool to assess their thermal resistance, durability and potential risks. In our work, the polystyrene insulation boards have been investigated at different heating rates. Fig. 5 illustrate the comparison of the DTG curves of polystyrene when

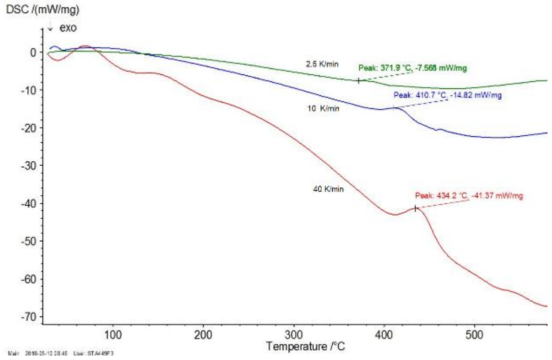

Fig. 5. DSC curves of EPS heated at various heating rates.

heating at 2.5, 10 and 40 K/min under air atmosphere.

As seen in Fig. 5, the rate of heating affects the decomposition temperatures a thus the thermal behavior of polystyrene is of great importance regarding its application.

4. Conclusion

Three different application of thermal analysis methods in environmental engineering have been presented in the paper. Based on the results, it can be concluded that the thermal analysis is a very effective and valuable analytical tool which can actually widely used for research in environmental, civil and fire engineering.

Acknowledgments

The research has been supported by Grant No. 1/0648/17 of Scientific Grant Agency of the Ministry of Education, science, research and sport of the Slovak Republic and the Slovak Academy of Sciences.

References

[1] B. Wunderlich, Thermal Analysis, 1st ed., Academic Press, Elsevier, 1990.
[2] V.S. Ramachandran, R.M. Paroli, A.H. Delgado, Handbook of Thermal Analysis of Construction Materials, 1st ed., William Andrew Inc., 2002.
[3] M. Wagner, Thermal Analysis in Practice, 1st ed., Elsevier, 2017.
[4] P. Gabbott et al., Principles and Applications of Thermal Analysis, 1st ed., Blackwell Publishing Ltd, 2008.
[5] A. P. Marinov, L. Gonsalvesh, M. Stefanova, J. Yperman, P. Gadjanov, Thermochimica Acta, 497 (2010) 46.
[6] X.Wang, R.Ch. Ren, Y. Liu, Procedia Earth and Planetary Science, 1 (2009) 750.
[7] Y. Chen, S. Mori, W. P. Pan, Thermochimica Acta, 275 (1996) 49.
[8] O. Francioso, D. Montecchio, P. Gioacchini, L. Cavani, O.Trubetskaya, Geoderma, 152 (2009) 264.
[9] T. Ahmad, K. Ahmad, M. Alam, Materials Research Express 5 (2018) 035511.
[10] L.D. Torquato, S. de Almeida, J.E. de Oliveira, M.S. Crespi, S.I. Maintinguer, Journal of Thermal Analysis and Calorimetry, 127 (2017) 1267.
[11] L. Findoráková, O. Šestinová, J. Hančuľák, E. Fedorová, A. Zorkovská, IOP Conference Series: Earth and Environmental Science, 44 (2016) 052024.
[12] H.M.I. Hasan, M.S.Masoud, International Journal of Chemical Sciences, 12 (2014) 11.
[13] S. Chakraborty, S. Nair, International Journal of Pavement Engineering, (2018) 1.
[14] J. Lv, T. Zhou, Q. Du, H. Wu, Construction and Building Materials, 157 (2017) 253.
[15] J.A. Teixeira, W.D.G. Nunes, R.P. Fernandes, A.L.C.S. do Nascimento, M. Ionashiro, Journal of Analytical and Applied Pyrolysis, 128 (2017) 261.
[16] S. Top, H. Vapur, A. Ekicibil, Journal of Molecular Structure, 1163 (2018) 4.
[17] N. Števulová, J. Čigášová, A. Eštoková, E. Terpáková, A. Geffert, F. Kačík, E. Singovszká, M. Holub, Materials, 7 (2014) 8131.
[18] N. Števulová, A. Eštoková, J. Čigášová, I. Schwarzová, F. Kačík, A. Geffert, Journal of Thermal Analysis and Calorimetry, 128 (2016)1649.

Compositions of volatile organic compounds emitted from natural and synthetic polymers

Aleš Ház[a*] – Michal Jablonský[a] – Anton Lisý[a]

[a]*Department of Wood, Pulp and Paper, Institute of Natural and Synthetic Polymers, Faculty of Chemical and Food Technology,*
Slovak University of Technology in Bratislava, Radlinského 9, Bratislava 812 37, Slovakia,

Abstract

Analysis of volatile organic compounds (VOCs) is an important method for understanding the chemical processes involved in polymer degradation and for the identification of materials. Many times is this type of analysis closely connected with thermal degradation during processing or during unwanted conditions. VOCs emitted during thermal treatment of plastics were analyzed to indicate compounds which can caused unpleasant odor. In this work were compared different techniques for analyzing VOCs from ligning and lignin composite. Identification was focused on comparison emitted sulphuric compounds. Screening analysis were made at 80, 160 and 200°C by different atmospheres. To confirm which compounds are emitted from samples, experiments were conducted and volatile organic compounds (VOCs) emitted from samples were trapped by Tenax/Carbograph adsorption tubes and analyzed by TD-GC/MS or directly analyzed by py-GC/MS. In the present study rubber, lignin/PLA/PHB composite and lignin were tested.

Keywords: TD-GC/MS; VOC; polymers; thermal desorption

---

[*] Corresponding author. Tel.: +421 2 593 256 48; e-mail: ales.haz@stuba.sk.

1. Introduction

Thermal desorption (TD) is a highly sensitive alternative to conventional sample collection procedures for volatile and semivolatile compounds, such as solvent desorption tubes. It is more efficient than other extraction methods and allows the selective concentration of target analytes, making it ideal for trace-level analysis by gas chromatography (GC/MS) across a wide range of applications. Thermal desorption is a process of collection and desorption of analytes from solid sorbents using heat and a flow of inert gas, rather than solvent extraction. Analytes are then focused on a cold trap prior to entering the analytical column, resulting in higher responses and narrow, more symmetric peaks. This is accomplished by interfacing a thermal desorption unit with a GC/MS. TD is highly sensitive and can significantly lower detection limits, by as much as 10^3, as it allows water to be purged, further facilitating the selective concentration of the compounds of interest. Thermal desorption tubes can be sampled actively with a sampling pump, or passively with a diffusion cap, which are also reusable.

Plastics are extremely diverse in terms of chemical composition, properties and possible applications, and are widely distributed in the society and the environment. In the last two decades the global annual production has doubled, reaching 245 million tons in 2008. Several of the chemicals used to produce plastics are hazardous for human health and the environment. These, and their degradation products, may be released during the life cycle of a plastic product. The plastic polymers are not considered as toxic, but in plastic products there may be present non-bound residual monomers, polymerization chemicals, degradation products, and additives which have toxic properties [1-3].

Study of volatile organic compounds (VOCs) brings outputs/outcomes in several levels:

1) Environmental (toxicity, emitted hazardous compounds)
2) Processing (stability, bonding, efficiency of selected processes)
3) Conversation (preservation of cultural heritage artefacts)
4) Degradation (study of degradation and stabilization process)
5) Recycling (secondary usage of materials, converting waste materials into new materials and objects)

At every level of this distribution is useful VOCs analysis. Dependence of purpose is necessary to change the conditions and process of emitting and collecting VOCs. In case of polymer stability study is necessary to simulate typical conditions of material purpose.

Generally isolated kraft lignins have a potential to be a substance for bioplastics. Lignin acts as filler which is suitable replacement of carbon black in quite wide range of concentrations in rubber blend - the highest reinforcing effect was observed in case of lignin. Lignin improves rubber-to-metal and rubber-to-polyesters adhesion. Lignin and lignosulfonates has a great potential as antioxidant of rubber blends [1,4].

2. Experimental

In this article is shown possibilities of using some of capturing and analyzing VOCs from three types of polymers (rubber and lignin/PLA/PHB composite). Capturing right into the absorption tube (Tenax + Carbograph) in first and second case was used. In third case releasing of VOCs by analytical pyrolysis was used.

Conditions at capturing VOC’s from rubber: 80°C, atmosphere – air, flow 60ml/min, duration 2hod

Conditions at capturing VOC’s from composite (lignoplast): 160°C, atmosphere – CO_2, flow 70ml/min, duration 2hod.

Conditions at capturing VOC’s from lignin: 200°C, atmosphere – He, flow 70ml/min, duration 30sec.

2.1. Py-GC/MS analysis

The pyrolysis was performed with a Pyroprobe 5150 Series (CDS Analytical Inc.). The pyrolyzer interface temperature was 150°C. Approximately 1.5 mg of sample was inserted into the glass liner and placed immediately in the pyrolyzer probe. The pyroprobe temperature was initially set and held for 5 sec s at 60 °C, and then ramped at 10 °C/ms to a final temperature and held for 5 sec.

2.2. TD-GC/MS analysis

Sorbent tubes were thermally desorbed by a thermal desorption unit (Unity 2, Markes, UK) coupled to a gas chromatograph (GC 7890A gas chromatograph Agilent Technologies, USA) with ion trap mass spectrometer detector (MSD 5975C, Agilent Technologies, USA). Thermal desorption of sorbent tubes was carried out in a two-step mode. In the first step, collected compounds were desorbed from sorbent tubes for 4 min at 320 °C and a flow rate of 50 mL.min-1 of He, carried through a 100 mg Tenax™ TA cryogenic internal trap, cooled at -10 °C. Thereafter, in the second step, the trap was desorbed at 300 °C for 1 min with fast heating (900 °C min^{-1}).

For GC/MS analysis, a GC 7890A gas chromatograph Agilent Technologies was used. The separation was made on a 30 m x 250 µm x 0.25 µm i.d. fused silica capillary column HP-5MS. The oven temperature was held at 40°C for 2 min, and then heated by ramp 20 °C/min to 300°C. The final temperature was kept for 5 min. The injector temperature was 250°C with splitless mode. Helium was used as the carrier gas with flow 1,2 ml/min. The end of the column was introduced into the ion source of the Agilent Technologies model 5975C series mass selective detector (MSD) operated in electron impact ionization mode. The data acquisition system used ChemStation E software and analyzed compounds were identified with NIST and Wiley electronic libraries.

3. Results and discussion

It is possible to focus analyses according to which parameter is desired: for polymer stability, identifying toxic or odor compounds, checking polymerization process, identifying of compound which were used as catalyst/antioxidant/plasticizer during polymer production. The main purpose of the analysis of rubber was to identify compounds which can be toxic or may cause unpleasant odor. On the basis of identificated compounds is possible to execute sensoric evaluation of pure compounds and determinate compounds which generate unpleasant odor. The toxicity of compound can be evaluated according to known properties of each compound. Main emitted compounds from rubber sample were: aniline, cyclohexanone, 1,2-ethandiyl-bis(2-methylacrylat), N-cyclohexyl-1-phenylmethanimin, N-benzylidenaniline, etc

Table 1

Main compounds identified from lignin at 160°C

RT (min)	Area (Ab*s)	Hit Name	Mol. Weight (amu)	CAS Number
1,443	71777163	Carbon dioxide	43,99	000124-38-9
1,767	2952397	Unk	Unk	Unk
2,032	1265122	Butanal, 3-hydroxy-	88,052	000107-89-1
2,085	850631	Ethanethiol	62,019	000075-08-1
2,882	890485	Butanal, 3-methyl-	86,073	000590-86-3
2,953	632508	Benzene	78,047	000071-43-2
3,374	1008712	Furan, 2,5-dimethyl-	96,058	000625-86-5
3,776	79318503	Dimethyl sulfone	93,991	000067-71-0
4,022	9377160	Toluene	92,063	000108-88-3
4,391	593067	Hexanal	100,089	000066-25-1

*Unk – unknown

Table 2

Main compounds identified from pyrolysis of rubber at 80°C

RT (min)	Area (Ab*s)	Hit Name	Mol. Weight (amu)	CAS Number
5,408	12789125	Cyclohexanone	98,073	000108-94-1
5,875	1502906	Ethylidene norbornene	120,19	16219-75-3
6,134	2455993	Benzaldehyde	106,042	000100-52-7
6,244	92926129	Aniline	93,058	000062-53-3
7,262	885366	1-Methylene-2-vinylcyclopentane	108,094	006196-78-7
8,376	3267892	Cyclohexane, isothiocyanato-	141,061	001122-82-3
8,83	14684930	2-Propenoic acid, 2-methyl-, 1,2-ethanediyl ester	198,089	000097-90-5
8,953	611879	3-Hexene, 2,5-dimethyl-, (E)-	112,125	000692-70-6
9,128	1669792	Phenol, 2-(1,1-dimethylethyl)-4-methyl-	164,12	002409-55-4
9,303	447277	1-Undecene, 10-methyl-	168,188	022370-55-4
9,335	572574	2-Tetradecene, (E)-	196,219	035953-54-9
9,387	1021485	1-Octanol, 2-butyl-	186,198	003913-02-8
9,931	468310	Cyclopropane, 1-(1-methylethyl)-2-nonyl-	210,235	041977-39-3
10,573	2193801	Cyclohexanamine, N-(phenylmethylene)-	187,136	002211-66-7
11,214	2534039	Benzenamine, N-(phenylmethylene)-	181,089	000538-51-2

In case of identification VOC s products from lignoplast, the aim was to search compounds which can caused unpleasant odor.

This study measured the odor and VOC emissions of natural and synthetic polymers. Figure 1 shows the volatile odor compound emissions of precipitated lignin as an organic filler in case of third sample (composite). Purpose of this comparison was to show differences of emitted VOCs.

Odor production of the bio-composites can be caused by the matrix polymer or the natural-filler, or by a combination of the two. The matrix polymer can emit unwanted odors, caused by residual monomers or by decomposition products that occur in the production process of bio-composites due to the non-optimized heating temperatures [5-7].

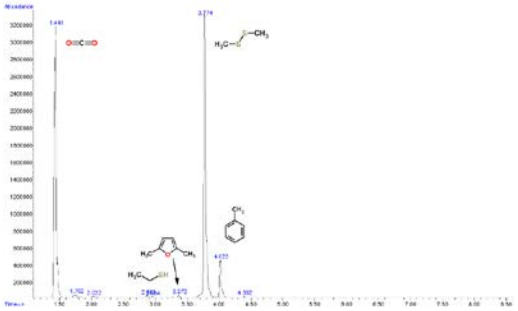

Fig. 1 TD-GC/MS analysis of VOCs from lignin at 160°C

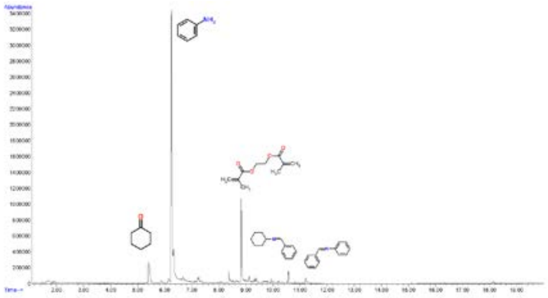

Fig. 2 TD-GC/MS analysis of VOCs from rubber with addition of stabilizer at 80°C

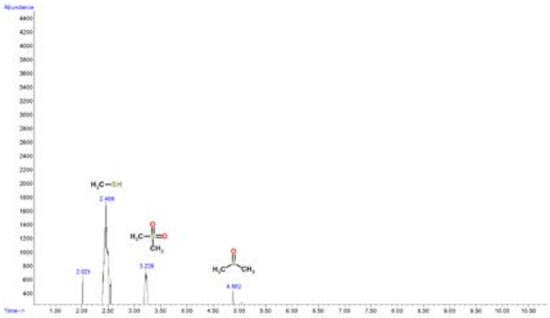

Fig. 3 Py-GC/MS analysis of VOCs from lignoplast at 200°C

Sulphuric content is the one of mains reason for generating the odor emitted by the bio- composites consist of kraft lignin. These compounds can be produced from natural-filler materials rich in aromatic polymer from wood. Lignin and PLA/PHB/lignin can emit odors caused by the thermal degradation due to the low degradation temperature. Tables 1 and 3 list the emission compounds, as detected by TD-GC-MS, of various VOCs from lignin and lignin/PHB and PLA bio-composites. The various VOC emissions of these bio-composites were mainly caused by the oxidation of the matrix polymer and the thermal degradation of natural polymer. In case of lignin analysis and biocomposite material made from lignin it is possible to observe lower emittion of sulphuric compounds which are undesirable by-products of biocomposite production. Methanethiol, Dimethyl sulfone, Dimethyl sulfoxide were identified in final material.

Table 3

Main compounds identified from pyrolysis of lignoplast at 200°C

RT (min)	Area (Ab*s)	Hit Name	Mol. Weight (amu)	CAS Number
2,021	6743	Carbon dioxide	43,99	000124-38-9
2,465	76549	Methanethiol	48,003	000074-93-1
3,226	24424	Dimethyl sulfone	94.01	000067-71-0
4,882	52826	Dimethyl sulfoxide	78.01	000067-68-5
6,581	6743	Unk	Unk	Unk

*Unk - unknown

4. Conclusions

The objective of this work was to analyze emissions of VOCs from the lignin, rubber and lignin/PHB/PLA composite. It has been found that for lignin the main identified emission at temperature 160°C consists of sulphuric compounds which are undesirable. At the highest temperatures were identified substituted phenol and benzene. After desorption from tubes was determined odorous substances from lignin. The main substances were identified as: methanethiol and dimethyl sulfone, methanethiol and dimethyl sulfoxide. This information allows us to use suitable treatment for elimination of that substance from lignin. Based on the results obtained from bio-composite VOC's the content of sulphuric compounds is still parameter which has to be solved. Application of these results can lead to the creation of rubber-lignin composites and application of compound which can act as emission stoppers. Recyclability and biodegradability of these composites are important part of future development in natural and synthetic polymer industries.

Acknowledgments

This work was supported by the Slovak Research and Development Agency under the contracts No. APVV-15-0052 and APVV-0393-14. This article was realized also thanks to the support for infrastructure equipment by the Operation Program Research and Development for the project "National Center for Research and Application of renewable energy sources" (ITMS 26240120016, ITMS 26240120028) for the project "Competence center for new materials, advanced technologies and energy"(ITMS 26240220073) and for the project "University science park STU Bratislava" (ITMS 26240220084), co-financed by the European Regional Development Fund. The authors would like to thank for financial assistance from the STU Grant scheme for Support of excellent Teams of Young Researchers under the contract no. 1663.

References

[1] Ház, A., Jablonský, M., Sládková, A., Feranc, J., & Šurina, I.: Key Engineering Materials, 688 (2016)

[2] Delilah Lithner, Ph.D. thesis, Environmental and health hazards of chemicals in plastic polymers and products (2011)

[3] Kubačková, J., Ferenc, J., Hudec, I., Šutý, Š., Jablonský, M., Annus, J., & Pret'o, J.: Elastomery, 17(3), 21-27 (2013).

[4] Feldman, D. (2002). Lignin and its polyblends—a review. In Chemical modification, properties, and usage of lignin (pp. 81-99). Springer, Boston, MA.

[5] Kim, H. S., Kim, S., Kim, H. J., & Kim, H. G. (2006). Physico-Mechanical Properties, Odor and VOC Emission of Bio-Flour- Filled Poly (propylene) Bio- Composites with

Different Volcanic Pozzolan Contents. Macromolecular Materials and Engineering, 291(10), 1255-1264.

[6] Šutý, Š., Ház, A., Lauko, T., Feranc, J., Plavec, R.:. Identification of odorous substances in kraft lignin for bioplastics. In PMA 2015 & SRC 2015, 56-59 (2015)

[7] Hodásová, Ľ., Jablonský, M., Škulcová, A., Ház, A.: Wood Research 60.6: 973-986 (2015)

Comparison of Forces and Means at the Fire of Selected Petroleum Large-Capacity Tanks

Ján Horváth[a*] – Jaroslava Štefková[b] – Martin Zachar[a]

[a] *Technical University in Zvolen, Department of Fire Protection, T. G. Masaryka 24, 960 53 Zvolen, Slovakia*

[b] *Technical University in Zvolen, Institute of Foreign Languages, T. G. Masaryka 24, 960 53 Zvolen, Slovakia*

Abstract

Fires of petroleum in large-capacity storage tanks belong to the most demanding fire interventions from the viewpoint of deploying the sufficient amount of forces and means. The article deals with forces and means necessary for a successful suppression of such fires for three real bulk storage tanks. The selected tanks are of a similar make but of different dimensions. The forces and means are calculated for the two most complicated scenarios. The calculations were performed according to the Regulation of the President of the Fire and Rescue Corps of the SR No. 39/2003. The results given in the table show that the necessary amount of forces and means grows directly with the dimensions of the tanks. In the present, it is not possible to exclude the risk of a real fire; therefore, it is necessary to consider the necessary deployment of the forces and means already at the beginning of its construction and/or installation.

Keywords:fire scenarios; fire suppression; large-capacity storage tank

---

[*] Corresponding author. Tel.: +421 455 206 827; e-mail: jan.horvath@tuzvo.sk.

1. Introduction

Currently, there are several variants of the large-capacity petroleum storage tanks in operation. The comparison of fire safety of individual tank types and possible solutions of fire suppression of these tanks is not definitely settled yet, at least in some European countries.

In Slovakia, petroleum is stored in large-capacity tanks whose storing capacity ranges from 30,000 to 100,000 m^3. At the pumping station in Tupá (in the proximity of Šahy – 6 km) there are large-capacity storage tanks in the above-ground make where the maximum content of the stored petroleum is 320,000 m^3. There are six tanks of the 30,000 m^3 capacity and two tanks with the capacity of 70,000 m^3.

The MERO Company (the Czech Republic) has the maximum capacity of 1,550,000 m^3 at the central supplies of petroleum in Nelahozeves. It consists of four tanks with the storage capacity of 50,000 m^3, six tanks with the capacity of 100,000 m^3 and six tanks with 125,000 m^3 capacity. Compared to the storage in Tupá, it stores five times bigger amount of petroleum.

Double-shell large-capacity tanks are in an above-ground make, standing, cylinder shaped, steel parts welded – all metal. They have chamber floating roof which floats on the surface of the stored liquid. The roof is also welded from steel parts. Created air cells enable floating of the roof on the surface of the stored liquid [1].

The main task of the fire forces arriving first to the scene is to perform the necessary measures to control the spread of fire. It mainly means to cool down the fire affected tanks, to cool down neighbouring tanks, measures to prevent ignition of vapours in neighbouring tanks, collection tanks (outer shell of the tank), pipelines, sewage, and technology piping. When neighbouring tanks are being cooled down, especially those tanks which are directly affected by flames from the burning tank are being cooled down on the adjacent side. Cooling the tanks placed on the sides or downwind in the distance equalling to the diameter of a burning tank is performed in the second step [2].

Considering that each storage tank at the PS4 (a pumping station) in Tupá (Fig1) and in Nelahozeves (Fig.2) would have at least two neighbouring tanks within the distance of two diameters of the burning tank, it is necessary to consider at least two neighbouring tanks to cool down. To simplify the comparison of calculations, the 30,000 m^3 storage tanks neighbouring the burning tank (applied also for the central supplies in Nelahozeves) are considered.

Fig. 1 Satellite image of the pumping station in PS4 in Tupá [author´s archive]

Fig. 2 Satellite image of the petroleum central supplies of the MERO company in Nelahozeves [author´s archive]

Cooling down is executed via deluge guns or solid stream nozzles. The advantage of the deluge guns is their higher reach and output.

The Regulation of the President No. 39 does not define the cooling down of the neighbouring tanks; therefore, only storage tanks are considered.

2. Methodology and calculation

Possible fire scenarios:

1 A fire in between the roof and outer shell of the tank – S1 scenario.

2 A fire of the collection tank and the space between the roof and the shell of the tank –S2 scenario.

3 A fire of the storage tank – complete surface (when floating tank roof is submerged) –S3 scenario.

4 A fire of an accident tank (when floating roof of the storage tank submerged and shell of the storage tank is damaged) - S4 scenario.

5 A fire of the accident tank (the space between the inner and outer shell of the tank) – S5 scenario.

The most complicated fires seem to be the scenarios S3 and S4. The forces and means are calculated for S3 scenario for the storage tank with the capacity of 30,000 m^3, the other results shall be recorded in the table for the comparison. In case of S4 scenario the cooling down of the accident tank (60 l.m^{-2}.min.$^{-1}$) shall be used for the calculations.

D – diameter of the storage tank (42.8 m)

D_h – radius of the accident tank (53.6 m)

S_h – area of the petroleum rim in the storage tank (1 439 m^2)

S_{hh} – area of the petroleum rim in the accident tank (2 256 m^2)

I_p – required volume of the extinguishing agent (heavy foam) (75 l.m^{-2}.min.$^{-1}$)

I^o_{ph} – required volume of the water supplies to cool down the burning tank (30 l.m^{-1}.min.$^{-1}$)

I^o_{phs} – required volume of the water supplies to cool down the tank when storage tank is burning (60 l.m^{-1}·min.$^{-1}$)

Q^h_p – required volume of the water supplies to cool down the neighbouring tank (12 l.m^{-1}.min.$^{-1}$)

– required supplies of an extinguishing agent (l.min.$^{-1}$)

The necessary supply of the extinguishing agent can be calculated from the relation (1):

$$Q_p^h = S_h \times I_p \qquad (1)$$

Q^h_p = 1 439 x 75 = **107 925** *l.min.$^{-1}$* = **108** m^3.min. $^{-1}$ *(foam)*

The volume of the necessary solution is determined by the ratio of the foam and the expansion rate. The expansion rate is within the interval of 0 to 20, the value of 7.5 was used for our calculations. It is the ratio of the created foam to the foaming solution from which the foam was created.

The volume of the foaming solution was calculated by the relation (2):

$$Q_{pr} = \frac{V_p}{\check{c}_n} \qquad (2)$$

V_p – required volume of the extinguishing foam *l.min.$^{-1}$*

$\check{C}_n$ – expansion rate for the selected stream (or other device) *7,5*

Q_{pr} = 107 925:7,5 = **14 390** *l.min.$^{-1}$*

The foaming solution consists of the water and foam concentrate. The percentage of adding the foam concentrate depends on the kind of the used foam concentrate, foam generator and mixing device. The foam concentrate producer suggests the suitable ratio of mixing, which usually is a few volume percents.

The amount of required volume of the foam concentrate was calculated by the relation (3) for the foam concentrate Sthamex – AFFF 1% F-15 with 1% ratio of mixing given by the producer.

$$V_p = Q_{pr} \times p_p \quad (3)$$

V_p – required volume of the foam concentrate per minute

P_p – percentage of mixing 1% *– (0.01)*

V_p = 14 390 x 0,01 = 143.9 = **144** *l.min.$^{-1}$*

To ensure the successful suppression of fire it is necessary to secure uninterrupted delivery of foam for 10 minutes.

The necessary amount of foam concentrate shall be calculated from the relation (4):

$$V_p = n_{pr} \times q_p \times t_n \times z \quad (4)$$

V_p – foam concentrate amount *(l)*

n_{pr} – number of foam making nozzles *(pcs)*

q_p – flow of an individual foam – making nozzle *(l.min^{-1})*

t_n – required time of suppression *– 10 min.*

z – foam concentrate supplies *– 3*

Deducting the foam concentrate amount from the required foaming solution the required volume of water supply to suppress the tank per minute according to the relation (5):

$$Q_V = Q_{pr} - V_p \quad (5)$$

Q_v – required amount of water per minute during extinguishing by foam

Q_{pr} – volume of foaming solution for the

Q_v = 14 390 – 144 = **14 246** *l.min.$^{-1.}$*

Amount of water required to cool down the water tank shall be calculated by the following relation (6):

$$Q_p^o = \pi \times D \times I_p^o \quad (6)$$

Q^o_p – required amount of water to cool down the particular tank *(l.min^{-1})*

D – tank diameter *(m)*

I^o_p – required amount of water for cooling *(l.m^{-1}.min^{-1})*

Q^o_p = 3.14 x 42.8 x 30 = **4 034** *l.min.$^{-1}$*

The water supply necessary for cooling down the neighbouring tanks shall be calculated by the relation (7):

$$Q_p^o = m \times 0{,}5 \times \pi \times D \times I_{phs}^o \quad (7)$$

Q^o_p – necessary amount of water for cooling neighbouring tanks *(l.min^{-1})*

m– number of cooled tanks *(they must be of the same diameter)*

D – diameter of the cooled tanks *(m)*

I^o_p – required amount of water for cooling *(l.m^{-1}.min^{-1})*

Q^o_p = 2 x 0.5 x 3.14 x 42.8 .12 = **1 614** *l.min^{-1}*

The total supply of water per minute shall be calculated by the relation (8) as the sum of necessary water supply for suppression (without foam concentrate) and water supply to cool down the burning and neighbouring tanks.

$$Q_C = Q_p^o + Q_v \quad (8)$$

Q_c = 14 246 + 4 034 + 1 614 = **19 894** *l.min^{-1}*.

To calculate the supplies, the Ambassador Monitor (Fig 3) shall be used. There are two in the firefighting equipment of the Fire Brigade in Tupá. The design of the mentioned monitor enables its use during a real fire threat.

Fig. 3 Ambassador Monitor

Multi-purpose monitor Ambassador with high, controllable performance is designed to suppress the large-scale fires. It concerns especially fires in the petroleum industry, where there are required big amounts of extinguishing agents necessary to deliver for bigger distances and heights in many cases. The monitor is manually controlled with the adjustable performance in the range from 3,700 to 22,700 *l.min^{-1}* at the pressure of 0,7 MPa. The intake of water for the monitor is provided by 4×150 mm ready for connecting of A type hoses. The 100 mm diameter hose can add foam concentrate or foam powder in the monitor.

To control the device, the producer recommends 5 people, the others are necessary to ensure continuous supplies of water and foam concentrate. It should be positioned in distance of 35 – 75 m from the fire sire depending on the diameter of the tank being extinguished [3]. The reach of Ambassador for different flow rates and connectors is given in Table 1.

Table 1

The reach of Ambassador

2 connectors	7 400 *l*.min.$^{-1}$	Reach of 70 m
3 connectors	14 800 *l*.min.$^{-1}$	Reach of 90 m
4 connectors	22 700 *l*.min.$^{-1}$	Reach of 120 m

The number of streams to suppress the fire is calculated from the equation (9):

$$N_{pr}^{h} = \frac{Q_p^h}{q_{pr}} \quad (9)$$

N^h_{pr} – number of streams to suppress the fire *(pcs)*
Q^h_p – necessary amount of extinguishing agent to suppress the fire *(l.min^{-1})*
q_{pr} – flow rate of the nozzles *(l.min^{-1})*

The number of the nozzles necessary to suppress the fire can also be calculated from the relation (10):

$$N_{pr}^{h} = \frac{S_p}{S_{pr}} \quad (10)$$

S_p – area of fire or the area of suppression *(m^2)*
S_{pr} – area which can be suppressed by one nozzle *(m^2)*

The number of nozzles for protection (for cooling) can be calculated from the relation (11):

$$N_{pr}^{o} = \frac{Q_p^o}{q_{pr}} \quad (11)$$

N^o_{pr} – number of streams necessary for protection - cooling *(pcs)*
Q^o_p – necessary amount of water for cooling *(l.min^{-1})*
q_{pr} – flow rate of the nozzles *(l.min^{-1})*

The total number of streams can be calculated from the relation (12):

$$N_{pr} = N_{pr}^{h} + N_{pr}^{o} \quad (12)$$

The number of firefighting vehicles (pumper trucks, water tender) is determined from the relation (13):

$$N_A = \frac{Q_c}{q_A} \quad (13)$$

N_A – number of firefighting vehicles *(pcs)*
Q_c – total necessary amount of water *(l.min^{-1})*
q_A – supply of one vehicle *(l.min^{-1})*

The number of necessary firefighters is determined from the relation (14):

$$N_p = \left(2 \times n_p^c + 3 \times n_p^b \right) \times 1{,}25 \quad (14)$$

n^c_p – number of „C“ nozzles (two firefighters per one nozzle)
n^b_p – number of „B“ nozzles (three firefighters per every nozzle) [4].

3. Results and discussion

To cool down the affected tank the turntable deluge gun WR30 with the nozzle diameter of 30 mm, flow rate of 1,660 *l.min^{-1}* at the pressure of 0.8 MPa, distance of the reach 60 m and height of the reach 45 m, while there are two firefighters counted to operate the deluge gun WR 30 according to the Regulation 39/2003. To cool down the neighbouring tanks the intervention was designed for nozzles of B type with the nozzle diameter of 18 mm at the pressure 0.4 MPa and flowrate 400 *l.min.$^{-1}$*. The number of water tenders/pumper trucks (CAS) necessary at the site is determined from the relation (13), while the calculations were made under the condition of the long-term supply of one vehicle 3,000 *l.min.$^{-1}$* without the need of remote of shuttle transport of water (an ideal case) including the corporate fire water piping and hydrant network with the sufficient flowrate and pressure. The calculated values of the observed parameters are given in Table 2.

Four firefighters in the turnout gear resistant to radiant heat were counted per one mobile Ambassador Monitor. Two firefighters in protective gear were counted per one turntable deluge gun WR 30. The number of intervening firefighters in protective gear is the sum of the number of firefighters to operate Ambassadors and the number of firefighters necessary to cool down the affected tank with the deluge gun WR 30.

Table 2

The calculation of forces and means

Calculated tank volume	29 062 m^3		72 803 m^3		*124 968 m^3*	
Scenario	S3	S4	S3	S4	S3	S4
Tank diameter (m)	42.80	53.60	66.00	80.00	84.47	90.47
Suppression area (m^2)	1 439	2 256	3 421	5 027	5 604	6 428
Foam (l.min.$^{-1}$)	107 925	169 200	256 575	377 025	420 300	482 100
Foaming solution (l.min.$^{-1}$)	14 390	22 560	34 210	50 270	56 040	64 280
Foam concentrate (l.min.$^{-1}$)	144	226	342	503	560	643
Necessary foam concentrate (l)	4 320	6 780	10 260	15 090	16 800	19290
Necessary water (l.min.$^{-1}$)	14 246	22 334	33 868	49 767	55 480	63 637
Cooling of the burning tank (l.min.$^{-1}$)	4 034	10 103	6 220	15 080	7 961	17 053
Cooling of neighbouring tanks (l.min.$^{-1}$)	1 614	1 614	1 614	1 614	1 614	1 614
Cooling total (l.min.$^{-1}$)	5 648	11 717	7 834	16 694	9 575	18 667
Water total (l.min.$^{-1}$)	19 894	34 051	41 702	58 921	65 055	82 304
Number of Ambassadors	1	1	2	3	3	3
Necessary WR 30 cooling top tank	3	7	4	10	5	11
Water for the number of WR 30	4 980	11 620	6 640	16 600	8 300	18 260
Number of B streams	4	4	4	4	4	4
Water for number of B- streams	1 600	1 600	1 600	1 600	1 600	1 600
Number of CAS	10	12	18	29	26	30
Number of equipped firefighters	14	18	16	32	22	34

4. Conclusion

To successfully suppress the fire, the firefighting technique and means were chosen so that there is the least demand for the intervening firefighters in the dangerous zone of radiant heat. The mobile monitor Ambassador was introduced for its sufficient reach and flow rate parameters. As the final results showed (Table 2), Ambassador is one of the most suitable alternatives for suppression of fires in large-capacity tanks.

During the calculations, we assumed there is always only one burning tank while there were chosen the scenarios which are more difficult for fire suppression. The tactic exercises are usually aimed at only one tank; however, it is not excluded that there can be the fire of more tanks as the fire can shift to other neighbouring tanks or the same ignition source can ignite other tanks as well. The deployment of firefighters in specialized gear protective against radiant heat (Table 2) suggests the high demand of intervening firefighters. The initial intervention should be carried out by the firefighters at the corporate fire brigade. Their number is, at present, rather low at the Fire Brigade in Tupá.

Acknowledgments

This paper was supported by the Cultural and Educational Grant Agency under contracts No. KEGA 012TUZ-4/2016 and No. KEGA 030UMB-4/2017.

References

[1] TRANSPETROL. 2008. Operatívny plán hasenia, vydanie 2. Tupá : 2008. 20 s.
[2] OLŠANSKÝ, J. 1976. Metodika hasenia ropy a ropných produktov v nádržiach. Bratislava : 1976, 43 s.
[3] ŠULEKOVÁ, J. 2002. Zařízení na hašení ropných nádrží. In 150 Hoří. 2002, č. 6 [cit.2012-03-12]. http://aplikace.mvcer.cz/archiv2008/casopisy/150hori/2002
[4] POKYN prezidenta Hasičského a záchranného zboru o obsahu a postupe pri spracúvaní dokumentácie o zdolávaní požiarov (transl. - The Regulation of the Prezident of the Fire and Rescue Corps of the SR on Content and Procedure for Documentation of Fire Suppression), č. 39.Bratislava. 2003

Earth in a Trap? 2018
Analytical Methods in Fire and Environmental Science

Input factor analysis for the use of special LKT for the transport of water to a forest fire area

Ivan Chromek[a*] – Richard Hnilica[b] – Michaela Hnilicová[c] – Jaroslav Matej[d] – Valéria Messingerová[c]

[a]*Department of Fire Protection, Faculty of Wood Sciences and Technology, Technical University in Zvolen, T. G. Masaryka 24, 960 53 Zvolen, Slovak Republic*

[b]*Department of Manufacturing Technology and Quality Management, Faculty of Environmental and manufacturing Technology, Technical University in Zvolen, Študentská 26, 960 53 Zvolen, Slovak Republic*

[c]*Department of Forest Harvesting, Logistics and Ameliorations, Technical University in Zvolen, T. G. Masaryka 24, 960 53 Zvolen, Slovak Republic*

[d]*Department of Mechanics, Mechanical Engineering and Design, Faculty of Environmental and Manufacturing Technology, Technical University in Zvolen, Študentská 26, 960 53 Zvolen, Slovak Republic*

Abstract

The forest wheeled skidder has been developed from its beginnings as a single-purpose machine for the needs of skidding in the forest. The paper deals with the analysis of input factors that predispose this type of construction to ensure the transport of water supply in case of fire brigades in forest fires. The input factors for the use of LKT mainly include analysis of the terrain, which is capable of this type of equipment to move, analyze the appropriateness of placing the adapter for the transport of water, the selection of appropriate materials, design and construction solutions. The aim of these analytical procedures is to conservation the original features and to extend the target use of special machines.

Keywords: forest wheeled skidder; adapter; duty of water; forest; forest fire fighting

---

[*] Corresponding author. Tel.: +421-45-5206826; fax: +421-45-5330027; e-mail:chromek@tuzvo.sk.

[1] LKT: Forest Wheeled Skidder,

[2] CAS: Pumping appliance.

1. Introduction

Design and development of pumping appliance for fire-fighting in inaccessible forest fire areas collides with high costs from point of view of development, and also with limited possibilities of mass production (piece production). The last question is utilization of such a one-purpose machine, mainly number of uses in relation to working life of the machine. This is the basic problem, that creates a room for alternative solutions. In this paper the solution is based on analysis of the terrain in which the machine operates, selection of a machine that exists in present, and is suitable for this environment, design of a body – adapter, based on water tank, selection of suitable materials from point of view of strength and low weight. Another criterion is a shape of the water tank with accent on conservation of native travel abilities of the base vehicle.

In the case of any forest fire, forest land in the conditions of the Slovak Republic, is characterized by under-dimensioned availability of the space. Recommended norms in relation to forest road network, for flat terrain 15 m*ha^{-1}, for hills 22.5 m*ha^{-1}, and for mountain conditions 27.5 m*ha^{-1}, are based on the needs of optimal forest management, where it is possible also include fire protection [1]. According to data from the Green Report 2015 [2], this status is basically persistent. In 2015, the share of 1L roads was only 17.35%, with the use of 1L foreign roads not more than 24%. More details are given in Table 1.

As it can be seen from these data, the basic space for the transport of water in the case of forest fires are mainly ground paths of class 3L + TPC and the forest background itself, with a high average stocking, characterized by windfall, gully, creating terrain inequalities even at relatively small altitudes outside alpine and mountain areas. In this area, it is possible to move only field vehicles with an emphasis on all aspects of accessibility, not excluding sloping accessibility, but also maneuverability in a limited space. This type of terrain is at least suitable for the movement of basic types of fire-fighting equipment, including the most advanced CAS[2], which is the TATRA 815-7 CAS 30 6x6 [3].

The main disadvantage of this machine is the high weight (25 t) and in particular the length of the vehicle, exceeding 9 meters (9.4 m). These two parameters, despite the amount of fire extinguishers onboard (9,000 l), significantly reduce the use of this type of vehicle, predestined for forest fires to maneuver outside the forest road network. Similarly, the CAS on the T 148 and T 815 chassis.

2. Material and methods

The main task of LKT[1] is to move wood from the forest to the place of further manipulation. In the case of a transport of an extinguishing agent, it is a change of the basic working algorithm. The space remains, the direction of movement changes only. For this reason, considering how to use LKT for these purposes, the following concepts of its use are taken into account:

1) the use of LKT in the form of a pulling device to increase the CAS’s accessibility (Figure 1),
2) the use of LKT as a pulling device for pulling a one-axle or two-axle trailer (Figure 2)
3) the use of LKT as a carrier for the transport of water – a special purpose machine (Figure 3)
4) the use of LKT as a carrier for a removable water transport superstructure (Figure 4).

Table 1

Forest opening with the transport network

Types of road		Year 2014	
		Length (km)	Density (m.ha^{-1})
Own roads	Haul forest roads class 1L (carriageway)	6 516	3,3
	Haul forest roads class 2L (metalled road)	15 051	7,7

	Earth forest road 3L + TPC	16 039	8,3
	All	37 606	19,3
Foreign roads – haul forest roads 1L		3 212	1,6
All (own a foreign)		40 818	20,9

As it can be seen from concept 1, LKT is used as a traction device to increase the uptake of fire-fighting equipment in the forest terrain. In this case, the MB UNIMOG CAS is drawn. Similarly, in the past, the traffic ability of CAS vehicles on ZIL 131 or Praga V3S chassis has increased. However, this solution is at the limit of the possibility of this technique with the risk of its damage or destruction.

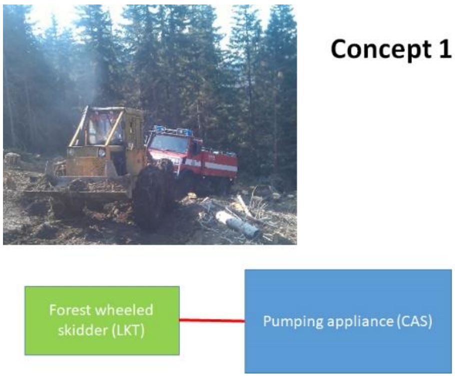

Fig.1 Utilization of LKT in the form traction gear to increase the endurance distance of CAS

Concept 2 hits a limited capability of the trailer, in relation to its stability when crossing the terrain (churning up the road, the tracks on the road, the stones or the root stones and the tires).

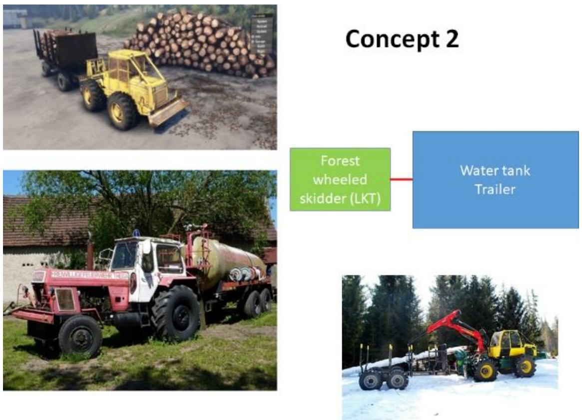

Fig.2 Utilization of LKT in the form traction gear to increase a one-axle or two-axle trailer

Fig.3 The use of LKT as a carrier of a fixed superstructure for water transport – a special purpose machine

---

[1] LKT: Forest Wheeled Skidder,

[2] CAS: Pumping appliance.

The concept 3 shows the uniqueness of such a machine, which significantly increases the costs of its production and operation. Small-scale or piece production does not ensure its presence in the area, in the event of a forest fire.

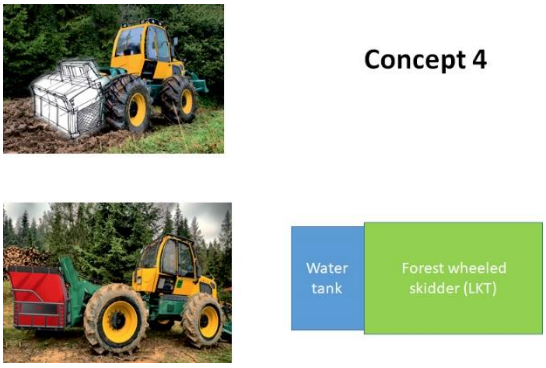

Fig.4 The use of as a carrier of detachable body for water transport

Under concept 4, the original purpose of LKT is preserved, with minimal constraints on driving characteristics. With a volume of carried fire-extinguishing material, approx. 2000 l replaces vehicles based on P V3S or MB UNIMOG chassis. In this way, the original LKT function is retained with minimal delay when applying the superstructure to the rear LKT shield. After transporting the superstructure into the space, the superstructure may be used as a water reservoir, with the possibility of possible aviation addition (top cover), or can be reused for LKT supply. Such an extension may also include accessories for the placement and transport of other technical means for the needs of firefighters in action.

3. Results

The design of the fire-fighting body must be adapted to the parameters of base machine LKT. The LKT will be carried on the inclinable rear log arch. The fire-fighting body must be further mobile, so it can be dismantled. The proposed fire-fighting body with its equipment will meet the criteria for forest fire interventions and monitoring of forest area.

The basic technical parameters for the fire-fighting body on LKT will be:

- water volume of about 2,000 liters,
- fire-fighting body equipment (high-pressure motor pump, fire extinguishing box),
- anchorage of the fire-fighting body on the inclinable rear log arch,
- the protective frame that ensures fire-fighting body handling (tank transfer, tank lifting),
- independent extinguishing after disconnecting the base-machine,
- possibility of transportation of parts to build a lake system of water relay of forest fires-fighting.

Based on the fact that the proposed fire-fighting body is to be used in the complicated terrain of mountain forests, its weight must be monitored in its design. In order to increase capacity weight base machine, but also to ensure maximum handling a four-member operator is therefore allowed for lightweight construction tanks of composite materials. [4]

Composite materials play an increasingly important role today in the selection of material for the production of specific parts. Their use comes mainly from the effort to replace steel and other metals, increase strength, reduce weight, chemical resistance, corrosion resistance, and so on. Composite material parts have excellent properties that impossible of achievement with other materials. Their use is very universal. They are mainly used in the aerospace, marine and automotive industries. Other applications are in electrical engineering, electronics, power engineering and mechanical engineering.

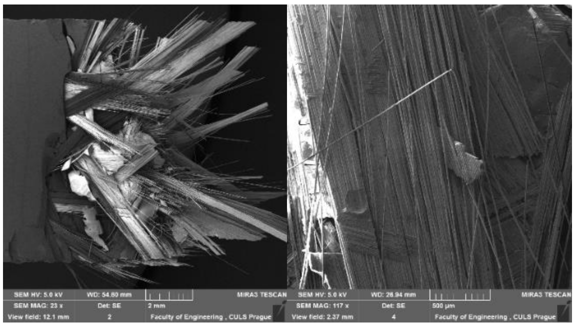

Fig. 5 SEM images of composite sandwich material (fiberglass)

According to [5], the properties of the fiberglass are given by the type of resin used and the type of reinforcement, the proportional share of glass fibers in the total volume and their arrangement. Strength increases with increasing fiber content and their arrangement in one direction. Good interaction of the glass fibres with the matrix in the form of epoxy is proved on the base of the conclusions of mechanical testing and subsequent results of the electron microscopy [6]. As early as in the design stage, the individual components are dimensioned to withstand many times greater loads and stresses than it is envisaged for operational conditions [7]. The analysis was needed to assess the suitability of the material proposed by the tank in terms of its strength and possible material savings in its production. The microstructure of the fibers of the composite used is shown in Figure 5. For this reason, the water tank does not exceed 130 kg. In the future we also see the possibility of producing composite water tanks using natural fibers, which are currently devoted to various authors in their research [8]; [9]; [10]; [11]; [12]; [13]; [14]; [15]; [16]. Replacing of the synthetic fibres by the natural ones has a lot of benefits which can be rationalized also by means of an ecological equilibrium [8].

For transport safety and prevention of vertical and horizontal movement of water in the water tank during transport, as shown in Figure 6, we considered the construction of internal wave-breaks. These breakwaters are part of the construction of the water tank itself, thereby increasing its overall strength. To simplify maintenance has been undertaken to construct a removable lid.

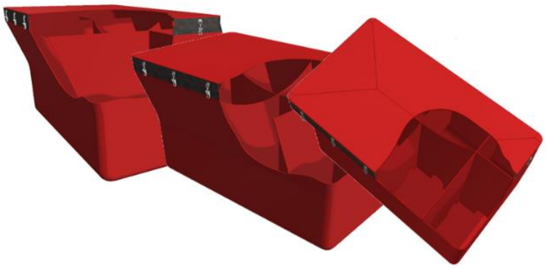

Fig. 6 Design of water tank construction with built-in wave-breaks [17]

Requirements for the transport of the tank in the forest terrain and the possibility of its damage required the structure of the protective frame (Fig. 7), which performs a protective function during transport, but also when manipulation the water tank outside the transport. In addition, in an emergency, it can serve as an improvised trailer for transporting other materials (fire hoses, pumps, etc.).

Fig. 7 The resulting design of an adapter for water transport

On the basis of the resulting amorphous model as a finite element mesh, we started the draft supporting frame of the fire-fighting body. The supporting frame will carry a fire-fighting body consisting of the composite water tank, the protective frame, the pump and the fire-fighting equipment. The resultant shape of the carrier frame is shown in Fig. 8. [18]

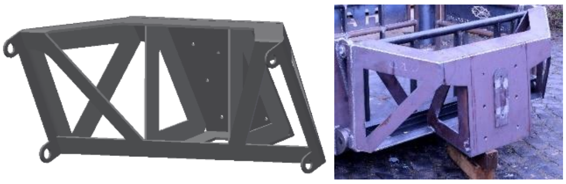

Fig. 8 Design of the supporting frame for the fire-fighting adapter

---

[1] LKT: Forest Wheeled Skidder,

[2] CAS: Pumping appliance.

Based on FEA analysis (Fig. 9), we simulated the load on the supporting frame from the full water tank while the load was at an acceptable level.

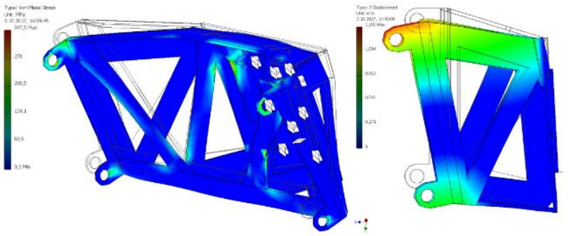

Fig. 9 FEA analysis – max Von Mess Stress 347 MPa, max z displacement 1,355 mm

Additional equipment of the portable water tank to the demands of accepted practice:

- water pump (suction head 8 m / total head 80 m / capacity -1 500 l.min^{-1} / suction and discharge port diameter 2“),
- 2" suction hose with strainer – length 0,25 m,
- hose "C" (fire hose with connector) 20 m and hose "D" (fire hose with connector) 20 m,
- dividing breeching 2xC+1xD,
- hand branchpipe ("C" Profi, "D" Profi),
- ball valve "C" with connector,
- the ax-hoe, the spade and the shovel.

This equipment is intended to ensure an autonomous capacity to refill the tank from the nearest natural water source, as well as to manage the intervention itself in a complicated terrain. The final version of the design is shown in Figure 10.

Fig. 10 The final version of the adapter design

4. Conclusions

In conclusion, we can say that at the present time the representation of LKT type machines is predominant in the Slovak forest but they do not have a similar fire-fighting body proposed in the present submission. Based on the above analysis, it would be appropriate to process the proposal, on the basis of which a fire-fighting body of the said structure would be incorporated into the fleet. The fire-fighting body would be quickly adaptable to the LKT base machine and would provide an effective fire-fighting tool, especially in difficult forest terrains.

Acknowledgments

This work was supported by the Slovak Research and Development Agency under the contract No. APVV-14-0468 „Development of an auxiliary device and its technological employment to increase the efficiency of extinguishing forest fires“.

References

[1] Sačkov, I. 2012. Analýza hustoty a parametrov lesnej cestnej siete v chránených územiach pre zabezpečenie ekologického obhospodarovania lesov. Záverečná správa predmetu zmluvy pre Lesy SR, š. p., Banská Bystrica. NLC – LVÚ Zvolen. September 2012. 14 s. <http://www.nlcsk.sk/download/epol/EPOL8b.pdf>.

[2] Zelená správa 2015. Správa o lesnom hospodárstve v Slovenskej republike za rok 2014. [online]. Dostupné na internete: <http://www.mpsr.sk/sk/index.php?navID=123&id=9795>..

[3] Protipožiarne. 2015. [online] Dostupné na internete: <http://www.protipoziarne.sk/c-752-CAS_30_TATRA_815_7_6x6.html>.

[4] Hnilicová, M., Hnilica, R. 2017. Využitie kompozitných materiálov za účelom zníženia hmotnosti nadstavieb pre bázové stroje. In *Kvalita, technológie, diagnostika v technických systémoch : zborník vedeckých prác*. - Nitra : Slovenská poľnohospodárska univerzita v Nitre, 2017. ISBN 978-80-552-1672-0, s. 69-74.

[5] Ehrnstein G. W. 2009. Polymerní kompozitní materiály. Praha, nakladatelství SCIENTIA v Prahe, 351s, 2009. ISBN 978-80-86960-29-6.

[6] Zavrtálek, J., Müller, M. Low-cyclic fatigue test of adhesive bond reinforced with biodegradable fabrics (2016)

Manufacturing Technology, 16 (5), pp. 1205-1211. ISSN 12132489.

[7] Kotek, L., Ťavodová, M., Jonák, M., Kalincová, D., Tůma, Z., Sujová, E. 2016. Using of high speed motion analysis for compression test of motorcycle forks arm. In *17th Mechatronika 2016 : proceedings of the 17th international conference on Mechatronics - Mechatronika (ME) 2016* - Praha : Czech Technical University in Prague, 2016. ISBN 978-80-01-05882-4, s. 291-294.

[8] Mizera, C., Hrabě, P., Muller, M., Herák, D. Creep behaviour of the polymer composite with false banana's fibres (Ensete Ventricosum) (2016) Manufacturing Technology, 16 (1), pp. 188-192. ISSN 12132489.

[9]] Poole, A.J., Church, J.S., Huson, M.G. Environmentally sustainable fibers from regenerated protein (2009) Biomacromolecules, 10 (1), pp. 1-8. DOI: 10.1021/bm8010648.

[10] Wambua, P., Ivens, J., Verpoest, I. Natural fibres: Can they replace glass in fibre reinforced plastics? (2003) Composites Science and Technology, 63 (9), pp. 1259-1264. DOI: 10.1016/S0266-3538(03)00096-4.

[11] Aziz, S.H., Ansell, M.P. The effect of alkalization and fibre alignment on the mechanical and thermal properties of kenaf and hemp bast fibre composites: Part 1 - polyester resin matrix (2004) Composites Science and Technology, 64 (9), pp. 1219-1230. DOI: 10.1016/j.compscitech.2003.10.00.

[12] Lee, B.-H., Kim, H.-J., Yu, W.-R. Fabrication of long and discontinuous natural fiber reinforced polypropylene biocomposites and their mechanical properties (2009) Fibers and Polymers, 10 (1), pp. 83-90. DOI: 10.1007/s12221-009-0083-z.

[13] Alves, C., Ferrão, P.M.C., Silva, A.J., Reis, L.G., Freitas, M., Rodrigues, L.B., Alves, D.E. Ecodesign of automotive components making use of natural jute fiber composites (2010) Journal of Cleaner Production, 18 (4), pp. 313-327. DOI: 10.1016/j.jclepro.2009.10.022.

[14] Keller, A. Compounding and mechanical properties of biodegradable hemp fibre composites (2003) Composites Science and Technology, 63 (9), pp. 1307-1316. DOI: 10.1016/S0266-3538(03)00102-7.

[15] Kalia, S., Thakur, K., Celli, A., Kiechel, M.A., Schauer, C.L. Surface modification of plant fibers using environment friendly methods for their application in polymer composites, textile industry and antimicrobial activities: A review (2013) Journal of Environmental Chemical Engineering, 1 (3), pp. 97-112. DOI: 10.1016/j.jece.2013.04.009.

[16] Hrabě, P., Herak, D., Mizera, Č. Utilization of the elementary mathematical model for description of mechanical behaviour of composites reinforced by ensete ventricosium fibres (2017) Agronomy Research, 15 (Special Issue 1), pp. 1006-1013. ISSN 1406894X.

[17] Chromek, I., Hnilica, R., Hnilicová, M., Messingerová, V. 2017. Funkčné nadstavby, jeden zo spôsobov zvýšenia efektívnosti dostupnej techniky pri hasení lesných požiarov. In *Požární ochrana 2017 : sborník přednášek XXVI. ročníku mezinárodní konference pod záštitou primátora města Ostravy ... a Českého národního výboru CTIF* - Ostrava : Sdružení požárního a bezpečnostního inženýrství, 2017. ISBN 978-80-7385-188-0. ISSN 1803-1803, s. 85-87.

[18] Hnilicová, M., Matej, J., Dado, M., Hnilica, R. 2017. Design of the supporting frame for the fire-fighting adapter using the shape generator. In *Proceedings of the 5th International scientific conference on advances in mechanical engineering (ISCAME 2017)* : University of Debrecen, 2017. ISBN 978-963-473-304-1, p. 198-202 [online]. Dostupné na internete: <http://old.eng.unideb.hu/gepesz/wp-content/uploads/2015/10/ISCAME_2017_Conference_Proceeding.pdf>.

---

[1] LKT: Forest Wheeled Skidder,

[2] CAS: Pumping appliance.

Earth in a Trap? 2018
Analytical Methods in Fire and Environmental Science

Reduction of fire risk indicators at oil and gas industry companies by use modified water-gel compositions for thermal protection of oil products tanks

Alexey Ivanov[a] – Farid Dali[a] – Valeria Mikhaylova[a] – Alexey Smirnov[a]

– Grigory Ivakhnyuk[a*]

[a]*University of State Fire Service of Emercom, Moskovskiy Avenue,149, Saint-Petersburg, 196105, Russia*

Abstract

There are represented the researching physical properties of modified hydrogel, prepared by polymers of acrylic acid marked «Carbopol ETD 2020», in conditions of thermal and electrophysical modification by the variable frequency modulated potential (VFMP). Data on changes of hydrogels density was came into the procession of gelling agent concentration, thermal and electrophysical modification by VFMP. Determined, that comparative time of modified hydrogels heating increases with increasing gel agent concentration in conditions of VFMP, also the comparative time of heating increases with thermal influence for modified hydrogels near the critical temperature value 4 °C. Concluded, that modified hydrogels may be used to improve the efficiency of the thermal protection of oil products tanks.

Keywords: hydrogel; electrophysical and thermal modification; thermal protection; variable frequency modulated potential; oil products fires;

---

[*] Corresponding author. Tel.: +7-921-889-9015; e-mail: hasfarid@inbox.ru.

1. Introduction

When eliminating fires of oil products in tank farms accompanied by significant heat release due to flaring combustion of steam-air mixture, it is necessary to cool and provide thermal protection of technological reinforcement of tanks adjacent to the burning [1].

Extinguishing of such fires is complicated by the fact that boiling and release of oil products is possible due to long heating of the tank walls [2]. For the purpose of thermal protection of the burning and adjacent tanks use standard fire-technical equipment (mainly manual and fire monitors trunks) [3].

Water is most often used as a cooling agent in case of fires in warehouses of oil products. Water is the most affordable fire extinguishing and cooling agent, with good thermophysical characteristics. However, low viscosity and low adhesion properties do not allow efficient use of water for thermal protection of metal structures of tanks.

Hydrogels have better adhesion to wood, metals, polymers and other materials than water, low corrosion activity and good performance [2]. In this regard, the development of technologies for obtaining effective water-gel compositions with improved technical and economic indicators is relevant.

2. Statement of research problem

In conditions of flaring combustion, the maximum average surface density of the flame torch radiation of the burning tank q_f can be determined by the formula [4]:

$$Q_1 = (335 + 7112/d_p) \cdot m_b \cdot 10^3$$

where d_p is the diameter of the burning tank; m_b is the mass rate of liquid burnout.

Modeling of the tank heating process with oil products in case of fire in the adjacent tank is described in [5]. Assuming that the roof and walls of the tank are heated evenly, the bulk of the heat is transferred from the burning tank to the neighboring one by radiation, the amount of heat energy Q_1 for heating the metal wall and the roof of the tank by temperature T_r is described by the ratio:

$$dQ_1 = S_k \cdot \delta_\mathrm{c} \cdot \rho_c \cdot c_c \cdot dT_k$$

where S_k, δ_c, ρ_c, c_c – the area, thickness, density and heat capacity of the steel material of the tank, respectively.

In the conditions of application of thermal insulating substances on the outer surface of the tank, the amount of heat Q_2 consumed by the heating layer of the protective substance at a temperature T_h can be determined by the ratio:

$$dQ_2 = S_h \cdot \delta_h \cdot \rho_h \cdot c_h \cdot dT_h$$

where S_h, δ_h, ρ_h, c_h is the area, thickness, density and heat capacity of the insulating substance, respectively.

Thus, the method of increasing the efficiency of protection against heating of vapor-gas mixture and liquid inside the tank in the conditions of external heat exposure, can be a change in the values of thermal capacity of hydrogels. The solution of this problem is possible with the modification of hydrogels with the help of temperature and electrophysical effects on water and gel-forming component included in its composition.

In the case of electrophysical influence on water systems, insignificant in its energy parameters influence can lead to changes, which increase the effect of influence by many times [6].

One way electrophysical impacts on the water system is frequency modulated potential (VFMP) [7]. In [8] the increase of oxidative-reducing potential of distilled water samples is noted, as well as the increase of pH of water-salt solutions in the conditions of electrophysical influence.

Application of extinguishing agents (AEA), modified with impact VFMP, in terms of the already developed diagrams of extinguishing fires is considered in [9]. It is established that the modified AEA can be applied in standard diagrams of fire extinguishing, do not demand change of a design of the standard equipment.

It is known that some anomalies are characteristic for water, in particular, the heat capacity of water decreases with temperature rise up to 40 °C, the viscosity of water decreases at a temperature from 0 to 25 °C. this allows using these properties for modification of water systems.

To assess the possibility of using modified water-gel compositions in thermal protection installations, the results of studies of molecular structure, heating dynamics under convection conditions for water-gel compositions modified under electrophysical and thermal action are presented.

3. Research materials.

Distilled water and hydrogels based on it were used as materials for the research. A lightly crosslinked acrylic polymer (LCAP) of the brand "Carbopol ETD-2020"was used as a gel-forming component.

In this research, the technology of water treatment included the impact VFMP with parameters 220 V, 50 Hz for 30 min. for 4 °C and 20 °C. Further, in the container of water was added to the sample LCAP in a concentration of from 0.1 to 1.0 wt. %. During the period of gelation (12 hours) continued impact VFMP. Stabilization of the hydrogels was carried out by introducing into a dispersion of 20% aqueous ammonia solution at a concentration of 0.1 – 1.0 wt.%.

4. The density of the modified hydrogels

Measurement of density of the hydrogels was carried out by measuring the mass of a substance using an analytical balance brand of "VIBRA LN3202CE" in a fixed volume of fluid. Data on the density of hydrogels depending on the concentration of LCAP are given in Table 1. A decrease in the density of hydrogels with an increase in the concentration of the gel-forming component was noted. When exposed VFMP a decrease in the density of the hydrogel.

Hydrogels obtained on the basis of water at 4 °C, as a rule, have a higher density than samples obtained at 20 °C. This effect can be explained by reducing the density of water with an increase in temperature [10] and fixing the structure of water with LCAP. The impact VFMP also contributes to a slight (0.2 – 0.3 percent) decrease in density of the hydrogels, due to additional electrostatic forces in the cross-linked polymer chains LCAP [11].

The heating time of the modified hydrogels to the maximum temperature increases with the increase in the concentration of the gel-forming component. The time of heating the hydrogel at a concentration of LCAP from 0.1 to 0.2 wt. % less time heating the distilled water by 30 – 50 %, while at higher concentrations of the modified hydrogels are heated much more slowly, with better results for gels with a concentration of LCAP 0.25 to 1.0 wt. %. For all samples of hydrogels, structured on the basis of water at a temperature of 4 °C, there is a significant (up to 60 %) increase in the heating time of the liquid [12].

Investigation of the mechanism of heating and boiling of modified hydrogels under thermal action

Researches of the mechanism of heating and boiling of hydrogels and determination of dependence of thermal conductivity on a method of modification of hydrogels and concentration of LCAP were carried out at chair of Safety of technological processes and productions of Saint Petersburg University of State Fire Service of Emercom of Russia [12].

Figure 1 presents data on the maximum temperature of modified hydrogels and distilled water, as well as the heating time to boiling point. From the above data, it can be concluded that the maximum heating temperature of hydrogels in the

Fig. 1. Maximum temperature and time to reach the temperature of hydrogels, °C.

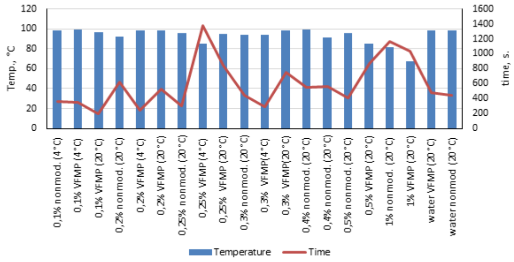

conditions of electrophysical and temperature modification is reduced.

Table 1

Physical parameters of the modified (VFMP) and unmodified (nonmod) hydrogels

Parameters Sample name	Density, kg/m^3	pH	Heat capacity, KJ/kg·C
0,25% VFMP (20 °C)	1048	5,97	16,88
0,3% nonmod (20 °C)	1045	8,46	8,17
0,3% VFMP (4 °C)	1042	7,06	5,6
0,3% VFMP (20 °C)	1041	7,06	13,57
0,4% nonmod (20 °C)	1040	5,76	10,08
0,4% VFMP (20 °C)	1038	5,97	11,77
0,5% nonmod (20 °C)	1033	5,73	7,61
0,5% VFMP (20 °C)	1029	5,06	19,44
1,0% nonmod (20 °C)	1016	6,18	27,64
1,0 % VFMP (20 °C)	1010	4,96	33,47
water nonmod (20 °C)	1000	-	4,3
water VFMP (20 °C)	998	-	4,55

Figure 2 presents the comparative dynamics of the heating of the hydrogels (with a concentration of 0,25 LCAP masses. %) modified and unmodified. From the obtained data, it can be concluded that the temperature increase of hydrogels modified under the conditions of VFMP exposure is slower, which allows using them as a thermal insulation material to block the transfer of energy from the heat source to the protected material [13-14].

Fig. 2. Kinetics of heating of modified and unmodified hydrogels at the concentration of LCAP from 0.25 mass%.

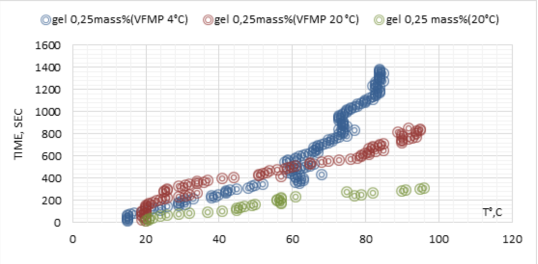

5. Conclusions

1. Key electrical and thermal modification are the terms of use VFMP, structural building of water at a temperature corresponding to the gelation process.
2. Application of electrophysical and temperature modification allows to change thermophysical characteristics of hydrogels that can be used for increase of efficiency of installations of thermal protection, both for increase of speed of removal of heat from a heating surface, and for providing thermal isolation of object of protection in the conditions of the hydrocarbon fire.

References

[1] Manual extinguishing oil and petroleum products in tank farms. VNIIPO. (1999) 86.

[2] A. Savchenko, Theoretical basis gelling cooling systems tank walls and tanks hydrocarbons against heat fire, Problems of fire safety, RU, 1991.

[3] A.F. Sharovarnikov, Kalan Publ., Moscow, 2002, 448.

[4] V. P. Suchkov, Fire risk assessment methods for technological processes, Academiy of GPS MChS Rossii Publ., Moscow , 2010. 155

[5] U. A .Abramov, Fire risk assessment of petroleum tank heated by near-burning tank. Radioelectronics and Informatics, 2005, no. 2, pp. 110 – 112

[6] V. I. Klassen, The impact of magnetic field on water systems, Moscow, Chem Publ., 1982, vol. 2, 296.

[7] G. K. Ivakhnjuk. Method and apparatus for controlling physical-chemical processes in a substance and on a phase boundary. Patent RF, no. 2479005, 2013

[8] A. V. Ivanov, Investigation of physical and chemical properties of modified water solutions to control the process of detoxification of soils in emergency on the oil and gas facilities. Problems of technosphere risk management, 2015, no. 1, 29 – 26.

[9] A. V. Ivanov, Research extinguishing and thermal insulation properties of hydrogels prepared from modified nanofluids. Vestnik St. Petersburg University of the State Fire Service of EMERCOM of Russia, 2014, no. 2, pp. 31 – 37. Available at: http://vestnik.igps.ru/wp-content/uploads/V62/4.pdf (Accessed 28 December 2017).

[10] N. P. Gorlenko, U. S. Sarkisov, Low-energy activation of dispersed systems]. Tomsk, TGSU Publ., 2011. 264 p.

[11] F. K. Oppong, R. Laurent, J. F. Barbara, E. B. Arthur, J. R. de Bruyn. Microrheology and structure of a yield-stress polymer gel. Physical Review E. 2006, vol. 73, no. 4, pp. 041405. doi: 10.1103/PhysRevE.73.041405.

[12] A. V. Ivanov, Investigation of the characteristics of modified hydrogels for thermal protection of petroleum products tanks. Fire and explosion safety, 2017, vol.26, no. 1, pp.58-68. doi: 10.18322/PVB.2017.26.04.58-67

[13] V. I. Mikhailova, The modified parameters effects for thermal protection properties of hydrogel in Jet fire conditions. Vestnik St. Petersburg University of the State Fire Service of EMERCOM of Russia, 2017, no. 3, pp. 79 – 87. Available at: http://vestnik.igps.ru/wp-content/uploads/V93/11.pdf (Accessed 28 December 2017).

[14] F.Abdulaliev , Proc. 1th Fire Protection, Safety and Security 2017. Conf., Scientific, Electrophysical mwthod of improving the fire-extinguishing and heat-shielding characteristics of water-based materials, 03-05 May., 2017; Zvolen, Slovakia, (2017) 86-92.

Environmentally Sustainable Access: Research Developments with a Focus on Softwood Bark Waste/By-products

Michal Jablonsky[a*] – Ales Haz[a] – Jozef Jablonsky[b] – Nikola Chupacova[a]

[a]*Department of Wood, Pulp, and Paper, Institute of Natural and Synthetic Polymers, Slovak University of Technology, Radlinského 9, 81237 Bratislava, Slovak Republic*

[b]*Central Military Hospital SNP Ruzomberok - Teaching Hospital, Gen. Miloša Vesela 21, 03426 Ružomberok, Slovak Republic*

Abstract

In recent times, focus on waste bark research has increased all over the world and a large number of evidence has collected to show immense potential of bark waste used in various pharmacological, food or protection systems. Over the last few years, researchers have aimed at identifying metabolic plant-derived substances which can be used as drugs or as leads for drug discovery. Phytochemical compounds, particularly polyphenols, are the most active compounds that are naturally present in softwood barks and show a unique combination of chemical, biological, and physiological, antioxidant, antibacterial, anti-inflammation, and cytotoxic activities.

Keywords: bark; softwood; waste; by-product

---

[*] Corresponding author. Tel.: +421 2 59 325 218; e-mail: michal.jablonsky@stuba.sk.

1. Introduction

Waste is defined as *any substance or object that the holder discards or intends/is required to discard* [1]. In a broad sense, *biowaste is the waste derived from living organisms or of organic origin (such as sewage, agricultural or forestry waste, manure, sawdust, or food scraps), which is composed chiefly of organic matter*.

The total annual arising of biowaste in the EU is estimated at 76.5-102 million tonnes of food and garden waste included in mixed municipal solid waste and up to 37 million tonnes from the food and drink industry [2]. In legal language, valorisation is defined as the process of creating value from knowledge by making it suitable and/or available for economic and/or societal use and translating it into competitive products, services, processes and entrepreneurial activity [3]. In the field of biomass and biowaste processing, valorisation can be broadly defined as the concept that covers such areas as cutting-edge research and experiences on the conversion of waste and biomass to energy, fuels and other useful materials, with particular focus on environmental indicators and sustainability goals [4].

Translated into more easily understandable and simpler words, *valorisation of biomass and biowaste means creation of surplus value and/or increase in value of biomass and biowaste through their partial purposeful decomposition to obtain value-added materials, substances or compounds with required properties enabling their real or potential utilization*.

The amount of lumbered roundwood worldwide is estimated at 3,591,142,000 m^3, while the estimated amount of bark resulting from wood processing is 10% from the wood mass [5]. Valorisation is a key component of an economic and environmental lignocellulosic biorefinery [6,7]. Lots of works during the last decades have focused on the extraction of bioactive compounds from different types of biomass or bio-waste, especially nutraceuticals as polyphenolic bioactive substances. Phytomass, such as bark and needles, plays a vital role in the prevention and cure of various diseases.

2. The use of the bark

With increasing industrialization, industrial by-products (wastes) are continuously accumulated, raising environmental and economic concerns related to their disposal and usability. The primary utilization of bark waste lies in its direct use. The simplest and least economical way is to combust it in order to obtain energy or to use it for surface mulching. However, particles of softwood bark have been also used as an insulation filling material for the thermal insulation of a timber frame wall [8]. In addition, they can be used for the production of particle- and fibreboard or plywood. Bark may also have utility as a source of adhesives and other chemicals (e.g., tannins, dyes, and waxes), or for environmental protection applications (e.g., absorption of spilled oil, industrial wastes, and sewage effluents). Bark is a source of compounds soluble in different non-polar and polar solvents, such as fats, saturated and unsaturated fatty acids, resins, resin acids, waxes, phenolic and polyphenolic compounds, stilbenes, flavonoids, terpenoids, alkaloids and ligands. Bioactive substances show antioxidant, antimycotic, cytotoxic, antiviral, antitumor, antimalarial, insecticidal, antimutagenic, tumorigenic, pharmacokinetic activities and other properties. The recovery of extractive compounds present in bark is affected by temperature, time and pressure of the extraction agent used (in terms of the nature of the characteristics - polar, non-polar), as well as by the choice of the solvent, the particle size and the content of water. The choice of a suitable method for obtaining chemicals from waste biomass depends on the objectives pursued [9]. One of the objectives is to obtain the largest possible content of compounds from waste, as well as to acquire biologically active substances. The assesment of biological activity represents a key tool for determining the choice of acceptable methods. In a recently published work, 237 bioactive compounds were identified in the bark of softwood. These compounds, especially polyphenols, present different biological actions and have been characterized with regard to their properties using the data available in the literature and by computation of ADME (Absorption, Distribution, Metabolism, and Excretion) [10]. It has been established that the amount and nature of the extracted substances is highly dependent on the isolation method adopted. While today most of the hundreds of millions tons of bark collected per year are incinerated, landfilled or used for thermal energy production, without being valorised, softwood and hardwood bark has been reported to comprise a wide variety of antioxidants, of which phenolic antioxidants are of particular interest from the point of view of fine chemicals products. Typical phenolic antioxidants comprise flavonoids, phenolic acids, stilbenes, tannins, lignans and lignin. Extraction is a fundamental process for separation and recovery of bioactive compounds from plants. Commonly used extraction methods include microwave assisted extraction (MAE), supercritical fluid extraction (SFE), pressurized liquid extraction (PLE), ultrasound assisted extraction (UAE), pulsed electric field assisted extraction (PEF) and enzyme assisted extraction (EAE). These techniques are known for their short extraction time, reduced volume of organic and hazardous solvents, ease to use, as well as the fact that they allow achieving a higher extraction yield with lower energy consumption [11]. A promising technology is the use of deep eutectic solvents as extractants [12]. The development of modern, environmentally friendly technologies and products utilizing wood waste as a source of extractive substances to develop value-added products has a high commercial potential. Nowadays, the utilization of extractives obtained from different types of biomass is widespread. The reason mainly lies in their broad spectrum of application in the food industry due to their antimicrobial, antibacterial, anti-inflammatory, antifungal, insecticidal or antioxidant effects. These extractive compounds may be also of great importance in the fields of nutrition, healthcare and medicine, where they may find application.

3. Conclusion

An environmentally appropriate approach to the use of bark should be to extract its bioactive substances, and thus turn the bark into value-added products. The extractive compounds of bark have high potential to be used in the production of special pharmaceutical preparations or of fine chemicals. Meanwhile, large bark particles may be used for production of particle- and fibreboard plywood, or filling materials.

Acknowledgments

This work was supported by the Slovak Research and Development Agency under the contracts No. APVV-15-0052, APVV-0393-14 and APVV-16-0088.

References

[1] Directive 2008/98/EC of the European Parliament and of the Council of 19 November 2008 on waste and repealing certain Directives, OJ L 312, 2008.

[2] FAOSTAT, http://www.fao.org/faostat/en/, 2017

[3] de Jong, S.P.L. Engaging Scientists – organising valorisation in the Netherlands, PhD Thesis, Rathenau Instituut, Den Haag, Netherlands, 2015.

[4] Nizhou, A. Waste Biomass Valor. 1 (2010) 2.

[5] Pásztory, Z., Mohácsiné, I. R., Gorbacheva, G., Börcsök, Z. BioResources 11 (2016)7888.

[6] Surina, I., Jablonsky, M., Haz, A., Sladkova, A., Briskarova, A., Kacik, F., Sima, J. BioResources 10 (2015) 1423.

[7] Jablonsky, M., Skulcova, A., Kamenska, L., Vrska, M., Sima, J. BioResources 10 (2015) 8047.

[8] Kreps, F., Burčová, Z., Jablonsky, M., Ház, A., Frecer, V., Kyselka, J., Schimdt, S., Surina, I., Filip, V. ACS Sustainable Chemistry & Engineering 5(2017) 8170.

[9] Kain, G., Barbu, M. C., Hinterreiter, S., Richter, K., Petutschnigg, A. BioResources 8 (2013) 3731.

[10] Jablonsky, M., Nosalova, J., Sladkova, A., Haz, A., Kreps, F., Valka, J., Miertus, S., Frecer, V.,Ondrejovic, M, Sima, J., Surina, I. Biotechnology advances 35 (2017) 750.

[11] Belwal, T., Ezzat, S. M., Rastrelli, L., Bhatt, I. D., Daglia, M., Baldi, A., Devkota, H.P., Orhan, I.E., Patra, J.K., Das, G., Anandharamakrishnan, C., Gomez-Gomez, L., Nabavi, S.F., Nabavi, S.M., Atanasov A.G. A TrAC Trends in Analytical Chemistry. 100 (2018) 102.

[12] Skulcova, A., Hascicova, Z., Hrdlicka, L., Sima, J., Jablonsky, M. Cellulose chemistry and technology (2018) accepted.

Effect of aging on reaction-to-fire of fibreboards

Juraj Jancík[a][*] – Linda Makovická Osvaldová[a]

[a]*University of Žilina, Faculty of Security Engineering, ul. 1.mája 32, 010 26 Žilina, Slovakia*

Abstract

This paper theoretically describes the observation process of changes in reaction-to-fire of fibreboards as insulation materials exposed under natural conditions of buildings. Samples are modified with flame retardant *"Ohňostop",* that have proved to enhance their reaction-to-fire. Research focuses on monitoring the ability to preserve this attribute in time.

Keywords: Fiberboards; Aging; Insulation; Reaction-to-fire; Flame-retarding

---

[*] Corresponding author. e-mail: juraj.jancik@fbi.uniza.sk

1. Introduction

Fibreboards as insulation materials are being widely used in various constructions all over the world. We might expect increased use of natural-based insulation materials assumed by the latest eco-friendly trends in general. Fibreboards have proved as insulation materials in time but questions about their fire resistance properties and behaviour in fire occur. Their classification of reaction-to-fire is set in class E, which shows the need to modify them in order to improve fire resistance properties.

After a successful experiment that improved their classification of reaction-to-fire to D class by using a water-based flame retardant *"Ohňostop"*, this research is focused on the aging process and ability to preserve fire resistance properties in time, using this flame retardant. During this experiment, samples will be exposed to natural conditions of building.

Observing of the preservation ability of samples will be assessed by the mass loss rate of the samples tested in different time lapse. All the methodology and specifications of the experiment and used materials are closely described in following chapters.

2. Basic fibreboard specification and flame retardant application

Fibreboard is a large-scale material made of wood fibres, using mostly spruce tree as a source (applies for central Europe). We recognize these three basic types of fibreboards according to their density [1]:

- Insulation fibreboards - 250 to 400 kg.m^{-3}
- Medium density fibreboards - 480 to 850 kg.m^{-3}
- Hardboard – over 850 kg.m^{-3}

Samples of the lowest density level, out of the mentioned types, will be used for the experiment. Their dimensions will be 90x80x60 stated in millimetres.

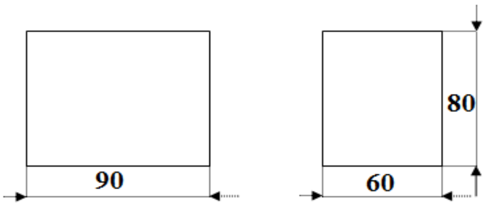

Fig.1 Dimensions of the samples

There are two basic processes of production of fibreboards. In this case samples were made with so called wet process, which is more energetically demanding than the dry one. Wood fibres are soaked in the water with binding additives like glue and hydrophobic additives like paraffin. Boards are pressed under low pressure which causes that their strength is lower than other types of fibreboards. This means that they can not be used as independent construction materials, however they outmatch other types of fibreboards in features such as thermal or acoustic insulation [2].

Some of the basic properties of insulation fibreboards are shown in Table 1. Vapour resistance factor is stated without unit because It is a measure of the material's relative reluctance to let water vapour pass through, and is measured in comparison to the properties of air.

Table 1
Density, thermal conductivity, specific heat capacity and vapour resistance factor of insulation fibreboards [3]

ρ	**250 - 400 kg.m^{-3}**
λ	0,038 – 0,050 W.m^{-1}.K^{-1}
c	1630 - 2510 J.kg^{-1}.K^{-1}
μ	5 - 10

3. Methodology of natural aging simulation and flame retardant application

Experiment includes 50 samples of insulation fibreboards in total. These are evenly divided into 5 groups, each by 10 samples according to their time of exposure to natural conditions. Groups are marked with letters A-E, where E group is exposed for the longest time period. Samples included in group A will be tested right after the drying process of flame retardant application and every next group will be tested after a 6 month period.

Placement of the simulation is set in the countryside area of north-west Slovakia. Samples will be placed outdoors on a spot protected from direct sunlight, rain and snow. The spot is located in the environment of real house to achieve genuine conditions. Samples will be separated by gaps to avoid contact with each other so conditions are equal for all samples regardless the position. Weight of the samples will be measured on a weekly basis in order to monitor its changes in time of exposure.

For the enhancement of fire resistance properties a flame retardant "Ohňostop" will be used. It´s a water-based flame retardant containing inorganic salts. Three ways of applications including spraying, coating and soaking have been examined. Out of these, soaking turned out to be the most effective way of application, therefore it´s been chosen for this experiment as well. [3].

Samples will be soaked 15mm deep into the flame retardant and left to absorb it for 15 minutes. Leaving the samples for longer could help to absorb more of the retardant, however there´s a risk of damaging the sample structure. Every sample will be loaded with a sinker to prevent it from floating and improve the absorption process. Samples will be weighed before and immediately after application to find out how much of flame retardant has been absorbed. After the soaking samples will be left to dry out for two weeks and placed on the exposure placement afterwards, where it will undergo influence of natural conditions for estimated time. Samples will be weighed again after the drying process.

4. Data collection and calculations

The main data collected will be the mass loss rate values. During the experiment each sample will be exposed to flame with direct contact for 2 minutes after which the source of flame will be removed. Weight of the sample will be recorded in 15 second intervals during the time of exposure and for subsequent 8 minutes after the flame source removal. These data have following characteristics:

- Primary
- Real
- Periodical
- Complete
- Experimentally gathered

All the collected data will be stored in tables in Microsoft Excel for further analysis and calculations.

4.1. Mass loss rate and burning rate calculatio0ns

Mass loss rate will be the decisive factor in this experiment. By gathering its values for each sample separately and comparing the results between groups of different time lapses, we will be able to identify whether aging has significant impact on the fire resistance properties of fibreboards. Burning rate is an important factor as well in this case as it expresses velocity of the combustion process in examined samples. Following formulae will be used for these calculations:

$$\delta_{mr}(\tau) = \frac{m(\tau)-m(\tau+\Delta\tau)}{m(\tau)} \cdot 100$$

(τ) – mass loss rate in time (τ) [%],
(τ) – weight of sample in time (τ) [g],
$m(\tau + \Delta\tau)$ – weight of sample in time $(\tau + \Delta\tau)$ [g].

$$v_r = \frac{\delta_m}{\Delta\tau}$$

v_r – burning rate [%/s],
δ_m – mass loss rate in time (τ) [%],
$\Delta\tau$ – time interval of weight recording [s]

4.2 ANOVA

Analysis of Variance is a statistical technique that assesses potential differences in a scale-level dependent variable by a nominal-level variable having 2 or more categories. [4] A single factor ANOVA will be used it this research to verify hypothesis whether different times of exposure cause changes in mass loss rate. For evaluation of ANOVA a Microsoft Excel tool will be used. As this is a draft, random fictional values were used to create and example of ANOVA outcome showed in the following figure.

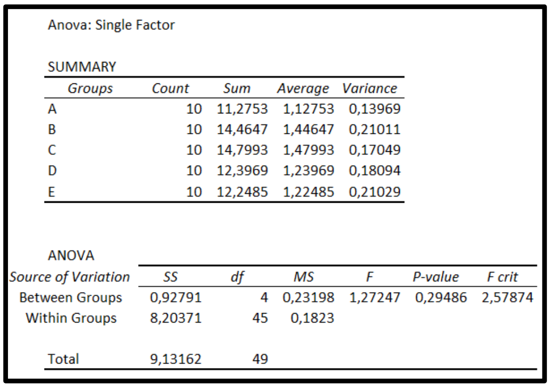

Anova: Single Factor

SUMMARY

Groups	Count	Sum	Average	Variance
A	10	11,2753	1,12753	0,13969
B	10	14,4647	1,44647	0,21011
C	10	14,7993	1,47993	0,17049
D	10	12,3969	1,23969	0,18094
E	10	12,2485	1,22485	0,21029

ANOVA

Source of Variation	SS	df	MS	F	P-value	F crit
Between Groups	0,92791	4	0,23198	1,27247	0,29486	2,57874
Within Groups	8,20371	45	0,1823			
Total	9,13162	49				

Fig. 2 Analysis of Variance of mass loss rate

From the results we can see the the P-value score is high, which means, that differences between values are rather stochastic than dependant, what was naturally expected as input values for this example were chosen randomly.

4.3. Correlation between mass loss rate and time exposure

Correlation between these factors will be evaluated through Microsoft Excel as well. The value of correlation will be assessed by the correlation coeficient R and a trendline which will show the predicted ongoing trend. Name of groups are transefered into numbers according to amount of months between the flame retardant application and testing to make the comparing factors both quantitative.

As we can see the correlation is inconsiderable and the trendline shows that mass loss rate remains approximately constant over time, which would mean that aging does not effect it.

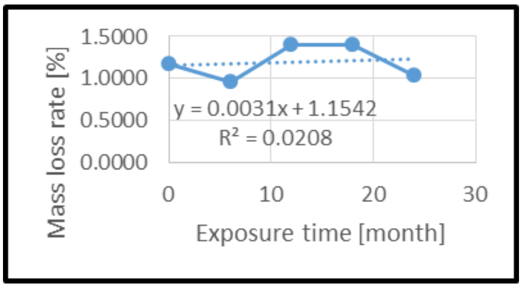

Fig. 3 Chart of correlation between mass loss rate and exposure time

However input values were fictional like in the previous calculation, because no real values have been gathered so far. The chart is just an example and should not be considered relevant for any further use except for illustration of evaluating.

Acknowledgements

This work was supported by the Slovak Grand agency VEGA. (Project 1/022/16|6| Fire safe insulation systems based on natural materials

References

[1] SVOBODA A KOL., 2013. Stavební hmoty. Praha: Jaga Group s.r.o, 2013. ISBN 978-80-260-4972-2.

[2] BÖHM, M., REISNER, J. 2010. Dřevovláknité desky (DVD). [online], [cit. 11.1.2016]. Available at: http://www.lesprace.cz/casopis-lesnicka-prace-archiv/rocnik-89-2010/lesnicka-prace-c-6-10/drevovlaknite-desky-dvd

[3] MARIENKA, A. 2016. Reakcia na oheň vybraných zatepľovacích materiálov na prírodnej báze – drevovláknitá doska. Žilina: University of Žilina, 2016. EN:28900220162023.

[4] The ANOVA Table [online]. The Pennsylvania State University : 2016. [cit. 2017-06-23]. Available at: https://onlinecourses.science.psu.edu/stat414/node/218.

Tropical wood facing material under fire conditions

Patrícia Kadlicová[a]* – Linda Makovická Osvaldová[a]

[a]*University of Žilina, Fakulty of Security Engineering, Department of Fire Engineering, Ul. 1. mája 32, 010 26 Žilina, Slovakia*

Abstract

This article describes the flammability of selected tropical wood. Data required for analysis are outputs of laboratory tested small wood samples. Experimental equipment was non-standardized laboratory equipment using a flame source of higher intensity (flame burner - propane-butane) affecting the test sample in an open environment. The above-mentioned laboratory outputs are presented by numerous clear graphs. Statistical analysis of dependence of important parameters and use of an appropriate analytical method reveals important parameters in assessing the flammability of the test sample.

Keywords: tropical wood; relative burning rate; flammability; analyze of dependence

---

* Corresponding author. Tel.: +421 513 6670; e-mail: patricia.kadlicova@fbi.uniza.sk.

Introduction

The use of tropical woods as cladding of building structures in interiors and exteriors is rapidly rising. The demand for foreign wood materials is mainly related to their more colorful design, which is significantly different from domestic.

Trees growing in the tropical climate zone have a different structure. These changes in the structure create better physical and mechanical properties [1]. From a fire security point of view, it is necessary to mention their high content of lignin, because alleviates the total flammability [2].

In this paper, we evaluate the flammability of the selected tropical wood. Results are based on data measured by laboratory tests of small test samples.

1. Laboratory testing

Samples used in laboratory tests were made of tropical wood called Merbau. This timber grows in the southeast Asia and is characterized by exceptional stability and hardness. When it swells and dries, only very small changes occur. It is a wood that has mostly straight fibers and gently shines [3].

Ten samples were made from the wood species described. Each sample had a size of 100x150x20 mm. The construction of a laboratory equipment consisted of scales, the sample holder, the holder of the Bunsen burner and the gas bomb (propane-butane) is on Fig. 1

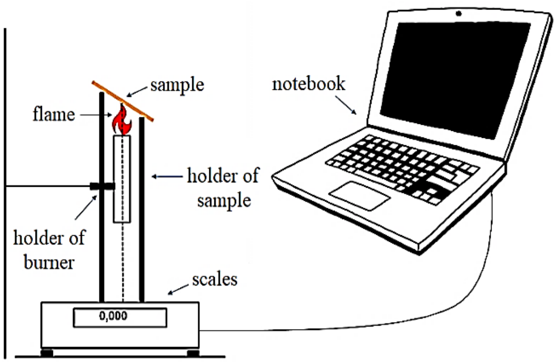

Fig. 2. Scheme of the laboratory equipment

Each sample was tested in the same manner, which lasted 10 minutes. During this time, sample changes were observed and every 15 seconds the weight loss was caused by continuous burning of the flame sample from the burner.

2. Processing results

The weight loss recorded during the test was adjusted to a relative burning rate v_r based on the relative weight loss δ_{mr}, using appropriate relationships. The resulting average values are presented in the figure 2.

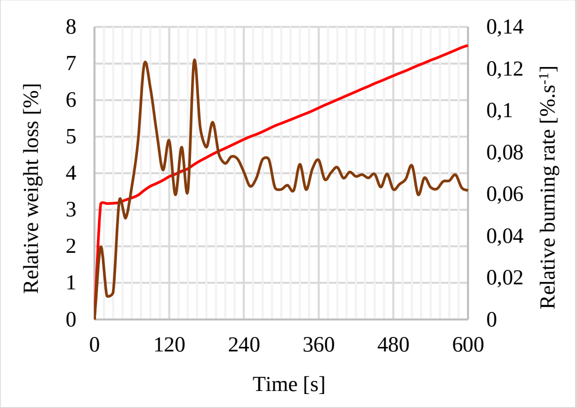

Fig. 1. Average values v_r and δ_{mr}

In the graph, we can be seen that on average the relative weight loss reached about 5,34 %, which does not represent a significant amount of the burned part of the material.

The samples burned with an average speed of 0,07 $\%.s^{-1}$. For each sample, we notice a significant increase in the rate of flame at the beginning of the 60th second, which either decreased and re-appeared around in the 150. second, or burning continued so that the values oscillated about the aforementioned average speed.

3. Spearman correlation

For ordinal variables, analysis of dependence based on comparison between units in a set, was performed. We have selected Spearman's rho (Spearman correlation) from several procedures, i. e., a correlation coefficient that is based on a sequence of variables and can be also applied to data that are not normally distributed. The coefficient will rise in the case of an indirect dependence from -1 to 0 and in the case of a direct dependence from 0 to 1. The very first step of the dependency determination process was to define hypotheses. In our case, for the zero H0 and the alternative H1 hypothesis, the following was true:

- H0 – The variation in weight loss of the Merbau sample depends only on its relative burning rate.
- H1 – The variation in weight loss of the Merbau sample does not depend only on its relative burning rate.

Next step was to determine the normality of samples. The Kolmogorov Smirnov test was used to verify it. Results interprets the Table 1 [4].

Table 1

Verifying the normality of the distribution of values

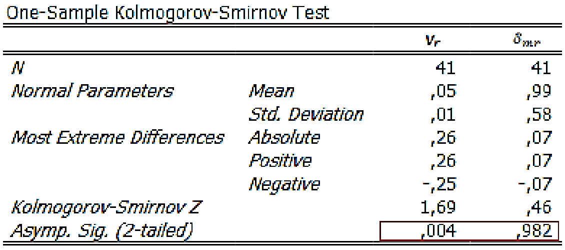

One-Sample Kolmogorov-Smirnov Test

		v_r	δ_{mr}
N		41	41
Normal Parameters	*Mean*	,05	,99
	Std. Deviation	,01	,58
Most Extreme Differences	*Absolute*	,26	,07
	Positive	,26	,07
	Negative	-,25	-,07
Kolmogorov-Smirnov Z		1,69	,46
Asymp. Sig. (2-tailed)		,004	,982

In this table, the level of significance which can be found in the last row is very important. This argument is true only for burning rate, not for relative weight loss. Based on the results of the test, we have found that data are not normally distributed, although the rule only belongs to one of the parameters and therefore, we have used Kenallovo tau (Table 2) [4].

Table 2

The resulting values of Kenall´s tau

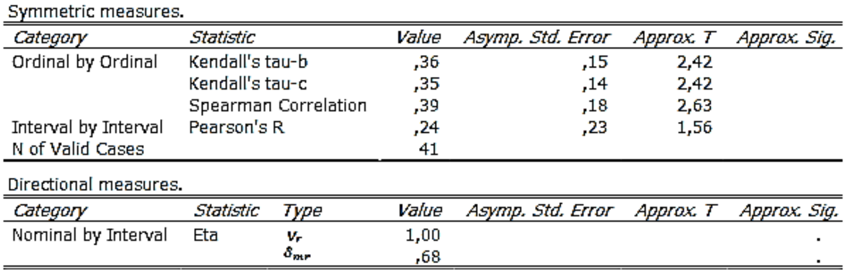

Symmetric measures.

Category	*Statistic*	*Value*	*Asymp. Std. Error*	*Approx. T*	*Approx. Sig.*
Ordinal by Ordinal	Kendall's tau-b	,36	,15	2,42	
	Kendall's tau-c	,35	,14	2,42	
	Spearman Correlation	,39	,18	2,63	
Interval by Interval	Pearson's R	,24	,23	1,56	
N of Valid Cases		41			

Directional measures.

Category	*Statistic*	*Type*	*Value*	*Asymp. Std. Error*	*Approx. T*	*Approx. Sig.*
Nominal by Interval	Eta	v_r	1,00			.
		δ_{mr}	,68			.

The result consists of two tables. In the first one Kenall's test shows outputs of different statistical method, the values of which differ from each other. These differences are because each method uses a different calculation equation. Therefore, the lowest value rule is used for the final evaluation. Since the values are not high because they are closer to 0 than 1, the relationship of the parameters exists, but is not very strong [4]. However, if we consider the dependence of the weight loss on the rate of degradation in general, then the value of the coefficient Eta = 0,68 in the second table shows a relatively strong relationship. Squaring the value to the second power and after conversion to the percent we can state, that 46,24 % of variability from δ_{mr} depends on v_r.

In the H1 hypothesis, we have argued that the variation in weight loss of the Merbau sample does not depend only on its relative burning rate, which has been confirmed, and therefore the H1 hypothesis is accepted and the H0 hypothesis is rejected.

Conclusion

Laboratory tests results indicate low flammability of tropical wood Merbau when its exposed to an open flame for ten minutes. This statement is based on the recalculated weight loss δ_m and its subsequent relative burning rate v_r.

Since measured and recalculated values were so-called ordinal variables, the dependence analysis was performed. The result of this analysis was an approval of the hypothesis H1. It has been argued that the variation in weight loss of the Merbau sample does not depend only on its relative burning rate, since it depends only on 46,24 % of variability.

Acknowledgments

„This work was supported by the Slovak Grand agency VEGA. (Project 1/022/16|6| Fire safe insulation systems based on natural materials).“

References

[1] OLORUNNISOLA, Abel O. *Design of Structural Elements with Tropical Hardwoods* [online]. Cham: Springer International Publishing, 2018 [cit. 2018-02-07]. ISBN 978-3-319-65342-6. Available on: doi:10.1007/978-3-319-65343-3.

[2] DE FREITAS ROCHA, Monique Amaro a Alexandre LANDESMANN. Combustion properties of Brazilian natural wood species: PROPERTIES OF BRAZILIAN NATURAL WOOD SPECIES. *Fire and Materials* [online]. 2016, p. 219–228. ISSN 03080501. Available on: doi:10.1002/fam.2281.

[3] OLORUNNISOLA, Abel O. Anatomy and Physical Properties of Tropical Woods. In: *Design of Structural Elements with Tropical Hardwoods* [online]. Cham: Springer International Publishing, 2018 [cit. 2018-02-05], p. 7–29. ISBN 978-3-319-65342-6. Available on: doi:10.1007/978-3-319-65343-3_2.

[4] Meranie vzájomných vzťahov u ordinálnych premenných. *Štatistika v PSPP* [online]. 7. February 2017 [cit. 2018-02-15]. Available on: http://statistikapspp.sk/meranie-vzajomnych-vztahov-ordinalnych-premennych/.

Portable Multifunctional Equipment for Control of the Employees' Working Activity

Gennady Korshunov[a] – Anatoly Romanov[a] – Andrei Nikulin[a] – Iliya Dolzhikov[a] – Qiang Xu[b]

[a] *Saint-Petersburg Mining University, Saint Petersburg, Russian Federation*

[b] *Nanjing University of Science and Technology, China*

Abstract

The article presents the results of the review of a workplace-related mortality record provided by the International Labour Organisation. More than 240,000 fatalities have been found to be caused by human error. The article contains examples of managerial and engineering solutions aimed at increasing the employee's accountability in the work process and describes the algorithms of interaction between portable multifunctional equipment and various personal protective equipment types used by employees. A universal structure has been determined for the equipment designed to control the use of personal protective equipment with 17 indicators that characterise the possibility of using and implementing a communication system based on portable multifunctional equipment for control of the employees' working activity.

Keywords: working activity; PPE; ILO; equipment; working conditions; arrangement of working time; statistics; labour.

---

1. Introduction

According statistics provided by the International Labour Organisation, workplace-related mortality totals 2.3 million per 3 billion people a year. Figure 1 shows main causes for employee mortality in 2017 caused by occupational diseases and fatal accidents [1].

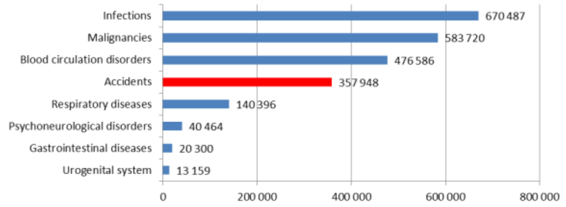

Fig. 1. Work-related mortality

Major occupational health and safety challenges:

- the highest mortality rates are due to work-related occupational diseases (exposure to harmful substances causes 651,279 deaths a year);
- the construction industry experiences an incommensurately high level of accidents;
- the review of the age of the injured shows that the most vulnerable groups are young and elderly workers.

A reduction in the number of deaths caused by industrial factors through the use of proper technical safeguards is one of the most popular and effective approaches and fosters:

- development of machines, tools, and technologies which minimise accident probability and
- development and implementation of special safeguards to protect, guard, and inform people of work-related hazards.

According to the statistics provided by the International Labour Organisation, about two thirds of accidents (about 240,000 fatalities a year) are not related to the operation of machinery or processes but are due to the worker's behaviour in the workplace. Failure to comply with occupational health and safety rules, safety misconduct in the workplace, and failure to use personal protective equipment are primarily caused by poor workplace management, otherwise speaking, human factor [2-3].

Such events mainly occur either through no fault of people or when workers are forced to violate rules in specific circumstances. Apparently, such incidents can be prevented solely by proper managerial and engineering measures implemented to [4]:

- enhance theoretical competence of personnel (training);
- focus on the severity of the consequences of wilful wrongdoing (increased price of mistakes for the community, company, and family); and
- fight tolerance to hazards and any needed or forced non-compliance with the occupational health and safety rules which have not entailed severe consequences (tolerance to violations).

Apart from main causes, there is a whole bunch of individual (personal) factors, which are mainly psychological: bravado, lack of discipline, understatement of risk, lack of interest to work done, family problems, etc. [5]

Consequently, potential errors (hazardous actions) can be identified in a timely manner and duly prevented by enhancing the technical capabilities of the employee's personal protective equipment (PPE).

It is also worth noting that existing PPE is passive equipment without any controlled protective properties. Furthermore, the reliability parameters of PPE as technical means of protection also change during their use and their protective properties worsen as a result of misuse [6-8].

2. Method

The experiment was conducted with the following objectives:

Research has been conducted at Cambridge University to demonstrate the incredible efficacy of placing personal video recorders at the police officers' chest level. The use of these cameras resulted in a 93% decrease in the citizens' complaints against policemen over a year. Researchers believe that such cardinal changes could have not been achieved in any other way [9]. Russian police officers adopt this practice and road traffic police has been equipped with personal recorders since 2017 (Fig. 2).

Fig. 2. A road traffic police officer with Dozor video recorder on a lapel pocket

These are compact devices which are transparent for users and resistant to misuse. They can record video and sound (Fig. 3).

Fig. 3. Kapkam and Dozor video recorders

The use and development of this practice in the industrial environment by using personal multifunctional equipment to control the employees' working activity will facilitate effective prevention of wilful misconduct. The improvement of this equipment and expansion of its functionality will support the correct use of the PPE issued to employees [10-12].

Let us consider the general structure of PPE/human/environment interaction to protect the human body against exposure to harms and hazards shown in Figure 4. In this case, environmental elements are understood as industrial infrastructure, production environment, aerodynamic and thermal characteristics, specific production factors, and so on. The PPE complex is understood as technical equipment intended to minimise exposure to adverse factors. The properties of the environment formed between the PPE and the employee's body result from the interaction between PPE protective properties and functional body systems. The parameters of this environment and their changes determine the degree of the employee's comfort and safety.

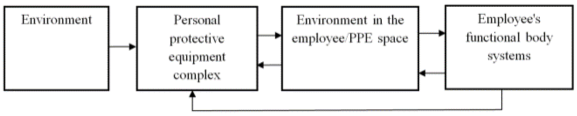

Fig. 4. General structure of PPE/human/environment interaction

Therefore, there is a risk of emergencies with the use of passive PPE due to lack of control over:

- correct use of PPE;
- changes in environmental parameters;
- changes in environment parameters in the PPE/employee space; and
- changes in the parameters that characterize the employee's health status.

Control of the above will increase the employee's accountability for working operations, reduce risks of the failure to use PPE, ensure control over working operations, and enable to identify causes of an emergency or accident involving an employee [13].

This can be technically implemented by using digital equipment based on advanced nanotechnology that support the smallest possible size of developed equipment, low power consumption, and relatively low cost with significant computational capacity.

The aforementioned properties of cutting edge equipment enable to design and use control units based on the transparency principle in relation to a PPE user. It means the minimum possible influence on the employee to ensure convenience. An employee must not be involved in the maintenance of these control units. The interaction between an employee and control unit must exist only in an emergency when the employee is alerted of an alarm or a hazard. Figure 5 presents the structure of a PPE control unit which is universal and unambiguous in relation to specific PPE.

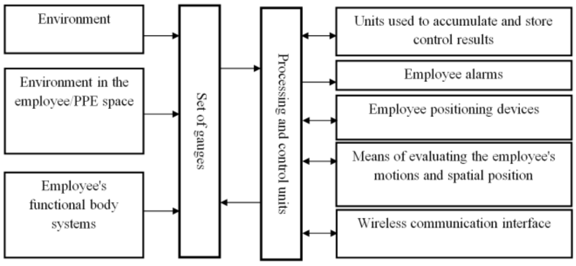

Fig. 5. Universal structure of a PPE use control unit

A control unit and its features depend on PPE purpose. The type of gauges and their location in the PPE space depend on the aggregate of tasks the control unit is intended to solve (e.g., atmospheric composition gauges). PPE location on an employee predetermines the ability of a control unit to record the activity of functional body systems. Processing and managing hardware is omni-purpose and its functions implement the algorithm related to the control over specific PPE use and contribute to the reduction of risks caused by PPE abandonment, control over working operations, and identification of causes of an emergency or accident involving an employee. Such universal properties include units used to accumulate and store control results, emergency alarms, as well as wireless communication interface between PPE and control units.

A control unit can be equipped with employee positioning devices based on GPS or GLONASS (when using PPE in the open air) and hardware used to evaluate the employee's motions and spatial position to obtain additional information on the employee's productivity. A control unit does not have any speciality elements, which could be provided additionally (e.g., intercom for verbal communication between employees via wireless interface). Moreover, wireless interface with alarms intended for employees (sound and/or light alarm) can be used to generate a distress signal over the radio to find an employee among rubble, in cavities, etc. [14]

All control units mounted on various-purpose PPE used by the same employee are combined into single hardware and information space via a distributed computer network. However, this combination for specific PPE can be achieved using wired connection with processing and managing units based on such standard protocols as SPI, I2C, USB, and COM, and for several PPE, via Zig Bee Pro network protocol (IEEE 802.15.4 standard) [15]. ZigBee technology enables to create a fairly complex structure with many PPE units which quantity varies. Figure 6 shows an arrangement option for the network that combines the PPE complex mounted on an employee to form unified information space.

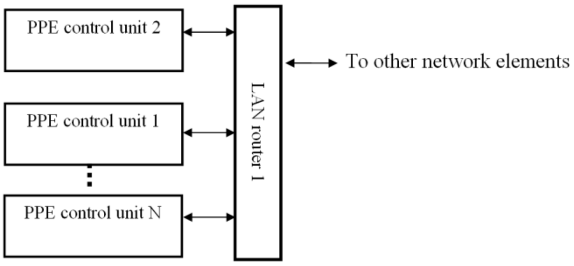

Fig. 6. Arrangement option for the network that combines the PPE complex mounted on an employee to form unified information space

Portable multifunctional equipment (PME) can be used as a local area network (LAN) router. It is issued to an employee before the start of a work shift and contains information on the organisational features of a production process (start of shift, routine breaks, end of shift, etc.).

Employee identification at the time of issuing PME can be an additional motivation factor that enhances the employee's accountability in the work process. Furthermore, PME is the main LAN device that supports PPE troubleshooting, time synchronisation of control units on all PPE units, accumulation and assessment of controlled information received from a PPE complex, emergency or accident identification, and generation of an alarm or emergency alert. The transfer of all functions from the PPE control unit to PME can significantly simplify its structure and optimise the set of elements required to support a specific task. An employee returns PME at the end of each shift. The information accumulated over the work shift is read by a controller using stationary hardware, evaluated using relevant control algorithms, and provided to controlling bodies in a document that determines the results of controlled information evaluation, type of violations, and time distribution over a completed work shift. [16–17]

3. Results

The use of proposed equipment aims at improving the effectiveness of PPE use by employees in the work process. The challenge stipulates fairly tough requirements for the design of control units for the

PPE mounted on one employee or a number of employees. Hardware must support:

1. automatic troubleshooting of equipment and generation of information on identified faults before the start of and during a work shift;
2. generation of astronomical time and time synchronisation with LAN units;
3. recording of the given set of parameters;
4. processing and evaluation of recorded information;
5. accumulation of control results in an energy-independent memory;
6. generation of an alarm and emergency signal in extreme conditions;
7. identification of unauthorised access to PPE control unit elements;
8. effective information exchange between PPE and PME/PME and a number of employees in the control process;
9. optimisation of energy consumption and continuous functioning using off-line power sources over an operation period;
10. modular design to enable prompt changing of a hardware structure;
11. use of Plug and Play technology to change a set of gauges;
12. prompt reprogramming of functions to meet a specific control objective;
13. prompt and ergonomic attachment to PPE elements;
14. explosion- and environment-proof design;
15. easy maintenance during scheduled and day-to-day examination, repair, and decommissioning;
16. minimum dimensions and weight; and
17. salvation of control results in case of a disaster (explosion, fire, flood, etc.).

It is worth noting that proposed PPE control units can be upgraded by improving control methods without changing hardware (through software update) and by reconfiguring the structure of used technical elements and their replacement whenever required.

4. Conclusions

The employee's safety can be improved in various production areas if control units based on state-of-the-art sensors are used additionally to passive PPE to characterise the environment, environment in the human/PPE space and parameters of various functional systems of the human body, as well as to ensure control over the correct use of PPE in various production processes. Cutting edge recording and processing units for the information in question and alarming employees have characteristics to meet the challenge subject to compliance with the transparency principles with regard to employees using PPE which makes the control procedure effective in standard and emergency conditions and during rescue operations required during emergency response.When choosing fabrics to make special clothes, including miner's overalls, clothes contamination during use must be taken into account.

References

[1] Women and men in the informal economy: a statistical picture (third edition) / International Labour Office – Geneva: ILO, 2018.
[2] K. C. Parsons (2007) Protective clothing: heat exchange and physiological objectives, Ergonomics, 31:7,991-1007, DOI: 10.1080/00140138808966738
[3] T.M. Zhigalova About heat and moisture exchange with between humans wearing special clothes and the environment. Text. / T.M. Zhigalova, Z.S. Chubarova, A.A. Zakharova // News of Higher Educational Institutions. Light Industry Technology. 1991. No. 4: pp. 55-60.
[4] L.V. Stepanova Peculiarities of the use of personal protective equipment by employees as protection against industrial contamination and mechanical damage // 3rd International Scientific and Practical Conference on Industrial Safety at Mineral Resources Companies in the 21st Century: scientific conference abstracts/St. Petersburg Mining University. St. Petersburg, 2016. p. 78.
[5] A.F. Davydov Russian working clothes market // Working clothes. 2010. No. 4: p. 12.
[6] Personal protective equipment. Textbook/Team of authors led by Yu.G. Sorokin. Moscow. 2007. 288 p.
[7] Batmanov V.P., Barsukov O.K. Laser and optic device to determine dust concentration and distribution of dust particles in the workplace air. Zapiski Gornogo instituta. 2017. Vol. 203: p. 146-149.

[8] Aude Morel, Gauthier Bedek, Fabien Salaün & Daniel Dupont (2014) A review of heat transfer phenomena and the impact of moisture on firefighters' clothing and protection, Ergonomics, 57:7, 1078-1089, DOI: 10.1080/00140139.2014.907447

[9] Lomakin, D. Za gaishnikami prismotrit «Dozor» / Gazeta.ru. URL: https://www.gazeta.ru/auto/2016/12/08_a_10412891.shtml

[10] S. Lee & S. K. Obendorf (2010) Barrier effectiveness and thermal comfort of protective clothing materials, The Journal of The Textile Institute, 98:2, 87-98, DOI: 10.1533/joti.2005.0143

[11] A.G. Shailkov, G.M. Volokhov, T.N. Abramenko, V.P. Kozlov Methods of determination of thermal conductivity and temperature conductivity Edited by A.V. Lykov Moscow: Energy. 1973. 336 p.

[12] Kovshov, S., R. Istomin, A. Nikulin and A. Sotiriu, 2014. Industrial injuries appraisal in mines of JSC "SUEK Kuzbass". Advanced Materials Research Volume 1001: 414-420.

[13] Nikulin, A., A.Yu. Nikulina Assessment of occupational health and safety effectiveness at a mining company. Eco. Env. & Cons. 23 (1): 2017, pp. 533-537.

[14] Kazakov B.P., Levin L.Yu., Shalimov A.V., Zaitsev A.V. Development of Energy-Saving Technologies Providing Comfortable Microclimate Conditions for Mining. Zapiski Gornogo instituta. 2017. Vol. 223: p. 116-124. DOI: 10.18454/PMI.2017.1.116

[15] Baskakov, S Standart ZigBee и platform MeshLogic: routing efficiency in mode "Many to One" //First mile. 2008. Vol. 2-3. Pages 32-37.

[16] Lobnik, A. Optical chemical sensors and personal protection / TUT Textiles a Usages Techniques.Volume 4, Issue 63, March 2007, Pages 34-3

[17] Construction Program Employee Safety Manual. NYS ACCIDENT REPORTING SYSTEM (ARS). Department of transportation. URL: https://www.dot.ny.gov/main/business-center/contractors/construction-division/construction-repository/CPE_Handbook_web.pdf

Kettle thermal damage monitoring by thermovision

Ivan Kubovský[a*]– Peter Lačný[a]

[a]*Technical University in Zvolen, Faculty of Wood Sciences and Technology, T.G.Masaryka 24, Zvolen 960 53, Slovak Republic*

Abstract

The paper deals with monitoring the temperature of the plastic kettle. The simulated fault has been induced on the kettle thermostat, which has led to its gradual overheating to the state of thermal degradation of its vessel. Non-contact temperature fields measurement and their visualization were performed using the FLIR i7 thermal camera. Monitoring has lasted 17 minutes. The maximum pot surface temperature reached approximately 154 ° C.

Keywords: kettle; temperature; thermal camera; thermal degradation

---

[*] Corresponding author. Tel.: +0-000-000-0000 ; fax: +0-000-000-0000 ; e-mail: kubovsky@tuzvo.sk.

1. Introduction

Thermovision offers relatively wide application possibilities. We can detect locations with elevated temperature by means of thermal cameras, which can pose a potential fire risk in the event of a malfunction. In fire and rescue practice, in fire interventions as well as in prevention, the thermal camera is used quite often. With the ability to visualize temperature fields, it can provide information about the magnitude of the fire and reveal its hidden sources. Helps people search in confined spaces, identify free escape routes, and search for lost people in disarranged terrain [1]. An important place is also in the field of fire prevention (electrical equipment, heat distribution, mechanical parts of machinery, landfills of bulk materials). The monitoring of technical devices with the thermal camera enables the detection of high temperature locations in time. This will give the broader scope to decide whether it is a failure or just a short-term overload of the device [2,3]. The heat generated in many types of devices does not pose any immediate danger unless the temperature exceeds the pre-load values. With its disproportionately large increase, it usually means overload or failure, which can cause damage to the device and, in the extreme case, fire [4]. Thermal imaging will instantly reveal temperature anomalies and conditions that could lead to serious disruptions and fire in the future. Thermal imaging can be processed on a computer and then analyzed.

2. The basics of thermovision

Thermovision uses electromagnetic radiation emitted by each substance with a temperature above absolute zero (-273.15 ° C). In particular, infrared radiation (IR) forming part of the electromagnetic spectrum with wavelength above 780 nm is exploated (Fig.1). The area of IR wavelengths is usually divided into several smaller bands - near infrared (0.7-1.4 μm), short wave IR (1.4-3.0 μm), medium infrared (3-8 μm) and distant (8-1000 μm) [5]. Sometimes a long-lived area with a range of 8-15 μm is inserted in front of the remote zone.

A body with a temperature of several hundred to thousands of degrees Celsius radiates part of the energy even in the visible area of the spectrum (Figure 2 - vertical colour strip in the graph). For this reason, we see, for example, glowing metal objects in red to white.

However, In the infrared range of the spectrum up to 105 times more energy is emitted, which is preferably used in thermovision. The theoretical foundations relating to body radiation are described by several laws. Planck's radiation law expresses the dependence between the amount of energy radiated by the body, its temperature and the wavelength of electromagnetic wave radiation. As can be seen in FIG. 2, the increase of temperature growes the intensity of the radiation and its maximum of which is shifted to the shorter wavelengths (Wien's shift law). The amount of radiated energy increases with the fourth power of temperature (Stefanov - Boltzmann Law). As a result, it is possible to determine the temperature uniquely from the electromagnetic wave, radiated by the heated body. However, the surface temperature of the object is not directly measured. Temperature is calculated based on measured infrared radiation and specified boundary conditions). The most important boundary condition is surface emissivity (ε). It is a dimensionless number from interval 0 (glossy surfaces) to 1 (absolute black body). It represents the ratio of the energy emitted by the object to the energy emitted by the ideal body (the so-called black body) at a given temperature. Other boundary conditions include the distance between the subject and the camera, atmospheric permeability, relative humidity and air temperature [5]. Thermal cameras effectively translate heat - that is, thermal energy - into visible light to analyze surroundings. The colour picture displaying of temperature fields provided by the thermal camera is called the thermal image. The device, which only allows display of temperature fields, is called thermovision. When the thermal image also contains the temperature of the measured surface, it is a thermometry. The range of commercially available thermal cameras covers a temperature range from −40 to +2000 °C, with a sensitivity of better than 0.05 °C. The main parts of the thermal camera are shown in Fig. 3.

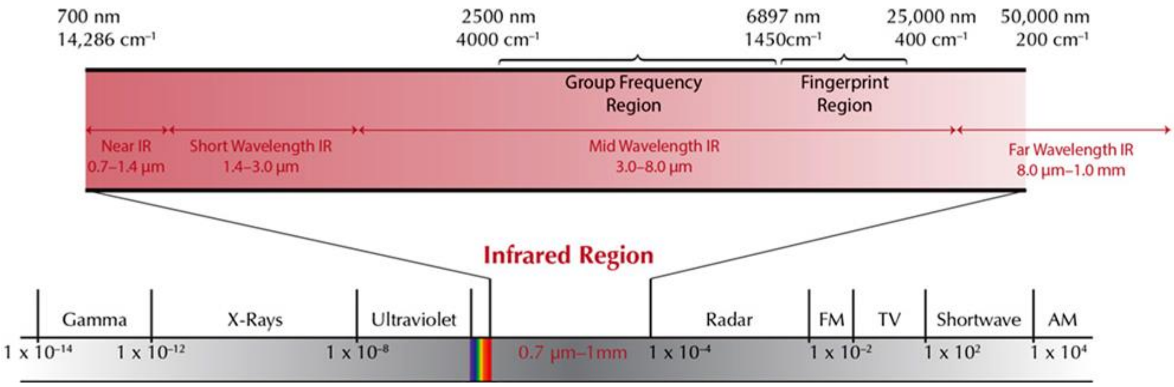

Fig. 1 Electromagnetic radiation spectrum (modified according to [6])

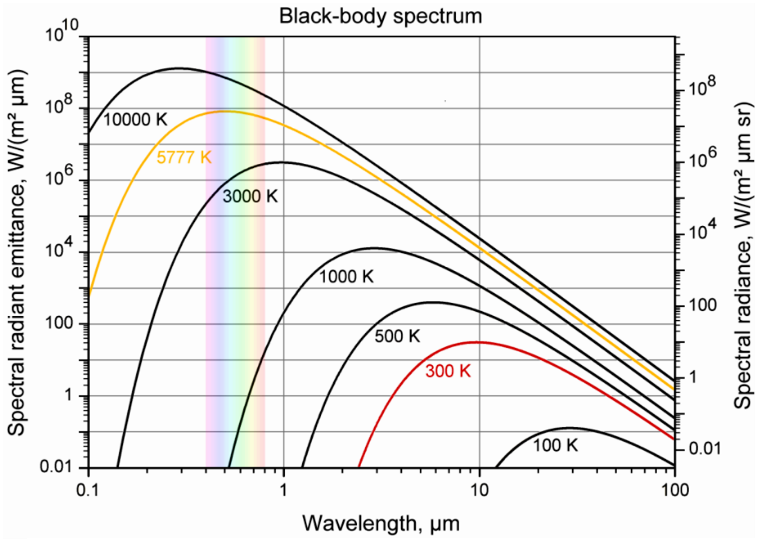

Fig. 2 Dependence of radiant intensity on black body temperature (modified according to [7])

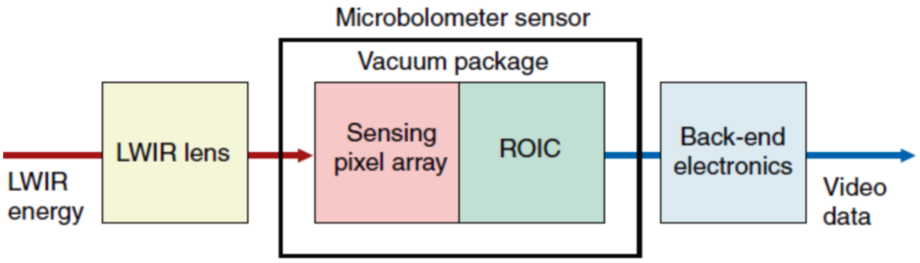

Fig. 3 Block diagram of the thermal camera [8]

3. Material and methods

The measuring object was a 1.2 liter Solac electric kettle. The heating element in the kettle is a resistive helix with a power of 1000 W, which includes a wound conductor made of a high resistivity material located in a protective anti-corrosion tube. By passing the electric current through the conductor there is produced a heat which heats the water inside the kettle. The kettle is equipped with a thermostat with a thermal fuse. The thermostat will ensure safe shutdown when boiling. Danger can arise if the kettle is switched on without sufficient volume of water. In this case, the thermal fuse responds and the current to the spiral is interrupted. Before the experiment, a fault was purposely caused on a thermal fuse and a thermostat to simulate one of the common faults in practice. A manual FLR i7 camera with a 120 × 120 pixel resolution to monitor and record the temperature fields was used. The camera has a temperature sensitivity below 0.1 °C with emissivity correction from 0.1 to 1 (we used 0.95 for our measurements). The temperature range is from -20 ° C to +270 ° C. Thermal images are displayed on the 2.8-inch colour display and stored on a 2 GB SD card [9]. The 16 MPix Kodak FZ151 camera was used to visualize the experiment.

Fig. 4 Kettle and thermal camera i7 [9]

Prior to the start of the monitoring, the kettle was water filled, completely covering their heating body, and was placed on a horizontal pad. At a distance of 1m, a thermal camera and camera were placed on the tripod. The surface of the plastic container of the kettle (the area of the heater and the gap under the lid of the kettle) was monitored. The experiment began when the power switch was turned and the camera and thermal camera were started. Images were stored at regular intervals (5 s). After destruction and self-disconnection from the electricity, monitoring was terminated. Ambient air temperature during the measurement was + 8 °C.

4. Results and discussion

Attached thermal imagines displayed the temperature at a given location and time. In FIG. 5 (left side of the picture) is the thermal image recorded at the time of commissioning (connecting the power cord to the wall socket). The right part of this image shows the stage obtained at the end of the first minute of the measurement. The surface temperature in the heater area increased approximately threefold (to 46.6 °C) from the initial temperature. The temperature under the cover rose to 12.7 °C). At the end of the second minute (left part of Figure 6), we recorded a rise in temperature at both observation points (64.5 °C and 26.1 °C). The temperature in both observed places has steadily increased. At the end of the third minute it reached 82.3 °C and 97.7 °C (right part of Figure 6). The same trend continued as shown in Fig. 7 (the area around of the heater element was heated from 90.9 ° C to 135.1 ° C, area under the cover from 107 ° C to 151.1 ° C). We found the highest temperature at the end of the 11th minute when it rose to 135.4 ° C in the heater area and even to 153.8 ° C under the cover (left side of Figure 8). The next period of the measurement had changed the temperature. At the end of the 13th minute we found that the value decreased at both of the monitored points (right part of Figure 8). The ambient temperature of the heating element decreased to 114.5 °C and the temperature below the cover at 106.6 °C). The decrease in the temperature measured values confirms the assumption that between 12 and 13 minutes there was a burning of the conductor of the heating coil and thus the interruption of the electricity supply. As a result, the temperature had steadily declining trend (Figure 9). This finding has led to an experiment being terminated.

The demaged kettle was dismantled after cooling and disposed into bins for recyclable waste. Thermal images and videos of the exposed heater immediately after the experiment is completed are shown in Fig. 10 and 11.

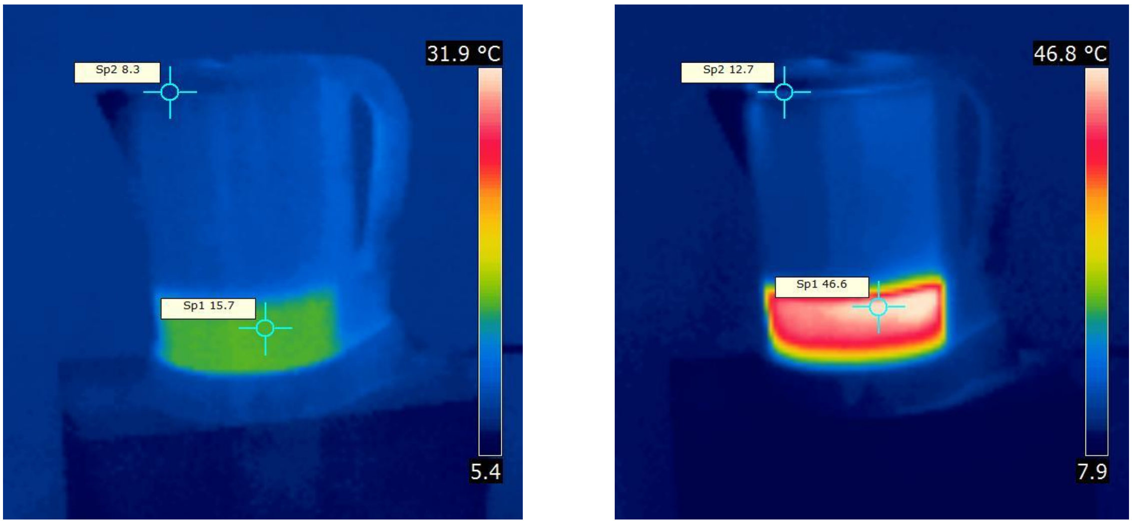

Fig. 5 Thermal images at startup and at the end of first minute from the beginning of the experiment

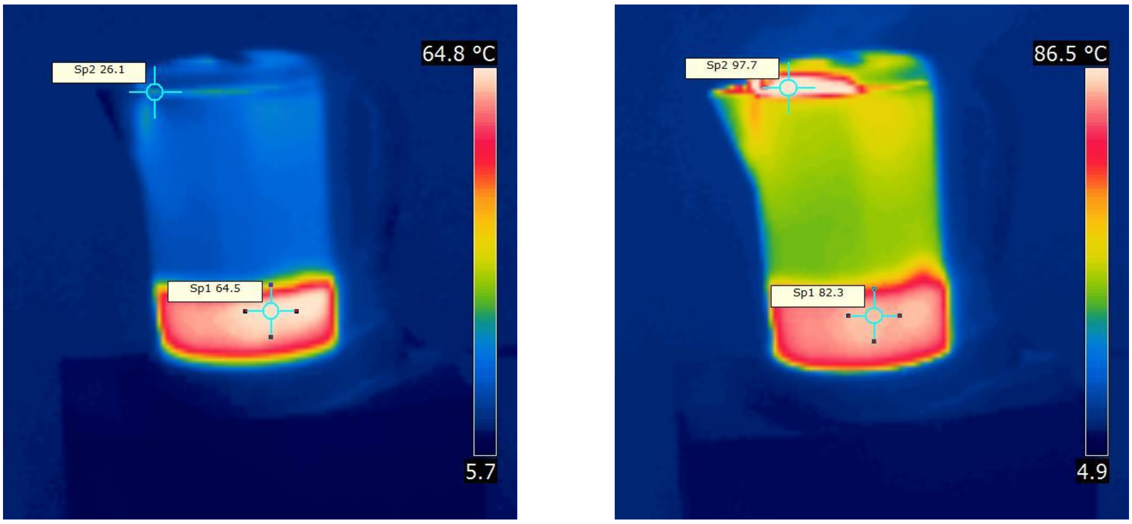

Fig. 6 Thermal imaging at the end of 2nd and 3rd minutes

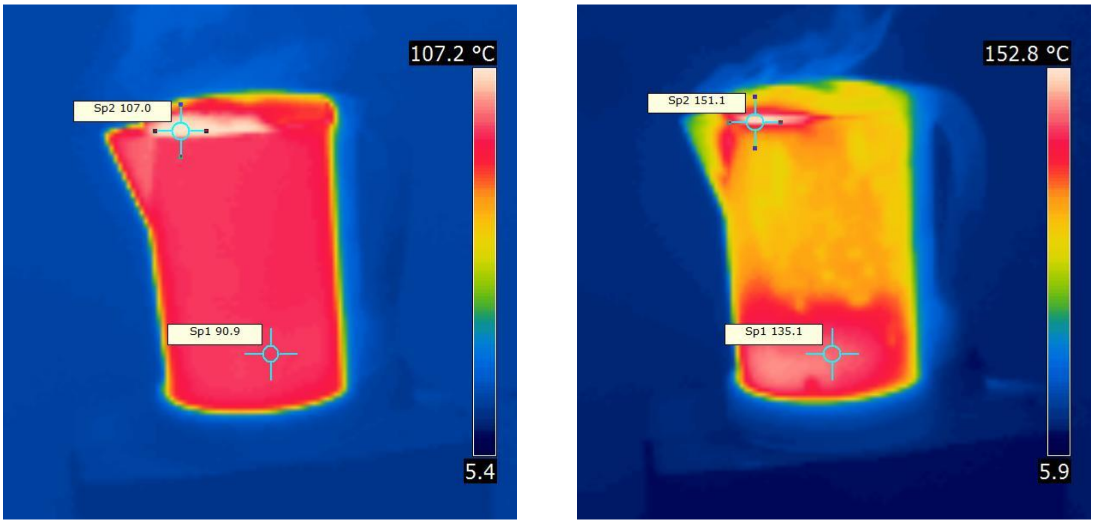

Fig. 7 Thermal images at the end of 5th and 10th minutes

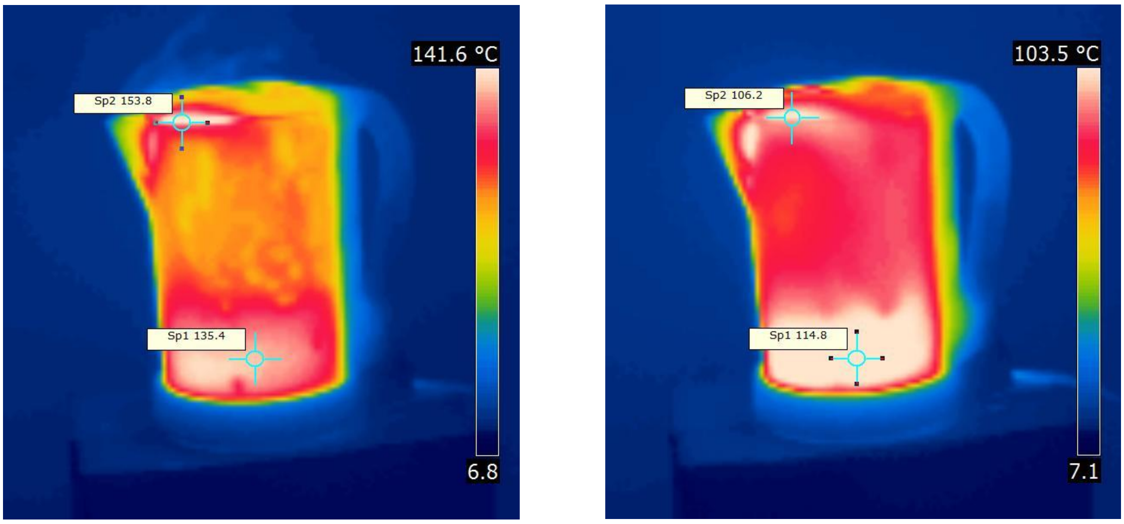

Fig. 8 Thermal images at the end of 11th and 13th minutes

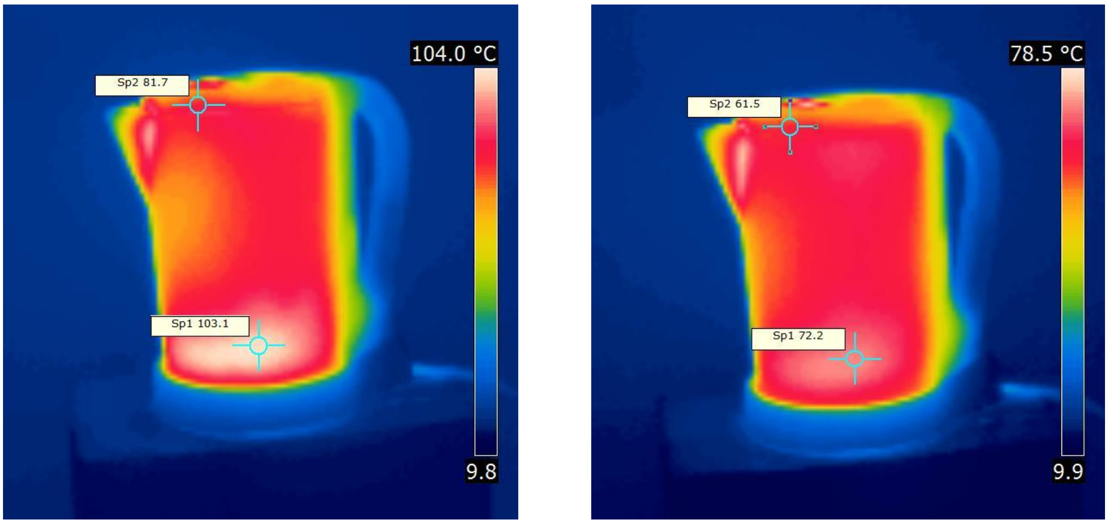

Fig. 9 Thermal images at the end of 15th and 17th minutes

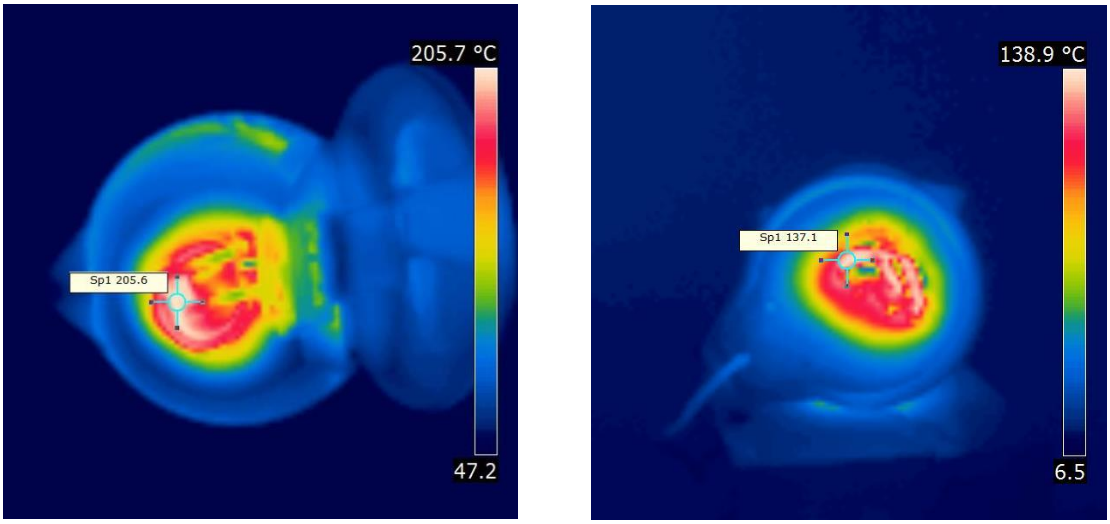

Fig. 10 Thermal images of the uncovered heater immediately after the experiment

Fig. 11 View of an uncovered heater element immediately after the experiment

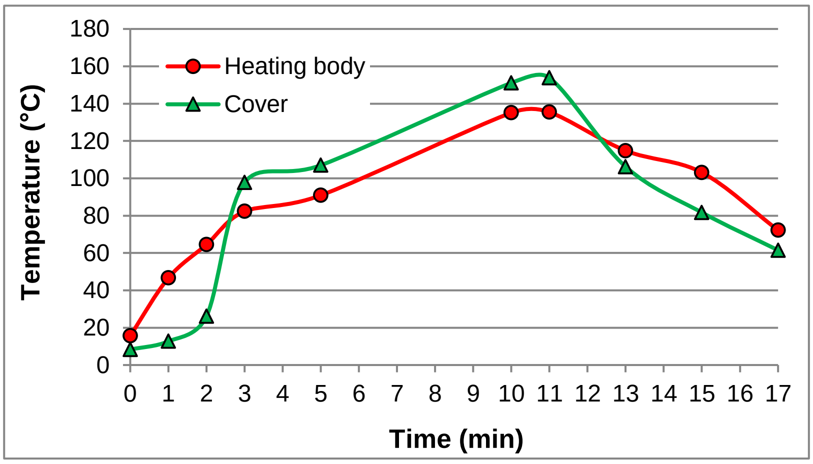

Fig. 12 Time dependence of temperature on the observed points

In Fig. 12 is a graphical representation of the time course of temperature on the observed points of the kettle surface.

5. Conclusions

As can be seen from the measured values, the temperature at both observation points had an initially upward trend. The reversal occurred only when the power supply was interrupted [10]. Thermal protection malfunctions caused a gradual increase in temperature. In the event that the power supply is not interrupted, it can be assumed that the temperature would continue to rise, creating the conditions for the fire eventually. A kettle is an appliance that is used several times a day in almost every household. A similar type of malfunction that has been deliberately triggered in our case may result in the occurrence of large-scale damage or endanger the health and life of its users.

Acknowledgments

This work was supported by the VEGA agency of the Ministry of Education, Science, Research and Sport of the Slovak Republic (No. 1/0806/17).

References

[1] KVANT, s. r. o. 2014. *Termovízna technika pre hasičov*. Dostupné na: http:// www.termokamery.sk/aplikacie-a-galeria/termovizna-technika-pre-hasicov/

[2] ŠIMKO, M. 2015. Aplikačné možnosti termovízie v praxi. *ELEKTRO: Časopis pre elektroniku*. Dostupné na: http://www.odbornecasopisy.cz/ index.php? id_document =26599

[3] ŠIMKO, M, CHUPÁČ, M. 2007. *Termovízia a jej využitie v praxi*. 1. vyd. Žilinská univerzita v Žiline : EDIS, 2007. 110 s. ISBN 978-80-8070-654-8

[4] Infrared Imaging Services LLC. Dostupné na: http:// www. infraredimagingservices.com /electrical-infrared

[5] http://www.opticsforhire.com/blog/2015/7/15/design-of-ir-lenses

[6] http://www.lotusgemology.com/index.php/library/articles/294-ftir-in-gem-testing-ftir-intrigue-lotus-gemology

[7] http://www.sun.org/encyclopedia/black-body-radiation

[8] OSTROWER, D. Optical Thermal Imaging - replacing microbolometer technology and achieving universal deployment. III-Vs Review 19(6), 2006, 24- 27. doi.org/10.1016/S0961-1290(06)71764-1

[9] FLIR. Datasheet 2012, 17 s. http://flir.custhelp.com /app/ fl_download_ datasheets.

[10] LAČNÝ, P. Využitie termovíznej kamery pri inšpekcii elektrotechnického zariadenia. Zvolen: Technická univerzita vo Zvolene. Drevárska fakulta. 2017. 59 s.

Earth in a Trap? 2018
Analytical Methods in Fire and Environmental Science

Current trends in flame-retardant treatment of selected polymers – a review

Andrea Majlingová[a*] – Danica Kačíková[a] – Qiang Xu[b] – Cong Jin[b]

[a]*Technical University in Zvolen, T.G. Masaryka 24, 960 53 Zvolen, Slovakia*

[b]*Nanjing University of Science and Technology, 200 Xiao Ling Wei, Nanjing 210014, P.R. China*

Abstract

Polymer based materials are used as in industry as in households. They are rapidly developing. Due to their cost, they often replace the traditional materials. The disadvantage of its use, both natural and synthetic polymers, is their sensitivity to flame because of their main constitute element, i.e. carbon. In general, the flammability of polymer materials depends on their chemical composition. Their flammability can be reduced by interfering the combustion process at any stage. A common approach to improve the flame-retardant properties of polymers is to apply the flame retardants. Those are used to prevent, minimize, suppress or stop the combustion process of polymer materials. They act to break the self-sustaining polymer combustion cycle and consequently reduce the burning rate or extinguish the flame in several ways. This paper compiles current research findings and results related to wood and wood composites, fabrics and PU/PUR foams flammability reduction, applying the flame-retardant treatment.

Keywords: fabrics; flammability; flame retardant; PU/PUR foam; wood; wood composite

---

[*] Corresponding author. Tel.: +241-45-5206065; e-mail: majlingova@tuzvo.sk.

1. Introduction

The number of high rise building fires and the resulting loss has been fast increasing over the past decade. The most recent shocking example is the Grenfell Tower fire on 14 June 2017, resulting in at least 80 deaths and over 70 injuries. Other significant high-rise building fires include the 2005 Winsor Tower fire in Madrid, the 2015 residential fire in Baku, the 2009 CCTV tower fire in Beijing, the 2010 Shanghai Jingan fire, the series high rise building fires in Dubai in 2016 and 2017, etc.

The rapid spread of those fires is situated along the external façade, which is almost all traced to the cladding systems, which include combustible insulation materials, such as the commonly used wood and wood-based materials, foams of polyurethane (PU/PUR), polystyrene (PS) and polyisocyanurate (PIR); and constitutes potential fire hazards. Its flammability and fire risk have drawn increasing attention from both scientific and industrial communities.

For the residence fire, bedding and upholstered furniture are the first item ignited in roughly 19% of fatal fires. In a white paper launched at the EU parliament in 2014, entitled “Europe is playing with fire”, Fire Safe Europe called on the European Commission to act to improve fire safety in buildings.

When talking about the of fire protection in buildings, the optimal level depends on a large extent on the amount and type of flammable materials and substances that occur in them. As mentioned above, flammable materials, which are relatively common in building sites, include polymeric materials (e.g. wood, wood-based materials, plastics, linen and upholstery fabrics).

Some polymers, especially porous polymers with a large specific surface area, such as polyurethane foam [1-3], fabrics [4-7], and wood [8], burn easily, releasing a large amount of heat, flame and smoke in association with generation of many droplets during the burning process, and thereby threatening people’s lives and property.

A common approach to reduce the flammability of polymers is to apply the flame retardants.

But, there are still some problems also in the use of the flame-retardants themselves. Those are mostly used in the form of additives with relatively high potential toxicity to human health and environment [9-15].

Therefore, also highly effective and environmentally benign flame-retardant techniques are attracting research attention increasingly.

Thus, not only the improvements of the chemical flame-retardant properties, but also the ways of application to polymers are urgently needed [16, 17].

2. Polymers and their flame-retardant treatment

When we talk about polymers, we exactly mean matters, which consist of several ordered monomer repeated units, the molecules of which have molecular weight in the range of several thousand or more.

Polymers, in general, are widely used in everyday life. Among the polymers belong also wood, fabrics, plastics. Those materials we can find in buildings, e.g. in furniture, building constructions, insulation, flooring; in industry, e.g. aerospace, automotive, packaging; but also, outside the buildings, e.g. in streets, parks, etc.

Most of these polymers are combustible materials and thus increase fire hazard [18], so their flammability should be critically considered and limited in practical applications [19].

To reduce the flammability of polymers, three typical strategies have been mainly developed and used [18], including the use of inherently flame-retardant polymers [20-22], flame retardants [23-34], flame-retardant nanocomposites [34-44] and surface treatment/coating [17, 46-52].

First, the halogen containing flame retardants were applied to reduce the flammability of polymers. They were mostly used in furniture, mattresses and electronics [53, 55]. The disadvantage of their use was the fact that those halogenated compounds produce carcinogenic substances in the combustion process, which are harmful for human health, and for environment [54].

To enhance this situation new flame retardants, i.e. halogen-free flame retardants, were developed. Those involves phosphorus, nitrogen, silicone, boron, zinc, iron and aluminum flame retardant additives.

The principle of phosphorus-containing flame retardation lies in a fact that they can undergo dehydration and carbonization to form protective carbon layers and thereby effectively reduce the polymers flammability [17, 55-59].

Nitrogen-containing flame retardants absorb heat and produce non-combustible gases to dilute the concentration of combustibles during the decomposition process of polymers [58, 60-62].

Silicone-containing flame retardants form an insulating layer on the polymer surface upon burning. Thereby, they are effectively impeding the transmission of oxygen, heat and mass and reducing the flammability of polymers [17, 63-65].

Quite limited in engineering is the application of boron, zinc, iron and aluminum-containing flame retardants. They can suppress smoke and retard flame only to some extent. They have also the other disadvantages: increasing viscosity, high loading and potential toxicity to human health and environment [54, 65, 67-73].

Nowadays demands for eco-friendly materials requires also application of "green" fire-retardancy treatments, which offer opportunity for implementation of nanotechnologies.

Various application ways are being used to enhance the flame retardancy of polymers. Among the basic belong soaking [74], coating [76], spraying [77-79], preparing one (e.g. sol-gel) or more layers of flame retardant treatment. The most progressive approach, the layer-by-layer method seems to be [17, 51, 78, 80].

As mentioned by Qiu et al. [17], compared with the traditional flame retardant method, the layer-by-layer method offers several advantages: the flame retardant multilayer films are constructed between a substrate and the exterior, which can directly interfere with the combustion process and eliminate the challenges associated with processing or adversely modifying mechanical behavior when incorporating flame retardants into the substrate itself; if the positively and negatively charged functional polyelectrolytes or nanoparticles are properly selected, the layer-by-layer method, which is simple and versatile, can be readily adopted to fabricate multilayer films with controllable thickness, composition, and function. In addition, the layer-by-layer method relies on mild experimental conditions such as room temperature, atmospheric pressure and a low concentration of to-be-assembled materials (bellow 1 wt%), which often means it is a cost-effective route for fabricating coatings.

Further, we introduce the flame retardants types and application ways used for the polymer material such as wood and wood composites, fabrics and polyurethane foams. This information is completed on review of current research works focusing the flame/retardant issue and concerning the selected types of polymers.

There are introduced only those included in Web of Science citation database.

3. Wood and wood composites flame-retardant treatment

Wood is one of the most sustainable, esthetically pleasing and environmentally benign engineering materials, and is often used in structures found in buildings. Unfortunately, the fire hazards related to wood are often limiting its application. In addition, for example, the mechanical properties of wood have up till now been impaired by the most common flame/fire retardants, and therefore, the investigation of wood modification with not-weakening flame retardants is essential currently.

In general, we distinguish among the five essential mechanisms of flame retardants for wood: 1. changing the pyrolysis of wood; 2. protecting the surface of wood with isolating layers; 3. changing the thermal properties of wood; 4. reducing combustion by diluting pyrolysis gases; 5. reducing combustion by inhibiting the chain reactions of burning

Practical techniques for flame/fire retardance of wood include: 1. pressure impregnation; 2. surface treatments (intumescent varnishes and paints and non-intumescent coatings); 3. addition of a fire retardant during manufacturing process; and 4. other flame/fire retardant treatment methods (e.g. nanocomposite systems, boron gas treatment or modification of wood using e.g. the chemoenzymatic method for modifying cellulose materials.

There are further introduced several current works which focus on flame retardancy of wood and its testing.

Altun, Dogan and Bayramli [81], used red phosphorus (RP) to improve the fire performance of wood flour - low density polyethylene (LDPE) composites containing ammonium polyphosphate (APP). The fire performance of LDPE-based composites was investigated by using limiting oxygen index (LOI), UL-94 standard, thermogravimetric analysis, and cone calorimeter. The addition of 30 wt% APP increased the LOI value from 17.5 to 24.2 and still burned to clamp (BC) in UL-94 test. The RP showed beneficial effect when combinedly used with APP. The maximum beneficial effect was seen at ratio of 5:1 (APP:RP) with the highest LOI value of 27.2 and UL-94 rating of V0. RP showed its beneficial effect via increasing the gas phase action of the flame-retardant system.

Bogdanova, Kobets and Kirlitsa [61] studied the factors exerting a significant influence on the termination of the combustion of natural materials (wood and peat) with the use of synthetic nitrogen- and phosphorus-containing fire retardants with different efficiencies. With the use of a mathematical experimental design method, it was confirmed that the inhibition of gas-phase radical processes by volatile nitrogen-containing products is the predominant process of combustion suppression. It was found that the synergism of the nitrogen-phosphorus flame retardants is determined by their complex action: phosphorus mainly enters organomineral structures in the condensed phase, and nitrogen inhibits reactions in a gas phase.

Carosio et al. [82] used the transparent cellulose nanofiber (CNF)/clay nanocomposites, with unique brick-and-mortar structure, as a sustainable and efficient fire protection coating for wood. Fire performance was assessed by cone calorimetry. When exposed to the typical 35 kW/m^2 heat flux of developing fires, the time to ignition of coated wood samples increased up to about 4.30 min, while the maximum average rate of heat emission (MARHE) was decreased by 46% thus significantly reducing the potential fire threat from wood structures.

Elvira-Leon et al. [29] investigated the effect of epsomite as flame retardant for wood has been investigated and compared it with a commercial boron salt. Both flame retardants have been introduced into wood samples by vacuum impregnation. Flame retardancy was evaluated by means of the limiting oxygen index, the dripping test and the exposition to a direct flame (Bunsen test). The results showed that the addition of epsomite increases the limiting oxygen index, delays the time to ignition and the evolution of the temperatures trough the wood.

Chambhare, Lokhande and Jagtap [62] synthetized multifunctional phosphorus and nitrogen containing tris-diethanolamine spirocyclic pentaerythritol bisphosphorate reactive diluent (TDSPBRD) for epoxy acrylate oligomer from spirocyclic pentaerythritol bisphosphorate diphosphoryl chloride, diethanolamine, and allyl chloroformate. The synthesized reactive diluent was utilized to formulate ultraviolet (UV)-curable wood coating. The weight fraction of reactive diluent in the coating formulation was varied from 5 to 25 wt% with constant photoinitiator concentration. The molecular structure of the reactive flame retardant was confirmed by Fourier transform infrared (FTIR), H-1 nuclear magnetic resonance (NMR) and P-31 NMR spectral analysis and energy dispersive spectroscopy (EDAX). Further, the effectiveness of the flame-retardant behavior of the coatings was evaluated using the limiting oxygen index and UL-94 vertical burning test. Thermal stability was estimated from thermogravimetric analysis and differential scanning calorimetry. The effects of varying the concentration of TDSPBRD on the viscosity of the coating formulation along with the optical, mechanical and chemical resistance properties of the coatings were evaluated. The coatings gel content, water absorption behavior, and stain resistance were also studied.

Gao and Xu [83] treated the wood with guanyl urea phosphate (GUP) to impart flame retardant. The flame retarding behavior of samples was valued by cone calorimeter and thermalgravimetric analysis. The flammability parameters, including rate of heat release (RHR), total heat release (THR), total mass loss (TML) and mass loss rate (MLR), yield of CO and CO_2, smoke production rate (SPR) and total smoke production (TSP) were recorded simultaneously. By analyzing these data, it was concluded that most combustion parameters of wood were decreased by the treatment.

He et al. [84] studied the poplar samples, which were impregnated with ammonium polyphosphate fire retardant at various pressures and durations after they were pretreated with microwave heating. The effects of the pressure and duration on the flame-retardation and smoke-suppression properties were investigated with cone calorimeter analysis. The peak heat release rate (pk-HRR), total heat release (THR), and total smoke product (TSP) of treated woods were measured for samples of pretreated and untreated with microwave. After the impregnation, the poplar wood showed the significant improvement in its fire resistance. Compared with non-impregnation wood, the pk-HRR, THR, and TSP of wood impregnated with ammonium polyphosphate at pressure of 0.4MPa and duration of 10 min were 48.29%, 35.58%, and 68.64% less, respectively. The pk-HRR, THR, and TSP of microwave pretreated wood was 15.89%, 5.69%, and 13.59% less than those without microwave pretreated sample. They stated that the microwave pretreatment of wood can increase fire retardant effectiveness of ammonium polyphosphate-impregnated wood.

Jin and Chung [85] tested the combustive properties of Pinus rigida specimens treated with the mixed phosphorus (P)-nitrogen (N) additives. Each Pinus rigida specimen was painted three times with 15 wt% mixed P-N additive solutions at room temperature. After drying the specimen treated with chemicals, the combustive properties were examined using a cone calorimeter (ISO 5660-1). The time to ignition (TTI) for the specimens treated with the mixed additives was in the range, 70-109 s. The specimens treated with the mixed P-N additives showed a lower peak heat release rate by 3.8-25.5% and lower total heat release by 6.1-22.1% than those of the samples treated with the pure P-N additives. The effective heat of combustion (EHC) for the sample treated with the mixed P-N additives was 15.68-18.70 MJ/kg, which was lower than that of the pure P-N additive plate. Among mixed P-N additives, N,N'-piperazine bis(methylene phosphonic acid) (PIPEABP)/pyrophosphoric acid (PP)/4NH(4)(+) (2:1) had the highest fire performance index (FPI) and lowest fire growth index (FGI). The fire risk of all the samples treated with the P-N additives except sample 2 is much smaller than that of untreated sample and it shows improved fire safety.

Lahtela and Karki [86] investigated the effects of melamine impregnation and heat treatment on the fire performance of Scots pine (Pinus sylvetris L.). The treated samples were tested with a cone calorimeter, and the following features were studied: time to ignition, heat release, smoke production, and mass loss. The heat-treated samples became more homogenous about the results of fire performance. Some of the examined fire behavior values decreased because of heat treatment, while the same values increased after the combination of melamine impregnation and heat treatment. The smoke production was reduced the most for the samples that were both impregnated and heat treated. Although the influence of treatment on the fire behavior properties of solid wood was relatively marginal, it was assumed that these treatments will not have a negative impact on the fire-resistance properties of pine wood.

Merk, Chanana and Gaan [87] studied the precipitation of CaCO3 mineral in Norway spruce and European beech wood by alternating impregnation with aqueous and alcoholic electrolyte solutions. Microstructural imaging by SEM and confocal Raman microscopy showed the distribution of calcite and vaterite as two CaCO3 polymorphs, which were deposited deep inside the cellular structure of the wood. The confined microenvironment of the wood cell wall seemed to favor a formation of vaterite, as visible by XRD and Raman spectroscopy. In view of a practical application, they stated that the mineralization of wood opens ways for sustainable wood-based hybrid materials with a significantly improved fire resistance, as proven via pyrolysis combustion flow calorimetry and cone calorimetry tests. Beyond that, this versatile solute-exchange approach provides an opportunity for the incorporation of a broad range of different mineral phases into wood for novel material property combinations.

Makovicka Osvaldova et al. [88] were investigating the influence of density while evaluating the efficiency of wood flame retardants. They pointed out the fact that test methods evaluating wood flame retardant efficiency are comprised of a parameter, which is often considered to be an evaluation criterion, and its calculation includes the weight of the test specimen or considers the change of its weight during the test. In such a case, the overall result may be affected not only by the weight of the test specimens, but also by their density.

Seo et al. [89] tried to improve the flame-retardant performance of wood-based materials through the development of a coating material using carbon-based materials. The coating materials were applied to the surfaces of wood-based materials used for interior materials and furniture. They measured fire characteristics of the coated wood-based materials using a cone calorimeter. The coating materials were prepared by the mixing of carbon materials, such as natural graphite, expandable graphite, and exfoliated graphite nanoplatelets, in water-based coating materials. TG analysis revealed that water-based coating materials/carbon material-blended composites had good thermal durability in the working temperature ranges. The flame-retardant performance was confirmed through cone calorimeter experiments, and the result of the experiment satisfied the standard for flame-retardant performance in ISO 5600-1.

Wang et al. [90] studied the new flame-retardant plywood that was manufactured by adding expanded vermiculite (EVMT) in the adhesive and by surface treatment as a flame-retardant coating. They discussed the effect of EVMT to the limited oxygen index values of samples. The thermal degradation process of plywood samples has been investigated by thermal analysis. The result showed that EVMT increased all the limited oxygen index values of the treated samples and decreased the thermal activation energy at a high degree of degradation. Scanning electron microscope (FEI, Holland, The Netherlands) images showed that EVMT could form a protective coating, which improved the flame retardancy of plywood.

Wang et al. [91] studied thermal degradation and fire performance of plantation Chinese fir wood treated with low molecular weight phenol melamine urea formaldehyde (PMUF) resin, boron compounds (BB), and the mixture of PMUF/BB (PMUF-BB). The fire performance and thermal degradation of wood was measured by limiting oxygen index instrument, cone calorimeter, and simultaneous thermal analysis. The results showed that the limiting oxygen index increased to 50.7%, 43.5%, and 55.0% for BB, PMUF, and PMUF-BB samples, respectively. The PMUF resin decreased the heat release rate of wood but increased the total heat release compared with the control samples. The thermal analysis results demonstrated that PMUF resin enhanced the thermal stability of wood, however, had little impact on the residual chars. Combinative treatment with boron compounds could substantially reduce the fire risk for PMUF-modified wood, making them especially useful for application in public settings.

Altuntas, Karaogul and Alma [71] studied the effects of fire retardants on the fire, thermal and mechanical properties of wood plastic composites using recycled fibers. They compared the effects of boron-based fire retardants and synergistic influential compounds used in medium-density fiberboard waste (MDFw) filled high-density polyethylene (HDPE) composites. The aim of the study was to improve the use of boron based and fire-retardant materials in wood plastic composite. Fiber waste, HDPE and boron-based compounds were used to produce wood plastic composites. Mechanical thermal and fire properties of the produced composites were investigated. The results pointed out the fact that, when fire retardants were used in composites, the mechanical properties of composite with MAPE increased slightly, also the modulus of elasticity of composites increased considerably. Boron-based fire retardants and other synergistic influential compounds decreased the burning rate and limiting oxygen index (LOI) properties of the composites. The use of the zinc borate in the MDFw-based wood plastic composite had the best results on the mechanical and fire-retardant properties.

Altuntas, Narlioglu and Alma [70] investigated synergic effects of different fire-retardant compounds and zinc borate on wood-plastic composites filled with polypropylene (PP) and medium-density fiberboard (MDF) waste fibers. For this purpose, zinc borate, synergic compounds (antimony trioxide, ammonium phosphate, and magnesium hydroxide), and a coupling agent, i.e., maleic anhydride-grafted polypropylene (MAPP), were used in the production of wood-plastic composites (WPCs). The composite samples were characterized in terms of the burning rate and limiting oxygen index (LOI) analyses, thermal gravimetric analysis (TGA), and differential scanning calorimetry (DSC) along with mechanical tests, i.e., flexural properties, tensile properties, elasticity modulus, and impact strength. It was found that the synergic influence of the combination of zinc borate, antimony trioxide, and magnesium oxide on WPCs increased the heat resistance according to the burning rate, LOI, TGA, and DSC tests. Also, the mechanical properties of the WPCs decreased slightly, but their elasticity modulus increased.

Chu, Mu and Zhang [92] studied the improvement of the W-HT, Populus beijingensis W. Y. Hsu wood properties, using the nitrogen-phosphorus (NP) fire retardant (10% aqueous solution). The effects of the combined NP treatment and HT were also observed. Control groups included native wood and samples from W-HT200 °C,W - 120 min and W-HT220 °C,W- 120 min. The surface color, dimensional stability, and combustion properties of the treated samples were examined. NP pre-treatment intensified the effectivity of HT150 °C, where the treatment time decreased by 75%. The decomposition and catalytic dehydration of NP treatment enhanced the dimensional stability and darkened the wood surface. After HT, the NP fire retardant was transformed from dispersive particles into a uniform layer on the inner surfaces of wood. The heat release rate (HRR) decreased by 60.3% and the residual mass (RM) increased by 61.1% in W (NP, HT) compared to normal W-HT200 °C poplar.

Fu et al. [93] used nanostructured wood hybrids, prepared by clay impregnation into the cell wall, for fire-retardancy. Balsa wood (Ochroma pyramidale) was delignified to form a hierarchically structured and nanoporous scaffold mainly composed of cellulose nanofibrils. This nanocellulosic wood scaffold was impregnated with colloidal montmorillonite clay to form a nanostructured wood hybrid with high flame-retardancy. The nanoporous scaffold was characterized by scanning electron microscopy and gas adsorption. Flame-retardancy was evaluated by cone calorimetry, whereas thermal and thermo-oxidative stabilities were assessed by thermogravimetry. The location of well-distributed clay nanoplatelets inside the cell walls was confirmed by energy-dispersive X-ray analysis. This unique nanostructure dramatically increased the thermal stability because of thermal insulation, oxygen depletion, and catalytic charring effects. A coherent organic/inorganic charred residue was formed during combustion, leading to a strongly reduced heat release rate peak and reduced smoke generation.

Li et al. [94] studied the smart thermo-responsive wood that was developed by depositing thermochromic materials on wood surfaces. The as-fabricated wood composites can reversibly change their colors with the changing temperature. The scanning electron microscope showed that the wood surface was made up of even spherical particles. The attenuated total reflectance Fourier transform infrared spectroscopy spectra demonstrated that the thermochromic materials were successfully settled onto wood surfaces, and the cross-cut test results further proved that all samples can meet general application in the furniture industry. As the concentrations of thermochromic materials increased from 0 to 4.0%, the total color changes (Delta E*) of samples remarkably increased from 1.81 to 39.56, exhibiting a good thermo-responsive property. TG results showed that the sample had the excellent thermal stability below the temperature of 216 A °C. Furthermore, the accelerated UV-aging tests demonstrated that the thermo-responsive property of the samples was highly efficient when it was exposed under the UV irradiation for 100 h.

Lokhande, Chambhare and Jagtap [52] studied synthesis and properties of phosphate-based diacrylate reactive diluent applied to UV-curable flame-retardant wood coating. The diacrylate reactive diluent was synthesized by reacting glycidyl methacrylate, piperazine, and cyclic ethylene chlorophosphate. The synthesized reactive diluent was utilized to formulate UV-curable wood coating. The weight fractions of reactive diluent were varied from 0 to 25% in coating formulation with constant photo initiator concentration. The molecular structure of reactive flame retardant was evaluated by FTIR, mass spectroscopy, (PNMR)-P-31, and (HNMR)-H-1 spectral analysis. The flame-retardant behaviors of the cured film were evaluated from limiting oxygen index and UL-94 vertical burning test. Thermal stability was estimated from thermogravimetric analysis and differential scanning calorimetry. The effects of varying concentrations of reactive diluent on the viscosity of the formulation along with optical, mechanical, and chemical resistance properties of coatings were evaluated. The gel content, water absorption behavior, and stain resistance of coatings were also studied.

Luneva et al. [59] developed a flame retardant for wood impregnation based on a magnesium complex containing phosphorus and nitrogen. As they stated in their work, it considerably reduces the wood loss in fire tests. Application of the flame retardant in an amount of 300 g/m2 allowed preparation of materials with the fire performance corresponding to group I of materials. The mechanism of the fireproofing action of the flame retardant on wood and the thermal degradation of the impregnated wood were further studied.

Gasparik et al. [95] focused flammability characteristics of thermally modified oak wood treated with a fire retardant. The flammability characteristics were determined for oak wood (Quercus robur L.), which was thermally modified at 160, 180, and 210 °C. Subsequently, the thermally modified and unmodified wood was treated with a fire retardant. The effect of the thermal modification (TM) and fire-retardant treatment (FRT) on the weight loss (WL), burning rate (BR), maximum burning rate (MBR), and time to reach the maximum burning rate (TRMBR) were evaluated. The FRT had an expected positive effect on all the flammability characteristics, where the WL, BR, and MBR decreased, and the TRMBR increased. The TM temperature did not have a clear effect. As the TM temperature increased, the WL and BR decreased. The highest differences were found at 160 and 180 °C. As the TM temperature increased for the wood without the FRT, the TRMBR decreased. During the burning of the thermally modified wood with the FRT, the trend was the exact opposite.

Guidice and Canosa [96] in their study formulated, developed, and determined the performance of flame-retardant systems for wood protection. Flame-retardant systems involved wood impregnation and intumescent coating application. The impregnation was made in two retention levels using silanes of low and high hydrophobicity (methyltriethoxysilane and n-octyltriethoxysilane, respectively); these silanes were conducted to polymerize by sol-gel process in wood pores. The intumescent coatings were formulated with a polymeric binder (hydroxy-functional acrylic resin) modified with n-octadecyltriethoxysilane in two w/w ratios to combine the individual characteristics of each film-forming material. In this research, Pinus radiata panels were selected to study the performance of quoted flame-retardant systems. The results indicated excellent flame-retardant performance of some studied systems in two-foot tunnel, in oxygen index cabin, and in horizontal-vertical chamber.

Grzeskowiak [97] studied effectiveness of new wood fire retardants using a cone calorimeter. Analysis was conducted for two preparations, A1 containing guanidine carbonate and A2 with urea, in accordance with the standard ISO 5660-1 and nonstandard method using Mini Fire Tube. Samples of Scots pine (Pinus sylvestris L.) wood were protected using the above-mentioned mixtures applied under vacuum. Recorded results for pine wood impregnated with the tested preparations at a concentration of 15% showed that they have high fire-retardant effectiveness at the intensity of the radiant heat of $35kW/m^2$. An increase in the number of nitrogen atoms in the preparation provides greater fire-retardant effectiveness of the agent.

He et al. [98] used the silica sol (SiO_2 sol) and K_2CO_3 as flame retardants for wood. The synergistic effect of SiO_2 sol and K_2CO_3 on the flame retardancy, leaching resistance, and thermal properties of wood was investigated. The limiting oxygen index results revealed a significant improvement in the flame retardancy and leaching resistance of the wood sample treated with K_2CO_3 and SiO_2 sol using the double bath technique. The thermal analysis results showed that the synergistic effect of K_2CO_3 and the SiO2 sol effectively prolonged the degradation of the wood sample during the charring stage and improved the stability of the char residue. The thermogravimetry-mass spectrometry analysis and scanning electron microscopy results showed that K_2CO_3 catalyzed the degradation reaction of the wood sample at lower temperatures resulting in an increase in the water and carbon dioxide output, and the SiO_2 sol formed a compact and melted barrier on the surface of the char residue, which hindered the transfer of heat and combustible gases in the condensed phase. Thus, the combination of K_2CO_3 and SiO_2 sol they proved to be a promising flame-retardant system for wood.

Milanko et al. [99] used the sodium silicate as a fire-retardant coating of wood. The aim of study was to determine the resistance to flame action of wood coated with protective material alkaline silicates (water glasses).

Mitterova, Zachar and Majlingova [100] focused the assessment of the chemical substance with fireproof function application effect on the thermal resistance of spruce wood. The results showed the change in effect of the protective substance at varying concentration and method of application (coating, retting), and thus also the different values of observed variables (weight loss, time of ignition) of tested spruce samples.

Wang et al. [101] investigated the effects of water bath temperature, dye concentration, flame retardant concentration and dipping time on dye uptake and limited oxygen index of simultaneously dyed and fire-retardant-treated fast-growing poplar wood veneer. Through comprehensive analysis, an improved process was obtained and wood with these improved properties was prepared. Analyses of chemical structure and thermal stability of prepared wood samples were conducted, as well as crystallinity and microscopic morphologies using Fourier transform infrared spectroscopy, thermogravimetric, plus X-ray diffraction and scanning electron microscopy and energy-dispersive X-ray spectroscopy. Results showed that dye uptake and limited oxygen index had a similar increasing tendency with increased water bath temperature and dipping time. Moreover, dye uptake improved upon addition of flame retardant, while limited oxygen index decreased as dye concentration increases. Flame retardant combined with the wood fiber and was in the absence of chemical reaction with the dye used. Dye and flame-retardant molecules diffused into the cell cavity, wood vessel and aperture. Furthermore, the fire-retardant properties and crystallinity of wood simultaneously treated with dye and flame retardant were both improved.

Wu, Wang and Guo [102] studied the synergistic flame-retardant effects of different zeolites on intumescent fire-retardant coating for wood. To investigate the fire-retardant properties of intumescent fire-retardant coatings of wood modified by different zeolites, tests were conducted by a cone calorimeter with poplar samples whose surfaces were covered by an intumescent fire-retardant coating modified by 3A, 4A, 5A, 13X zeolites, respectively. Results indicated that the ignition time (TTI) of the intumescent fire-retardant coating modified by 3A zeolite was prolonged 120 s, while the total smoke production (TSP) increased 60.1% as compared with the untreated group. The intumescent fire-retardant coating modified by the 13X zeolite had a smaller smoke production rate (SPR) and was the last to reach the peak-SPR. Its TSP remained in a very low state until 410 s and decreased 25%. Thus, 3A zeolite and 13X zeolite were of complementarily synergistic effects on improving the fire-retardant properties of an intumescent fire-retardant coating for wood. They suggested the alternative types of zeolites for flame-retardant coatings.

Zhang et al. [103] studied effect of biochar on mechanical and flame-retardant properties of wood. Biochar/wood/plastic composites were prepared with different biochar content by the extrusion method, and the mechanical properties and flame-retardant properties were tested. They indicated that with the increase of biochar content, the mechanical properties of the composites tended to rise at first and then fell. They also found that the appropriate amount of biochar can promote the mechanical properties of the biochar/wood/plastic composites. Both $Mg(OH)_2$ and $Al(OH)_3$ could improve the flame-retardant properties of the material evidently. $Mg(OH)_2$ obtained better results than $Al(OH)_3$. When the adding amount of $Mg(OH)_2$ is 40 wt%, the flame-retardant effect is the best. $Al(OH)_3$ can reduce the mechanical properties of the material, while $Mg(OH)_2$ could evidently promote the tensile strength and impact resistance strength of the material.

4. Fabrics flame-retardant treatment

Fabrics play an important role in everyday life. One of their main drawbacks refers to their structure, as they are mainly made of organic polymers, which conversely, if not inherently flame-retarded, they are flammable and potentially dangerous. The ease of flammability of fabrics has been faced by designing and synthesizing suitable flame retardants, i.e., additives that are able to suppress or delay the appearance of a flame and/or reduce the flame-spread rate (flame retardants) or delaying ignition or reducing the rate of combustion when needed (fire retardants).

Depending on the chemical composition and on their thermal and fire properties, textile fibers and fabrics need substances such as halogen, sulfur, phosphorus, nitrogen, boron, metals, etc. to attain flame retardancy [104, 105]. These additives can be directly introduced into synthetic fibers during the spinning process or can be deposited on the synthetic or natural fiber/fabric surface [106, 107].

These surface treatments can be performed either using finishing or coating techniques: the former involve the impregnation of the fabric in a solution/stable suspension of the flame-retardant additive; the latter involve the application of a continuous or discontinuous layer/film on both the outer surface and back of the fabric [51].

Further, we introduce results of current research focusing the fabrics flame retardants issue.

Cayla et al. [108] introduced, that the possible way to improve sustainable development for the textile industry is using the bio-based polymers to replace the polymers from petrochemicals in the manufacture of textile fibers. Polylactic acid (PLA) is one of the available bio-based polymers. A way to improve the fire behavior of this bio-based polymer is to add an intumescent formulation mainly composed of acid and carbon sources. To optimize the amount of bio-based product in the final material composition, lignin from wood waste can be used as the carbon source.

Chen et al. [109] focused on development and further application of intumescent flame-retardant and self-healing superhydrophobic coatings on cotton fabric. While, the flame-retardant and self-healing superhydrophobic coatings are fabricated on cotton fabric by a convenient solution-dipping method, which involves the sequential deposition of a trilayer of branched poly(ethylenimine) (bPEI), ammonium polyphosphate (APP), and fluorinated-decyl polyhedral oligomeric silsesquioxane (F-ROSS). When directly exposed to flame, such a trilayer coating generates a porous char layer because of its intumescent effect, successfully giving the coated fabric a self-extinguishing property. Furthermore, the F-POSS embedded in cotton fabric and APP/bPEI coating produces a superhydrophobic surface with a self-healing function. The coating can repetitively and autonomically restore the superhydrophobicity when the superhydrophobicity is damaged. The resulting cotton fabric, which is flame-resistant, waterproof, and self-cleaning, can be easily cleaned by simple water rinsing. Thus, the integration of self-healing superhydrophobicity with flame retardancy provides a practical way to resolve the problem of washing durability of the flame-retardant coatings. The flame-retardant and superhydrophobic fabric can endure more than 1000 cycles of abrasion under a pressure of 44.8 kPa without losing its flame retardancy and self-healing superhydrophobicity, showing potential applications as multifunctional advanced textiles

Chan et al. [33] synthesized the series of boron-nitrogen polymers (PEIPAs) to provide a green alternative for flame retardant finishing on cotton fabrics.

Cheng et al. [110] applied a novel phosphorus-rich hybrid organic-inorganic silica coating for improving the flame retardancy of silk fabric, which was prepared using naturally occurring phytic acid as phosphorus precursor and catalyst for the hydrolysis of tetraethoxysilane. In addition, they added three silane coupling agents in the hybrid sol as cross-linkers, with the aim of developing hydrophobic coatings and improving the washing durability of the treated silk fabric.

Dong et al. [34] successfully synthesized a novel antibacterial and flame-retardant agent, monochlorotriazine triethylphosphite guanidine (MCTPG). The chemical structure of MCTPG was characterized by FTIR and H-1 NMR. The flame retardancy of treated cotton fabric was evaluated by limiting oxygen index (LOI), the vertical burning test and cone calorimeter, respectively. The treated cotton fabric obtained good flame retardancy with a LOI value of 31.2%, and the char length decreased to 8.5 cm. The ignition time increased, and the values of total heat release, heat release rate, mass loss decreased. The thermal stability and surface morphology of treated cotton fabric were investigated by thermogravimetric analysis and scanning electron microscope (SEM), respectively. The results showed that MCTPG played a protective role in the degradation of cotton fabrics, hindered the formation of volatile species and favored the formation of char. Furthermore, the antimicrobial activity of treated cotton fabrics was tested. And it showed that the inhibition zone of the treated cotton fabrics base to Escherichia coli and Staphylococcus aureus reached to 2.9 mm and 2.8 mm, respectively.

Feng et al. [111] synthesized a plant-based non-formaldehyde flame retardant containing high phosphorus ammonium phytate (APA) for cotton fabric. The char length of treated cotton sample decreased to 31 mm from the original 300 mm. The LOI value of finished cotton fabric was of 43.2%, and after 30 laundering cycles, it remained of 30.5%, suggesting that APA could be used as an effective semi-durable flame retardant. The TG analysis in air demonstrated that the thermal oxidation stability of treated fabric was significantly improved. Cone calorimetry results showed that the peak of heat release rate and total heat release of treated sample reduced obviously, comparing with reference sample. The SEM morphologies suggested that the APA molecule penetrated the inner space of cotton fibers. FTIR spectra implied the APA molecule grafted onto cotton fibers. Then, the effective flame-retardant APA has significant potential in practical application.

Jimenez et al. [112] studied an innovative way to improve fire-retardant properties of different polymers by applying intumescent coatings on their surface has been studied. Two polymers have been investigated: polypropylene and polycarbonate. The surfaces were first subjected to a flaming treatment to clean them and to increase their wettability and thus improve the adhesion of the coatings. Two different formulations were then applied: a transparent intumescent varnish, based on an acrylic resin, and an intumescent coating based on polyvinyl acetate resin. Different parameters have been obtained using several fire tests. The cone calorimeter, the limiting oxygen index and UL94 tests have been carried out to evaluate the fire-retardant properties obtained for both the intumescent coating and the intumescent varnish. Results clearly showed an outstanding improvement of the fire-retardant properties using intumescent coatings without any incorporation of flame retardants in the bulk.

Liu et al. [113] tested and evaluated the combustion performances of pure cotton fabric, respectively, enriched with graphene oxide, phosphorus-doped graphene oxide, and nitrogen-doped graphene oxides. The results show that phosphorus-doped graphene oxide acts as the most promising flame retardant, which can effectively reduce the burning rate and heat release rate of the combustion process, with excellent smoke suppression effect. Based on the relevant parameters obtained from the experimental results of phosphorus-doped graphene oxide, Simtec simulation was performed to demonstrate vertical combustion of thin fabric before and after flame-retardant treatment, and the results were consistent with the trend of the experimental results and suggest a magnifying effect of phosphorus-doped graphene oxide.

Rehan et al. [114] addressed an innovative approach for benign development of environmentally synthesis of chitosan-based nanocomposite. The synthesis involved the inclusion via interaction of AgNPs and clay with chitosan (Cs) giving rise to Cs/AgNPs and Cs/AgNPs/clay nanocomposites which when applied independently induce super functionalities. Comparison was made among the two nanocomposites with respect to their intimate association with the in-depth cotton fiber-fabric surfaces and the onset of this on the multi-functionalization of cotton fabrics. They emphasized that Cs/AgNPs/clay nanocomposites prove unequivocally that its use in one-step treatment process for cotton fabrics results in imparting very appreciable good technical properties which, in turn, are reflected on all the gained functionalities of cotton fabrics: high strength, uniform morphology, increased thermal stability, successful deposition of the composite on the surface of cotton fabrics, high water absorption, antimicrobial activity, flame retardant, controlled release of fragrance and UV protection. The data obtained indicated that the treatment for cotton fabrics with these nanocomposites is stable against washing even after 20 washing cycles. Based on encourage data, the environmental benign synthesis of Cs/AgNPs/clay nanocomposites was considered as a promising nanocomposite for the multifunctional finishing textiles.

Shan et al. [115] prepared and tested a novel flame-retardant monomer DDPSi-FR, containing organophosphorus and silicon. The chemical structure of DDPSi-FR was characterized by Fourier transform infrared spectroscopy (FT-IR) and X-ray photoelectron spectroscopy (XPS). Subsequently, after treating the wool fabrics, the effects of the monomer on the flame retardancy, thermal stability, and mechanical properties were studied. The flame retardant and thermal properties were evaluated by conducting vertical flame tests, limiting oxygen index (LOI) determination, and thermogravimetric analysis (TGA). The results showed that improved flame retardancy and thermal stability were achieved. Notably, the flame retardancy was retained even after 15 washing cycles. The mechanical properties were evaluated using the bursting strength, and the results indicated that DDPSi-FR treatment improved the breaking strength.

Zope et al. [116] reported on the development of water-based flame-retardant coating based on phosphonitrogen combination for cotton fabrics. A one-step spray-on process was employed to coat the fabrics by taking advantage of the spontaneous reaction between para-phenylenediamine (PDA) and tetrakis (hydroxymethyl) phosphonium chloride (THPC) resulting in an instantaneous precipitation of poly[1,4-diaminophenylene-tris(dimethyl hydroxymethyl)phosphine] (PApP) on the fabric surface. The effectiveness of PApP in improving the flame-retardant properties like ignition resistance and lateral flame spread were evaluated in accordance with ASTM D6413 and BS EN ISO 15025 flammability tests. Despite the early (thermal) decomposition, the onset for coated fabrics under both oxidative and pyrolytic conditions, remarkably the self-extinguishing behavior (<3 s) without any lateral flame spread was observed. Possible reaction scheme was also proposed to correlate flame retardant mechanism of the coated fabrics with the observations. Additional analysis via pyrolysis combustion flow calorimetry and vertical flame testing before and after washing showed that flame retardant efficiency did decrease with washing, but the overall performance was still promising.

Zhang et al [117] developed a method to impart polyacrylonitrile (PAN) fabric durable flame retadancy. PAN fabric was modified with hydroxylamine hydrochloride (HA) to prepare amidoxime PAN fabric (A-PAN) followed by phosphorylation with phosphoric acid (PA) to obtain flame-retardant PAN fabric (P-A-PAN). Thermogravimetric (TG) analysis, differential scanning calorimetry (DSC), microscale combustion calorimetry (MCC) and pyrolysis-gas chromatography-mass spectrometry (Py-GC/MS) were used to analyze the thermal degradation process and flame-retardant mechanisms. The structure of the fabrics was characterized by Fourier transform infrared spectroscopy (FTIR) and X-ray Photoelectron Spectroscopy (XPS). The surface morphology of fabrics was observed by scanning electron microscope (SEM). Moreover, the flame retardancy of fabrics before and after washing was evaluated by Limiting oxygen index (LOI) and horizontal burning test. The results showed that the P-A-PAN possessed an excellent thermal stability with the highest LOI value of 34.1% and the highest char residue of 55.67% at 800 °C. Most importantly, the P-A-PAN possessed a wonderful flame-retardant durability with a little decrease of LOI after 20 washing cycles. When they were ignited, the P-A-PAN fabrics before and after washing were both nonflammable due to the char residue formation of modified fabric.

5. Polyurethane foam flame-retardant treatment

Recent trends in flame retardancy of polyurethane foams (PUR) and, in general of polymers, have been deeply influenced by regulation requirements and by the concept of "sustainable development" which implies that the fire retardants should present a low impact on human health and environment during the whole life cycle of the polymer; it concerns then also the toxicity and the density of smoke developed during burning of the materials. Therefore, the reduction of the amounts of brominated compounds used in flame retardancy formulations is one of the main aims of the research in this field, although this reduction is not very easy because of their very high effectiveness [118].

Modesti et al. [118] reviewed and discussed novel halogen-free flame-retardant systems for polyurethane foams. They studied the charring compounds which may lead to the development of different char morphologies: compact, intumescent and "glassy-like" char layers. The advantages and disadvantages of each system on fire behavior and thermal stability of polyurethane foams was analyzed. Attention was put on possible synergistic effects arising from suitable mixing of them. In the flame retardants analyses, there were involved the phosphorus-based compounds (phosphates, elementary phosphorous and novel hypophosphites), intumescent systems (for example expandable graphite) as well as glass precursors like borates, alumino-silicates and glass modifiers. The recent interest in nanocomposites, potential application and benefits of layered silicates on fire behavior and thermal stability of PUR foams was also reported. To assess the effectiveness of the systems considered in enhancing the fire behavior and thermal stability, PUR and PIR-PUR (polyisocyanurate-polyurethane) foams containing different amounts of them were prepared and tested in several ways. The thermal stability, both in inert and oxidizing atmosphere, and fire behavior through the limiting oxygen index (LOI) and use of cone calorimeter (CC) were analyzed. Some results of SBI (Single Burning Item) test were also reported. Also, the char morphology and composition were studied using scanning electron microscope (SEM) and elementary analysis (EDX, Energy Dispersive X-ray spectroscopy).

Yang and Nelson [65] developed flame retardant flexible polyurethane foams through four different approaches including the utilization of inorganic flame retardant, phosphorus-containing flame retardants, a combination of phosphorus compounds and inorganic additives, and the combination of phosphorus compounds and reactive silicone. Cone calorimetry results of the obtained flexible foams strongly supported "synergism" among the combined systems. With 15 pbw of phosphorus flame-retardant, Antiblaze (R) 230, an alkyl arylphosphate/phosphonate, in PUR, the peak heat release rate was reduced by 23% However, the combined use of Antiblaze (R) 230 with zinc stannate (ZS) reduced the PHRR of the resulting PUR foams by over 40%. Moreover, the combined use of ZS or zinc hydorxystannate (ZHS) with Antiblaze (R) 230 significantly reduces smoke generation. Flame retardant flexible foams are also successfully obtained with functionalized silicone component, and with the combination of silicone and phosphorus-containing flame retardant, which follow a different flame-retardant mechanism.

Hu and Wang [119] prepared two series of polyisocyanurate polyurethane (PIR PUR) foams (i.e., EG foams filled with different amounts of EG alone and APEG foams containing different amounts of expanded EG and APP), using expandable graphite (EG) and ammonium polyphosphate (APP) as flame retardants, and evaluated the effect of the additives on the physical mechanical property, fire behavior and thermal stability of the foams based on compressive strength test, limiting oxygen index (LOI), cone calorimeter test, thermogravimetric analysis (TGA) and scanning electron microscopy (SEM). The addition of EG alone or both EG and APP into the foam greatly influences the physical mechanical property. The compressive strength of APEG foams was closely related to the apparent density. The LOI value showed good improvement in both EG and APEG foams. The addition of APP in APEG foams gave better fire behavior than the EG foams with an obvious decrease in PHRR and increase in residue. In addition, the TGA curves illustrated that APP might be an effective charring agent to promote char formation. The SEM results showed that the incorporation of APP and EG allowed the formation of a cohesive and dense char layer, which inhibited the transfer of heat and combustible gas and increased the thermal stability of PIR-PUR.

Chen and Jiao [26] studied smoke suppression properties and synergistic flame-retardant effect of ferrite yellow (FeOOH) on flame retardant thermoplastic polyurethane (TPU) composites, using ammonium polyphosphate (APP) as a flame-retardant agent. Smoke suppression properties and synergistic flame-retardant effect of FeOOH on flame retardant TPU composites were intensively investigated by smoke density test (SDT), cone calorimeter test (CCT), scanning electron microscopy (SEM), and thermal-gravimetric analysis (TGA). Remarkably, the SDT results showed that FeOOH can effectively decrease the amount of smoke production with or without flame. On the other hand, the CCT data revealed that the addition of FeOOH can apparently reduce heat release rate (HRR), total heat release (THR), and total smoke release (TSR), etc. Here, Fe0OH was an effective smoke suppression agent and a good synergism with APP in flame retardant TPU composites, which can greatly improve the structure of char residue realized by TGA and SEM results.

Liu et al. [120] successfully synthesized three types of ferrites zinc ferrite, copper ferrite and nickel ferrite via coprecipitation. The morphology of ferrites and foams was studied by X-ray diffraction (XRD), transmission electron microscopy and scanning electron microscopy. The flame retardancy and potential smoke and toxicity suppression effects of ferrites on flame-retardant polyurethane-polyisocyanurate (FPUR-PIR) foams with dimethylmethylphosphonate and tris (2-chloropropyl) phosphate were investigated by thermogravimetric analysis (TG), limiting oxygen index, smoke density rating (SDR), cone calorimeter and X-ray photoelectron spectroscopy. Meanwhile, the detailed reaction between ferrite and phosphonate, ferrite and polyurethane-polyisocyanurate was examined by thermogravimetry coupled with FTIR spectrophotometry, XRD, TG and FTIR. The results showed that ferrites significantly decreased the smoke production of FPUR-PIR, and reduced SDR per unit mass by 25.1-41.6 %. Notably, ZnFe2O4 (ZF) showed an excellent performance in smoke and toxicity suppression in this study. Moreover, ZF not only can restrained the release of groups containing phosphorus and kept more P in condensed phase, but also can accelerated the dehydration of PUR-PIR and facilitated the crosslinking of pyrolysis fragments to form thermal oxidation stable char layer. This study has provided insight into possible modes of smoke and toxicity suppression action in FPUR-PIR incorporated ferrites.

Liu, He, Yang [56] prepared a series of flame-retarded PIR-PUR foams, using a novel phosphorus containing flame retardant, 9,10-dihydro-9-oxa-10-phosphaphenanthrene 10-oxide (DOPO)-Mg. The thermal stability and pyrolytic gases of the PIR-PUR foam with and without DOPO-Mg were detected by TG and TGA-FTIR. The results indicated that DOPO-Mg can significantly reduce the combustible gases released during decomposition of the PIR-PUR foams, such as carbonyl group containing, methyl and methylene containing flammable gas. The Py-GC-MS results proved that DOPO-Mg changed the thermal degradation process of the PIR-PUR foam and prevented a highly toxic flammable gas from being generated. The flame retardancy of the PIR-PUR foams was tested using the LOI and cone calorimeter test. The LOI and heat release rate values of the PIR-PUR sample without DOPO-Mg were 21.2 % and 190.7 kW/m^2, respectively. 25 phr DOPO-Mg incorporation into the PIR-PUR foam resulted in a LOI value of 23.2 %. In addition, 5 phr DOPO-Mg incorporation into the PIR-PUR foam resulted in a peak heat release rate of 154.9 kW/m^2. The foams with DOPO-Mg showed more compact residues. The SEM test showed that spherical material formed on the surface of the char to hinder flame and heat transmission, which can be used to explain the flame-retardant effect.

Liu et al. [121] also investigated the catalysis of boron phosphate (BP) on the thermal stability and char forming in flame-retardant PUR-PIR foams with dimethylmethylphosphonate (DMMP) and tris(2-chloropropyl) phosphate (TCPP). The flame-retardant performance and thermal stability of FPUR-PIR were evaluated by cone calorimetry (CONE), thermogravimetric analysis (TG) and microscale combustion calorimetry (MCC). Gas-phase products of FPUR-PIR during the thermal decomposition were investigated via thermogravimetric analyzer coupled with FTIR and mass spectrometry (TG-FTIR-MS). Elemental composition and content of the charred layer in detail were analyzed by X-ray photoelectron spectroscopy (XPS). It was observed that the incorporation of 3 mass% BP in FPUR-PIR decreases the heat release rate, total smoke released and CO production. Meanwhile, the addition of 3 mass% BP advances the release of gaseous products and lower the production of smoke and toxic products like -NCO compounds, PO* and cyanic acid in the gas phase. It can accelerate the dehydration of hydroxyl compounds and promote the char formation of -NCO compounds. This can improve the thermal and oxidation resistance of condensed phase. The catalytic behavior of the dehydration and char formation of BP in the thermal degradation of FPUR-PIR is attributed to Bronsted and Lewis acidic sites on BP.

Lorenzetti et al. [122] compared several expandable graphites (EGs), differing in expansion volume but with the same mean size, used as flame retardants in polyurethane (PUR) foams. Not only common sulfur-intercalated graphites were investigated, but also a new one intercalated with phosphorus. They studied the properties of EG, which are important for its flame retardancy effectiveness in PUR foams. Thermal stability, flammability, and fire behavior were analyzed through limiting oxygen index and cone calorimeter tests. Detailed characterization of the phosphorus-intercalated graphite was also provided as well as physical-mechanical characterization. The results showed that the well-known sulfur-intercalated graphites and the one with phosphorus both enhance the residue yield, induce a protective layer, and thus efficiently flame-retard PUR foams. While the expansion volume of the EGs had a surprisingly limited influence on the performance of the foams, at least in the range tested, the most important feature controlling the effectiveness of EG in terms of flame retardant PUR foams was the type of intercalant. The presence of EG affected the physical-mechanical properties of the foams; however, no significant effect of the expansion volume or intercalant type has been revealed on the physical-mechanical properties of the foams.

Yue et al. [123] focused the utilization of sustainable forestry waste resources in the production of polyurethane (PU) foam, which seems to be a promising green alternative to the use of un-sustainable resources. They reported the liquefaction of waste pine wood at different reaction temperatures and its application in synthesizing a melamine phosphate modified wood type polyurethane foam (designated as MWPU). Their strategy was to obtain liquefied pine-based polyol at an optimum reaction temperature and apply the polyol in synthesizing a flame retardant (MWPU) foam via the incorporation of a melamine phosphate (MP) filler. Spectroscopic and microscopic analyses were conducted to investigate the structure characteristics and the morphology of the liquefied waste pine wood polyol and the synthesized (MWPU) foam. An optimum liquefaction temperature of 160 °C was obtained and the glass transition temperature (T-g) for 10 wt% incorporated MP foam was 43.8 °C. The as-prepared

(MWPU) foam showed higher glass transition temperature and storage modulus than pine wood-based PU foam without MP. The MWPU foam withstood heating at 300 °C without significant degradation and exhibited a higher thermal stability and limited oxygen index (LOI) value than pine wood-based PU foam. These results provided an insight into the physical and structural properties of the as-prepared bio-based foam and paved the way toward preparing bio-based PU foam, which could further expand its potential applications.

Byard et al. [32] used the phosphorus-containing epoxides to generate several oligomeric polyether diols, which were in turn utilized in the preparation of model polyurethane (PU) samples, either as comonomers in the polymerization (Prep samples) or solvent blended into a priori prepared PU (Blend samples). The resultant samples were evaluated for heat release reduction potential using micro combustion calorimetry. Several variables were investigated in the oligomerization of the original epoxides, such as presence of initiator, epoxide comonomer, and solvent. The oligomer mixtures were thoroughly characterized, using NMR, mass spectrometry (MS), elemental analysis, and viscosity measurements. The final PU Prep samples were carefully analyzed to demonstrate and evaluate the degree of chemical incorporation of the polyether diols into the PU main chain. Results from the heat release studies demonstrated that incorporation of the phosphorus-containing diol did lower flammability, but the structure of the original epoxide, as well as the oligoimerization conditions, influenced heat release reduction.

Eceiza et al. [72] reported on the fire behavior of isophorone diisocyanate-based polyurethane foams containing different conventional flame retardants (FRs) such as melamine, ammonium polyphosphate, aluminum hydroxide, expandable graphite, and their combinations. The foams were obtained in a laboratory scale and characterized in terms of their morphology, density, thermal stability, and fire behavior. According to atomic force microscopy, the incorporation of FRs decreased the phase separated domain size. The cellular structure of the foams was examined qualitatively by scanning electron microscopy while the quantitative analysis of the surrounding skin was performed by optical microscopy and Image J. The flame retardant containing foams showed more and smaller cells. The thermogravimetric analysis showed that the flame retardants had no influence in the initial degradation temperature of the foams. However, the obtained residue values were higher than the theoretical ones, indicating that there was some type of interaction between the flame retardants and the foams. The fire behavior of polyurethane foams was studied by the cone calorimeter and the data showed that the introduction of expandable graphite and combinations of ammonium polyphosphate/melamine to the reference foam gave rise to a significant reduction in the total heat release.

Wang et al. [124] synthesized and characterized a phosphorous-nitrogen intumescent flame-retardant, 2,2-diethyl-1,3-propanediol phosphoryl melamine (DPPM) by Fourier transform infrared spectroscopy and nuclear magnetic resonance. Flame-retardant rigid polyurethane foams (RPUFs) with DPPM (DPPM-RPUF) as fire-retardant additive were prepared. Scanning electron microscope (SEM) and mechanical performance testing showed that DPPM exhibited a favorable compatibility with RPUF and negligibly negative influence on the mechanical properties of RPUF. The flame retardancy of DPPM on RPUF was investigated by the limiting oxygen index (LOI), vertical burning test and cone calorimeter. The LOI of DPPM-RPUF could reach 29.5%, and a UL-94V-0 rating was achieved, when the content of DPPM was 25 php. Furthermore, the DPPM-RPUF exhibited an outstanding water resistance that it could still obtain a V-0 rating after water soaking. Thermogravimetric analysis showed that the residual weight of RPUF was relatively low, while the charring ability of DPPM-RPUF was improved greatly. Real-time Fourier transform infrared spectroscopy was employed to study the thermo-oxidative degradation reactions of DPPM-RPUF. The results revealed that the flame-retardancy mechanism of DPPM in RPUF was based on the surface charred layer acting as a physical barrier, which slowed down the decomposition of RPUF and prevented the heat and mass transfer between the gas and the condensed phases.

6. Conclusions

The paper gives an overview on current state of research focusing the flame retardancy of natural and synthetic polymers, especially wood and wood composites, several fabrics, as well as PU/PUR foams. It was created as a compilation of current scientific works included in Web of Science database. In compilation totally 124 literature sources were involved.

Acknowledgments

This work was supported by the VEGA Grant Agency under projects No. VEGA 1/0493/18 (25%); No.1/0387/18 (25%), the Slovak Research and Development Agency under the Agreements No. APVV-16-0326 (25%) and No. APVV SK-CN-2017-0018 (25%).

References

[1] Luo, F., Wu, K., Li, Y. et al. 2015. Reactive flame retardant with coreshell structure and its flame retardancy in rigid polyurethane foam. J. Appl. Polym. Sci. 132 (2015) 42800–42808.

[2] Xu, .Z., Liu, L., Wang, SQ., Hu, Y. 2015. Synergistic effect of expandable graphite and aluminum hypophosphite on flame-retardant properties of rigid polyurethane foam. J. Appl. Polym. Sci. 132 (2015): 42842–42851.

[3] Xu, W., Wang, G., Zheng, X. 2015. Research on highly flame-retardant rigid PU foams by combination of nanostructured additives and phosphorus flame retardants. Polym. Degrad. Stab. 111 (2015): 142–150.

[4] Alongi, J., Carletto, RA., Di Blasio, A. et al. 2013. Intrinsic intumescent-like flame retardant properties of DNA-treated cotton fabrics. In Carbohydr. Polym. 96 (2013): 296–304.

[5] Reddy, PRS., Agathian, G., Kumar, A. 2005. Ionizing radiation graft polymerized and modified flame-retardant cotton fabric. Radiat. Phys. Chem. 72 (2005): 511–516.

[6] Chen, DQ., Wang, YZ., Hu, XP., et al. 2005. Flame-retardant and anti-dripping effects of a novel char-forming flame retardant for the treatment of poly(ethylene terephthalate) fabrics. Polym. Degrad. Stab. 88 (2005) 349–356.

[7] Didane, N., Giraud, S., Devaux, E. 2012. Fire performances comparison of back coating and melt spinning approaches for PET covering textiles. Polym. Degrad. Stab. 97 (2012) 1083–1089.

[8] Phanphanich, M., Mani, S. 2011. Impact of torrefaction on the grindability and fuel characteristics of forest biomass. Bioresource Technology, 2011, 1029(2): 1246-1253.

[9] Stapleton, HM., Klosterhaus, S., Eagle, S. et al. 2009. Detection of organophosphate flame retardants in furniture foam and U.S. House Dust. Environ. Sci. Technol. 43 (2009) 7490–7495.

[10] Suppakarn, N., Jarukumjorn, K. 2009. Mechanical properties and flammability of sisal/ PP composites: effect of flame retardant type and content. Compos. B Eng. 40 (2009) 613–618.

[11] Cequier, E., Marce, RM., Becher, G., Thomsen, C. 2013. Determination of emerging halogenated flame retardants and polybrominated diphenyl ethers in serum by gas chromatography mass spectrometry. J. Chromatogr. A 1310 (2013) 126–132.

[12] Li, WL., Liu, LY., Song, WW. et al. 2016. Five-year trends of selected halogenated flame retardants in the atmosphere of Northeast China, Sci. Total Environ. 539 (2016) 286–293.

[13] Stieger, G., Scheringer, M., Ng, CA., Hungerbuhler, K. 2014. Assessing the persistence, bioaccumulation potential and toxicity of brominated flame retardants: data availability and quality for 36 alternative brominated flame retardants. Chemosphere 116 (2014) 118–123.

[14] Bongiovanni, R., Turcato, EA., Di Gianni, A., Ronchetti, S. 2008. Epoxy coatings containing clays and organoclays: effect of the filler and its water content on the UV-curing process. Prog. Org. Coat. 62 (2008) 336–343.

[15] Kemmlein, S., Herzke, D., Law, RJ. 2009. Brominated flame retardants in the European chemicals policy of REACH-Regulation and determination in materials. J. Chromatogr. A 1216 (2009) 320–333.

[16] Malucelli, G. 2016. Surface-Engineered Fire Protective Coatings for Fabrics through Sol-Gel and Layer-by-Layer Methods: An Overview. Coatings 2016, 6(33): 23 p; doi:10.3390/coatings6030033.

[17] Qiu, X., Li, Z., Li, X., Zhang, Z et al.. 2018. Flame retardant coatings prepared using layer by layer assembly: A review. In Chemical Engineering Journal 334(2018): 108–122.

[18] Bourbigot, S., Duquesne, S. et al. 2007. Fire retardant polzmers>recent development and opportunities. J. Mat. Chem., 2007, 17: 2283-2300).

[19] Wu, Q., Zhang, Q., Zhao, L et al. 2017. A novel and facile strategy for higly flame retardant polymer foam composite materials: Transforming silicohne resin coating into silica self-extinguishing layer. Journal of Hazardous Materials, 2017, 336: 222-231.

[20] Chen, MJ., Chen, CR, Tan, Y. et al. 2014. Inherently flame-retardant flexible polyurethane foam with low content of

phosphorus/containing cross/linking agent. Ind. Eng. Chem. Res., 2014, 53: 1160-1171.

[21] Ding, H., Xia, C., Wang, J. et al. 2016. Inherently flame-retardant flexible bio-based polyurethane sealant with phosphorus asnd nitrogen-containing polyurethane prepolymer. J. Mater. Sci, 2016, 51: 5006-5015.

[22] Ruan, CP., Shen, MX, Ren, XY et al. 2016. A versatile and scaleable approach toward robust superhydrophobic porous materials with excellent absorbency and flame retardancy. Sci. Rep., 2016, 6.

[23] Liang, S., Neisius, NM., Gaan, S. 2013. Recent developments in flame retardant polymeric coatings. Prog. Org. Coat., 2013, 76: 2533-2542.

[24] Han, J., Liang, G., Gu, A. et al. 2013. A novel inorganic-organic hybridized intumescent flame retardant and its super flame retarding cyanate ester resins. J. Mat. Chem., 2013, A1: 2169-2182.

[25] Cequier, E., Ionas, AC., Covaci, A. et al. Occurrence of a Broad Range of Legacy and Emerging Flame Retardants in Indoor Environments in Norway. Environmental Science & Technology, 2014, 48(12): 6827-6835.

[26] Chen, XL., Y. Jiang, YF., Jiao, CM. 2014. Smoke suppression properties of ferrite yellow on flame retardant thermoplastic polyurethane based on ammonium polyphosphate. Journal of Hazardous Materials, 2014, 266: 114-121.

[27] Yang, H., Wang, X., Song, L. et al. 2014. Aliminum hypophosphite in combination with expendable graphite as a novel flame retardant system for rigid polyurethane foams. Polym. Adv. Technol., 2014, 25: 1034-1043.

[28] Zhang, M., Luo, Y., Zhang, J. et al. 2015. Effects of a novel phosphorus-nitrogen flame retardant on rosin-based polyurethane foams. Polym. Degrad. Stab., 2015, 120:427-434.

[29] Elvira-Leon, JC., Chimenos, JM., Isabal, C. et al. 2016. Epsomite as flame retardant treatment for wood: Preliminary study. Construction and Building Materials, 2016, 126: 936-942.

[30] Qiu, S., Wang, X., Yu, B. et al. Flame-retardant - wrapped polyphosphazene nanotubes: A novel strategy for enhancing the flame retardancy and smoke toxicity suppression of epoxy resins. Journal of Hazardous Materials, 2017, 325: 327-339.

[31] Altuntas, E., Narlioglu, N., Alma, M. H. 2017. Investigation of the Fire, Thermal, and Mechanical Properties of Zinc Borate and Synergic Fire Retardants on Composites Produced with PP-MDF Wastes. Bioresources, 4: 6971-6983.

[32] Byard, B., Wang, K., Morgan, A. et al. 2018. New polyether diols as flame retardants for polyurethane: Derivatives of epoxy-functionalized phosphonates and phosphates. Fire and Materials, 42(1): 3-17.

[33] Chan, SY., Si, LP., Lee, KI.et al. 2018. A novel boron-nitrogen intumescent flame retardant coating on cotton with improved washing durability. Cellulose, 25(1): 843-857.

[34] Dong, CH., He, PS., Lu, Z. et al. 2018. Preparation and properties of cotton fabrics treated with a novel antimicrobial and flame retardant containing triazine and phosphorus components. Journal of Thermal Analysis and Calorimetry, 2018, 131(2): 1079-1087.

[35] Kiliaris, P., Papaspyrides, CD. 2010. Polymer/layered silicate (clay) nanocomposites: An overview of flame retardancy. Progress in Polymer Science, 2010, 35(7): 902-958.

[36] Lewin, M., 2011. Flame retarding polymer nanocomposites: synergism cooperation, antagism. Polym. Degrad. Stab., 2011, 96: 256-269.

[37] Gu, H., Guo, J., He, Q. 2013. Flame -retardant epoxy resin nanocompositesd reinforced with polyaniline-stabilised silica nanoparticles. Ind. Eng. Chem. Res., 2013, 52: 7718-7728.

[38] Yuan, BH., Bao, CL. Song, L. et al. 2014. Preparation of functionalized graphene oxide/polypropylene nanocomposite with significantly improved thermal stability and studies on the crystallization behavior and mechanical properties. Chemical Engineering Journal, 2014, 237: 411-420.

[39] Ge, H., Tang, G., Hu, WZ. et al. 2015. Aluminum hypophosphite microencapsulated to improve its safety and application to flame retardant polyamide 6. J. Hazard. Mater., 2015, 294: 185-194.

[40] Gu, HB., Ma, C., Gu, JW. et al. 2016. An overview of multifunctional epoxy nanocomposites. Journal of Materials Chemistry C, 2016, 4(25): 5890-5906.

[41] Feng, JB., Sun, YQ., Song, PG. et al. 2017. Fire-Resistant, Strong, and Green Polymer Nanocomposites Based on Poly(lactic acid) and Core-Shell Nanofibrous Flame Retardants. Acs Sustainable Chemistry & Engineering, 2017, 5(9): 7894-7904.

[42] Gu, JW., Liang, CB. Zhao, XM.. et al. 2017. Highly thermally conductive flame-retardant epoxy nanocomposites with reduced ignitability and excellent electrical conductivities. Composites Science and Technology, 2017, 139: 83-89.

[43] Guo, BT., Liu, YZ., Zhang, Q. et al. 2017. Efficient Flame-Retardant and Smoke-Suppression Properties of Mg-Al-Layered Double-Hydroxide Nanostructures on Wood Substrate. Acs Applied Materials & Interfaces, 2017, 9(27): 23039-23047.

[44] Yuan, BH., Hu, Y., Chen, XF. et al. 2017. Dual modification of graphene by polymeric flame retardant and Ni (OH)(2) nanosheets for improving flame retardancy of polypropylene. Composites Part a-Applied Science and Manufacturing, 2017, 100: 106-117.

[45] Jena, DK., Sahoo, PK. 2018. Development of biodegradable cellulose-g-poly(butyl acrylate)/kaolin nanocomposite with improved fire retardancy and mechanical properties. Journal of Applied Polymer Science, 2018, 135(11):

[46] Li, YC., Kim, YS., Shields, J. et al. 2013. Controlling polyurethane foam flammability and mechanical behaviour by tailoring the composition of clay-based multilayer nanocoatings, J. Mater. Chem., 2013, A 1: 12987–12997.

[47] Malucelli, G., Carosio, F., Alongi, J. et al. 2014. Materials engineering for surface-confined flame retardancy. Materials Science & Engineering R-Reports, 2014, 84: 1-20.

[48] Wei, C. Zeng, S. Tan, Y. et al. 2015. Impact of Layer-by-Layer selfassembly clay-based nanocoating on flame retardant properties of sisal fiber cellulose microcrystals. Adv. Mater. Sci. Eng. 2015: 1–7.

[49] Carosio, F., Negrell-Guirao, C., Di Blasio, A. et al. 2015. Tunable thermal and flame response of phosphonated oligoallylamines layer by layer assemblies on cotton. Carbohydrate Polymers, 2015, 115: 752-759.

[50] Carosio, F.; Alongi, J. 2016. Ultra-Fast Layer-by-Layer Approach for Depositing Flame Retardant Coatings on Flexible PU Foams within Seconds. Acs Applied Materials & Interfaces, 2016, 8 (10): 6315-6319.

[51] Maluceli, G. 2016. Surface-engineered fire protective coatings for fabrics through Sol-Gel and Layer-by-Layer methods: an overview. Coatings, 2016, 6(33): 23 p.

[52] Lokhande, G., Chambhare, S., Jagtap, R. 2017. Synthesis and properties of phosphate-based diacrylate reactive diluent applied to UV-curable flame-retardant wood coating. Journal of Coatings Technology and Research, 2017, 14(1): 255-266.

[53] Dvir, H. 2003. Optimization of a flame-retarded polypropylene composite, Compos. Sci. Technol., 2003, 63: 1865–1875.

[54] Zhang, MM., Buekens A., Li, XD. 2016. Brominated flame retardants and the formation of dioxins and furans in fires and combustion. Journal of Hazardous Materials, 2016, 304: 26-39.

[55] Stapleton, HM., Klosterhaus, S., Eagle, S. et al. 2009. Detection of organophosphate flame retardants in furniture foam and U.S. House Dust. Environ. Sci. Technol., 2009, 43: 7490–7495.

[56] Levchik, SV. 2006. A review of recent progress in phosphorus-based flame retardants, J. Fire Sci., 2006, 24: 345–364.

[57] Altun, Y., Dogan, M., Bayramli, E. et al. 2016. The effect of red phosphorus on the fire properties of intumescent pine wood flour - LDPE composites. Fire and Materials, 2016, 40 (5): 697-703.

[58] Liu, YL., He, JY., Yang, RJ. et al. 2016. The Thermal Properties and Flame Retardancy of 9,10-Dihydro-9-oxa-10-phosphaphenanthrene 10-Oxide (DOPO)-Mg/Polyisocyanurate-Polyurethane Foam Composites. Bulletin of the Chemical Society of Japan, 2016, 89(7): 779-785.

[59] Luneva, NK., Onufreichuk, AV., Ezovitova, TI. et al. 2017. Composition of a Wood Combustion Inhibitor Based on a Magnesium Complex Containing Phosphorus and Nitrogen. Russian Journal of Applied Chemistry, 2017, 90(9): 1459-1468.

[60] Feng, YZ., He, CG., Wen, YF. 2018. Superior flame retardancy and smoke suppression of epoxy-based composites with phosphorus/nitrogen co-doped graphene. Journal of Hazardous Materials, 2018, 346: 140-151.

[61] Bogdanova, VV., Kobets, OI., Kirlitsa, VP. 2016. The mechanism of action and the synergistic effect of nitrogen and phosphorus-containing fire retardants in fire protection and wood and peat fire suppression. Russian Journal of Physical Chemistry, 2016, 10 (2): 306-312.

[62] Chambhare, SU., Lokhande, GP., Jagtap, RN. 2016. UV-curable behavior of phosphorus- and nitrogen-based reactive diluent for epoxy acrylate oligomer used for flame-retardant wood coating. Journal of Coatings Technology and Research, 2016, 13 (4): 703-714.

[63] Chan, SY., Si, LP., Lee, KI. et al. 2018. A novel boron-nitrogen intumescent flame retardant coating on cotton with improved washing durability. Cellulose, 2018, 25(1): 843-857.

[64] Wang,, X., Hu, Y., Song, L. et al. 2010. Thermal degradation behaviors of epoxy resin/Poss hybrids and phosphorus-silicon synergism of flame retardancy, J. Polym. Sci., Part B: Polym. Phys., 2010, 48: 693–705.

[65] Yang, F. Nelson, G. L. 2012. Halogen-Free Flame Retardant Flexible Polyurethane Foams via a Combined Effect of Flame Retardants. In Fire and Polymers VI: New Advances in Flame Retardant Chemistry and Science. ACS Symposium Series, 2012, 1118: 139-149.

[66] Gao, M., Wu, WH., Xu, ZQ. 2013. Thermal degradation behaviors and flame retardancy of epoxy resins with novel silicon-containing flame retardant. J. Appl. Polym. Sci., 2013, 127: 1842–1847.

[67] Butt, C. M., Congleton, J. , Hoffman, K. et al. 2014. Metabolites of Organophosphate Flame Retardants and 2-Ethylhexyl Tetrabromobenzoate in Urine from Paired Mothers and Toddlers. Environmental Science & Technology, 2014, 48(17): 10432-10438.

[68] Costa, L.G., De Laat, R., Tagliaferri, S. et al. 2014. A mechanistic view of polybrominated diphenyl ether (PBDE) developmental neurotoxicity. Toxicology Letters, 2014, 230(2): 282-294.

[69] Fromme, H., Becher, G., Hilger, B. et al. 2016. Brominated flame retardants - Exposure and risk assessment for the general population. International Journal of Hygiene and Environmental Health, 2016, 219(1): 1-23.

[70] Altuntas, E., Narlioglu, N., Alma, MH. 2017. Investigation of the Fire, Thermal, and Mechanical Properties of Zinc Borate and Synergic Fire Retardants on Composites Produced with PP-MDF Wastes. Bioresources, 2017, 12(4): 6971-6983.

[71] Altuntas, E., Karaogul, E., Alma, MH. 2017. Effects of Fire Retardants on the Fire, Thermal and Mechanical Properties of Wood Plastic Composites Using Recycled Fibers. Kastamonu University Journal of Forestry Faculty, 2017, 17(2): 334-342.

[72] Eceiza, I., Barrio, A., Martin, L. 2018. Thermal and fire behavior of isophorone diisocyanate based polyurethane foams containing conventional flame retardants. Journal of Applied Polymer Science, 2018, 135(10)

[73] Zhang, JL., Mei, CT., Huang, RZ. et al. 2018. Comparative mechanical, fire-retarding, and morphological properties of high-density polyethylene/(wood flour) composites with different flame retardants. Journal of Vinyl & Additive Technology, 2018, 24(1): 3-12.

[74] Laufer, G.,Carosio, F. Martinez, R. et al. 2011. Growth and fire resistance of colloidal silica-polyelectrolyte thin film assemblies. Journal of colloid and interface science, 2011, 356 (1): 69-77.

[75] Yan, L., Xu, Z., Wang, X. 2017. Influence of nano-silica on the flame retardancy and smoke suppression properties of transparent intumescent fire-retardant coatings. Progress In Organic Coatings., 2017, 112: 319-329.

[76] Chen, W., Liu, P., Min, L. et al. 2018. Non-covalently Functionalized Graphene Oxide-Based Coating to Enhance Thermal Stability and Flame Retardancy of PVA Film. Nano-Micro Letters, 2018, 10(3): Article Number: 39.

[77] Farag, Zeinab R.; Krueger, Simone; Hidde, Gundula; et al. 2013. Deposition of thick polymer or inorganic layers with flame-retardant properties by combination of plasma and spray processes. Surface & Coatings Technology, 2013, 228: 266-274.

[78] Seo, S., Lee, S., Park, YT. 2016. Note: Automatic layer-by-layer spraying system for functional thin film coatings. Review of Scientific Instruments, 2016, 87(3): Article Number: 036110.

[79] Zope, IS., Foo, S., Seah, DGJ. et al. 2017. Development and Evaluation of a Water-Based Flame Retardant Spray Coating for Cotton Fabrics. ACS Applied Materials & Interfaces, 2017, 9 (46): 40782-40791.

[80] Carosio, F., Di Pierro, A., Alongi, J. et al. 2018. Controlling the melt dripping of polyester fabrics by tuning the ionic strength of polyhedral oligomeric silsesquioxane and sodium montmorillonite coatings assembled through Layer by Layer. Journal of Colloid and Interface Science, 2018, 510: 142-151.

[81] Altun, Y., Dogan, M., Bayramli, E. 2016. The effect of red phosphorus on the fire properties of intumescent pine wood flour - LDPE composites. Fire and Materials, 2016, 40(5): 697-703.

[82] Carosio, F., Cuttica, F., Medina, L., Berglund, L. A. 2016. Clay nanopaper as multifunctional brick and mortar fire protection coating-Wood case study. Materials & Design, 2016, 93: 357-363/

[83] Gao, M., Xu, YX. 2016. Flame Retardancy of wood treated with GUP by Cone Calorimetry. Proceedings of the 2016 3rd International Conference on Mechatronics and Information Technology (ICMIT), 2016, 49: 496-500.

[84] He, X., Li, XJ., Zhong, Z. et al. 2016. Effectiveness of impregnation of ammonium polyphosphate fire retardant in poplar wood using microwave heating. Fire and Materials, 2016, 40(6): 818-825.

[85] Jin, E., Chung, YJ. 2016. Combustion characteristics of Pinus rigida specimens treated with mixed phosphorus-nitrogen additives. Journal of Industrial and Engineering Chemistry, 2016, 36: 74-79.

[86] Lahtela, V., Karki, T. 2016. The influence of melamine impregnation and heat treatment on the fire performance of Scots pine (Pinus sylvetris) wood. Fire and Materials, 2016, 40(5): 731-737.

[87] Merk, V., Chanana, M., Gaan, S. et al. 2016. Mineralization of wood by calcium carbonate insertion for improved flame retardancy. Holzforschung, 2016, 70(9): 867-876.

[88] Makovicka Osvaldova, L., Gaspercova, S., Mitrenga, P. et al. 2016. The influence of density of test specimens on the quality assessment of retarding effects of fire retardants. Wood Research, 2016, 61(1): 35-42.

[89] Seo, H. J., Kim, S., Huh, W. et al. 2016. Enhancing the flame-retardant performance of wood-based materials using carbon-based materials. Journal of Thermal Analysis and Calorimetry, 2016, 123(3): 1935-1942.

[90] Wang, F., Gao, ZZ., Zheng, M. et al. 2016. Thermal degradation and fire performance of plywood treated with expanded vermiculite. Fire and Materials, 2016, 40(3): 427-433.

[91] Wang, F., Liu, JL., Lv, WH. 2017. Thermal degradation and fire performance of wood treated with PMUF resin and boron compounds. Fire and Materials, 2017, 41(8): 1051-1057.

[92] Chu, D. M., Mu, J., Zhang, L. et al. 2017. Promotion effect of NP fire retardant pre-treatment on heat-treated poplar wood. Part 1: color generation, dimensional stability, and fire retardancy. Holzforschung, 2017, 71(3): 207-215.

[93] Fu, Q. L., Medina, L., Li, YY. et al. 2017. Nanostructured Wood Hybrids for Fire-Retardancy Prepared by Clay Impregnation into the Cell Wall. Acs Applied Materials & Interfaces, 2017, 9(41): 36154-36163.

[94] Li, YY., Hui, B., Li, GL. et al. 2017. Fabrication of smart wood with reversible thermoresponsive performance. Journal of Materials Science, 2017, 52(13): 7688-7697.

[95] Gasparik, M., Makovicka Osvaldova, L., Cekovska, H. et al. 2017. Flammability Characteristics of Thermally Modified Oak Wood Treated with a Fire Retardant. Bioresources, 2017, 12(4): 8451-8467.

[96] Giudice, C. A., Canosa, G. 2017. Flame-Retardant Systems Based on Alkoxysilanes for Wood Protection. Wood in Civil Engineering, 2017, p. 75-89.

[97] Grzeskowiak, W. L. 2017. Effectiveness of new wood fire retardants using a cone calorimeter. Journal of Fire Sciences, 2017, 35(6): 565-576.

[98] He, S. R., Wu, W. H., Zhang, M. J. et al. 2017. Synergistic effect of silica sol and K2CO3 on flame-retardant and thermal properties of wood. Journal of Thermal Analysis and Calorimetry, 2017, 128(2): 825-832.

[99] Milanko, V., Mrackova, E., Laban, M. et al. 2017. The use of sodium silicate to create fire retardant woods. Fire Protection, Safety and Security 2017, International Scientific Conference on Fire Protection, Safety and Security, May 03-05, 2017, Zvolen, Slovakia, p. 117-127.

[100] Mitterova, I., Zachar, M., Majlingova, A. 2017. Effect of flame retardants on selected fire parameters of spruce wood. Fire Protection, Safety and Security 2017, International Scientific Conference on Fire Protection, Safety and Security, May 03-05, 2017, Zvolen, Slovakia, p. 128-132.

[101] Wang, XQ., Zhang, Y., Yu, ZM. et al. 2017. Properties of fast-growing poplar wood simultaneously treated with dye and flame retardant. European Journal of Wood and Wood Products, 2017, 75(3): 325-333.

[102] Wu, J., Wang, MZ., Guo, HW. 2017. Synergistic Flame Retardant Effects of Different Zeolites on Intumescent Fire Retardant Coating for Wood. Bioresources, 2017, 12(3): 5369-5382.

[103] Zhang, QF., Cai, HZ., Yang, KY. et al. 2017. Effect of biochar on mechanical and flame-retardant properties of wood - Plastic composites. Results in Physics, 2017, 7: 2391-2395.

[104] Okubayashi, S., Griesser, UJ., Bechtold, T. 2005. Moisture sorption/desorption behavior of various manmade cellulosic fibers. J. Appl. Polym. Sci., 2005, 97: 1621–1625.

[105] Hearle, JWS., Morton, WE. 2008. Tensile properties. In Physical Properties of Textile Fibres, 4th ed. Woodhead Publishing Series in Textiles: Cambridge, UK.

[106] Bajaj, P. 2000. Heat and flame protection. In Handbook of Technical Textiles. 1st ed. Woodhead Publishing Limited: Cambridge, UK, pp. 223–263.

[107] Horrocks, AR. Flame retardant challenges for textiles and fibres: New chemistry versus innovatory solutions. Polym. Degrad. Stab., 2011, 96: 377–392.

[108] Cayla, A., Rault, F., Giraud, S. et al. 2016. PLA with Intumescent System Containing Lignin and Ammonium

Polyphosphate for Flame Retardant Textile. Polymers, 2016, 8(9).

[109] Chen, SS., Li, X., Li, Y. et al. 2015. Intumescent Flame-Retardant and Self-Healing Superhydrophobic Coatings on Cotton Fabric. Acs Nano, 2015, 9(4):4070-4076.

[110] Cheng, XW., Liang, CX., Guan, JP. et al. 2018. Flame retardant and hydrophobic properties of novel sol-gel derived phytic acid/silica hybrid organic-inorganic coatings for silk fabric. Applied Surface Science, 2018, 427: 69-80.

[111] Feng, YJ., Zhou, Y., Li, DK. et al. 2017. A plant-based reactive ammonium phytate for use as a flame-retardant for cotton fabric. Carbohydrate Polymers, 2017, 175: 636-644.

[112] Jimenez, M., Guin, T., Bellayer, S. et al. 2016. Microintumescent mechanism of flame-retardant water-based chitosan-ammonium polyphosphate multilayer nanocoating on cotton fabric. Journal of Applied Polymer Science, 2016, 133(32).

[113] Liu, H., Du, Y., Yang, GH. 2018. Flame retardance of modified graphene to pure cotton fabric. Journal of Fire Sciences, 2018, 36(2): 111-128.

[114] Rehan, M., El-Naggar, ME., Mashaly, HM. et al. 2018. Nanocomposites based on chitosan/silver/clay for durable multi-functional properties of cotton fabrics. Carbohydrate Polymers, 2018, 182: 29-41.

[115] Shan, GH., Jia, LX., Zhao, T. et al. 2017. A novel DDPSi-FR flame retardant treatment and its effects on the properties of wool fabrics. Fibers and Polymers, 2017, 18(11): 2196-2203.

[116] Zope, I. S., Foo, S., Seah, DGJ. et al. 2017. Development and Evaluation of a Water-Based Flame Retardant Spray Coating for Cotton Fabrics. Acs Applied Materials & Interfaces, 2017, 9(46): 40782-40791.

[117] Zhang, Y., Ren, YL., Liu, XH. et al. 2018. Preparation of durable flame retardant PAN fabrics based on amidoximation and phosphorylation. Applied Surface Science, 2018, 428: 395-403.

[118] Modesti, M., Lorenzetti, A. 2010. Recent trends in flame retardancy of polyurethane foams. Flame Retardants: Functions, Properties and Safety. Book: P 185-218.

[119] Hu, XM., Wang, DM. 2013. Enhanced fire behavior of rigid polyurethane foam by intumescent flame retardants. Journal of Applied Polymer Science, 2013, 129(1): 238-246.

[120] Liu, X., Xu, DM., Wang, YL. et al. 2016. Smoke and toxicity suppression properties of ferrites on flame-retardant polyurethane-polyisocyanurate foams filled with phosphonate. Journal of Thermal Analysis and Calorimetry, 2016, 125(1): 245-254.

[121] Liu, X., Wang, JY., Yang, XM. et al. 2017. Application of TG/FTIR TG/MS and cone calorimetry to understand flame retardancy and catalytic charring mechanism of boron phosphate in flame-retardant PUR-PIR foams. Journal of Thermal Analysis and Calorimetry, 2017, 130(3): 1817-1827.

[122] Lorenzetti, A., Dittrich, B., Schartel, B. et al. 2017. Expandable graphite in polyurethane foams: The effect of expansion volume and intercalants on flame retardancy. Journal of Applied Polymer Science, 2017, 134(31).

[123] Yue, D. Z., Oribayo, O., Rempel, G. L. et al. 2017. Liquefaction of waste pine wood and its application in the synthesis of a flame retardant polyurethane foam. Rsc Advances, 2017, 7(48): 30334-30344.

[124] Wang, C., Wu, Y. C., Li, Y. C. et al. 2018. Flame-retardant rigid polyurethane foam with a phosphorus-nitrogen single intumescent flame retardant. Polymers for Advanced Technologies, 2018, 29(1): 668-676.

Specification of a representative value for fire load density accumulated in building compartment

Mariusz Maslak[a]* – Michal Pazdanowski[a]

[a]*Cracow University of Technology, Warszawska 24, 31-155 Cracow, Poland*

Abstract

Two alternative approaches to the specification of fire load density representative for the considered fire zone are considered in this paper. The first approach is based on the direct inventory of combustible materials stockpiled in the fire zone. Here the nominal value obtained by direct measurements constitutes the measure of sought density. The possible inventory taking methods and the interpretation of results obtained are described in detail. The second approach is based on the statistically justified characteristic value. This measure seems to be more universal in application, though not so individualized as the first one. It is calculated as the appropriate quantile of the fire load density probability distribution, treated as the random variable. Procedure of this type takes into account the statistical variation of densities determined in zones used in the same manner. Thus the obtained value is interpreted as authoritative for fire zone of particular type, instead of being associated with analyzed zone in a specific building.

Keywords: building compartment; fire load density; inventory of combustible materials; nominal value; random variable; probability distribution; quantile; characteristic value.

---

* Corresponding author. Tel.: +48-12-641-5673; fax: +48126282033; e-mail: mmaslak@pk.edu.pl.

1. Introduction

Fire load of a fire zone $Q\,[\mathrm{MJ}]$ is usually interpreted as quantitative amount of energy which, at the combustible materials stored in the zone and constituting potential fuel, will be released during the anticipated fire. Accompanied by opening factor $O\,[\mathrm{m}^{0,5}]$, which characterizes the geometry of considered zone and quantifies the possible exchange of exhaust gases with surroundings, i.e. the ventilation of such a zone, it determines the course of the authoritative fire, and more precisely the heat release rate HRR, which in turn directly affects the effective fire intensity. In the design practice precise specification of the total amount of this energy would be useful in estimating the safety level of zone users changing during fire only after unequivocal specification of fire material distribution within this zone is obtained. It is important to specify, whether the combustible materials are distributed rather evenly over the whole area, or clustered generating local maxima substantially exceeding the averaged reference value. Because of this the fire load should be expressed with respect to the floor area of analysed fire zone $A_f\,[\mathrm{m}^2]$, and therefore the fire load density should be given as $q_f\,\left[\mathrm{MJ/m}^2\right]$. Thus:

$$q_f = \frac{Q}{A_f} \tag{1}$$

The density q_f should be in the quantitative sense distinguished from the density $q_t\,[\mathrm{MJ/m}^2]$ related to the total surface area of all partitions delimiting the fire compartment $A_t\,[\mathrm{m}^2]$ (i.e. both floor and ceiling as well as walls). Both quantities are used interchangeably in the subject literature, however the relationship:

$$q_f = q_t\left(\frac{A_t}{A_f}\right) \tag{2}$$

always holds, while also:

$$q_t = \frac{Q}{A_t} = \frac{Q}{2A_f + HC} \tag{3}$$

where H and C denote the height and circumference of the considered fire zone, respectively.

At least two qualitatively different approaches to the specification of fire load density q_f (and the corresponding density q_t) authoritative for fire safety analysis may be found in the literature. The first one is based on detailed inventory of contents contained within the analyzed zone and determination of the nominal value q_{fn}, while the second one is based on the statistically justified characteristic value q_{fk} identified for the assumed density probability distribution treated as random variable q_f and estimated with respect to homogenous and representative population of fire zones used in a similar manner. The presentation and comparison of both approaches constitutes the basic objective of current paper.

2. Specification of nominal fire load density based on the detailed inventory of a fire zone

According to the code PN-B-02852:2001 [1], and Appendix E to the code EN 1991-1-2 [2], in order to estimate the fire load Q one should take the inventory of combustible materials gathered in the considered fire zone, give the mass $m_i\,[\mathrm{kg}]$ and assign the effective combustion heat value $H_{u,eff,i}\,[\mathrm{MJ/kg}]$ for each of these materials. Consequently, with n materials taken into account, one obtains:

$$Q = \sum_{i=1}^{n} m_i H_{u,eff,i}\ \left[\mathrm{MJ}\right] \tag{4}$$

The adjective "effective" is related to the imperfect conditions of combustion in fire, where the reduction $H_{u,eff,i} = \chi_i H_{u,i}$ occurs, with $\chi_i \le 1$. The perfect conditions occur only during laboratory calorific experiment, during which the net combustion heat value $H_{u,i}\,[\mathrm{MJ/kg}]$ is measured. In the engineering practice the coefficient χ_i is usually disregarded in calculations (c.f. for instance the example [2]). This may be justified by difficulties in unequivocal determination of its value, but the simplification of this type leads to unnecessary overestimation of Q value determined from (4), though one has to admit, that this results in the estimate located on safe side. One has to admit as well, that the energy Q estimate is made subject to the assumption that all the materials taken into account are perfectly dry. If this is not true, and the humidity of *i*-th material expressed as a percentage of its dry mass is equal to u, one should perform the correction according to the formula:

$$H_{u,i} = H_{u0,i}\left(1 - 0{,}01u\right) - 0{,}025u \tag{5}$$

where the value $H_{u0,i}$ is determined for perfectly dry material.

The quantity Q is currently specified in terms of energy units expressed in the SI system in MJ. In older elaborations the interested readers may find the units like calories, or even kilograms of dry normalized wood. Expressing the so calibrated values in terms of currently obligatory units results in many ambiguities, especially if a large diversity of materials is considered in the analysis. Detailed discussion of these issues would require a separate elaboration. The papers [3] and [4] seem to represent an interesting introduction into this problem.

The basic methods of collecting data used in the inventory of the fire zone in question include:

- the direct weighting method – according to which the masses of identified combustible materials are determined by simple weighting, and subsequently appropriate combustion heat is assigned to them,
- the indirect inventory method – in this method the masses sought are determined via volumetric measurements of objects containing combustible materials, subsequent assignment of authoritative density, which yields an estimate of mass, later on the values of combustion heat are assigned,
- the questionnaire method – identified combustible materials and their masses are determined based on the questionnaire delivered by the direct user of the compartment to an expert,
- real estate website review – estimation of combustible materials and their masses based on photos or videos taken in the fire compartment.

In order to assure sufficient reliability, the code [5] requirements allow for application of only those data gathering methods in which direct presence of an expert is required during data acquisition. Let us note, that when the questionnaire method is used, an expert analyzes the data gathered by a third party not necessarily competent in evaluation. On the other side application of videos or photographs is of very limited reliability as well, as even the best video represents only a part of the reality. Thus the reliable estimation of mass or volume of analyzed object may be difficult. Both methods recommended by the code [5], i.e. the direct weighting method and the indirect inventory method have many limitations. First of all, it may be difficult to weigh many combustible materials gathered in the fire zone in real life. This is especially true in case of combustible materials built into the bearing structure. On the other hand, in the case of movable combustible objects it may be much easier to estimate the mass than the volume. For instance, how a chair should be dealt with, which is in part made of metal, and in part of man made materials? Taking into account all the limitations listed above, it is assumed, that a combined method merging the indirect inventory method with weighting offers the best solution.

Based on the recommendations of the code [5], while making an inventory of the real fire load characterizing the fire zone under consideration, a distinction is made between:

- the density of movable fire load – for instance furniture, books, carpets, curtains and similar objects are assigned there,
- the density of fixed fire load – the combustible structural materials and for instance materials used to finish the floors, walls, ceilings and similar are assigned to this group.

As it has been indicated above the fire density value obtained from inventory is understood as the nominal value q_{fn}, specific to the analysed fire zone.

3. The idea of statistically based estimating the representative quantile of random fire load density in a fire zone

Practical application of the formula (4) in the case of analyzing the safety level in fire, related to a specific building, with fire zones of different character, is undoubtedly tedious and in addition not very useful, as during the service time the users may change the way the individual rooms are used and almost certainly will change individual furniture or components of the interior design during the useful life of the building. Because of this fact replacement of the traditional deterministic approach by the statistically based one supplemented with components of risk management is postulated. The change of this type results in replacement of the value q_{fn}, specified individually for each considered case, by the related to this value characteristic value q_{fk} determined as statistically justified quantile of suitable probability distribution. In order to do that the fire zones subjected to analysis are grouped into zones of similar character, especially having the same function or being used in the same way. Subsequently appropriate values of q_{fk} are assigned to each group. The determination of sought quantile results in the need to determine the distribution type of random variable q_f, the central value of this distribution and at least one dispersion parameter. In order to perform such analysis the first step must be taken, which is to gather a homogeneous and reliable data population related to each of the identified groups. It turns out, that the mode of gathering such data directly affects the obtained results [6]. The quantitative differences obtained during the analysis of the fire zones belonging to the same group using all the methods mentioned above are often very significant [7]. *C. Culver* [8] paid attention to these differences in results for the first time.

4. The factors affecting the distribution of statistical sample within the homogenous research group

The statistical data analysis technique selected to estimate the authoritative fire load density generates the need to specify the homogenous research groups, i.e. sets grouping the particular fire zone types, having similar designation and service mode. The grouping of this type must be performed very carefully, as it critically affects final evaluation of fire safety. One may find many recommended grouping methods in the bibliography on the matter, very often substantially divergent. Two of these methods have to be distinguished, as they were included in normative acts commonly used in engineering practice. In the Annex E to the code EN 1991-1-2 [2] dwellings, hospital rooms, libraries, offices, classrooms, shops and shopping centers, cinemas and theaters, as well as facilities for transportation services (for instance such as railway and bus terminals) are defined as separate groups. On the other hand the code NFPA 557 [5] designates in this case:

- offices and business occupancies,
- religious properties,
- eating and drinking establishments,
- educational buildings,
- facilities that care for the sick,
- stores and mercantile buildings,
- places where people sleep, other than homes,
- other public assembly buildings.

In the second case dwellings are not distinguished as a separate group, this is probably a result of the specific US fire regulations.

On the other hand the analysis of combustible materials should be grouped and generalized. Usually these materials are assigned to one of three (or four) basic groups such as: paper or wood (often combined into one group as manufactured materials on cellulose base), man made materials and textiles. The groupings listed above are not perfect due to obvious reasons. The detailed analysis of office spaces indicates that typical offices and conference rooms designated for meetings of many people should be distinguished [9]. Additionally an important difference between the skewness of fire load density histograms obtained for offices operating in private and public sectors has been documented in [8]. American estimates made in late seventies of previous century [8] reported, that the share of paper and wood in the fire load of office spaces accounted for 99,8%. The similar value (i.e. precisely 98.7%) is given by *S. Kumar* [10] for offices located in India in mid nineties. Meanwhile the most recent research only a few years old, cited for US conditions by *E. Zalok* and *J. Eduful* [6] suggest the following distribution: cellulose materials 70% (including 24% paper and 46% wood), man made materials 22%, textiles 8%. Substantial increase in the share of man made materials is an obvious result of the presence of computers, printers, TV sets, radios and similar devices in the contemporary offices. So are the estimates obtained a few decades ago still reliable, especially in the era of ever faster social and cultural changes?

Detailed analysis of rooms intended for housing constitutes another example well illustrating the ambiguity in the estimation of parameters describing the fire load density distribution in a homogeneous statistical sample. The authors of paper [11] cite the research of *C. Holm* and *P. Oksanen* [12] dating back to the early seventies of previous century. They indicate the differences in the sought density, should the living room, bedroom and kitchen be considered separately instead of an apartment being treated as a whole. The comparison of proposed distributions with distribution related to the whole apartment and recommended currently by the code [2] shows, that in current times the fire load of apartments is substantially higher. The conclusion of this type is confirmed by the comparison of a distribution obtained in 1970 for apartments located in the USA [13] with much later distribution, obtained in 2004 for apartments located in Canada [14].

The area of a fire zone represents an additional factor determining the distribution of fire load density. In general it is indicated [8], that the fire load Q in fire zone increases with increasing area A_f only up to the area approximately equal to $A_f = 30\,\mathrm{m}^2$, and drops substantially in bigger spaces.

5. The question of fitting appropriate probability distribution to random fire load density

Availability of appropriate statistical data set, constituting an uniform sample, allows for representative analysis. In order to do that the histogram and cumulative empirical distribution of analyzed variable are generated after an assignment of the results to the a priori defined classes and analysis of each class size. Matching the empirical distribution thus obtained in the most precise way to one of the continuous probability distributions described by mathematicians constitutes the primary task of the evaluator. Usually the probabilistic moments are applied to do that, while the moments of the sample (the mean value and the standard deviation) are treated as estimators (preferably compatible, unbiased and the most effective) of the moments of distribution against which the empirical distribution is compared. The graphical collocation method at the limit point may be applied to this purpose and rectify the empirical cumulative distribution on subsequent probabilistic meshes or seek the maximum possible likelihood, out of these calculated during the comparison of empirical distribution to subsequent probability distributions [15]. Both *S. Kumar* with *C. V. S. K. Rao* [10] as well as *A. C. Bwalya* with *M. Sultan* and *N. Benichou* [16] report good fitting of the results obtained during research with the log-normal probability distribution. The observation of this type would indicate, that common logarithm of random fire load density distribution conforms to the normal distribution, On the other hand, as the fire is an extraordinary occurrence, and thus an infrequent one, which should not occur more than once during the whole service life of the building, it is postulated to assign the properties of one of the distributions specified for the extreme values, such as the *Gumbel* distribution [17] or the *Weibull* distribution [18] to the fire load density. It was shown, that in the case of both of these distributions the fitting is sufficiently good, though the *Weibull* distribution yields the best fitting (in the sense of *Kolmogorow – Smirnov* test) when the indirect inventory method is applied, and the *Gumbel* distribution is better when direct weighting method is used. The skewness of empirical distributions obtained during the inspections seems to favor the distribution of the extreme type.

6. Interpretation of the characteristic value of random fire load density in fire compartment

Both in the Eurocode [2] and in the code [5] the random fire load density in fire compartment q_f is characterized by the *Gumbel* probability distribution. This means that its characteristic value q_{fk} has been defined as the quantile of this distribution determined at the level of probability of not exceeding p. In order to specify this value one should first determine the average value $\overline{q_f}$ and standard deviation σ_{qf} of the sample, using the following formulae:

$$\overline{q_f} = \overline{q_{f,f}} + \overline{q_{f,c}} \tag{6}$$

and

$$\sigma_{qf} = \sqrt{\sigma_{qf,f}^2 + \sigma_{qf,c}^2} \tag{7}$$

where the density $q_{f,f}$ is related to the combustible materials representing the fixed fire load, and the density $q_{f,c}$ with the potential fuel representing the contents fire load. In the subsequent step these parameters are transformed into the corresponding parameters of *Gumbel* distribution, i.e. the modal value $\tilde{q}_f$ (in other words the most probable value in the reference period assumed for analysis) and the *Gumbel* standard deviation u_{qf}. After application of the classical method of probabilistic moments [15], one obtains:

$$\tilde{q}_f = \overline{q}_f - 0{,}577\frac{\sqrt{6}}{\pi}\sigma_{qf} = \overline{q}_f - 0{,}45\sigma_{qf} \tag{8}$$

as well as:

$$u_{qf} = \frac{\sqrt{6}}{\pi}\sigma_{qf} = 0{,}78\sigma_{qf} \tag{9}$$

where the coefficient 0.577 represents the so called *Euler* constant. The sought quantile q_{fk}, i.e. such value of the random density q_f, which in random realization may be exceeded with given probability q (and this in turn means that this value will not be exceeded with probability $p = 1 - q$), is determined by the following formula:

$$\begin{aligned} q_{fk} = {} & \tilde{q}_f - u_{qf}\ln[-\ln(p)] = \\ & \overline{q}_f - \frac{\sqrt{6}}{\pi}\sigma_{qf}\{0{,}577 + \ln[-\ln(p)]\} \end{aligned} \tag{10}$$

Thus, now the authoritative level of not exceeding the probability p has to be determined. In the Annex E to the Eurocode it was assumed, that the characteristic value q_{fk} represents such level of random density q_f, which will not be exceeded in random realization with warranted probability of 80%, this means that $p = 0.8$, and thus $q = 1 - 0.8 = 0{,}2$. Such arbitrary decision raises doubts, as in reality the value of probability p should be specified based on the detailed analysis of fire initiation risk. Let T_r denote the return period of the characteristic value, i.e. the mean time (expressed in years) between subsequent times when the value q_{fk} is exceeded. Then, subject to the assumption, that the probability q does not change in time, the following holds:

$$q = P(q_f > q_{fk}) = \frac{1}{T_r} \tag{11}$$

in turn yielding:

$$p = P(q_f \le q_{fk}) = 1 - q = 1 - \frac{1}{T_r} \tag{12}$$

The value q should at the same time measure the failure probability, usually understood as exhaustion in fire of the capability to safely support the external loads applied to the structure accompanied by the loads generated by the restrained thermally induced expansion. However, not every case when the characteristic load q_{fk} is exceeded ends up in structural failure. Should one prefer the probability q to cover such failure scenario, due to the fire, which has been initiated in the considered fire zone, then this probability has to be expressed as the product of fire initiation probability q_{ini}, and a conditional failure probability q_{fail}, subject to the condition that the failure occurred as a consequence of this fire. The value of probability q_{ini} is determined by the frequency of fires f_s, expressed in number of fires per year per square meter of fire zone used in a given manner. One has to keep in mind, that the frequency f_s refers to the so called structurally significant fires, jeopardizing the safety of the bearing structure, and not small and local fire incidents. This frequency should be determined based on the representative statistical analysis. Should the value f_s be replaced by the value f_{ss}, such that $f_{ss} = f_s A_f$, where A_f is measured in square meters of the floor area in specific fire zone located in the considered building (see the formula (1)), then the number of fires per year will constitute the measure of f_{ss}. Thus:

$$q_{ini} = \frac{1}{f_{ss}} = q_{ini,1} \tag{13}$$

Let us note, that with this approach the probability $q_{ini} = q_{ini,1}$ should be interpreted as probability referring to a single so called one year long unit period and not to the whole service time of a building. Of course, should one assume that the value q_{ini} is constant in time and the service period is equal to m years, the probability referring to that time period $q_{ini,m}$ may be expressed as:

$$q_{ini,m} = (q_{ini,1})^m \tag{14}$$

On the other hand, the regulations contained in the code [5] assume that the measure of conditional probability q_{fail} is expressed by the risk, that the bearing structure would fail in a fire that was earlier initiated in the considered fire compartment. This risk is denoted by the symbol R_s and, if the detailed data is missing, is set at the constant level of $1 \cdot 10^{-6}$ per year. Thus, finally:

$$q = q_{ini,1} q_{fail} = \frac{R_s}{f_{ss}} \tag{15}$$

and after taking into account the formula (11), one may state that:

$$T_r = \frac{f_{ss}}{R_s} \tag{16}$$

The combination of formulae (10), (11), (12) and (16) leads to the estimate of the characteristic value q_{fk}, listed in the code [5] as:

$$q_{fk} = \overline{q_f} - \frac{\sqrt{6}}{\pi}\sigma_{qf}\left\{0{,}577 + \ln\left[-\ln\left(1 - \frac{R_s}{f_{ss}^*}\right)\right]\right\} \tag{17}$$

The frequencies f_{ss} authoritative for each fire zone type and given in that code have been empirically estimated as follows:

- offices and business occupancies – six fires per one million of square meters per year,
- religious properties – six fires per one million of square meters per year,
- eating and drinking establishments – eighty one fires per one million of square meters per year,
- educational buildings – ten fires per one million of square meters per year,
- facilities that care for the sick – sixteen fires per one million of square meters per year,
- stores and mercantile buildings – sixteen fires per one million of square meters per year,
- places where people sleep, other than homes – forty three fires per one million of square meters per year,
- other public assembly buildings – ten fires per one million of square meters per year.

These values, before application in the formula (17) have to be corrected to the value $f_{ss}^* = \chi f_{ss}$ due to the type of the structure and fire protection scheme applied. The correction factors χ are listed in the appropriate tables of the code [5] assigned to the types of authoritative fire zones.

7. Concluding remarks

This paper is an extended version (preceded by papers [19], [20] and [21]) of authors' comments to the procedures used in engineering practice to specify the representative value of fire load density in a fire compartment, authoritative for forecasting the real safety level in fire. However in the case of a particular fire compartment the traditional inventory taking seems to be the advised procedure to follow, as it yields in the common sense the most reliable value, i.e. the nominal value coming out of direct measurements and thus taking into account the materials actually gathered in the considered compartment and the real spatial distribution of these materials, the observation of this type may not always be true. It has been shown, that the inventory taking method applied directly affects the results obtained. This influence is so large, that in any case it should not be disregarded. Therefore preparation of unequivocal guidelines in this domain, recommended for application in the design practice, seems to be pressing. Let us note as well, that the quantitative estimate obtained during inventory, i.e. in a direct manner, will be valid only for a relatively short time span after. Any change in the fire compartment use, and even only a resupply of the combustible materials gathered in the fire compartment would result in making the prior results out of date. In view of the arguments listed above the traditional procedure seems to represent a rather impractical and undoubtedly tedious approach. The alternative solution, recommended for application by the recommendations and regulations pertaining to the evaluation of fire safety, especially in the codes [2] and [5], is by substitution of the conventional deterministic approach with analysis of the probabilistic character. This allows for well justified statistical calibration of characteristic value for fire load density, treated in this case as random variable. One has to take into account the fact, that this authoritative value is representative for formally homogeneous group of fire compartments, subjected to the same service regimen, and not for a particular fire compartment, selected in the analyzed building. Nevertheless, the reliability of results obtained this way has been positively verified experimentally many times, though this is only a confirmation in the statistical sense. In considering the probabilistic procedure recommended for the use in this field, the authors tend to recommend the American algorithm, formalized in the code [5]. In contrast to the analogous approach proposed in Europe [2], it takes into account the failure risk estimated on a sufficiently large statistical sample, and understood as exceeding in the random implementation of the previously specified characteristic value. This risk is differentiated depending on the use of the fire compartment, the type of the bearing structure defining and delimiting the fire compartment as well as the applied fire protection scheme against direct fire exposure. The simple direct transfer of American risk estimates of this type to Europe seems to be very risky, though. The specifics of material and structural solutions used in Europe, the social and cultural conditions affecting the way buildings are used as well as the legal regulations are different. In addition, due to the obvious reasons mainly of economic nature, the unified requirements should not be drawn for all European countries which differ substantially in between. Introduction of the slightly expanded risk analysis into the algorithm for action recommended in the Eurocode [2] would result in the need for prior preparation of the statistical material adapted to European reality. This would undoubtedly raise the reliability of obtained estimates, but on the other hand, such relatively small, complication of the computational procedure could raise the objections within the group of experts dealing with evaluation of safety in fire. The transparency of interpretation of the authoritative characteristic value q_{fk} requires two additional simplifying assumptions. At first, one should assume, that the value arrived at via statistical calculations (or in any other manner justified by the nature of the phenomenon) is evenly distributed over the whole considered fire compartment, and this in reality usually is not true. Secondly, it is assumed, though this assumption is a conservative one, that all the materials taken into consideration when this value is determined would actually burn in fire, and this may not necessarily occur.

References

[1] PN-B-02852:2001 - Ochrona przeciwpożarowa budynków. Obliczanie gęstości obciążenia ogniowego oraz wyznaczanie względnego czasu trwania pożaru.
[2] EN 1991-1-2 - Eurocode1: Actions on structures. Part 1-2: General actions – Actions on structures exposed to fire.
[3] H. W. Yii - Effect of surface area and thickness on fire load. Fire Engineering Research Report 2000/13, March 2000, University of Canterbury, Christchurch, New Zealand.
[4] N. E. Khorasani, M. Garlock, P. Gardoni P. - Fire load: Survey data, recent standards and probabilistic models for office buildings, Engineering Structures, 58/2014, 152-165.
[5] NFPA 557 - Standard for determination of fire loads for use in structural fire protection design, 2012 Edition, National Fire Protection Association, Quincy, MA 02169-7471, USA.
[6] E. Zalok, J. Eduful - Assessment of fuel load survey methodologies and its impact on fire load data, Fire Safety Journal, 62/2013, 299-310.
[7] National Fire Protection Association (NFPA) - Validation of methodologies to determine fire load for use in structural fire protection – final report. The fire protection research foundation – research on support of the NFPA mission. Carleton University, May 2011.
[8] C. Culver - Characteristics of fire loads in office buildings. Journal of Fire Technology, 14(1), 1978, 51-60.
[9] VKF and AEAI - Note explicative de protection incendie – Evaluation en vue de la determination de la grandeur des compartiments coupe-feu. Vereinigung Kantonaler Feuerversicherungen (VKF) and Association des établissements cantonaux d'assurance incendie (AEAI), 2007.
[10] S. Kumar, C. V. S. K. Rao - Fire loads in office buildings. Journal of Structural Engineering, 123 (3), 1997, 365-368.
[11] J. Hietaniemi, E. Mikkola - Design fires for fire safety engineering, VTT Working Paper 139, VTT, Finland, 2010.
[12] C. Holm, P. Oksanen - Palokuorman määrä kerrostalojen asuinhuoneistoissa. Palontorjuntatekniikka, 2/1970, 1-4.
[13] J. A. Campbel - Confinement of fire in buildings. Fire Protection Handbook. NFPA Handbook, USA, 1981.
[14] A. C. Bwalya - An extended survey of combustible contents in Canadian residential living rooms. Research Report No 176. National Research Council, Ottawa, Canada, 2004.
[15] J. Murzewski - Niezawodność konstrukcji inżynierskich. Arkady, Warszawa, 1989.
[16] A. C. Bwalya, M. Sultan, N. Benichou - A pilot survey of fire loads in Canadian homes. Research Report No 159. National Research Council, Ottawa, Canada, 2004.
[17] G. Ramachandran - Properties of extreme order statistics and application in fire protection and insurance problems. Fire Safety Journal, 5 (1), 1982, 59-76.
[18] K. Korpela, J. Kushner - Fire loads in office buildings. Proceedings of the 3rd International Conference on Performance-Based Codes and Fire Safety Design Methods, Bethesda, MD, USA, Society of Fire Protection Engineers (SFPE), 2000.

[19] M. Maślak - Probabilistyczna interpretacja wartości charakterystycznej losowej gęstości obciążenia ogniowego strefy pożarowej, Materiały Budowlane, 10/2014, 90-92.

[20] M. Maślak - Characteristic value of the random fire load density. Probability-based specification depending on the way how the building compartment is used. In: Wald F., Burgess I., Jelčić Rukavina M., Bjegović D., Horová K. (Eds.) – Proceedings of the International Conference "Applications of Structural Fire Engineering" (ASFE 2015), Dubrovnik, Croatia, October 15-16, 2015, Publisher: Czech Technical University in Prague, Czech Republic, 2015, 68-73.

[21] M. Maślak – Miarodajna gęstość obciążenia ogniowego strefy pożarowej. Wartość nominalna z pojedynczej inwentaryzacji czy raczej statystycznie uzasadniona wartość charakterystyczna, Bezpieczeństwo i Technika Pożarnicza, Vol. 44, Issue 4, 2016, 119-128.

Alternative approaches to critical temperature evaluation for axially compressed steel column exposed to fire

Mariusz Maślak[a] – Michał Pazdanowski[a] – Maciej Suchodoła[a]

[a]*CracowUniversity of Technology, Warszawska 24, 31-155 Cracow, Poland*

Abstract

Four alternative procedures used to estimate the critical temperature of axially compressed steel column exposed to the direct action of a fully developed fire with equalized temperature of combustion gases in the nearest vicinity of this column are presented and compared in detail. The first two procedures are based on the recommendations of the code EN 1993-1-2 with application of the so called degree of utilization, computed for the accidental load combination rule. The difference between the first and the second method lies in the fact, that the critical temperature is determined without and with application of an iterative algorithm. The third procedure, applied by the authors to verify the results obtained by the analytical approaches presented above is based upon the application of nonlinear numerical analysis performed within the ANSYS computational environment for a column model discretized with 3D finite elements. In the last approach a purely bar model of the column is analyzed, but the conventional stability analysis is replaced by a second order bearing capacity analysis conducted for an imperfect element and taking into account the amplification of initially assumed bow imperfections.

Keywords: Axially compressed steel column; fully developed fire; critical temperature; degree of utilization; iterative procedure; numerical analysis; bow imperfection; second-order bearing capacity analysis.

---

1. Introduction – description of the steel column analyzed in the example

In the design practice the time during which, after engulfing by fire, the structural element, in spite of the weakening due to increasing temperature, will be able to safely resist the external loads applied to it and the additional internal forces induced by the restrained capability to undergo thermal deformations, is considered to be the measure of fire resistance. However, the value of this type may hardly be considered objective, unequivocally assigned to the considered element. In this sense the fire resistance depends on the characteristics of acting fire, and especially on the course and intensity of heating. Each change in the reference fire taken into account would result in this approach in an immediate change in the estimated fire resistance. Therefore the classical fire resistance, expressed in the units of time is replaced in the calculations by an alternative, and in the authors' opinion more universal value, interpreted as the critical temperature correlated with the analyzed element reaching the fire resistance limit state [1]. One has to keep in mind, however, that the sought temperature in general will not be determined unequivocally. The obtained result will depend on the numerical model applied, and this will be shown in a present paper.

Let us consider the axially compressed column, pinned on both ends, and having the height of $H = 6.0\ m$. This column is made of S235 steel and a HEB180 I-beam for which the cross sectional area is equal to $A = 65.3\ cm^2$. This cross section conforms to the requirements of class 1 both for the persistent as well as for the accidental fire scenario. In order to fulfill the requirement of constant load effect $E_{fi,d,t}$ during the whole fire, it was assumed, that the considered column may extend in the longitudinal direction in an unconstrained manner. This is ensured by allowing for the unconstrained displacements in the vertical direction at the top support. Thus no additional internal forces are generated in the considered column heated by the fire action. It is also assumed, that this column is loaded by a perfectly axially applied compressive force comprising of a constant load having the characteristic value of $G_k = 100\ kN$, and by a single additional live load having the characteristic value of $Q_k = 250\ kN$. Thus the ratio of $Q_k / G_k = 2.50$.

It may be easily shown that the considered column is capable of safely resisting the loads applied to it in the conditions of persistent design scenario. In this case the bearing capacity will be exhausted by the flexural buckling along the so called „weak” axis of symmetry of the cross section (i.e. the „z” axis). As for the HEB180 $i_z = 4.57\ cm$, thus the slenderness:

$$\overline{\lambda}_z = \frac{600}{4.57\cdot 93.9} = 1.398 \qquad (1)$$

Should one assume the buckling curve „c”, for which $\alpha = 0.49$, one obtains

$$\varphi_0 = 0.5\cdot\left[1 + 0.49\left(1.398 - 0.2\right) + 1.398^2\right] = 1.771 \qquad (2)$$

resulting in the authoritative buckling coefficient:

$$\chi_z = \left(1.771 + \sqrt{1.771^2 - 1.398^2}\right)^{-1} = 0.339 \qquad (3)$$

and thus:

$$N_{b,Rd} = 0.339\cdot 65.3\cdot 10^{-4}\cdot\frac{235\cdot 10^6}{1.0} = 520.21\ kN \qquad (4)$$

This bearing capacity is sufficient, as:

$$N_{Ed} = 1.35\cdot 100 + 1.50\cdot 250 = 510\ kN < N_{b,Rd} \qquad (5)$$

2. Specification of the critical temperature for considered column according to the code

In the safety analysis the fire is considered as an accidental design situation. Thus the authoritative effect $E_{fi,d,t} = E_{fi,d,t}^{accidental}$ is determined according to the rules holding for the accidental load combinations. Therefore, having the value $E_{d,t} = E_{d,t}^{persistent}$ determined in traditional analysis for persistent design scenario, without taking the action of fire into account, one may express the sought value of $E_{fi,d,t}$ in terms of $E_{d,t} = E_{d,t}^{persistent}$ using the formula:

$$E_{fi,d,t} = \eta_{fi} E_{d,t} \tag{6}$$

Let us note, that the relation (6) will hold, provided that the effect $E_{fi,d,t}$ would be created by the same components, which were accounted for in the effect $E_{d,t}$, and this in turn would be true only if during fire no additional internal forces would be generated in the considered structural components. Thus then $E_{fi,d,t} = E_{fi,d,0} = \underset{t_{fi}}{const}$. In this approach the coefficient η_{fi} represents a conversion factor between the persistent and the accidental design situations. According to the recommendations contained in the code EN 1990 [2], during the selection of the authoritative component $\psi_{2,1}$ for the leading live load, and associated with its quasi-permanent value (this corresponds to the recommendations of Polish national annex), in general case the following holds:

$$\eta_{fi} = \frac{\sum_{j\geq 1} G_{k,j} + \sum_{i\geq 1} \psi_{2,i} Q_{k,i}}{\sum_{j\geq 1} \gamma_{G,j} G_{k,j} + \gamma_{Q,1} Q_{k,1} + \sum_{i>1} \gamma_{Q,i} \psi_{0,i} Q_{k,i}} \tag{7}$$

In the scenario, where one has to deal with only one dead and a single live load, and both these loads act in the „congruent" manner increasing the authoritative effect of action, i.e. when one may assume that $\gamma_{G,j} = 1.35$ and $\gamma_{Q,i} = 1.50$, the formula (7) may be simplified to the following:

$$\eta_{fi} = \frac{G_k + \psi_{2,1} Q_{k,1}}{1.35 G_k + 1.50 Q_{k,1}} = \frac{1.0 + \psi_{2,1} \dfrac{Q_{k,1}}{G_k}}{1.35 + 1.50 \dfrac{Q_{k,1}}{G_k}} \tag{8}$$

Should one consider now the accidental design scenario related to the fire acting on the considered column, then beginning with (8), in the considered example the following was obtained:

$$\eta_{fi} = \frac{1 + \psi_{fi} \cdot 2.50}{1.35 + 1.50 \cdot 2.50} = \frac{1 + 2.50 \psi_{fi}}{5.10} \tag{9}$$

As the analyzed live load is a payload, in the following calculations the coefficients ψ_{fi} were associated with the consecutive coefficients $\psi_{2,1}$ attributed to the quasi-permanent values of this load, and subsequently with coefficients $\psi_{1,1}$ accompanying the analogous frequent values. Obviously the values of assumed coefficients correspond to the load categories, according to the recommendations of the code [3].

During the calculations conducted for fire conditions one should take into account the changes in effective column slenderness induced by the progressive weakening of steel used to make it. This occurs according to the formula:

$$\overline{\lambda}_{\Theta} = \overline{\lambda} \left(\frac{k_{y,\Theta}}{k_{E,\Theta}} \right)^{0.5} \tag{10}$$

where the coefficient $k_{y,\Theta}$ is a measure of the reduction in nominal yield limit f_y of structural steel subjected to fire temperature Θ_a, and the coefficient $k_{E,\Theta}$ - a measure of the reduction in longitudinal limit of elasticity E_a for the said steel. The values of both coefficients, corresponding to the selected values of temperature Θ_a for typical low-carbon steels are listed in the table 4.6 of the code [4]. The authoritative buckling curve specific for the fire conditions, according to the code [4], is determined as:

$$\chi_{fi,\Theta} = \frac{1}{\varphi_{0,\Theta} + \sqrt{\varphi_{0,\Theta}^2 - \overline{\lambda}_{\Theta}^2}} \tag{11}$$

where $\chi_{fi,\Theta}$ stands for the buckling coefficient determined for fire conditions, while:

$$\varphi_{0,\Theta} = 0.5 \left(1 + 0.65 \sqrt{\frac{235}{f_y}} \overline{\lambda}_{\Theta} + \overline{\lambda}_{\Theta}^2 \right) \tag{12}$$

Finally:

$$N_{b,fi,\Theta,Rd} = \chi_{fi,\Theta} A k_{y,\Theta} \frac{f_y}{\gamma_{M,fi}} \tag{13}$$

The critical temperature of the considered column will be estimated in this case in a manner recommended in the code [4], thus directly from the formula:

$$\Theta_{a,cr} = 39.19\ln\left[\frac{1}{0.9674\mu_0^{3.833}} - 1\right] + 482\,[\,^{o}\mathrm{C}\,] \tag{14}$$

where μ_0 represents the degree of utilization determined for the structural components assigned to the class 1, 2, or 3 in fire conditions based on the ratio:

$$\mu_0 = \frac{E_{fi,d,t}}{R_{fi,d,0}} \tag{15}$$

where $E_{fi,d,t}$ represents the design value of the authoritative load effect, specified for the moment t_{fi} of the forecast fire, while $R_{fi,d,0}$ stands for the design bearing capacity of the considered structural component, determined for the fire initiation moment, i.e. $t_{fi} = 0$, and thus not taking into account the reduction of bearing capacity in fire temperature.

While complementing the values necessary to determine the coefficient μ_0 based on the formula (15), one may at first determine the value of correlated parameter μ equal to the ratio $N_{Ed} \big/ N^{(20)}_{b,fi,\Theta,Rd}$. The symbol $N^{(20)}_{b,fi,\Theta,Rd}$ denotes the bearing capacity of the column determined as it should be done for the accidental fire scenario and in its initial moment $t_{fi} = 0$, and thus simply for the temperature $\Theta_a = 20\,^{o}\mathrm{C}$, assumed to represent the room temperature. Because of various forms of the formula (2) typical for the persistent design scenario, and corresponding formula (12) applied during fire related calculations the value of $N^{(20)}_{b.fi,\Theta,Rd}$ will be quantitatively different than the value of $N_{b,Rd}$ calculated earlier, based on the formula (4). For the column analyzed in the example the following holds:

$$\varphi^{(20)}_{0,\Theta} = 0.5\left(1 + 0.65\sqrt{\frac{235}{235}}1.398 + 1.398^2\right) = 1.931 \tag{16}$$

this in turn, based on (11), yields:

$$\chi^{(20)}_{fi,\Theta} = \frac{1}{1.931 + \sqrt{1.931^2 - 1.398^2}} = 0.306 \tag{17}$$

and subsequently:

$$\begin{aligned} N^{(20)}_{b,fi,\Theta,Rd} &= 0.306 \cdot 65.3 \cdot 10^{-4} \cdot \frac{235 \cdot 10^6}{1.0} = \\ &= 469.57\ kN < N_{b,Rd} = 520.21\ kN \end{aligned} \tag{18}$$

Finally:

$$\mu = \frac{N_{Ed}}{N^{(20)}_{b,fi,\Theta,Rd}} = \frac{510}{469.57} = 1.086 \tag{19}$$

The above equality does not indicate, that the bearing capacity of the column, even at the room temperature, is insufficient to safely resist the applied axial compressive force, as in order to analyze the fire safety the coefficient $\mu_0 = \eta_{fi}\mu < \mu$ is authoritative.

Should one for instance assume that $\psi_{fi} = \psi_{2,1} = 0.6$, which according to [2] corresponds to the live load belonging to the category C or D, one would obtain $\eta_{fi} = 0.490$ based on (9), and this in turn yields $\mu_0 = 0.490 \cdot 1.086 = 0.532 < 1.0$, which after application of (14) leads to the following estimate for $\Theta_{a,cr} = 574.6\ ^{o}C$. A complete range of results obtained after application of consecutive values of coefficient ψ_{fi} is listed in the table 1.

At last one should verify how reliable are the estimates obtained this way. In order to do that for each value of the temperature $\Theta_{a,cr}$ listed in the table 1 it has been checked in the classical manner, i.e. in accordance with the recommendations contained in the code EN 1993-1-2 [4], whether the fire resistance limit state has been reached. The results of the performed verification are listed in the table 2. The design value of the resultant compressive force in the column, authoritative for the fire scenario and consecutive values of the coefficient ψ_{fi}, has been determined by the formula:

$$N_{E,fi,d} = G_k + \psi_{fi}Q_k \tag{20}$$

As may be easily observed, the temperature $\Theta_{a,cr}$ determined directly from the formula (14) and related in the table 1 to successive values of the coefficient

ψ_{fi} considered in the example in any way may not be treated as the critical temperature of the considered column. This temperature could not be correlated with the column reaching the fire resistance limit state. The design value of the column resistance $N_{b,fi,\Theta,Rd}$ proved to be substantially insufficient to safely resist the computational loads $N_{E,fi,d}$ applied to it. This means, that the forecast fire resistance, and thus the warranted fire safety estimate is overly optimistic. The overestimated bearing capacity in many cases was in excess of 30%, and this in principle disqualified the obtained estimates.

Table 1

Estimates of critical temperature $\Theta_{a,cr}$ for the column considered in the example, obtained directly from (14) for various categories of live load, with authoritative values of coefficient $\psi_{fi} = \psi_{1,1}$ and alternatively $\psi_{fi} = \psi_{2,1}$.

Live load category	A and B	C and D	E	A and B	C and D	E
ψ_{fi}	$\psi_{fi} = \psi_{1,1}$			$\psi_{fi} = \psi_{2,1}$		
	0.5	0.7	0.9	0.3	0.6	0.8
η_{fi}	0.441	0.539	0.637	0.343	0.490	0.588
μ_0	0.479	0.586	0.692	0.373	0.532	0.639
$\Theta_{a,cr}$ $\left[{}^oC\right]$	591.5	558.5	528.0	630.7	574.6	543.1

Table 2

Verification of the critical temperature $\Theta_{a,cr}$ estimates listed in the Table 1 for the column considered in the example based on the classical, code based approach according to the recommendations [4].

ψ_{fi}		$\Theta_{a,cr}$ $\left[{}^oC\right]$	$k_{y,\Theta}$	$k_{E,\Theta}$	$\overline{\lambda}_{\Theta}$	$\chi_{z,fi,\Theta}$	$N_{b,fi,\Theta,Rd}$ $[kN]$	$N_{E,fi,d}$ $[kN]$	$\dfrac{N_{E,fi,d}}{N_{b,fi,\Theta,d}}$
$\psi_{1,1}$	0.5	591.5	0.496	0.335	1.703	0.231	175.58	225	1.28
	0.7	558.5	0.599	0.430	1.649	0.242	222.28	275	1.24
	0.9	528.0	0.693	0.519	1.616	0.249	265.11	325	1.23
$\psi_{2,1}$	0.3	630.7	0.396	0.255	1.744	0.222	135.17	175	1.29
	0.6	574.6	0.549	0.384	1.672	0.237	199.67	250	1.25
	0.8	543.1	0.646	0.475	1.631	0.246	243.88	300	1.23

3. Code procedure taking into account iterations

Explanation of the differences between $\Theta_{a,cr}$ temperature estimates obtained by direct application of the formula (14), and those obtained in an alternative manner by associating this temperature with the fact that the considered column reached the fire resistance limit state is in this case relatively simple. The formula (14) should not be applied here, as in the fire resistance limit state the equivalence:

$$\mu_0 = k_{y,\Theta} \tag{21}$$

used to derive this formula does not hold. While looking for the critical temperature specified for the axially compressed steel column engulfed by fire, the safe load transfer condition develops into [5]:

$$\mu_0 \le \frac{R_{fi,d,t}}{R_{fi,d,0}} = k_{y,\Theta}\,\frac{\chi_{z,fi,\Theta}}{\chi^{(20)}_{z,fi,\Theta}} \tag{22}$$

The buckling coefficient $\chi_{z,fi,\Theta}$ here relates to the accidental fire condition, thus its value does change following the changes in temperature Θ_a. The value of analogous buckling coefficient $\chi^{(20)}_{z,fi,\Theta}$ is determined for the moment of fire initiation. This means, that this value remains constant regardless of the considered fire exposure time. In addition, as it has been shown before, these two coefficients are differentiated by the way the ancillary value φ_0 is determined, thus indirectly affecting the shape of buckling curve assumed for analysis. The level μ_0 to which the bearing capacity is used is determined for the moment $t_{fi} = 0$, thus it remains constant for the whole fire exposure time, and so it remains unaffected by the changing temperature of structural steel. As a result of the correction described by the formula (22) the bearing capacity reduction level of the considered column in fire conditions is no longer directly proportional to the corresponding reduction in strength of the structural steel used to make it. It is now somehow increased by the value of an authoritative buckling coefficient $\chi_{z,fi,\Theta}$ which decreases with the increasing steel temperature. This in turn means, that the $k_{y,\Theta}$ reduction factor value, acceptable from the safety standpoint must be appropriately raised, according to the inequality:

$$k_{y,\Theta} \geq \mu_0 \frac{\chi_{z,fi,\Theta}^{(20)}}{\chi_{z,fi,\Theta}} \tag{23}$$

Thus, since the value of the critical temperature $\Theta_{a,cr} = 574.6\ {}^oC$ presented in the Table 1 and obtained subject to the assumption that $\psi_{fi} = \psi_{2,1} = 0.6$, proved to be substantially overestimated after the verification performed in the Table 2, the iterative procedure will be applied now to get a more precise estimate of it. For the temperature $\Theta_{a,cr} = 574.6\ {}^oC$ and for corresponding data listed in the Table 2, the formula (19) yielded:

$$\begin{gathered} k_{y,\Theta}^{(574.6)} \geq 0.532 \frac{0.306}{0.237} = 0.687 \Rightarrow \\ \Rightarrow \Theta_{a,cr} = 530.0\ {}^oC \end{gathered} \tag{24}$$

At this temperature:

$$k_{E,\Theta}^{(530.0)} = 0.513 \tag{25}$$

as well as:

$$\begin{gathered} \bar{\lambda}_{\Theta}^{(530.0)} = 1.398 \sqrt{\frac{0.687}{0.513}} = 1.618 \Rightarrow \\ \Rightarrow \chi_{z,fi,\Theta}^{(530.0)} = 0.249 \end{gathered} \tag{26}$$

which in turn yields:

$$\begin{gathered} N_{b,fi,\Theta,Rd}^{(530.0)} = 0.249 \cdot 65.3 \cdot 10^{-4} \cdot 0.687 \cdot \frac{235 \cdot 10^6}{1.0} = \\ = 262.5\ kN > N_{E,fi,d} = 250\ kN \end{gathered} \tag{27}$$

The critical temperature $\Theta_{a,cr} = 530.0\ {}^oC$ obtained in this step is evidently underestimated. Subsequent application of the formula (22) yields the temperature:

$$\begin{gathered} k_{y,\Theta}^{(530.0)} \geq 0.532 \frac{0.306}{0.249} = 0.654 \Rightarrow \\ \Rightarrow \Theta_{a,cr} = 540.6\ {}^oC \end{gathered} \tag{28}$$

for which:

$$k_{E,\Theta}^{(540.6)} = 0.482 \tag{29}$$

and

$$\begin{gathered} \bar{\lambda}_{\Theta}^{(540.6)} = 1.398 \sqrt{\frac{0.654}{0.482}} = 1.628 \Rightarrow \\ \Rightarrow \chi_{z,fi,\Theta}^{(540.6)} = 0.247 \end{gathered} \tag{30}$$

thus finally yielding:

$$\begin{gathered} N_{b,fi,\Theta,Rd}^{(540.6)} = 0.247 \cdot 65.3 \cdot 10^{-4} \cdot 0.654 \cdot \frac{235 \cdot 10^6}{1.0} = \\ = 247.9\ kN < N_{E,fi,d} = 250\ kN \end{gathered} \tag{31}$$

The above inequality indicates, that the resultant temperature $\Theta_{a,cr} = 540.6\ {}^oC$ is close to reality, though again overly optimistic. In the subsequent step the following have been obtained:

$$\begin{gathered} k_{y,\Theta}^{(540.6)} \geq 0.532 \frac{0.306}{0.247} = 0.659 \Rightarrow \\ \Rightarrow \Theta_{a,cr} = 539.0\ {}^oC \end{gathered} \tag{32}$$

thus meaning that:

$$k_{E,\Theta}^{(539.0)} = 0.487 \tag{33}$$

and

$$\overline{\lambda}_{\Theta}^{(539.0)} = 1.398\sqrt{\frac{0.659}{0.487}} = 1.626 \Rightarrow \tag{34}$$
$$\Rightarrow \chi_{z,fi,\Theta}^{(539.0)} = 0.247$$

finally, as the result:

$$N_{b,fi,\Theta,Rd}^{(539.0)} = 0.247 \cdot 65.3 \cdot 10^{-4} \cdot 0.659 \cdot \frac{235 \cdot 10^{6}}{1.0} = \tag{35}$$
$$= 249.8\ kN < N_{E,fi,d} = 250\ kN$$

In the authors' opinion the estimate $\Theta_{a,cr} = 539.0\ {}^{o}C$ may be assumed as relatively reliable. The difference between the column bearing capacity determined for this temperature and the effect of actions of loads applied to it and summed according to the rules holding for the accidental load combinations is now very small.

Juxtaposition of analogous estimates for the critical temperature of the considered column, and obtained by the iterative procedure for the remaining cases listed in the Table 2 is shown in the Table 3.

Table 3

Estimates of the critical column temperature for the case considered in this paper, obtained via iterative procedure for various categories of live load and authoritative values of coefficients corresponding to frequent or quasi-permanent values of this load, listed above in the Table 1.

Imposed load category	A and B	C and D	E	A and B	C and D	E
ψ_{fi}	$\psi_{fi} = \psi_{1,1}$			$\psi_{fi} = \psi_{2,1}$		
	0.5	0.7	0.9	0.3	0.6	0.8
$\Theta_{a,cr}$ $\left[{}^{o}C\right]$	556.6	521.1	465.9	592.0	539.0	503.3

Comparison of critical temperature estimates for the considered column with respect to the initial relative slendernesses $\overline{\lambda} = \overline{\lambda_{20}}$, those obtained after application of the iterative procedure described above and listed in the Table 3, with those shown before in the Table 1 and determined for the same slendernesses after direct application of the formula (14) with no iterations applied, are shown in the Fig. 1. The compared curves are related to the values of $\psi_{fi} = \psi_{2,1} = 0.6$ assumed in the example. As may be observed the differences in results are very substantial, especially in the case of relatively slender columns, for which the buckling coefficient decreasing in fire with decreasing steel strength plays a decisive role. In Fig. 2 the influence is depicted of the selected category of live loads and of the way the computational effect of combining actions applicable in the case of accidental fire scenario exert on the critical temperature of the considered column. The knowledge of this type in the computational model described above is determined by the properly assumed value of the coefficient ψ_{fi}.

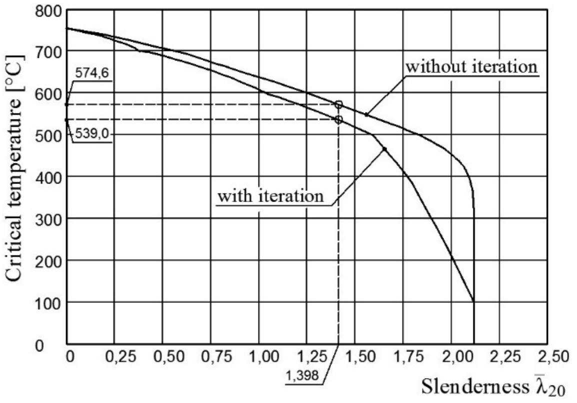

Fig. 1 Estimate of the critical temperature $\Theta_{a,cr}$ for the column considered in the example at various initial slendernesses $\overline{\lambda}_z = \overline{\lambda}_{20}$, obtained via direct application of formula (14) and after application of the iterative procedure. The factor $\psi_{fi} = \psi_{2,1} = 0{,}6$ was assumed. The results obtained in presented calculations are indicated.

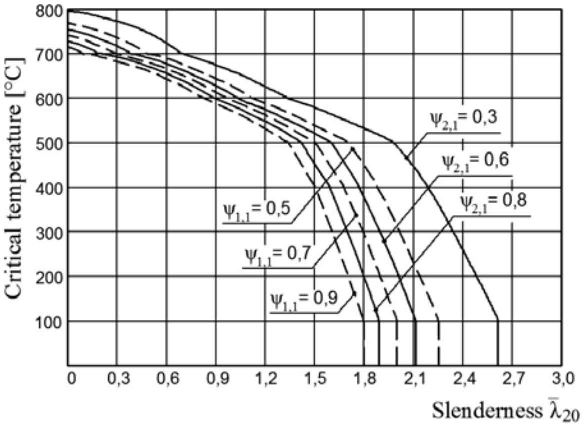

Fig. 2 Influence of the live load category and load combination specific to the accidental fire scenario applied during calculations on the estimates of critical temperature for column considered in the example, obtained after application of the iterative procedure.

4. Estimate of the critical temperature for the column obtained by application of the numerical analysis

A 3D numerical model has been developed in the ANSYS computational environment [6] in order to verify the estimates of the critical temperature $\Theta_{a,cr}$ obtained for the column analyzed in this paper by application of analytical procedures. Obviously the same column geometry and the same heating conditions have been applied during numerical analysis. The shell elements of the Shell181 type have been used, allowing for geometrically and physically nonlinear analysis. Finite elements of this type allow for taking into account the local phenomena such as local yielding in the wall of the I-beam undergoing analysis by appropriate selection of the number of integration points. An elastic plastic material model exhibiting kinematic hardening has been assumed for the structural steel subjected to analysis. The dependence of yield limit f_y and the longitudinal modulus of elasticity E_a for the steel on the temperature Θ_a has been introduced into the model according to the recommendations [4]. An initial bow imperfection conforming to the first global form of instability for the considered column – obtained by the conventional local buckling analysis (LBA) has been also introduced into the model. The size of this imperfection has been assumed according to the recommendations contained in the code [4], at the level of L/1000, where L stands for the column height. The boundary conditions at both ends of the column completely restricted the displacements in the plane perpendicular to the column longitudinal axis (i.e. U_x as well as U_y), and in addition at one end of the column the displacements along the longitudinal axis (U_z) have been blocked as well. In order to determine the critical temperature $\Theta_{a,cr}$ the loads have been applied to the column in sequence, in two steps. During the first step the static load having the value of $N_{E,fi,d}$ had been applied, and in the second step, after stabilization of deformations, the column has been monotonically heated with the temperature Θ_a increasing in time, until the column lost the capability to safely resist the loads applied to it. Thus the numerical calculations have been terminated when the limit point on the static equilibrium path delimited in the space by the axes: averaged temperature of the column cross section at the mid height of the column – horizontal displacement of the column axis at the mid height has been reached. In Fig. 3 the static equilibrium paths are depicted in detail, these obtained for selected models after conducted simulations with values of critical temperature $\Theta_{a,cr}$ listed along the curves corresponding to the models loaded by forces $N_{E,fi,d}$ having the values of 175 kN, 250 kN and 300kN, respectively (see Table 2 for $\psi_{fi} = \psi_{2,1}$). The shape of obtained equilibrium paths allows for estimation of the temperature Θ_a, above which the plastic deformation of structural steel started to dominate the situation.

The complete juxtaposition of critical temperature estimates for the column considered in the example, both those specified for $\psi_{fi} = \psi_{2,1}$ and depicted in Fig. 3, as well as those relating to the assumption that $\psi_{fi} = \psi_{1,1}$, is listed in the Table 4. There these results are compared with analogous estimates obtained by the purely analytical approach, with application of the iterative procedure recommended by the authors, and presented above in the Table 4.

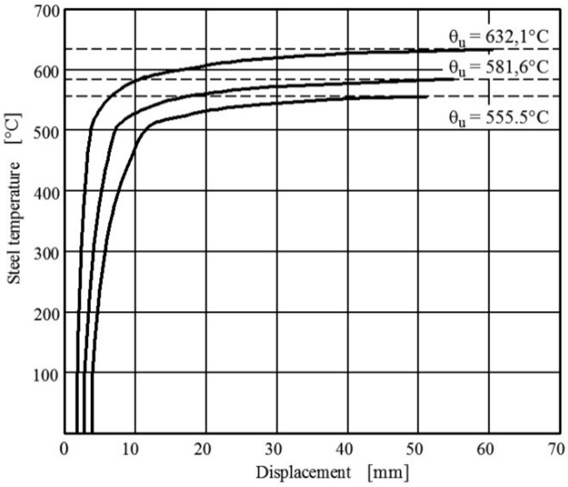

Fig. 3 Static equilibrium paths obtained after simulation conducted for three numerical models of the column considered in the example, loaded with three values of axial force $N_{E,fi,d}$: 175 kN, 250 kN and 300kN, accompanied by the values of critical temperature determined in each case.

5. Alternative critical temperature specification method for a column based on a second order analysis with the amplification of initial bow imperfection

In this approach the conventional stability analysis is replaced by the second order bearing capacity analysis of a column with imperfect geometry and taking into account the amplification of initial bow imperfection, assumed in an analogous manner as before in the numerical model described in the preceding chapter of current paper [7]. The condition for safe transfer of loads in fire conditions assumes the form of the following inequality:

$$\frac{N_{E,fi,d}}{Af_{y,\Theta}}+\eta_{\Theta}\frac{N_{E,fi,d}}{W_{pl}\,f_{y,\Theta}}\leq 1.0 \qquad (36)$$

where the parameter η_{Θ} stands for the amplification coefficient, and is determined via the following formula:

$$\eta_{\Theta}=\frac{1}{1-\dfrac{N_{E,fi,d}}{N_{cr,\Theta}}} \qquad (37)$$

In order to simplify the considerations, it is assumed during the analysis that the amplification is made based on the purely elastic Euler critical force, and not on the critical force specific to the elastic–plastic buckling, thus:

$$N_{cr,\Theta}=\frac{\pi^2 E_{a,\Theta} J_z}{L^2} \qquad (38)$$

Table 4

Estimates of the critical temperature for the columns considered in the example, obtained after application of the second order analysis juxtaposed with analogous estimates obtained by iterative analytical approach and numerical simulations.

Imposed load category	A and B	C and D	E	A and B	C and D	E
ψ_{fi}	$\psi_{fi}=\psi_{1,1}$			$\psi_{fi}=\psi_{2,1}$		
	0.5	0.7	0.9	0.3	0.6	0.8
$\Theta_{a,cr}\ \left[{}^{o}C\right]$	553.6	521.5	480.7	587.6	538.4	505.1
$\Theta_{a,cr}^{ANSYS}\ \left[{}^{o}C\right]$	594,6	568,5	542.4	632.1	581.6	555.5
$\Theta_{a,cr}^{II}\ \left[{}^{o}C\right]$	599.6	575.0	550.1	638.3	587.3	562.5

In the presentation of this computational approach one has to underline, that the fire temperature affects not only the yield limit of the structural steel, but also the accompanying changes in the flexural rigidity of the considered column.

The replacement of inequality (36) by the equality related to the considered column reaching the fire resistance limit state allows for the determination of the temperature $\Theta_{a,cr}^{II}$ related to this state. Juxtaposition of the temperature values obtained for all the cases considered in current paper is presented in the Table 4 as well.

6. Concluding remarks

Juxtaposition of the critical temperature estimates specified for the columns analyzed in the example considered here, and arrived at via different computational methods for the same heating conditions allows for quantitative comparison of these results, and drawing more general conclusions. As one may easily observe, the values of the critical temperature $\Theta_{a,cr}$ derived by the analytical iterative approach, for each of the considered cases proved to be by at least $40\,^{o}\mathrm{C}$ lower than the estimates $\Theta_{a,cr}^{II}$ obtained after application of the second order bearing capacity analysis or application of the numerical analysis. This proves, that the iterative procedure based on the conventional analysis of the stability type usually yields very safe, and thus relatively conservative results. The key parameters of this method, i.e. primarily the classical buckling coefficients are calibrated for fire conditions in such manner as to yield the results located always on the safe side. Should one assume, that the most precise estimates of the sought critical temperature are yielded by the analysis of the appropriate numerical models developed for the considered columns, one would have to admit, that the corresponding results derived by the application of relatively simple in use second order analysis are relatively close. Overestimates in the range of $5^{\circ}\mathrm{C}$ to the detriment of the safety do not seem to have any practical importance in this case. Thus it seems, that all the computational approaches considered in present paper, within the scope of analysis performed, proved their reliability and applicability for practical use in analysis of safety related to the accidental design scenario of a fully developed fire.

References

[1] M. Maślak: Temperatura krytyczna konstrukcji stalowej, Ochrona Przeciwpożarowa, 2/2014.

[2] EN 1990: Eurocode - Basis of structural design.

[3] EN 1991-1-1: Eurocode 1 - Actions on structures, Part 1-1: General actions.

[4] EN 1993-1-2: Eurocode 3 – Design of steel structures, Part 1-2: General rules – Structural fire design.

[5] M. Maślak, M. Suchodoła: O wyznaczaniu temperatury krytycznej stalowych słupów ściskanych ogarniętych pożarem, Inżynieria i Budownictwo, 2/2018.

[6] P. Kohnke (Ed.): ANSYS®: Theory reference. Release 5.6. Canonsburg, PA, USA, November 1999.

[7] N. Boissonade, R. Greiner, J. P. Jaspart, J. Lindner: Rules for Member Stability in EN 1993-1-1: Background documentation and design guidelines, ECCS, Brussels, 2006.

Earth in a Trap? 2018
Analytical Methods in Fire and Environmental Science

Evaluation of the TETRA K board for the fire protection and safety needs

Iveta Mitterová[a] – Václav Kasan[a]

[a]Faculty of Wood Sciences and Technology, Technical University in Zvolen, T. G. Masaryka 24, 960 53 Zvolen, Slovak Republic

---

Abstract

The process of waste reuse also leads to a significant saving of natural resources, energy and, finally, efforts to ensure a clean environment.

An interesting solution in this regard is the recycling and processing of Tetra Pak (beverage cartons) for products that find use in the construction of tile boards, or so-called dry construction products. It is precisely the type of product that has become our study object, to find out what properties of the Tetra Pak boards, such as the Tetra K standard board, have in terms of fire. For this purpose, experiments were carried out, where samples of the material were subjected both to the ignition testing according to STN EN ISO 11925-2 and evaluated for their ability to spread a flame on their surface, as well as a non-standard testing method for the detection of mass loss and ignition time. The work methodology and the results achieved are the content of the paper.

When, on the basis of the same evaluation criteria (mass loss, ignition time, flame propagation) and constant testing conditions, we mutually compare the Tetra K boards with e.g. OSB boards, having a similar use, we can say that both materials at the same time of thermal loading have the relative mass loss: Tetra K board of 70.3 ± 6.9 % and OSB board of 67.7 ± 5.6% on average; average ignition time: Tetra K of 81 ± 14 s and OSB of 63 ± 11 s. The both materials, according to STN EN 13501-1 + A1, met reaction to fire classification criterion $Fs \leq 150$ mm in 60 s. This means that the two materials do not differ significantly from the point of view of the comparison of the fire properties. The advantage of the Tetra K board is probably a lower price.

Keywords: Flame spreading; mass loss; one-flame source; radiant source; recycling; Tetra Pak boards

---

1. Introduction

Beverage carton also popularly called "Tetra Pak", has become an indispensable part of our households as it is packed with ordinary foods - milk, dairy products, juices, baby drinks, etc. Around 1,500,000 beverage cartons are sold in Slovakia a year and approximately 9,000 tonnes are marketed each year [1].

Cardboard packaging is one-off packaging. Their re-use on food packaging is excluded, therefore the empty ones ends in waste and can be disposed of or used other way.

Drinking cartons belong to the so-called multilayer composite materials. All carton layers, which are the paper fibres (more than 70%), polymer (more than 20%), and sometimes aluminium (4%) can be recycled by simple processes and this way to give them a new life.

The process of recycling beverage cartons is also known as pulping, in which paper fibres are separated from the polymer and aluminium. The fibres are long and firm, which means they are especially suited to different paper products. Polymer and aluminium are separated by pyrolysis. In this process the polymer changes to gas, the aluminium scales are pressed into briquettes and further used as a raw material to produce various aluminium products [2].

Another and interesting solution is the recycling and processing of "Tetra Pak" for products that are used in construction in the form of tiles and panels - dry construction.

Right this way the of waste reuse caught our attention, and respecting the use of those products, we have decided to implement own experiments to find out the fire properties of the “Tetra Pak” boards, particularly the Tetra K standard boards.

Tetra K standard “Tetra Pak” board

The producer of this board is the Slovak company Kuruc Company Ltd., and it belongs to its basic products. The sorted waste from the beverage cartons used is washed, the raw material is crushed to the desired fractions and subsequently pressed to the boards at the specified temperature, defined humidity and high pressure, without the addition of adhesives or other binders. The surface of the boards can be adjusted according to the customer's requirements (washable, furniture, etc.).

The boards are characterized by good strength, flexibility and low absorption. However, they are not suitable for use in spaces where they may be exposed to a long-term effect of moisture and direct exposure to water. According to the input raw material, they are environmentally, health and hygienically harmless, characterized as recyclable material [3].

They are used for the construction of light structures and shelters. In conjunction with the insulation material - PUR foam. the Tetra K panels are made of these, which can be used in less loaded structures such as partitions and prefabricated walls. In combination with EPS, they are used as facing panels for internal and external insulation [4, 5].

2. Experiment

Tetra K boards from the abovementioned manufacturer were subjected to two testing methods for the fire performance evaluation: the ignition test, according to STN EN ISO 11925-2 [6] (Figure 1a), and the non-standard test method using the radiant heat source (Figure 1b). The observed parameters were: flame propagation over the surface of the tested samples, mass loss and ignition time.

Testing samples

According to the requirements of the selected testing methods, the Tetra K „Tetra Pak“ board samples dimensions were of 90 x 250 mm for the ignition test and of 50 x 40 mm for the radiant source test. The sample thickness was of 10 mm, i.e., such as these boards are commonly produced.

Testing apparatus used

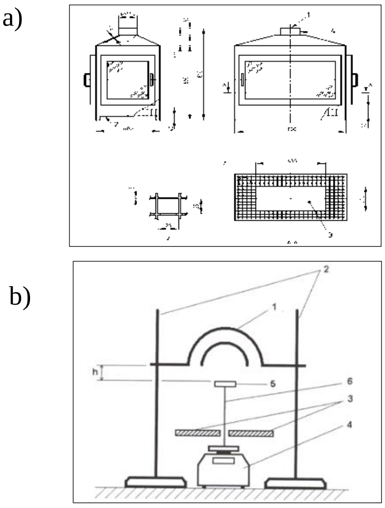

Fig. 1 Schematic representation of testing apparatus used

a) For the ignition test [6]

b) For radiant heat source test
1– infrared, 2 – metal stand, 3 – scale protection, 4 – electronic scales, 5 – testing sample, 6 – samples holder

Testing methods

The ignition test - the principle is the effect of a small flame (20 mm height) on the vertically oriented samples for 15 s or 30 s (depending on the classification class). If the flame application time is of 15 s, the total duration of the test is 20 s from the moment the flame starts. If the flame application time is 30 s, the total duration of the test is 60 s from the moment the flame occurrence. The tests may be performed by exposing the main surface and / or by exposing the side surface (edge) of the samples to the flame.

During the test (20 s or 60 s - depending on the classification class), it is observed whether the sample was ignited, the flame peak is 150 mm above the flame attachment point and the time at which it occurs, the physical behaviour of the tested sample is also observed.

The Radiant Heat Source Test – the experiment consists of exposing the test samples to the effect of a 1000 W thermal infrared heater, at a distance of 30 mm from the surface of the radiating body, for 600 seconds. During the test, the mass loss of the test material is recorded at regular 10-s intervals, and ignition of the samples is monitored visually, with a time-record being performed if the phenomenon would occur.

The evaluation criterion for the test is the relative mass loss, according to the following equation [7]:

$$\delta_m(\tau)=\frac{m(\tau_0)-m(\tau)}{m(\tau_0)}*100\quad(\%)$$

Where:

δ_m - relative mass loss over time (τ) [%]
$m(\tau_0)$ - original sample weight [g]
$m(\tau)$ - sample weight over time (τ) [g]

3. Results

Results of the ignition test according to STN EN ISO 11925-2

This evaluation is documented in Tab. 1 and 2, where the results of two exposures (surface, edge) of samples to the flame, with a loading time of 30 s and a total test duration of 60 s, are introduced.

Tab. 1

The results of the evaluation criteria for surface loading

Sample		Sample ignition yes/no	Reaching a height of 150 mm above the flame attachment point (STN EN ISO 11925-2)	Meeting the Classification Criterion $F_s \leq 150$ mm in 60 s (STN EN 13501-1 + A1)
1	4	no	no	met
2	5			
3	6			

Tab. 2

The results of the evaluation criteria for edge loading

Sample		Sample ignition yes/no	Reaching a height of 150 mm above the flame attachment point (STN EN ISO 11925-2)	Meeting the Classification Criterion $F_s \leq 150$ mm in 60 s (STN EN 13501-1 + A1)
1	4	no	no	met
2	5			
3	6			

Radiant source test results

The evaluation is documented in Tab. 3, which shows the results of the total mass loss as well as the ignition time of the samples tested. Figure 3 is a graphical representation of the mass loss over time of the samples tested.

Tab. 3

The results of the evaluation criteria for test with a radiant source

Criteria	Samples					Mean
	1	2	3	4	5	
Mass loss (%)	59.15	74.97	73.93	68.14	75.43	70.3 ± 6.9 %
Ignition time (s)	97	82	80	86	60	81 ± 11 s

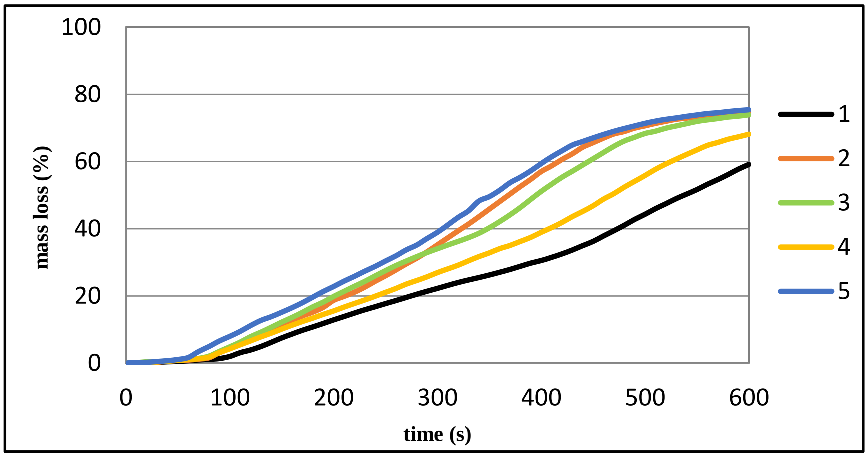

Fig. 3 Dependence of mass loss on time of the Tetra K board samples

4. Discussion

The ignition test, we used to evaluate the Tetra K "Tetra Pak" board is one of the valid methods for evaluation of construction products from the reaction-to-fire point of view. Its results are used for classification of construction products into the reaction-to-fire classes.

In this test, the Tetra K board did not spread a flame on its surface (see Figure 4a), and that is why it met the Fs ≤ 150 mm in 60 s classification criterion. According to STN EN 13501-1 + A1 [8], the compliance with this criterion is one of the requirements for classification into the classes B, C and D (see Tab. 4).

The manufacturer of the "Tetra Pak" board reports its evaluation using the invalid degree of flammability C1, which is currently class C classification according to NA.1 of the National Annex to the standard EN 13501-1 + A1.

However, we cannot clearly confirm this classification, because according to the classification requirements of the STN EN 13501-1 + A1 standard, in addition to meeting the Fs criterion ≤ 150 mm in 60 s (according to the ignition test), the Tetra K boards would have to meet the test criteria according to STN EN 13823 [9] - see tab. 4.

Tab. 4

Classification criteria and test methods for reaction classes B, C and D – selection from Table 1 of the 13501-1 + A1 standard [8]

Class	Testing method	Classification criteria	
B	EN 13823	FIGRA ≤ 120 W/s	Smoke production and burning droplets / particles
		LFS < edge of the test sample	
		THR_{600s} ≤ 7.5 MJ	
	EN ISO 11925-2 **loading = 30 s**	**F_s ≤ 150 mm in 60 s**	
C	EN 13823	FIGRA ≤ 250 W/s	Smoke production and burning droplets / particles
		LFS < edge of the test sample	
		THR_{600s} ≤ 15 MJ	
	EN ISO 11925-2 **loading = 30 s**	**F_s ≤ 150 mm in 60 s**	
D	EN 13823	FIGRA ≤ 750 W/s	Smoke production and burning droplets / particles
	EN ISO 11925-2 **loading = 30 s**	**F_s ≤ 150 mm in 60 s**	

In evaluation of the radiant source test we found that the “Tetra Pak” board samples lost on average of 70.3 ± 6.9% of their original mass over the 600 s period (this variability we assign to the structure of the recycled material), and they were ignited in a relatively short time (81 ± 14 s). In Fig. 4b, there is shown how the structure of the material has changed after the thermal loading against the original structure. The samples were very fragile. There remined only the remains of the aluminium foil, as mentioned in the introduction, the beverage cartons contain.

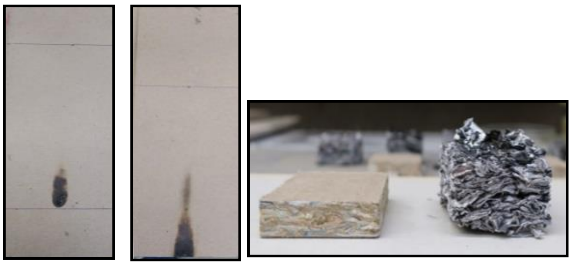

a) b)

Fig. 4 Photo documentation of Tetra K samples after the test
a) In the ignition test (exposed area and edges)
b) In the radiant source test

When comparing the results of the Tetra K board and e.g. OSB board (mass loss: 67.7 ± 5.6%, ignition time: 63 ± 11 s, Fs criterion ≤ 150 mm in 60 s), evaluated by Vyletelová in her work [10], we can state that both materials under constant test conditions had not achieved very different results, i.e., that the two materials do not differ significantly from the fire safety point of view.

5. Conclusions

Recycling is important for the environment in many respects, in particular it provides many significant ecological and economic benefits. It prevents, e.g., storage of materials in landfills, re-use reduces the need for new resources, and usually the re-use of raw materials requires less energy than their recovery.

The fact that even “Tetra Pak” does not have to be a waste is evident from this paper. We introduced a product of a Slovak company that has been engaged in the recycling and processing of beverage cartons for a long time and which supply the market with

"Tetra Pak" boards, which are used as building or insulating elements in the construction industry. However, our objective was to evaluate how such a material, the Tetra K "Tetra Pak" board, will behave in the conditions of thermal loading.

Experiments have shown that this material, when exposed to a heat source, does not spread a flame on its surface, and therefore is not supposed to contribute to the development of the fire. On the other hand, it loses the bulk of its weight (70.3% on average in time of 600 s) and becomes fragile.

For comparison, we also reported the results of the OSB board (material with a similar use in constructions), and we can conclude that the Tetra K and OSB boards had similar results in terms of the same evaluation criteria, but with the difference that the OSB board remained more compact after the test. The decision, which of these materials choose, if necessary, remains on the customer. The favour of Tetra K boards a lower price may indicate.

Acknowledgement

This work was supported by the Slovak Research and Development Agency under the contract No. APVV-16-0326 (50 %) and No. VEGA 1/0493/18 (50 %).

References

[1] We sort the beverage cartons. Tetrapak (Triedime nápojové kartóny)= [online]. [cit. 2018-05-01] Dostupné na internete: http://www.napojovy-karton.sk

[2] Beverage cartons recycling. (Recyklácia nápojových kartónov) [online]. [cit. 2018-05-01] Dostupné na internete: http://www.napojovy-karton.sk/recyklacia

[3] TETRA K Standard Board (Štandardná doska TETRA K). Kuruc Company spol. s r.o. [online]. [cit. 2018-05-01]. Dostupné na internete: http://www.kuruc.sk/vyroba-dosiek/standardna-doska-tetra-k/

[4] MIKA, O. 2005: TETRA K boards from the recycled laminated packaging (Desky TETRA K z recyklovaných vrstvených obalů). In Materiály pro stavbu (časopis). Roč. 11, č. 5, s. 28-30 ISSN 1213-0311

[5] HRÁZSKÝ, J, - KRÁL, P. 2009: Desky TETRA K – boards - a top environmental product made from waste (TETRA K špičkový ekologický produkt vyráběný z odpadu). In Stolársky magazín (časopis). Roč. 10, č. 4, s. 6-8 ISSN 1335-7018

[6] STN EN ISO 11 925-2:2011 Reaction to fire tests. Ignitability of products subjected to direct impingement of flame. Part 2: Single-flame source test (Skúšky reakcie na oheň. Zapáliteľnosť stavebných výrobkov vystavených priamemu pôsobeniu plameňového horenia. Časť 2: Skúška jednoplameňovým zdrojom)

[7] KLEIN, T. – BAHÝL, V. – VACEK, V. 1999. Introduction to probability and mathematical statistics. (Základy pravdepodobnosti a matematickej štatistiky), Zvolen: ES TU, 1999. 236 s. ISBN 80-228-0115-1.

[8] STN EN 13501-1 + A1: 2010 Fire classification of construction products and building elements. Part 1: Classification using data from reaction to fire tests (Klasifikácia požiarnych charakteristík stavebných výrobkov a prvkov stavieb. Časť 1: Klasifikácia využívajúca údaje zo skúšok reakcie na oheň)

[9] STN EN 13823: 2011 Reaction to fire tests for building products. Building products excluding floorings exposed to the thermal attack by a single burning item.(Skúšky reakcie stavebných výrobkov na oheň. Stavebné výrobky okrem podláh vystavené tepelnému pôsobeniu jednotlivého horiaceho predmetu)

[10] VYLETELOVÁ, A. 2014: Effectiveness of the retardant depending on its application to wood material (Účinnosť retardačnej látky v závislosti od jej aplikácie na drevný materiál). Zvolen: TU vo Zvolene, 2014, 81 s.

Comparison of synthetic and natural sorbents in engine oil spills

Miroslav Mojžiš[a] – Miriama Šuleková[a] – Martin Zachar[a] – Danica Kačíková[a]

[a]*Technical university in Zvolen, Slovak Republik*

Abstract

The leak of petroleum substances has harmful effects and negative impact on the ecosystem. The most frequent petroleum pollutants with a small range (up to 1 $dm^3.h^{-1}$) or spills which do not exceed 1 m^2 and thickness of 1mm, include leakage due to various accidents or negligence. Prevention or intervention that employs sorbents to handle oil leakage situations. The paper is focused on sorbents in bulk state and on their quantitative use by leakage of petroleum substances, especially in traffic accidents on roads. Bulk sorbents were chosen based on their origin: natural and synthetic. Synthetic sorbents include Absodan plus, PeWaS Sorb, Sorp Reo and Spilkleen Plus. Sawdust, leaves residues, needles and mosses were used as natural sorbents. Sorbents were tested for sorption capacity according to standardized method ASTM F 726. Sorbent samples were tested for engine oil 10W 40, which is the most commonly used oil in motor vehicles. According to the sorption properties due to the standard, sorption capacity of adsorbents were measured in the short term. Based on the obtained results, it was found that synthetic sorbents have better sorbtive capacity represented by Sorbtive Grass Reo with a value of 14.98 g/g. Among natural sorbents, leaves residues of 7.43 g/g have better capacity. In the accordance of obtained results, synthetic sorbents have higher sorption capacity than natural sorbents as they are manufactured for sorption purposes.

Key words: oil spills; natural sorbents; synthetic sorbents; ecosystem

1. Introduction

Leak of petroleum substances has a negative effect on the ecosystem [1]. Petroleum can mainly leak out in various traffic accidents, but it is important to point out that under certain conditions, even small quantities can cause severe damage to individual components of the ecosystem, particularly water, soil and air. Petroleum products are a product of petroleum processing, which is processed and transformed into a variety of products. The best-known oil products include lubricants, oils and fuels, which are very common in practice. In practice, we can quite often come across the leak of petroleum substances in various traffic accidents. These substances usually include the working fluids in motor vehicles. There are several ways and technologies for extracting petroleum from nature [2]. These techniques and processes for removing or purifying the environment from petroleum can be divided into biodegradation, chemical or manual removal[3], [4], [5], [6]. Different types of sorbents are used on a natural or synthetic basis as a cleaning agent for petroleum substances.

2. Sorbents

Sorbents are substances of a solid state, which can absorb gaseous or liquid substances due to their physical and chemical composition. The characteristic property of sorbents is the ability to absorb a certain amount of liquid in relation to its own weight [7]. The sorbents are divided according to the form into the bulk sorbents and those made of microfibers like a fabric. Other criterium for sorbent distribution is their origin: natural or synthetic sorbents. Also, sorbent structure is very important for its sorption capacity. The capacity of the sorbent mainly depends on the size of the surface area to which the dangerous substance, oil product can adhere as well as surface type (surface structure). The size of the surface of the sorbents and the increase in their sorption capacity is influenced by various cracks such as pores and capillaries. The average surface area of the sorbent is expressed in units of area (m^2) per unit mass (g, kg). Sorbents have a surface area most often about 1 000 000 $m^2 \cdot kg^{-1}$ [8]. Sorbents are considered to be good with such a surface and effective. Because of the size of the surface, sorbents have the ability to bind both physically and chemically on their surface and also into the pores, capillaries and substances of organic or inorganic origin.

The principle of sorption substances can be described as follows. Adsorption consists of several processes, which take place at the same time. In particular, it is a saturation of the sorbed substance on the surface and into the pores directly in the beads or granules and the saturation between the various granules. By adsorption in a monomolecular layer, only a small amount of liquid can be collected on the surface of the solid. The amount of liquid can be increased by surface enlargement of the solid particles. Figure 1 shows the mechanism of adsorption.

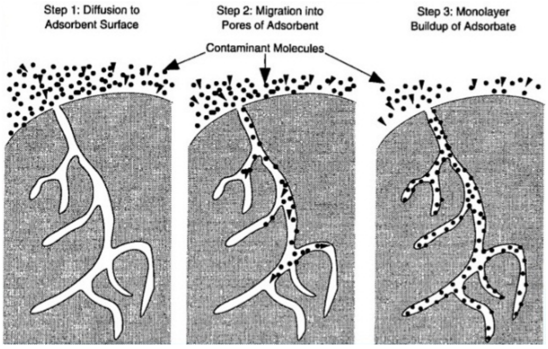

Fig. 1 Mechanism of adsorption (https://www.slideshare.net/VivekKumar36/adsorption-regenerationvivek-kumarneeri) [9]

At present, most of the commercial sorbents are synthetic materials and are of a hydrophobic nature, due to their excellent sorption capacity for a variety of oil-based materials [10]. To remove leaked working fluids, it is also possible to use materials in the vicinity of the leakage, which are natural sorption materials in the case of leakage of operational fluids in forestry or leakage during handling of wood in forest stores. When some substances leak into the environment, natural sorbents are preferredfor their biological degradability. Many other authors dealt with the use of various inorganic and organic natural sorbents to remove oil stains [11], [12].

2.1. Natural sorbents

Natural sorbents include wood sawdust, peat, hedges, leaves residue, sand, and others. They generally have low absorption capacity and are suitable only for small leaks. On the other hand, they are affordable because they are in sufficient quantity in the natural environment at the site of intervention. Subsequent ecological disposal is difficult, because syntheticly produced and prepared sorbents are are favoured. Both natural and synthetic sorbents can be modified by so-called hydrophobization, which increases the absorption of non-polar liquids such as oil and petroleum products [13].

2.2. Synthetic sorbents

Synthetic sorbents include ash and coconut dust. They were not intended for sorption purposes and absorbency of oil or water based liquids, but were only a side effect due to their pore-containing structure. These by-products of production have begun to be processed into high-quality sorption materials. As a result of the above, the substances based on rocks (perlite, clay, limestone), cellulose and plastics (polypropylene, polymer) were also produced. Synthetic sorbents are deliberately manufactured and treated for the purpose of removing petroleum products or for chemical contamination. They can be chemically treated similarly to natural sorbents by hydrophobization. This treatment makes the sorbents hydrophobic and oleophilic. Sorbents are used in the industry but also in the Fire and Rescue Services intervention.

Sorbents are further divided according to the bulk and textile form. Bulk sorbents have a varied form of preparation such as granules or powder. The size of the loose sorbents is most often from 0.1 mm to 5 mm. The structure is porous and contains different pores and cracks. An important sorbent parameter is the surface size. The advantage of loose sorbents is the possibility of use on broken surfaces but their disadvantage is dustiness and inappropriate use in strong winds. Textile sorbents are usuallymade from polypropylene or polyethylene and are produced in the form of fibers or other fibrous forms. Use is similar to bulk sorbents. Textile sorbents have several advantages, e.g. they are dust-free, they can be used in stronger wind and they can be reused.

3. Materials and methods

The selection of the material for examination is represented by synthetic and natural sorbents as follows: Synthetic sorbents - Absodan plus, PeWaS sorb, Sorp Reo and Spilkleen Plus.

Natural sorbents - sawdust, leaves, needles and mosses.

Selected sorbents were tested for engine oil 10W40, which is one of the most common oils for small spills up to 1 dm^3.h^{-1}, or the spill does not exceed 1 m^2 of film formed by a thickness of 1 mm.

Samples of both natural and synthetic sorbents were tested in the original state of Fig. 2.

Fig. 2 Synthetic sorbents

Prior to testing, their shape and shape were preserved. The natural sorbents were surface-picked and untreated. see Fig. 3.

Fig. 3 Natural sorbents

The sorption capacity of the sorbents was determined according to the standard adsorbent adsorption assay method (ASTM F 726). The sorption capacity of the individual sorbents in the bulk state will be reported in the graphical comparison below.

4. Oil sorbent sorption capability tests

Sorbents were tested according to the American Society of Testing and Materials F 726 Standard Test Method for Sorbent Performance of Adsorbents.

This test method describes laboratory tests that describe the "Short-term Oil-Absorption Test" and other non-emulsion floating, non-emulsion liquids from the water level. Type II adsorbents (loose) were tested according to the method. sorbent test specimens were conditioned at a temperature of 23 ± 4 ° C and a relative humidity of 70 ± 20% for at least 24 hours. before testing in a completely uncovered state without overlapping to allow the samples to obtain a balance with the laboratory environment (ASTM F 726).

5. Results and discussions

Both natural and synthetic sorbents were conditioned and weighed to a weight of 4g. A crystallization vessel of adequate diameter was filled with a layer of engine oil at least up to 2.5 cm. The dry mesh basket was immersed in the oil for a specified time and left to drip. This slight modification is not a part of the method, but it has produced more accurate measurement results because the differences in trapping oil on the trays of the basket have been eliminated. The repeatability of the individual sample measurements was three times. The values obtained were averaged by the mass of the adsorbed petroleum in the adsorbent. The sorbents were used after testing, and the oil was ecologically discarded.

In order to represent the average values of the maximum sorption capacities of selected natural sorbents for engine oil, we used a graph. see. Fig. 4.

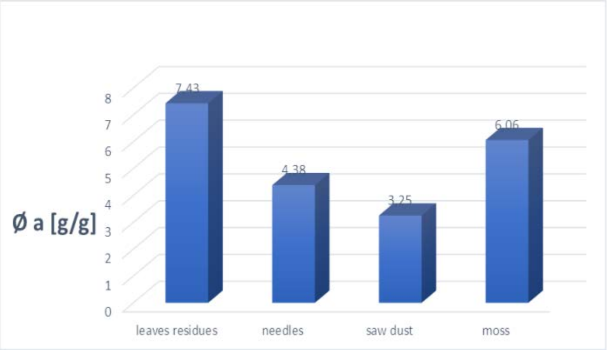

Fig. 2 Average sorptive capacity of natural sorbents

Ø a - average sorptive capacity of the petroleum to adsorbent weight [g /g]

From the ASTM F 726 tests, it was found that the best sorption capacity reached leaves residue of 7.43 [g/g]. Among the good natural sorbents we can include a moss that has a value of 6.06 [g/g], needles with a value of 4.38 [g/g]. As the least effective natural sorbent, sawdust has a value of 3.25 [g/g].

Fig. 5 shows the average values of the maximum sorption capacities of synthetic sorbents for engine oil.

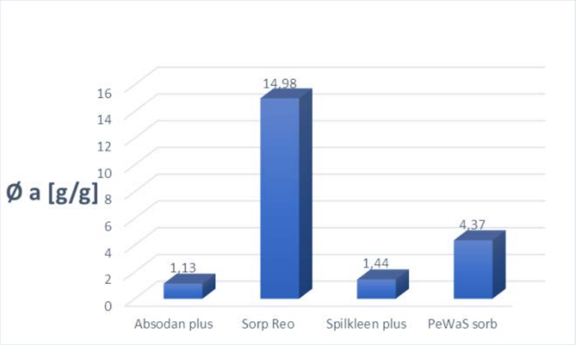

Fig. 3 Average sorptive capacity of synthetic sorbents

The graphical representation is the most efficient Sorptive Grain Reo with an average adhesion of 14.98 g / g of adsorbent. Sorp Reo is treated by hydrophobic treatment and is therefore suitable as an intervention for leakage of hydrocarbon greases in a wet environment or directly on water surfaces. The second in the order of 4.37 g / g is PeWaS sorb. Less efficient sorbents include Spilkleen plus with 1.44 and Absodan plus at 1.13 g /g.

6. Conclusions

The contribution is aimed at comparing synthetic and natural sorbents, which are a means of eliminating escaping petroleum substances that have an adverse environmental impact on the environment. In the case of rapid deployment of sorption agents, greater leakage of petroleum substances will be avoided and also the size of the negative environmental impact will be reduced. For testing according to the chosen method, 10W 40 engine oil has been selected and used, which has a large quantity of small quantities of operating fluids from motor vehicles. Selected types and types of sorbents were compared to sorption capacity according to the standard ASTM F 726 test method according to which the maximum short-term sorption capacity was found. From the measurement results we can conclude that the sorbent is usable and suitable for Fire and Rescue Services interventions. By sorbent comparison and testing it was found that with the sorption ratio of the synthetic sorbents the sorptive Sorptive Grain Reo sorbent has the best sorption properties with 14.98 g of adsorbed oil per 1 g of adsorbent. Said synthetic sorbent is treated by hydrophobic treatment, which means that it improves the properties of sorbent and allows its use on water surfaces. In case of leakage in the forest environment, it is possible to use selected natural sorbents. With the ratio of natural sorbents, the sorption capacity of the leaves of sorbent with the value of 7.43 g of absorbed used oil per gram of adsorbent has the highest sorption capacity.

Other natural as well as synthetic sorbents tested have good sorption capacity. Compared to natural and synthetic sorbents, synthetic sorbents are more efficient because they are specially formulated and modified for sorption purposes. Another possible advantage of synthetic sorbents is their ability to retain the absorbed substance in its content as opposed to natural sorbents where the possibility of subsequent leakage due to mechanical action on the sorbent used is possible. On the other hand, natural sorbents have the advantage of being near leakage and economically unattractive. The choice of a suitable sorbent depends on the amount of oil escaping and the complexity of the leakage situation. A suitable sorbent selection can quickly and efficiently prevent leakage and spreading of the oil into the environment. Sorbent comparison is important in terms of suitability for use, biodegradability and other important factors that are important for the effective removal of hazardous events with the presence of a hazardous substance.

Acknowledgements

This paper was supported by the Cultural and Educational Grant Agency under contracts No. KEGA 012TUZ-4/2016 (50%) and No. KEGA 030UMB-4/2017 (50%).

References

[1] DOERFFER, W. J. 2013. Oil Spill Response In The Marine Environment. U. K.: Pergamon Press, 2013. First edition 1992. 398 s. ISBN: 0-08-041000-6..

[2] DONG, X., et al. 2012: Superhydrophobic and superoleophilic hybrid foam of graphene and carbon nanotube for selective removal of oils or organic solvents from the surface of water. Chemical Communications, 2012, 48.86: 10660-10662..

[3] OLALEKAN, A. et al. 2014: silica aerogel as a viable absorbent for oil spill remediation. Journal of Encapsulation and Adsorption Sciences, 2014, 4.04: 122.

[4] GERTLER, C., et al. 2009: Microbial consortia in mesocosm bioremediation trial using oil sorbents, slow-release fertilizer and bioaugmentation. FEMS microbiology ecology, 2009, 69.2: 288-300.

[5] YU, L., et al. 2015: Fe 3 O 4/PS magnetic nanoparticles: Synthesis, characterization and their application as sorbents of oil from waste water. Journal of Magnetism and Magnetic Materials, 2015, 394: 14-21.

[6] YOON, H., et al. 2014: Gravity-driven hybrid membrane for oleophobic–superhydrophilic oil–water separation and water purification by graphene. Langmuir, 2014, 30.39: 11761-11769.

[7] ANKOWSKI, A. et al. 2011, Theuse of Sorbents in Actual Conditions for Elimination of Oil Derivative Spillages. In: Požární ochrana 2011. vol. 20. p. 5 – 9. 2011.

[8] ZACHAR, M. 2010: Mutual comparison of sorbents. In: Fire engineering: proceedings. Zvolen:, s. 439-445. 2010.

[9] Fig. [10.5.2018] https://www.slideshare.net/VivekKumar36/adsorption-regenerationvivek-kumarneeri

[10] RADETIC, Maja, et al. 2008: Efficiency of recycled wool-based nonwoven material for the removal of oils from water. Chemosphere, 2008, 70.3: 525-530.

[11] ADEBAJO, Moses O., et al. 2003: Porous materials for oil spill cleanup: a review of synthesis and absorbing properties. Journal of Porous materials, 2003, 10.3: 159-170.

[12] SINGH, V., et al. 2014: Novel natural sorbent for oil spill cleanup. Industrial & Engineering Chemistry Research, 2014, 53.30: 11954-11961.

[13] ORINČÁK, M. et al. 2012: Účinnosť sorpčných materiálov pri dekontaminácií kyselín a zásad. In: Advances in Fire & Safety Engineering. [CD-ROM]. p. 181 – 196. 2012.

Evaluation of selected food dusts from the standpoint of fire safety

Eva Mračková[a]* – Emília Orémusová[a] – Michal Danek[a]

[a]*Technical University in Zvolen, Masaryka 24, 960 53 Zvolen, Slovakia*

Abstract

The article deals with dust – air mixtures of selected food dusts and the determination of their selected fire - technical characteristics. The aim of this thesis is to experimentally determine the lower explosive limit of food powder samples consisting of smooth flour, powdered sugar and cocoa using the VK 100 explosion chamber and the gross calorific value measurement using the IKA C5000 calorimeter according to the methodology given in STN ISO 1928. State exams belong analytical methods used in fire and safety engineering. By conducting experiments and evaluating samples, it was concluded that all samples of food dusts examined are explosive and present a high risk of explosion and fire in technologies. The test sample of cocoa showed the most reactive, with the lowest lower explosive limit and the highest gross calorific value. Gross calorific value values contribute to the spread of fire, therefore the manufacturing operations of food products must be assured by the design elements of the explosion protection.

Key words: dust explosion; lower explosion limit; explosion chamber; gross calorific value; calorimetric apparatus

---

* Corresponding author. Tel.: +0-420-4552-06831 ; fax: +0-420-4553-21811 ; e-mail: mrackova@tuzvo.sk.

1. Introduction

One of the main issues that we can encounter in the food industry but also in industry in general is the issue of occurrence of flammable dust. It is result from graining, grinding and machining of material [1]. The dust is a major, side product or waste in many industry sectors. It comes into air by mutual relative movement of air particles. Solid particles of dust are dispersed and floating in the air - so called air particle (aerosol) [2]. The sedimentation time of solid dust particles in relatively quiet environment depends on their weight and size [3].

The dust dispersion has significant impact on its flammability and explosiveness. Dispersed dust has a large surface, a lower self-ignition temperature, and the dust mixture has extensive intervals of explosiveness [4].

Production in the food industry in terms of raw material but also from the view point of processing technology is various [5]. The share of the food industry in industrial production of Slovakia at present is 4.6%. Processing of raw materials such as grain, sugar beet and cocoa beans creates a dispersive environment with the risk of explosion [6].

The aim of the work in article is to evaluate selected fire-technical characteristics of food dusts [7]. The lower explosive limit and the gross calorific value were selected for experimental determination from the fire-technical characteristics (flash point, burning point, ignition temperature, caloricity, gross calorific value and concentration limits of explosiveness) [8, 9]. We determine selected fire - technical characteristics of food dusts using the explosion chamber VK 100 in accordance with the methodology of the manufacturer of the equipment and the automatic calorimeter IKA C5000 according to Slovak Technical Standard STN ISO 1928 [10]. The fire - technical properties are not physical constants except for exceptions, but conventional quantities whose reproducibility depends to a great extent on the quality of material, the method of execution of tests, and on conditions of testing itself.

2. Methodology of the work and material

From Selected samples of food dusts were experimentally tested by two methodologies in devices described below.

2.1. Explosion chamber VK 100

The laboratory equipment, the explosion chamber VK 100, is designed to determine the lower explosion limit of dusty flammable substances dispersed in the air [2]. The explosion chamber is a cubic container having its length (height) less than or equal to twice its diameter d:1 ≤ 2:d. The laboratory equipment, the explosion chamber VK 100, is designed to determine explosive limits of dusty or liquid flammable substances dispersed in the air. The main parts of the explosion chamber VK 100 are the explosion chamber itself and control device. The measurement methodology was performed according to manufacturer's instructions, which is in accordance with global agreements of measurements in cubic vessels. The experiment was repeated three times for each charge of the food dust sample due to statistical evaluation of results.

2.2. Automatic combustion calorimeter IKA C5000

The calorimeter IKA C5000 is a compact semi-automatic calorimeter determined to measure the gross calorific value and caloricity of solid and dust samples. The heat released in burning of the material, together with the physical properties of the material and the influence of surrounding environment indicates the ability of the material to spread the flame, so significantly affecting reaction of material to fire, gross calorific value indicates the maximum possible heat that is chemically released from the substance. It is the physical - chemical constant of particular material, which can be calculated as the sum of combining heats of products of combustion of individual elements contained in particular material. Gross calorific value is the amount of the heat released in perfect combustion of the weight or volume unit of the substance in pure oxygen at certain pressure, while the water produced in combustion is in the liquid state. The measurement was performed with using of adiabatic method according to the Slovak Technical Standard STN ISO 1928, Solid Fuels. Determination of gross calorific value by calorimetric method in the pressure vessel and calculation of caloricity [10].

The total gross calorific value is expressed in $MJ.kg^{-1}$ or in $J.kg^{-1}$. An automatic calorimetric apparatus will evaluate total gross calorific value directly in the apparatus and resulting value of total gross calorific value will be displayed as a result of measurement. The total gross calorific value is calculated by following relation:

$$Q_{PCS} = \frac{E(T_m - T_i + c) - b}{m} \qquad (1)$$

where:

Q_{PCS} – total gross calorific value, ($MJ.kg^{-1}$)
E – water equivalent of calorimeter ($MJ.kg^{-1}$)
Ti - initial temperature, (K)
Tm – maximum temperature (K)
b - correction needed to take into account the gross calorific value of additional fuels ($MJ.kg^{-1}$)
c - correction factor of temperature (K)
m - the weight of the test sample (kg) [10].

2.3. Experimental material

We used for experiments samples of the smooth flour T650, the powder sugar and the cocoa powder. The reason to select used food dust samples was that they had comparable size of fractions and they are the most frequently used in the food industry. Examined food dusts, according to statistical records from previous years represent a high risk of the danger of explosion, followed by spreading the fire [11, 12].

The smooth flour T650 is floured inner part of the cereal grain with a smaller portion of the bran particles. It consists from saccharides, the farina is on main place (70-80% of the weight) and proteins which in combination with water form so called gluten. The wheat flour contains 10-12% of proteins. The water content in the flour is about 14.5% (according to the Decree of the Ministry of Agriculture and Rural Development of the Slovak republic on the edible grain and the mill products from the grain may not exceed 15%). The flour also contains a small amount of fat (1-2%) and fibres (1-2%), which are formed from cellulose and other polysaccharides, in addition to mentioned ingredients. It contains important minerals, so called ash (0.4-1.8%), further it belongs here especially calcium, phosphorus, magnesium, potassium, sulphur, selenium. The flour also contains vitamins, mostly from the B-complex, which are dissolved in the water (B1, B2, B3 and B6). It is mainly vitamin E from among vitamins soluble in fats.

The powder sugar as the natural sweetener consists from 99.7 % of the pure sucrose. It consists from one molecule of glucose and one molecule of fructose. We know it in the pure state as a white crystalline substance having the sweet taste. The sucrose is very widespread in nature, and it is an important metabolic product of all green plants where it serves as a transport soluble saccharide. The starch (3%) is often added into the powdered sugar as an anti-nodulizing substance [13, 14]. The sucrose is made from the sugar beet in Slovakia, it contains 17% of sucrose on average, it is more than in the sugar cane.

The basic raw material for production of cocoa are cocoa beans. They grow in the tropical climatic zone at an altitude of up to 600 m. It needs a temperature of 20-35 ° C, it can grow freely in nature up to height of 15 m, but the height is modified to 6-8 m. Fruits having weight of 300-500 g have a shape of a rugby ball, they grow to the length of 30 cm and to the width of 12 cm. Their colour is gradually changing by maturing from green to brown. There are 20-50 beans in five rows inside the fruit. 100 g of the content of cocoa powder contains 10.5 g of fat, 23.5 g of saccharides, 33.5 g of fibre, 23.5 g of proteins and 2.9 g of salt. correct design of the suction equipment [15].

3. Results

3.1. Experimental results of determination of the lower explosive limit of selected food samples of dust

We have proceeded from higher weights of the food samples of dust to lower when determining the lower explosive limit. We recalculated concentration for the each weight of the dust sample. We visually evaluated the course of experiments with individual samples of the smooth flour, powdered sugar and cocoa by observation through inspection holes in walls of the explosion chamber VK 100 and after bursting of the paper membrane we recorded results into the Table 1.

3.2. Experimental results of determination of the gross calorific value of selected food samples of dust

Particular weights of test samples of the food dusts weighed before the experiment were listed in the Table 2 together with measured values of the gross calorific value determined using of calorimetric apparatus IKA C5000.

We calculated the mean value of the total gross calorific value within the sense of the Slovak Technical Standard STN ISO 928 from the first and the second experiment of measurement the gross calorific value of the smooth flour T650. Colours are highlighted in the Table 2, where the high value of the gross calorific value of the cocoa powder is obvious, while values of the gross calorific value of the smooth flour and powdered sugar are comparable.

Table 1

The lower explosive limit of selected food samples of dust

Measurement No.	Charge (g)	Concentration ($g.m^{-3}$)	Results of tests **The smooth flour** N-negative, P-positive			Results of tests **The powder sugar** N-negative, P-positive			Results of tests **The cocoa** N-negative, P-positive		
			The number of the experiment			**The number of the experiment**			**The number of the experiment**		
			1	**2**	**3**	**1**	**2**	**3**	**1**	**2**	**3**
1	6	60	P	P	P	P	P	P	P	P	P
2	5.2	52	N	P	P	P	P	P	P	P	P
3	4	40	P	N	N	P	P	P	P	P	P
4	3	30	N	N	N	P	P	P	P	P	P
5	2	20	N	N	N	P	N	P	P	P	P
6	1.5	15	N	N	N	N	N	N	P	N	N
7	1	10	N	N	N	N	N	N	N	N	N

It is possible to evaluate from results of the experiment, that the lower explosive limit ranges from 40 g.m-3 for the smooth flour, 20 g.m-3 for the sample of the powdered sugar and 15 g.m-3 for the cocoa powder; it shows, that all dust samples in the swirly condition represents the danger of explosion in the food industry. Resulting concentration of the low explosive limit are shown in the Table 1.

Values of lower explosive limit of selected food dust samples and their values of gross calorific value after series of measurements in the explosion chamber VK 100 and the calorimeter IKA C5000 are shown in Figure 1. These values were used as input data for compilation of diagram, where the dependence of low explosive limit on the value of gross calorific value is shown.

Table 2

Gross calorific value of selected food samples of the dust

Experiment No.	The smooth flour The weight (g)	Gross calorific value Q_{pcs} (J/g)	The powder sugar The weight (g)	Gross calorific value Q_{pcs} (J/g)	Cocoa The weight (g)	Gross calorific value Q_{pcs} (J/g)
1	9.9016	16 221	9.9026	16.488	9.9008	21 492
2	9.9012	16 298	9.9019	16 413	9.9014	21 449
The average	9.9014	16 221	9.9022	16 450.5	9.9011	21 470.5

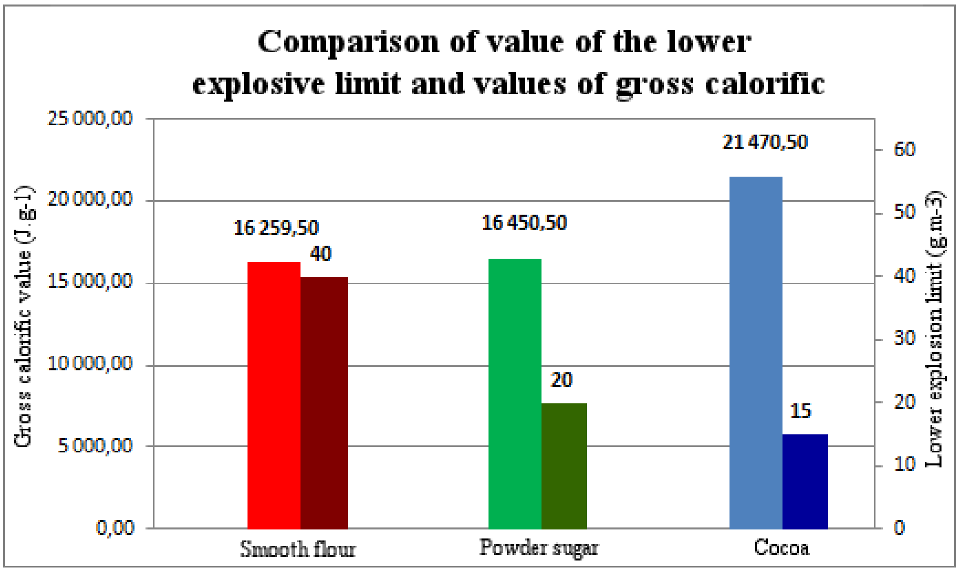

Figure 1 Comparison of value of the lower explosive limit and values of gross calorific of investigated dust samples

We experimentally determined the lower explosive limit for the flour sample to 40 g.m^{-3}, the lower explosive limit for powdered sugar represents value of concentration of 20 g.m^{-3} and the cocoa had determined the lowest explosive limit of 15 g.m^{-3} and it represents the highest risk of explosion. Values of gross calorific value for these materials ranged from 16 259.5 to 21 470.5 J.g^{-1}, where the cocoa powder clearly manifested the highest potential of the gross calorific value and it contributes the most to spreading of fire from investigated samples of food dust.

4. Conclusion

- selected experimental food flammable powders are of organic origin,
- samples of food dust particles are classified by departmental and corporate standards into classes according to size of particles,
- the lower explosive limit of the smooth flour having the lowest value of gross calorific value of 16 259.5 J.g^{-1} reaches the highest value of the lower explosive limit

- of 40 g.m^{-3}, which can be attributed to its 14.5 % of water content,
- samples of powdered sugar showed a higher value of gross calorific value
- of 16 450.5 J.g^{-1}, but lower value of the lower explosive limit of 20 g.m^{-3},
- the highest value of gross calorific value was measured at the sample of cocoa having
- 21 470.5 J.g^{-1}, its value of the lower explosive limit represents only 15 g.m^{-3}, Specified values correspond to the difference of the content of the cocoa which contains fats and there is minimum content of the fat in other food flammable dusts,
- we attribute specified lowest value of LEL to the finest composition of the dust fraction of the cocoa sample,
- the experiment is included into original results,
- assumed dependence of the lower explosion limit on the value of gross calorific value , i.e. the lower concentration of the lower explosive limit, the higher value of gross calorific value was confirmed after evaluation of measurement results,
- it is clear from measured results that cocoa has been shown to be the most reactive food dust among rated food dusts, it represents the highest risk of explosion and subsequent spreading the flame in the food industry,
- values of gross calorific value contribute to spreading of fire, so it is necessary to secure operations for processing and production of these foodstuffs with structural components of the counter-explosion protection [10].

Acknowledgments

This This work was supported by the Cultural and Educational Grant Agency of the Ministry of Education, Science, Research and sport of the Slovak Republic on the basis of the project No. KEGA 009TUZ-4/2017 (40 %), No. KEGA 012TUZ-4/2016 (30%) and by the Slovak Grant Agency under contract No. VEGA 1/0806/17 (30 %).

References

[1] I. Tureková (2008) Význam požiarnotechnických vlastností potravinárskych prachov v praxi. In: Manažérstvo životného prostredia 2008. Žilina : Strix et VeV, 2008, s. 161-166. ISBN 978-80-89281-34-3.

[2] P. Štroch. (2010) Procesy hoření a výbuchů. Žilina : EDIS - vydavateľstvo ŽU, 2010 156 stran : ilustrace. ISBN: 978-80-554-0187-4

[3] J. Damec. (2005) Protivýbuchová prevence. Ostrava: SPBI, 2005, 188 s. ISBN 80-86111-21-0

[4] R. Brázda, J. Zegzulka (2011) Wall Pressure Issues in the Aeration of Bulk Material Silos, Powder Technology. 206 (2011) 252-258.

[5] I. Tureková, E. Mračková. (2016) The dimensional characteristics of the particles of wood dust of selected deciduous trees considering to explosion. In: Key Engineering Materials: 11th International Symposium on Selected Processes at the Wood Processing, 2015; Dudince; Slovakia; 9 September 2015 through 11 September 2015. ISBN 978-303835569-4. ISSN 1013-9826. Vol. 688, sp. iss (2016), p. 182-189.

[6] I. Slabá, I., I. Tureková. (2012) Smouldering and Flaming Combustion od Dust Layer on Hot Surface. Dersden (Germany): Scientific monographs, 2012. 88 s. ISBN 978-3-9808314-5-1

[7] S. Kovshov, A. Nikulin, V. Kovshov, E. Mračková (2015) Application of equipment for aerological researching of characteristics of wood dust, Acta Facultatis Xylologiae Zvolen. 57 (2015) 111-118.

[8] R. Eckhoff. (2005) Expolosin hazard in the process industries. Houston Texas: Gulf Publishing Company, 2005. 457 s. ISBN 0-9765113-4-7.

[9] H. Groh. (2004) Explosion protection. Germany: Expert Verlag GmbH, 2004. 524 s. ISBN 0-7506-4777-9

[10] STN ISO 1928 (2003) Tuhé palivá. Stanovovanie spalného tepla kalorimetrickou metódou v tlakovej nádobe a výpočet výhrevnosti.

[11] V. Ebadat. (2010) Dust explosion hazard assessment. Journal of loss prevention in the process industries, 23(6), 907-912.

[12] M. Hitka, V. Mačkayová, M. Sirotiaková, Adjustment of employee evaluation in wood processing company Zvolen Corp, Drvna Industrija. 58 (2007) 69-76.

[13] U.S. Chcemical safety and hazard investigation board. (2006) Combustibe dust hazard study. U.S. Chemical safety and hazard investigation board, 2006.108 s. Report no. 2006-H-1.

[14] J. Barton. (2002) Dust explosion prevention and protection. Massachusets USA: Gulf Professional Publishing, 2002. 352 s. ISBN 0-7506-7519-3.

[15] M. Hudáková, I. Coneva, K. Hollá. (2016) Hodnotenie environmentálnych rizík vyplývajúcich z emisií horenia pri požiaroch v budovách. In. Krízový manažment – 1/2016, 15. ročník. Žilinská univerzita v Žiline, Fakulta bezpečnostného inžinierstva. s. 26-34. ISSN 1336-0019.

Earth
in a Trap?
2
0
1
8

Earth in a Trap? 2018
Analytical Methods in Fire and Environmental Science

A scientific approach to determination of the cause of fire

Miroslava Nejtková[a*]

[a]*Ministry of the Inteiror – Directorate General Fire Rescue Service Czech republic, Population Protection Institute, Czech republic*

Abstract

The paper deals with a scientific approach to determination of the cause of fire. It focuses on one of the most important tasks – collection of veritable information relevant to proposing versions of the causes of fire. The first part of the paper deals with the tools for documentation and digitization of the fire scene. The second part of the paper focuses on sampling, laboratory investigation and subsequent elaboration of a Fire-Technical Expertise. The also paper mentions non-destructive X-ray testing, which is a great contribution in investigations.

Keywords: cause of fire; analysis; documentation; fire scene; sample; investigation

---

[*] Corresponding author. Tel.: +0-420+950 350 355; e-mail: miroslava.nejtkova@ioolb.izscr.cz

1. Introduction

A Regional Fire Rescue Service performs state fire inspection duties according to the Section 26 (2) b) and § 31 of the Act No. 133/1985 Coll., on Fire Protection, as amended [1]. Determination of the causes of fires is one of the tasks of the state fire inspection, which is carried out for legal persons, business individuals, ministries and other state bodies, municipalities and natural persons. Specifics concerning determination of the causes of fires are defined in the Section 50 of the Regulation No. 246/2001 Coll., on Determining terms of fire safety, and duties of the state fire inspection (Fire Prevention Regulation) [2]. Fire is considered to be any undesired burning that kills or injures humans or animals, damages properties, belongings, or environment. It also means an undesired combustion where persons, animals, properties or environment are under an immediate threat [2]. A fire within the meaning of this definition is also considered to be an explosion of a mixture of flammable gases or vapours of flammable liquids or dusts with gaseous oxidant. A physical explosion, an explosion of explosives if there is no subsequent burning after the explosion, is not considered to be a fire [3].

The General Directorate of the Fire Rescue Service of the Czech Republic ensures implementation of fire-technical expertise. Therefore a workplace was set up at the Population Protection Institute to carry out expert activities for determining the origin of a fire. The expert group operates nationwide and assists with explaining the cause of a fire at a fire scene. The assistance is provided during inspecting, documenting and digitizing fire scenes, taking samples for laboratory examinations, determining hypothesiss of fire causes, and laboratory examination of samples from fire scenes. Subsequently, conclusions are processed into fire-technical expertise in the form of a professional statement that is part of a fire report.

2. Scientific approach to determining the cause of fires

A key requirement for a fire to originate is presence of a flammable substance, initiating source and oxidizing agent, called a flammable triangle. The energy of the initiator source must be sufficient enough to be able to ignite a flammable substance in ambient conditions (free oxygen / fired oxygen). In the event of an explosion, the so-called flammable triangle is transformed into the so-called explosive pentagon, where the effect of the environment (vessel shape) and particle dispersion also arises.

In order to determine the cause of fire or explosion, it is necessary to collect all required data concerning the emergency situation. The collected data need to be analysed and evaluated. Only then feasible hypothesis of the fire causes can be established. When verifying the hypothesis of the fire cause, fire investigators have to rely on obtained data and information. They must not confuse the obtained information and their assumptions or speculations. Similarly, they must not adjust proven facts to proposed hypothesis.

Testing the hypothesis is carried out by comparing an assumed development of the fire (development scenario) with the evidence found at the fire scene. The assessment is done for all proposed hypothesis. In the process of verifying the hypothesis, each hypothesis must be gradually ruled out on the basis of found evidence rather than its nonexistence. If the hypothesis does not comply, it can be excluded and other hypothesis can be verified. There may also be a situation that no proposed hypothesis will fully correspond to any possible fire scenario, i.e. it is a time to re-collect or complete the data, and re-evaluate and design new hypothesis. Should there be additional hypothesis that explains development of the fire and damage caused by it as well as the previous one, a more detailed assessment is required. This procedure is repeated until all available hypothesis are reviewed. Ideally, there will be only one hypothesis that corresponds to all the facts and is the only possible cause of the fire. The general procedure reported in NFPA 921 [4] is illustrated in Fig.1

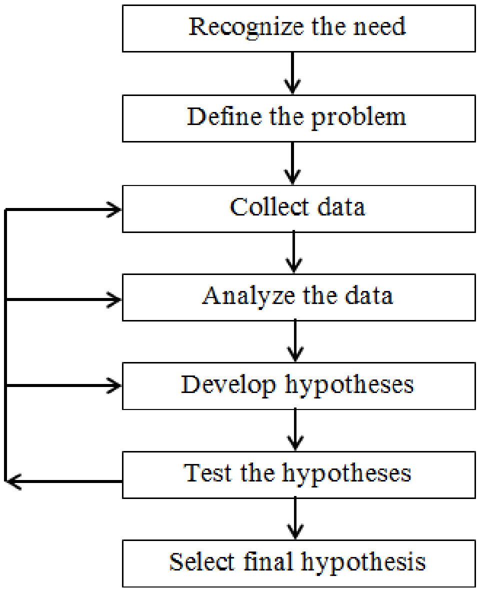

Fig 1 Scientific procedure for determining the cause of fire according to NFPA 921 [4]

3. Collection of relevant data

In order to properly determine the cause of fire, the first step should be a systematic reconnaissance of a fire scene. All the evidence obtained at the fire scene should then be documented, not only using a camera but also video cameras, thermal cameras, drones, lidar, spatial scanners, etc.

If a burner accelerant is suspected, it is possible to use a trained dog that is able to detect presence of substances that are commonly used as flame accelerants. The process is followed by taking samples, which were marked by the trained dog. The obtained samples are sent to one of the designated laboratories of the FRS CR, where they are analysed.

Should an electrical installation or use of electric appliances be suspected as the cause of fire, it is possible to use multimeters to measure physical values; as well as portable X-ray systems. After the sampling, it is possible to carry out further technical-physical examinations in the designated laboratories of the FRS CR.

Attention should be paid to witnesses' observations and statements. Thorough interviews of witnesses who could provide useful and accurate information concerning development of the fire, or activities that took place before the occurrence of the fire, must be conducted. Investigators must further address the facts and activities that were carried out prior to the occurrence of the fire. Various operational documentation, work procedures and standard specifications are suitable for this task.

3.1. Dokumentation of the fire scene

A digital camera is currently standard equipment of fire investigators. One of the ways to achieve a 3D image view is to use spherical images. Spherical imagery can generally be obtained directly by using spherical camera or panoramic heads on which the digital camera is positioned.

The Population Protection Institute specifically utilizes two instruments, an automatic panorama head and a spherical camera.

The fully automatic panorama head allows both sector-scanning or full sphere panoramic scanning. The automatic head accelerates and simplifies the process of image capture and subsequent image processing. It also ensures that the images concur and overlap sufficiently. It also offers cutting-edge features such as HDR photography or exposure bracketing.

A spherical camera enables users to capture a spherical 360 ° x 137 ° ± 5 ° photo in HDR quality. HDR capture is highly suitable for fire documentation of places with considerable differences in exposure (large luminosity differences); thereupon in places where there is a dark corner and sunny sky, or where bright light goes through the window, door, or missing structures. The resulting spherical images taken with a spherical camera or camera combined with a panoramic head can be published in a same way as a standard photo. It is also possible to cut a segment from the spherical image with a detail of the fire.

Each spherical image is then merged into a virtual walk-through, which connects individual places and rooms of the scene of a fire.

Fig. 2: Example of a spherical photo in HDR quality at the scene of fire [5]

3.2. Digitalization of the fire scene

Spatial ground laser scanning method is a suitable and proven technique of a precise, detailed and well documented scene of fire.

Spatial scanning is a geodetic method of measuring spatial coordinates. It is based on automatic and precise tracking of a large number of points that define an area in the tri-axial coordinate system. These points are generally called a point cloud, where every point is defined by coordinates X, Y, Z. The system is capable of obtaining up to 976,000 spatial points per second from the surrounding area. In this way it is possible to define an object, room, multileveled house, street, and even an entire city. When using this type of scanner, the measuring is performed at a distance of 130m from its location and it locates everything within its direct visibility. The scanner is stationary and during scanning it is statically placed on a tripod and can be ejected up to 4,5 meters high.

The spatial scanner operates in a contactless manner. It emits a laser monochromatic beam at a wavelength of about 1550 nm. The beam falls on a rotating oblique mirror; the angle of incident is 90°, which ensures scanning the area in the vertical direction. Scanning in the horizontal direction is provided by rotating the scanner around its own vertical axis. The laser scans the area horizontally (360 degrees) and vertically (305 degrees), or a sector specified by the operator. The scanner is also able to scan in an inverted mode by 180 °, i.e. upside down, and thus digitizes the space beneath.

The accuracy of the data collection directly depends on the reflectivity of the materials the scanned objects are made of. The worst precision of the scanner is defined as +/- 2 mm at a distance 25 m at 90% reflectivity of the surface.

The outputs are standard 3D data appearing in the infrared spectrum in a shade of grey. The scanner has a built-in internal camera, which is also able to document colour information from the visible electromagnetic spectrum. The resulting colour photograph, which when processed is applied to the 3D data, is then at a resolution of up to 70 million spatial points (megapixels). The mentioned spherical camera is also fully compatible with the scanner, which allows users to implement a better quality color photo to precisely obtained 3D data.

To scan complete data, site scanning is performed and the resulting data are merged into one final project. The output is an accurately documented scene of an accident (fire scene), created 3D digitization of a fire scene, and virtual measurements obtained from the 3D data. At the same time, it is possible to perform surface measurements. The Fire Investigator herewith acquires accurate 2D scale plans, orthogonal views, 2D slots, and ground plan views.

This measurement system greatly improves the process of surveying the scene of a fire. It is not necessary to complicatedly re-measure the rooms, technology within the fire scene, and manually sketch them. A comprehensive visual information that is represented by a virtual tour in an HTML forms another outputs.

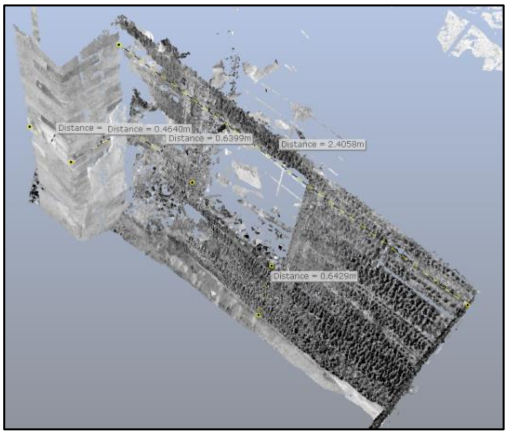

Fig. 3: Measurement of spatial data [5]

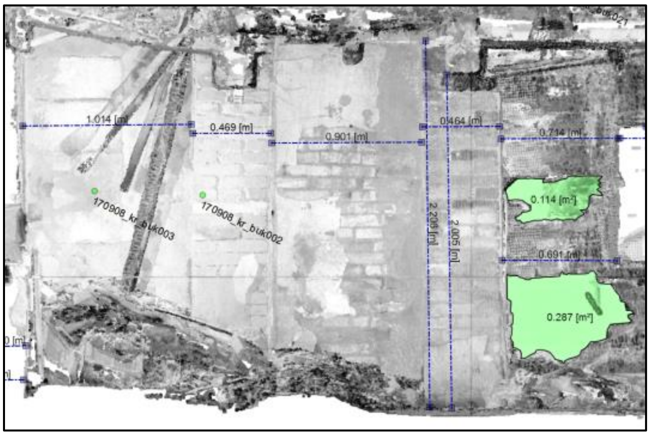

Fig. 4: Example of measuring proportions and areas [5]

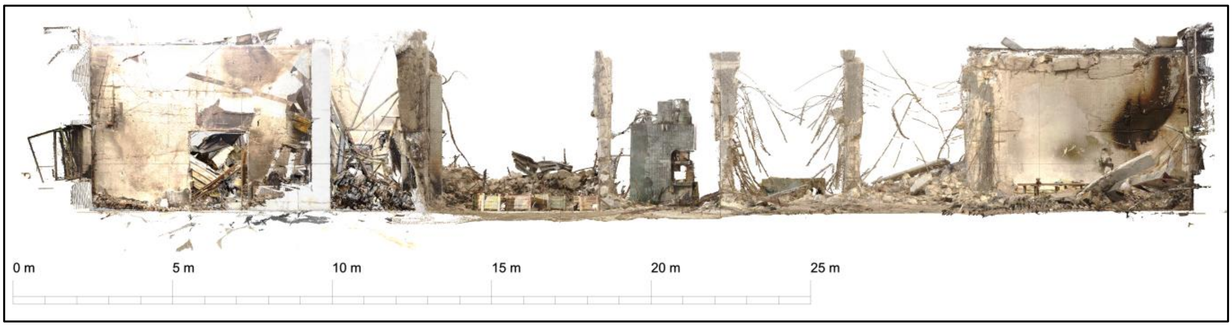

Fig. 5: Sample of a building section with an enclosed scale [5]

4. Evaluation of appliance and wiring

4.1. Sampling

Where necessary, samples, which are considered to have an effect on the origination of the fire, are taken from the scene of a fire. This paper will further deal with samples of electrical equipment, wiring, etc., which can be further subjected to physical-technical testing.

All electrical power installations (e.g. power grids, transformers, dynamos), low-voltage electrical appliances (home distributions, etc.), electrical appliances (e.g. TVs, refrigerators, heaters) and electrical installations such as switchboards, faxes, etc. can be submitted to testing and detecting for their defects.

It is possible to carry out basic investigation concerning a physical-technical field directly within the scene of a fire, for example using multimeters to test circuit closing, or perform thermodiagnostics, etc

More frequently samples are taken from the scene of a fire and sent to an expert workplace, such as the Population Protection Institute.

Samples at the fire scene are collected by trained members of the Czech Fire Rescue Service or by police officers of the Czech Police. On-site samples are taken after a risk of electric shock during collection of samples is eliminated. Subsequently, samples must be collected in a correct way. To prevent collecting an inappropriate electrical equipment, reconnaissance of the fire scene is conducted with a focus on V-patterns, arc mapping, unusual heating, ground faults and damaged electrical cables [6].

Arc mapping is an investigative tool that can provide information on the direction of fire spread. It relies on determining where electrical arc and other faults occurred during the fire. Evidently the electrical circuit involved had to be energized at the time of the fire for the arcing to occur. Faults to ground inadvertent connections to any grounded item are one of the most common sources of electrical fires. Uninterrupted runs of copper wires or electrical cable very rarely cause fires unless the wire or cable is damaged. Investigators have to look for potential points of damage, for sharp bends and places where a nail or staple may have been driven into the wire.

For electro technical investigations it is also essential to know the chronological course of events, description of the wiring, the building structures, determine forensic and fire point of origin, collect electrical equipment and obtain the review reports. If the sample is only sent for analysis, it is necessary to know the exact location where the sample was collected, its placement in relation with the surrounding objects, the position of the sample, its orientation and photographic documentation.

The data on the sampling site must always be collected. Such data include the patterns produces by the fire, which is a visible or measurable physical change or identifiable shape formed by the fire effect (mass loss of material, char, spalling, colour changes, melting of materials, thermal expansion and deformation of materials, deposition of smoke on surfaces, e.g.)

4.2. Laboratory testing

The laboratory tests will assist the investigator in making an accurate assessment of the condition of appliances or wiring and the contribution they may have made to a fire. For instance, whether a switch was on or off at the time of the fire, examination of the contacts, housing and switch mechanism.

In the laboratory testing, it is possible to carry out analysis of electrical conductors using methods of optical microscopy, electron microscopy, energy dispersive X-ray spectrometers, diffraction X-ray analysis, infrared spectroscopy and Raman spectroscopy.

When handling the sample, it is important to know how the sample has been manipulated with throughout the whole time. Further damage to the sample must be avoided. It is necessary to examine the sample using available methods and when combining them proceed from non-destructive to destructive methods. However, destructive methods are frequently used in laboratories to separate off the burned parts so that only the connecting elements of the appliance themselves remain

Non-destructive testing is indisputably very important. Non-destructive methods of laboratory examination include x-ray analysis, which can reveal important points for further investigation without causing additional damage to the sample.

An X-ray analysis uses not only changes in absorption of X-ray radiation through different materials, but also ray bending, diffraction, etc. Thus, it is possible to determine for instance structure, or surface tension. However, an absorption is the most frequent method. An X-ray absorption occurs in materials according to an atomic number of each element. The second factor influencing absorption is the thickness of the material at the radiation site. Two basic method, depending on the way of use, are prevalent today: radiography and radioscopy. Radioscopy works within real time. An examined object is placed between an X-ray lamp and an image converter (which converts X-rays into a visible light area, vacuum image amplifiers, flat panels). The manipulates rotates the object, so it is possible to evaluate the object immediately and within the real-time. [7].

X-ray tomography is considered to be a higher level of radioscopy. The technique looks similar to the standard radioscopy method. A semiconductor panel is almost exclusively used as a sensor nowadays and is more accurate. When you rotate an object, several hundred images are taken from which the software reconstructs the image. While in the standard image the value of each pixel corresponds to the blackening value, for tomography the value of each voxel (three-dimensional pixel) corresponds to the absorption value at a given point. Unlike a conventional X-ray image, where we see the darkness immediately when viewed, we need a software to view a tomography image. With its help we can examine each layer, make cuts.

At the Population Protection Institute, a study was carried out to verify usability of X-ray radiation for the purpose of examining samples of electrical appliances damaged by fire. A better option is to use an X-ray cabin in which a sample is placed rather than using a portable X-ray apparatus used at the fire scene (similar to a device used by the Police of the Czech Republic for pyrotechnics). When using an X-ray cabin, more accurate results are obtained and the X-ray system is referred to as a small source [8].

If a small portable X-ray system is used in an X-ray cabin, the cabin is usually designed in a way to allow the X-ray system to be removed and used in the field. However, to use an X-ray system outside the cabin is legislatively more complicated. While an X-ray system (irrespective of its size, even 450 kV) is in the cabin, it is classified as a so-called small source and the user is only obliged to report its use to the State Office for Nuclear Safety. If an X-ray system device is used outside the cabin, in the field, it is classified as a so-called simple source. In this case a number of requirements have to be fulfilled e.g. the user must be accompanied by a qualified person certified by the State Office of Nuclear Safety, and must have an approved emergency plan, a monitoring plan, a controlled area, etc. [8].

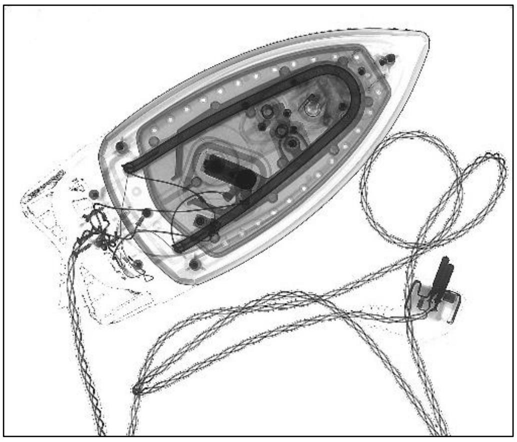

Fig. 6: An X-ray Output - a sample of a burned iron [5]

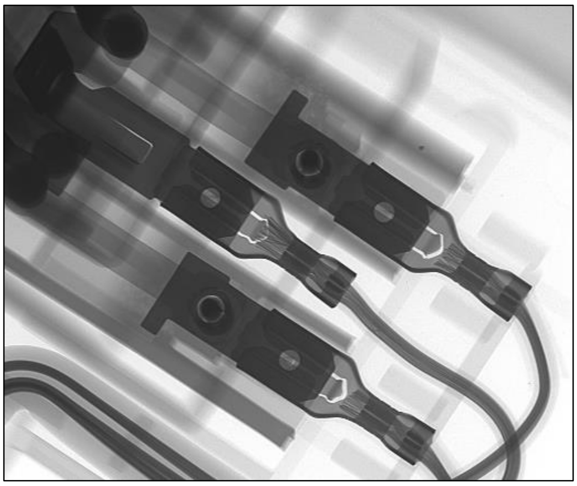

Fig. 7: Picture acquired using an X-ray system - details of kettle connection [5]

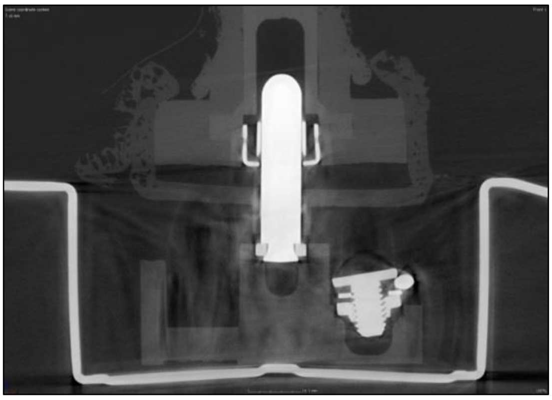

Fig. 6: An X-ray Output - a sample of a burned socket [5]

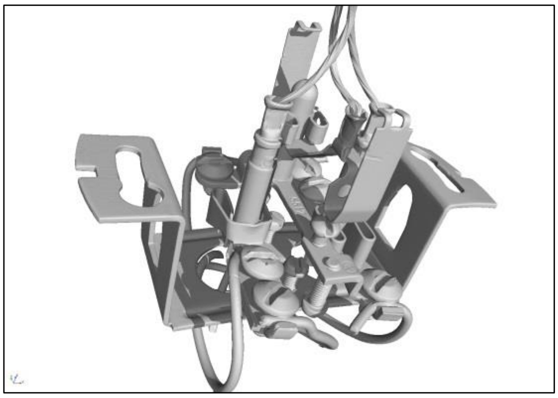

Fig. 8: Illustration of a 3D model of burned sockets using CT [5]

5. Conclusion

The paper focused on one of the most important steps for determining the cause of fire, namely the collection of correct relevant information. Facts and information about the incident are collected through direct observations, measurements, photographs, evidence collection, testing, experimentations. All collected data should include the documentation of the property, construction and occupancy, fuel loading, the preloading and layering of the debris and evidence as well as the extinction of the heat and smoke patterns, char depths and calcination, and the application from electrical arc mapping surveys where relevant. This includes, among other things, also high quality photographic documentation and digitization of a fire scene.

If fire-technical expertise is to be performed correctly, the samples must be collected in a correct way. The relevance of fire-technical expertise outputs depends on many factors. First of all, it is the correct sampling of the fire scene, its packaging, and the documentation of all the details at the scene of fire. After considering all the possibilities and risks, the method of packaging and transportation of the sample to the laboratory can be decided. The laboratory subsequently verifies physical values, and carries out non-destructive and destructive testing. The results of the laboratory testing are presented in the Fire Technical Expertise, which is consequently sent to the Investigators of the Regional Fire Rescue Service. The investigators will then include the information from the Report into the data obtained, on the basis of which he is able to propose and verify the hypothesis of the cause of the fire.

References

[1] Statute n. 133/1985 Sb., about fire safety, as amended by current law In: The collection of laws of the Czech (in czech)
[2] Decree n. 246/2001 Sb., about settings fire safety conditions and state supervision (Fire prevention decree), as amended by current law In: The collection of laws of the Czech Republic. (in Czech)
[3] Ministry of interior - Instruction of the General Director of the FRS of the Czech Republic No. 46, 2013. Procedure of fire investigation at the Fire Rescue Service of the Czech Republic, updated by Guideline No. 49/2015
[4] NFPA 921: Guide for Fire and explosion invetigations. 2017
[5] author´s archive
[6] R.A. Yereance, T. Kerkhoff, 3rd ed., Electrical fire analysis, 2010, ISBN 978-0-398-07955-0.
[7] J.D.DeHaan, D. J, Icove, Kirk´s fire investigation, 7th ed. ISBN 978-0-13-508263-8, 2012, p. 590-591.
[8] Statute n.18/1997 Sb., atomic low, as amended by current law. In: The collection of laws of the Czech (in czech)

Testing of Alginite as a sorbent of heavy metals from soil and above – ground biomass of plants

Jana Oravcová[a] – Martin Dráb[b] – Hana Ollerová[b] – František Kačík[a,c*]

[a] *Technical University in Zvolen, Faculty of Wood Sciences and Technology, Zvolen, Slovakia*

[b] *Technical University in Zvolen, Faculty of Ecology and Environmental Science, Zvolen, Slovakia*

[c] *Czech University of Life Sciences in Prague, Department of Wood Processing, Praha, Czech Republic*

Abstract

The aim of the thesis is to determine the content of mercury in soil and in plants grown in contaminated soil with the addition of Alginite. Samples of soil contaminated with mercury were taken from locality of *Malachov* and then mixed with Alginite in a 1: 3 and 1: 1 ratio. In these substrates, we performed an experiment with *Brassica napus L. var. napus*. (rape). Plant and soil samples were analyzed on a dedicated spectrophotometer - AMA 254. In the samples of substrates used for growing rape we found a mercury content from 0.0929 mg.kg^{-1} to 2.9085 mg.kg^{-1}. The mercury content in the above – rape biomass from 0.0425 mg.kg^{-1} to 03302 mg. kg-1. The sorption properties of Alginite were most pronounced in the above – mentioned rape biomass when a drop-in mercury content of 0.2005 mg.kg-1 was recorded. We compared the resulting values with the limit values that were exceeded in many cases. From the values we have found, we can say that Alginite has confirmed its sorption properties, which can be further used in the treatment of the physical – chemical properties of lighter soils, the decontamination of soils devastated by anthropogenic activity.

Keywords: mercury; Alginite; Brassica napus L. var. napus; AMA 254

---

[*] Corresponding author. František Kačík: email: kacik@is.tuzvo.sk; kacik@fld.czu.cz.

1. Introduction

With the increasing number of inhabitants on the planet, problems arise with the production of agricultural crops, which are further processed into food. To keep the hygiene limits in these crops, the state of the environment (soil, water, air) is very important. Risk factors that negatively affect the quality of the environment include heavy metals, including mercury. Mercury in the form of organic compounds is used as a pesticide and fungicide. The environment comes in the form of many objects and chemicals, batteries, thermometers, agrochemicals, pharmaceutical products, dental metals and others. Due to the low solubility of most inorganic compounds, mercury is not the usual pollutants in waters hazard but are industrial accidents and formation of soluble organic compounds as volatile substances thus becoming the atmospheric pollutants.

2. Issues

Mercury in the medium occurs in three oxidation states (0, + I and + II) and seven stable isotopes (196 Hg, 198 Hg, 199 Hg, 200 Hg, 201 Hg, 202 Hg and 204 Hg). The largest inorganic forms are mercury (Hg + and Hg2 +). Mercury salts (e.g., HgCl2) are soluble in water, whereas organic Hg compounds are insoluble and do not react with weak acids and low carbon sulphide-containing bases. Mercury contained in soil and in the atmosphere can be in different forms in plants [1]. The dominant form of mercury in the atmosphere is the gaseous elemental force (Hg0) [2]. Atmospheric mercury is obtained in the plants through the trickles, trichomes or cracks in the curriculum, the role of sheet morphology is also important. An important form of accumulation of mercury in the plant organism is the entry of wet and dry deposits of meruti from the atmosphere [3]. The soils and sediments of watercourses, seas, oceans and reservoirs belong to those substrates that are of great importance in the mercury cycle. The content of mercury in sediments often points to the overall contamination of the site better than the instantaneous concentration in water [4]. Exposure to mercury plants reduces the effectiveness of photosynthesis, transpiration rate, water absorption, and chlorophyll synthesis. Organic and inorganic forms of Hg have been shown to cause potassium, magnesium and manganese loss in the plant, and reduce iron accumulation [5]. At present, there is a high environmental burden on anthropogenic activity. For this reason, interest in different ways of cleaning and decontaminating devastated soil is also increasing. One of the possibilities of recovery is the use of available natural resources. Alginit is an organic-mineral rock that has a realistic perspective of wide use in the rich locality of Lučenec. Alginite contains fossil algae that formed a continuous sediment in the Pannonian lake system during volcanic changes 3-4 million years ago, along with eroded rocks [6]. **Alginit** from locality of *Pincina* is a clay-rich rock rich in organic matter. Its main suppliers were the yellow-green algae *Botriococcus braunii*, which lived in the colonies in the forested zone of the *Maar lake*, and after the death they fell to the bottom where they were deposited together with the clay material. fallen from the engraving maar ring. The high content of organic matter, enhanced by the presence of the clay smectite minerals, is associated with an important Alginite property - a high water absorption capacity [7].

3. Material and methods

To carry out our research, soil contaminated by mercury must be secured. Since manipulation with elemental mercury can cause a health hazard as well as damage to laboratory equipment, soil samples containing mercury were collected at locality of *Malachov*, where cinnabarite was harvested in the past - from which the bulk of mercury is extracted, only significantly smaller quantities of schwazite - tetrahedrity furthermore from ores containing mercury.

3.1. Samples of soil

Soil samples were taken in October 2016 (autumn) at the end of the vegetation period in accordance with STN 48 1000 (Sampling and Preparation of Forests for Forest Health Surveys). We took it to locality of *Malachov* site, where we predicted an increased concentration of merkte in the soil. Soil samples are taken from 10 - 30 cm depths using hoe and rice into plastic bags. Subsequently, the soil could dry at room temperature for several days. After drying, we removed the rough skeleton, organic residues from the soil, and then we had to homogenize soil samples. Their form was significantly varied and could consequently cause distortion of the results.

3.2. Samples of Alginite

Alginite samples were taken at locality of Pincina deposit near Lučenec in February 2016 (winter). To obtain a representative sample of Alginite, we have followed standard laboratory procedures for sampling. At the selected collection site, we set a square-shaped area with a length of one side of 5 meters. This was then divided into partial squares measuring 30 x 30 cm. From each square we removed the same amount of Alginite using a blade. The thus obtained Alginite sample could dry at room temperature. Since Alginite is characterized by its high-water adsorption, the drying time of the Alginite was significantly longer than in the soils. Alginite samples also had a diverse form, so we had to homogenize them similarly to soil samples.

3.3. Realization of container experiments

Modified soil samples and Alginite were used to grow test plants. In our research, we have decided for *Brassica napus L. var. napus*. (rape). This plant is the most widely grown crop in Slovakia with the largest representation and utilization. When growing rape we have prepared four different substrates in gardening containers, namely - horticultural substrate freely available for sale, soil naturally contaminated with mercury taken at locality of *Malachov* site, contaminated soil with the addition of Alginite in the ratio 1: 1 and 1: 3. To the substrates thus prepared, we sowed 2 g of seed, which was evenly distributed over the entire surface and then covered with a small layer of substrate and poured. We repeated this procedure three times for each substrate.

After drying, the above-ground portions were homogenized with a mill and analyzed on a single-purpose atomic spectrophotometer AMA 254. The substrate samples were removed from the plants in which the plants were grown. The substrates were also homogenized in the mortar, sieved through a 2 mm sieve, and then quartz was performed to obtain an average sample which was subsequently analyzed on a single-purpose atomic spectrophotometer AMA 254.

After performing the previous steps, we proceeded to analyze the samples. We analyzed each sample at least three times. The weights of the individual samples ranged from 30 mg to 60 mg. Samples of substrates containing naturally contaminated soil from Malachov were weighed in combination with sand, to add approximately 2 mg of substrate to the sand to give a final weight of about 50 mg. For samples of above-ground parts of plants, we set the times for the individual phases of analysis as follows: drying 45 s, thermal decomposition 150 s and temperature adjustment 45 s. We used different times for substrate samples: 45 with drying, 180 with thermal decomposition, and 45 with temperature adjustment.

The AMA 254 analyzes in two ranges, among which it selects the software automatically so that the absorbance value is not exceeded by 0.8.

4. Results and discussions

4.1 Concentration of mercury in above-ground biomass

The value of the arithmetic average of the total mercury content in the above – ground plant organs of the rape is 0.1721 mg.kg^{-1} ± 0.1137 mg.kg^{-1}. The measured values of mercury concentration (Fig. 1) in above – ground rape biomass measured in individual growing substrates decrease in the following order contaminated soil from *Malachov* > contaminated soil with Alginite in a ratio of 1: 3 > contaminated soil with Alginite in a 1: 1 ratio > horticultural substrate freely available on sale.

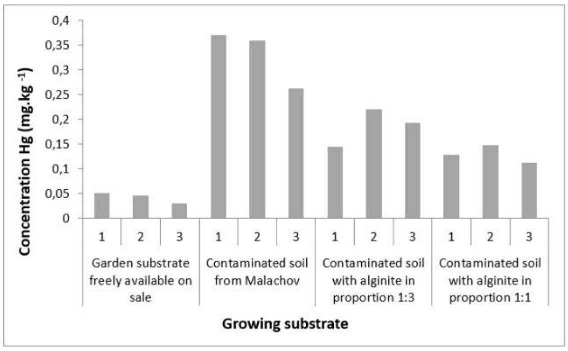

Fig. 1 Concentration of Hg in above-ground rape biomass

The highest mercury concentration was recorded in the above – ground parts of the rape grown in the substrate – contaminated soil from *Malachov*. The concentration value is 0.3302 $mg.kg^{-1}$ ± 0.0593 $mg.kg^{-1}$. This concentration is directly related to the ancient extraction of mercury in *Malachov*. The lowest value of mercury concentration was recorded in the above – ground rape organs grown in the substrate – the garden substrate is freely available on the market. The concentration value is 0.0425 $mg.kg^{-1}$ ± 0.0106 $mg.kg^{1}$.

The mercury concentrations of 0.1858 $mg.kg^{-1}$ and 0.1297 $mg.kg^{-1}$ ± 0.0382 $mg.kg^{-1}$ and 0.0181 $mg.kg^{-1}$ were measured in the above – ground parts of the rape cultivated in the substrate - contaminated soil with the addition of Alginite in the ratio 1: 3 and 1: 1. Compared with contaminated *Malachov* soil, these concentration values are smaller by 0.1444 $mg.kg^{-1}$ and in the other case by 0.2005 $mg.kg^{-1}$, so we can assume that Alginite has shown its sorption properties. In above – ground rape biomass, the maximum allowable amount (NPM) for other foods (0.05 $mg.kg^{-1}$) was exceeded for all substrates contaminated with *Malachov* soil. This value was maintained in biomass grown in the garden substrate. Also, NPM for feed materials (0.1 $mg.kg^{-1}$) were exceeded in the above – ground rape organs on substrates using contaminated soil from. When adding Alginite to this soil in a 1: 1 ratio, we have achieved a result approaching this value.

4.2 The concentration of mercury in the used growing substrates

The mean value of the total mercury content of the growing substrates used for rape production is 1.7979 $mg.kg^{-1}$ ± 1.2079. Mercury concentrations (Fig. 2) found for individual growing substrates used to grow barley fall in the following order – contaminated soil from *Malachov* > contaminated soil with Alginite in 1: 3 ratio > contaminated soil with 1: 1 Alginite added > gardening substrate freely available on sale.

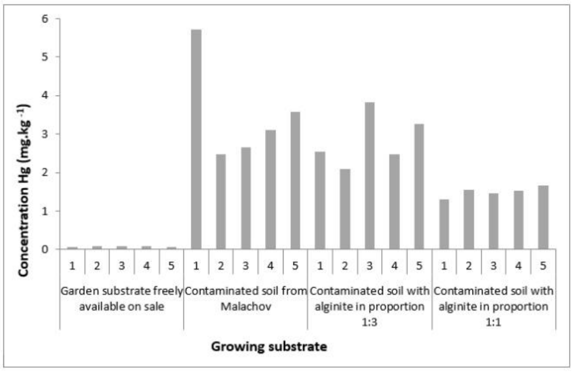

Fig. 2 Content Hg in growing substrates used for the cultivation of rapeseed - Brassica napus L. var. napus

The highest value of mercury concentration in growing substrates was recorded at the substrate – contaminated soil from *Malachov*. Its value is 2.9085 $mg.kg^{-1}$ ± 0.2138 $mg.kg^{-1}$. To the above – ground parts of the rape grown on this substrate was accumulated 0.3302 $mg.kg^{-1}$ ± 0.0593 $mg.kg^{-1}$. The lowest value of mercury concentration in growing substrates used for rape husbandry was recorded at the substrate – the garden substrate, freely available on the market. The concentration value in this substrate reached 0.0929 $mg.kg^{-1}$ ± 0.0113 $mg.kg^{-1}$. Gardening substrate, freely available in the market, should be suitable for growing different crops and should be hygienically safe, which has been confirmed.

For contaminated soil with 1: 3 and 1: 1 Alginite, we used mercury concentrations of 2.6318 $mg.kg^{-1}$ ±

0.5665 mg.kg^{-1} and 1.6218 mg.kg^{-1} ± 0.1637 mg.kg^{-1}. These values are lower by 0.2767 mg.kg^{-1} and 1.2867 mg.kg^{-1} compared to contaminated soil from *Malachov*. In this case, we have also confirmed the sorption properties of Alginite, and we can conclude that when Alginite occurs in contaminated soil, it can absorb more risk factors than our mercury.

5. Conclusions

This work provides partial information on the determination of the concentration of mercury in above-ground biomass of rapeseed - Brassica napus L. var. napus. From the measured values, the applied substrate directly influences the concentration of mercury in the above-mentioned plant biomass. From the values we have found, we can also say that Alginite has confirmed its sorption properties, which can be further used in the treatment of the physico-chemical properties of lighter soils, the decontamination of soils devastated by anthropogenic activity.

Acknowledgement

This work was supported by the grant VEGA No. 1/0387/18 (50%) and grant KEGA 030UMB-4/2017 (50%).

References

[1] A. Kabata-Pendias, A.B. Mukherjee. Trace Elements from Soil to Human. Springer-Verlag, Berlin. 2007.

[2] Lodenius M.Dry and wet deposition of mercury near a chloralkali plant.Sci Total Environ; 213:53 –56. 1997.

[3] A. W. Rea, S. E. Lindberg, T. Scherbatskoy, G.J. Keeler. Mercury accumulation in foliage over time in two northern mixed - hardwood forests. In: Water, Air and Soil Pollution 133. 2002.

[4] J.E. Fergusson. The Heavy Elements. Chemistry, Environmental Impact and Health Effects, Pergamon Press, Oxtford. 1990.

[5] D.W.Boening. Ecological effects, transport, and fate of mercury: a general review, Chemosphere, vol. 40, no. 12, pp. 1335–1351, 2000.

[6] J. Kulich et al. Perspektíva využitia alginitu vo výžive rastlín . Perspective of exploitation of alginit in plant nutrition. Journal of Central European Agriculture, 2.3-4: 200. 2001

[7] C. Ravasz, G. Solti, C. Tóth. Report presenting the results of the research work caried out in the are of the maar craters at Pinciná in the year 1994. Manuskript, Geonconsult, Bratislava. 1994

Earth in a Trap? 2018
Analytical Methods in Fire and Environmental Science

Assessment of biological degradability of agricultural substrates

Juraj Poništ[a] –Dagmar Samešová[a]

[a]*Department of Environmentla Eingennering, Faculty of Ecology and Environmental Sciences, Technical University in Zvolen, T. G. Masaryka 24, 960 53 Zvolen*

Abstract

This work focuses on research of the biological degradation of the agricultural substrates, namely the cattle manure and the corn silage. We evaluated the suitability and on the contrary unsuitability of the selected substrates in the process of the biodegradability. Research methods used activated sludge from the wastewater plant to evaluate the potential of selected substrates in the process of the biodegradability. The significant indicators, which include O_2, CO_2, BOD_5 and COD_{Cr} were used for analysis on biological degradability of agricultural substrates. The corn substrate achieved the highest decomposition rate. Used tests and deviations between them, confirmed the requirements for a combination of the different tests of biodegradation. It was problematic to have only respirometric assays that showed a very similar pattern, although the percentage of biodegradation was different.

According to determination of selected indicators, corn silage and cattle manure can be defined as average biodegradable substrates. Addition of the active sludge made degradation faster of both samples.

Keywords: manure; anaerobic digestion; biodegradability;corn silage

---

1. Introduction

Generally, biodegradability refers to the breaking down of a product via microbial activity. This can be realized by aerobic catabolic pathways, during which are producing CO_2, water, and biomass or anaerobically, producing CO_2 and CH_4 [1].

Composting process together with anaerobic digestion are examples of aerobic and anaerobic biodegradation processes respectively, resulting in the formation of gases (e.g. CO_2, CH_4 and N_2O), water and compost or digestate [2].

The residue of anaerobic digestion, called digestate, is used as soil amendments, and its biological stability is an important indicator of the environmental risk posed by the digestate [3]

Difference between the aerobic and the anaerobic process is from stoichiometry of degradation biomass [4].

Composting has been used mostly in treating municipal sewage sludge, but has also been used to treat several industrial solid wastes. These include industrial wastewater treatment sludge, food processing wastes, and some industrial wastes containing low levels of pesticides [5, 6].

The production of biogas is widely used by modern society for the treatment of livestock manure and slurries. Biogas is today standard technology for stabilisation of primary and secondary sewage sludge, for treatment of organic industrial waste from food-processing and fermentation industries as well as for the treatment of the organic fraction of municipal solid waste [7].

Biogas is one of the important renewable energy resources [8], which contains in general about 60% methane (CH_4), and about 40% carbon dioxide (CO_2) [9], while the hydrogen sulfide (H_2S), as a malodorous and sour impurity gas in biogas, which is spanning from 100 to 2400 ppm. [10].

Generally, biogas can be produced from nearly all kind of biological feedstock types. European agriculture handles more than 65% of livestock manure as slurry, a liquid mixture of urine, feces, water, and bedding material. Another agricultural substrate suitable for anaerobic digestion is represented by energy crops, of which most common are grain crops, grass crops and maize. Maize silage is among the most promising energy crops for biogas production [11].

2. Methods

Before evaluating of biodegradability was necessary characterization of initial agricultural substrates, which includes analysis of total solid (TS) and COD.

To evaluate of biological degradability of agricultural substrates were used significant indicators, which includes BOD_5 and COD_{Cr} (Table 1) [12, 13].

To evaluate the potential of selected substrates in the fermentation process were chosen testing method using activated sludge from the wastewater treatment plant. Supporting indicators in the analysis of biological degradability are O_2, CO_2, BOD_5 and COD_{Cr} [14].

Change of BOD was observed during 28 days of incubation with determination of BODn and COD_{Cr}. Substrates were leached according to values of COD. Substrates were leached 24 hours with shaking followed by filtration of samples.

BOD was measured in interval 5, 10, 15 days with manometric method according to STN EN ISO 5814 (Water quality).

Determination of degradation was occurred during one-time cultivation with constant stirring. For evaluating of biological degradability with addition of active sludge were used 2 L vessels in concentration of substrate 400 mg COD/l and active sludge 100 mg/l.

In chosen time interval were taken samples for determination of COD (figure 1, 2) according to STN ISO 6060 (Water quality).

The respirometric analysis was performed with manometric OxiTop Control^W system (WTW, Germany) according to STN EN ISO 9408: 2001.

Main advantage of this method is that can be performed without dilution of samples with modelling condition like by biological treatment.

3. Results and discussion

Characteristics of substrates can be found in Table 1.

Table 1

Determination of the dry matter and COD of the maize silage and cattle manure

Agricultural substrate	Dry matter (%)	COD_{Cr} (mg/l)
Maize silage	31	100 000
Cattle manure	14	81 000

In maize silage was observed higher value of COD. Both values of COD can involve biodegradable substrates.

Measuring of BOD and COD_{Cr} was occurred in the same interval time (each 5 days). The results first analysis of biodegradability represents Table 2.

Table2

BOD and COD_{Cr} of the maize silage and cattle manure during incubation

Agricultural substrate	BOD_n(mg/l)	COD_{Cr} (mg/l)
Maize silage	40 000^a	96 000
	42000^b	96 000
	43000^c	95 000
Cattle manure	27 000^a	79 800
	27 500^b	79 000
	28 000^c	78 500

[a] 5 days

[b] 10 days

[c] 15 days

Maize silage		Cattle manure	
BOD_n [mg/l]	COD_{Cr} [mg/l]	BOD_n [mg/l]	COD_{Cr} [mg/l]
40 000*	96 000	27 000*	79 800
42 000**	96 000	27 500**	79 000
43 000***	95 000	28 000***	78 500

*5 days; **10 days; ***15 days

After 15 days was observed higher increase of BOD in maize silage. After 15 days of incubation was not observed important changes.

During incubation of maize silage BOD/COD ratio was moving in range 0.45 to 0.42. During incubation of cattle manure BOD/COD ratio was moving in range 0.34 – 0.35. These values are defined for average biodegradable substrates.

Influence of added active sludge in process of biodegradability represents Figure 1 and 2.

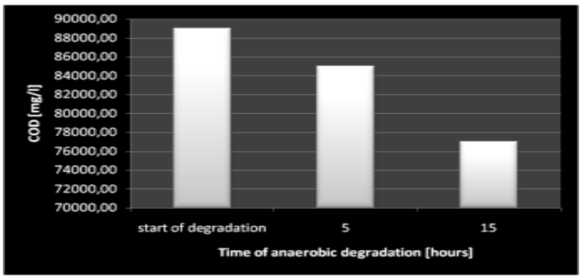

Fig.1. COD during one-time cultivation of the maize silage with the addition of activated sludge

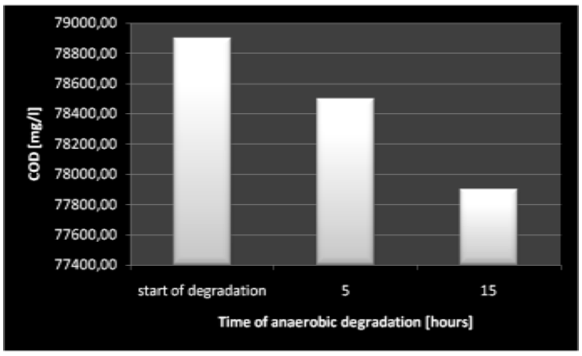

Fig. 2. COD during one-time cultivation of the cattle manure with the addition of activated sludge

Addition of active sludge contributed to faster degradation both of samples.

During respirometric assay was observed changes of consumption of oxygen under aerobic condition (Fig. 3).

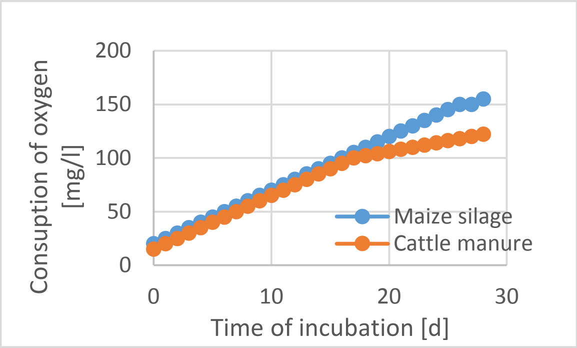

Fig.3. Respirometric assay of biological degradability

The maize silage reached sharper curve consumption of oxygen (Fig. 3). The maize silage can be considered as better biodegradable substrate in comparison with the cattle manure.

Acknowledgments

Authors are grateful for financial support of the project KEGA 018TU Z-4/2017 (The increasing of knowledge level of students in the area of life cycle valuation).

References

[1] HAYES, D.G., Commentary: The Relationship Between “Biobased,” “Biodegradability” and “Environmentally-Friendliness (or the Absence Thereof)", In: The Journal of the American Oil Chemists' Society, vol. 94, no. 11, 2017, pp. 1329-1331.

[2] HERMANN, B.G.et al., "To compost or not to compost: Carbon and energy footprints of biodegradable materials’ waste treatment", In: Polymer Degradation and Stability, vol. 96, no. 6, 2011, pp. 1159-1171.

[3] ZHENG, W,et al., Relationship between anaerobic digestion of biodegradable solid waste and spectral characteristics of the derived liquid digestate. In: Bioresource Technology. 2014, vol. 161, pp. 69-77.

[4] LIU, X., et al., Evaluation of the correlations between biodegradability of lignocellulosic feedstocks in anaerobic digestion process and their biochemical characteristics. In: Biomass and Bioenergy. 2015, vol. 81, pp. 534-543.

[5] CHEREMISINOFF, N.P.,Biotechnology for Waste and Wastewater Treatment**,** Published by Elsevier Inc., 1997, p.51, ISBN: 978-0-8155-1409-1

[6] HYBSKÁ,H., VACEK,V., TOMANICOVÁ,N., Degradation rate of the hydraulic oil in the soil. In Studia Oecologica, 2013, roč. 7, č. 2 (2013), s. 10-17.- ISSN 1802-212X. –

[7] AL SEADI,T., et al., Biogas Handbook, Denmark: Esbjerg, 2008, pp. 30-31. ISBN 978-87-992962-0-0

[8] Zhou, Q., Jiang, X., Li, X., Jiang, W., The control of H2S in biogas using iron ores as in situ desulfurizersduringanaerobicdigestionprocess. In: AppliedMicrobiology and Biotechnology. 2016, vol. 100(18), pp. 8179-8189.

[9] RODRIGUEZ, C et al., Pre-treatment techniques used for anaerobic digestion of algae. In: Fuel Processing Technology. 2015, vol. 27(5), pp. 765-779.

[10] HAO, X., HOU,G., ZHENG,P., LIU, R., LIU, Ch., H_2S in-situ removal from biogas using a tubular zeolite/TiO_2 photocatalytic reactor and the improvement on methane production. In: Chemical Engineering Journal. 2016, vol.192, pp.105-110.

[11] Holm-Nielsen, J.B., Al Seadi, T., Oleskowicz-Popiel, P., The future of anaerobic digestion and biogas utilization, In: BioresourceTechnology, 2009, vol. 100, no. 22, pp. 5478-5484.

[12] HORÁKOVÁ, M.,Analytika vody, druhé vydanie, Praha: VŠCHT, 2007, 335 s., ISBN 978-80-7080-520-6

[13] ZÁBRANSKÁ, J.,Laboratorní metody v technologii vody. Praha: VŠCHT, 1997, s. 9-11, ISBN 80-7080-272-3

[14] Hybská, H., Základy ekotoxikológie, Zvolen : Technická univerzita vo Zvolene,. 2015, 116 s., ISBN 978-80-228-2798-0

Preliminary results of "Environmental biomonitoring by bees" network at University of Sopron

Tamás Rétfalvi[a][*] – Ferenc Lakatos[b] – Piroska Szabó[a] – Zoltán Kovács[c]

[a]*University of Sopron, Faculty for Forestry, Institute of Chemistry, Bajcsy-Zs. 4. Sopron, 9400, Hungary*

[b]*University of Sopron, Faculty for Forestry, Institute of Sylviculture and Forest Protection, Bajcsy-Zs. 4. Sopron, 9400, Hungary*

[c]*Forestexpert Ltd, Jókai 7. Bajna, 2525, Hungary*

Abstract

Activity of Honey bees (*Apis mellifera*) has many beneficial properties, which make them particularly suitable for environmental biomonitoring. Examination of vital signs, chemical analysis of collected and stored materials, such as pollen, honey, propolis and wax provide us lots of information for evaluation of environmental status. For this purpose University of Sopron started a new project in 2015. We are developing an environmental monitoring system based on bee families. Our target is to establish the basic parameters and methods of a novel monitoring network, which is appropriate for fast, reliable indication and detection of contaminants with relatively low costs. Concerning the forgoing results Polycyclic Aromatic Hydrocarbons (PAH) were correlated with the pollution originated from waste combustion, while in case of metal content significant effects of road traffic were found. Our future plans include installation and development of "smart beehives" equipped different measuring instruments in order to implement real-time environmental biomonitoring.

Keywords: biomonitoring; bee; honey; propolis; wax; heavy metal content

---

[*] Corresponding author. Tel.: +36-99-518-175; e-mail: retfalvi.tamas@uni-sopron.hu

1. Introduction

Nowdays increasing social awareness is observable to focus on our environmental status, regarding to prevent and reduce different pollution processes (Lagadic et al. 1997). Protection of clean and sustainable environment became a major aim not only for civil society organizations but also for industrial sector. Lot of technologies and methods were developed to measure the negative effects. Emission limits, alert thresholds are existing, although alterations of the ecosystem react more sensitively to the adverse impacts compared to the instrumental apparatus in many cases. Today University of Sopron's new project, as GreenBee has two installed apicultures at industrial partners and there is a control area in botanical garden of main campus. The aim of this project is to establish a honey bee-based biomonitoring system, which is able to support the evaluation of environmental reliability, throughout extension of experiences on environmental effects.

It is necessary to select suitable and practical bioindicators and determine their reactions to the pollutants (Kargar et al. 2017). Honey bee (*Apis mellifera*) plays critical role in agriculture and the global ecosystem by pollinating plant, while producing bee products with high economic value (Li et al. 2015). Beehive matrices (pollen, honey, wax, propolis) can be used as bioindicators of the presence and levels of pesticides, (Rissato et al. 2007) heavy metals (Leita et al. 1996) and other environmental pollutants (Ponikvar et al. 2005). They represent good witness of environmental health and their presence could be considered as highly informative (Badiou-Bénéteau et al. 2013).

This research focuses on measurement of polycyclic aromatic hydrocarbon (PAH) content and elemental analysis. PAH compounds are a large groups of organic chemicals containing two or more aromatic rings and belonging to the food and environment contaminants (Lambert et al. 2012). PAHs generally occur in complex mixtures which may consist of hundreds of compounds. Among these compound sixteen were identified as a priority by United States Environmental Protection Agency (US EPA). In this study we performed the analysis with the respect of these 16-EPA listed PAHs.

2. Material and methods

2.1. Sample collection

Samples were originated from the north part of Transdanubia area, county of Győr-Moson-Sopron, Hungary. Two sampling zone were chosen: an urban-industrial and an agricultural area.

In case of PAH analysis the sampling period was March, 2016, for heavy metal content determination samples were collected in March, 2017.

During the sampling procedure honey, propolis, pollen and wax samples were stored frozen, then delivered to the laboratory.

2.2. Sample preparation and PAH analysis

After sample collection the frozen samples were prepared at once.

Liquid extraction from matrix was the first step of sample preparation, which is determined by the chemical feature of sample. In case of honey after a dilution of distilled water the PAH compounds were transferred from the hydrophilic phase to the hydrophobic phase by liquid-liquid extraction (LLE) of ethyl acetate and cyclohexane (ratio of 1:1) solvent mixture (*Sigma-Aldrich Ltd*.). In case of preparation of samples with low water content (pollen, wax, propolis) first step was dilution with cyclohexane-acetone (ratio of 1:1) (*Sigma-Aldrich Ltd*.). LLE and organic solvent extraction were performed by intensive stirring with magnetic mixing during 6 hours. Next step was purification, we have separated the interfering matrix components, and samples were concentrated by solid phase extraction with Enviro-P column. After desorption gas chromatographic measurement was executed. Identification of PAH compounds was done by 16 element-standard solution (suggested by EPA), while quantitative measurement was performed by internal standard method. The applied instrument was Shimadzu GC-MS QP-2010.

2.2. Measurement of heavy metal content

Determination of heavy metal content from the samples after a HNO_3-H_2O_2 destruction was applied by ICP-OES instrument (iCAP 6300 Duo ICP-OES), which is wild-use method in practise. Qualitative determination was done by standards, quantitative analysis was performed by calibration method. Following standards were applied for determination: Multi-element standard solution for ICP, Ref.No. M8A96.K1.5N.L1, (*CPAchem Ltd*.).

3. Results and discussion

3.1. PAH compounds

The highest five of PAH compounds concentration from quantitative analysis (executed by EPA 610 polinuclear aromatic hydrocarbons mixture) are shown in Table 1. Among the examined samples propolis contained the highest concentration regarding to the total value of 16 PAH compounds. Lowest levels were observed in honey samples. This is explained that honeybees collect the propolis from resinous, gummy products of plants, such as tree buds, pine resins, etc. This sticky raw material binds well the airborne dust particles and related organic materials, such as PAH compounds.

Anthropogenic effect can be found by comparing the sampling areas. PAH concentrations of samples from urban area exceeded the levels from agricultural area in all cases, which suggests the artificial origin of PAH compounds.

PAH compounds are originally found in products of combustion, in fume gases and exhaust gases, as a result of incomplete combustion (Veyrand et al. 2007). Another sources could be the petrol industry related to the oil-refinery process. They spread in the air and sediment to the soil and water, which explains their appearance in propolis samples.

3.2. Elemental analysis

During the elemental measurements, the composition of pollen samples showed the highest concentration values related to all of the elements (Table 2, 3). This observation can be explained by plan physiology, different elements are absorbed from the soil, thus pollen is the best indicator.

Significant anthropogenic effect was found in case of Zn, the highest difference was measured between the urban and agricultural fields. The reason of that can be the application of Zn-containing surface treatment by industrial company from urban area.

Table 1

Concentrations (μgkg^{-1}) of detected PAH compounds from honey, pollen, propolis, wax samples from agricultural and urban sampling area (BDL-below detection limit)

	naphthalene	acenaphtelene	fluorene	pyrene	benzopyrene	Total
honey agriculture	BDL	0.45	BDL	0.30	BDL	0.75
pollen agriculture	0.31	BDL	0.70	0.25	0.34	1.60
propolis agriculture	0.84	BDL	1.50	BDL	0.70	3.05
wax agriculture	BDL	1.10	0.37	BDL	BDL	1.63
honey urban	0.08	0.28	0.53	BDL	BDL	0.89
pollen urban	0.41	0.57	1.95	1.03	0.18	4.34
propolis urban	0.51	2.33	1.41	0.27	0.54	7.73
wax urban	0.32	1.57	0.76	0.66	BDL	4.95

Table 2

Concentrations (mgkg^{-1}) of heavy metals from honey, pollen, propolis, wax samples from agricultural and urban sampling area (BDL-below detection limit)

	Al	B	Ba	Cd	Co	Cr	Cu	Ga
honey agriculture	8.0	10.2	6.8	0.90	BDL	0.08	2.65	0.70
pollen agriculture	66.2	14.2	4.9	4.33	BDL	0.36	7.15	BDL
propolis agriculture	16.2	3.7	11.3	3.53	0.44	0.86	3.42	0.31
wax agriculture	15.2	4.7	5.8	4.14	0.16	0.34	2.66	0.58
honey urban	6.1	6.3	8.0	2.42	BDL	0.08	4.19	BDL
pollen urban	22.0	17.4	8.0	2.08	BDL	0.29	14.2	BDL
propolis urban	28.7	4.1	40.2	BDL	0.02	0.98	5.36	0.35
wax urban	11.9	6.0	8.3	BDL	BDL	0.78	3.12	0.10

Table 3

Concentrations (mgkg-1) of heavy metals from honey, pollen, propolis, wax samples from agricultural and urban sampling area (BDL-below detection limit)

	Li	Mn	Mo	Ni	Pb	Se	Sr	Zn
honey agriculture	BDL	0.91	BDL	0.25	0.63	0.18	2.04	6.4
pollen agriculture	BDL	22.33	0.19	0.66	1.22	BDL	5.27	61.2
propolis agriculture	0.56	1.45	0.60	0.26	1.79	BDL	3.38	25.9
wax agriculture	0.04	1.19	0.25	0.05	1.52	BDL	2.32	34.8
honey urban	BDL	0.60	BDL	0.12	0.56	BDL	2.45	13.4
pollen urban	BDL	23.16	0.10	0.57	1.16	BDL	4.54	84.1
propolis urban	BDL	4.22	0.22	0.44	2.64	BDL	2.87	98.2
wax urban	BDL	1.48	0.08	0.23	1.25	BDL	2.27	46.1

4. Conclusion

Based on our preliminary results, chemical analysis of different beekeeping products provides an indication method of various anthropogenic pollution impacts. In case of organic contaminants propolis appears to be the most efficient accumulator, while highest concentration of elements were detected from pollen samples. Further researches are needed in order to follow the alterations of vegetation period.

Acknowledgments

This research was funded by EFOP 3.6.2-16-2017-00018 project.

References

[1] Baciou-Bénéteau, A., Benneveau, A., Géret, F., Delatte, H., Becker, N., Brunet, J. L., Reynaur, B., Belzunces, L. P., Honeybee biomarkers as promising tools to monitor environmental quality. Environmental International. 60 (2013) 31-41.

[2] Kargar, N., Matin, G., Matin, A. A., Buyukisik, B. H., Biomonitoring, status and source risk assessment of polycyclic aromatic hydrocarbons 8PAHs) using honeybee, pine tree leaves, and propolis. Chemosphere. 186 (2017) 140-150.

[3] Lagadic, L., Caquet, T., Amiard, J.C., Ramade, F., Biomarquers en Ecotoxicologie, Aspects Foundamentaux, Paris:Masson (1997) 419

[4] Lambert, O., Veyrand, B., Durand, S., Marchand, P., Bizes, L. B., Piroux, M., Puyo, S., Thorin, C., Delbac, F., Pouliquen, H., Polycyclic aromatic hydrocarbons: Bees, hones and pollen as sentinels for environmental chemical conatminants. Chemosphere. 86 (2012) 98-104.

[5] Leita, L., Muhlbachova, G., Cesco, S., Barbattini, R., Mondini, C., Investigation of the use of honeybees and honey bee products to asses heavy metals contamination. Environ. Monit. Assess. 43 (1996) 1-9.

[6] Li, Y., Kelley, A.R., Anderson, D.T., Lydy, J.M., Development and comparison of two multi-residue methods for the analysis of select pesticides in honey bees, pollen and wax by gas chromatograohy-quadrupole mass spektrometry. Talanta. 140 (2015) 81-87.

[7] Ponikvar, M., Snajder, J., Sedej, B., Honey as a bioindicator for environmental pollution with SO_2. Apidologie. 36 (2005) 403-409.

[8] Rissato, S.R., Galhiane, M.S., de Almeida, M.V., Gerenutti, M., Apon, B. M., Multiresidue determination of pesticides in honey samples by gas chromatography-mass spectrometry and application in environmental contamination. Food Chem. 101 (2007) 1719-1726.

[9] Veyrand, B. Brosseaud, A., Sarcher, L., Varlet, V., Monteau, F., Merchand, P., Andre, F., Bizec, L. B., Innovative method for determination of 19 polycyclic aromatic hydrocarbons in food and soil samples using gas chromatography couples to tandem mass spectrometry based on an isotope dilution approach. Journal of Chromatography A. 1149 (2007) 333-344.

Automatic Control of Using Safety Helmets by Workers

Anatoly Romanov[a] – Andrei Nikulin[a] – Dmitry Ikonnikov[a] – Iliya Dolzhikov[a] –
Stanislav Kovshov[a]

[a]*St. Petersburg Mining University, St. Petersburg, Russian Federation*

Abstract

The article addresses ways to automate the process of controlling compliance with the rules for safety helmet use to improve the safety of employees working in harmful or hazardous conditions. Authors have proposed to consider the employee/safety helmet system as a physical object/biotechnical system. It has been shown that in cases when only the information that characterises a physical object is controlled, the information can be imitated by unprincipled workers. It has been resolved that the process should be complemented with the information that characterises the employee's activity (as a biological object). A suggestion has been made that proposed information spaces should be combined to improve the reliability of a control result. The article offers a method to generate a decision rule that integrates the assessment obtained based on the review of information from different sources. A structure of information process interaction has been developed to solve the task. The scope and purpose of main hardware that implement long-term automatic control over compliance with the rules for safety helmet use have been determined.

Keywords: occupational safety; Industrial safety helmets; smart PPE; safer equipment; health; safety.

---

1. Introduction

In accordance with national standard of the Russian Federation 12.4.011-89, Occupational Safety Standards System. Means of Protection. General Requirements and Classification, personal protective equipment (PPE) should be used by employees when work safety cannot be provided by equipment design, process flow, architectural and planning solutions or collective protective equipment.

Head injury prevention is based on the use of industrial safety helmets that meet relevant requirements taking into account working conditions for separate jobs. According to Rosstat, 10% to 20% of all industrial accidents occur due to a failure to wear PPE or the low quality of PPE. Head injuries are relatively common and account for 3% to 6% of all accidents. They are sometimes severe and cause significant loss of work time due to disability lasting up to three weeks [1]. Injuries are caused by:

– objects with sharp angles, such as tools or attachment bolts, falling from a height of several meters;

– hitting the head on the ground or against fixed objects when falling.

There is a risk of head injury at all industrial sites. Slippery oily floors, falling building materials or objects near workers, mechanisms and equipment are just a short list of causes of accidental loss of health and disability. The right head protection used in the right way and worn during the work day is a simple and reliable solution to handle the problem.

The review of accidents among builders who wear safety helmets show that head injuries occur if impact energy exceeds 100 J. Other injuries are less common but should also be taken into account. Such injuries include burns caused by splashing hot or aggressive liquids, melt metals, or injuries caused through accidental contact of the head with current-carrying elements. It is worth noting that up to 30% of workplace accidents is the result of a lateral rather than a vertical impact, e.g. when a worker collides with hard objects. The list of affected jobs is long. The risk of a lateral impact is more common in personnel involved in the repair of various equipment at facilities, e.g. in freight handlers. Hazards are known to be intrinsic in handling of large-sized equipment, with the presence of many protruding parts, permanent body movements and change of posture when carrying out different operations. Furthermore, a significant share of head injuries is observed during falls at industrial sites and in case of accidental blow on the head during construction and repair and when performing work in the constraint environment. Therefore, the risk of blows, contusion, and falling is significant and the need to protect the head (including lateral blow protection) is well justified.

Pursuant to Order of the Ministry of Healthcare and Social Development of the Russian Federation No. 290n dated 1 June 2009 on the approval of inter-industry rules for providing employees with special clothes, special shoes, and other personal protective equipment, an employer shall ensure proper control over the issuance of PPE within an established period of time. The employer makes sure its employees use PPE when they: work in harmful or hazardous working conditions and are exposed to special temperatures or contamination [2]. Structural unit managers appointed by the employer and occupational health and safety specialists control the correct use of PPE, its timely replacement, inspections, and testing.

In reality, the use of PPE, including safety helmets, involve a number of formalities and compromises related to the human factor. Responsible employees are not always conscientious enough and do not punish others for not using PPE and so on.

A relevant occupational safety challenge is to have transparent remote control over employees and prevent human factor impact on performance. This requirement is an important area for the improvement of methods and the upgrade of hardware aimed at ensuring employee safety in the environment presenting increased hazards for human health. An effective solution will ensure continuous control over compliance with mandatory requirements for PPE use thus increasing the level of employee safety in the working process.

2. Materials and Study Methods

The employee's head and a safety helmet together form an information space which is the aggregate of two sources that contain information required to control safety compliance when wearing the safety helmet in the industrial environment. The worker's head as type 1 source of information is regarded a physical object with specific geometrical proportions, mechanical properties, volume, and substances filling this space.

The sources of information that consider the employee/safety helmet system as a physical object include:

- changes of dielectric properties of the object;
- changes in the optical conditions in the object; and
- change in the characteristics of an ultrasound signal passing through the object.

The information on the presence of this physical object in the internal space of the safety helmet can be extracted with sensors that respond to changes in the characteristics. The following information can be recorded:

- changes in the dielectric permanent environment in the safety helmet space when the said object is present;
- interruption of a light beam by an object geometry;
- changes in the characteristics of an ultrasonic transmitter caused by the impact of mechanical properties and substances in the object;

and so on.

The benefit of the considered method of control over safety compliance is the relative simplicity of head identification in the safety helmet space using such sensor systems but the method disregards a subjective factor, such as the possibility of an unprincipled worker to impact a control result artificially by substituting a physical object. This requires an additional source of information (type 2 information) that would reduce the probability of a false control result.

The second proposed source of information is the information generated by an employee as a biological being and a working process participant.

The sources that characterise the details of the employee/safety helmet status as a biotechnical system include:

- changes in the rhythmic activity of body systems in a biological object;
- changes in heat exchange conditions between the biological object and the environment; and
- spontaneous and organised motor activity of a biological object.

In this case required assessment control criteria generated based on the review of type 1 information are complemented with adequate factor-based criteria, which are significantly hard to imitate. The type of recorded information is selected based on its value and potentially comfortable implementation of the recording process (which does not affect productivity).

It may include:

- rhythmic activity of core functional body systems (cardiovascular system and external respiratory system);
- main vital constants (body temperature, oxygen blood content, etc.);
- electrical brain activity;
- spontaneous and organised (professional) motor activity;
- heat exchange with the environment;

and so on.

Since these processes are hard to imitate, it is almost impossible to generate false information about the use of a safety helmet.

Furthermore, in accordance with the theory of reliability of technical systems, two technical systems used simultaneously and independently for the same purpose are properly backed up and significantly improve sustainability.

Reliable recording of required information forms a basis for its reliable assessment. The basis for this assessment is the generation of decision rules and their relevant algorithms. Type 1 information can be presented in the analogous and discrete form. A change in the dielectric permanent environment inside the safety helmet caused by the employee's head inside it is analogous information and entails a change in the electric capacity formed by a dielectric material and capacitor coating inside a safety helmet structural element. The electronic circuit of the impulse generator where the condenser in question is a time-setting element can change an impulse sequence period. It is an informative sign used in the decision rule. If an optoelectronic method is used to identify the employee's head inside the safety helmet, assessed information is discrete. In both cases, the result of assessment must be discrete (e.g., $Y_1 = 1$ means that the employee's head is not inside the safety helmet; $Y_1 = 0$ means that the employee's head is inside the safety helmet).

The decision rules used to analyse biomedical information are normally more complex but are finally transformed into a discrete code (e.g., $Y_2 = 1$ means that the employee's head is inside the safety helmet; $Y_2 = 0$ means that the employee's head is not inside the safety helmet).

The assessment, which includes decision rules obtained during the review of type 1 and type 2 information, forms the aggregate of logic equations solved to obtain more reliable additional information on the employee/safety helmet system (e.g., $F_1 = \bar{Y}_1 \wedge Y_2 = 1$ corresponds to the double confirmation that the safety helmet is on; $F_2 = Y_1 \wedge \bar{Y}_2$ corresponds to the double confirmation that the safety helmet is off).

The assessment of mandatory safety helmet wearing rules cannot be adequate enough if not "tied-in" with the working process stages. In such conditions, it is crucial to record the astronomical time at the point when a safety helmet is put on (t_{poi}) (where i=1,2,3….n means the number of time intervals of active safety helmet use) and the time when its use ends (a safety helmet is taken off) (t_{toi}). The review of safety helmet use time intervals ($€ = f(t_{poi}, t_{toi})$) helps to establish control over the adequate use of/failure to use head protection (stipulated by the rules and regulations in specific process areas) in the working time. Therefore, the aggregate of decision rules must be complemented with continuous generation of a time sequence which helps to export to the decision rule information on the legality of the employee/safety helmet system status at different stages of the work shift.

When the safety helmet is used in the wrong way, the situation is corrected in two ways. First, an employee is informed on the current violation as soon as possible with a sound message generated as a verbal or sound alarm. This message motives the employee to correct the situation. Second, the time intervals corresponding to the employee/safety helmet system status during the work shift are saved. The result of the posterior estimation of saved information can include additional social and disciplinary measures taken by relevant control departments.

3. Results

Processes combined in a common information space help to handle employee safety challenges (Fig.1).

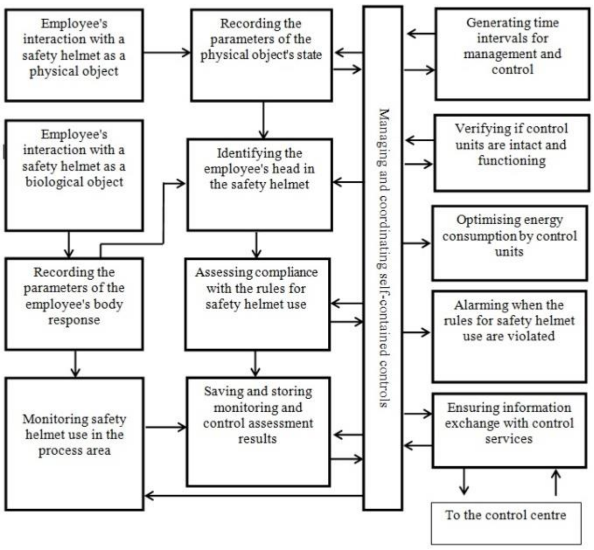

Fig. 1 Structure of the process of automatic control over compliance with the rules for safety helmet use.

In each production case, a specific set of functions and relevant processes can be determined to address the challenge. Automatic control over adherence to the rules for safety helmet use is possible using hardware specifically aimed at improving the following three areas:

1. Control over compliance with the rules for safety helmet use in the working process.

2. Information exchange between the employee/ safety helmet system and a stationary computer hardware (SCHW) after process completion and return of safety helmets for storage.

3. Processing of information from the SCHW in accordance with the regulator's requirements

This hardware must consist of a set of control units (CUs) mounted in the structural element of the safety helmet worn by each employee involved in the process and in the SCHW installed in the area where safety helmets are stored after work completion. All CUs in the SCHW form a common information space shown in Fig. 1 which supports a number of operations, such as:

- transfer of the information accumulated during control from the CUs to the SCHW upon request;
- transfer of internal information on the element status of each CU to SCHW; and
- receipt of management information from the SCHW to prepare each CU for the next operation period.

While processing the information from CUs, the SCHW supports:

- generation of a database with controlled data on safety helmet use by each process participant;
- assessment of controlled information based on given criteria; and
- submission of assessment results to relevant control services in a convenient format.

Automatic control over compliance with the rules for safety helmet use implies that the procedure is implemented independently from the employee over a long period of operation. Based on task conditions, each automatic control unit must operate from a self-contained power source over a given period of time (as long as possible), so that the selection of hardware for a self-contained control unit is limited and the optimisation of energy consumption is required through hardware and algorithm solutions, apart from the optimisation of overall hardware support.

At the hardware level, optimisation involves the selection of a process element base for a self-contained control unit. State-of-the-art elements are equipped with long-term functional energy consumption saving option. Energy consumption can be further minimised by selecting an active control principle in discrete time points. The time interval between two adjoining active control moments ($T_{оп}$) is selected in a way to rule out continuous control, on the one hand, and to prevent the loss of significant portion of controlled information, on the other hand. If the total time required per single control procedure is $T_и$, the total active time of operation of a self-contained control unit during a work day will be:

$$T_w = K \cdot T_и = (T_p / T_{оп}) \cdot T_и \qquad (1)$$

If there are T_g work days in a year, the total time of active work will be:

$$T_{w1} = T_g\, T_w \qquad (2)$$

This period of continuous operation will be supported by a source with energy capacity E, Ah, equal to:

$$E = T_{w1}\, I_n \qquad (3)$$

Where: I_n means current consumed by the unit during active operation.

Further optimisation of energy consumption is related to the control of a charge level by a self-contained control unit used and control of energy reserves when supporting and maintaining the hardware in general.

Each CU has its unique number which is analysed by SCHW in a special room designated for safety helmet storage after the process. The concept proposed implies that information exchange between CU and SCHW is independent from the user and is done automatically. For this purpose, the hardware consisting of CUs exchanges information as initiated by the SCHW server using a virtual main line (e.g. Wi-Fi). Once the transfer of information accumulated in each CU is completed, their hardware switches to the energy-saving (sleep) mode until the next shift.

The information transferred to the SCHW is saved in a database and analysed using developed algorithms. The intactness of the hardware in each CU is assessed together with data accumulated over the previous operation period. A log of past events is generated and the user's actions are evaluated for a monitored period.

Conclusions

Continuous automatic control over compliance with the PPE use requirements is key to work safety improvement. A special focus is on control over the protection of such vital organs as brain. A safety helmet connected to the employee's head becomes a source of information which can be used to control compliance with the rules for PPE use in various industrial environments.

For control purposes, it is recommended to use the information sources considering the employee/safety helmet system both as a physical object and a biotechnical system. The information received from a physical object is shown to be relatively easy to record and does not require complex decision rules to identify the violation of the rules for safety helmet use. However, this control method disregards the ability of an unprincipled worker to impact the control result by substituting a physical object. This method of identification is considered a basic (necessary) one and should be complemented with the review of information received from an employee as a biological object thus forming the aggregate of inimitable information flows. It is proposed to improve identification reliability by creating a backed-up system which must improve the credibility of the control procedure in question.

A resulting information field may be recorded and processed with hardware in the analogous and digital form but the decision rule must yield a discrete response based on the assessment of information from considered information sources and measured working process stages.

It is demonstrated that the violations of the rules for safety helmet use must be promptly reported to an employee to motivate corrective actions and later to relevant control services for post hoc review.

Developed interaction principles between various information processes can be implemented using state-of-the-art hardware to be operated automatically independent of an employee to ensure the long-term operation of all control unit elements. The authors have proposed processes, instrumentation, and algorithms to minimise energy consumption during automatic control.

Acknowledgments

The research is executed at the expense of a grant of the President of the Russian Federation for young scientists and graduate students.

References

[1] Korycki, R., 'The Damping of Off-Central Impact for Selected Industrial Safety Helmets Used in Poland', JOSE, volume 8, number 1, 2002, p. 51-70.

[2] Baszczyński, K., 'Industrial safety helmets – protection of the head against side impact', Occupational Safety, CIOP - PIB, Warsaw, May 2002, number 5, page. 10-13.

[3] Gilchrist, A., Mills, N.J., 'Improved side, front and back impact protection for industrial helmets', School of Metallurgy and Materials, University of Birmingham, HSE Contract Research Report, No.13/1989 Available at: /1989/crr89013.pdf

[4] Mills, N.J., Gilchrist, A., 'Proposals for side-impact and retention tests for industrial helmets', School of Metallurgy and Materials, University of Birmingham, 1990.

[5] K. C. Parsons (2007) Protective clothing: heat exchange and physiological objectives, Ergonomics, 31:7,991-1007, DOI: 10.1080/00140138808966738

[6] T.M. Zhigalova About heat and moisture exchange with between humans wearing special clothes and the environment. Text. / T.M. Zhigalova, Z.S. Chubarova, A.A. Zakharova // News of Higher Educational Institutions. Light Industry Technology. 1991. No. 4: pp. 55-60.

[7] L.V. Stepanova Peculiarities of the use of personal protective equipment by employees as protection against industrial contamination and mechanical damage // 3rd International Scientific and Practical Conference on Industrial Safety at Mineral Resources Companies in the 21st Century: scientific conference abstracts/St. Petersburg Mining University. St. Petersburg, 2016. p. 78.

[8] A.F. Davydov Russian working clothes market // Working clothes. 2010. No. 4: p. 12.

[9] Personal protective equipment. Textbook/Team of authors led by Yu.G. Sorokin. Moscow. 2007. 288 p.

[10] Batmanov V.P., Barsukov O.K. Laser and optic device to determine dust concentration and distribution of dust particles in the workplace air. Zapiski Gornogo instituta. 2017. Vol. 203: p. 146-149.

[11] Aude Morel, Gauthier Bedek, Fabien Salaün & Daniel Dupont (2014) A review of heat transfer phenomena and the impact of

moisture on firefighters' clothing and protection, Ergonomics, 57:7, 1078-1089, DOI: 10.1080/00140139.2014.907447

[12] S. Lee & S. K. Obendorf (2010) Barrier effectiveness and thermal comfort of protective clothing materials, The Journal of The Textile Institute, 98:2, 87-98, DOI: 10.1533/joti.2005.0143

[13] A.G. Shailkov, G.M. Volokhov, T.N. Abramenko, V.P. Kozlov Methods of determination of thermal conductivity and temperature conductivity Edited by A.V. Lykov Moscow: Energy. 1973. 336 p.

[14] Kovshov, S., R. Istomin, A. Nikulin and A. Sotiriu, 2014. Industrial injuries appraisal in mines of JSC “SUEK Kuzbass”. Advanced Materials Research Volume 1001: 414-420.

[15] Nikulin, A., A.Yu. Nikulina, A. Yu. Assessment of occupational health and safety effectiveness at a mining company. Eco. Env. & Cons. 23 (1): 2017, pp. 533-537.

[16] Kazakov B.P., Levin L.Yu., Shalimov A.V., Zaitsev A.V. Development of Energy-Saving Technologies Providing Comfortable Microclimate Conditions for Mining. Zapiski Gornogo instituta. 2017. Vol. 223: p. 116-124. DOI: 10.18454/PMI.2017.1.116

Emission Modeling of Exhaust Gases from Typical Parking House Operation

Jozef Salva[a] – Miroslav Vanek[a] – Marián Schwarz[a] – Miroslav Dado[b]

[a] *Department of Environmental Engineering, Faculty of Ecology and Environmental Sciences, Technical University in Zvolen (Slovakia), jsallva@gmail.com, Tel: (+421) 455 206 830*

[b] *Department of Manufacturing Technologies and Quality Management, Technical University in Zvolen (Slovakia), dado@tuzvo.sk, Tel: +421 455 206 864*

Abstract

This paper deals with air emissions modeling of exhaust gases associated with a standard parking house during its operation. The dispersion study evaluates the immission load from the mobile sources of air pollution and from stationary sources of air pollution (operating air-conditioning). The pollutants were evaluated as CO, NO_2, SO_2, PM_{10} and benzene. The authors also point to the possible side effects associated with ototoxicity of CO and NO_2 (as a part of a group of asphyxiants within ototoxic substances) and benzene (as part of solvent group within ototoxic substances). Outputs of the modeling software did not detect the exceedance of the limit values under the legislation on human health protection.

Keywords: exhaust gases; emissions modeling; MODIM; ototoxicity; parking house

---

1. Introduction

The objective of this paper is the air emission modeling of pollutants associated with the operation of a typical parking house.

In this dispersion study we assess the immission impact associated with the operation of the model parking house at the level of the immission burden from the transport (mobile sources of air pollution) and the controlled exhalations discharge from the building of the parking house through the air-conditioning device (stationary sources of air pollution).

The assessment is in the results interpreted as an immission contribution, which is evaluated as a percentage of the legislation limit value for each pollutant.

2. Characteristics of the Assessed Building Object of the Parking House

2.1. Layout

For purpose of immission modeling, a model of a typical parking house was developed based on the study and documentation of existing parking houses, especially in the Slovak Republic.

The object of a typical parking house that is the subject of the study has two parking levels at the ends of which is a walking exit to the surrounding reinforced areas. The upper parking level is opened. The lower parking level is closed and ventilated through air-conditioning system (see Chapter 2.2 for details) [1].

The following number of parking places are available within the considered typical parking house [1]:

- 85 parking places - lower parking level;
- 84 parking places - 1st floor (upper parking level)

Together, the parking house has a capacity of 169 parking places.

The dimension of parking place is considered in accordance with STN 73 6056/Z2 [2].

2.2. Operating Air-conditioning

The requirement for ventilation of underground garages is based on the technical standard STN 73 6058 [3]. Based on this, the amount of exhaust air is 300 $m^3.h^{-1}$ per parking place. The total required ventilation quantity for the modeling of a typical parking house is 85 x 300 = 25,500 $m^3.h^{-1}$. The parameters of the air-conditioning system are summed up in Table 1.

Ventilation is proposed as axial fans located on the side walls of the building of the parking house, so that the fans on one side of the building provide a supply and on the other side the air outlet [1].

Table 1

Parameters of air-conditioning system

	Unit	Air volume
Input	$m^3.h^{-1}$	25 000
Outlet	$m^3.h^{-1}$	25 00

3. Methodics

The objective of immission modeling is to evaluate the contribution of a standard parking house to ambient air pollution (immission concentrations) during its operation. The dispersion study evaluates the immission load from the following sources:

- mobile sources of air pollution (movement of vehicles);
- stationary sources of air pollution (operating air-conditioning - polluted air from the lower parking level).

3.1. Modeling Software

The MODIM computation program, developed by Envitech Slovakia, is used to model the immission load. The program is based on the US EPA-ISC2 methodology (ISC 2 Dispersion model).

In the immission load modeling process, the modeling for the annual average concentration field is performed under neutral dispersion conditions (Pascal-Gifford's D stability class) and average wind speed over the year in terms of used wind rose (see Figure 1) [4]. As a model a wind rose for city of Zvolen is used.

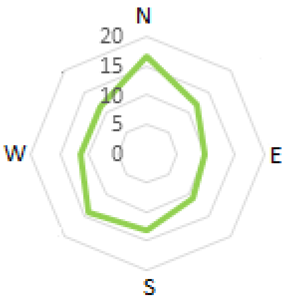

Figure 1 Wind rose for city of Zvolen

3.2. Evaluated pollutants

The resulting numerical values of the immissions are compared with the current legislative limits of the immission impact in accordance with the Decree of the Ministry of Environment of the Slovak Republic no. 244/2016 Coll. on air quality, which is documented in Table 2 [5].

For the field of maximum short-term concentrations, the calculation is carried out at the most unfavourable dispersion conditions for all wind speeds in the C-stability class (slightly labile) [4].

Table 2

Limit values for human health protection and deadlines for their achievement [5]

Pollutant	**Average Time**	**Limit Value**
PM_{10} [a]	24 hours	50 $\mu g.m^{-3}$
	1 year	40 $\mu g.m^{-3}$
SO_2	1 hour	350 $\mu g.m^{-3}$
	24 hours	125 $\mu g.m^{-3}$
NO_2	1 hour	200 $\mu g.m^{-3}$
	1 year	40 $\mu g.m^{-3}$
CO	8 hours	10 000 $\mu g.m^{-3}$
benzene [b]	1 year	5 $\mu g.m^{-3}$

[a] PM_{10} is a 83% fraction of solid particles smaller than 10 µm. The PM_{10} concentration will be 0.83 times the concentration of the solid particles (the MODIM program calculates the solid particles as PM_{20}).

[b] Benzene produced by automotive transport is evaluated as part of volatile organic compounds (VOCs), which make up 1 % of all VOCs

Regarding the pollutants listed in Table 2, it should be noted that some of them have the potential to cause toxic effects on the structures of the inner ear in long-term exposure, which often results in irreversible hearing loss. These chemicals are the so-called ototoxic substances [6].

Specifically, CO and NO_2 (generally NO_X), as the main components of exhaust gases, which are included in the group of asphyxiants (ototoxic substances) are characteristic of preventing the body from using oxygen. The ototoxicity of these substances is explained as a consequence of hypoxia (oxygen deficiency) in the cochlea [7, 8].

Carbon monoxide, as opposed to CO_2, is lighter than air, and in enclosed spaces it can accumulate in the upper layers of the space. In the case of long-term exposure to ototoxic substances, this leads to health issues. It is important to note that, according to the World Health Organization (WHO), up to 1/3 of all registered occupational diseases within the EU is associated with hearing loss [6, 9].

The confirmed ototoxic substance within the pollutants listed in Table 2 also include benzene (within the group of solvents). Combustion of fossil fuels is one of the most important sources of this carcinogen in the environment [10, 11].

3.3. Categorization of source of air pollution

According to Act No. 137/2010 Coll. the mobile sources of pollution (movement of vehicles during parking house operation) and stationary sources of air pollution (representing by ventilation of exhaust gases from the lower level of parking) are assessed as sources of air pollution. The upper level of parking is opened and therefore the emissions from this space are not diverted by controlled exhaust to the surrounding environment [12].

We do not consider any energetical or technological source of air pollution in the parking house. The only sources of emissions are exhaust gases produced by vehicles - it is a small source of air pollution according to legislation [12].

3.4. Computing Area

The object of a parking house is not situated into defined area, because it is not strictly necessary for the purpose of immission evaluation. However, the immission characteristics are influenced by the airflow character represented by the wind rose, which was described in Chapter 3.1 as a model for the purposes of this dispersion study.

For the immission modeling process, the calculation area is 1,000 x 1,000 m in 50 m increments in both (x, y) directions.

3.5. Input Parameters for Modeling

Mobile Sources of Air Pollution

The transport contribution for the operation of the parking house is based on the increase in the number of vehicle passes through the parking house (arrival, parking and departure of vehicles). Operating hours are considered between 7:00^{AM} and 10:00^{PM} (16 hours per day). The transport balance, which is documented in Table 3, was carried out with a conservative estimate in order to obtain the most unfavourable variant of the immission load.

Table 3

Estimated frequency of daily traffic associated with operation of a model parking house

Parameter	**Value**
Number of parking places	169
Estimated frequency of vehicle replacement on 1 parking place	1 vehicle/4 hours
Total daily frequency on 1 parking place	4 vehicles/1 place a day
Total daily frequency of parking house	676 vehicles / day
Total daily frequency of parking house (80 % capacity of parking house)	540 vehicles / day

Emission parameters of mobile sources of air pollution (emission factors or mass flow of pollutants) are integrated directly in MODIM.

Stationary Sources of Air Pollution

The upper parking level is designed as opened with natural ventilation, and in terms of legislation it has the character of a line, respectively area emission source.

Lower parking level is considered enclosed with forced ventilation by operating air-conditioning system and it is a point source of air pollution.

The requirement for ventilation of underground garages is based on STN 73 6058 [3]. Based on this, the total amount of airflow is 25,500 $m^3.h^{-1}$. The ventilation is considered by axial fans located on the side walls of the building, so that fans on one side of the object provide air extraction and clean air will be drawn through the ventilation holes on the opposite side of the building. According to the prevailing wind directions, air flow in the east → west direction is considered.

We are considering the simplest suction solution in three separate sections of a parking house. In each section, the exhaust will be provided with a single axial fan designed to provide the maximum required amount of exhaust air exiting directly through the wall on the building facade, respectively. to an appropriate height of 3.0 m above the terrain. Horizontal direction is, in terms of pollution dispersion, a more adverse variant compared to the vertical orientation of exhaust because the initial air flow rate increases the effective stack height. Horizontal discharge is a frequent technical solution, and we consider this as the most undesirable variant for the needs of dispersion.

According to the available data from air-conditioning manufacturers, the exhaust diameter at the capacity of airflow 8,500 $m^3.h^{-1}$ varies from 500 to 700 mm [1].

Under the exhaust air parameters for dispersion study purposes, we understand the concentration of modeling pollutants under standard conditions and the exhaust air temperature. In the dispersion study, we must make the most favourable estimate because we do not have measured data and an estimate based on average vehicle emissions would be burdened by a large uncertainty of input data. In this case, the most unfavourable estimate is based on the assumption of the maximum concentration of pollutants in garage (even assuming that the ventilation system is at full capacity) which does not cause a health hazard to the customers and to the operating personnel of the parking house.

The Maximum Permissible Exposure Limit (MPEL) for individual pollutants (see Table 4) is set out in Government Regulation no. 355/2006 Coll. on the protection of workers from the risks related to exposure to chemical agents at work. Specially for the benzene, because of its carcinogenic effect, the MPEL is expressed as a technical guideline value [13].

Table 2

Maximum permissible exposure limits for the pollutants

Pollutant	**CAS**	**MPEL**[a]			
		Long-term		**Short-term** [c]	
		ppm	**mg.m**$^{-3}$	**ppm**	**mg.m**$^{-3}$
CO	630-08-0	30	35	60	70
NO_2	10102-44-0	2	4	-	-
SO_2	7446-11-9	0.5	1.3	1	2.7
benzene [b]	71-43-2	1	3.25	-	-
PM_{10}	-	-	10	-	-

[a] The MPEL for gases, vapors and aerosols with toxic effects are determined independently of temperature and pressure in ppm and dependent on these variables in $mg.m^{-3}$ at 20 °C and 101.3 kPa.

[b] For benzene, the technical guideline value is used instead of the maximum permisseible exposure limit.

[c] MPEL short-term is the time-weighted average (TWA) of the concentrations measured over the 15-minute reference period to which employees may be exposed at any time during work change (up to 4 times for change and only for systemically active substances).

The input parameters of the parking house as a stationary source of air pollution are summarized in the following Table 5.

Table 3

Summary of parameters of stationary source of pollution

	Value	**Unit**
Number of exhausts	3	-
Orientation of exhausts	axial	-
Height of the exhausts above terrain	3.0	m
Exhaust diameter	700	mm
Maximum airflow by one exhaust	8,500	$m^3.h^{-1}$
Flow rate at maximum flow	6.13	$m.s^{-1}$
Total airflow	3x 8 500 = 25 500	$m^3.h^{-1}$
Air temperature	20	°C
The maximum permissible CO concentration	70	$mg.m^{-3}$
The maximum permissible NO_2 concentration	4	$mg.m^{-3}$
The maximum permissible SO_2 concentration	2.7	$mg.m^{-3}$
The maximum permissible PM_{10} concentration	10	$mg.m^{-3}$
The maximum permissible benzene concentration	3.25	$mg.m^{-3}$
Mass flow of pollutants for 1 exhaust		
CO	0.165	$g.s^{-1}$
NO_2	0.009	$g.s^{-1}$
SO_2	0.006	$g.s^{-1}$
PM_{10}	0.024	$g.s^{-1}$
benzene	0.008	$g.s^{-1}$

4. Results

The immission load from the operation of the standard parking house as mobile source of pollution is summarized in the following Table 6. The pollutants were evaluated as CO, NO_2 and benzene and the data express the maximum values of the pollution concentration in the entire computing area.

Table 6

Immission load from the parking house operation - mobile sources of air pollution

Pollutant	**Immission concentration [µg.m^{-3}]**		**Comparison with the limit value for the protection of human health [% of limit]**	
	Average	**Maximum**	**Average**	**Maximum**
CO	-	7.33 (8 h)	-	0.08
NO_2	0.40	0.98 (1 h)	1.00	0.49
benzene	0.13	-	2.60	2.60

From the data presented in Table 6, it is clear that the contribution of the parking house as a mobile source of pollutants is only minimal, at most 2.6 % of the limit value for benzene.

The result of the immission assessment for a parking house as a stationary source of air pollution is documented in Table 7. Pollutants were evaluated in the form of CO, NO_2, SO_2, PM_{10} and benzene.

The calculated values of the immission concentrations are compared and reported as a percentage of the limit value for the protection of human health. These are data of the maximum detected short-term concentrations and average values of immissions in the entire computing area.

Table 7

Immission load from the parking house operation - stationary sources of air pollution

Pollutant	**Immission concentration [µg.m^{-3}]**		**Comparison with the limit value for the protection of human health [% of limit]**	
	Average	**Maximum**	**Average**	**Maximum**
CO	-	687.72 (8h)	-	6.88 %
NO_2	6.35	56.81 (1h)	15.88 %	28.41 %
SO_2	4.24 (1year) 20.08 (24h)	37.88 (1h)	16.06 %	10.82 %
PM_{10}	3.11	20.71 (24h)	7.76 %	41.42 %
benzene	1.25	-	25.00 %	-

From the above-mentioned results it is obvious that the operation of the building of the parking house does not exceed the prescribed health protection limit values for stationary sources.

It is necessary to emphasize that this is a numerical simulation of the most unfavourable variant in terms of the proposal of stationary sources of air pollution, which is described in Chapter 3.5. The highest immission concentrations, especially in the case of maximum short-term concentrations, practically occur in all the pollutants considered only in the immediate vicinity of the building of the parking house, at a distance of approximately 50 to 100 m (this is due to the low height of the exhausts above the terrain and also the low temperature of the exhaust air). At the remote points of the computing area, significantly lower pollutant concentrations can be observed.

5. Conclusion

According to results there is no exceedance of the assessed limit values set in the field of human health protection during the operation of model parking house. The increase of immission concentrations can be considered to be acceptable with respect to the calculated values.

However, the interpreted results of the immission modeling should be seen primarily in the context of the existing pollution of the site (background concentrations), especially with the emphasis on air quality management regions where the immission contribution of the parking house itself should not be negligible and in addition to the existing pollution it is possible to exceed the relevant legislation limits.

The emphasis on the location of a similar building of a parking house should also be placed on the location of the nearest settlement units and public areas, as evidenced by the maximum contribution of the immission concentrations listed in Table 7.

It is also necessary to take into account inverse situations which significantly increase the ground concentration levels of pollutants, which cannot be sufficiently objectively captured by numerical simulation.

In the next period, it will be necessary to focus on research into the exposure of the parking house operating personnel to ototoxic substances. This scientific area has not yet received any closer attention within the Slovak Republic, especially for ototoxic substances in the form of CO, NO_X and benzene, which are provably contained in exhaust gases from combustion engines.

Acknowledgments

The paper is based on work performed under research contract VEGA 1/0377/17 which support is gratefully acknowledged.

References

[1] Drkal, F., „Návrh větrání garáží (II). [online] [cit. 2018-04-22]. Dostupné na internete: < https://vetrani.tzb-info.cz/teorie-a-vypocty-vetrani-klimatizace/4738-navrh-vetrani-garazi-ii>

[2] STN 73 6056: Odstavné a parkovacie plochy cestných vozidiel, Bratislava: SÚTN, 1987.

[3] STN 73 6058. Hromadné garáže. Základné ustanovenia, Bratislava: SÚTN, 1987.

[4] Závodský, D. - Medveď, M. - Ďurec, F. 2001. Chémia atmosféry a modelovanie znečisťovania ovzdušia. Prvé vydanie, Banská Bystrica : Univerzita Mateja Bela, 2001. 126 s. ISBN 80-88784-34-4.

[5] Vyhláška č. 244/2016 Z. z. Ministerstva životného prostredia Slovenskej republiky z 19. augusta 2016 o kvalite ovzdušia

[6] Schwarz, M., Dado, M., Hnilica, R. Ototoxické látky : časť 1, Časopis výzkumu a aplikací v profesionální bezpečnosti, vol. 7, no. 4, 2014.

[7] Schwarz, M., Dado, M., Salva, J., Frič, M., Synergism of noise and ototoxic substances in wood-processing industry, Akustika: odborný časopis o akustice a vibracích, pp. 18-22, 2017.

[8] M. Schwarz, M. Dado and R. Hnilica, Ototoxické látky : časť 2, Časopis výzkumu a aplikací v profesionální bezpečnosti, vol. 7, no. 4, 2014.

[9] Hybská, H., Samešová, D.. Ecotoxicology. Technical University in Zvolen, 2015. - 164 p. ISBN 978-80-228-2750-8

[10] Šuta, M. Účinky výfukových plynů z automobilů na lidské zdraví, Český a Slovenský dopravní klub 1996, ISBN 80-901339-4-0.

[11] Hybská, H. Základy ekotoxikológie. Technická univerzita vo Zvolene, 2015. - 116 s. ISBN 978-80-228-2798-0

[12] Zákon č. 137/2010 Z. z. Národnej rady Slovenskej republiky zo dňa 3. marca 2010 o ovzduší.

[13] Nariadenie Vlády Slovenskej republiky č. 355/2006 Z. z. z 10. mája 2006 o ochrane zamestnancov pred rizikami súvisiacimi s expozíciou chemickým faktorom pri práci

Human thermal comfort in miner’s overalls

Ilya F. Sidakov[a] – Andrei Nikulin[b] – Lyudmila V. Stepanova[b] – Nikulina Anni Yulievna[b]

[a]*Kovcheg-Ural LLC, 29-1 Timiryazeva Str., Chelyabinsk 454091, Russian Federation*

[b]*Saint-Petersburg Mining University, Saint Petersburg, Russian Federation*

Abstract

The article presents the results of the experimental surveys of the thermal conductivity of two types of fabrics used to make special clothes for mine workers (miner's overalls) depending on the degree of clothes contamination with coal dust. Thermographs of the cooling process have been obtained and a thermal conductivity factor has been calculated for each sample. The impact of miner's overall contamination on the miners' thermal comfort has been reviewed.

Keywords: human ressources; Arctic; special clothes; safety; corporate social responsibility coal dust; thermal comfort; fabric thermal conductivity

---

1. Introduction

Jobs at mining companies and particularly in the Arctic climate involve hard work that demands high concentration and stamina. For mining companies to show good performance, management is expected to care for and attend to the needs of their workers. This implies both compliance with necessary basic legal requirements and search for and use of additional methods to ensure occupational health and workplace safety which are part of the corporate responsibility programme. These methods include improvement of special clothes for miners to provide them with thermal comfort.

The main function of human clothes is to maintain the thermal balance between the environment and the human body. This requirement applies both to everyday and special clothes and is essential for work in coal mines due to small confined spaces and high energy input when carrying out work [1,14,20].

The quality of special clothes is assessed by a number of requirements but the main indicator is its thermal insulation capacity that ensures thermal comfort under the clothes [2].

Thermal insulation properties of fabrics have been extensively studied [3,4,16]. These surveys address the overall process of heat transmission from the human body through a special clothes package to the environment and facilitate the calculation of thermal resistance of the clothes package depending on the environment. However the surveys conducted do not take into account the contamination of special clothes in real operational environment. Coal dust contaminates the surface of the miner's overalls and penetrates fabric fibres thus increasing its thermal insulation properties.

Excessive thermal insulation of special clothes impairs mental and physical performance, results in rapid fatigability, reduces mental alertness, and leads to active sweating [5,15]. In this case, a person feels discomfort which may result in partial or complete abandonment of special clothes [18]. The results of the surveys conducted at coal companies in Russia show that 48 % of mine workers fail to use personal protective equipment for short-term activities and 4% of workers do not use personal protective equipment at all [19]. The main reasons for the abandonment of special clothes is the worsening of their protective properties (more than 33 %) and increased temperature and humidity in the workplace (over 60 %) [6]. A failure to wear special clothes results in micro-injuries and purulent skin diseases of various degree up to temporary disability [7].

The main indicator of thermal comfort and an indirect indicator of human thermal condition is the density of a thermal flow from the human body through special clothes to the environment. One of key factors influencing the thermal flow is the thermal conductivity factor of the fabric the miner's overalls are made of [8]. However, a fabric thermal conductivity factor is currently determined for new fabric samples only and its change during real-time use of special clothes is disregarded [9].

Therefore, the survey aims at the experimental assessment of a change in the thermal conductivity factors of the fabrics used in miner's overalls depending on the degree of their contamination with coal dust.

2. Method

Objectives of the experiment:

1. Determine the temperature fields on the surface of studied fabric samples subject to cooling.
2. Calculate a thermal conductivity factor for the samples of the fabric used to make miner's overalls.
3. Identify a correlation between the thermal conductivity factor of fabric samples and fabric contamination with coal dust.

Two fabrics were sampled for the surveys: Gorizont T40 and FAS: the summary of their characteristics is provided in Table 1.

Table 1

Characteristics of Gorizont T40 and FAS

Characteristics	Gorizont T40 fabric	FAS fabric
Density, g/m^2	370	390
Composition	75% cotton and 25% polyester	100% cotton
Particles confinement class	IV	IV

Gorizont T40 is the main fabric used to make miner's overalls in Russia. It meets GOST 12.4.110-82, Miner's Overalls for Protection against Mechanical Impacts and Overall Industrial Contamination [10].

FAS is one of the most popular fabrics used to make special clothes in European countries, including special clothes for the mining industry. It is certified in Russia as per GOST 12.4.142-84, System of Occupational Health and Safety Standards. Fabrics for Special Protective Clothes. Classification of Particles Confinement Norms, and GOST 12.4.110-82, Miner's Overalls for Protection against Mechanical Impacts and Overall Industrial Contamination [11].

The methodology developed at the Industrial Thermal Energy Department of Kosygin Moscow State Textile University (Methodology for the determination of thermal and physical characteristics is based on non-stationary thermal mode methods for the experimental assessment of the thermal properties of materials clothes are made of through regular thermal treatment based on free cooling of a heated sample in a gaseous environment (air)) [12] was used to determine the thermal physical characteristics.

The surveys were conducted in the quality control laboratories of Kovcheg Highly Efficient Home Laboratory company in Chelyabinsk. A laboratory unit is shown in Figure 1.

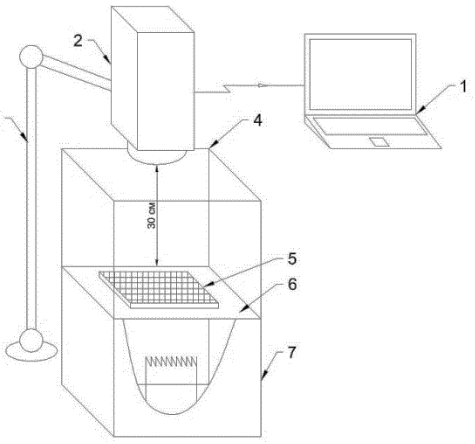

Fig. 1. Thermal vision system to determine the thermal and physical properties for fabrics:
1 – laptop for data processing 2 – FLIR E60 IR chamber; 3 – IR chamber tripod; 4 – protective screen; 5 – fabric sample; 6 – heating surface; 7 – insulated cabinet

Source parameters for the experiment:

- emissivity of a reference object (emissivity factor) – 0.95;
- ambient temperature – 25°C;
- distance between the object and the thermovision chamber – 30 cm;
- relative air humidity – 27%.

Characteristics of FLIR E60 IR chamber:

- a temperature measurement range: -20°C to 650°C;
- detector: uncooled microbolometric matrix, 320x240 elements;
- temperature sensitivity threshold is less than 0.05°C at 30°C;
- temperature measurement error: ±2°C;
- spectral range: 7.5 to 13 μm;
- image sweep frequency: 60 Hz (9 frames per second).

Main experiment stages:

1. Heat a fabric sample on a metal plate to a fixed temperature of 100°C (a smaller fibre deformation temperature).
2. When the temperature field is evenly distributed over the sample surface, disconnect the electric heater (control the uniformity of heating of a studied sample using FLIR E60 IR chamber).

3. Record thermographic images of the sample cooling process at a rate of one frame per second.
4. Replace clean fabric samples by a sample contaminated with coal dust and repeat measurement steps.

Samples were contaminated with coal dust with a particle size of up to 100 µm, which corresponded to the most common values for the production units at Russian mines [13]. Contamination involved the following stages:

- preparation of a white paper sheet sized to match a tested fabric sample;
- weighing of a fabric sample using laboratory scales accurate to 0.01 g;
- a required amount of coal dust was weighed using laboratory scales (+0.05-0.08 g taking into account loss during contamination and depending on a fabric sample size);
- dust was evenly distributed across the white paper sheet with a blade;
- a prepared fabric sample was put with its face down onto the sheet of paper with coal dust and turned with the sheet over;
- a 300 g glass cylinder was used to roll the sheet of paper ten times;
- the sample was turned again, the sheet of paper was separated and re-weighed, and the degree of contamination was determined based on the difference between the weight of a clean and contaminated sample;
- if a required contamination degree was achieved, measurements were started; if required contamination density was not achieved, the above steps were repeated and more coal dust was added if necessary.

3. Results

The experiments yielded thermographic images of the sample cooling process. They were processed in FLIRTools software. Cooling thermographs were built based on the average values across the fabric sample area thus minimising any error due to potentially uneven contamination of the samples (Fig.2).

Once cooling thermographs were received, the thermal conductivity factor was calculated for each sample. The first stage involved the determination of the reflecting power for each sample since the reflecting degree changed depending on the level of fabric contamination with coal dust. Results obtained for each sample were used to build a semilogarithmic cooling chart. A straight section on the curve corresponds to the regular mode. Six points with relevant coordinates were marked on this straight line.

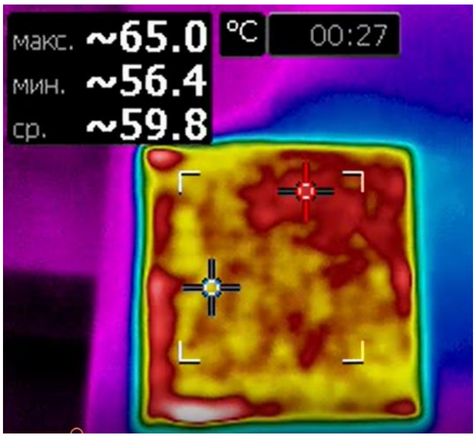

Fig. 2. Processing of sample cooling thermographs in FLIR Tools software.

Then formula 1 was applied to determine a cooling rate for each of the five selected sections and formula 2 was used to find the mean cooling rate for the entire sample.

$$m_n = \frac{\ln v_n - \ln v_{n+1}}{\tau_{n+1} - \tau_n}, \text{c}^{-1} \qquad (1)$$

where,

υ1 is the difference between the temperature in this point and the external environment at time point τ1; υ2 is the difference between the temperature in this point and the external environment at time point τ2.

$$m_{\text{cp}} = \frac{m_1+m_2+m_3+m_4+m_5}{5},\ \text{c}^{-1} \qquad (2)$$

A fabric sample conditionally takes the form of a rectangular block with L1, L2, and L3 edges, therefore a fabric form factor was determined using the following formula (3):

$$K = \frac{1}{\pi^2\left(\frac{1}{L_1}+\frac{1}{L_2}+\frac{1}{L_3}\right)} \qquad (3)$$

where,

L1 is sample width, mm;

L1 is sample length, mm;

L3 is sample height (fabric thickness), mm.

Temperature conductivity was determined using the following formula (4), m^2/s:

$$a = \frac{K - m_{\text{cp}}}{10^6} \qquad (4)$$

The overall density of samples was determined using the following formula (5), kg/m^3:

$$\gamma = \frac{M}{L_3} \qquad (5)$$

where,

M is sample surface density, g/m^2.

A fabric thermal conductivity factor was determined using the following formula (6), W/m·deg:

$$\lambda = a * c * \gamma \qquad (6)$$

where,

c is fabric specific conductivity, kJ/kg deg.

The specific thermal capacity of the samples was calculated as thermal conductivity of an even mixture of substances. Gorizont T40 (75% cotton, 25% polyether) s =1.35 kJ/kg deg; FAS (100% cotton) s=1.3 kJ/kg deg [17].

The results for the calculated thermal conductivity factor of source samples and samples contaminated with coal dust are shown in Fig. 3.

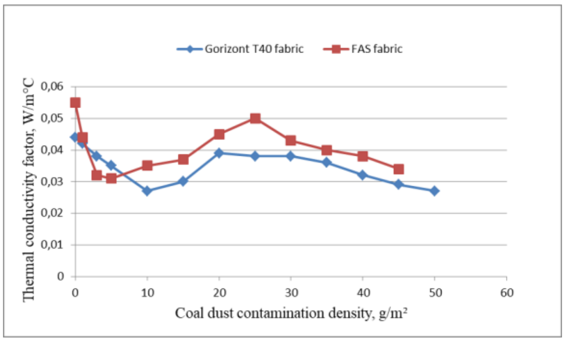

Fig. 3. Correlation between a thermal conductivity factor and degree of contamination with coal dust

4. Discussion

The analysis of obtained results showed that fabric thermal conductivity changed depending on the degree of its contamination with coal dust. Minor contamination results in a reduction of the thermal conductivity factor. Then, with contamination density of 10 to 25 g/m^2, the thermal conductivity factor increases but starts to decrease without achieving source values in proportion to an increase in fabric contamination density.

Heat transfer is facilitated by the thermal conductivity of fibres, air and convection via through pores, radiation of heat by pore walls. Therefore, resulting thermal conductivity factor values characterise material capacity to transmit thermal energy by convection and heat radiation additionally to its thermal conductivity.

We have these results since the fabrics used to make miner's overalls are not homogeneous layers despite their high density, but are systems consisting of many fibres separated by air-filled pores of various forms and sizes. When a fabric is contaminated with coal dust, air is displaced from fabric pores and as air has a low thermal conductivity factor, fabric heat-conducting capacity increases. With more intensive contamination, fabric becomes thicker and its thermal conductivity factor decreases, respectively. Therefore, contamination of miner's overalls with coal dust slows down heat loss by workers and prevents normal evaporation of moisture from the skin surface which affects thermal comfort and leads to full or partial abandonment of miner's overalls in the work process.

Conclusions

1. Mining companies and especially those operating in severe environmental conditions of the Arctic need to focus on the miners' thermal comfort.
2. Contamination of miner's overalls with coal dust results in a reduced heat flow from the human body to the environment which may affect the worker's thermal comfort.
3. When choosing fabrics to make special clothes, including miner's overalls, clothes contamination during use must be taken into account.
4. The use of 100% cotton in miner's overalls, even when they are contaminated with coal dust, brings less thermal discomfort than when a blended fabric is used.

Acknowledgments

The research was funded by the Russian Scientific Foundation, Project No. 17-78-20145, Social and Economic Levers for Mobilizing Human Resources to the Arctic Region of the Russian Federation. Saint-Petersburg Mining University.

References

[1] M. A. Montoliu, V. Gonzalev & L. Palenciano (2007) Cardiac frequency throughout a working shift in coal miners, Ergonomics, 38:6, 1250-1263, DOI: 10.1080/00140139508925186

[2] K. C. Parsons (2007) Protective clothing: heat exchange and physiological objectives, Ergonomics, 31:7,991-1007, DOI: 10.1080/00140138808966738

[3] T.M. Zhigalova About heat and moisture exchange with between humans wearing special clothes and the environment. Text. / T.M. Zhigalova, Z.S. Chubarova, A.A. Zakharova // News of Higher Educaitonal Institutions. Light Industry Technology. 1991. No. 4: pp. 55-60.

[4] L.B. Kazantseva Dependence of the human thermal condition and thermal properties of clothes from air-permeability, length, and type: Author's abstract from Ph.Sci. thesis. M: 1969.

[5] Jiao, Yi Li, Lei Yao, Yajun Chen, Yueping Guo, Stephen H. S. Wong, Frency S. F. Ng & Junyan Hu (2017) Effects of body-mapping-designed clothing on heat stress and running performance in a hot environment,Ergonomics, 60:10, 1435-1444, DOI: 10.1080/00140139.2017.1306630

[6] M.L. Rudakov, L.V. Stepanova Peculiarities of the use of personal protective equipment by employees as protection against industrial contamination and mechanical damage // 3rd International Scientific and Practical Conference on Industrial Safety at Mineral Resources Companies in the 21st Century: scientific conference abstracts/St. Petersburg Mining Univesity. St. Petersburg, 2016. p. 78.

[7] A.F. Dolzhenkov Assessment of wear resistance of special clothes based on a change in purulent disease and micro-injury morbidity in mining workers / A.F. Dolzhenkov, S.L. Tarasenko // Methods and means of creating safe and healthy working conditions in coal mines: collection of academic papers /MacNII: Makeevka, 2013. Issue 2 (32): pp. 198 – 205

[8] R.A. Del, R.F. Afanasyeva et al. Clothes hygiene, Moscow: Legprombytizdat, 1991.160 p.

[9] GOST 12.4.110-82, System of labor safety standards. Miner's overalls for protection against mechanical action and general industrial contaminations. Specifications.

[10] A.F. Davydov Russian working clothes market // Working clothes. 2010. No. 4: p. 12.

[11] Personal protective equipment. Textbook/Team of authors led by Yu.G. Sorokin. Moscow. 2007. 288 p.

[12] S.Yu. Boiko, M.V. Nazarov Research of thermal conductivity of woven fabric depending on its thickness and fibre composition of refined threads // International Journal of Applied and Fundamental Research. 2014. No. 9-2: pp. 11-15; URL: http://applied-research.ru/ru/article/view?id=5821 (accessed on: March 22, 2018).

[13] Batmanov V.P., Barsukov O.K. Laser and optic device to determine dust concentration and distribution of dust particles in the workplace air. Zapiski Gornogo instituta. 2017. Vol. 203, p. 146-149.

[14] Glen P. Kenny, Matthieu Vierula, Joseph Maté, Francois Beaulieu, Stephen G. Hardcastle & Francis Reardon(2012) A Field Evaluation of the Physiological Demands of Miners in Canada's Deep Mechanized Mines,Journal of Occupational and Environmental Hygiene, 9:8, 491-501, DOI: 10 (1080) 154596242012693880

[15] Aude Morel, Gauthier Bedek, Fabien Salaün & Daniel Dupont (2014) A review of heat transfer phenomena and the impact of moisture on firefighters' clothing and protection, Ergonomics, 57:7, 1078-1089, DOI: 10.1080/00140139.2014.907447

[16] S. Lee & S. K. Obendorf (2010) Barrier effectiveness and thermal comfort of protective clothing materials, The Journal of The Textile Institute, 98:2, 87-98, DOI: 10.1533/joti.2005.0143

[17] A.G. Shailkov, G.M. Volokhov, T.N. Abramenko, V.P. Kozlov Methods of determination of thermal conductivity and

temperature conductivity Edited by A.V. Lykov Moscow: Energy. 1973. 336 p.

[18] Kovshov, S., R. Istomin, A. Nikulin and A. Sotiriu, 2014. Industrial injuries appraisal in mines of JSC "SUEK Kuzbass". Advanced Materials Research Volume 1001: 414–420.

[19] Nikulin, A., A.Yu. Nikulina Assessment of occupational health and safety effectiveness at a mining company. Eco. Env. & Cons. 23 (1): 2017; pp. 533-537.

[20] Kazakov B.P., Levin L.Yu., Shalimov A.V., Zaitsev A.V. Development of Energy-Saving Technologies Providing Comfortable Microclimate Conditions for Mining. Zapiski Gornogo instituta. 2017. Vol. 223, p. 116-124. DOI: 10.18454/PMI.2017.1.116

Comparison of the Gross Caloric Value of the Selected Wood Species

Nikoleta Szirmaiová[a*] – Danica Kačíková[a] – Martin Lieskovský[b]

[a]*Faculty of Wood Sciences and Technology, Technical University in Zvolen, T. G. Masaryka 24, 960 53 Zvolen, Slovak Republic*

[b]*Faculty of Forestry, Technical University in Zvolen, T.G. Masaryka 24, 960 53 Zvolen, Slovak Republic*

Abstract

The article deals with the defining of the parameter influencing the ignition and the speed of the fire spreading in the woodland area. The aim of this paper is to experimentally define gross caloric value using the calorimeter IKA C200. The procedures of measurements were carried out according to the STN ISO 1928. Spruce wood and beech wood was used for the experiment. Samples from selected tree species were extracted in the area of Zvolen. Roots, trunks and branches were examined. The representative samples were dried at the temperature 103 ± 2 ° C before the testing to ensure humidity 0 %. The highest gross caloric values were observed with spruce wood branches (21 150 J/g), spruce wood roots (20 939 J/g), and a spruce wood trunk (20 386 J/g). The representative samples of beech wood (root, trunk and branches) showed lower gross caloric values than spruce samples. The results confirm that soft wood (like spruce) shows remarkably higher gross caloric values than hard wood. Based on obtained results, it can be said that spruce wood is easily combustible and shows higher values of gross caloric value and thus more dangerous according to forest fires than beech wood.

Keywords: Beech; Forest fires; Gross caloric value; Spruce

---

* Corresponding author. Tel.: +421 455 206 827; e-mail: xszirmaiova@is.tuzvo.sk

1. Introduction

Slovak Republic is one of the 7 most forested European countries. Wood is the strategic raw material in our economy. Approximately 42 % of the country area is forested and forests are considered to be the most valuable part of the state fortune. The overall yeld of hard wood is 59 % and of soft wood 41 %. The most common are beeches (31 %), spruces (26,3 %), oaks (10,9 %), pines (7,2 %), hornbeams (5,7 %) and firs (4,1 %) [1].

Vast complexes of woods and forests close to residental areas are important part of air regeneration and the oxygen production. They also minimalise harmful effects of pollution and dust. Moreover, diversity and complexity of colours during the season is considered to be aesthetic and relaxing [2].

However, besides positive qualities forest ecosystems bring threat of forest fires. This fact is confirmed by cases from the past years. Climatic and geografic changes create environment inclinable to frest fires. In the past occurred destructive fires caused by lightning strikes or self combustions. However it can not be stated that in general forest fires bring only negative effects. During a forest fire enormous amounts of nutritive substances are freed, what is inevitable requirement for growing and regeneration of various types of wood species. Smoke and heat caused by fire helps the seeds to germ. Nowadays the most forest fires are caused by a people. Especially it is careless using of free flame (grass burning, hiking, camping, smoking). According to these facts forest fires are nowadays considered to be an anthropogenic harmful element or an harmful natural element [3,4].

Not only fire, but also wind is one of the natural elements that can lead to damage of an individual tree, tree groups or vast forests (natural disasters). As a reason of perishing of crown canopy as a consequence of natural disasters microclimatic conditions are changed – more rainfalls, sunlight and heat reach the soil and more intensive exchange of air occurs.

As a consequence of wind throw disaster and fire as well some soil qualities change. Micro topography of the area is changed, elevations and depressions occur, in which organic material, water etc. can be accrue.

Windtrhows as results of strong wind lead to soil-forming process changes (slowing down or fastening of the processes – e. g. organic material changes) or to mixing of the soil horizonts [5,6].

These changes occur mosaically, a forest fire influences full-area and can influence physical, physically-chemical or biological qualities of soils (hydrophobiness, soil structure, volume weight, colour, soil pH, amount and quality of organic material, nutritiens supplies, biomass and retreat of microbial communities etc.) in accordance with burning intensity and the length of fire [7].

In last decades te amount of forest fire increases worldwide. It is assumed nowadays, that approximately 600 000 ha of forests are damaged or destroyed by forest fires [8].

One of the wood advantages is, that when stored properly it preserves its energy content. In first two or three years is the energy content comparatively higher. It is caused by drying of wood. This fact is very important because humidity in wood is released only when burning whereas caloric power lowers. While humid wood burning the burning temperature lowers as well and it leads to abnormal oxidation of all burning elements and it leads to smoking [3,4]. While burning at optimal wood humidity, wood burns almost without smoke and it is easily flammable. During manipulation are no dirts and little ash (approximately 1 % of original weight) which can be used as fertilizers [9,10].

Forestry produces biomass for energy use primarily in form of wood chips. Wood chips were among the first renewable fuels used to substitute fossil fuels, as they are similar to solid fossil fuels in many ways and thermal energy plants can be relatively easily adapted for their use. Wood chips are a product of chipping wood with size up to 120 mm (STN 48 60 0057 2004; STN 48 0058 2004) with varying calorific value, moisture content, bark content, and impurities content [11].

Gross caloric value is an amount of heat that is released during fully burning of weight or volume measure of flammable material in pure oxygen at specific pressure. Water included in flammable material is released in liquid condition.

The aim of this work is to determine and evaluate gross caloric value of some of the most grown wood species in Slovak Republic. For soft woods it is spruce and for hard woods beech. The goal of the experimental part is to set gross caloric value for wood, root and branches on their own.

2. Material and methodology

2.1. Beech (Fagus sylvatica L.*)*

Beech is non-nucleated wood species and false nucleus occurs very often. Beech (*Fagus sylvatica* L.) is the most economically important deciduous wood-species in Central Europe. Red heartwood and its forms are important factors which influence the quality of trunks and products made from them, the pricing of these wood products, and due to its negative effect on quality is responsible for economic losses in silviculture and in the wood processing industry [12]. Root system creates a shape of heart. Young bark is brown or brown-gray and it evolves in light grey rhitydome. Branches are usually angle-wise to trunk. A runk is thin. Leaves are petiolated, egg-shaped or eliptic, very slightly irregularly lobed, almost solid. The age of beech is 200 to 500 years. Beech tree is rarely seen in urban areas because it cannot grow in the atmosphere rich in carbon monoxide.

2.2. Spruce (Picea abies L.*)*

Spruce is the most common and economically important soft wood in our country. Spruce can grow 24 to 30 meters tall and spread 7,5 to 12 meters. Small-diameter branches sweep horizontally from the straight trunk which can grow to four feet thick. Branchlets droop from the branches toward the ground in a graceful, weeping fashion forming a delicate pyramid. Many small-diameter roots originate from the base of the trunk and they are often found fairly close to the surface of the soil. The root system is shallow and often dense, particularly close to the trunk which makes growing grass difficult.

Wood is without visible nucleus and shortly after cutting a zone of adult wood can be seen. The color is white or white-yellow, it gets more yellow in light. Age-bands borders are sharp, thin summer wood gets gently to thick summer wood. Resin canals are small, scattered, can be seen with naked eye only at length wise well trimmed cuts as slight, darker shiny tears. Fir-needles are square spiky and they grow on the whole twig [13].

2.3. Determination of the gross caloric value

Gross caloric value is defined as a heat released by the fully burning (oxidation of active elements of fuel) 1 kg of fuel and cooling of residues of combustions and ash to the initial temperature (20°C).

During forest fires all parts of trees are combustible. Our representative samples are roots, trunk and branches. When setting the gross caloric value 3 measurements were carried for each of the samples. The weight of samples was from 0,63 to 1,23 g.

To determine the gross caloric value IKA C200 oxygen bomb calorimeter (IKA Werke, GmbH&CO.KG, Staufen, Germany) was used. The process of measurements was carried out in accordance with STN ISO 1928: 2003-07: Solid fuels – setting of the gross caloric value by calorimetric method in a pressure vessel and calculation of calorific value [14].

Prior to testing the samples were dried at the temperature 103 ± 2 ° C to reach desired humidity 0% and consequently were kept at desiccator at temperature 20 ± 1 °C during 24 hours. The prepared sample is placed in a loop holder. A cotton fuse is attached to the fuse wire (a standard fixed part of the bomb calorimeter). If the sample material does not burn fully, it must be briquetted. Pressure which ensures the briquette’s compactness is sufficient. If the measured material has very low calorific value, the sample is mixed with benzoic acid. The ratio of individual components corresponds to the expected calorific value of the tested material During testing a weighed sample is burnt in a pressure vessel of calorimeter filled with oxygen at pressure of 3 – 5 MPa. The results show the average value of these measurements.

3. Results and Discussion

Our representative samples are roots, trunk and branches. When setting the gross caloric value 3 measurements were carried for each of the samples. Samples of hard wood (beech) and soft wood (spruce) were compared.

Firstly we interpreted gross caloric value of beech and spruce. The results show the difference between gross caloric value of the roots, trunks and beech branches. The lowest values of spruce wood were measured on the samples of trunk and the highest values were measured on the sample of branches. Graphical representation can be seen in the Tab. 1.

The results seen in Fig. 1 show the difference between approximate gross caloric value of beech and spruce wood.

Spruce samples reached the highest numbers of gross caloric value in branches 21 150 ± 103 (J/g). The second highest numbers occurred in root samples 21 204 ± 500 (J/g) and the lowest measured numbers are in a trunk with results 20 426 ± 90 (J/g).

Beech wood reached the highest gross caloric value numbers in trunk samples 19 845 ± 20 (J/g). The second highest numbers occurred in branches 19 515 ± 10 (J/g). The lowest gross caloric value was measured in beech roots, 19 320 ± 5 (J/g).

Tab. 1

Gross calorific value of selected wood species

Wood species	Gross calorific value J/g								
	Root			Trunk			Branches		
	1.	2.	3.	1.	2.	3.	1.	2.	3.
Beech	17611	19875	20065	19807	19845	19837	19511	19515	19488
Spruce	21204	20938	20675	20332	20426	20401	21246	21051	21154

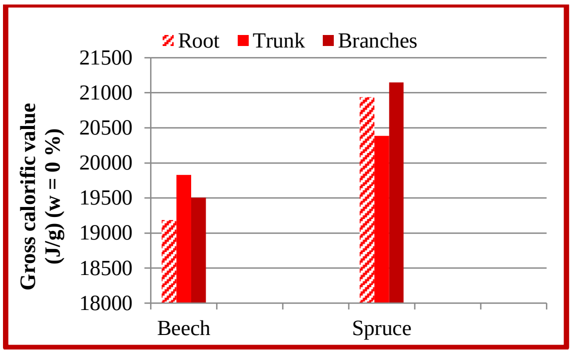

Fig. 1 Gross calorific value (average)

The authors [15,16,17,18,19,20,21,22] were concerned with establishing the gross caloric value of various wood species (soft and hard as well). Their results are comparable with ours and confirm that spruce wood (belonging to soft wood) shows higher gross caloric value numbers than beech wood (hard wood type).

The authors indicate [23,24] that hard wood shows lower gross caloric value (20 J/g) than soft wood (20,5 - 21 J/g). This theory was confirmed in our case as well. The values of gross caloric value of spruce wood (soft wood) are higher than values of hard wood (beech).

Dry wood heating capacity values are approx. 18.7 MJ·kg^{-1} for conifers and 18.4 MJ·kg^{-1} for broadleaf species. These data allow us to assume that it is moisture content, not the respective tree species, which will affect the heating capacity of energy woodchips most significantly. The difference in heating capacities of individual dendromass components or tree species respectively, is to a major extent caused by the existing moisture content in wood [25]

The highest risk is in crown fires but root systems cannot be underestimated as well. Underground fires can cause significant damages since the localization is much more difficult. Because of these facts it is important to pay attention to protection and maintaining of the forest economy.

4. Conclusion

The aim of this experiment was to assest gross caloric value of branches, trunk and roots of chosen wood species at 0 % humidity. According to measurements we can confirm the significant difference between gross caloric value temperatures of chosen tree parts. This finding is important when characterizing of combustible (wood) which burns during forest fires represents a risk of forest fires. Based on obtained results, it can be said that spruce wood is easily combustible and shows higher values of gross caloric value and thus more dangerous according to forest fires than beech wood.

Acknowledgements

This work was supported by the Slovak Research and Development Agency under the contract No. APVV-0057-12 (50 %). This work was supported by the VEGA Agency under the project No. 1/0493/18 (50 %).

References

[1] Possibilities of local heating and electric energy production from biomass. Forest Research Institute, Zvolen:[2018-04-12] http://www.nlcsk.sk/nlc_sk/ustavy/ulzi.aspx

[2] J. Pagan, D. Randuška, Atlas of wood species 1 (Original woody plants). Bratislava: Obzor, 1987. 360 pp. ISBN 65-013-87

[3] M. Stolina et al., Protection of forest. Zvolen: Technická univerzita vo Zvolene, 2000, p. 67-75.

[4] A. Majlingová, Forest fires - The current state of solving problems in the conditions of Slovakia. Crisis Management, 2015 (1): p.47-56.

[5] R. J. Schaetzel, D. L. Johnson, S. F. Burns, T. W. Small, Tree uprooting: review of terminology, process. 1989.

[6] N. G. Ulanova, The effects of windthrow on forests at different spatial scales: a review. For. Ecol. Managem., 135: 2000, p. 155-167

[7] G. Certini, Effects of fire on properties of forest soils: a review. Oecologia 143: 2005, p. 1-10.

[8] J. Albers, Comparative Analysis of the Forest Fire Situation in Central-Eastern Europe. Master thesis. Vienna: Institute of Silviculture, Department of Forest- and Soil Sciences, University of Natural Resources and Life Sciences (BOKU). 2012, 82 pp.

[9] J. Ladomerský, Emission analysis and minimization from the wood waste combustion. Wood Research 45 [4]: 2000, p. 33–44.

[10] J. Martinka, T. Chrebet, I. Hrušovský, K. Balog, Assessment of the impact of heat flux density on the combustion efficiency and fire hazard of spruce pellets. European Journal of Environmental and Safety Sciencis. ESRI. Vol. 1, Issue 1. 2013. ISSN 1339-472X

[11] M. Lieskovský, M. Jankovský, M. Trenčiansky, J. Merganič, J. Dvořák: Ash Content vs. the Economics of Using Wood Chips for Energy: Model Based on Data from Central Europe, BioResources 12(1), 1579-1592. ISSN 1930-2126

[12] M. Trenčiansky , M. Lieskovský , J. Merganič , R. Šulek, Analysis and evaluation of the impact of stand age on the occurrence and metamorphosis of red heartwood. In iForest_ms16_2116, doi: 10.3832/ifor2116-010
http://www.sisef.it/iforest/contents/?id=ifor2116-010

[13] E. F. Gilman, D. G. Watson, Fact Sheet ST-448, a series of the Environmental Horticulture Department, Florida Cooperative Extension Service, Institute of Food and Agricultural Sciences, University of Florida. 1994

[14] STN ISO 1928:2003-07. Solid fuels. Determination of gross caloric value and calculation of heating value.

[15] L. Núñez-Regueira, J.A. Rodríguez-Aon, J. Proupín-Castieiras, A. Vilanova-Diz, N. Montero-Santovea, Determination of calorific values of forest waste biomass by static bomb calorimetry. In: Thermochimica Acta 371 (1-2), 2001. p. 23-3.

[16] A. Friedl, E. Padouvas, H. Rotter, K. Varmuza, Prediction of heating values of biomass fuel from elemental composition. In: Analytica Chimica Acta 544 (1-2), p. 191-198.

[17] M.Erol, H. Haykiri-Acma, S. Kücükbayrak, Calorific value estimation of biomass from their proximate analyses data. In: Renewable Energy 35 (1), 2010. p. 170-173.

[18] C.D. Everard, K.P. McDonnell, C.C. Fagan, Prediction of biomass gross calorific values using visible and near infrared spectroscopy. In: Biomass and Bioenergy 45, 2012. p. 203-211.

[19] E. Orémusová, Ľ. Tereňová, R. Réh, Evaluation of the gross and net calorific value of the selected wood species. Advanced materials research. Environmental and safety aspects of renewable materials and energy sources. Vol. 1001 (2014), p. 292-299.

[20] M. Aniszewska, A. Gendek, Comparison of heat of combustion and calorific value of the cones and wood of selected forest trees species. Leśne Prace Badawcze. 2014, Vol. 75 (3): p. 231–236.

[21] E. Orémusová, L. Makovická Osvaldová, A. Osvald, Gross calorific value of leaves, bark, and branches of selected deciduous trees. Transactions of the VSB - Technical University of Ostrava, Safety Engineering Series (TSES). Vol. VII, No. 1, 2012. p. 32 – 36. ISSN 1805-3238.

[22] F. Kačík, J. Ďurkovič, D. Kačíková, Chemical Profiles of Wood Components of Poplar Clones for Their Energy Utilization. In Energies. 2012. Vol. 5 (12). p. 5243 – 5256. doi:10.3390/en5125243

[23] D. Fengel, G. Wegener. Wood chemistry ultrastructure reactions. Walter de gruyter, Berlin and New York: 1984

[24] Wood handbook. Wood as an engineering material. Gen. Tech. Rep. FPL-GTR-113. 1999, 463 pp.

[25] M. Lieskovský [et al.], Analysis of woodchip heating capacity calculated according to technical standards and measurements of calorific value - APVV-SK-CZ-0194-11 ; 7AMB12SK015. - SCOPUS. In Journal of forest science. - ISSN 1212-4834. - Vol. 60, no. 11 (2014), p. 451-455. (2014).

Reaction to fire of façade heat insulating materials

Ľudmila Tereňová[a] – Emília Orémusová[b]*

Department of Fire Protection, Faculty of Wood Sciences and Technology, Technical university in Zvolen, T. G. Masaryka 24, 960 53 Zvolen, Slovak Republic

Abstract

Nowadays the most important requirements for construction of buildings are energy economics and heat saving. The market offers many thermal insulation materials used in the external thermal insulation composite systems of buildings which also need to comply with the requirements of the fire safety. In the paper are evaluated two samples of the insulation cork boards and boards from the expanded polystyrene (EPS) from the point of view of the reaction to fire. The reaction to fire is the basic coefficient of their possible use in the external thermal insulation composite systems of renewed buildings. For both thermal insulation materials were used the testing method for evaluation of ignitability according to the standard STN EN 11925-2 and for the determination of the gross calorific value according to the standard STN EN 1716. Based on the results of the test of ignition were both materials ranked in the class of reaction to fire E. With the expanded polystyrene EPS sample appeared extensive deformation of shape. Higher or in other words less favourable values of the gross calorific value were detected with the samples from EPS. Cork insulation boards reached from the overall evaluation of their reaction to fire more favourable results than the boards from the expanded polystyrene. The cork boards had better results also in the regard of the gross calorific value evaluation. The average rate of the gross calorific value of two different cork boards in the reference state i.e. considering actual humidity varied from 25 711 J/g to 29 248 J/g. Meanwhile, the EPS samples had markedly higher average rates of gross calorific value namely from 40 673 J/g to 40 839 J/g.

Keywords: reaction to fire, cork boards, expanded polystyrene, ignitability, gross calorific value, external thermal insulation composite systems

---

[*] Ing. Ľudmila Tereňová, PhD. Tel.: +421 455 206 828; e-mail: ludmila.terenova@tuzvo.sk
Ing. Emília Orémusová, PhD. Tel.: +421 455 206 820; e-mail: emilia.oremusova@tuzvo.sk

1. Introduction

The most widely used thermal insulation materials in the market of the external thermal insulation composite systems (ETICS) are mineral wool and expanded polystyrene. The mineral wool thermal insulation composite system corresponds to the class $A2_{s1,d0}$ and second one on the basis of polystyrene to the class $B_{s1,d0}$. This classification directly affects usage of the materials with the regard to the fire height of the building and the thickness of the thermal insulation layer.

The external thermal insulation composite systems with the flammable thermal insulation such as expanded polystyrene EPS then naturally pose a higher risk of fire spreading in the thermal insulation system and consequently also through the facade of a building. Therefore, it is very important to deal with mentioned materials and examine their fire-technical characteristics. One of the flammable materials, which is currently used in the constructions of thermal insulation composite systems of buildings, is cork. However, current manufacturers of the cork insulation materials do not have clearly stated their class of reaction to fire. Only a few of them declare fire class E but mostly they state fire class B2 according to the German standards. We have chosen to compare these materials on the basis of results of the ignition test according to the standard STN EN 11925-2 [1] and at the same time gross calorific value test according to the standard STN EN 1716 [2], which are among the European test methods used to classify materials into the classes of reaction to fire.

2. Experimental part

Two sorts of insulation materials were subjected to testing: cork board (facade and insulating) and expanded polystyrene (EPS and Perimeter). These are flammable materials in practice classified into the class of reaction to fire E in terms of classification standard STN EN 13 501-1 + A1/O1 [3]. The experiments were carried out at the testing laboratory of the Department of Fire Protection at the Faculty of Wood Sciences and Technology of the Technical University in Zvolen, Slovakia.

2. 1 Tested material

Facade cork board (Fig. 1) is made out of the natural insulation material from selected cork bark which is compressed by exposure to the high temperature of the water vapour without the usage of any bonding materials other than its own resin. Expansion reduces bulk density, reduces absorption (0-3%) and improves thermal insulation capacity. It is free of expanding ingredients. Then it is processed and cut to the required measure and weight.

Fig. 1 Facade cork board

It is used as system tested diffusion insulation board for external thermal insulation (according to ETAG 004) and it is designed for older buildings as well as for new buildings. The boards are attached to the base either by adhesive on the basis of cement or mechanically with connecting elements. The bulk density is 100 - 120 kg / m^3according to standard EN 1015-10. The coefficient of thermal conductivity at the temperature of 23 ° C and 50% of relative air humidity is 0.056 W/m.K. Concerning the content or release of dangerous substances, according to the manufacturer's data, the insulation boards do not contain dangerous substances [4].

Insulation cord board (Fig. 2) is an expanded cork board which has remarkable anti-vibration properties for its elasticity. It is made out of cork pulp linked permanently by elastic bonds on the basis of resin. Thanks to the high content of waxes contained in the wood pulp structure it retains long-term technical stability.

Fig. 2 Insulating cork board

In the building industry, the antivibration insulation is used under industrial machines and devices, under road girders, on top of the bridge dilatations, rail tracks and into floor structures in civil, residential and industrial buildings. In households is damping down of oscillations and vibrations useful for people suffering from rheumatism and sore joints. The bulk density varies from 170 to 255 kg / m^3, depending on the recommended compressive stress. Depending on the bulk density, the thermal conductivity coefficient is at 20° C degrees 0.047-0.052 W / m.K [4].

Expanded polystyrene (Fig. 3)

Polystyrene EPS EPS 70 F (Polyform) samples of the thickness 10 and 50 mm were made from expanded polystyrene. Another sample from expanded polystyrene was the new type of EPS 200 with increased solidity made also from recycled parts of the thickness 30 mm. This type of polystyrene we can find in our market under the name Perimeter (Polyform).

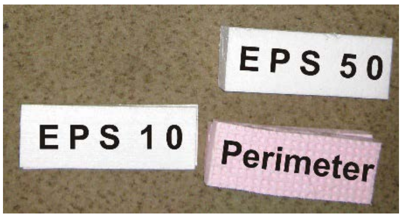

Fig. 3 Expanded polystyrene

Polystyrene EPS 70 F has the optimal use for thermal insulation of the external thermal insulation composite systems. The coefficient of thermal conductivity is λ = max. 0.038 W / m.K and bulk density ranges between 14 and 18 kg / m^3[5].

EPS 200 Perimeter is designed for thermal insulation of building constructions that reach the ground, especially for thermal insulation of constructions of the depth from 3 to 6 m. The coefficient of thermal conductivity is λ = max. 0.032 W / m.K, bulk density ranges between 29 and 32 kg / m^3. It has lined surface for faster and more precise division [5].

2. 2 Testing methods

Test of ignition

The testing procedure is defined according to the standard STN EN 11925-2 [1]. The testing method is determining ignition of the construction products subjected to the direct exposure of guided single torch flame burning under the conditions of zero added radiation using samples tested in a vertical orientation. During this test of a small flame, the samples are tested also in the area of surface and edge of the sample. The testing time determined by the regulation is 15 or 30 seconds according to the requirements of the test requester.

In the course of the testing the following attributes are observed:

- if the sample ignites after application of flame and ignition time,
- in a case, that sample ignites, if the flame is expanding by more than 150 mm in the vertical direction from the point of flame attachment,
- the time when this limit is reached and in a case of short-term burning is this time recorded,
- the time of the forced sample spraying and the behaviour of the sample in the case of ignition,
- whether the filter paper located at the bottom of the testing device is ignited,
- weight loss of samples.

All tested samples were tested in the surface area only, both cork boards of 3 pieces of samples and samples from the expanded polystyrene of just 2 pieces of samples, although the test standard prescribes at least 6 representative samples. The samples had prescribed dimensions of 250 x 90 mm (height x width). When the thickness is less than or equals to 60 mm the samples are tested using their actual thickness, as in our case. The flame application time specified for the classification of the material in the class of reaction to fire E according to the standard STN EN 13 501-1 + A1 / O1 [3] is 15 seconds. In a case that the sample ignites during this time, the flame spread must not exceed the borderline of 150 mm. The overall duration of the test is 20 seconds from the moment when the application of flame begins.

In order to be able to register the changes and differences appearing on the samples resulting from flame application, the samples of cork boards were tested also within the time frame of 30 seconds, that is the time determined by the standard for the classification into the class D and also a non-standard time of 300 seconds. All tested samples of the expanded polystyrene were exposed to the application of fire for the duration of 15 seconds. Before each measurement, the flame attachment border line was marked 40 mm above the lower edge of the sample. After weighing, the tested samples were fastened to the holder that was inserted into the combustion chamber. During the testing on the surface area of the sample the flame was applied to the axis of the sample. After the ignition of the flame torch, the desired flame height was set to 20 mm ±0,1 mm using the flame height measuring device. In the horizontal direction the flame torch (at the angle of 45°) was shifted to the sample. At the moment, when the flame of the torch reached the sample the digital stopwatch started to measure the time. After the determined time of flame application expired the troch was pulled away and the required parameters were monitored. The test was performed in the room under standard laboratory conditions. The testing device is shown in the Fig. 4.

Fig. 4 Testing device according to STN EN 11925-2 [1]

Test of the gross calorific value

The gross calorific value was set in a full-automatic IKA C 5000 control calorimeter in an adiabatic working mode in terms of the STN ISO 1716 [2] designated for the construction products and manual of the device [6]. The basis of determining the gross calorific value lies in the total burning of the sample in a calorimetric pressure vessel in the oxygen under the pressure of 3 MPa, in measuring of the water temperature increase in the calorimetric vessel and in determining corrections to heat. When the measuring has finished the software of the device calculates automatically the rate of gross calorific value according to the formula:

$$H_0 = \frac{C.\Delta T - Qz}{m} \qquad (1)$$

where:

H_O - rate of gross calorific value in the reference state of analytic humidity [J/g],

C - heat capacity of the calorimeter [J/°C],

ΔT - increase of the temperature in the device during the combustion experiment [°C],

Qz - excessive ignition energy [J],

m - mass of the combusted substance [g].

3. Evaluation of the results

In the following subchapters, the results of both tested materials will be shown in the form of tables, figures and graphs.

3.1. The cork boards ignition testing results

Facade cork board

During the testing of the flame application on the area of the surface no ignition occurred in none of the tested samples, just on the sample number two a clear flame appeared, which after pulling the torch away immediately went out. On the samples and the spaces where the flame was applied appeared only black areas without any deformation, that means, there was no reason why even the ignition of the filter paper did not occur. In the Fig. 5 is shown the sample of the facade cork board during the testing. Recorded results: weight loss in grams Δm, percentage weight loss M, ignition (yes/no) are shown in the tab. 1. The differences in the results were manifested in weight loss, which naturally increased with longer flame duration. During the time of 15 seconds of fire application the average weight loss was measured of only 0.15 g (0.11%), during the time of 30 seconds the average weight loss was increased to 0.25 g (0.17%) and the average weight loss that occurred during the time of 300 seconds was 0,52 g (0,34 %).

Insulating cork board

In the Tab. 2 are recorded results from the testing of insulating cork board that was tested on the surface of the sample. While with the facade cork board no ignition was recorded in any of the six samples, three spontaneous combustions were observed in the samples of insulating cork board that were tested on the surface of the sample. In the 5minute test, no burning was observed, just in the contact area with flame appeared smoked spots, but there were no hollows due to flame exposure. During the time of 15 seconds of fire application the average weight loss occurred of 0,22 g (0,1 %), during the time of 30 seconds the average weight loss was increased just to the value of 0.25 g (0.17%) and the average weight loss that occurred during the time of 300 seconds was 0,52 g (0,34 %). In the Fig. 6 is pictured sample of insulation cork board in the course of testing.

The main result of the cork boards testing with a single flame source performed according to the standard EN 11252 [1] is that on none of the tested samples flame did not reach the border 150 mm within the given time and also none of the samples caused ignition of the filter paper, which means, that the classification criteria were met for the categorization into the class of reaction to fire E in terms of STN EN 13 501-1 + A1/O1 [3]. While we mutually compare the weight loss results of both tested samples, during all the tested times (15 s, 30 s, 300 s) when measuring was done on the surface of the sample the bigger weight loss was recorded in the insulating cork board than in the facade cork board.

Tab. 1 The testing results of the facade cork board

Samples of facade cork board									
Time	15 s			30 s			300 s		
Sample number	1	2	3	4	5	6	7	8	9
Weight loss Δ *m*(g)	0,13	0,18	0,14	0,34	0,23	0,19	0,56	0,44	0,57
Percentage decrease *M* (%)	0,09	0,13	0,1	0,23	0,16	0,12	0,38	0,3	0,33
Ignition (yes/no)	no	no	no	no	no	no	no	no	no

Tab. 2 Testing results of the insulating cork board

Samples of the insulating cork board									
Time	15 s			30 s			5 min		
Sample number	1	2	3	4	5	6	7	8	9
Weight lossΔ*m*(g)	0,2	0,15	0,31	0,26	0,24	0,26	0,53	0,79	0,62
Percentage decrease *M*(%)	0,09	0,07	0,15	0,12	0,12	0,12	0,26	0,39	0,31
Ignition (yes/no)	no	yes	no	yes	yes	no	no	no	no

Tab. 3 Testing results of the expanded polystyrene EPS

Type of the expanded polystyrene	Sample marking	m_1(g)	m_2(g)	Δm(g)	M (%)	Spontaneous combustion of the sample	Reaching of border line 150 mm	Ignition of filter paper
EPS 70 F	EPS_50 1	14,38	14,38	0	0	no	in the 10th second	no
EPS 70 F	EPS_50 2	14,41	14,41	0	0	no	in the 10th second	no
EPS 200	Perimeter 1	21,94	21,94	0	0	no	no	no
EPS 200	Perimeter 2	22,62	22,62	0	0	no	no	no

Fig. 5 Facade cork board in the course of testing

Fig. 6 Insulating cork board in the course of testing (ignition of the sample with the bright flame)

3.2. *The results of the ignition testing of the expanded polystyrene EPS*

The following test results were recorded during the measurements: sample weight before the testingm_1, sample weight after the testingm_2, weight loss Δm, percentage weight loss M, spontaneous combustion of the sample (yes, no), time for reaching the border line of 150 mm and ignition of the filter paper (yes, no), that are stated in the tab. 3. In the Fig. 7 and Fig. 8 is the documented behaviour of individual samples during testing. For samples of expanded polystyrene EPS 70 F, that has special retardation treatment, no spontaneous combustion occurred during the determined time which was set by the standard (Figure 7). Likewise, the EPS 200 Perimeter has reached good results, although in practice it is mainly used for thermal insulation of structures that are in contact with the ground. Its positive result is that the resulting deformation did not reach the border line of 150 mm in the time of thermal stress for 15 seconds (Fig. 8). In none of the tested samples of the expanded polystyrene occurred the ignition of the filter paper during the testing.

Fig. 7 Sample EPS 70 F during the testing
(reaching of the border line of the 150 mmm without spontaneous combustion)

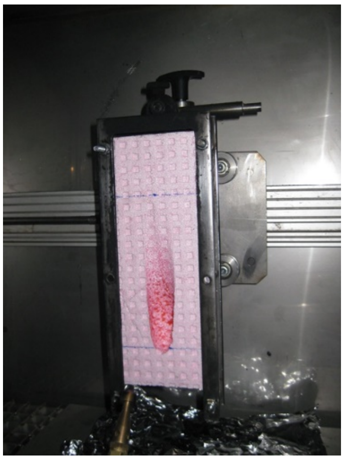

Fig. 8 Samples EPS 200 Perimeter in the course of the testing
(sample after the pulling away of flame without spontaneous combustion)

3.3. Testing results of the gross calorific value of cork boards

The results of average rates of the gross calorific value are displayed graphically in the Fig. 9. Each material was measured on the basis of three samples. The gross calorific values of all individual tested samples are shown in the graph for the reference samples, i.e. at their actual moisture content determined after drying of the samples in the oven dryer at (103 ± 2) ° C: EPS 200 and EPS 70 F - humidity 0.45%, CO-F - humidity 2.86%, CO-I - Humidity 4, 85%.

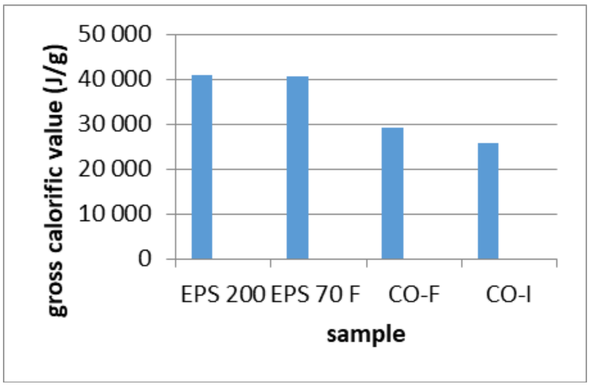

Fig. 9 Gross calorific value of polystyrene and cork boards

The gross calorific value represents the maximal amount of heat per unit of weight, that the material is able to release during the complete combustion in the oxygen when the water is produced in the liquid state. The results show that considerable higher values of the gross calorific value reached the EPS samples in the average of 40 756 J / g, while the difference between the individual types of polystyrene boards was only 166 J / g. The higher value of 40 839 J / g was reached by the sample EPS 200, EPS 70F had the value of 40 673 J / g. Fricke [7] is stating the gross calorific value of the polystyrene 40,000 J / g, Walters et al. [8] 41 960 J / g.

The cork boards reached in average the rate of the gross calorific value of 27 479 J/g. The differences in results were more differentiated between the individual types of cork boards. Higher gross calorific value rate of 29 248 J/g was reached by facade board CO-F despite the higher value of ash - 1,22 %, while the insulation cork board CO-I had average gross calorific value rate of 25 711 J/g and of ash 0,53 %. Mateus et al. [9] and [10] state the value of the cork waste of 21.6 MJ / kg, but at the humidity of 20%.

Conclusion

When we want to compare cork boards and expanded polystyrene from the ignition point of view according to STN EN 11925-2 [1], the overall result, that is, the categorization in the reaction class of fire E has come out the same. In relation to their use in the external thermal insulation composite systems, both materials can be used for additional thermal insulation of facades up to fire height of 22.5 m. However, the specific behaviour of both materials during the testing was different. There was no ignition and no visible deformations observed on the samples of the facade cork board even with prolonged times of flame application. In comparison with the results of EPS, significant deformations have already occurred even in the initial flame application on the samples. Different results of the tested EPS and cork materials mainly resulted from their totally different origin and composition. Regarding to the inconsistency and ambiguity in stating of the reaction to fire of cork boards from the side of manufacturers, therefore our intention is to test this material thoroughly according to STN EN 13823 [11].

The testing results of gross calorific value have shown that considerably higher values were reached by EPS samples. The gross calorific value of cork boards was much lower, therefore, more favourable values. The cork boards generally achieved a much better result by both testing methods. By comparing these materials, we wanted to point out that with the same classification into the class of reaction to fire, different materials can behave differently and may have a different effect on the possibility of spreading the fire in the thermal insulation system.

Acknowledgments

"This paper was supported by the grant agency of MŠVVaŠ SR KEGA, no. of the project 009TU Z-4/2017 (50%) and VEGA, no. of the project 1/0493/18 (50%) ".

References

[1] STN EN 11925-2: 2011 Skúšky reakcie na oheň. Zápalnosť stavebných výrobkov vystavených priamemu pôsobeniu plameňového horenia. Časť 2: Skúška jednoplameňovým zdrojom.
[2] STN ISO 1716: 2003 Skúšky reakcie stavebných výrobkov na oheň. Stanovenie spalného tepla.
[3] STN EN 13 501-1+A1/O1: 2012 Klasifikácia požiarnych charakteristík stavebných výrobkov a prvkov stavieb. Časť 1: Klasifikácia využívajúca údaje zo skúšok reakcie na oheň (Konsolidovaný text)
[4] JELINEKCORKGROUP: *Technický list korok-fasádna izolačná doska, 2012.*
[5] Polyform, s.r.o. Expandovaný polystyrén (EPS). Tepelné a zvukové izolácie. [online]. 2015, [cit.2015.04.08]. Dostupné na internete: http://www.polyform.sk/sk/eps-technicke-informacie
[6] IKA. 2007. IKA. Calorimeter system C 5000 control/ C 5000 duo-control: Operating Instructions. [online]. [cit. 2011-12-08]. Dostupné na internete: <http://www.ika.com/ika/product_art/manual/ika_c_5000_englisch.pdf>
[7] Fricke, K. et.al. 2009. Stoffliche oder Energetische Verwertung – Ressourceneffizientes
[8] Walters, R.N. – Hackett, S.M. – Lyon, R.E. 2001. Heats of Combustion of hith Temperature Polymers. New Jersey : Galaxy Scientific Corporation, 2001. 13 s.
[9] Mateus, M.M - Bordado Rui, J.C. - Santos, G. Potential biofuel from liquefied cork – Higher heating value comparison. ELSEVIER. Volume 174, 2016, pages 114-117, ISSN: 0016-2361
[10] E. World Conference on Biomass for, Industry, S. Kyritsis, EnergiaTa, Wip, 1st World Conference on Biomass for Energy and Industry: proceedings of the conference held in Sevilla, Spain, 5–9 June 2000, James & James, London.
[11] STN EN 13823: 2011 Skúšky reakcie stavebných výrobkov na oheň. Stavebné výrobky okrem podlahových krytín vystavené pôsobeniu osamelo horiaceho predmetu

Earth in a Trap? 2018
Analytical Methods in Fire and Environmental Science

Effective Prevention of Hazardous Waste Industrial Dusts

Ivana Tureková[a] – Eva Mračková[b*]

[a]*Constantine the Philosopher University in Nitra, Tr. A. Hlinku 1, 949 74 Nitra, Slovakia*

[b]*Technical University in Zvolen, Masaryka 24, 960 53 Zvolen, Slovakia*

Abstract

Development of new technologies along with the use of new materials also requires new approaches to risk assessment. In practice, it means that by processing new materials, particular types of waste with characteristics involving environmental, as well as health and safety risks emerge. This paper deals with technologies related to the occurrence of abrasive dusts from processing of plastics related to the environmental protection, health protection of workers and explosion protection. These seemingly different fields require common and complex approach to protection solutions. It is proven that only by testing of dust characteristics and by determining their most significant hazards which have shown to be explosion characteristics as well, it is possible to suggest effective technological measures.

Key words: dust clouds; plastic; hazard; safety characteristics

---

[*] Corresponding author. Tel.: +0-420-4552-06831 ; fax: +0-420-4553-21811 ; e-mail: mrackova@tuzvo.sk.

1. Introduction

Industry 4.0 is the name for the current trend of automation and data exchange in manufacturing technologies. It includes cyber-physical systems, the Internet of things, cloud computing [1] [2] [3] [4] and cognitive computing. Industry 4.0 is commonly referred to as the fourth industrial revolution [5], which also significantly relates to the Slovak automotive industry.

New technologies bring new materials and hazards necessitate new assessment of hazards. Abrasive processes from plastics and composites with the help of CNC machinery lead to the occurrence of dust matters which might be explosive [6].

Dust belongs to the most common injurants to which humans are exposed to in ordinary life as well as at their work activities. The scope of harmful effects of dust on humans is very broad. Their assessment depends on the origin, characteristics and size of the dust particles, its concentration in the air, the length and conditions of its action and the individual sensitivity to dust. In this matter, there is extensive legislation which encompasses legislation on the working environment, the external environment as well as indoor living spaces [7].

Therefore, it is an essential prerequisite to know the materials used for work as well as the physical and chemical properties along with safety characteristics which also predict health and environmental properties of waste.

2. Industrial dust hazards

From a health point of view, industrial dust is a polydisperse solid aerosol created by human activity during the mechanical processing of solid materials [8]. The size of dust particles is 1 to 100 μm, the particles larger than 30 μm are referred to as coarse dust and they sediment rapidly. The size of particles is determined by the actual or aerodynamic diameter. Particles larger than 10 μm are settled in close proximity to the source site after a few minutes of their origin (or re-emergence). Therefore, particles smaller than 10 μm predominate in contaminated air. Particles with the size of 1 μm settle only very slowly and particles smaller than 0,1 μm almost do not settle at all [9], [10].

Depending on the external conditions, dusts act bimodally, they can burn and they may also have explosive properties in the whirled state [11]. Dust explosions in the industry might arise from many sources of initiation including friction and burning or smouldering materials [12].

In general, all types of dust are harmful and can cause serious health problems. Particles smaller than 10 μm are especially dangerous for humans as they can penetrate deep into the airways and by inhaling of air they get into the lung alveoli. For measurements in practice, it is functional to divide dust into two size fractions (i.e. components) – respirable and non-respirable [13].

While the larger particles (above 10 μm) can only cause upper respiratory irritation with coughing and sneezing and irritation of ocular conjunctivas, smaller particles can enter lower airways and particles of below pod 2,5 μm can permeate into lung passages and either settle in lungs or penetrate into the blood stream. Based on this aspect, the dust indicator can be divided into:

- Total Suspended Particle – TSP,
- Particles smaller than 10 μm (Particle Matter – PM10),
- Particles smaller than 2.5 μm (PM 2.5) [14].

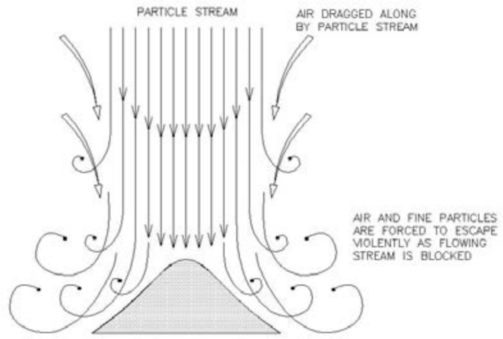

Figure 1 Example of dust generation during powder handling [16]

The mechanisms that generate dust and keep it suspended in air arise from aerodynamic forces [15]. Any dust that is generated can be carried away to another place as a result of air currents. Ventilation air flows or air streams generated during material drops act on fines in the material (dust), and separate them from the main stream, Figure 1. Thus, even if dust generation may occur at one location, dust problems may be experienced at another location, away from the source [16].

In terms of explosion hazard, combustible dust is comprised of small solid particles in the air that settle down by their own weight or might remain suspended in the air for some time. In general, particle size is defined by two dimensions smaller than 500 µm [17].

With particles of mean size larger than 400 µm, most dusts can no longer be initiated by standard energy. However, an addition of 5 to 10 % by weight of fine dust particles with a mean particle size of approximately 40 µm and the mixture can again become explosive. It is important to bear in mind that when handling dust, larger particles become smaller as a result of abrasion [18].

Risk management is a decision-making process that is based on the result of the risk assessment and aims to reduce risk while:

- an objective assessment of the safety risk of dust explosion is a thorough method encompassing identification of all hazards, the probability of their occurrence and severity of their potential consequences,
- health risk assessment is a process of assessing the probability and severity of a harmful effect on humans resulting from an exposure to a risk factor under defined conditions and from defined sources of risk consisting of hazard identification, exposure assessment, dose and effect relationship assessment and the characterization of the risk assessment uncertainties [19].

The first step is to determine the predisposition of equipment and technology to explosion of the equipment and consequently, take precautions to avoid the explosion (Figure 2).

Depending on the level of danger that potential explosions threaten, additional steps may be needed to safeguard nearby equipment and personnel from unlikely, yet calamitous, explosions that transpire in spite of preventive techniques [20].

The dust and its suspending atmosphere must exhibit several characteristics. If any of the following fire conditions is not present, a dust-cloud explosion cannot occur:

- the dust must be combustible,
- the oxygen content of the surrounding atmosphere must be sufficient to sustain combustion,
- the dust concentration must be within the upper and lower explosion limits,
- the particle-size distribution must be capable of supporting energy,
- an ignition source of sufficient energy must be present to initiate explosion [17], [18].

3. Materials and methods

The industrial dust sample was made of a composite plastic material in combination with resin. As this was an industrial environment, the representative sample was taken from several locations at the CNC 5-axis machining plant, type MX 5, used not only for machining of plastics but also composites. The machining area was secured by continuous suction into a single central suction system. The filter elements were cleaned by compressed air.

3.1. Sieve analysis of dust sample

The sieve analysis is a fractional or separation technique of particle size analysis. It is based on the use of a set of sieves with a particular size of openings which is assembled in the direction of gravitational transfer of the analysed matter into the block with a gradually decreasing size of openings. After completion of fractionation, each sieve contains a particular portion of the original sample within the ranges determined by the size of the upper and lower sieve openings. The residues on the sieves are then weighed and evaluated. The sieve analysis was carried out on a RETSCH AS 200 in accordance with STN ISO 3310-1: 2007-03 (25 9610). Coarse

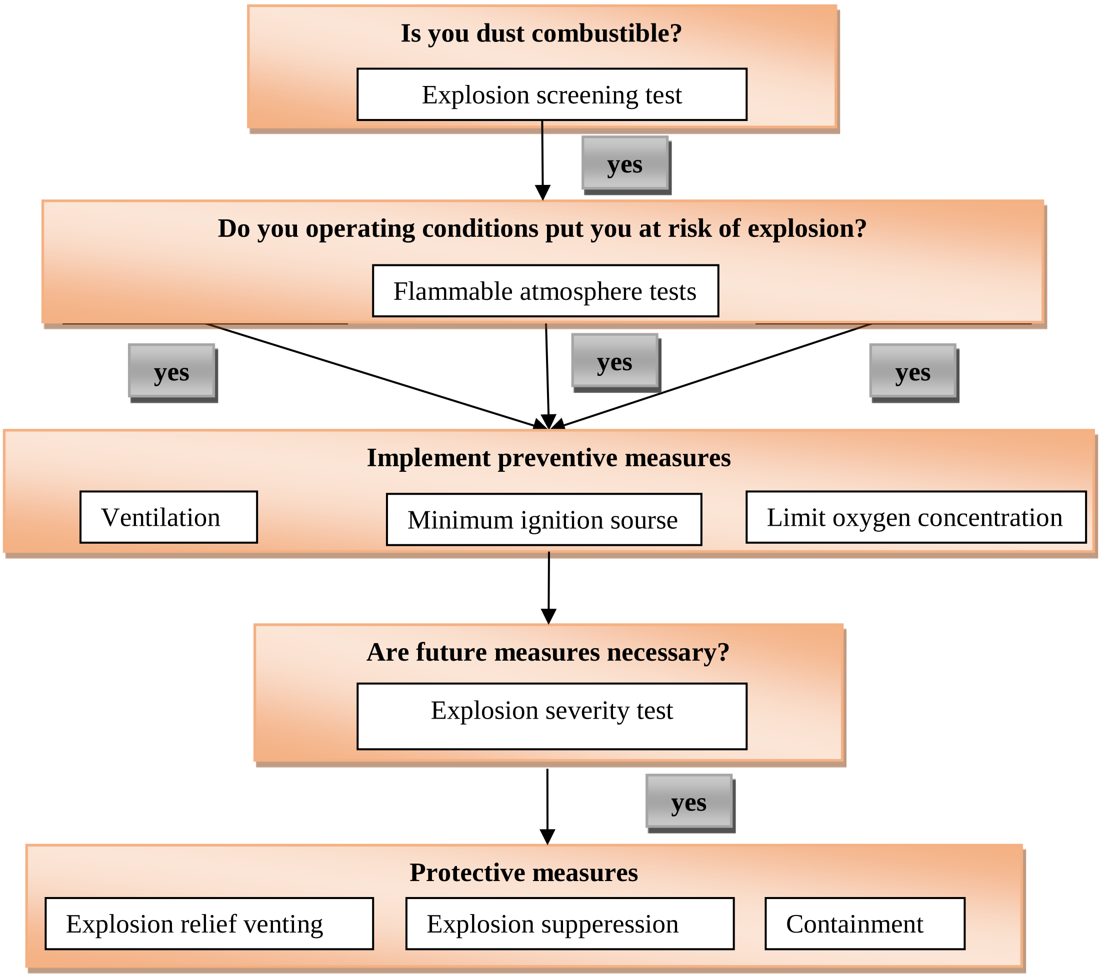

Figure 2 Procedure for applying preventive measures [19]

impurities were removed by fraction separation of < 0,400 mm, using a sieve set of openings between 0,040 mm and 0,400 mm. Once sieve analysis was completed, the analytical balance (KERN PLT 450-3M) was used to measure the weight of each sieve fraction which gave us information about the percentages of the particles present in the analysed sample [21].

3.2. Thermal analysis of dust sample

Thermogravimetry (TG) and differential scanning calorimetry (DSC) were used. These are analytical methods as the weight of analysed samples is in milligrams. These methods find application in observations and comparisons of thermal decomposition of matter and in the observation of the changes of conditions of the course of chemical reactions.

Thermogravimetry (TG) studies the course of thermolysis and polymer burning and records the changes in the weight of the heated sample.

Differential scanning calorimetry provides information on endothermic and exothermic processes during the controlled thermal decomposition.

By means of differential scanning calorimetry, the reaction heat dissolution temperature of the test sample was identified in the temperature interval of 35 – 600 °C in a dynamic air atmosphere.

3.3. Combustible dust characteristics

With regard to the fire and explosion prevention, the following parameters can be considered as dust safety characteristics:

- lower explosive limit (LEL),
- maximum explosion pressure p_{max},
- maximum rate of pressure rise (dp/dt)max,
- explosion constant K_{St}.

The cubic constant allows assessment of the effects of the explosion in the given closed vessel and is the basis for classification of dust explosion according to classes St 1, St 2 and St 3 (Table 1).

Table 1

The industrial dust explosion classes based on KST value [22]

Explosion class	**K_{st} (bar.m.s^{-1})**
St 1	≤ 200
St 2	200 – 300
St 3	> 30

The Kst value is calculated from the Cubic law according to a defined relationship between (dp /dt) max and the volume (V) in which the explosion occurs:

$$K_{st} = (dp/dt)_{max} \,.\, V^{1/3} \qquad (1)$$

Where:

K_{st} - cubic constant for the mixture of dust and air (bar.m.s^{-1})

$(dp/dt)_{max}$ - maximum rate of pressure rise (bar.s^{-1})

V - volume of the cubic container (m^3)

Determination of these characteristics, with the exception of the cubic constant, is not yet possible; therefore the most reliable results are determined experimentally as well as for the needs of the practice, in the accredited laboratory. If the matter composition is known, we can roughly determine these characteristics, for instance from tables. In real practice, in cases of new materials and their changes, these characteristics must be determined to ensure the correct design of the suction equipment [23].

4. Results

4.1. Results of the sieve analysis

The results of the sieve analysis of the dust particles smaller than > 0,400 mm show that their weight representation is 93,8 %. The average size of dust subjected to the sieve analysis was (0,049 ± 0,01) mm. This uncertainty is standard expanded uncertainty, corresponding to 95% confidence level.

4.2. Results of thermal analysis - Thermogravimetry (TG)

The sample was stabilized for 24 hours under standard conditions; the test was carried out on a Mettler TA 3000 with TC 10A processor and TG 50 thermogravimetric weights module in the air and flow rate of 200 ml.min^{-1}.

The thermogravimetric analysis was performed in the heat interval of 35 – 600 °C and based on the results of the measurement in the dynamic atmosphere, the individual degrees of decomposition and corresponding resistant residuals of the analysed test samples were defined. The results of measurements are shown in the Figure 3 and Table 2.

The thermal decomposition of the industrial dust took place in two stages. The active dust decomposition phase was conducted at 510 °C. Thus, it can be noted that the amount of dust sample that was not subject to degradation in the first stage of

Table 2

Temperature characterization of individual degrees of decomposition of industrial dust sample by TG analysis [15]

Sample weight	Degrees of decomposition	Heat interval (°C)	Weight loss (%)	T_{max} (°C)	Resistant C (%)
10.095 mg	I. degree	139 - 407	22.40	350	75.93
	II. degree	407 - 584	34.41	511	41.52
Residual weight			0.175 mg		

Note: For temperature calibration, materials with given Curie temperatures were used: Isatherm (144.5 °C), Nickel (357.0 °C), a Trafoperm (748.0 °C).
Accuracy of test equipment was determined from calibrations: (-2.4 to + 8.2) %

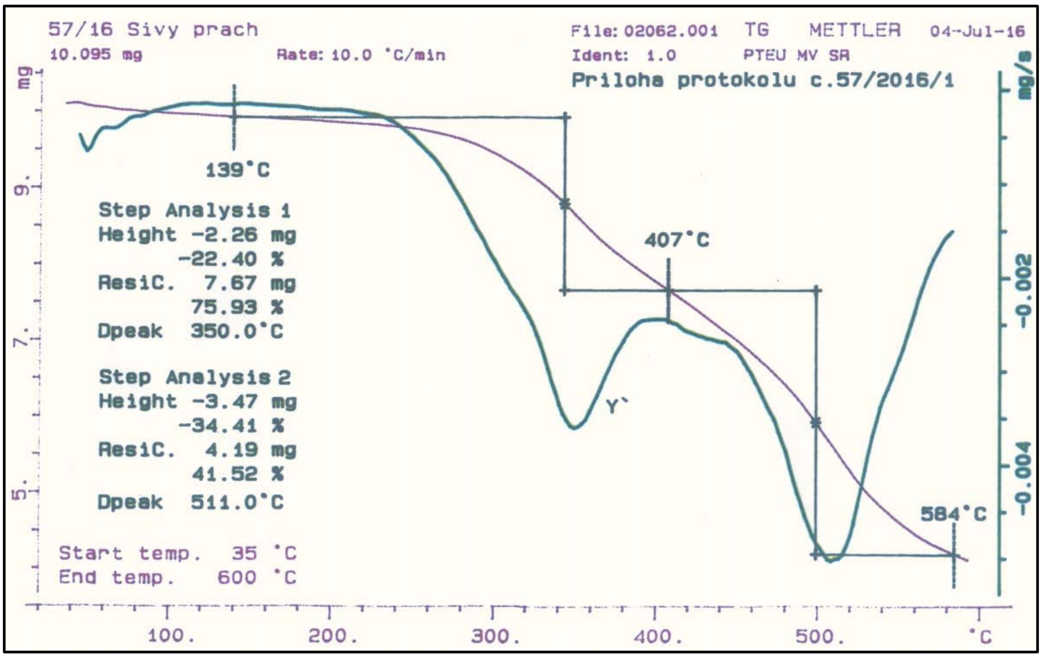

Figure 3 TG a DTG analysis of the industrial dust

Table 3

Dependence of changes in reaction enthalpy of industrial dust samples on temperature

Sample, bank sample	Heat interval (°C)	Change of reaction enthalpy ($J.g^{-1}$)	Maximum peak temperature (°C)
Industrial dust	190 - 458	3997.9 (exo)	435.9
4.560 mg	458 -596	5175.0 (exo)	537.2

thermal decomposition was decomposed in the second stage at much higher temperatures where the highest weight loss was recorded.

4.3. Results of thermal analysis - DSC results

The DSC method was used to measure changes in the reaction enthalpy of the fuel forming and thermal generation processes in thermal decomposition of dust.

In the chosen interval of exothermic reactions, the reaction heat was determined and the maximum heat generation rate was characterized by the maximum exothermic peak temperature on the thermal analytic curve in the temperature range of 35 – 600 °C in a dynamic air atmosphere (Table 3).

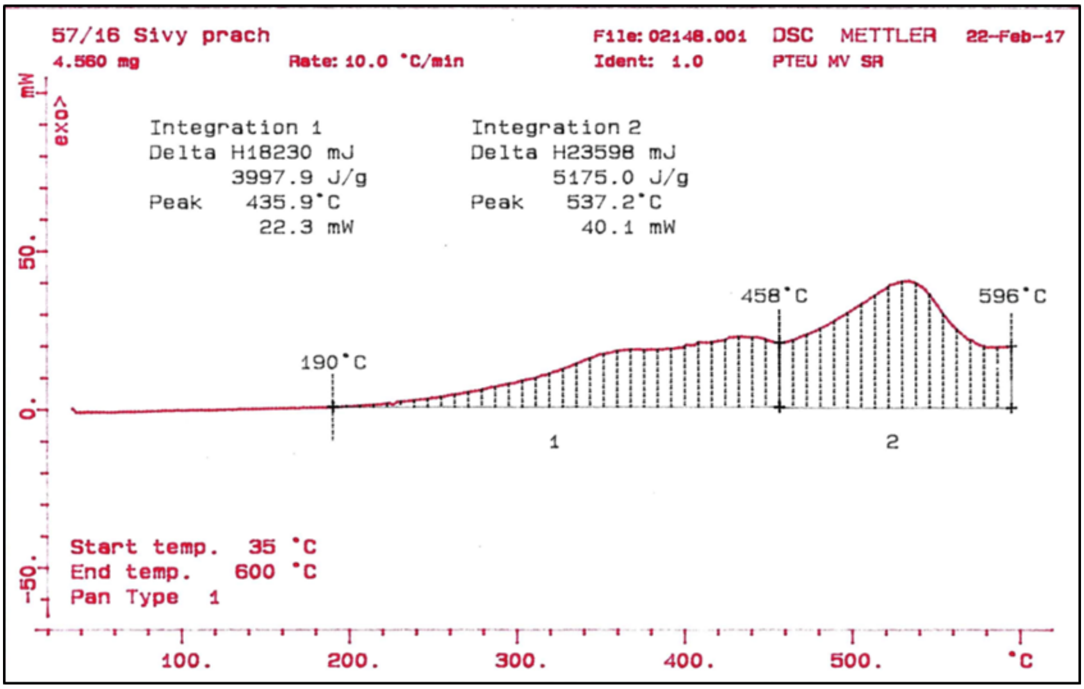

Figure 4 DSC analysis of industrial dust

In the chosen interval of exothermic reactions, the reaction heat was determined and the maximum heat generation rate was characterized by the maximum exothermic peak temperature on the thermal analytic curve in the temperature range of 35 – 600 °C in a dynamic air atmosphere (Table 3).

By the use of DSC, temperature intervals of the exothermic reaction were observed, the course of the reaction enthalpy during heating without endothermic reactions is shown in Figure 4.

The reaction enthalpy changes determined by this means are not consistent with enthalpy measurements in a calorimetric bomb, but provide substantial information about the heat release in thermal degradation process and allow us to collect information about the thermal colour reactions in the individual degrees of thermal decomposition of the test sample.

4.4. Results of safety characteristics

The explosion characteristics of industrial dust are shown in Table 4, including comparisons of similar industrial dusts. In terms of explosion class, industrial dust sample is classified as explosion class 1.

Table 4

Explosive characteristics of industrial dusts

Type of dust	LEL (g.m^{-3})	p_{max} (bar)	$(dp/dt)_{max}$ (bar.s$^{-1)}$)	K_{st} (bar.m.s$^{-1)}$)	Explosion class
Industrial dust	**20**	**5.9**	**213**	**58.0**	**St 1**
Polyester dust	-	9,3	-	237.0	St 2
Black coal	70	9	147	120.0	St 1
Toner	40	9.1	255	164.0	St 1

5. Discussion

The average particle size of 0,049 mm points out the fact that particles can settle, but it is important to ensure that there is no excessive accumulation of a dust pile and no explosive concentration is reached, especially by primary or secondary dust leakage from equipment.

- Primary dust leakage can be caused by opening of equipment which is a part of a routine technological process, i.e. opening due to filling or removing of the material but also from all open places from which dust can escape the equipment. Premises of CNC machinery and storage containers of filter units are the most critical.
- Secondary leakages, on the other hand, represent occasional opening for the purpose of taking samples, control, e.g. changing of the filter cartridges on filter units, maintenance and repairs of equipment in case of breakdowns, cleaning and control openings in pipelines.

The results acquired by testing should be implemented in the form of technical measures using engineering instruments into real technology or supplemented with further testing.

- provide sufficient suction from the grinding process,
- prevent the formation of continuous layers of dust with thickness greater than 1mm by suitable cleaning regime,
- the operational filter unit must be designed for suction of combustible dusts and dimensioned to the explosion characteristics of the collected dust,
- the filter unit and pipping must withstand maximum explosion pressure in accordance with STN EN 14460 [24], alternatively, explosion-proofing equipment or explosion suppression equipment must be installed,
- separating explosion on the supply line from the filters must be ensured (to prevent the transmission of an explosion through pipeline to operator crew,
- develop explosion protocol.

The results from TG and DSC methods demonstrate that industrial dust releases sufficient energy and is, therefore a suitable waste to be used for energy recovery by combustion. However, it is important to acquire enough information about the actual amount of generated waste, the exact chemical composition of the product of thermal combustion (including dust captured from the filter) and propose the mode of transport, i.e. pre-treatment by e.g. tableting.

Dustiness in the workplace, caused by dust generation, has detrimental effects on the human organism [25] and represents one of the basic problems in the field of occupational safety and health at the workplace. In terms of health risk, a more detailed analysis of the operation with the aim of particle PM 2.5 and PM10 particle capture in the operator's respiratory zone and to assess the length of exposure at the workplace.

6. Conclusion

This article pointed out the fact that new technologies bring new risks, whether safety, environmental or health. Creation of new components brings waste which cannot be just classified as waste but needs to be assigned a catalogue number since it can cause an explosive atmosphere in the form of dust and, in the form of respirable fractions it also exhibits negative effect on human´s health in case of long-term exposure. In particular, in the CNC machining process, all available testing techniques must be used to obtain the necessary information for the design of suitable suction technologies, in this case suction system suitable for potential explosive atmospheres.

Acknowledgments

This paper was supported by the Cultural and Educational Grant Agency of the Ministry of Education, Science, Research and sport of the Slovak Republic on the basis of the project no. KEGA 009TUZ-4/2017.

References

[1] P. Minet, I. Khoufi, A. Laouiti. (2017) Increasing reliability of a TSCH network for the industry 4.0, Network Computing and Applications (NCA) 2017 IEEE 16th International Symposium on, pp. 1-10, 2017.

[2] J. Jasperneite. (2012) Was hinter Begriffen wie Industrie 4.0 stecktin Computer & Automation. https://www.computer-automation.de/steuerungsebene/steuern-regeln/artikel/93559/0/

[3] H. Kagermann. W. Wahlster and J. Helbig, eds. (2013) Recommendations for implementing the strategic initiative Industrie 4.0: Final report of the Industrie 4.0 Working Group

[4] H. Lasi, H. G. Kemper, P. Fettke, T. Feld, M. Hoffmann: Industry 4.0. In: Business & Information Systems Engineering 4 (6), pp. 239-242

[5] B. Marr. (2018) Why Everyone Must Get Ready For The 4th Industrial Revolution. Forbes. Retrieved 2018-02-14.

[6] R. Komanduri, D. A. Lucca, Y. Tani, (1997). Technological advances in fine abrasive processes. CIRP Annals, 46(2), 545-596.

[7] B. Lighty, J. Slama, J. M. Veranth, and A. F. Sarofim. (2000) Combustion aerosols: factors governing their size and composition and implications to human health. Journal of the Air & Waste Management Association 50.9 (2000): 1565-1618.

[8] A. Očkajová, I. Marková. (2016) Particle size analysis of selected wood dust species particles generated in the wood working environment. In: Acta Universitatis Matthiae Belii : sekcia Environmentálne manažérstvo. - ISSN 1338-4430. - Roč. 18, č. 2 (2016), pp. 15-23.

[9] A. Paulíková. (2011) Prašnosť pracovného prostredia. TZB portál. http://www.tzbportal.sk/kurenie-voda-plyn/prasnost-pracovneho-prostredia.html

[10] E. Mračková, (2006) Výbušnosť drevného prachu: (smrek, buk, dub, topoľ, drevotriesková doska). 1. Vyd. Zvolen: Technická univerzita, 91 s. ISBN 80-228-1698-1

[11] M. Hudáková, I. Coneva, K. Hollá. (2016) Hodnotenie environmentálnych rizík vyplývajúcich z emisií horenia pri požiaroch v budovách. In. Krízový manažment – 1/2016, 15. ročník. Žilinská univerzita v Žiline, Fakulta bezpečnostného inžinierstva. s. 26-34. ISSN 1336-0019.

[12] I. Tureková (2008) Význam požiarnotechnických vlastností potravinárskych prachov v praxi. In: Manažérstvo životného prostredia 2008. Žilina : Strix et VeV, 2008, s. 161-166. ISBN 978-80-89281-34-3.

[13] I. Tureková, E. Mračková. (2016) The dimensional characteristics of the particles of wood dust of selected deciduous trees considering to explosion. In: Key Engineering Materials : 11th International Symposium on Selected Processes at the Wood Processing, 2015; Dudince; Slovakia; 9 September 2015 through 11 September 2015. - ISBN 978-303835569-4. - ISSN 1013-9826. - Vol. 688, sp. iss (2016), p. 182-189.

[14] R. R. Sayers, (1938) Harmful industrial dusts. Public Health Reports (1896-1970), 217-228.

[15] J. H. S. Lee, F. Zhang, R. Knystautas. (1992) Propagation mechanisms of combustion waves in dust-air mixtures. Powder Technology, 71(2), 153-162.

[16] J. Khambekar, B. H. Pittenger. (2013) Understanding and preventing metal-dust hazards. International Journal of Powder Metallurgy. Volume 49, Issue 4, pp. 39 – 47.

[17] ČSN EN 14034-1+A1 (2011) Stanovení výbuchových charakteristik rozvířeného prachu: Část 1: Stanovení maximálního výbuchového tlaku pmax rozvířeného prachu. Praha: Úřad pro technickou normalizaci, metrologii a státní zkušebnictví, 2011.

[18] J. Damec. (1998) Protivýbuchová prevence. 1. vyd. V Ostravě: Sdružení požárního a bezpečnostního inženýrství, 1998, 188 s. Spektrum (Sdružení požárního a bezpečnostního inženýrství). ISBN 80-86111-21-0.

[19] Lele, Damodar Vishnu. “Risk Assessment: A Neglected Tool for Health, Safety, and Environment Management.” Indian Journal of Occupational and Environmental Medicine 16.2 (2012): 57–58. PMC. Web. 24 Apr. 2018.

[20] F. Kadri, B. Birregah, E. Châtelet. (2014) The impact of natural disasters on critical infrastructures: a domino effect-based study. Journal of Homeland Security and Emergency Management, 11(2), 217-241.

[21] R. M. Harrison, J. Yin. (2000) Particulate matter in the atmosphere: which particle properties are important for its effects on health?. Science of the total environment, 249(1-3), 85-101.

[22] V. Ebadat. (2010) Dust explosion hazard assessment. Journal of loss prevention in the process industries, 23(6), 907-912.

[23] I. Tureková, Z. Szabová, T. Chrebet, I. Kasalová. 2013). Determination of Inductive Ignition Period and Activation Energy of Food Dust. Advanced Materials Research. - ISSN 1022-6680(P). - Vol. 750-752, pp. 1860-1863.

[24] STN EN 14460: (2006) Explosion resistant equipment.

[25] P. Štroch. (2010) Procesy hoření a výbuchů. Žilina : EDIS - vydavateľstvo ŽU, 2010 156 stran : ilustrace. ISBN: 978-80-554-0187-4

METAL flammable dust as dangerous substances

Miroslava Vandlíčková[a]

[a]University of Žilina, Faculty of Security Engineering, 1st May Street 32, 010 01, Žilina, Slovak Republic

---

Abstract

A number of industrial technologies are accompanied by the presence of flammable metal dust, which can occur in the seated or whirled state. From the point of view of occupational safety, their fire-technical characteristics, their impact on workers' health and the environment must be taken into account. This article deals with the properties of chosen flammable industrial metal dusts, especially from the point of view of fire safety, anti-explosion protection and environmental risk. The group of toxicological properties of metallic dusts is also included in the article as mankind is also an inseparable part of the environment. The conclusion of this article deals with preventive measures to prevent fire and explosion of such flammable metal dusts as effectively as possible, and also to prevent acute and chronic diseases caused by human exposure to metal dust in factories or at another possible space.

Keywords: metal; flammable dust; environmental hazard; fire; explosion; occupational safety; dangerous substances

---

1. Introduction

An explosion of dust can be defined as a rapid combustion of fine particles suspended in the air, particularly in an enclosed location. It can appear where any dispersed powdered combustible material (flour, sugar, cinnamon, wood, cellulose, coal, zinc, magnesium, aluminum, titanium, etc.) is present in high enough concentrations in the atmosphere. Flammable dust can be defined as a set of pulverized particles of the solid substance which exist in the gassy environment. These dust particles have the dimensions lower than 0,5 mm. Dusts as products in the branch of industry arise in the process aimed, for example, at food production, or can arise as secondary raw materials at the solid substance processing. [1] The metal dusts can be generated by the activities like grinding, sawing, cutting, sanding or brushing. The combustible metal dusts present extra risks and hazards to workplaces, and setting up tandards to mitigate those risks is crucial to ensuring the safety of a location. [2] But still combustible dust is a topic that remain on the periphery of fire safety in many industry areas in spite the fact that the consequences of such fires and explosions can have a catastrophic impact on material values, technology and, of course, workers' health and lives. That is why it is important to know the biological, environmental, physical, chemical and fire - technical properties of the industry metal dust it has been working with. Finer particles burn readily when their ignition point is reached, and tend to ignite the coarser particles as well. Examples of potential sources of ignition are open flames, welding equipment and cutting torches, matches, and cigarettes, faulty electrical equipment and static electrical discharges. Such conditions must be avoided in areas where dust producing operations are carried out. [3]

The mechanisms that generate dust and keep it suspended in the air arise from aerodynamic forces. Any dust that is generated can get carried away to another place as a result of air currents. Ventilation air flows or air streams generated during material drops act on fines in the material (the dust), and separate them from the main stream as it is possible to see at Figure 1. Thus, even if dust generation may occur a tone location, dust problems can be experienced at another location, away from the source. [4]

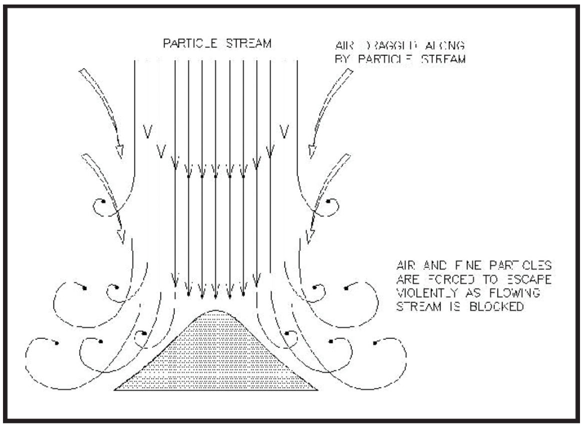

Fig. 1. Example of dust generation during powder handling. [4]

2. Properties and fire – technical characteristics of particular combustible metal dust

Metal dusts have many similar chemical and physical properties, but still some of them are depending on the particular metal.. In the Figure 2 it is possible to see, for example, various colour of metal dust at their burning. Some of them are used e.g. in pyrotechnics and fireworks.

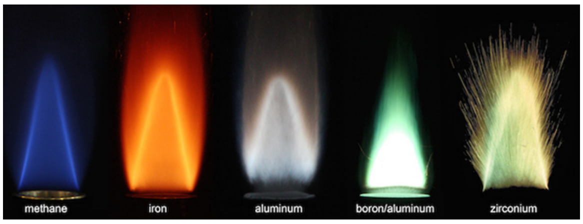

Fig. 2. Chemical properties of metal dusts - colours of particular metal dusts [5]

In general, combustible metals are more prone to ignition and produce a faster burn, with higher peak pressures than the other combustible dusts. Resulting deflagrations and explosions can be much more violent and special precautions must be taken.

Aluminum, magnesium, and titanium are by far the most common combustible metals. [6]

In order to cause explosion of flammable dust, the following elements are present at the same time: flammable dust, ignition source, oxygen (air), dispersion of flammable dust particles and their occurrence in a closed space (e.g. in a container, etc.).

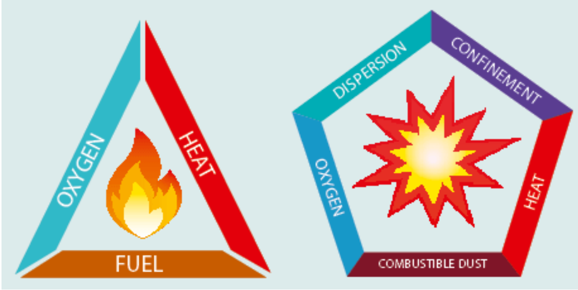

Fig. 3 Fire triangle and explosion pentagon [7]

Experimental examinations can provide information on many basic fire - technical characteristics of dust, among which we list, for example, lower explosive limit, maximum explosion pressure, maximum rate of pressure increasing, deflagration index K_{St}, maximum explosive pressure, minimum ignition energy, ignition temperature of the settled dust, ignition temperature of the whirled dust, limiting oxygen content, minimum explosible concentration, etc.

Deflagration index is the maximum rate of pressure increasing, maximum explosive pressure means the highest pressure created by a dust explosion in an enclosed vessel. The lowest concentration of dust required for the combustion is known as minimum explosible concentration. Minimum ignition temperature is value of the lowest temperature which is able to ignite a dust cloud or dust layers on a hot surface. Minimum ignition energy is the lowest energy electric spark required to ignite a dust cloud and the lowest percent oxygen concentration that can support combustion of a dust is limiting oxygen concentration. [8].

For a large number of flammable dusts, these fire - technical characteristics can be found in tables or literature. However, it should be remembered that these values are of the character of intervals, therefore they should be understood just as approximate values. The safety parameters of flammable dusts depend on the specific technology and handling of the substance (metalworking, energetics, woodworking, waste processing, etc.) [9]. For example it is possible to see burning and explosion behavior and properties of nanotitanium in the next Figure 4

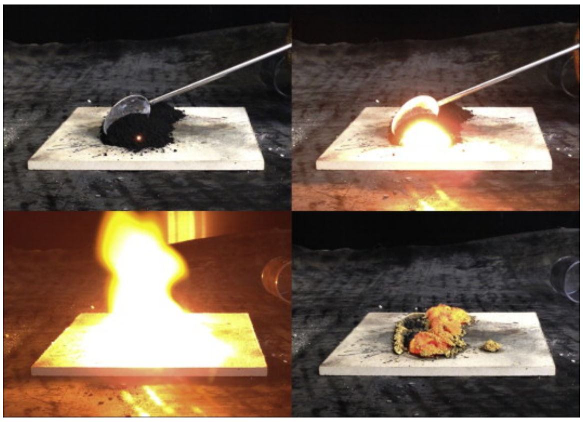

Fig. 4. Burning and explosion behavior of nanotitanium [10]

In metal working and recycling operations, processing machines such as cutting tools or metal shredders constantly generate heat and often sparks, which can cause ignition. Even in the absence of sparks, the dust can spontaneously ignite if the temperature of the dust or a surface reaches the dust’s minimum ignition temperature. While this is true for all combustible materials, the risk of fire and explosions is higher with metal dusts because the processes that generate metal dusts are more likely to create conditions leading to self-ignition. Even with a wet dust collection system, a water-based cooling emulsion could react with the metal dust and generate hydrogen, which has a very low ignition energy and could lead to self-ignition. Metals and metal dusts have a much higher energy content than organic materials. This leads to a very long burning time and a higher burning temperature. Also, a regular extinguishing agent such as water or sodium bicarbonate can’t be used for a metal dust fire because it could generate chemical reactions with the metal and actually accelerate combustion. Only a Class D extinguishing agent is effective. However, even a Class D extinguishing agent can only keep a metal fire under control; it can't completely extinguish the flame because the heat is too great. [11] Experimentally obtained values of explosibility of many metal dusts according to Jacobson, Cooper and Nagy are seen in the Table 1. [12]

The lungs are protected by a series of defense mechanisms in different regions of the respiratory tract. When a person breathes in, particles suspended in the air enter the nose, but not all of them reach the lungs. The nose is an efficient filter. Most large particles are stopped in it, until they are removed mechanically by blowing the nose or sneezing. Some of the smaller particles succeed in passing through the nose to reach the windpipe and the dividing air tubes that lead to the lungs. These tubes are called bronchi and bronchioles. All of these airways are lined by cells. The mucus they produce catches most of the dust particles. [13] Dust generally is able to cause a damage to the lungs and the respiratory system, but some types can cause cancer, too. Major diseases associated with inhalation of hazardous dust are, for example, benign pneumoconiosis which means the disease caused by inhalation of seemingly harmless dust that settle in the lungs to such extent that it is visible in X-ray examination. The dust does not cause damage to the lung tissue and therefore the disease does not lead to a disability or to a serious health damage. Such condition is most commonly associated with metal dust such as iron and tin. Pneumonitis, or inflammation of lung tissues or bronchioles, is caused mainly by the inhalation of dust of certain metals. Symptoms are similar to pneumonia, but vary in severity, depending on the fact which metal is inhaled. This disease is most often caused by the cadmium and beryllium dust. [14]

Table 1

Experimentally obtaine values of explosibility of metal dusts according to Jacobson, Cooper and Nagy [12]

Material	Ignition temperature [°C]		Minimum explosive concentration [oz/cu ft]	Minimum ignition energy for dust cloud [mJ]	Maximum pressure [PSIG]	Maximum rate of pressure rise [PSI/s]	Index of explosibility
	Cloud	Layer					
Aluminum, atomized	650	760	0,045	50	73	20 000+	>10
Aluminum-magnesium alloy	430	480	0,02	80	86	10000	>10
Magnesium	620	490	0,04	40	90	9000	>10
Thorium hydride	260	20	0,08	3	60	6500	>10
Zirconium	20	190	0,045	15	55	6500	>10
Uranium hydride	20	20	0,06	5	43	6500	>10
Titanium	330	510	0,045	25	70	5500	>10
Uranium	20	100	0,06	45	53	3400	>10
Thorium	270	280	0,075	5	48	3300	>10
Titanium hydride	480	540	0,07	60	96	12000	6
Zirconium hydride	350	270	0,085	60	69	9000	3,7
Aluminum-silicon alloy	670	/	0,04	60	74	7500	3,6
Calcium silicide	540	540	0,06	150	73	13000	2
Iron, carbonyl	320	310	0,105	20	41	2400	1,6
Ferrotitanum	370	400	0,14	80	53	9500	1,3

Boron	470	400	<100	60	90	2400	0,8
Aluminum-nickel alloy	950	540	0,19	80	79	10000	0,6
Aluminum-lithium alloy	470	400	<100	140	96	3700	0,6
Aluminum-cobalt alloy	950	570	0,18	100	78	8500	0,4
Ferromanganese	450	290	0,13	80	47	4200	0,4
Aluminum-copper aaloy	/	830	0,1	100	68	2600	0,3
Chromium	580	400	0,23	140	55	4000	0,1
Manganese	460	240	0,125	305	48	2800	0,1
Tantalum	630	300	<200	120	50	2600	0,1
Tin	630	430	0,19	80	37	1300	0,1
Zirconium alloy	420	340	/	30	43	300	/
Aluminum-iron alloy	870	750	/	720	62	1800	/
Zinc	680	460	0,5	960	48	1800	<0,1
Gold-bronze	370	190	1	/	44	1300	/
Ferrosilicon	860	/	0,425	400	50	700	<0,1
Vanadium	500	490	0,22	60	48	600	<0,1
Antimony	420	330	0,42	1 920	8	100	<0,1
Cadmium	570	250	/	4000	7	100	/
Iron ore, pyrite	420	/	/	/	/	/	/
Ferrovanadium	440	400	1,3	400	/	/	<0,1
Ferrochromium	790	670	2	/	/	/	/
Lead	710	270	/	/	/	/	<< 0,1
Manganese ore (sulfide)	320	300	/	/	/	/	<< 0,1
Tellurium	550	340	/	/	/	/	<< 0,1
Nickel ore (sulfide)	/	340	/	/	/	/	<< 0,1
Molybdenum	720	360	/	/	/	/	<< 0,1
Cobalt	760	370	/	/	/	/	<< 0,1
Copper ore (sulfide)	/	390	/	/	/	/	<< 0,1
Tungsten	730	470	/	/	/	/	<< 0,1
Lead ore (sulfide)	/	< 500	/	/	9	200	<< 0,1
Beryllium	910	540	/	/	/	/	<< 0,1
Copper	700	/	/	/	/	/	<< 0,1
Aluminm-bronze alloy	/	990	/	/	/	/	/
Beryllium-copper alloy	/	/	/	/	/	/	/
manganese-bronze alloy	/	910	/	/	/	/	/
Nickel	/	/	/	/	/	/	/
Selenium	/	/	/	/	/	/	/
Stainless steel	/	/	/	/	/	/	/

3. Fire and explosion safety

In the field of explosion protection, prevention is divided into active and passive. The first group includes measures that prevent the explosion itself from exploding, while passive protection includes construction measures, which limit the effects of the explosion of flammable dust to a safe level. Active protection can be performed as:

- Primary protection – measures to prevent or to minimize the formation of an explosive mixture, it is to eliminate at least one of the factors necessarily present in the explosion of flammable dust.
- Secondary protection - measures to prevent ignition of the explosive mixture.

To eliminate an explosive dust-oxygen mixture it is possible to use industrial vacuum cleaners or adding inert substances (e.g. nitrogen, carbon dioxide, water vapor, limestone) to areas with an explosive atmosphere to keep the oxygen concentration below the limit (eg in mills, dryers, etc.).

Secondary protection is the elimination of initiating resources, which may be, for example, hot surfaces, flame, hot gases, mechanical sparks, electrical operating equipment. The particular initiation source is eliminated by complete exclusion from the explosive atmosphere, by alternative substitution and by the choice of more appropriate initiating source or by an adherence of stringent safety measures when operating in an explosive atmosphere. In the case of the impossibility of using active protection, the devices must be designed in such way that the effects of the explosion are limited to the safety level. Such measures include the explosion-durable construction of a device, then explosion-easing, explosion-suppression or preventing of flame and explosion on other parts of the device and the environment. The explosion-endangered part of the device must be constructed with a certain pressure resistance that corresponds to the expected explosive pressure in the relevant part of the device.

4. Conclusion

Safety in industrial installations with the appearance of flammable metal dust is linked to the observance of principles, including a detailed analysis of the relevant technological process and consideration of the possibility of emergencies. The practical application of all legislation applicable to the relevant technological operation can greatly prevent the occurrence of extraordinary events associated with the explosion of flammable metal dust, thereby saving the human lives, protecting the health of workers as well as specific technological facilities and operations.

Acknowledgments

„This work was supported by the Slovak Grand agency VEGA. (Project 1/022/16|6| Fire safe insulation systems based on natural materials).“

References

[1] P. Štroch, Combustion and explosion processes, Žilina: University of Žilina, 2010, 157 p., ISBN 978-80-554-0187-4
[2] J. Bradley, Consideration for Working with Combustible Metal Dusts, 2010-10-10, [cit. 2018-04-10], available at http://www.ccohs.ca/oshanswers/chemicals/lungs_dust.html
[3] Guidelines for Handling Aluminum Fines Generated During Various Aluminum Fabricating Operations, [cit. 2018-04-10], available at http://www.aluminum.org/sites/default/files/Safe%20Handling%20of%20Aluminum%20Fine%20Particles.pdf
[4] J. Khambekar, B.H. Pittenberg, Understanding and Preventing Metal – Dust Hazards, In: International Journal of Powder Metallurgy, 2013, Vol. 49, Issue 4, [cit. 2018-04-17], available at http://jenike.com/files/2013/09/IJPM_Article_11.13.pdf
[5] J. Moravec, Kovový prach jako alternativní palivo budoucnosti?, 2016 – 01-14, [cit. 2018-04-10], available at http://oenergetice.cz/technologie/kovovy-prach-jako-alternativni-palivo-budoucnosti/

[6] R. Wynn, Safely Collecting Combustible Metal Dusts, 2009-07-31, [cit. 2018-04-10], available at http://www.powderbulksolids.com/node/36981

[7] [cit. 2018-04-17], available at https://c1sinc.com/blog/dust-collection-industrial-promotes-quality-safety-health/dust-explosion-pentagon-fire-triangle/

[8] J. Micheli, Controlling your plant´s combustible dust hazards, 2016, [cit. 2018-04-10], available at http://www.middough.com/Middough/files/f9/f9e7c5a1-796d-4b9d-af61-6d863383ed27.pdf

[9] K. Kořínek, Požárně technické charakteristiky prachů a jejich význam v technické praxi. Výzkumný ústav bezpečnosti práce. Knihovna BOZP, čítárna [online], 22. decembra 2006, [cit. 2018-04-10]. Available at http://www.bozpinfo.cz/win/knihovna/bozp/citarna/clanky/pozarni_ochrana/prach_vybuchy_pozary.html

[10] A. Krietsch at all, In: Explosion behaviour of metallic nano powders, Journal of Loss Prevention in the Process Industries Volume 36, July 2015, Pages 237-243, [cit. 2018-04-10]. available at https://www.sciencedirect.com/science/article/pii/S0950423015000923

[11] G. Mayer et all., Explosion protection for dust collection systems handling metal dust, 2015, [cit. 2018-04-10], available at https://www.powderbulk.com/enews/2015/editorial/story_pdf/pbe_11_04_15RIHF.pdf

[12] M. Jacobson et all, Explosibility of metal Powders, United States Department of the Interior, 1964, [cit. 2018-05-02], available at http://www.dtic.mil/dtic/tr/fulltext/u2/b270510.pdf

[13] What are the Effects of Dust on the Lungs, [cit. 2018-04-10], available at http://www.ccohs.ca/oshanswers/chemicals/lungs_dust.html

[14] Dust and nanoparticles [cit. 2018-05-02], available at http://ec.europa.eu/taxation_customs/dds2/SAMANCTA/SK/Safety/Dust_SK.htm

Earth in a Trap? 2018
Analytical Methods in Fire and Environmental Science

Safecast bGeigie Nano as a tool for teaching students to understand monitoring environmental radioactivity

Miroslav Vanek[a*] – Anna Ďuricová[a] – Jozef Salva[a]

[a] *Technical University in Zvolen, Faculty of Ecology and Environment, Department of Environmental Engineering, T.G. Masaryka 24, 960 53 Zvolen, Slovakia*

Abstract

Safecast is a volunteered geographic information project based on the public participation in data collection and upload to a publicly available online database. This paper provides brief introduction to the Safecast database and bGeigie Nano device, with the detailed information available in the relevant references. While the main purpose of the Safecast database and bGeigie Nano is to provide publicly available data on the environmental radioactivity, we believe, that this concept is also a valuable tool for teaching university students to understand the complex aspects of environmental radioactivity monitoring, through unique personal experience. Proposed activities have a potential to become a part of the education process for the course of Radioecology. We intend to provide the opportunity for students to use the bGeigie Nano device to collect data and participate in the worldwide environmental radioactivity monitoring network. This experience itself would be a valuable asset, besides the obvious benefit of contributing to the database with our own new data.

Keywords: Safecast; bGeigie Nano; environmental radioactivity

---

[*] Corresponding author. Tel.: +421 45 520 6830; fax: +421 45 520 6279; e-mail: vanek@tuzvo.sk.

1. Introduction

Safecast is a volunteered geographic information project based on the public participation in data collection and upload to a publicly available online database. [1] The database is freely available under Creative Commons license and GPS tracked data can be displayed on the interactive online map. Device used to collect data is a bGeigie Nano, which is basically a digital Geiger Müller counter with GPS tracking and data logger.

Safecast project was initiated after Fukushima Daichi Nuclear Power Plant disaster, which occurred in March 2011. The inadequacy of the available information on the radiological situation from the government and power plant operator has led to the creation of volunteer based group devoted to monitoring and openly sharing information on environmental radiation. Since then the group has implemented participatory, open-source, citizen-science-centered radiation mapping solutions developed through a process of collaborative open innovation [2].

Even though the main purpose of the Safecast database and bGeigie Nano device is a monitoring of environmental radioactivity and sharing of the obtained data, we believe it has also a high potential as a teaching tool for university students. This paper briefly describes the properties of the bGeigie Nano device and Safecast database, and aims on its possible use for teaching environmental radioactivity related courses.

This paper aims on the process of teaching students of environmental engineering at the Technical University in Zvolen, Slovak Republic, in the field of radioecology and environmental radioactivity. Technical education at the Technical University in Zvolen, Slovak Republic is constantly evolving, integrating several new approaches, such as interactive methods [3], development of conceptual thinking by the use of video analysis [4] and other new methods [5]. Proposed course is part of the subject called Radioecology provided by the Department of Environmental Engineering at the Faculty of Ecology and Environmental Sciences. The main purpose of the course is to familiarize students with environmental radioactivity.

2. Material and methods

2.1. Safecast database

Fig. 1. Safecast map with results of measurement

The database serves two primary purposes. One, it is intended to provide an archive of independent data that can be freely used by anyone for any purpose. Two, it is used to generate the widely accessible visualizations, primarily maps, that Safecast publishes. [2] Details of the data processing methodology, including schematic diagrams, are openly available online. [6]

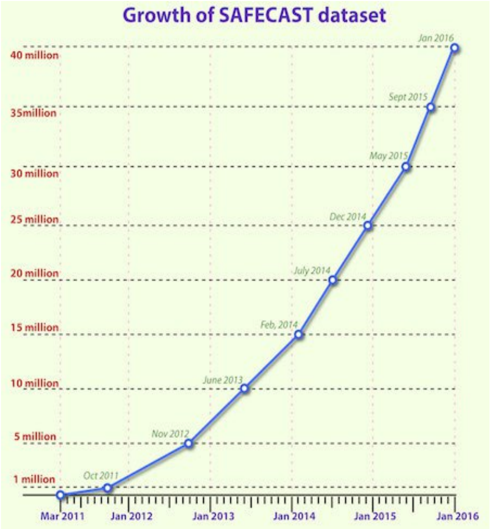

Fig. 1. Growth of Safecast dataset from 2011 to 2016

The database has grown rapidly since its first deployment and it is now considered to be the largest publicly available database of environmental radiation measurement data.

2.2. bGeigie Nano

The Safecast bGeigie Nano is a mobile, GPS enabled, logging, radiation sensor used by anyone that wants reliable radiation readings including scientists, first responders and citizens. It is designed for mounting on the outside of a car window but can be used on bicycles, trains, planes, and other modes of transportation. [7] bGeigie Nano is available as a kit from KitHub web based e-shop. It is possible to purchase also fully assembled device for significantly higher price. As a kit it provides unique opportunity to assemble the device by the enthusiast volunteers who are the main target group. However, assembly can be provided by any skilled technician.

The core part of the device is a state of art Geiger Müller tube from one of the leading manufacturers of radiation detectors – LND, INC. Oceanside, New York, USA.

Device measures counts per second, which is then converted to equivalent dose rate in $\mu Sv.h^{-1}$ according to calibration.

Fig. 2. Safecast bGeigie Nano assembled in protective case

bGeigie Nano units have periodically been put through stringent calibration tests at QualTek in the US, at the Jülich Research Centre in Germany, and at the IAEA testing laboratory in Seibersdorf, Austria. In all cases the measured accuracy has been shown to be compatible with the SAFECAST specifications (Accuracy: +/- 10% typical, +/- 15% maximum) [8].

Table 1

Basic parameters of the LND 7317 pancake GM detector

Parameter	Value	Unit
Type of detector	G-M pancake	
End window material	Mica	
End window areal density	2.0	$mg.cm^{-2}$
Gas filling	Ne + Halogen	
Diameter	53.6	mm
Operating voltage	475 - 675	V
Minimum dead time	40	µs
Gamma sensitivity ^{60}Co	58	CPS/MR/HR

Data available from manufacturer [11]

Research [9] recently published describes how the standard Safecast static transformation function overestimates the official measurements because it fails to capture the presence of two different Cesium isotopes and their changing magnitudes with time. However, the difference is minor and can be corrected by the published methodology. Another paper [10] compares the Safecast data with official authoritative data collected by U.S. authorities and the conclusion is, that the two datasets are highly correlated, with Safecast data slightly lower values.

2.3. Student activities

Safecast bGeigie Nano provides all features of a modern digital GM counter with data logging, enhanced with the GPS geo-referencing the measurement results. Besides the obvious use as a handheld GM counter, it can be used as a static device with the time series measurement. However, the most powerful feature is the GPS module integrated in the device. Based upon the availability of the bGeigie Nano devices, the proposed student activities may vary but following is the basic proposed concept.

Exploring the Safecast system

Students are expected to familiarize with the basic principles of operation and basic parameters of bGeigie Nano, as well as with the Safecast database. The whole topic is divided into subchapters, based on the number of students working groups. Each group prepares a short presentation on the topic and after the presentation a short moderated discussion guides students to find answers to a prepared set of questions.

Design of the monitoring plan

Each student group is required to prepare a preliminary measurement plan, based upon availability of the devices and local conditions. Map with the previous data readings is consulted. The basic rules on how to use the device must be a part of the plan.

Measurement and data upload

Students make the measurement. The data can be collected either in the school campus, or on the voluntary basis even during the weekend trip home or other convenient location. Data upload is performed with the teacher assistance through a single purpose account. Students acquire the data for further analysis.

Data analysis

Data analysis will be a part of the activity report. It can be done by simple spreadsheet software. As a part of the educational project, we are preparing a set of virtual experiments using MatLab software environment for various lab experiments.

3. Conclusion

Open source and public volunteer initiatives play an important role in our society. Safecast is a unique intersection of open source data, volunteer science project and environmental radiation monitoring.

In our neighbor country Czech Republic, the official National Radiation Protection Institute have lunched a project [12], based on the use of bGeigie Nano mobile devices, as well as designing their own static devices to create a monitoring network. They obtained 30 bGeigie Nano devices and supplied them to participating schools and other institutions to collect data. In the map shown in Fig. 1 it is clearly visible that the resulting data coverage in Czech Republic is far superior compared to Slovakia.

We intend to provide the opportunity for students to use the bGeigie Nano device to collect data and participate in the worldwide monitoring network. This experience itself would be a valuable asset, besides the obvious benefit of contributing to the database with new data.

Acknowledgments

This work was supported by Cultural and Educational Grant Agency of the Ministry of Education, Science, Research and Sport of the Slovak Republic for the project KEGA No. 021TU Z-4/2017; project KEGA No. 012TU Z-4/2017 and by Science Grant Agency for the project VEGA No. 1/0377/17.

References

[1] Safecast. *Safecast* [online]. [Accessed: 2018-05-15]. Available from: <https://blog.safecast.org/>

[2] BROWN, Azby, Pieter FRANKEN, Sean BONNER, Nick DOLEZAL, Joe MOROSS. Safecast: successful citizen-science for radiation measurement and communication after Fukushima. *Journal of Radiological Protection* [online]. 2016, **36**(2), S82 [vid. 2018-05-15]. ISSN 0952-4746. Available from: <doi:10.1088/0952-4746/36/2/S82>

[3] KRIŠŤÁK, Ľuboš, Miroslav NĚMEC, Zuzana DANIHELOVÁ. Interactive Methods of Teaching Physics at Technical Universities. *arXiv:1302.2863 [physics]* [online]. 2013 [Accessed: 2018-05-15]. Available from: <http://arxiv.org/abs/1302.2863>

[4] HOCKICKO, Peter, Ľuboš KRIŠŤÁK, Miroslav NĚMEC. Development of students' conceptual thinking by means of video analysis and interactive simulations at technical universities. *European Journal of Engineering Education* [online]. 2015, **40**(2), 145–166 [vid. 2018-05-15]. ISSN 0304-3797. Available from: <doi:10.1080/03043797.2014.941337>

[5] NĚMEC, Miroslav, Ľuboš KRIŠŤÁK, Peter HOCKICKO, Zuzana DANIHELOVÁ and Klára VELMOVSKÁ. Application of Innovative P&E Method at Technical Universities in Slovakia. *Eurasia Journal of Mathematics, Science and Technology Education* [online]. 2017, **13**(6),

2329–2349 [Accessed: 2018-05-15]. ISSN 1305-8223. Available from: <doi:10.12973/eurasia.2017.01228a>

[6] *Safecast Tile Map - Data Processing Methodology* [online]. [Accessed: 2018-05-15]. Available from: <http://safecast.org/tilemap/methodology.html>

[7] Safecast bGeigie Nano - Mobile Radiation Monitoring Device. *KitHub* [online]. [Accessed: 2018-05-15]. Available from: <https://shop.kithub.cc/products/safecast-bgeigie-nano>

[8] About Calibration and the bGeigie Nano. *Safecast* [online]. [Accessed: 2018-05-15]. Available from: <https://blog.safecast.org/faq/about-calibration-and-the-bgeigie-nano/>

[9] CERVONE, Guido, Carolynne HULTQUIST. Calibration of Safecast dose rate measurements. *Journal of Environmental Radioactivity* [online]. 2018, **190–191**, 51–65. ISSN 1879-1700. Available from: <doi:10.1016/j.jenvrad.2018.04.018>

[10] COLETTI, Mark, Carolynne HULTQUIST, William G. KENNEDY, Guido CERVONE. Validating Safecast data by comparisons to a U. S. Department of Energy Fukushima Prefecture aerial survey. *Journal of Environmental Radioactivity* [online]. 2017, **171**, 9–20. ISSN 1879-1700. Available from: <doi:10.1016/j.jenvrad.2017.01.005>

[11] 7317| Nuclear Radiation Detectors. *LND | Nuclear Radiation Detectors* [online]. [Accessed: 2018-05-15]. Available from: <http://www.lndinc.com/products/geiger-mueller-tubes/7317/>

[12] *Detektor záření SAFECAST a jeho využití pro veřejnost — Státní ústav radiační ochrany, v.v.i.* [online]. [Accessed 2018-05-15]. Available from: <https://www.suro.cz/cz/vyzkum/vysledky/safecast>

Study of forest fire behaviour under the meteorological conditions changed

Rastislav Veľas[a*] – Andrea Majlingová[a] – Danica Kačíková[a]

[a] *Technical University in Zvolen, Faculty of Wood Sciences and Technology, T.G.Masaryka 24, Zvolen 960 53, Slovak Republic*

Abstract

In recent years, the forest fires issue has been addressed by many experts, who contributed a development of knowledge on forest fire behaviour. For forest fire behaviour modelling, it is especially important to have the information on meteorological conditions, weather conditions and the influence of fuel and topography. The main objective of this work is to describe and evaluate the effect of selected meteorological and weather conditions on the area of the fire site. For modelling and simulation, we used the data on forest fire that occurred in the Koč locality, situated in the National Park Slovenský raj, in 2007. In the FARSITE programme, the input data related to the air temperature, wind speed, precipitations totals were changed to study the effect of the increasing values of meteorological factors studied. The forest fire behaviour was modelled for the first 24 h of its duration. The computer modelling results and analyses of the courses of fire site area growth showed that with the increasing wind speed the fire site area grows. However, wind speed had the most significant influence on the development of the fire during the day. During the night the area of fire site was growing very slowly (only few m^2/h), probably because the fire intensity significantly decreased. There was almost no effect of change in air temperature on forest fire behaviour. When studying the effect of precipitations totals on forest fire spreading, we also considered the impact of the time of precipitations occurrence, either from 5.00 a.m. to 7.00 a.m. or from 12.00 p.m. to 14.00 p.m., before the fire ignition, except the precipitations totals. Larger fire site area occurred in the case of precipitations totals of 0 $mm/m^2/h$ than 3 $mm/m^2/h$ and when the precipitations occurred before the fire initiation, i.e. from 12.00 p.m. to 2.00 p.m. When considering the precipitation totals of 8 and 40 mm $mm/m^2/h$, the fire was not initiated in FARSITE programme, due to the high moisture content of forest fuel available in the study area. We also performed a correlation analyses between wind speed (precipitations totals) and fire site area to statistically confirm the dependency between the meteorological factors change and the fire site area growth. The results showed the very tight dependence between all the meteorological factors considered and the fire site area growth.

Keywords: forest fire; modelling; FARSITE; fire behaviour; meteorological conditions

---

[*] Rastislav Veľas. Tel.: +421-45-5206827; e-mail: xvelasr@tuzvo.sk.

1. Introduction

From the social point of view, the most important feature of large forest fires is their potential to seriously and irreversibly harming of areas of significant importance. The extent and severity of such fires can also significantly affect the population and the environment in adjacent areas [1]. An increasing number of forest fires is not only due to global warming, but according to the FAO [2], the most frequent cause is intentional and unintentional human activity. According to Cohen [3], the fires most often occur at the interface of the wildland-urban area. This area is defined as the transition zone between wildland, urban and industrial environment [4].

Modelling and simulation of forest fires spread is an interesting domain that is used to understand and predict possible fire behaviour. The fire models are categorized to different types: to stochastic and deterministic models, i.e. empirical model, or to physical models [5]. In the world, there are several systems used to model and simulate forest fires such as FARSITE, FlamMap, BehavePlus and Wildland Fire Dynamic Simulator (WFDS). Their outputs are the data showing the fire site area and perimeter, the speed and direction of fire spread, flame length and fire intensity. To predict the fire behaviour, it is especially important to have the information on effect of changing meteorological conditions (air temperature, relative air humidity, fuel moisture, as well as speed and direction of the wind), fuel (models, types, volume, spatial distribution) and topography (elevation, slope, aspect) [6].

The moisture content of fine fuel is a key element affecting forest ignitability and closely related to the probability of fire occurrence. It further also affects the intensity and the severity of the fire [7-8].

Boer et al. [9], in their study, indicated that forest fire danger assessment systems should be based on a reliable prediction of the fuel moisture content, the so-called critical moisture threshold of the fuel represented by the moisture of extinction. They came to this value based on research carried out in central Portugal in June 2017, where catastrophic forest fires broke out, shortly after the region's fuel had dried to the so-called threshold value of critical humidity.

Prat-Guitart et al. [10] investigated the influence of moisture content and peat density on the horizontal propagation of smouldering fire in laboratory conditions. The results showed that the moisture content had a greater effect on the spread rate than bulk density.

Fang et al. [11] investigated the impact and contribution of weather, topography and vegetation on the size and severity of fire in the Chinese coniferous forest ecosystem. The results showed that the main causative factor of the size of the fire was weather, while vegetation and topography had a stronger impact on the severity of the fire. The size of the outbreak (< 130 ha) is mainly influenced by vegetation, but in the case of outbreaks (> 200 ha), they are more affected by extreme weather conditions. Also, their study has suggested that fuel modification will have little effect on reducing the range of fire, but it can work to mitigate the severity of future fires.

Mendes-Lopes et al. [12] examined how the flame affects the tree trunk, especially at the bottom of the tree under windy conditions to include this information in the model and into the cells due to computational modelling of fire spread. Fernández-Alonso et al. [13] in the modelling deal with the influence of the wind on the severity of the fire. They report that more intense fire occurred more frequently in areas with high simulated wind speed and more pronounced in the case of wind-driven fires.

Bar Massada et al. [14] considered the risk of fire at the wildland-urban interface. For the spatial mapping of the probability of occurrence of the fire, they performed 6,000 simulations. Simulations have been conducted under normal and extreme weather conditions to assess the impact of weather on fire spreading, the likelihood of burning and the risk for buildings. The results highlight the fact that extreme weather conditions not only cause a higher risk of fire than normal weather, but also change the location of high-risk areas in the country, which has major importance for fire management in wildland-urban interface areas.

The main objective of this study is to describe and evaluate the impact of changes in air temperature, relative air humidity and precipitation totals on forest fire spreading during the 24 h of fire duration.

The subject of this study was the fire behaviour of forest fire that occurred in the locality of Koč, situated in the Slovenský raj National Park, in 2007. For modelling and simulation of fire behaviour the FARSITE programme. The modelling results were further used to create trend of fire site area growth during the 24-hours period and to determine the dependence between the evaluated factors and fire site area in the STATISTICA 10 programme.

2. Methodology

2.1. Model forest fire

The modelled fire belongs to the most extensive forest fires in Slovakia. It occurred in the National Park Slovenský raj, in the locality of Koč over Štvrtocká píla, in the cadastre of Vernar village of Vernár, in Poprad district. The forest fire damaged forest area with extent c.a. 18 ha. This area was represented by mixed forest stands, composed mostly from fir, spruce, pine, beech tree species, 70 - 160 years old.

The fire was initiated on 22.7.2007 at 2.45 p.m. by employees of the Vernár Municipality Administration Office, who at that time cleaned the tourist footpath, in the Predná Hoľa locality. The forest fire occurred in a rugged mountain terrain at an altitude of 930 m.a.s.l. With the use of aerial attack and the pond water transport system to the fire, the fire-fighting activities were terminated after five days, i.e. on 29.7.2007 at 9.00 p.m. The most likely cause of the forest fire was the lightning which affected a tree crown on the top of the hill on 21.7.2007 at 2.45 p.m. [15].

The fire site area consists of the following fuel models: PM 25 - Herbs up to 15 cm, PM 29 - Grass and herbs up to 30 cm dry SLT series D and PM 30 - Grass and herbs up to 30 cm wet SLT series D.

The most represented fuel model on a fire affected area was PM 30 - Grass and herbs up to 30 cm wet SLT series D.

2.2. Experiment

In the FARSITE programme, input data relating to air temperature (together with relative air humidity), wind speed, precipitation totals were changed. The impact of the individual parameters on the resulting fire site area (ha) was analysed and evaluated. The impact of the amount of precipitation at the individual air temperatures on the ignition and consequent spread of fire was also evaluated. The proposed model conditions (air temperature, precipitation totals, wind speed, relative air humidity) entering modelling were such as introduced in Table 1.

In modelling the forest fire behaviour was studied at different combinations of meteorological factors values. The only independent variable was the air temperature, i.e. the other meteorological factors change was studied in dependency on specified air temperature value (20 °C, 25 °C, 30 °C and 35°C). The fire burning period was represented only by the first 24 h period of fire duration. It was simulated from 22.7.2007 from 2.45 p.m. until the next day, 23.7.2007 to 2.45 p.m. In modelling, the precipitations occurrence period was set either from 5.00 a.m. until 7.00 a.m. or from 12.00 p.m. to 14.00 p.m. The following input data were required to work with the program: terrain data, meteorological data and the data on fuel volume, spatial distribution and fire properties. The results of modelling in FARSITE were used to determine the dependency between the fire site area and individual meteorological factors at a given time step from the fire ignition. This analysis was processed in the STATISTICA 10 program.

Table 1

FARSITE input weather and wind values at individual air temperatures

Considered meteorological and fuel factors	Considered air temperature values (°C)			
Maximum temperature (°C) at 3.00 p.m.	20	25	*30*	*35*
Minimum temperature (°C) at 5.00 a.m.	5	12	*15*	*20*
Precipitations totals (mm/m^2/h)	0	0	0	0
Maximum air humidity (%) at 3.00 p.m.	65	60	55	50
Minimum air humidity (%) at 5.00 a.m.	55	50	45	40
Fuel moisture content of herbal fuel (%)	100	90	80	65
Fuel moisture of woody fuel (%)	75	75	75	70
Precipitations totals (mm/m^2/h)	3	3	3	3
Maximum air humidity (%) at 3.00 p.m.	70	65	60	55
Minimum air humidity (%) at 5.00 a.m.	60	55	50	45
Fuel moisture content of herbal fuel (%)	110	100	95	75
Fuel moisture of woody fuel (%)	90	90	85	80
Precipitations totals (mm/m^2/h)	8	8	8	8
Maximum air humidity (%) at 3.00 p.m.	80	75	70	65
Minimum air humidity (%) at 5.00 a.m.	70	65	60	55
Fuel moisture content of herbal fuel (%)	140	140	140	130
Fuel moisture of woody fuel (%)	100	100	95	90
Precipitations totals (mm/m^2/h)	40	40	40	40
Maximum air humidity (%) at 3.00 p.m.	95	90	85	80
Minimum air humidity (%) at 5.00 a.m.	85	80	75	70
Fuel moisture content of herbal fuel (%)	220	220	220	200
Fuel moisture of woody fuel (%)	130	130	125	120
Wind speed (km/h)	0	19	38	-

3. Results and discussion

3.1. Effect of increasing wind speed on forest fire behaviour

In the analysis focusing the effect of the wind speed changed on forest fire spreading, we focused the correlation between the influence of wind speed and fire site area (ha). The effect of wind speed on fire site area growth was studied based on fire site area data obtained from modelling in 1 h intervals. A graphical representation of the course of the fire site area growth in relation to the wind speed at air temperature of 20 °C is shown in Figure 1.

From the course of the individual curves, shown in Figure 1, we see a gradual increase of the fire site area from the fire initiation at 2.45 p.m., until 7.45 p.m. In the upcoming hours, the size of the fire area at windless (0 km/h) was growing very slowly, due to the decreased fire intensity during the night. At 7.15 a.m., next day, after the sunrise, the fire intensity increased, and the area of the fire site increased too.

At a wind speed of 19 km/h, the fire spread rate increased again at 6.15 a.m., the second day of fire duration. At a wind speed of 38 km/h, the fire site area growth increased at 5.45 a.m. In the next hours, until 2.45 p.m., i.e. the end of fire duration, the fire site area continually grew up. The largest fire site area was reached at wind speeds of 38 km/h (137.05 ha). At the wind speed of 19 km/h the fire site area after 24 h of fire duration was of 92.55 ha. The smallest fire site area was at wind speed of 0 km/h (59.37 ha).

It should also be noted that the area of the fire site proportionally grew up with the increasing wind speed. With increasing wind speed also the fire intensity in the morning increased earlier.

The reason why the fire site area was growing up slowly during the night was the lower air temperature, increased relative air humidity and this way also the moisture content of forest fuel available. Gradual spread of fire occurred in the early morning hours, when forest fuel began to lose moisture was due to the increase of the air temperature and a decrease in relative air humidity.

Based on this fire behaviour results, we can state that the wind speed has a significant impact on the development of the fire site area, especially during the day.

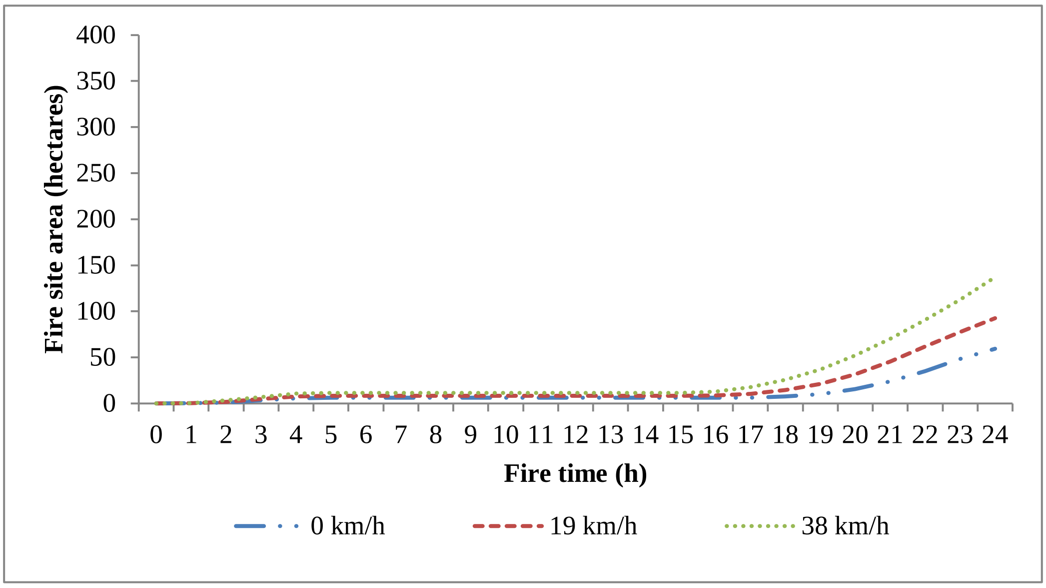

Fig. 1 Course of fire area development depending on wind speed

Using the statistical analyses, the correlation coefficients between wind speed and fire site area were calculated for all the wind speeds at given air temperatures and for the time steps 2, 5, 17, 20, 24 h from the fire initiation.

The results of the correlation analysis between the wind speed and fire site area, at air temperature of 20 °C, are shown in Table 2.

Based on the results of the correlation coefficients, which determine the tightness of the correlation, it is obvious that it is a very close dependency between the wind speed and the area of the fire site. Similar results of the correlation analysis were also at air temperatures of 25 °C, 30 °C and 35 °C.

Table 2

Correlation matrix representing the dependency between the wind speed and fire site area

Wind Speed (km/h)	0	19	38
0	-	0.995860	0.991038
19	0.995860	-	0.999012
38	0.991038	0.999012	-

3.2. Effect of the precipitations totals increase and time of occurrence on forest fire behavior

When studying the effect of precipitations totals on forest fire spreading, we focused on evaluating the dependency between the precipitations totals and fire site area (ha) of the model fire. We had also considered the impact of the time of precipitations occurrence, either from 5.00 a.m. to 7.00 a.m. or from 12.00 p.m. to 14.00 p.m., before the fire ignition, on 22.07.2007.

We studied the effect of precipitations totals on fire site area growth during the first 24 h of fire duration. In Figure 2, there is shown the course of fire site area growth in dependency on precipitations totals occurring from 5.00 a.m. to 7.00 a.m., at air temperature of 20 °C.

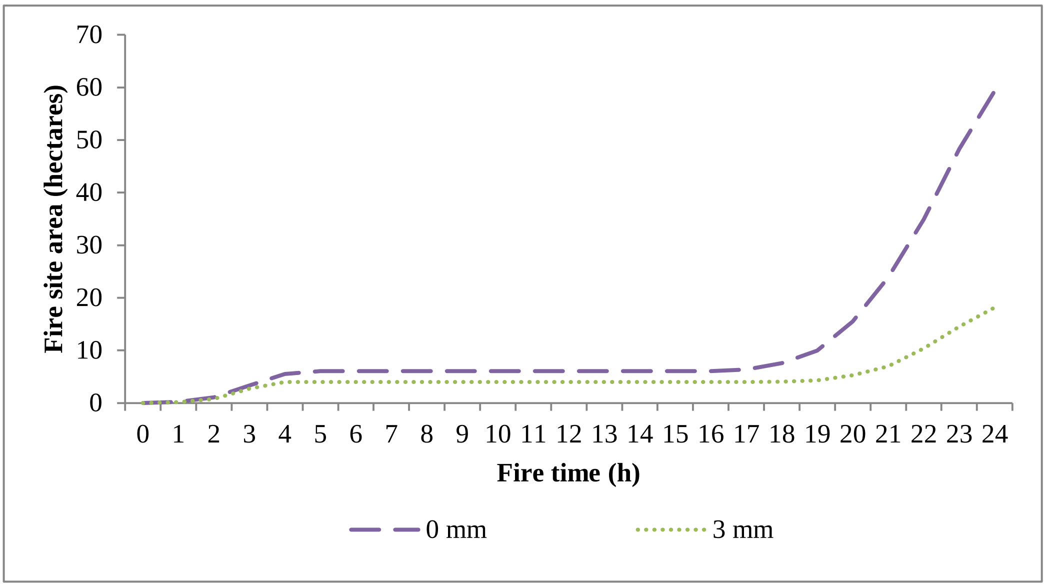

Fig. 2 Course of the fire site area grow thin dependency on the precipitations occurring from 5.00 a.m. to 7.00 a.m.

From the course, shown in Figure 2, is evident the gradual increase in the fire site area at precipitations totals of 0 mm/m^2/h and 3 mm/m^2/h, in period from the initiation of the fire (2.45 p.m.) up to 7.45 p.m., i.e. 5 h after fire initiation (for 0 mm/m^2/h), and 6.15 p.m., i.e. more than 3 h after the fire initiation (for 3 mm/m^2/h). In the next hours, the fire site area was growing very slowly (only in m^2/h), until 7.15 a.m. (for 0 mm/m^2/h), when the fire intensity grew up again, and the fire site area was gradually increasing again. At a precipitation totals of 3 mm/m^2/h, the fire intensity grew up from 8.45 a.m., i.e. after 18 h from fire initiation. An explanation of the reason, why the area of the fire site was not spreading as intensively as during the day has been already mentioned in Section 3.1. Further, we can notice that the spread of the fire did not occur immediately in the morning, but in the afternoon. It was caused probably because we modelled the fire at wind speed of 0 km/h.

The total area of fire site after the 24 h of burning was of 59.37 ha at precipitations totals of 0 mm/m^2/h and 18.17 ha at precipitations totals of 3 mm/m^2/h. The difference was of 41.20 ha.

In the study we focused also the precipitations totals of 8 and 40 mm/m^2/h. Those precipitations totals were too high to initiate the fire in the study area and therefore it was not possible to model and to get the data on fire site area from the FARSITE programme. That is the reason, why we do not introduce the results for those precipitations totals, too.

A similar course of the fire site area growth in dependency on changed precipitations totals value, occurring from 12.00 p.m. to 2.00 p.m., at air temperature of 20 °C, is shown in Figure 3.

Similar courses were also observed at air temperatures of 25 °C, 30 °C and 35 °C.

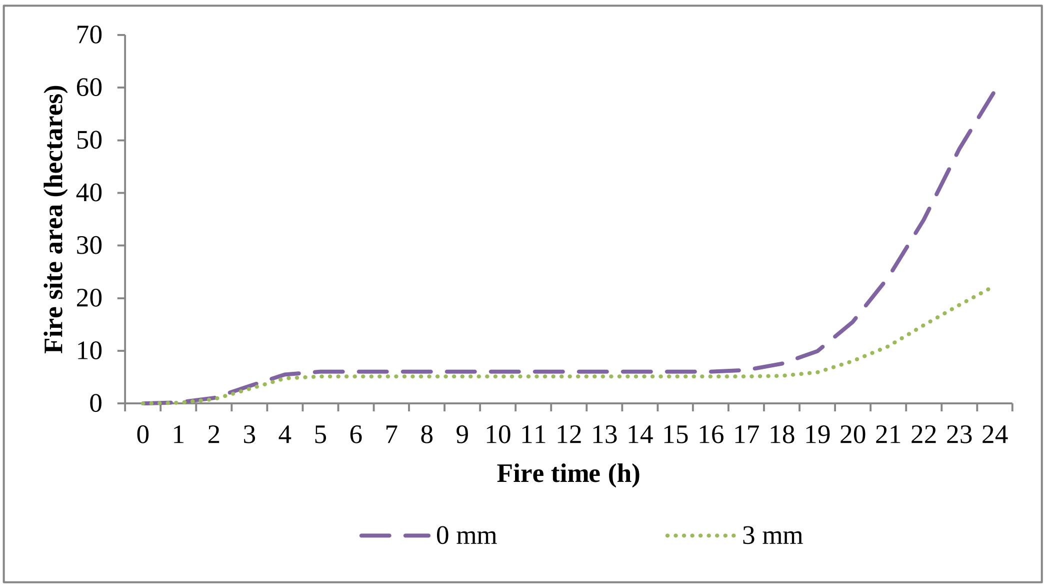

Fig. 3 Course of the fire site area growth in dependency on the precipitations occurring from 12.00 p.m. to 2.00 p.m.

In this case, it is necessary to note that larger area of fire site occurred in the case of precipitations that appeared in the time from 12.00 p.m. to 2.00 p.m. The fire site area at precipitations totals of 0 mm/m^2/h was the same as in previous case (59.37 ha), but it was of 22.27 ha at the precipitations totals of 3 mm/m^2/h.

When considering the other air temperature values, i.e. 25 °C, 30 °C and 35 °C, a larger fire site area was observed in the case of precipitations that occurred in the morning (from 5.00 a.m. to 7.00 a.m.).

According this fire behaviour results, we can conclude that the precipitations totals and the time of occurrence of precipitations has a significant impact on the development of the fire and the resulting fire area.

In the statistical analysis, the correlations were calculated for both above-mentioned precipitations totals occurring from 5.00 a.m. to 7.00 a.m. and from 12.00 p.m. to 2.00 p.m., at specified air temperatures and fire site area at specified time steps (2, 4, 19, 22, 24 h from the fire ignition).

Here, we present only the results of the correlation analysis between precipitations totals and the fire area at air temperature of 20 °C. Similar results of the correlation analysis were also observed at air temperatures of 25 °C, 30 °C and 35 °C.

In Table 3, there are shown the results of the correlation analysis between precipitations totals occurring from 5.00 a.m. to 7.00 a.m. and the fire site area, at air temperature of 20 ° C.

Table 4 shows the results of the correlation analysis between precipitations totals in the time from 12.00 p.m. to 2.00 p.m. and a fire site area at temperature of 20 ° C.

Table 3

Correlation matrix introducing the correlation coefficients expressing the tightness of the dependency between precipitations totals occurring from 5.00 a.m. to 7.00 a.m. and fire site area

Precipitations totals (mm/m^2/h)	0	3
0	-	0.993187
3	0.993187	-

Table 4

Correlation matrix introducing the correlation coefficients expressing the tightness of the dependency between precipitations totals occurring from 12.00 p.m. to 2.00 p.m. and fire site area

Precipitations totals (mm/m^2/h)	0	3
0	-	0.993541
3	0.993541	-

Based on the results of the correlation analyses, which determine the tightness of the correlation between the precipitations totals and the fire site area, it is obvious that it is a very close dependency.

4. Conclusions

The forest fire behaviour modelling results, considering the change in the selected meteorological factors, were used to study the effect and dependency of change in meteorological situation on forest fire behaviour. Based on the results obtained, we should confirm the following facts. With the increasing wind speed also, the fire site area is increasing. This fact was confirmed also by the correlation analyses results. the area the fire site is increasing. The effect of wind speed on the fire spreading is most evident during the day. During the night the fire site area grows slowly due to the low fire intensity. We can also assume that the fire behaviour in the night is probably also influenced by the moisture content of the forest fuel, which is over the critical value of moisture of extinction as stated e.g. Cohen [16].

Results of forest fire behaviour modelling under the changed values of precipitations totals and the different time of their occurrence showed the fact, that a larger fire site area occurred in the case of precipitations occurring before the fire initiation, from 12.00 p.m. to 2.00 p.m. When considering the precipitation totals of 8 and 40 mm mm/m^2/h, the fire was not initiated in FARSITE program due to the high moisture content of forest fuel available in the study area.

The effect of air temperature changed was not very significant. The courses of fire site area growth were very similar.

In the future, it will be necessary to study more the effect of precipitations totals depending on the period of their occurrence, but also in relation to the fuel moisture content change.

Acknowledgments

This work was supported by the Slovak Research and Development Agency under the contract No. SK-CN-2017-0018 (50 %). This work was supported by the KEGA Agency under the project No. 012TU Z-4/2016 (50 %).

References

[1] D. Vakalis, H. Sarimveis, C.T. Kiranoudis, A. Alexandridis, G. Bafas, A GIS based operational system for wildland fire crisis management II. System architecture and case studies, Appl. Math. Model. 28 (2004) 411-425.

[2] FAO, Fire management-Global assessment 2006, FAO Forestry Paper (2007) 151.

[3] J.D. Cohen, Preventing Disaster: Home Ignitability in the Wildland-Urban Interface, J. For. 98 (2000) 15-21.

[4] M. Calviño-Cancela, M.L. Chas-Amil, E.D. García-Martínez, J. Touza, Interacting effects of topography, vegetation, human activities and wildland-urban interfaces on wildfire ignition risk, For. Ecol. Manag. 397 (2017) 10-17.

[5] J.K. Adou, A.D.V. Brou, B. Porterie, Modeling wildland fire propagation using a semi-physical network model, Case Stud. Fire Saf. 4 (2015) 11-18.

[6] A. Bar Massada, A.D. Syphard, T.J. Hawbaker, S.I. Stewart, V.C. Radeloff, Effects of ignition location models on the burn patterns of simulated wildfires, Environ. Model. Softw. 26 (2011) 583-592.

[7] J.G. Cawson, T.J. Duff, K.G. Tolhurst, C.C. Baillie, T.D. Penman, Fuel moisture in Mountain Ash forests with contrasting fire histories, For. Ecol. Manag. 400 (2017) 568-577.

[8] A. Malcolm Gill, P. Zylstra, Flammability of Australian forests, Aust. For. 68 (2005) 87-93.

[9] M. Boer, R. Nolan, V. Resco de Dios, H. Clarke, O. Price, R. A. Bradstock, Changing weather extremes call for early warning of potential for catastrophic fire, Earth's Future. 5 (2017) 1196-1202.

[10] N. Prat-Guitart, G. Rein, R.M. Hadden, C.M. Belcher, J.M. Yearsley, Propagation probability and spread rates of self-sustained smouldering fires under controlled moisture content and bulk density conditions, Int. J. Wildland Fire. 25 (2016) 456-465.

[11] L. Fang, J. Yang, J. Zu, G. Li, J. Zhang, Quantifying influences and relative importance of fire weather, topography, and vegetation on fire size and fire severity in a Chinese boreal forest landscape, For. Ecol. Manag. 356 (2015) 2-12.

[12] J. Mendes-Lopes, J. Ventura, N. M. G. Santos, Proc. 1th Int. Conf. Model. Monit. Manag. For. Fires, 17-19 September, 2008; Model. Monit. Manag. For. Fires, (2008) 131-141.

[13] J.M. Fernández-Alonso, J.A. Vega, E. Jiménez, A.D. Ruiz-González, J.G. Álvarez-González, Spatially modeling wildland fire severity in pine forests of Galicia, Spain, Eur. J. For. Res. 136 (2017) 105-121.

[14] A. Bar Massada, V.C. Radeloff, S.I. Stewart, T.J. Hawbaker, Wildfire risk in the wildland–urban interface: A simulation study in northwestern Wisconsin, For. Ecol. Manag. 258 (2009) 1990-1999.

[15] A. Takáč, P. Sedlák, Zdolávanie lesného požiaru v Slovenskom raji v júli 2007, Spravodajca – Protipožiarna ochrana a záchranná služba. 2 (2008) 14-18.

[16] R. J. Coleman. Management of Fire Service Operations. Massachusetts: Breton Publishers, North Scituate, 1978, 560 pp.

Assessing the adsorbents suitability for removing of solid surface oil pollution

Veronika Veľková[a]* – Tatiana Bubeníková[a] – Patrik Tajnai[a]

[a]*Technical University in Zvolen, Zvolen, Slovak republic*

Abstract

The article is dealing with the assessment of the effectiveness of selected adsorbents to remove oil pollution. The aim was In the experiment was simulated leakage of diesel oil and engine oil on a solid surface. On the oil compounds were three kinds of adsorbents (Cansorb, Josyp Plus and Experlit) applicate. Application of selected adsorbents determines the effect of kinematic viscosity on the efficiency of adsorption. The influence of the origin of the adsorbent was also confirmed. It was the most effective adsorbent of organic origin CANSORB applied at leakage of engine oil and even diesel. Adsorbent of natural origin JOSYP PLUS with an efficiency of 55.86% not recommended for use to remove escaped diesel from a solid surface.

Key words: adsorbent; engine oil; diesel oil; solid surface; oil pollution

---

[*] Corresponding author. Veronika Veľková, Tel.: +421 45 52 06 533; e-mail: veronika.velkova@tuzvo.sk.

1. Introduction

Oil products and crude oil are the basic raw material for industrial purposes. Their impact on all components of the environment is not negligible. Contamination of the components of the environment (air, soil or aquatic ecosystem) there is a leak from the leakage of equipment, various accidents or mishandling them. In relation to the ecosystem of hydrocarbons characterized by the following risk factors: negatively affect aquatic fauna and flora, in contamination of the soil layer they affect the vegetation, the air is contaminated by volatile fractions, causing unpleasant odour effects, threaten and devalue drinking water sources and causing fire risks [1-2]. Already mentioned accidents have an adverse impact to living organisms and ecosystems. Question of emergency prevention has become was a topical issue for the whole society, which for this purpose creates adequate legislation [3].

Waste disposal causes potential danger to the environment. It constitutes the basic expenditure of excessive funds. Incineration of oils has a negative effect on air cleanliness and thus also to ecosystems and significantly negatively affects people's health. Various components of mineral oils are considered carcinogenic and that's why it is important to know the destination and persistence of these substances in nature [4]. Traffic accidents on roads are often associated with leakage of fuel, operating fluids. They pose a danger for contamination of soils and groundwater. Therefore, it is necessary to prevent their further escape and team to eliminate other negative consequences for the environment.

Sorbents are special substances and materials, which are capable of binding many liquid contaminants, pollutants and thus reduce the negative impact on the environment, e.g. oil products [5]. When disposing of the accident the most important sorbent property is its sorption property. Assessment sorption capacity should be considered, its applicability to a solid surface or on water. From the point of view of environmental protection, whether the absorbed substances are not released mechanical handling of the sorbent. Another important factor is the volume, their dustiness, the rate of reaction with the pollutant, easy of removal and as well as their method of disposal [6].

Sorbents can be natural or synthetic. Natural adsorbents are divided into organic materials such as peat or wood based products; and inorganic vermiculite or clay. The synthetic sorbents are made of polypropylene, polyurethane.

Adsorbents are available in bulk form, such as granules, powder, flakes and cubes, they are often packed in bags, meshes or sacks. They are also available in the form of tampons, rolls, pads. Currently, modern sorption materials are used, which are characterized by a high sorption capacity. By origin are divided into sorption means for natural and synthetic [7].

Absorption is mainly used for the isolation of unsaturated hydrocarbons obtained by cracking, or to separate the methane by absorption in the hydrocarbon absorbent. There is a great deal on the market. In the presented article we are dealing with the experiment evaluation of the effectiveness of selected types of absorbents.

2. Material and Methods

For adsorption process it is important to have an adsorbent with the largest active surface, which is created by the developed porous structure. Adsorbents are used in the form of beads or granules with dimensions from 0.1 mm to 6 mm, optionally in the form of a powder.

Here are some of the best-known industrial adsorbents. Most often are separated by adsorption polar and nonpolar compounds. The most commonly used the non-polar adsorbent is activated carbon, on which nonpolar substances are captured the better, the higher the mole weight. From polar adsorbents are used natural or synthetic aluminosilicates, alumina and others.

Frequently used adsorbents are molecular sieves with characteristic dimensions of cavities and canals. In addition to capturing multiple gaseous impurities they allow them to separate from each other. In the experimental part in laboratory conditions was simulated leakage of selected oil products on a solid surface.

The used contaminants were: diesel oil and engine oil.

Diesel fuel is a fuel for diesel engines. The baseline data is shown in Table 1.

Table 1

Physical and chemical properties of Diesel fuel [8]

Physical and chemical properties	
State	Liquid
Colour	Clear, colourless to yellowish
Odour	Specific
Density (g.m^{-3})	0.820 – 0.845 at 15°C
Kinematic viscosity	2 – 4.5 mm^2.s^{-1} at 20°C

Engine oil is specially designed for use in combustion engines. The basic data are shown in Table 2.

Table 2

Physical and chemical properties of Engine oil [9]

Physical and chemical properties	
State	Liquid
Colour	Amber
Odour	Weak
Density (g.m^{-3})	0.840 at 15°C
Kinematic viscosity	69.9 mm^2.s^{-1} at 40°C

To remove oil pollution were used the sorbents: CANSORB, EXPERLIT and JOSYP PLUS A. As a solid surface were used concrete cubes with dimensions 20 x 20 cm. Hard surface contamination was performed under laboratory conditions. The assay was evaluated gravimetrically.

A concrete cube was weighed. Concentration of the contaminant on the solid surface was 1000 g of contaminant per area of 1m^2. After the time has passed from the surface took off the applied sorbent and concrete cube was reweighed. From the difference in weight was calculated contaminant residue on a solid surface unabsorbed sorbent.

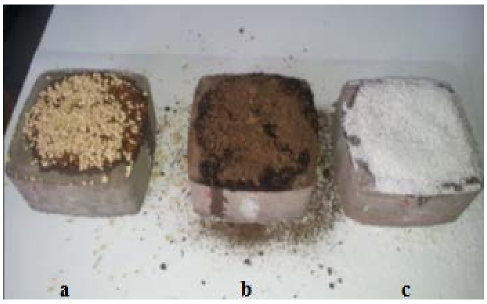

a – JOSYP PLUS **b** – CANSORB **c** – EXPERLIT

Fig. 1 The contaminated solid surface after application of sorbents

3. Results and discussions

In the solid surface contamination experiment there were performed three repetitions of the simulation of contamination of the concrete surface motor oil and diesel (each separately). Before contamination concrete cubes with petroleum products all concrete cubes dared and their mass was recorded. The solid surface of the concrete cube was contaminated by concentration 14 grams of contaminant to an area of 144 cm^2 (conversion to the desktop from selected initial contamination of 1000 g.m^{-2}).

The sorbents JOSYP PLUS, CANSORB A EXPERLIT were applied on the surface of the concrete cube, each separately.

The sorbents were removed from the surface after adsorbing oil products and contaminated concrete cubes were again weighed. From the weight difference from contamination and after contamination and after removing the sorbent from the surface the remainder of the contaminant was calculated not captured adsorbent. The amount of adsorbents, which were applied to the site, was not determined on the basis of its weight or volume, but its sufficiency was assessed visually. Sorbent created the entire surface sites applications continuous layer. The periods of action of the sorbent on the contaminant the following were chosen: diesel fuel - 3 minutes and engine oil 10 minutes [10]. Adsorbents used in experiments are commonly used substances during the interventions by the Fire and Rescue Service units, which also provided them with us.

From the results shown in Table 3, the highest efficiency had sorbent CANSORB. This is a sorbent of organic origin, which is made of fiber peat moss. It is fully biodegradable with the ability to absorb quickly and efficiently hydrocarbons and it is also able to repel water. These properties make it ideal for removing hydrocarbon contamination as a dry, also on the water surface [11-12].

Satisfactory results were obtained also with the adsorbent Josyp plus, whereby the manufacturer indicates the sorption capacity of the substance: 1 liter of the sorbent collected 0.46 liters of oil [13].

The lowest sorption efficiency was determined after use of Expertlite, natural material produced by expanding volcanic rock of perlite, of inorganic origin [14].

Table 3

Evaluation of solid surface decontamination of engine oil and diesel fuel

Adsorbent	Engine oil		Diesel fuel	
	Residue after removal (g)	Efficiency, %	Residue after removal (g)	Efficiency, %
JOSYP PLUS	2.77	80.21	4.18	70.14
CANSORB	2.04	85.43	3.75	73.21
EXPERLIT	3.63	74.,07	3.83	72.64

Based on the experimentally obtained results we can say:

- differences in sorption power between diesel fuel and engine oil were caused by their different density and viscosity (diesel fuel applied to a solid surface occupied a larger area with less thickness than engine oil),
- engine oil is better adsorbed on all sorbents used than diesel fuel,
- from sorption preparations were the best results used at CANSORB, it was confirmed for both contaminants,
- the highest efficiency, 80.2%, was, when the JOSYP PLUS sorbent was used in the experiments with engine oil,
- sorptive efficiency of EXPERLIT was in both experiments comparable (difference of 1.7%).

For the quality of the environment and human health is not so much important content of hazardous elements in soils, as their mobile and mobilizable share. It can get into the water, it can receive plants and then enter into the food chain. Natural contamination is equally dangerous as a contamination from the air pollution.

4. Conclusion

To address emerging crisis situations, such as accidents, various environmental accidents are deployed the units of the Fire and Rescue Service who are involved in the removal of hazardous substances. Oil products, due to anthropogenic activities one of the most widespread substances, affect the atmosphere, lithosphere, hydrosphere and biosphere. They are characterized by risk factors, which adversely affect aquatic fauna and flora. Contaminants of the soil layer affect the vegetation, the air is contaminated by volatile fractions. They cause unpleasant odor effects, threaten and degrade drinking water sources and cause fire risks. Based on our results more attention needs to be paid selection of sorbents for the purpose of their use, e.g. in relation to a particular dangerous substance. Interventions by the Fire and Rescue Service in case of extraordinary events to mitigate environmental pollution hazardous materials, substances, which include oil products. The use of sorbents solves surface contamination. Because that the present brings with it many repeated interventions, especially during accidents, leakage of petroleum substances occurs into the environment. This results to the cumulation of dangerous substances in the environment. Hydrocarbons have negative effects on the flora and fauna in the water, cause changes in microbial biodiversity in the soil. Through the food chain may also adversely affect human health and so it's the issue it required in the future sufficient attention.

Acknowledgments

This work was supported by the Slovak Research and Development Agency under the contract No. APVV-16-0326 (20%) and by the Cultural and Educational Grant Agency under contract no. KEGA 012TUZ-4/2016 (80%).

References

[1] H. Hybská, Základy ekotoxikológie, Technická univerzita vo Zvolene, 1. vyd. (2015) 117.
[2] D. Samešová, H. Hybská, Výskum environmentálnych impaktov ropných látok v prírodnom prostredí. Technická univerzita vo Zvolene (2011) 98.
[3] A. Daloš et al., Nebezpečné látky a ekologické havárie, Technická univerzita v Žiline (2003) 22-63.
[4] H. Hybská, D. Samešová.. Ecotoxicology, Technical University in Zvolen (2015) 164.
[5] I. Coneva, 10 let FBI. In SPEKTRUM. 12 (2012) 53-58. [online].
[6] Š. Galla, B. Štefanický. Prostriedky a technika pre likvidáciu nebezpečných látok (2007) [Online] http://www.sszp.eu/wp-content/uploads/b_07-Galla-Stefanicky.pdf
[7] D. Samešová, H. Hybská, A. Ďuricová, 15th International multidisciplinary scientific geoconference SGEM: Ecology and environmental protection, (2015) 275.
[8] Karta bezpečnostných údajov motorovej nafty. Dostupné: http://www.petroltrans.com/wp-content/uploads/2016/06/SDS-M
[9] Karta bezpečnostných údajov motorového oleja. Dostupné: file:///C:/Users/Hybska/Downloads/GSAP_msds_00058181.PDF
[10] Vestník Ministerstva životného prostredia Slovenskej republiky, čiastka 4. (2015). Oznámenie o osobitných podmienkach na udelenie národnej environmentálna skupina produktov: Sorpčné materiály.
[11] Zaraďovací list výrobku CANSORB. Príloha k č. p.: PHZ-603/OS-2007. Dostupné: www.minv.sk.
[12] H. Hybská, M. Villárová. Účinnosť vybraných produktov pri odbúravaní ropného znečistenia. In Acta Facultatis Ecologiae: Technical University in Zvolen. Vol. 27 (2012) 55-59.
[13] Josyp plus. ap-2000-dekra-prüfbericht-05-2014 (1).pdf
[14] Perlit. http://www.lbkperlit.sk/-expandovany-perlit.

Earth in a Trap? 2018
Analytical Methods in Fire and Environmental Science

Impact of foaming agents on vegetation

Veronika Veľková[a][*] – Danica Kačíková[a] – Viera Špureková[a]

[a]*Technical University in Zvolen, Department of Fire Protection*

Abstract

In the article, we have reported about experimental monitoring of the effects of foaming agents on plant organisms. Three kinds of foaming concentrates (protein, synthetic and AFFF) were used for low-expansion foam production. Prepared low-expansion foam was applicate on grass samples. Visual changes in grass samples and changes that have led to grass samples drying have been observed. The seasonal effects of meteorological factors were also observed in the experiment. We determined massive differences between foam stability of AFFF foam in the summer and winter time (foam was compact in December 20 times longer than in August). Also the impact of AFFF foam on the grass samples was influenced by the surrounding temperature conditions (extinction of grass after 2 days in summertime and 6 days in wintertime).

Key words: aqueos film forming foaming agent; protein foaming agent, synthetic foaming agent, low-expansion foam, grass

---

[*] Corresponding author: Veronika Veľková, Tel.: +421 45 52 06 533; e-mail: veronika.velkova@tuzvo.sk.

1. Introduction

The using of new materials, such as plastics, composites, carbohydrate fuels and other oil products necessitates the use of other extinguishing media in the case of fire. The history of foam is known from the end of 19th century. From that time on the methods of foam preparing and producing and, of course, also the composition of foaming agents has been improved. Nowadays the surface active compounds – tensides present the main foam forming substance, which are widely used in households and in industry.

Surfactants are diverse group of compounds built of polar, water soluble, and nonpolar, carbohydrate chain, part. Residual surfactants are after use discharged into sewage or directly into water and contaminate various components of environment (water, sediments, soil). [1]

Tensides are made of natural and petrochemical raw materials.

Surfactants are compounds with significant biological activity. Anion surfactants may bind to bioactive macromolecules, such as peptides, enzymes and DNA. Binding to proteins and peptides may alter polypeptide chain and surface molecule charge. This causes the change of biological function. Cation surfactants attack cytoplasmatic membrane of bacteria. Non-ionic surfactants exhibit antimicrobial activity by binding to various proteins and phospholipid membranes. This binding increases the permeability of the membranes and the vesicles resulting in the leakage of low molecular mass compounds. The result is cell death or damage through ion or amino acid loss. Concerns about surfactants ecotoxicity stem from their enormous use in everyday life. A large part of these compounds is degraded in sewage treatment plants, but a certain amount ends in surface water, soil or sediment. There is also concern about the accumulation of surfactants when cleaning waste sludge [1, 2]

It seems that surfactants, even at low concentrations, may significantly alter the physical and chemical properties of the soil environment and have a significant impact on soil biological agents. Surfactants primarily affect roots, with a relatively low inhibition of wheat shoots. The use of water contaminated with detergent for cultivation reduces photosynthetic rate and chlorophyll content in plants. Continuous deposition of anionic surfactant on soil enhanced acid and alkaline phosphatase activity and allyl sulfatase activity, while soil dehydrogenase activity increased with continuous LAS exposure. [3, 4]

The chronic and sub-lethal toxicity of anionic and non-ionic surfactants for aquatic animals occurs at concentrations typically higher than 0.1 mg/L. Unfavorable biological effects on aquatic organisms occur especially when surfactants occur at relatively high concentrations. The effects of surfactant exposure can be clearly displayed in various organs such as the glands, the liver, the kidney and the spleen. Exposure to a high concentration of surfactants leads to epithelial balls breaking, causing subsequent asphyxiation or nebulous failure, while exposure to sub-lethal concentrations of surfactants causes epithelial radiation hyperplasia, oxidative stress and mucus membrane damage that predispose to microbial attack. [3, 5]

The objective of this paper is to observe impact of various kinds of fire-fighting foams on the environment. We will observe changes of grass samples after application of protein, synthetic and AFFF low-expansion foam.

2. Material and methods

As a sample of the plant material was used Grass Forestina grass, which is excellent for growing new lawns or for trimming bare spots. It is a universal mix that is tailored to our climatic conditions.

Three types of foaming agents were used to observe the effects on plant organisms: Schaumgeist protein foam agent, Fomtec synthetic aqueous film forming foam agent and synthetic foam agent Sthamex.

Schaumgeist is a protein-based high-foaming agent based on natural renewable protein carriers, foam stabilizers and anti-freeze mixtures. It is used to produce low-expansion foam. According to the manufacturer, it is physiologically harmless and biodegradable [6, 7], but it can cause damage to aquatic fauna when leaking into surface water, it can damage activated sludge (bacteria) and foam formation at the sewage treatment plants. When released into the soil, the mixture is mobile and can cause groundwater pollution.

Fomtec AFFF is an aqueous film-forming foam concentrate consisting of fluorocarbon and hydrocarbon surfactants mixed with various solvents, preservatives and stabilizers. It is very important that a large amount of concentrated product does not accumulate in the sewage system and near water courses [7]. The foam agent is intended for use in the firefighting of Class B fires – hydrocarbon fuels such as oil, diesel and aviation fuels. It can be used with suction or exhaust discharge lamps. Fomtec AFFF is formulated using raw materials specifically selected for their fire performance and their environmental profile. It is biodegradable. The foam agent does not contain PFOS or PFOA. [8]

Sthamex foam agent is included among synthetic agents made as a viscous liquid based on 2-butoxyethanol, hydrocarbon surfactants and synthetic AFFF surfactants. The mixture is not classified as dangerous for the environment but contains hardly bio-degradable fluorinated surfactants. If leaked into water, it can cause damage to aquatic fauna, it can damage activated sludge in sewage treatment plants. [9]

By mixing of water and foam agent the 3 % foaming solution was formed. Subsequently, low-expansion foam was produced using a Foambox. By connecting the low-expansion foam nozzle to the Foambox it was possible to apply foam on the grass samples.

Foambox is a Sthamer device. The device is designed to test foaming agents. The pack contains two wells one for low-expansion foam and the other for medium-expansion foam, a foaming solution container, a compressor, a power supply, a pump, connecting hoses. The pump pressure is manually adjustable via the pump bypass valve. [39]

Two seasons were selected for the experiment to observe changes of grass samples after foam application due weather conditions.

The first part of experiment began in June, when grass was planted in 40x30 cm plastic crates. The first foam was applied after two months, in August at an air temperature of 37 °C. Protein (Schaumgeist) and synthetic (Fomtec) foam agents were used

The second part of the experiment began in October, when grass was planted in 40x30 cm plastic crates. The foam was applied after two months, in December at an air temperature of 3 °C. In this part were used only synthetic foam agents.

The aqueous film forming foam agent Fomtec was used in both of experiment variants to observe the effect of ambient conditions on the effect of foam on plant samples.

3. Results and discussion

The aim of the tests was to determine the impact of selected foaming agents on the environment (plant organism). Solutions of the same concentration were used for the preparation of foams, and grass samples were covered with the prepared low-expansion foam. The tests were realized in August and in December, what allows us to consider impact of weather on the foam stability and on the foam influence.

Table 1

The comparison of changes of grass samples after application of protein and synthetic foam in August.

The visible change	Fomtec		Schaumgeist	
	20 min	2 hours	20 min	2 hours
Foam degradation	-	+	+	+
Yellow color of grass	+	+	-	-
Dry up of grass	+	+	-	+
Changes on the soil bottom	-	-	-	-
Straw degradation	-	-	-	-

"+" with change
"-" without change

Table 1 shows the results of observations during the summer period. The foaming concetrate forming water film (Fomtec) and protein foaming agent (Schaumgeist) were used. Differences can be seen with the stability of the applied foam when the Schaumgeist foam has been degraded after 20 minutes after application. Degradation of Fomtec foam appears after 2 hours.

Changes of grass samples were observed visually. The first changes (yellow color of grass) appeared when the Fomtec foam influenced 20 min. Schaumgeist foam did not have this effect. We can assume that it was the action of tensides, as they are the main component of Fomtec foaming agent. Grass samples were dried 2 days after application of both kinds of foam.

In the second experimental part in December we compared two synthetic foaming agents – Sthamex and aqueous film forming foam Fomtec. We can see in the table 2 that the stability of foam was better and time of foam degradation was larger than in August.

Comparison of Sthamex and Fomtec shows more stability for aqueous film forming foam, the time of foam degradation was longer of Fomtec foam than Sthamex foam, where the foam was degradeted after 7 hours after application.

Visible changes of grass samples (yellowing of grass blades) could we see earlier after application of Fomtec foam. Sthamex foam caused only little color differences. Grass samples were dried after 6 days (Fomtec) respective 8 days (Sthamex) after foam application.

Table 2

The comparison of changes of grass samples after application of synthetic foam in December.

The visible change	Fomtec		Sthamex	
	7 hours	9 hours	7 hours	9 hours
Foam degradation	-	+	+	+
Yellow color of grass	+	+	+	+
Dry up of grass	-	+	-	+
Changes on the soil bottom	-	-	-	-
Straw degradation	-	-	-	-

"+" with change

"-" without change

Based on the comparation of results of AFFF Fomtec we can say that the surroundings temperature (temperature of the atmosphere) influences behavior and impact of foam on the vegetation. We can see in the tables 1 and 2 massive differences between foam stability in August (foam degradation 20 min) and in December (foam degradation 7 hours). We can assume that the weather could affect the changes of grass samples. At 37 °C the samples were dried faster and the degradation of the foam appeared faster.

Based on the results in Tables 1 and 2, it can be argued that surfactant-containing foaming agents, especially AFFF, significantly negatively affect the environment. According to Montagnolli [10] research, the presence of AFFF in the soil causes a decline in plant growth, when seed germination of lettuce and rucola were observed and seeds exposed to AFFF did not germinate even after 240 days. A high risk of surfactants is highlighted by research in Australia and Finland, where fluorinated tenzides have been determined in blood and urine of firefighter, which used to use fire extinguishing foams for training or fire suppression. [11, 12]

4. Conclusions

In the article, we have reported about experimental monitoring of the effects of foaming agents on plant organisms. Visual changes in grass samples and changes that have led to grass samples drying have been observed. The seasonal effects of meteorological factors (extinction of grass after 2 days in summertime and 6 days in wintertime) were also observed in the experiment.

There is impossible to get away tenzides from our life because of their widely using in household, industry and last but not least for fire suppression. Taxing the advantageous effects of surfactants and adversely impacting on the environment, we can ensure as little damage as possible to water, soil and living organisms.

Acknowledgements

This work was supported by the Slovak Scientific Grant Agency VEGA under contract No. VEGA 1/0806/17 (50%) and by the Slovak Research and Development Agency under the contract No. APVV-14-0468 "Development of an auxiliary device and its technological employment to increase the efficiency of extinguishing forest fires" (50%).

References

[1] T. Ivankovic, J. Hrenovic. Ssurfactants in the environment. University of Zagreb Faculty of Science. Arh Hig Rada Toksikol 2010;61:95-110. DOI: 10.2478/10004-1254-61-2010-1943

[2] H. Hybská, D. Samešová. Ecotoxicology. Zvolen. Technical University in Zvolen, 2015. - 164 p. ISBN 978-80-228-2750-8

[3] S. Rebello,A. K. Asok, S. Mundayoor, M. S. Jisha. Surfactants: toxicity, remediation and green surfactants. Environ Chem Lett (2014) 12: 275.

[4] H. Hybská, D. Samešová, H. Ollerová. Impact of organic pollutants on the environment. Zvolen : Technical University in Zvolen, 2015. - 186 s.

[5] D. Samešová, H. Hybská. Water technology. Technical University in Zvolen, 2015. - 170 p. ISBN 978-80-228-2816-1

[6] SCHAUMGEIST: Technical sheet

[7] FOMTEC AFFF 3%: Technical sheet

[8] STHAMEX AFFF 1%: Technical sheet

[9] FoamBox: FoamGenerators/PicoFoamGenSTHAMER-/TM100OperatingInstructionsFoamboxenglish.pdf

[10] R. N. Montagnolli, P. R. Matos Lopes, J. Matos Cruz, E. M. Turini Claro, G. M. Quiterio, E. D. Bidoia. The effects of fluoride based fire-fighting foams on soil microbiota activity and plant growth during natural attenuation of perfluorinated compounds. ISSN: 1382-6689. Environmental Toxicology and Pharmacology 50 (2017) 119-127.

[11] A. Rotander, L.-M. L. Toms, L. Aylward, M. Kay, J. F. Mueller. Elevated levels of PFOS and PFHxS in firefighters exposed to aqueous film forming foam, Environment International 82 (2015) 28-34. ISSN 0160-4120.

[12] J. A. Laitinen, J. Koponen, J. Koikkalainen, H. Kiviranta. Firefighters exposure to perfluoroalkyl acids and 2-butoxyethanol present in firefighting foams. Toxicology Letters 231 (2014) 227-232. ISSN 0378-4274.

Earth in a Trap? 2018
Analytical Methods in Fire and Environmental Science

Research of fabric air permeability for miner’s overalls

Oksana A. Vigelina[a] – Irina V. Andreeva[a] – Andrei Nikulin[b] –

Lyudmila V. Stepanova[b] – Anni Yu. Nikulina[b]

[a]*St. Petersburg State University of Industrial Technologies and Design, 18, Bolshaya Morskaya Str., St. Petersburg 191186, Russian Federation*

[b]*Saint-Petersburg Mining University, Saint Petersburg, Russian Federation*

Abstract

The article describes an algorithm of fabric contamination with coal dust and presents the results of the experimental surveys of the air permeability of two types of fabrics used to make special clothes for mine workers depending on the degree of clothes contamination. The peculiarities of coal dust particle distribution in material fibres have been identified and the impact of contamination on fabric physical and hygiene properties has been evaluated.

Keywords: human ressources; safety; Arctic; corporate social responsability; PPE; coal dust; fabric air permeability; fabric; OHSAS; labor.

---

1. Introduction

The miners' arduous working conditions in the Arctic severe climate require from mining companies to care for and attend to the needs of their human resources to retain workforce. The corporate social responsibility programmes of the companies with operations in the North aim at reducing industrial injuries and occupational disease rates. This is driven by research focused on the enhancement of the protective properties of personal protective equipment and special working clothes.

The main properties of fabrics used to make special clothes include physical and hygiene properties, which ensure normal thermal regulation within the workers' bodies in the course of work. With optimal values of these properties, workers feel comfort which is possible when a specific ratio of heat generation and heat loss is maintained in the human body [1]. Apart from providing thermal comfort, the hygiene property of clothing materials is related to the need to eliminate the waste products of the human body from under the clothes [2]. Metabolic products are excreted through the respiratory tract and from the skin surface to the environment as gas and drops of liquid [3]. These products may have adverse and even toxic effects on the human body which may result in a change in fabric properties and irritation of skin [18-19].

Hygiene requirements increase for the materials used in special clothes worn at coal mines due to confined space and performance of high-energy work [4, 16]. One of the ways of heat loss during intensive physical exercise is convection. Therefore fabric air permeability is one of the most important properties to be taken into account when making special clothes for coal miners. Apart from physical and hygiene properties, special clothes must have protective functions and protect employees against industrial contamination and especially coal dust [17]. It means that additionally to a high air permeability level, fabrics must have low dust permeability.

The most comprehensive research of fabric air permeability is presented in the works by N.A. Arkhangelskiy who introduced as one of property characteristics an air permeability factor with a specific given pressure differential and a technical air permeability factor with a pressure differential of 1 mm WG and developed a classification for textiles based on their air permeability including a wide list of materials from the most permeable (gauze or net) to the densest ones (thick cloth or woollen cloth). N.A. Arkhangelskiy studied how structure characteristics, in particular through porosity, impacted the air permeability of thin cotton fabrics with a plain or twill weave [5].

Later, research focused on the influence of various factors on fabric air permeability: the study of fabric density on air permeability, the nature of fibre distribution in a material, type of fabric weave, fibre geometry, temperature influence, and degree of fabric wear [6-11]. However, a change in the air permeability of fabric contaminated with coal dust is still understudied. The air permeability of fabrics is measured in standard conditions which are significantly different from real operation conditions which may lead to results that do not correlate to these properties in real conditions.

An experiment has been conducted to study this subject with the aim to assess changes in the air permeability of the fabrics used in special clothes worn by coal miners depending on the degree of their contamination with coal dust.

2. Method

The experiment was conducted with the following objectives:

- Sample and contaminate fabrics with coal dust of various density;
- Determine air permeability of each sample; and
- Identify a correlation between fabric air permeability and the degree of fabric contamination with coal dust.

Two fabrics were sampled for the study: Gorizont T40 and FAS(Table 1):

Table 1

Characteristics of Gorizont T40 and FAS

Characteristics	**Gorizont T40 fabric**	**FAS fabric**
Surface density, g/m^2	370	390
Fibre composition	75% cotton and 25% polyester	100% cotton
Particles confinement class	IV	IV

Gorizont T40 is the main fabric used to make miner's overalls pursuant to GOST 12.4.110-82, Miner's Overalls for Protection against Mechanical Impacts and Overall Industrial Contamination. It meets the requirements of the Technical Rules of Procedure of the Customs Union on the Safety of Personal Protective Equipment [12-13].

FAS is one of the most popular fabrics used to make special clothes in European countries, including special clothes for the mining industry. The fabric is certified in Russia as per GOST 11209-2014, Fabrics for Protective Clothing. Technical General Requirements. Methods for Testing [14].

Preparation for tests:

- A total of five FAS samples and six Gorizont T40 samples were collected in accordance with GOST 20566-75, Fabrics and Textile Items. Rules for Acceptance and Sampling Method.
- The fabric samples were contaminated with coal dust as follows: A required quantity of white paper sheets sized to match a tested fabric sample was prepared. Then, each sample was weighed using laboratory scales accurate to 0.01 g, a required amount of coal dust with particles sized 0 to 80 µm was weighed using laboratory scale (+0.05 to 0.08 g taking into account loss during contamination and depending on a fabric sample size) and distributed evenly across the white sheet of paper. A prepared fabric sample was put with its face down onto the sheet of paper with coal dust and turned with the sheet over using a glass cylinder with a weight of 300 g. The sheet of paper was then rolled for ten cycles and the fabric sample was then overturned, separated from the paper and weighed. If required contamination density was achieved, measurements were started. Otherwise, the contamination procedure was repeated.
- A total of five fabric samples were prepared with contamination density of 10, 20, 30, 40, and 50 g/m2.

Air permeability was tested in the testing laboratory of Univers-Test of the St. Petersburg State University of Industrial Technologies and Design based on GOST 12088-77, Textile Materials and Articles of Them. Method of Determination of Air Permeability [15] using FF-12 (Fig. 1)

Fig. 1. FF-12 used to measure air permeability

The main process flow chart for the device is shown in Fig. 2.

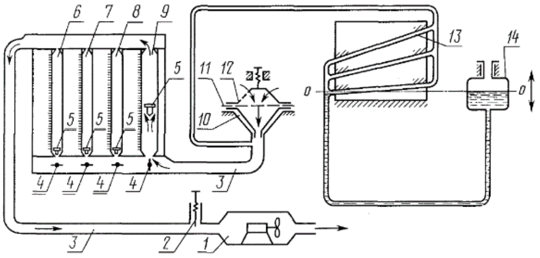

Fig. 2. Device components: 1 – electrical fan, 2 – needle valve, 3 – connecting tubes, 4 – variable area flowmeter handles, 5 – variable area flowmeter floats, 6, 7, 8, and 9 – variable area flowmeters, 10 – replaceable table, 11 – fabric used, 12 – counter ring, 13 – micropressure gage, 14 – vessel with distilled water [15].

Replaceable table 10 with an area of 10 cm^2 was used for testing. The testing involved depression under the spot sample of 49 Pa. A variable area flowmeter was selected based on fabric air permeability. Number of tests: 10.

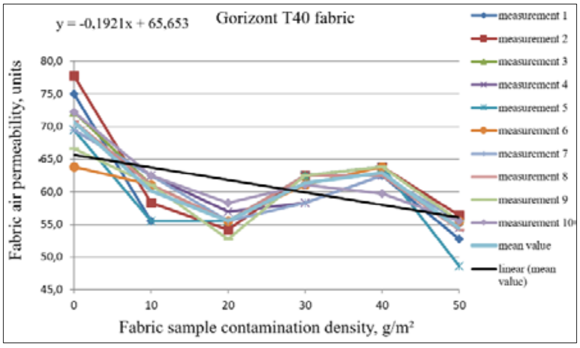

Fig. 3. Correlation between a thermal conductivity factor and degree of contamination with coal dust

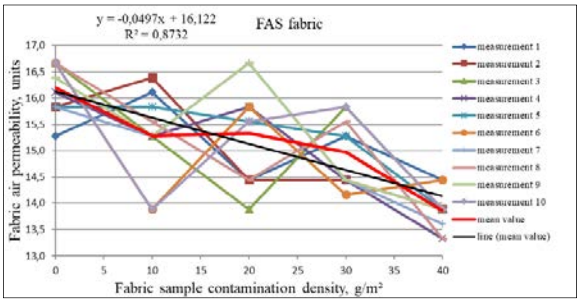

Fig. 4. Correlation between the air permeability of FAS fabric and degree of contamination with coal dust

A test result was a mean air permeability value from all measurements per spot sample.

Mean air permeability values for fabric Q in dm^3/m^2 from each spot sample are calculated using formula 1.

$$Q = \frac{100*V}{36*S} \quad (1)$$

where,

V is the arithmetic mean of an air flow from all spot sample measurements (variable area flowmeter readings), dm^3/hour;

S is a tested area, cm^2.

The result was calculated accurate to 0.1 dm^3/m^{2}s.

The results were used to build a correlation between fabric air permeability and contamination density. Relevant data is shown in Fig. 3 and 4.

Figures 5 and 6 show pictures of each fabric sample with various contamination density made using MBS-9 microscope.

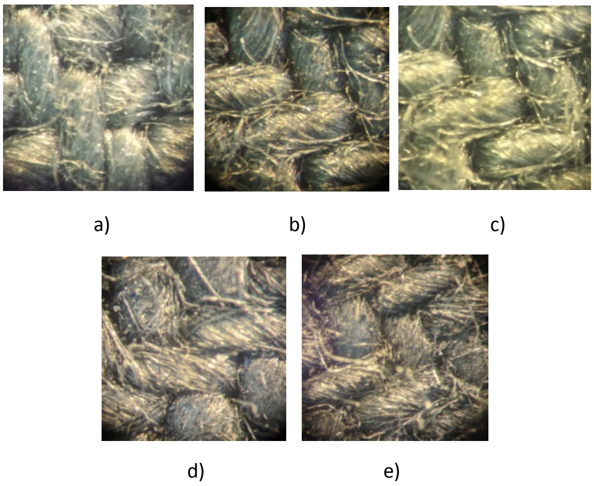
a) b) c)

d) e)

Fig. 5. Pictures of FAS fabric with various contamination density under the microscope: a) clean fabric b) 10 g/m^2 c) 20 g/m^2 d) 30 g/m^2 e) 40 g/m^2

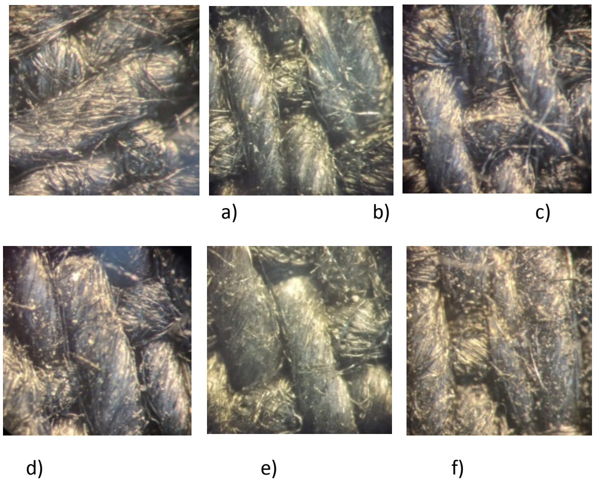
a) b) c)

d) e) f)

Fig. 6. Pictures of Gorisont T40 fabric with various contamination density under the microscope: a) clean fabric b) 10 g/m^2 c) 20 g/m^2 d) 30 g/m^2 e) 40 g/m^2 f) 50 g/m^2

4. Discussion

The results obtained certify that air permeability decreases when fabric samples are contaminated with coal dust (Fig. 3 and 4) since air permeability indicators, i.e. the number of pores in the structure and their size, are affected by material porosity. With minor contamination, pore size decreases, while more significant contamination reduces their number (Table 2).

Moreover, when air passes through fabric pores, a portion of energy is consumed for air friction against fabrics and it decreases with minor fabric contamination with coal dust, which makes fibres more oiled. Larger contamination density increases fabric resistance to airflow and therefore impairs fabric air permeability.

Therefore, contamination of miner's overalls with coal dust slows down heat loss by workers and prevents normal evaporation of moisture from the skin surface which affects thermal comfort and leads to full or partial abandonment of miner's overalls in the work process.

5. Conclusions

1. Miners employed by the companies with operations in the Arctic work and live in severe environmental conditions and their employers must be very sensitive to their needs. One of the essential areas for corporate social responsibility is provision of safe and comfortable working conditions.
2. Contamination of miner's overalls with coal dust results in a reduced heat flow from the human body to the environment which may affect the worker's thermal comfort. It is especially relevant during high-energy works.
3. When choosing fabrics to make special clothes, including miner's overalls, clothes contamination during use must be taken into account.
4. The test has revealed that the air permeability of Gorizont T40 fabric changes depending on the degree of contamination from 70 dm^3/m^2 s to 50 dm^3/m^2 s (a 25% reduction), while respective figures for FAS fabric are 16 dm^3/m^2 s to 14 dm^3/m^2 s (a 15% reduction). It means that the air permeability of Gorizont T40 is larger but its reduction is more expressed as compared to that for FAS fabric.

Acknowledgments

The research was funded by the Russian Scientific Foundation, Project No. 17-78- 20145, Social and Economic Levers for Mobilizing Human Resources to the Arctic Region of the Russian Federation. Saint-Petersburg Mining University.

References

[1] Jurgen Haase. Testing and Assessment of the Hygiene Properties of Textile Items. //Textiltechnik. 1980. - Bd. 30. - No. 3. - P. 314–318.

[2] Clothing Comfort. Interaction of Thermal, Ventilation, Construction and Assesment Factors. Edited by N.R.S. Hollies, R.F. Goldman. The Fiber Society Inc. Comfort Symposium Proc. Ann Arbor Science Publishers Inc. USA. — 1977.

[3] Slonevskiy, S.I., Mironova, A.I. Study of Clothing Microclimate //Collection: Studies of Clothing Hygiene. Works of the AMS of the USSR. T.ZO. — Moscow: Medgiz. -1953.

[4] M. A. Montoliu, V. Gonzalez & L. Palenciano (2007) Cardiac frequency throughout a working shift in coal miners, Ergonomics, 38:6, p. 1250–1263.

[5] Arkhangelskiy, N.A. Fabric Air Permeability. Operational properties of fabrics and current research methods. — Rostekhizdat. 1960. - P. 376-413.

[6] Korotkova, I.V., Bukharin, V.I. Theoretical and experimental studies of textile porosity. — Moscow: 1983. Dep. in TsNIITEIlegprom. - No. 868.

[7] Skvortsova, V.N. Dependence of fabric air permeability on the maximum length of covering //Textile industry. 1968. No. 6 P. 75–76.

[8] Kondratskiy, E.V. Regarding Fabric Porosity // Izvestiya vuzov. Textile Industry Technology, 1971, No. 3, pp. 27–31.

[9] Hearle J.W.S., Konopasek M. Newton A. On some general features of a computer-based system for calculation of the mechanics of textile structures // Text. Res. J. r v.42, N10, 1972, p.613-626.

[10] Sumit Mandal, Guowen Song An Empirical Analysis of Thermal Protective Performance of Fabrics Used in Protective Clothing, The Annals of Occupational Hygiene, Volume 58, Issue 8, 1 October 2014, p.1065–1077.

[11] Shustov, Yu. S., Mikheev, A.A. Impact of Wearing on Cotton Fabric Porosity. Design and Technologies. 2010. No. 17 (59). P. 127-134.

[12] GOST 12.4.110-82, System of Labor Safety Standards. Miner's Overalls for Protection against Mechanical Action and General Industrial Contaminations. Specifications.

[13] Technical Rules of Procedure of the Customs Union, TRP CU 019/2011, On the Safety of Personal Protective Equipment.

[14] GOST 11209-2014, Fabrics for Protective Clothing. Technical General Requirements. Methods for Testing.

[15] GOST 12088-77, Textile Materials and Articles Made of Them. Method of Determination of Air Permeability.

[16] Kazakov B.P., Levin L.Yu., Shalimov A.V., Zaitsev A.V. Development of Energy-Saving Technologies Providing Comfortable Microclimate Conditions for Mining. Zapiski Gornogo instituta. 2017. Vol. 223: p. 116-124. DOI: 10.18454/PMI.2017.1.116

[17] Korshunov G., Rudakov M., Stepanova L. Validation of requirements to miner suit on the basis of human heat exchange at performance of underground works, Pollution Research, Vol. 35, Issue 4, 2016; P. 919-922.

[18] Parchanski J. Risk of injuries among coal mine workers and its hysteresis. Zapiski Gornogo instituta. 2016. Vol. 222: p. 869-876. DOI 10.18454/PMI.2016.6.869

[19] Nikulin, A., Nikulina, A. Yu. Assessment of occupational health and safety effectiveness at a mining company. Eco. Env. & Cons. 23 (1): 2017, pp. 533-537.

Agroforestry as a tool for sustainable land use in Central European countries

Andrea Vityi[a*] – Nóra Kiss Szigeti[a] – Tamás Rétfalvi[b] – Emes Dominkó[b] – Bohdan Lojka[c] – Radim Kotrba[d,e] – Jaroslav Jankovič[f] – Michal Pástor[f] – Robert Borek[g]

[a]University of Sopron, Faculty for Forestry, Institute of Forest and Environmental Techniques,, Bajcsy-Zs. 4. Sopron, 9400, Hungary

[b]University of Sopron, Faculty for Forestry, Institute of Chemistry, Bajcsy-Zs. 4. Sopron, 9400, Hungary

[c]Czech University of Life Sciences Prague, Faculty of Tropical AgriSciences, Department of Crop Sciences and Agroforestry, Kamycka 129, Praha 6, 165 00, Prague, Czech Republic

[d]Czech University of Life Sciences Prague, Faculty of Tropical AgriSciences, Department of Animal Science and Food Processing, Kamycka 129, Praha 6- Suchdol, 165 00, Prague, Czech Republic

[e]Institute of Animal Science, Department of Ethology, Pratelstvi 815, Praha- Uhrineves, 104 00, Prague, Czech Republic

[f]National Forest Centre, Forest Research Institute in Zvolen, Department of Silviculture and Forest Production, T. G. Masaryka 22, 960 92 Zvolen, Slovak Republic

[g]Institute of Soil Science and Plant Cultivation, State Research Institute, ul. Czartoryskich 8 , 24-100 Pulawy, Poland

---

Abstract

Agroforestry systems can increase resource efficiency, enhance productivity, and improve the overall resilience of agro-ecosystems. Agroforestry has a long tradition, however their widespread use has been interrupted by introduction of industrial agriculture and in some countries by political changes connected with collectivization and land consolidation. As reflection to unsustainable use of land by post-communist co-operations/enterprises, agroforestry has become a rediscovered practice of mainly family farmers in the countries of Central Europe in the last years. Traditional agroforestry systems in this region represent traditional land use systems with a high environmental and cultural value. This region also has a high potential for establishment of modern agroforestry systems which could be a great source of inspiration to learn about interactions, symbioses, biodiversity and agroforestry strategies and practices in such multifunctional systems under adaptation to climate change. The paper gives a general overlook of the role of agroforestry in Hungary, Slovak Republic, Czech Republic and Poland with special regard on the following issues:

- the main reasons that make it necessary to investigate the potential of modern agroforestry practices and technologies to alleviate/mitigate the environmental problems in the Central European region
- the new initiatives with the aim of preserving traditional and establishing modern agroforestry systems
- main drivers and barriers regarding the adaptability and legalisation of agroforestry systems
- the potential of agroforestry practices in sustainable land management.

Keywords: agroforestry; sustainable land use; efficiency, productivity

---

[*] Corresponding author. Tel.: +36-99-518-966; e-mail: vityi.andrea@uni-sopron.hu

1. Introduction

Agroforestry (AF) is the land use practice of integrating woody vegetation with crops and/or livestock systems to optimise the benefits from their ecological and economic interactions. As multi-purpose mixed and integrated system, agroforestry has thousand of types with different combination of woody, herbaceous and animal components, adapted to local conditions. Furthermore, AF practices may vary both by spatial and temporal point of view. (Mosquera-Losada et al., 2016)

A recent study from EU-JRC compared the ecological benefits of eighteen of the EFA elements[1] and found agroforestry highest in almost all countries surveyed. (Tzilivakis et al., 2015). In the Ricardo/IEEP study published recently (Martineau et al. 2016), in total 22 mitigation actions were assessed in a meta-review of mainstreaming climate action in the Common Agricultural Policy (CAP) and concluded that agroforestry is among the mitigation actions having the greatest potential. Also new results of project SOLMACC[2] (Guttinger, 2016) proves that it is possible to reduce GHG emission from agriculture practices such as agroforestry, improved on farm nutrient recycling, or improved crop rotation and among all agroforestry had the highest record in greenhouse gas saving. The FP5[3] Silvoarable Agroforestry for Europe (SAFE) research project (2001-2005) used field experiments and modelling to show that agroforestry could increase land resource use efficiency by up to 40%, relative to “standard” monoculture arable or monoculture woodland systems (Dupraz et al., 2005).

The introduction of agroforestry practices can greatly contribute to increase the sustainability of farming and diversifying production (e.g. fruits, woody biomass, fibres) making farms more resilient to market changes and more profitable. All these aspects are key to recognize the important role that AF has to play as a technique for mitigation and adaptation of rural areas to climate change. To reach the goals of maintaining and protecting national resource services may be possible through agroforestry programmes carried out in cooperation with rural populations. (Szedlák, 1993).

2. State of Agroforestry in Central Europe

Agroforestry has been practiced from the beginning of agriculture in the whole of Europe. Despite of its presence as a traditional land use practice in the Central region of Europe as well, it has been regressed and disappeared from large areas of the countryside during the last decades. This is mainly due to the mechanization and intensification of agriculture in the second half of the 20th century as a result of which majority of tree components, such as protective green belts and hedges from agricultural land had been removed, leading to gradual disappearance of agroforestry from the landscape of the Central European post-communist countries.

Today, there is limited information available on the extent of agroforestry in the Central region, especially as regards the modern practices. At the same time recent studies (Hartel and Plieninger, 2014; den Herder et al., 2016) implies that agroforestry – both in traditional and modern form – might be present to a notable extent in the landscape of this region.(Table 1)

The remnants of traditional agricultural systems can be seen in the landscape of all the examined countries. Silvopastoral systems exists in whole of Central Europe but varies by countries. In the Czech Republic the extensive fruit orchards grazed by sheep , cattle, or deer are among the most widespread practice used in areas less favourable for intensive agricultural activity (e.g. mountains – regions of

---

[1] An Ecological Focus Area (EFA) is an area of land upon which agricultural practices that are beneficial for the climate and the environment are carried out by using six EFA options on their own or in combination: fallow land, buffer strips, field margins, catch crops, green cover, nitrogen-fixing crops

[2] SOLMACC (Strategies for organic and low-input farming to mitigate and adapt to climate change) is a LIFE-co-funded project that runs from 2013 to 2018. Web: http://solmacc.eu/

[3] Fifth Framework Programme (set out the priorities for the European Union's research, technological development and demonstration activities for the period 1998-2002)

White Carpathians and Bohemian Forest). (Zelba et al. 2015) Large part of mountain areas in Polish Carpathians and to some extent on lower areas is covered by traditional varieties of fruit trees, growing individually or in clumps on mid-field bulks or as orchards nearby households, here often grazed by cattle or sheep. Recently, there is a growing interest in planting traditional varieties of fruit trees across Poland (e.g. by projects of AgriNatura Foundation) and new silvopastoral orchards started to appear as well. Herzog (1998) defines it as fruit trees dispersed on cropland, meadows and pastures in a rather irregular pattern. Woodpastures including also forest tree species and wild fruit trees are important landscape elements in all four countries. (Zajączkowski 2005; Varga-Bölöni, 2009; Vityi – Varga 2014; Bobiec and Koziarz 2017; Jankovič – Čaboun, 2017) These semi-natural ecosystems are usually grazed or mown while trees have several role: provide shade, wind protection, fodder and fruit while at the same time offering habitat to a great variety of insects and birds e.g. hermit beetles, bumblebees, little owls and hoopoes. By shade and wind protection, trees reduce heat stress of animals and subsequently reduce food requirements, improve numbers of calves and intervals between calves (Quam et al. 1994). Providing additional leaf foliage or fruit deliver plenty of valuable nutrients and substances increasing resistance, they are also important in times of drought (Smith et al. 2012a, b). High-quality meat products (beef, lamb) can be produced here. Therefore, these systems have high economic, environmental and cultural value and serve as in situ conservation of traditional germplasm.

As regards traditional silvoarable systems, Central European countries are characterized again by a high degree of variation. In the Czech Republic and Poland the intercropped fruit orchards present in the landscape but to a lower extent. Mainly organic farmers are interested in re-implementation of this practice. This kind of practice – in a smaller scale - is also used in household gardens or kitchen gardens recently be considered as agroforestry systems. This is commonly used in the Czech, Hungarian, Polish and Slovak rural areas where mixed fruit and vegetable gardens with grazing animals are part of traditional households. Apart from these typical agroforestry systems, scattered trees and small woodlots on farmlands are found commonly in many areas. The fragmented structure of farms and diverse topography favour the presence of small groups of trees on agricultural land, especially in the central and eastern parts of Poland or the hilly areas of Hungary. (Borek, 2015; Vityi et al. 2017)

The use of hedges and live fences along the field borders, streams and slope contours has also a long tradition in the Czech Republic and similarly windbreaks in agricultural lands, buffers along watercourses and lakes as well as along linear infrastructures (roads, channels etc.) in Czech Republic, Hungary, Poland and Slovakia. (Vityi et al. 2015; Frank - Vityi 2016, Kędziora 2015; Zajączkowski 2005) Unfortunately, the era of collectivization led to their drastic reduction, however remnants can still be found. The importance of these systems for biodiversity conservation (so called ecologic networks or green infrastructure), environmental protection and climate adaptation is now recognized (Ryszkowski 2001) and therefore new establishment or conservation of these landscape elements is supported from various programs at different levels (e.g. RDPs[4] , greening subsidies or local grants) depending on the country.

Other agroforestry systems such as intercropping of forest trees and forest farming/gardening can also be found in the landscape of the region but with lower extension. Intercropping of forest trees involves interplanting trees in forest during first years after establishment. It was practiced in various forms until the 19th century and even promoted by foresters e.g. in Southern Moravia and Hungary. Currently the system is practiced only in small part of floodplain forest in the Czech Republic and in few sites in Hungary where crop cultivation helps weed reduction and protection of seedlings against extreme weather and wild animals. (Vityi et al. 2016)

We can find also a few examples of forest farming/gardening in each countries, however,

---

[4] National Rural Development Programs

usually as hobby farming or experimental plots based on classification of land and ownership (on forest land is illegal to let graze livestock in Poland and Czech Republic). Nevertheless breeding of game animals in fenced areas mainly on forest land for improvement of trophies for hunting has a long tradition (Bartoš et al, 2010). The collection of wild fruits, mushrooms and medicinal plants is widespread in Czech, Hungarian and Polish forests; however, it is not managed as agroforestry and therefore is not considered as AF in this region.

Table 1

Estimation of the extent of AF systems in the examined CE-countries (based on den Herder et al. 2016.)

Country	Total territorial area	Utilised Agricultural area (UAA[5])	High value tree agroforestry	Livestock agroforestry	Arable agro-forestry	All agroforestry	Estimated proportion of total territorial area	Estimated proportion of UAA
	1000 ha	1000 ha	1000 ha	1000 ha	1000 ha	1000 ha	%	%
CZ	7887	3484	7.2	45.8	0.0	45.8	0.6	1.3
HU	9302	4686	2.0	36.1	2.0	38.1	0.4	0.8
PL	31268	14447	14.3	97.5	2.9	100.4	0.3	0.7
SK	4904	1896	2.0	41.9	2.0	43.9	0.9	2.3

---

[5] Source: Eurostat online data sources: Farm structure statistics (2010)

Currently, no data are available about extension of modern agroforestry systems, as these are rather rare and non-formal. Among systems recognized as modern agroforestry alley cropping for quality timber production (e.g. wild cherry, walnut) and wood biomass (e.g. poplar) exists in the countries of the Central region. During the last years a growing potential and interest appeared in establishment of timber production agroforestry systems as well as in short rotation coppice systems (SRC) based on fast-growing species of willows and poplars (as well as black locust in Hungary). These systems provides energy biomass or quality wood besides the annual yield of agricultural crops grown in alleys of SRC but can be also combined with animals (eg. poultry, chickens and pigs) for quality meat and organic egg production. Czech and Hungarian experiments prove the multiple positive effects of animals on tree growth (eg. increase of soil nutrients and decrease of some harmful pest insect’s development stages) and the favourable effects of trees and tree fodder on animal welfare (eg. shelter against predatory birds, improvement of fodder quality).

3. Perspectives

Increased emphasis on the environmental aspects of agriculture is one of the most significant changes in the new common agricultural policy (CAP) of the EU.(Lawson et al., 2015) Agroforestry systems seen in the context of "green economy" ensure the efficient use of natural resources and effective management to prevent environmental degradation and minimize waste. Effective use of natural resources will undoubtedly be a decisive factor of competitiveness in the private sector too. In agriculture, when switching to green economy principles, agroforestry systems could play an important role in solving current challenges such as climate adaptation, biodiversity conservation, water cycle improvement (Ellison et al. 2017) and sustainable use of marginal and erosion-prone areas. In addition, trees and agroforestry systems are more carbon-safety (Zomer et al. 2016) than conventional agricultural systems, they can provide higher incomes for farmers, give job opportunities to rural people, and thus help solve the negative consequences of the persistent rural depopulation trend.

The recent shift in the European and the national agricultural policies leading to more environmentally friendly agricultural production and sustainable rural development could support tree growing on agricultural land. Therefore, it is crucial to raise awareness of policy makers and practitioners to agroforestry systems where trees can play number of positive roles. The EURAF is striving for agroforestry systems to play an important role in agriculture, with an ambitious goal to use agroforestry in Europe by 50 % of farmers until 2025.

Acknowledgments

We acknowledge the support of the AFINET project, which receives funding from the European Union Framework Programme under grant agreement no 727872, the EFOP-3.6.2-16-2017-00018 „Agrárerdészet - termeljünk együtt a természettel” project co-financed by the European Social Fund. Authors were also supported by the Faculty of Tropical AgriSciences – CULS Prague IGA-20185017 and by Ministry of Agriculture of the Czech Republic, institutional support MZE-RO0718. The authors state that there are none existing financial and personal conflicts of interest.

References

[1] Bartoš L., Kotrba R., Pintíř J. 2010. Ungulates and their management in the Czech Republic, In: European Ungulates and their Management in the 21st century, (Eds.) Apollonio M., Andersen R., Putman R., Cambridge University Press, London, UK, p. 243-261.

[2] Bobiec A., Koziarz M. 2017. Potential of oak (Quercus robur) regeneration in the rural landscape of the Carpathian foothills in SE Poland. The case of PLH180012 Natura 2000 site. Wooded Rural Landscapes in Central and Eastern Europe: Biodiversity, cultural legacy and conservation. 20-22 September, University of Rzeszów, Poland.

[3] Borek, R (2015): Agroforestry in Poland – the current state and policy perspectives. In: 3rd European Agroforestry Conference: Celebrating 20 years of Agroforestry research in

Europe. Book of abstracts. Montpellier, 2016. (pp.439-441) European Agroforestry Federation

[4] den Herder, M., Moreno, G., Mosquera-Losada, M.R., Palma, J.H.N., Sidiropoulou, A., Santiago Freijanes, J.J., Crous-Duran, J., Paulo, J., Tomé, M., Pantera, A., Papanastasis, V., Mantzanas, K., Pachana, P., Papadopoulos, A., Plieninger, T., Burgess, P.J. (2016). Current extent and trends of agroforestry in the EU27. Deliverable Report 1.2 for EU FP7 Research Project: AGFORWARD 613520. (15 August 2016). 2nd Edition. 76 pp.

[5] Dupraz, C, Burgess, PJ, Gavaland, A, Graves, AR, Herzog, F, Incoll, LD, Jackson, N, Keesman, K, Lawson, G, Lecomte, I, Mantzanas, K, Mayus, M, Palma, J, Papanastasis, V, Paris, P, Pilbeam, DJ, Reisner, Y, van Noordwijk, M, Vincent, G, van der Werf, W (2005). SAFE (Silvoarable Agroforestry for Europe) Synthesis Report. SAFE Project (August 2001-January 2005).

[6] Eichhorn M, Paris P, Herzog F, Incoll L, Liagre F, Mantzana K, et al. 2006. Silvoarable systems in Europe – past, present and future perspects. Agroforestry Systems 67: 29-50.

[7] Ellison D, Morris CE, Locatelli B, Sheil D, Cohen J, Murdiyarso D, Gutierrez V, van Noordwijk M, Creed IF, Pokorny J, Gaveau D, Spracklen DV, Tobella AB, Ilstedt U, Teuling AJ, Gebrehiwot SG, Sands DC, Muys B, Verbist B, Springgay E, Sugandi Y, Sullivan CA. 2017. Trees, forests and water: Cool insights for a hot world. Global Environmental Change-Human and Policy Dimensions 43: 51-61.

[8] Frank N., Vityi A, (2016): Shelterbelts in Hungary. In: 3rd European Agroforestry Conference - Book of Abstract. European Agroforestry Federation, Montpellier. pp 42-44

[9] Guttinger, A. (2016): How can (organic) farming practices reduce greenhouse gas emissions? Seminar on CAP and Climate Change - How can the CAP drive climate change mitigation and adaptation in the agriculture sector? 09/11/2016, Brussels. http://solmacc.eu/wp-content/uploads/2016/11/SOLMACC-presentation_Andreas-Gattinger.pdf

[10] Hartel, T, Plieninger, T (ed., 2014): European Wood-pastures in transition. A Social-ecological Approach. Routledge, 2014.

[11] Herzog F. 1998. Streuobst: a traditional agroforestry system as a model for agroforestry development in temperate Europe. Agroforestry Systems 42: 61–80. doi: 10.1023/A:1006152127824

[12] Jankovič, J., 2015: Agrolesnícke systémy v Európe a perspektíva ich využívania na Slovensku [Agroforestry systems in Europe and their perspective in Slovakia]. In: Aktuálne problémy v zakladaní a pestovaní lesa. Zborník referátov z 3. medzinárodnej konferencie, ktorá sa konala 5.-6. októbra 2015 v Liptovskom Mikuláši. NLC, Zvolen 2015. ISBN 978-80-8093-203-9, pp. 106-113 (in Slovak).

[13] Jankovič, J.: Aká je perspektíva využívania agrolesníckych systémov na Slovensku? [What is the perspective of utilization of agroforestry systems in Slovakia?] Les & Letokruhy. 11-12/2015, pp. 16-18 (in Slovak).

[14] Jankovič, J., Čaboun, V., (2017): Poznatky z mapovania borievkových porastov na Slovensku [Findings from the mapping of Common juniper stands in Slovakia]. In: Sitková, Z., Pavlenda, P. (eds.), 2017: Dlhodobý ekologický výskum a monitoring lesov – súčasné poznatky a výzvy do budúcnosti. Zvolen, Národné lesnícke centrum – Lesnícky výskumný ústav Zvolen, pp. 67-71 (in Slovak).

[15] Kędziora, A. (2015). The network of shelterbelts as an agroforestry system controlling the water resources and biodiversity in the agricultural landscape. Papers on Global Change IGBP: 22 pp. 63-82. 10.1515/igbp-2015-0016

[16] Lawson, GJ, Balaguer, F, Palma, JHN, Papanastasis, V (2015): Options for agroforestry in the CAP 2014-2020. In: 3rd European Agroforestry Conference: Celebrating 20 years of Agroforestry research in Europe. Book of abstracts. Montpellier, 2016. (pp.424-427) European Agroforestry Federation

[17] Mosquera-Losada MR, Santiago-Freijanes JJ, Rois M, Moreno G, Pisanelly A, Lamersdorf N, den Herder M, Burgess P, Fernández-Lorenzo JL, González-Hernández P, Rigueiro-Rodríguez A (2015): CAP and agroforestry practices in Europe. In: 3rd European Agroforestry Conference: Celebrating 20 years of Agroforestry research in Europe. Book of abstracts. Montpellier, 2016. (pp.428-430) European Agroforestry Federation

[18] Quam, V., Johnson, L., Wight, B., & Brandle, J. R. (1994). Windbreaks for livestock operations. Papers in Natural Resources, 123.

[19] Ryszkowski L ed. (2001) Landscape ecology in agroecosystems management. CRC Press, pp. 29-56.

[20] Smith, J., Pearce, B. D., Wolfe, M. S. (2012) a. A European perspective for developing modern multifunctional agroforestry systems for sustainable intensification. Renewable Agriculture and Food Systems, 27(4), 323-332.

[21] Smith, J., Leach, K., Rinne, M., Kuoppala, K. (2012) b. Integrating willow-based bioenergy and organic dairy production–the role of tree fodder for feed supplementation. Agriculture and Forestry Research, (362), 394-397.

[22] Tzilivakis J, Warner DJ, Green A, Lewis KA (2015) : Guidance and tool to support famers in taking aware decisions on Ecological Focus Areas. University of Hertfordshire.

[23] Varga A. – Bölöni J. (2009): Erdei legeltetés, fás legelők, legelőerdők tájtörténete. [Landscape history of the forest grazing and wood pastures] Természetvédelmi Közlemények, Magyar Botanika Társaság, Budapest. 68-79. pp.

[24] Vityi A, Frank N (2016): Shelterbelt as a best practice of improving agricultural production In: 3rd European Agroforestry Conference - Book of Abstract. European Agroforestry Federation, Montpellier. pp 211-212

[25] Vityi A, Marosvölgyi B, Kiss A, Schettrer P (2015): Research and Development Protocol for Arable Agroforestry in Hungary Group. Milestone MS16 Part of Experimental Protocol for Arable Farmers for EU FP7 Research Project: AGFORWARD 613520. 10 pp.

[26] Vityi A. ,Kovács K.,Dufla F., Bácsmegi L., Nagy I (2016): Improve the efficiency of afforestation by the use of

agroforestry practices. In: 3rd European Agroforestry Conference: Celebrating 20 years of Agroforestry research in Europe. Book of abstracts. Montpellier, 2016. (pp.145-146.) European Agroforestry Federation

[27] Vityi A., Marosvölgyi B., Kiss-Szigeti N. (2017): Az agroerdészet hazai helyzete, potenciálja, és korlátozó tényezői. VI. Kari tudományos konferencia. Előadás. Soproni Egyetem, 2017. 10. 24.

[28] Vityi, A (2014). Initial Stakeholder Meeting Report: Alley Cropping Systems in Hungary. 23 October 2014. EU FP7 Research Project: AGFORWARD 613520. 11 pp. Available online: http://www.agforward.eu/index.php/en/alley-cropping-systemsin-hungary.html

[29] Vityi, A., Varga A. (2014): Initial Stakeholder Meeting Report - High Natural and Cultural Value AF Systems in Hungary. EU FP7 Research Project: AGFORWARD 613520. 14 pp.

[30] Zajączkowski K., 2005, Regionalizacja potrzeb zadrzewieniowych w Polsce, (Regionalization of agricultural landscape needs for shelterbelts and woodlots in Poland), Prace IBL, Rozprawy i Monografie, (Papers of Forest Research Institute, Monographs), 4, 131 pp.

[31] Zelba O, Lojka B, Houska J, Kotrba R, Martiník A, Weger J (2015): Inventory of Agroforestry in Czech Republic. In: 3rd European Agroforestry Conference: Celebrating 20 years of Agroforestry research in Europe. Book of abstracts. Montpellier, 2016. (pp.439-441) European Agroforestry Federation

[32] Zomer RJ, Neufeldt H, Xu JC, Ahrends A, Bossio D, Trabucco A, van Noordwijk M, Wang MC. 2016. Global Tree Cover and Biomass Carbon on Agricultural Land: The contribution of agroforestry to global and national carbon budgets. Scientific Reports 6: 12.

Earth in a Trap? 2018
Analytical Methods in Fire and Environmental Science

Study of thermal degradation of selected materials using ATR-FTIR spectroscopy

Eva Výbohová[a*] – Veronika Veľková[b]

[a]*Department of Chemistry and Chemical Technologies, Technical University in Zvolen, T.G. Masaryka 24, 960 53 Zvolen, Slovakia*

[b]*Department of Fire Protection, Technical University in Zvolen, T.G. Masaryka 24, 960 53 Zvolen, Slovakia*

Abstract

This paper focuses on the possibility to use attenuated total reflectance - Fourier transform infrared (ATR-FTIR) spectroscopy in fire engineering. The key advantages and limitations of this technique are discussed. As examples, the study of thermal degradation of PUR foam, and wood are used. The assignment of characteristic absorption bands in the investigated materials is presented. Additionally, the changes in spectra due to thermal degradation of examined materials were discussed. In the case of PUR foam, the degradation of NCO, formation of new carbonyl groups, loss of CH_2 groups, and the loss of aromatic rings were observed. In samples of wood the structural changes in lignin macromolecule as well as the degradation of polysaccharides, mainly hemicelluloses were occurred.

Keywords: ATR-FTIR spectroscopy; thermal degradation; PUR foam; wood

---

[*] Corresponding author. Tel.: +421-45-5206534; fax: +421-45-5330027; e-mail: eva.vybohova@tuzvo.sk

1. Introduction

Attenuated Total Reflectance (ATR) is currently the most widely used FTIR sampling tool. This technique requires minimal or no sample preparation prior to spectral measurements. Whereas there are also portable devices, it allows you to get quick results even in the field.

Attenuated total reflectance is based on measuring the changes that occur in a totally internally reflected infrared beam when the beam comes into contact with a sample (Fig. 1). An infrared beam is directed onto an optically dense crystal with a high refractive index at a certain angle [1]. The beam penetrates a fraction of a wavelength beyond the reflecting surface and when a material that selectively absorbs radiation is in close contact with the reflecting surface, the beam loses energy at the wavelength where the material absorbs. The resultant attenuated radiation is measured and plotted as a function of wavelength by the spectrometer and gives rise to the absorption spectral characteristics of the sample [2].

The depth of penetration of the infrared beam into the sample at the contact position is given by the following equation [3]:

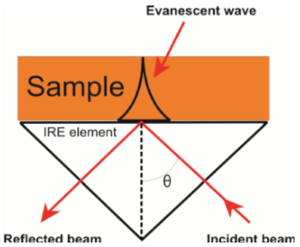

Fig. 1. Scheme of a single reflection ATR-FTIR [1]

$$DP = 1/[2\pi W n_c(\sin 2\theta - n^2_{sc})^{1/2}] \qquad (1)$$

Where DP is the depth of penetration,
W is wavenumber,
θ is the angle of incidence,
n_c is refractive index of crystal,
n_{sc} is the ratio $n_{sample}/n_{crystal}$.

From the equation above, it can be concluded that:

- The penetration depth increases at lower wavenumbers (longer wavelengths). This implies that, the peak intensities at the low-wavenumber side of the ATR spectrum are higher than in the transmission spectrum.
- The penetration depth decreases as the angle of incidence increases.
- If the same sample is measured using crystals of different refractive index, the depth of penetration is lowest for the crystal with the highest refractive index. Therefore, as n_c goes up, the depth of penetration goes down.

The crystals used in ATR cells are made from materials that have low solubility in water and are of a very high refractive index. The properties of commonly used materials for ATR crystals are summarized in Table 1. It is important to choose the correct ATR crystal for a given application. When selecting a suitable crystal, it is necessary to focus on its refractive index, wavenumber range, pH sensitivity, durability and toughness.

According to [3] diamond is in some ways the excellent ATR crystal material. Diamond is chemically inert, impervious to strong acids and bases. Diamond is the hardest substance known to man, so samples will not scratch it. Due to its tough even under great pressure the diamond crystal will not break.

ATR enjoys a number of advantages compared to the other sampling techniques. It is a fast and easy technique to measure many different types of samples including liquids, semi-solids, polymers, powders, and solids. Only gases cannot analyze using ATR technique. This accessory provides for the non-destructive measurement of samples with little or no preparation. Liquid samples can be applied directly to the ATR crystal, one drop is enough to analyze. Other samples can be directly applied to the ATR crystal without time-consuming dilution with matrices such as Nujol or KBr [3, 4].

Table 1

Properties of infrared crystals

Material	Useful range for ATR (cm^{-1})	Refractive index	pH range	Hardness (Knoop#)	Remarks
Diamond	4200-200	2.4	1-14	7000	very hard, withstands high pressure, chemically inert
Ge	5500-675	4.0	1-14	550	hard & brittle, good ATR material, temp. sensitive
KRS-5	20000-400	2.37	5-8	40	deforms under pressure, conventional ATR material
ZnS	17000-950	2.2x	5-12	178	good ATR material, withstands shock
ZnSe	20000-650x	x	5-9	137	hard & brittle, good ATR material

Semi-solids (e. g. paste, viscous liquids) can simply smear on the ATR crystal, and after analyze the crystal it is needed cleaning with an appropriate solvent. Spectrum of any polymer sample, including polymer films, pieces, pellets, and parts, can be obtained if it is clamped to the ATR crystal. All solids will generally need to be clamped to the ATR crystal to promote good contact of the sample with crystal surface. In the case of powders, high pressure is needed to flatten samples so they make good contact with the ATR crystal surface. This much pressure can bend or break softer ATR crystals, therefore for powder analyze the diamond crystal is recommended.

For all its advantages ATR technique has important disadvantages. The crystal must be scratch-free. Problem can be in the case of softer ATR crystals such as ZnSe that can be scratched by some samples. Another issue with ATR is its limited wavenumber range. Many ATR crystals absorb in the mid-infrared region. For example, diamond absorbs between 2200 and 2000 cm^{-1} and ZnSe absorbs below 700 cm^{-1}, masking sample features in these regions. Another disadvantage of ATR is its lack of sensitivity. In general, ATR can only detect molecules present in concentrations greater than 0.1 %. Finally, ATR is probably the most expensive FTIR sampling technique available. Especially, this concerns about diamond ATR accessories [3].

In fire engineering, the ATR-FTIR can be used to identification of materials from fire debris, study of thermal degradation of materials, detection of flame accelerators (ignitable liquids) or observing the effect of fire retardants on material properties [5, 6, 7, 8, 9, 10, 11].

The purpose of this paper is to demonstrate the possibility to use ATR-FTIR spectroscopy for analysis of thermal degradation of two various materials – polyurethane (PUR) foam and wood.

2. Materials and methods

2.1. The thermal degradation of PUR foam samples

The samples of PUR foam (Penosil Premium Foam) were heat-loaded in laboratory experimental equipment. The heating was achieved by two heating spirals. The temperature in the reaction zone was controlled by a digital thermometer. The samples were heat-loaded for 15 min at temperatures 180 °C, 200 °C, and 220 °C.

2.2. The thermal degradation of wood samples

Air-dried lumber from a common ash trunk (*Fraxinus excelsior* L.) was used to prepare samples with dimensions 32 mm × 32 mm × 120 mm. The samples were conditioned in a chamber at 20 ± 2 °C and 65 ± 5% relative humidity to the moisture content of about 12 %. Test samples were heat treated in a laboratory oven at temperature of 220 °C under atmospheric pressure in the presence of air for 150 minutes. One group of control samples was left without treatment (20 °C) and compared to thermally modified samples.

2.3. ATR-FTIR analysis

The samples of PUR foam as well as of wood were analyzed using ATR-FTIR spectroscopy. The measurements were performed using a Nicolet iS10 FTIR spectrometer equipped with a Smart iTR attenuated total reflectance (ATR) sampling accessory with a diamond crystal (Thermo Fisher Scientific, Madison, WI). The resolution was set at 4 cm^{-1} for 64 scans for each steaming technique and following analysis. The wavenumber range varied from 4000 to 650 cm^{-1}. Four analyses were performed per sample. OMNIC 8.0 software (Thermo Fisher Scientific, Madison, WI) was used to evaluate the spectra.

3. Results and discussion

ATR-FTIR analysis of PUR foam

On the Fig. 2 the FTIR spectrum of original sample of PUR foam is depicted. The wavenumbers of the most representative absorption bands are marked. Band assignment was made according to the references [12, 13, 14], as shown in Table 2.

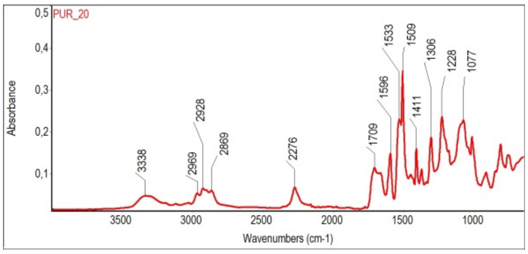

Fig. 2. FTIR spectrum of untreated PUR foam

Table 2

Assignment of infrared absorption bands in spectrum of PUR foam [according to 12, 13, 14]

Wavenumber (cm^{-1})	Spectral characteristic
3338	N-H stretching
2969	C-H in CH_2 and CH_3 stretching
2928	C-H in CH_2 and CH_3 stretching
2869	CH_2 and CH_3 stretching
2276	NCO stretching
1709	C=O non-bonded urethane stretching, associated urethane and isocyanurate ring stretch
1596	C=C aromatic
1509	H-N-C=O Amide II combined motion
1411	isocyanurate ring
1228	C-O-C
1077	ester C-O-C stretching

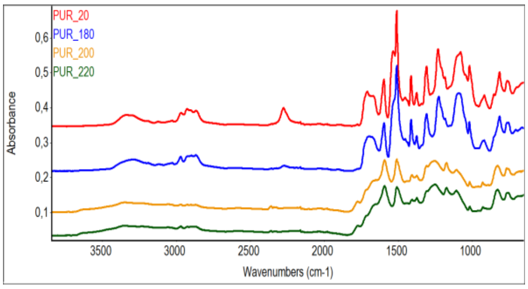

Fig. 3. Comparison of FTIR spectra of untreated (PUR_20) and heat treated (PUR_180, PUR_200, PUR_220) PUR foam samples

From the evaluation of the obtained spectral records (Fig. 3), it can be stated that during the heat treatment of PUR foam, firstly the degradation of NCO was observed. This is evident from the decrease in the intensity of absorption band at 2276 cm^{-1} in the spectrum of PUR foam treated at 180 °C and its loss in spectra of PUR foam treated at higher temperatures. At temperatures above 180 °C key observations are loss of the N-H groups (peaks around 3338 cm^{-1}, and 1509 cm^{-1}), loss of CH_2 and CH_3 groups (peaks between 2969 and 2869 cm^{-1}), formation of new carbonyl groups (peak around

1772 cm^{-1}), loss of urethane linkage (peak around 1709 cm^{-1}), loss of aromatic rings (peak around 1596 cm^{-1}), and loss of isocyanurate rings. According to Yarahmadi *et al.* (2017) the formation of new carbonyl groups together with the loss of CH_2 groups provides a clear indication of the thermo-oxidative degradation processes taking place in the soft segment of the PUR foam. In addition, the loss of aromatic rings suggests that there are changes also in the hard segment. The degradation of hard segment of PUR monomer is more pronounced at temperatures of 200 °C, and 220 °C.

ATR-FTIR analysis of wood

In the FTIR spectra of wood (Fig. 4) absorption bands appertaining to all wood components (cellulose, hemicelluloses, lignin, extractives) are observable. Assignment of them according to literature [15, 16] is in the Table 3.

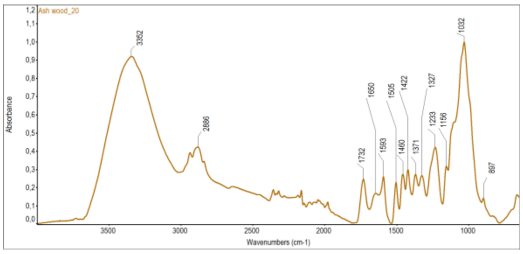

Fig. 4. FTIR spectrum of untreated ash wood

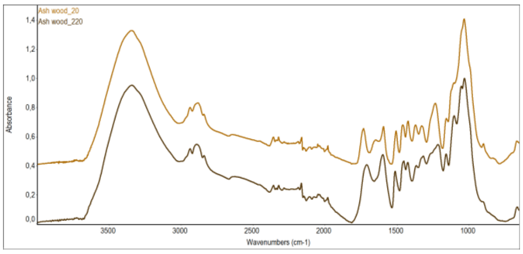

Fig. 5. Comparison of FTIR spectra of untreated (Ash wood_20) and heat treated (Ash wood_220) ash wood

Table 3

Assignment of infrared absorption bands in wood spectrum [15, 16]

Wavenumber (cm^{-1})	Spectral characteristic
3352	O–H stretching
2886	Symmetric/ asymmetric C–H stretching in – CH_2 and CH_3
1732	Unconjugated C=O stretching of acetyl, carboxylic groups and aldehydes
1650	Conjugated C=O stretching, absorbed water
1593	Aromatic skeletal vibrations in lignin
1505	Aromatic skeletal vibrations in lignin
1460	C–H deformations in lignin and carbohydrates
1422	C–H deformations in lignin and carbohydrates
1371	C–H in-plane bending in carbohydrates
1327	OH in-plane bending, CH_2 wagging in cellulose, syringyl ring
1233	Syringyl ring and C–O stretch in lignin and xylan
1156	C-O-C asymmetric bridge stretching
1032	C-O stretching in polysaccharides
897	Stretching at the β-(1,4)-glycosidic linkage, and C-H deformation in cellulose

In infrared spectrum of wood most of the specific vibrations in the fingerprint region (from 1800 to 700 cm^{-1}) are presented. There are also considerable changes due to heat treatment (Fig. 5).

Absorption band at 1732 cm^{-1} corresponds to the unconjugated C=O stretching vibrations. According to [16] its increasing and shifting to smaller wavenumbers due to heat treatment may be due to an increase of carbonyl or carboxyl groups in wood components by oxidation. Their formation contributes to the darkening of thermally loaded wood [17]. On the other hand, the decrease in intensity of absorption band of conjugated carbonyl groups at 1650 cm^{-1} was observed. The increase of the band at 1732 cm^{-1} in relation to 1650 cm^{-1} means that non-conjugated C=O groups increased in relation to conjugated groups. Similar results were described by other authors [16, 18].

From comparison of FTIR spectra of untreated and heat treated ash wood samples the increase in intensity of characteristic absorption bands of aromatic rings in lignin at 1593 cm^{-1} was observed. This can be due to an increase in the percentage of lignin in treated wood [16, 19]. Furthermore, the shifting of the maximum of absorption band from 1505 cm^{-1} to about 1512 cm^{-1} was observed. This can be due to structural changes in lignin macromolecule. Whereas at about 1505 cm^{-1} the vibrations of hardwood lignin (guaiacyl and syringyl units), at about 1512 cm^{-1} the vibrations of softwood lignin (guaiacyl units) are proved [20]. The shifting to greater wavenumber can be due to decrease of the methoxyl groups in lignin which would lead to a lignin more similar to softwood (guaiacyl units).

Due to heat treatment also the degradation of polysaccharides was observed. This is evident from the decrease in intensity of their characteristic absorption bands at 1371, 1327, 1233, and 897 cm^{-1}. In the spectrum of untreated wood it is evident the overlapping of two absorption bands around 1233 cm^{-1}. One of them (at 1233 cm^{-1}) represents the vibrations of hemicelluloses (xylan), and second (at 1264 cm^{-1}) the guaiacyl ring breathing with C–O stretching. We suggest that the decrease in its height due to heat treatment might be caused by degradation of thermally labile hemicelluloses, and its broadening by formation of new groups.

4. Conclusions

This paper deals with the possibility to use ATR-FTIR spectroscopy in fire engineering. ATR is a fast and easy technique to measure many different types of samples including liquids, semi-solids, polymers, powders, and solids. This accessory provides for the non-destructive measurement of samples with little or no preparation. In our experiment we demonstrate the use of ATR-FTIR technique for analysis of thermal degradation of natural and synthetic polymeric materials. We have analyzed the untreated and heat treated samples of PUR foam as well as wood. There are assigned the vibrations of characteristic groups of both materials. Additionally, the changes in FTIR spectra due to thermal degradation of examined materials were discussed.

Acknowledgments

This work was supported by the Slovak Scientific Grant Agency VEGA under contract No: 1/0806/17.

References

[1] Z.M. Khoshhesab, in: T. Theophanides (Ed.), Infrared Spectroscopy, IntechOpen, Rijeka, 2012, Ch. 11.
[2] B.H. Stuart, Infrared Spectroscopy: Fundamentals and Applications, 1st ed., John Wiley & Sons, Ltd., 2004.
[3] B.C. Smith, Fundamentals of Fourier transform infrared spectroscopy, 2nd ed., Taylor & Francis Group, Boca Raton, FL, 2011.
[4] V. Milata, P. Segľa, V. Brezová, A. Gatial, V. Kováčik, M. Miglierini, Š. Stankovský, J. Šíma, Aplikovaná molekulová spektroskopia, 1st ed., Vydavateľstvo STU v Bratislave2008.
[5] T.J. Kerr, K.L. Duncan, L. Myers, Vib. Spectrosc. 68 (2013) 225.
[6] L.S.G. Teixeira, F.S. Oliveira, H.C. dos Santos, P.W.L. Cordeiro, S.Q. Almeida, Fuel 87 (2008) 346.
[7] M. Khanmohammadi, A.B. Garmarudi, M. de la Guardia, Trends Anal. Chem. 35 (2012) 135.
[8] Bruker Optics, Application Note AN # 59. Identification of brominated flame retardants in polymers, 2009.
[9] D. Bakirtzis, V. Tsapara, S. Liodakis, M.A.Delichatsios, Thermochimica Acta 550 (2012) 48.
[10] C. Martín-Alberca, F. E. Ortega-Ojeda, C. García-Ruiz, Analytica Chimica Acta 928 (2016) 1.
[11] C. Martín-Alberca, F. E. Ortega-Ojeda, C. García-Ruiz, Applied Spectroscopy 70 (2016) 520.
[12] S. Radice, S. Solexis, M. Bradley, Application Note: 51255, Thermo Fisher Scientific, Madison, WI, 2007.
[13] N. Yarahmadi, A. Vega, I. Jakubowicz, Polymer Degradation and Stability 138 (2017) 192.
[14] R.C.M. Dias, A.M. Góes, R. Serakides, E. Ayres, R.L. Oréfice, Materials Research. 13 (2010) 211.
[15] D.N. Hon, N. Shiraishi, Wood and Cellulosic Chemistry, Marcel Dekker, New York, NY, 2001.
[16] B.Esteves, A. Velez Marques, I. Domingos, H. Pereira, Maderas, Cienc. tecnol. 15 (2013) 245.
[17] Y. Chen, J. Gao, Y. Fan, M.A. Tshabalala, N.M. Stark, BioResources 7, (2012) 2236.
[18] M.M. González-Peña, S.F. Curling, M.D.C. Hale, Polymer Degradation and Stability 94 (2009) 2184.
[19] R. Kotilainen, T. Toivannen, R. Alén, Journal of Wood Chemistry and Technology 20 (2000) 307.
[20] O. Faix, Holzforschung 45 (1991) 21.

Assessment of possible environmental risks of old dumps

Ivana Knapcová[a] – Dagmar Samešová[a]

[a]*Department of Environmental Eingennering, Faculty of Ecology and Environmental Sciences, Technical University in Zvolen, T. G. Masaryka 24, 960 53 Zvolen*

Abstract

The environmental risk study of the gudron´s dump
The technological stream, which is the most environmentally harmful during the refinery production, are wastes from acid refining - gudrons. Gudrons are produced in the processing plant at the treatment and pretreatment of crude oil by the use of sulphonation technologies. In the past, gudrons have been landfilled without security, and the problem of contamination remains as an environmental burden. The risk of contamination spreading has some migration pathways in general: land, surface runoff, groundwater, air. The aim of the paper is to assess the potential risk of dumps by means of ecotoxicological tests (acute toxicity test on daphnias - Daphnia magna and the growth inhibition test of the root of the higher cultural crops - Sinapis alba) of the aqueous and solid waste phases. There was evaluated the dependence of inhibition and immobilization on the concentration of the oil which was defined as unpolar extractable oil content (NEL). The results show that the waste is toxic to both aquatic and terrestrial organisms. In terrestrial tests, 50% inhibition was confirmed at NEL values of 79 mg.l^{-1} for the solid phase and 0.2 mg.l^{-1} for the aqueous phase. In the aqua test, 50% immobilization was confirmed at NEL concentrations of 5.4 mg.l^{-1} (solid phase) and 0.1 mg.l^{-1} (aqueous phase).

Key words: ecotoxicity, dump, environmental risks

1. Introduction

The technological stream that has the most environmental burden during refining of the petroleum fractions are acid refining residues - gudrons.

In the past, they were mostly landfilled without security and the problem of environmental contamination persists to this day.

This wastes are produced in the processing plant for the treatment and processing of crude oil by the use of sulphonation technologies.

These are processes in which the concentrated sulfuric acid is used for the sulfonation of the compounds. The sulfuric acid allows easier separation and regeneration of benzene, toluene and xylene fractions, modification of hydrocarbon materials [1], benzene refining, re-refining and white oil production [2].

Gudrons are a thick, highly viscous substance with a pungent, acidic odor [3], with a high degree of mobility [4], which gradually separates sulfuric acid [5].

These wastes have been deposited without modification in the natural environment, into artificial or naturally created lagoons.

In this way, landfills of hazardous industrial waste were originated (Predajná I and Predajná II) in the municipality of Predajná in the Slovak Republic [6].

Gudron waste dumped in landfills is a mixture of sulphonic acids, mineral oils, sulphonates (Ca, Na), chlorides, free sulfuric acid and water.

There is a three-phase stratification process according to a different specific weight:

1. the oil layer is the topmost, it consists of the various oils found in the waste,
2. the aqueous layer is below the oil phase, it is composed mainly of aqueous sulfuric acid, water and water-soluble substances (detergents, chlorides, sulphates),
3. the solid layer is at the bottom of the dump where all the solids forming the polymers are deposited [7].

Landfills of the hazardous industrial waste (acidic gudrons) Predajná I and II represent high risk sites in the Slovak Republic.

In the framework of the systematic identification of environmental burdens loads, they have been included among the high risk area.

Landfills Predajná I and II lie in the protection zone of the Low Tatras National Park with a second degree of protection.

The volume of gudron landfills represents about 225,000 m^3 of solid waste phase and several thousands of m^3 of liquid waste.

2. Methods

Preparation of model samples

The ecotoxicological tests were performed in the leachate from the solid layer and in the aqueous layer of gudron waste from the landfill Predajna II.

A sample of the bottom layer was taken from a depth of approximately 0.5 m.

The water layer was collected from the surface into the relevant samples according to the instructions for the sampling of waste water [8].

The basic physical and chemical characteristics of the individual layers are shown in Table 1.

Table 1 Selected physico-chemical indicators of gudrons from landfill Predajná II

Samples	Dry matter [%]	Residue after annealing [%]	pH	ChSK$_{cr}$ [mg.l^{-1}]	conductivity [mS.m^{-1}]
Solid layer	37,71	1,14	2,38	49 320,00	0,53
Water phase	1,62	0,12	2,10	18 560,00	2,70

Ecotoxicological tests

Toxicity tests are experimental methods for determining toxic effects of stressors (toxins) on natural organisms [9-10].

Onwurah (2007)[11] in his study, states that aquatic and terrestrial organisms (bio-organisms) have a high sensitivity to oil and petroleum product compounds, and therefore are suitable for assessing the toxic effect of gudron waste.

Gudrons as petroleum products contain a significant proportion of non-polar extractable substances .

The following bioassays were used to determine ecotoxicological properties:

- Terrestrial root growth inhibition test of higher cultural plant *Sinapis alba*
- Aquatic toxicity test on Daphnia magna

In view of the effect of the content of petroleum substances in the gudrons, which were identified as non-polar extractable substances (NES) and their cumulative properties, the dependence of inhibition and immobilization (stimulation) were evaluated in the baseline test.

Determination of non-polar extractable substances (NES)

The sample was extracted with organic solvent S-316. The polar and nonpolar substances pass into the organic phase during extractions. The extract is dried over anhydrous sodium sulfate after separation of the aqueous and organic phases

The removal of polar substances from non-polar materials from the extract is carried out by sorption on activated silica gel.

The determination of NES in the IR region uses valence vibrations for the CH_3 bands at 2960 cm $^{-1}$, for the CH_2 bands at 2925 cm $^{-1}$ and at 3055 cm $^{-1}$ for aromatic hydrocarbons using an organic solvent (S-316) [12-13].

This determination is a group determination of petroleum substances, which is permitted under the Water Act No. 364/2004

The terrestrial root growth inhibition test of higher cultural plant *Sinapis alba*

The effect of water on seed germination and growth of white Sinapis alba roots is tested in the early stages of development.

The test is based on a comparison of a cultivation of the seed on substrates saturated by investgated substance with controlled-test (seeds grown on a dilution water) [14-15].

The acute toxicity test on water fleas

The acute toxicity test is the most commonly used aquatic immobilization test for small crustaceans of the Daphnia magna (petrified) crustaceans that belong to primary consumers.

The principle is to determine the concentration which, immobilize 50% of the exposed individuals under defined conditions, within 24 and 48 hours [15-16].

Daphnia magna water scabs are exposed to the test samples in the aquatic toxicity test according to STN 83 8303.

Processing of results

The program STATISTICA 12 was used to evaluate the results of the basic tests. We used an advanced non-linear estimation method with self-regression using the non-linear function $y = 100 * (1 - l^{-kx})$. 2D graphs were used to plot the % inhibition (immobilization) dependending on the NES concentration (mg.l^{-1}).

3. Results and discussion

The terrestrial root growth inhibition test of higher cultural plant *Sinapis alba*

The values determined by the preliminary root growth inhibition test of the higher cultivated plant Sinapis alba confirmed a positive result for both the solid and the aqueous layer of waste.

The test is positive with respect to the determined values and the evaluation of the test according to STN 83 8303 because inhibition of root growth is ≥ 30% (stimulation ≤ 75%) as compared to control as in our case. The inhibition of root growth was ≥ 50% compared to the control, therefore we determined the IC50 value of the aqueous extract, and we performed the baseline test [15, 17]. We proposed 5 suitable dilutions with the corresponding measured NEL content in mg.l^{-1} (Table 3) in the baseline test samples.

Table 3: NES content [mg.l^{-1}] for individual dilutions and set pH values

Solid waste layer			Water layer of waste		
Dilutin	**pH**	**NES [mg.l^{-1}]**	Dilution	**pH**	**NES [mg.l^{-1}]**
50	2,00	123,20	5	3,55	0,47
100	2,61	61,72	10	4,42	0,24
500	3,45	12,40	25	6,43	0,09
1000	4,70	6,17	50	6,45	0,04
2000	6,20	3,09	75	6,50	0,03

The values determined in the basic test for the water and solid layer are graphically represented by nonlinear regression (Figures 1 and 2). Calculated IC50 values (from nonlinear equations) for individual samples are given in Table 4.

Table 4 Overview of tested concentrations that inhibit 50% of the tested individuals

	NES [mg.l^{-1}]	
	Solid layer - the leachate	**Water layer**
Terestrial test *Sinapis alba*	76	0,2
Acute toxicity *Daphnia magna*	5,4	0,1

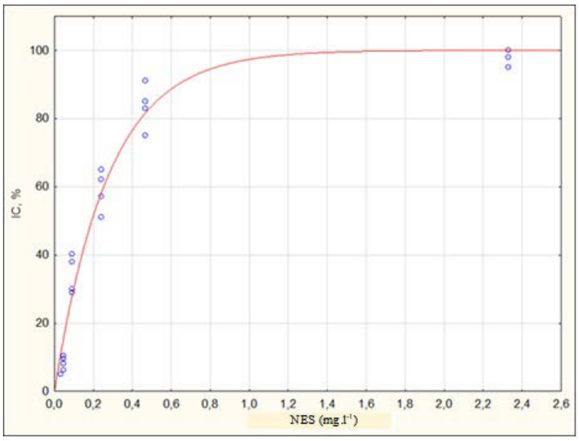

Figure 1: Graphical representation of the % inhibition in of aqueous layer samples of gudron (Sinapis alba root growth inhibition test)

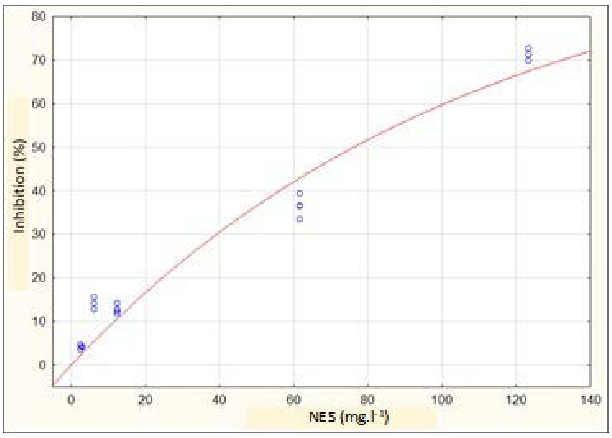

Figure 2: Graphical representation of the inhibition (%) according to NES (mg.l^{-1}) in solid-layer samples (root growth inhibition test)

The acute toxicity test on water fleas *Daphnia magna*

The preliminary test, in which the fleas were exposed to undiluted samples, showed a positive result for both test layers.

During the test, a mortality or immobilization of ≥ 50% of the fleas occurred in comparison with the control, in this case, it is necessary to set the EC50 value and to continue to set the basic test [9, 18, 19].

At the same time, we performed a control test where dilution water [15] was used instead of the sample. The number of mobilized subjects was evaluated after 24 and 48 hours. In the baseline test, were used the same dilutions as in the previous bioassay (Table 3). The set EC50 values for solid and water samples are given in Table 4 and the values are graphically recorded in Figures 3 and 4.

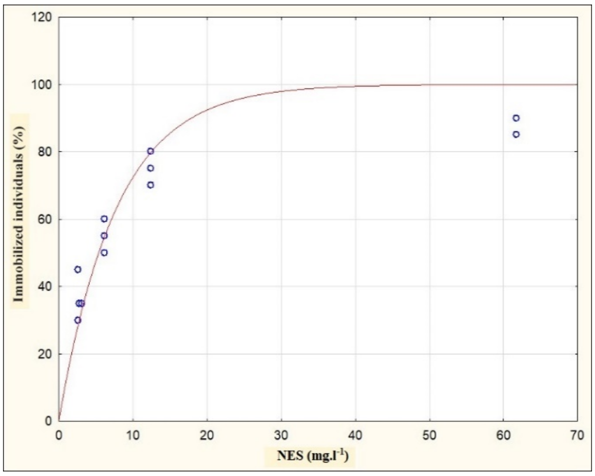

Figure 3 Immobilization dependence (%) of NEL (mg.l^{-1}) in samples of solids leachate (Daphnia magna acute toxicity test)

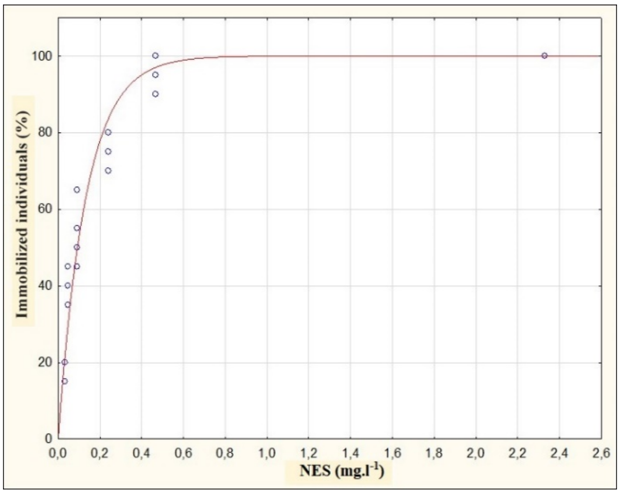

Figure 4 Immobilization dependence (%) of NES (mg.l^{-1}) in samples of the aqueous layer of gudron (acute toxicity test on Daphnia magna)

Conclusion

Based on the results, we can conclude that the analyzed samples are toxic to aquatic and terrestrial organisms. In terrestrial tests (Sinapis alba), 50% inhibition was confirmed at higher NEL values (76 mg.l^{-1}) and in the aquatic test 50% immobilization was confirmed at concentrations of 5.4 mg.l^{-1} compared with control.

We suppose that the toxicity of the water layer sample is primarily influenced by a different indicator as NEL because the concentration that causes 50% of the immobilization of individuals in the upper water layer is 0.1 mg.l^{-1}, which is the limit value of NEL in surface water [20].

External environmental impacts that can cause toxic compounds may significantly affect ecotoxicity.

We assume the significant impact of dilution and leaching due to precipitation, but also the formation of toxic compounds by the influence of solar radiation. Landfills are high in toxicity and further analysis is needed to assess the overall landfill risk.

Acknowledgments

Thanks to project KEGA 018TU Z-4/2017

References

[1] MILNE, D.D., CLARK, A.L., PERRY, R.: Acid Tars: their production, treatment and disposal in the U.K In: Waste Management and Research, 1986, Vol.4 issue:1, pp: 407-418. ISSN: 0734-242X.

[2] NASCARROW, D.J., SLADE, N.J., STEEDS, J.E. : Land Contamination: Technical Guidance on Special Sites: Acid Tar Lagoons, Environment Agency. 2001, pp11-50. ISBN 1 85705 583 7

[3] KOLMAKOV, G. A., ZANOZINA V. F., KARATAEY, E. N., GRISHIN, D. F., ZORIN, A. D.: Thermal Cracking of Acid Tars to Asphalts as a Process for Utilization of Refinery Wastes In: Petroleum Chemistry, 2006, Vol. 46, No. 6, pp. 384–388. Pleiades Publishing, Inc. ISSN 0965-5441.

[4] TUMANOVSKY, A. G., KOSOBOKOVA, E. M., RYABOV, G. A.: Current problems: production of energy carriers as a method of utilizing the bottom layer of acid tar. In: Chemistry and Technology of Fuels and Oils,. 2004, 6(40), pp 351-357. ISSN 1573-8310.UDC 677.4-486.32

[5] KRENÍKOVÁ, V. Odpady a druhotné suroviny I. Univerzita J. E. Purkyně v Ústí n. Labem, Fakulta životního prostředí. 2014, s.54-97. ISBN 978-80-7414-870-5.

[6] MASAROVIČOVÁ, M., SLÁVIK, I.: Komplexný monitoring odkalísk SR. Bratislava: STU, 2013 pp.10-26.

[7] JELÍNEK, R.: Monitorovanie environmentálnych záťaží na vybraných lokalitách Slovenskej republiky, 2015, In: Záverečná správa: Lokalita: MEZ č.59, Predajná- skládka 1. ŠGÚDŠ Bratislava

[8] STN ISO 5667-10 : Water quality. Sampling. Part 10: Guidance on sampling of waste waters

[9] FARGAŠOVÁ, A.: Ecotoxicological bioassays, Bratislava: Publishing Perspekt, 2012, pp.30-40.

[10] HYBSKÁ, H.: Základy ekotoxikológie. Zvolen: T echnická univerzita, 2015. 116 s. ISBN 978-80-228-2798-0

[11] ONWURAH, I., NOEL E., OGUGUA, V., OLAWALE, O.: Crude Oils Spills in the Environment, Effects and Some Innovative Clean-Up Biotechnologies. In: International Journal of Environmental Research.2007, pp. 307-320. ISSN 1735-6865.

[12] STN 830530-36 Chemický a fyzikálny rozbor povrchovej vody. Stanovenie ropy a ropných látok.

[13] HYBSKÁ, H., VILLÁROVÁ, M.: Účinnosť vybraných produktov pri odbúravaní ropného znečistenia.2012. In Acta Facultatis Ecologiae : Journal of Faculty of Ecology and Environmental Sciences Technical University in Zvolen. - ISSN 1336-300X. - Vol. 27 (2012), s. 55-59.

[14] HYBSKÁ, H.: Toxikológia a ekotoxikológia : návody na cvičenia. Zvolen: Technická univerzita, 2016, 101 s. ISBN 978-80-228-2298-5

[15] STN 83 8303 Skúšanie nebezpečných vlastností odpadov. Ekotoxicita. Skúška akútnej toxicity na vodných organizmoch a skúšky inhibície rastu rias a vyšších kultúrnych rastlín.

[16] HYBSKÁ, H.,VEĽKOVÁ,V., SAMEŠOVÁ D., FIALOVÁ J., KUČERA M.: Study of the regeneration clenaning of used mineral oils In: Ekotoxicological properties and biodegradation. 2017, pp. 473-481. DOI: 10.15255/CABEQ.2017.1109.

[17] PAVLOVSKY, J.: Toxikologie. VŠB Technická univerzita Ostrava, 2014, s. 183-184.

[18] BORODUlLINA T.S., POLONSKIY V.I., VLASOVA, E.S., SHASKOVA T.L.,GRIGOR.S. : Effect of oil pollution of water on delayded fluorescence of the alage Chlorella vulgaris Beijer and survival rate of the cladoceran Daphnia magna In: Sibirskii Ekologicheskii Zhurnal. N.18. pp.107-111. ISSN: 0869-8619.

[19] VOLPE, D.A., HAMED, S., ZHANG, L.K.: "Use of Different Parameters and Equations for Calculation of IC50 Values in Efflux Assays: Potential Sources of Variability in IC50 Determination", In: The AAPS Journal, 2014, vol. 16, no. 1, pp. 172-180. ISSN: 1550-7416.

[20] Nariadenie vlády č.269/2010 ktorým sa ustanovujú požiadavky na dosiahnutie dobrého stavu vôd časť. A - požiadavky na kvalitu povrchovej vody

All you need is ...
AMEDIS
www.amedis.sk

25-ročná tradícia v oblasti predaja a servisu laboratórnej a zdravotníckej techniky.

SCIEX

SCIEX LC-MS/MS systémy:
hmotnostné spektrometre SCIEX TripleQUAD,QTRAP, TripleTOF, Q-TOF, TOF/TOF, novinka – X500R QTOF s vysokým rozlíšením, kapilárna elektroforéza SCIEX pre chemické, farmaceutické a genetické analýzy

---

scion INSTRUMENTS

SCION Instruments GC-MS systémy:
SCION SQ single quadrupole GC-MS
plynové chromatografy SCION 456-GC a SCION 436-GC
kapilárne a náplňové GC kolóny

---

analytikjena

Analytik Jena MS systémy s indukčne viazanou plazmou:
ICP-MS systémy PlasmaQuant MS s hmotnostou detekciou PlasmaQuant MS Elite so zvýšenou cilivosťou vhodné pre pripojenie **Laser ablation, analýzu mikročastíc ...**

CEM

CEM Corp. laboratórne mikrovlnné systémy a procesné analyzátory
-mineralizácia tlaková – MARS 6 iWave, otvorená mineralizácia,
extrakcia, proteínová hydrolýza, kjeldahlizácia,
stanovenie vlhkosti a sušiny,
NMR bezkalibračné stanovenie tukov,
mikrovlnná organická syntéza, syntéza peptidov

LCTech

LCTech: **automatizovaná príprava vzoriek potravín, krmív, enironmentálnych a toxikologických vzoriek – systém FREESTYLE**
prístroje a imunoafinit. kolónky na stanovenie **mycotoxínov**
plne automatizovaná GPC a SPE, automatizovaná príprava vzoriek na stanovenie dioxínov a PCB – **DEXTech**
zariadenia na post-kolónovú derivatizáciu firmy Pickering

TELEDYNE ISCO
A Teledyne Technologies Company

TELEDYNE ISCO:
nízkotlaková LC, Flash chromatografia – CombiFlash NextGen
zberače frakcií
vysokotlakové lineárne čerpadlá

OXFORD INSTRUMENTS

OXFORD INSTRUMENTS:
líder v X-ray fluorescenčnej analýze, stolové XRF - spektrometre X-Supreme8000, Lab – X3500
stolové NMR systémy: Pulsar, QA/QC NMR analyzátor MQC+, MQR

ERWEKA
Quality through Experience
Since 1951

ERWEKA testovanie farmaceutických produktov:
disolučné systémy On-OFF line pre testovanie tabliet
fyzikálne testery (oder a pevnosť tabliet, rozpadavosť, tok práškov a granulátov, vákuové testovanie tesnosti obalov, testovanie čípkov)

---

unico®

UNICO:
UV- VIS a VIS spektrofotometre pre laboratóriá - SQ 4802
mikroskopy, centrifúgy

INFICON

INFICON:
prenosný GC/MS systém INFICON HAPSITE ER na detekciu, identifikáciu a kvantifikáciu chemických látok
prenosné mikro-GC systémy na analýzu plynov
INFICON 3000 Micro GC
kontinuálny monitorovací systém INFICON 5000 CMS

Kinesis
Scientific Experts

Kinesis **- široká ponuka spotrebného materiálu pre kvapalinovú a plynovú chromatografiu, pre AAS**

VUV ANALYTICS

VUV ANALYTICS - vákuová UV-spektrometria:
otvára široké spektrum výhod, väčšina zlúčenín má totiž malú alebo žiadnu absorpciu v UV-VIS, zatial čo všetky silno absorbujú vo vákuovej UV oblasti, **novinka - VGA-100** a **VGA-101 ideálne detektory pre plynovú chromatografiu** s možnosťou pripojenia na GC od rôznych výrobcov


Chemická analýza
chromatografia – hmotnostná spektrometria – spektroskopia – elektroforéza – kolóny – spotrebný materiál . . .


Genomika
expresia génov – microarray – QPCR – mutagenéza – klonovanie – SureFISH – bioreagencie – TapeStation . . .


Diagnostika
imunohistochémia – molekulárna patológia – špeciálne farbenia – pharmDx – EnVision . . .

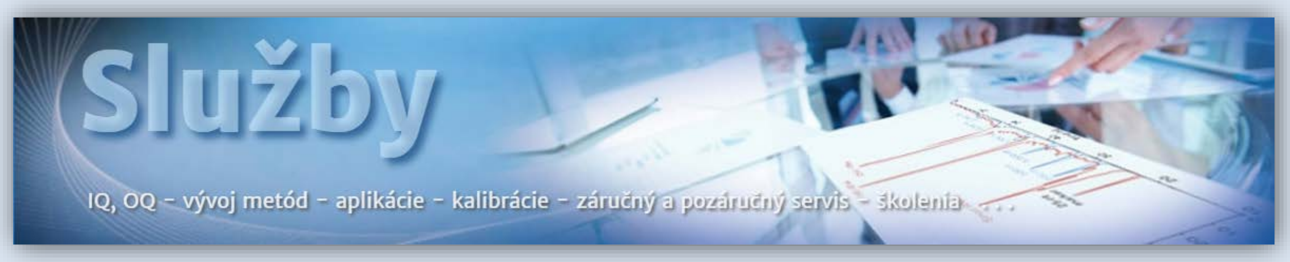
Služby
IQ, OQ – vývoj metód – aplikácie – kalibrácie – záručný a pozáručný servis – školenia . . .

Bruker - Remote Sensing

High Performance FT-IR Systems

Hyperspectral Imaging System Atmospheric and environmental research, volcanology, industrial surveillance and homeland security outline the wide range of applications of the HI 90 Hyperspectral Imaging System. The HI 90 is ideally suited for real-time identification, quantification, and visualization of gas clouds with high spatial resolution. Algorithms based on the combination of image processing and spectral analysis are implemented in the operating software. The system may also be used in a range of imaging applications for solids and liquids.

SIGIS 2

Scanning Imaging Remote Sensing System SIGIS 2 is a scanning imaging remote sensing system that allows rapid identi - fication, quantification and visualization of gas clouds from long distances. The system maps a predefined area and results of the analysis are visualized by a video image, overlaid by a chemical image. The SIGIS 2 is part of the equipment of emergency response forces around the world. In addition, SIGIS systems are applied in environmental applications, atmospheric research, volcanology, and industrial facility surveillance.

EM 27

Remote Sensing FT-IR The EM 27 is a ruggedized remote sensing system providing high performance spectroscopy in the field. The EM 27 can easily be deployed in the field for various air monitoring applications. Emissions from smoke stacks, waste disposal and hazardous emissions from chemical accidents can be observed with an operating range of typically several kilometers. The EM 27 SUN features a solar tracker for measurements of atmospheric gases by solar absorption spectroscopy. The tracker is controlled using an innovative camera-based feedback system (Camtracker). The outstanding tracking accuracy is the basis for high-precision quantification.

Armfield - Design and manufacture of equipment for engineering education and research. Constantly evolving f or the growing demands of the engineering education sector.

EM 27

SIGIS 2

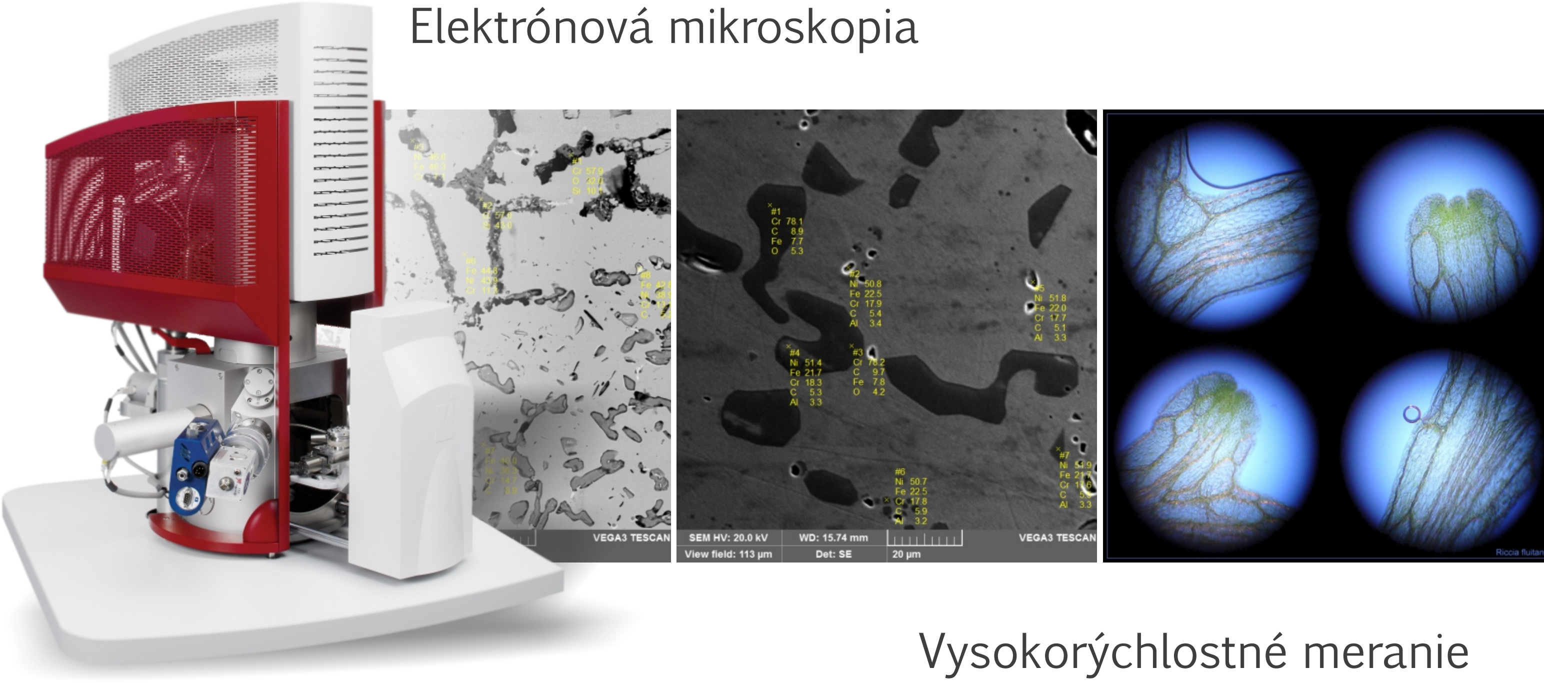
VEGA3 TESCAN
SEM HV: 20.0 kV
WD: 15.74 mm
View field: 113 μm
Det: SE
20 μm
VEGA3 TESCAN

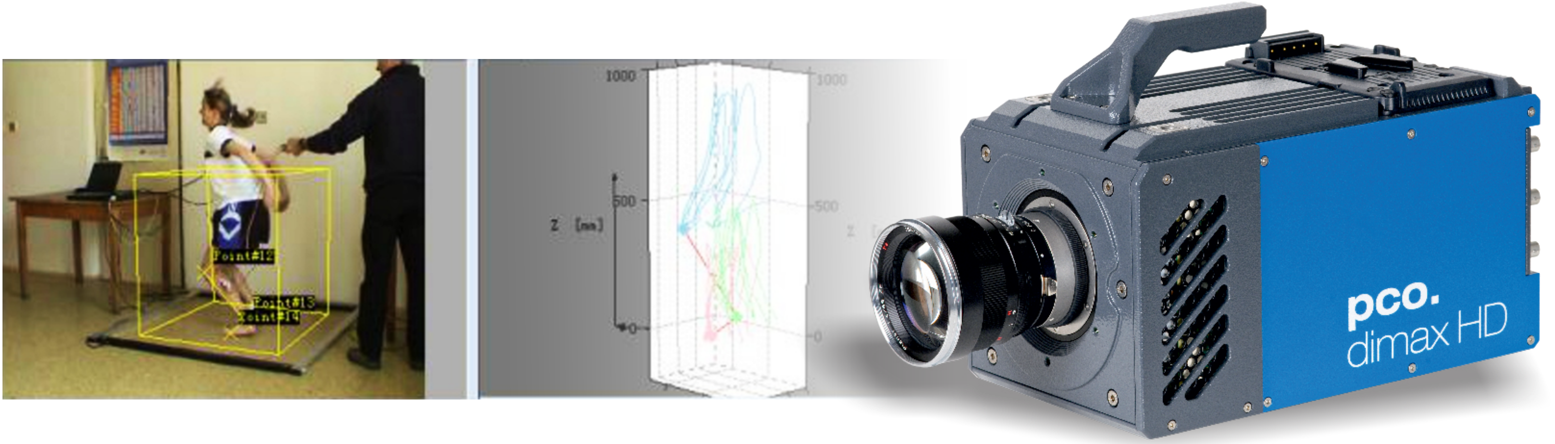
Point#12
Point#13
Point#14
Z [mm]
1000
500
0
pco.
dimax HD

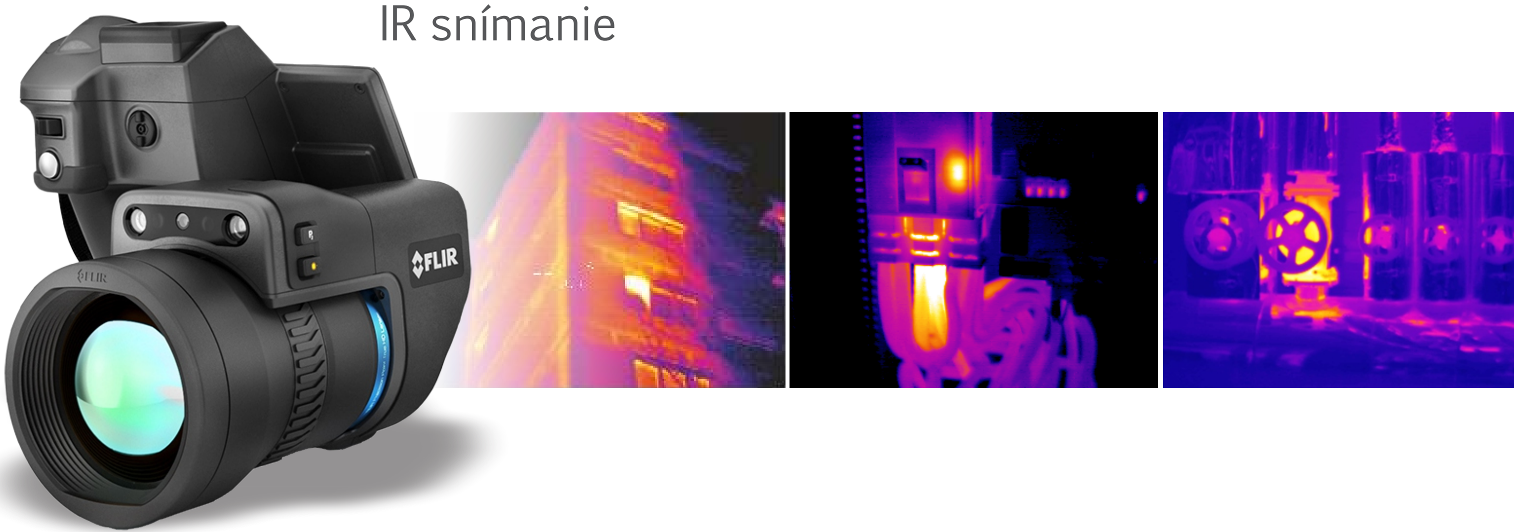
FLIR

JEDNORÁZOVÉ HYGIENICKÉ MATERIÁLY

– nová výzva pre čerpanie a čistenie odpadových vôd

Kúpeľné mesto Dudince trápil problém súvisiaci s čerpaním odpadových vôd dlhé roky. Veľká koncentrácia bytových domov, hotelov, sociálny dom a práčovňa majú za následok zmenu štandardného zloženia odpadovej vody. Okrem bežných problémov musel prevádzkovateľ verejnej kanalizácie na takmer každodennej báze riešiť problém upchatých čerpadiel v ČS na stokovej sieti a prevádzkové problémy, ktoré sa často posunuli až na producentov.

Čistenie upchatého čerpadla

Obyvatelia aj hoteloví návštevníci totiž, podobne ako aj v iných mestách, kanalizáciu využívajú ako odpadkový kôš pre bavlnené poplastované produkty, najmä hygienické výrobky a obväzy. Pre Stredoslovenskú vodárenskú prevádzkovú spoločnosť, a.s. (StVPS, a.s.) to znamenalo neustále zásahy a manuálne čistenie upchatých čerpadiel.

Upchávanie čerpadiel je dnes veľmi aktuálnou témou a zároveň výzvou v oblasti čistenia odpadových vôd. Nové druhy hygienických výrobkov a materiálov, ktoré sú zložené z bavlny a plastu (ako napríklad jednorazové utierky, plienky, vatové tyčinky, vlhčené obrúsky) obsahujú vo vode nerozložiteľné zložky, ktoré bežným čerpadlám v čerpacích staniciach a na ČOV spôsobujú výrazné problémy.

Na slovenskom trhu však pôsobia aj firmy, ktoré poznajú riešenie. Je ním unikátna hydraulika čerpadla, ktorá si vie s uvedeným problémom poradiť. Obežné koleso čerpadla a sacia doska tvoria v spojení s čepeľou z karbidu wolfrámu špeciálny rezací mechanizmus, ktorý zabraňuje upchatiu sacej časti čerpadla problematickými pevnými zložkami v odpadovej vode. Ak príde väčší zhluk pevných častí, toto zariadenie ho rozreže tak, aby jednotlivé pevné časti bez problémov prešli čerpadlom a zároveň nespôsobovali svojimi rozmermi upchávanie v následných výtlačných potrubiach. Táto skutočnosť je pre prevádzkovateľa veľmi dôležitá z hľadiska identifikácie a odstraňovania upchávok na výtlačných potrubiach, najmä väčších dĺžok, ktoré sú zle prístupné. Z hľadiska kontinuity prevádzky, podstatne nižších nákladov na údržbu čerpadiel, menšej náročnosti na personál a minimalizácie prerušení odvádzania odpadových vôd predstavujú tieto čerpadlá svetovú špičku a významne prispievajú k prevencii vzniku uvedených problémov.

Čerpadlo so štandardným rezacím zariadením

Firma PRAKTIKPUMP, s.r.o. sa zaoberá ponukou a dodávkami čerpadiel, ako aj servisnými a opravárenskými činnosťami v rámci vodárenských spoločností, ale aj priemyslu. Skúsenosti kombinuje s najmodernejšími riešeniami v oblasti čerpania kalovej aj čistej vody. V prípade problému, ktorý trápil mesto Dudince a prevádzkovateľa verejnej kanalizácie, firma na základe analýzy problému spoločne s prevádzkovateľom nahradila staré čerpadlá novými čerpadlami TSURUMI so špeciálnym rezacím zariadením. K výmene došlo v decembri 2013 a do dnešného dňa StVPS, a.s. nezaznamenala jediný výjazd spojený s jeho upchaním. Na základe týchto skúseností StVPS a.s. spoločne s firmou PRAKTIKPUMP, s.r.o. riešila týmto spôsobom aj ďalšie čerpacie stanice ako napríklad ČS Tajov, ČS Mlynská, ČS Iliaš a pod. Aj vďaka takýmto riešeniam firma PRAKTIKPUMP realizuje dodávky, opravy a servis čerpadiel v prevažnej väčšine vodárenských a priemyselných spoločností v Slovenskej a Českej republike.

Hydraulická časť TSURUMI so špeciálnym sekacím-trhacím zariadením s vysokou priechodnosťou

PRAKTIKPUMP, s.r.o.
JE VÝHRADNÝM ZÁSTUPCOM TSURUMI
NA SLOVENSKOM TRHU

☎ +421 (0)45 524 9011
✉ predaj@praktikpump.sk
🌐 www.praktikpump.sk

PRAKTIKPUMP
Profesionálny partner pre čerpacie technológie

TSURUMI PUMP

EDITOR`S NOTE

The Book is published in an electronic form. It consists of original scientific and professional papers written in English and formatted according to the editor`s requirements. All presented papers passed detailed review carried out by two reviewers at least.

All contributions in this Book of Proceedings were reviewed by two reviewers of Reviewing Committee.

REVIEWING COMMITTEE

The Reviewing Committee was composed of members of the Conference International Scientific Committee.

THE REVIEWING PROCESS

Manuscripts submitted for the inclusion in the **Earth in a Trap?2018: Analytical Methods in Fire and Environmental Sciences, Book of Proceedings** were subjected to the following review procedures:

- It was reviewed by editor for general suitability for this publication.
- If it was judged suitable, two reviewers were selected and a double blind review process took place.
- Based on the recommendations of the reviewers, the editor then decided whether the particular contribution should be accepted as it is, revised or rejected.

Book of Proceedings

International Scientific Conference

Earth in a trap? 2018: Analytical Methods in Fire and Environmental Sciences

23rd – 25th May, 2018

Hodruša-Hámre, Slovak Republic

ISBN 978-80-228-3062-1

Editors: Tatiana Bubeníková, Veronika Veľková

Technical editors: Rastislav Veľas, Martin Bednár

Published by Technical University in Zvolen, Slovak Republic, 2018